Physiological, cellular and molecular analysis of the role of mitochondrial dysfunction in people ageing with HIV

Matthew Hunt

BSc (Hons), MRes

Thesis submitted to Newcastle University for the Degree of Doctor of Philosophy

Wellcome Trust Centre for Mitochondrial Research

Institute of Translational and Clinical Research

September 2020

Author declaration

This thesis is submitted for the degree of Doctor of Philosophy at Newcastle University. The research was conducted in the Wellcome Trust Centre for Mitochondrial Research, as part of the Institute of Translation and Clinical Research, and is my own work if not stated otherwise. The research was completed under the supervision of Dr Brendan Payne, Dr Amy Vincent and Prof Sir Doug Turnbull from September 2017 to September 2020.

I certify that none of the material offered in this thesis has been previously submitted by me for a degree or any other qualification at any other university.

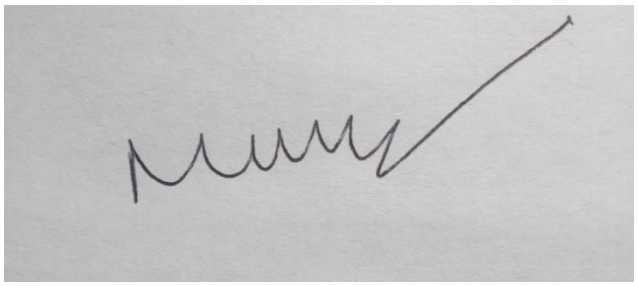

Matthew Hunt

Abstract

90% of people living with HIV (PLWH) in the UK are now on treatment in the form of antiretroviral therapy (ART) and 87% of these PLWH are virally supressed. Due to the success of ART, PLWH are now living longer, and the mean age of PLWH in the UK is now 48 years (Public Health England, 2019).

Despite successful ART, which has seen an increase in the quality of life for PLWH, some PLWH are living with an excess of frailty and reduction in physical function, as well as an increased susceptibility to acquiring age-related comorbidities (Guaraldi *et* al., 2011; Kooij *et al*., 2016; Desquilbet *et al*., 2007; Desquilbet et *al.,* 2009; Brothers *et* al., 2017). This phenomenon is understood to be highly heterogeneic, but while many of the risk factors are known, the exact pathological basis remains poorly understood. This could be due to the fact that there has been a lack of studies investigating the cellular and molecular causes in functionally relevant tissues such as skeletal muscle.

Mitochondrial dysfunction is one of the nine cellular and molecular hallmarks of ageing characterised by Lopez-Otin (Lopez-Otin *et al*., 2013). Mitochondrial defects are increased in HIV infection, despite viremia control as a result of ART (Payne *et al*., 2011), and PLWH have a high prevalence of mitochondrial-associated toxicities such as myopathy and peripheral neuropathy (Selvaraj *et al*., 2014; Cupler *et* al., 1995). These toxicities are strongly associated with nucleoside reverse-transcriptase inhibitors (NRTIs) such as zidovudine (AZT), zalcitabine (ddC), stavudine (d4T) and didanosine (ddI) (Dalakas *et al*., 1990; Arnaudo *et* al., 1991; Lim & Copeland, 2001; Lewis, 2003). However, mitochondrial dysfunction has also been demonstrated in individuals treated with newer antiretrovirals with a safter profile and low mitochondrial polymerase binding affinity, such as tenofovir disoproxil fumarate (TDF) (Samuels *et al*., 2017).

Given the close association between mitochondrial dysfunction and ageing (Lopez-Otin *et al*., 2013), and mitochondrial dysfunction in HIV infection (Erlandson *et al*., 2013; Payne *et al*., 2011; Chou *et al*., 2013), it is more than plausible to suggest that mitochondrial dysfunction plays a significant role in the accelerated ageing seen in PLWH. Due to the fact that there is a lack of concise studies which have investigated the role of mitochondrial dysfunction in ageing PLWH, I employed a wide range of cellular and molecular techniques to study mitochondrial dysfunction and other age-related pathology in skeletal muscle of older PLWH. This was correlated with clinical and treatment data, as well as physical function and body composition.

In addition, techniques established for the study of mitochondrial dysfunction in skeletal muscle were employed in a pilot study of mitochondrially-mediated renal disease in PLWH.

Acknowledgements

First and foremost, I would like to thank my supervisors Dr Brendan Payne, Dr Amy Vincent and Prof Sir Doug Turnbull for their support throughout my PhD and time at the MRG. Brendan, for trusting me and giving me the opportunity to undertake this PhD, which has been the best experience of my life. Thanks for giving me the confidence to allow myself to improve as a scientist and person. I have thoroughly enjoyed working with you. Apologies for the soppiness, but you have undoubtably changed my life for the better and I will always appreciate that. Amy, you have been a fantastic mentor and role model, and I greatly appreciate all the unwavering help you have given me over the past few years. A special mention to Grainne too, who as my panel member and later unofficial mentor has been a great source of encouragement.

Secondly, I would like to thank some of the other personnel who have helped me along the way. David McDonald, Andrew Fuller and the rest down at flow for the help over the years. Nicola at the clinic for constantly taking mine and everyone else's blood (thanks to all the willing and less willing participants too). Mrs Renfrew at Hummersknott, who helped me first really become interested in science. Thanks to Mike Glanville for letting me in and training me up in the CL3 lab. To Rob Taylor, Laura Bone and Gavin Falkous for the help with tissue and anything else that came with that. To Rad, Aarabi and Laura, it was a pleasure to help supervise you and the experience certainly taught me a lot. To Caroline Sabin and Alan Winston in London for their collaboration efforts. To David Chadwick, for allowing me to accompany him to Ghana for a once-in-a-lifetime experience. To Laura Greaves, working with you during my MRes really helped inspire me to pursue research. Thanks to Anna and Julia as well. Finally, to Angela – you are one of the nicest and most caring people I have ever met, as well as being an amazing scientist and support in the lab. It has been an absolute pleasure working with you.

Next to the MRG members who have made the last 3/4 years a real pleasure. To the office crew: Jack, Megan, Ruth, Hannah, Carla, Imogen, Alex and Roisin, who have been a constant source of support and banter. Shout out as well to Tasnim, Shane, Adam, Valeria, Chen, Charlotte, Nish, Lizzie and Ghazel who have been so kind, funny and friendly since I joined the lab – you made me feel welcome since day one.

To all my non-scientist friends. Firstly, a special thanks to Dan, Baker, Alex and Jay, who despite not fully understanding what I do, have unwittingly been a part of this whole journey with me and have been a massive support. I am so glad I have spent the last seven years of my life in Newcastle with

you lot. You guys know me better than anyone else and so know I will not overdo complements, but you all know how I really feel about you. Thanks as well to Ethan, Adam and Bulmer. Finally, a very special mention to Becca. You started this journey with me and although you may not realise, taught me a lot and made me a much better person. You were a great support and always tried to keep me grounded whilst motivating me to do better and I will always appreciate everything you did for me.

Next, I would obviously like to say thanks to my family. Firstly, thanks to my Durban and Darlington extended family for all the support and encouragement over the years. Thanks to Bud for being the best cat I know. Thanks to Paul for the being a great brother. I am very grateful to have a twin who wants to best for me whilst simultaneously trying your absolute hardest to keep me grounded (you are going to have to think of something else aside from “getting a real job” after this). The competitiveness that arises from having a twin has definitely served both of us well. Finally and most importantly, thanks to my Mum and Dad, who have supported me wholeheartedly throughout my life and especially over the last few years – you know as well as I do that I would not have been able to get this far without you. Special thanks to Mum, who has been my closest confidant, best friend and biggest inspiration. You have lived through nearly every aspect of the PhD with me and so this is as much for you as anyone else.

Courses and conferences attended

BHIVA 2017, Edinburgh, UK (*April 4th–7th 2018*). Poster presentation 'Muscle mitochondrial function and contemporary anti-retroviral therapy'.

- BHIVA/BASHH Science scholarship award 2018.

9th International Workshop on HIV & Aging, New York City, NY, USA (*September 13th–14th 2018*). Oral presentation 'Muscle mitochondrial function and contemporary anti-retroviral therapy'.

- Young investigator award 2018.

North East Postgraduate Conference 2018, Newcastle, UK (*November 9th, 2018*). Poster presentation. 'Muscle mitochondrial function and contemporary anti-retroviral therapy'.

NIHR showcase event, Newcastle, UK (*November 21st, 2018*). Three-minute oral presentation and poster presentation 'Molecular assessment of muscle function as a predictor of ageing phenotype in people living with HIV'.

10th International Workshop on HIV & Aging, New York City, NY, USA (*October 10th–11th 2019*). Oral presentation 'Cellular and molecular assessment of muscle mitochondrial function as a predictor of ageing phenotype in older people living with HIV'.

10th Annual Alliance for Healthy Ageing Conference, Hexham, UK (*October 24th–26th 2019*). Poster presentation 'Cellular and molecular assessment of muscle mitochondria function as a predictor of ageing phenotype in older people living with HIV'.

Northern BRC/NHSA Early Career Researchers Meeting, Leeds, UK (*November 8th, 2019*). Poster presentation 'Cellular and molecular assessment of muscle mitochondrial function as a predictor of ageing phenotype in older people living with HIV'.

North East Postgraduate Conference 2019, Newcastle, UK (*November 22nd, 2019*). Poster presentation 'Cellular and molecular assessment of muscle mitochondrial function as a predictor of ageing phenotype in older people living with HIV'.

SHINE Clinical Research Training Workshop, Amsterdam, The Netherlands (December 5th–6th 2019).

*Awarded the BHIVA Science scholarship award to attend BHIVA 2020 scheduled to be held in Manchester, UK in April 2020 but the conference was cancelled due to COVID-19 restrictions.

Publications

Hunt M, Zhu G, Greaves LC, Payne BAI (2018) – Muscle mitochondrial function and contemporary anti-retroviral therapy. *Reviews in Antiviral Therapy & Infectious Diseases*. 9, p7.

Hunt M, Zhu G, Greaves LC, Payne BAI (2018) – Muscle mitochondrial function and contemporary anti-retroviral therapy. *HIV Medicine.* 19 (Suppl. 2), s83.

Hunt M, McNiff MM, Sabin C, Winston A, Payne BIA (2019) – Cellular and molecular assessment of muscle function as a predictor of ageing phenotype in older PLWH. *Reviews in Antiviral Therapy & Infectious Diseases*. 11, p13

Hunt M & Payne BAI (2020) - Mitochondria and ageing with HIV. *Current Opinion in HIV & AIDS*. 15:2, 101-109. (**Appendix 6**).

Smith ALM, Whitehall JC, Bradshaw C, Hunt M, Greaves LC *et al*. (2020) – Age-associated mitochondrial DNA mutations cause metabolic remodelling that contributes to accelerated intestinal tumorigenesis. *Nature Cancer*. 1:976-989. (**Appendix 7**).

Abbreviations

2D-AGE – Two-dimensional agarose gel electrophoresis
3'OH – 3' hydroxyl group
^{31}P-MRS – Phosphorus magnetic resonance spectroscopy
3TC – Lamivudine
8-oxo-dG – 7,8-dihydro-8-oxo-2'-deoxyguanosine
ABC – Abacavir
ACEi – Angiotensin-converting enzyme inhibitor
Acetyl CoA – Acetyl coenzyme A
ACh – Acetylcholine
ACL – Anterior cruciate ligament
ADP – Adenosine diphosphate
AIDS – Acquired Immune Deficiency Syndrome
AKI – Acute kidney injury
ALIVE – AIDS Linked to the Intravenous Experience
AMPK – AMP-activated protein kinase
AMSI – Appendicular skeletal muscle mass/height
APAF1 – Apoptotic protease activating factor 1
APV – Amprenavir
ART – Antiretroviral therapy
ARV – Antiretroviral
AS160 – AKT substrate 160
ATN – Acute tubular necrosis
ATP – Adenosine triphosphate
ATV – Atazanavir
AZT - Zidovudine
AZT-MP – Monophosphorylated AZT
B2M – Beta-2-microglobulin
BIC – Bictegravir
BMD – Bone mineral density
BNIP3 – BCL2 interacting protein 3
BN-PAGE – Blue-native polyacrylamide gel electrophoresis
C – Complex
Ca^{2+} - Calcium
CaMKIV – Calcium-dependant protein kinase IV
CARD – Caspase recruitment domain
cART – Combination antiretroviral therapy
CD – Common deletion
CFS – Clinical Frailty Scale
CGA – Comprehensive geriatric assessment
CHS – Cardiovascular Health Study
CKD – Chronic kidney disease
CM – Cristae membrane

CMV – Cytomegalovirus
CN – Copy number
COX – Cytochrome c oxidase
CPEO – Chronic progressive external ophthalmoplegia
CRP – C reactive protein
CSA – Cross sectional area
d4T – Stavudine
DCT – Distal convoluted tubule
ddC – Zalcitabine
ddI – Didanosine
dH_2O – Deionised water
DII – Dietary inflammatory index
D-loop – Displacement loop
dNTP – deoxynucleotide triphosphate
DOR – Doravirine
dRN – Deoxyribonucleotide
DRP – Dynamin-related protease
DRV – Darunavir
DSBs – Double-stranded breaks
DTG – Dolutegravir
DXA – Dual-energy X-ray absorptiometry
E – Exit
eFI – Electronic Frailty Index
EFS – Edmonton Frailty Scale
EFV – Efavirenz
eGFR – Estimated glomerular filtration rate
EM – Electron microscopy
ER – Endoplasmic reticulum
ERRα – Oestrogen related receptor α
ETC – Electron transport chain
EtOH – Ethanol
ETR – Etravirine
EVG – Elvitegravir
EWGSOP – European Working Group on Sarcopenia in Older People
FDC – Fixed-dose combination
Fe-S – Iron-sulphur
FFP – Fried's frailty phenotype
FFPE – Formalin-fixed paraffin-embedded
FI – Frailty index
FII – Fusion inhibitor
FI-CGA – Frailty Index Derived From Comprehensive Geriatric Assessment
FIS1 – Mitochondrial fission protein 1
FMN – Flavin mononucleotide
FPV – Fosamprenavir
FTC – Emtricitabine

GALT – Gut-associated lymphoid tissue
GLUT4 – Glucose transporter isoform 4
H&E – Haematoxylin and eosin
H^+ - Proton
H_2O – Water
H_2O_2 – Hydrogen peroxide
HFRS – Hospital Frailty Risk Score
HIV – Human immunodeficiency virus
HIV+ – HIV positive
HIVAN – HIV-associated kidney disease
HIV-RT – HIV reverse transcriptase
HO· - Hydroxyl
hOAT – Human organic anion transporter
hOCT – Human organic cation transporter
HR – Hydrophobic heptad repeats
HSP – Heavy strand promoter
IBZ – Ibalizumab
IDV – Indinavir
IF2 – Initiating factor 2
IF3 – Initiating factor 3
IGF – Insulin-like growth factor
IL-6 – Interleukin-6
IMB – Inner boundary membrane
IMC – Imaging mass cytometry
IMCL- Intramyocellular lipid accumulation
IMF – Intermyofibrillar
IMM – Inner mitochondrial membrane
IMS – Intermembrane space
INI – Integrase inhibitor
IR – Insulin resistance
IR-HOMA – Insulin resistance-homeostatic model
IRS-1 – Insulin receptor substrate 1
K^+ - Potassium
Kg – Kilograms
KSS – Kearns-Sayre syndrome
LC3 – Light chain 3
LDHA – Lactate dehydrogenase
LIF – LC3-interacting region
LPV – Lopinavir
LRTI – Lower respiratory tract infection
LSP – Light strand promoter
LTR – Long terminal repeat
MACS – Multicentre AIDS Cohort Study
MAPK – Mitogen activated protein kinase
mCU – Mitochondrial calcium uniporter

MDC – Mitochondrial-derived compartments
MDV – Mitochondrial-derived vesicles
Mef2 – Myocyte enhancer factor 2
MELAS – Mitochondrial encephalopathy, lactic acidosis and stroke-like episodes
MERRF – Myoclonic epilepsy and ragged red fibres
MET – Metabolic equivalent expenditure
MFF – Mitochondrial fission factor
MFN – Mitofusin
MHC – Myosin heavy chain
MHMC – Modena HIV Metabolic Clinic
MID49 – Mitochondrial dynamics protein of 49 kDa
MIDD – Maternally-inherited diabetes and deafness
miRNA – Micro RNA
MPP – Mitochondrial membrane protease
MPTP – Mitochondrial permeability transition pore
mRNA – Messenger RNA
MRP4 – Multidrug resistance-associated protein type 4
MRPP – RNA processing protein
mtDNA – mitochondrial DNA
mTERF – Mitochondrial termination factor
mtLSU – Mitochondrial large subunit
mtRFs – Mitochondrial release factors
mtSSB – Mitochondrial single-stranded binding protein
mtSSU – Mitochondrial small subunit
mtUPR – Mitochondrial unfolded protein response
MVC – Maraviroc
Na^+ - Sodium
NCR – Non-coding region
nDNA – nuclear DNA
NFV – Nelfinavir
NGS – Normal goat serum
NICE – National Institute for Health and Care Excellence
NIX – NIP3-like protein X
NMJ – Neuromuscular junction
NNRTI – Nonnucleoside reverse transcriptase inhibitor
NO – Nitric oxide
NPC – No primary control
NRF – Nuclear respiratory factor
NRTI – Nucleoside reverse transcriptase inhibitor
NVP – Nevirapine
O_2^- - Superoxide
OD – Optical density
O_H – Origin of heavy strand replication
O_L – Origin of light strand replication
OMM – Outer mitochondrial membrane

Opa1 – Optic atrophy 1
OXPHOS – Oxidative phosphorylation
P – Peptidyl
PARL – Presenilin-associated rhomboid-like protein
PBS – Phosphate buffered saline
PCR – Polymerase chain reaction
PCT – Proximal convoluted tubule
PDK-1 – Pyruvate dehydrogenase kinase isozyme 1
PFA – Paraformaldehyde
PGC-1α - PPARγ coactivator-1α
PgP – P glycoprotein
Pi – Inorganic phosphate
PI – Protease inhibitor
PINK1 – PTEN-induced putative kinase 1
POLG – Polymerase gamma
POLRMT – Mitochondrial RNA polymerase
PPARγ - Peroxisome proliferator-activated receptor γ
PTEN – Phosphatase and tensin homologue
QOL – Quality of life
qPCR – Quantitative real-time PCR
RAL – Raltegravir
RFH – Royal Free London Hospital
RITOLS – RNA incorporation throughout the lagging strand
RN – Ribonucleotide
RNS – Reactive nitrogen species
ROS – Reactive oxygen species
RPV – Rilpivirine
rRNA – Ribosomal RNA
RT – Room temperature
RTV – Ritonavir
SAP – Secretory phenotype associated with senescence
SARCA – Sarcoplasmic/endoplasmic reticulum Ca^{2+} ATPase
SC – Satellite cell
SDH – Succinate dehydrogenase
SDM – Strand displacement model
SHARE – Survey of Health, Aging and Retirement in Europe
SIRT1 – Sirtuin 1
SNP – Single nucleotide polymorphism
SOD – Superoxide dismutase
SOD2 – Superoxide dismutase 2
SOF – Study of Osteoporotic Fracture
SPPB – Short Performance Physical Battery
SPRINTT – Sarcopenia and Physical fRailty In Older People multicomponenT Treatment strategies
SQ – Starting quantity
SQV – Saquinavir

SR – Sarcoplasmic reticulum
SS – Subsarcolemmal
T20 – Enfuvirtide
T2DM – Type 2 diabetes mellitus
TA – Tibialis anterior
TAF – Tenofovir alafenamide
TBST – Tris-buffered saline with tween 20
TCA – Tricarboxylic acid
TDF – Tenofovir disoproxil fumarate
TFAM – Mitochondrial transcription factor A
TFAM – Mitochondrial transcription factor A
TFB2M – Mitochondrial transcription factor 2B
TFV – Tenofovir
TIFF – Tagged-Image File Format
TIMM – Translocase of the inner mitochondrial membrane
TK – Thymidine kinase
TLR – Toll-like receptor
TNF – Tumour necrosis factor
TOMM – Translocase of the outer mitochondrial membrane
TPV – Tipranavir
tRNA – Transfer RNA
TUG – Timed-up and Go test
Ub – Ubiquitin
UCL – University College London
UVP – UV-sterilising cabinet
VACS – Veterans Aging Cohort Study
VDAC – Voltage-dependant anion channel
VNTR – Variable number of tandem repeats
WBC – White blood cell
WES – Whole exome sequencing
ΔΨm – Mitochondrial membrane potential

List of figures

List of tables

Table of contents

Chapter 1 – Introduction

1.1 Human immunodeficiency virus

1.1.1 Background and history

The human immunodeficiency virus (HIV) is a lentivirus within the Retroviridae family (Luciw, 1996) that is classified into HIV type I (HIV-1) and HIV type 2 (HIV-2). Due to the fact that HIV-1 is much more prevalent and significant for this work it will hereby be referred to as HIV in this thesis for brevity.

According to epidemiological and phylogenetic studies, HIV was first introduced into humans sometime between 1920-1940. HIV-1 evolved from non-human primate immunodeficiency viruses from the Central African chimpanzees (SIVcpz), most likely in Kinshasa in the Democratic Republic of Congo. In contrast, HIV-2 was introduced by the West African sooty mangabeys (SIVsm) (Gao *et al*., 1999; Sharp & Hahn, 2011; Faria *et al*., 2014).

HIV was first reported to be the causative agent of Acquired Immune Deficiency Syndrome (AIDS) in 1983, two years after AIDS was recognised as a new disease (CDC, 1981; Barre-Sinoussi *et al*., 1983; Popovic *et al*., 1984). This means that HIV spread for around 50 to 70 years before it was recognised.

1.1.2 Epidemiology

By the end of 2019, an estimated 38 million (range 31.6-44.5 million) people are thought to be HIV positive (HIV+), with ~690,000 HIV-related deaths occurring throughout that year. Approximately three quarters of HIV+ individuals reside in Sub-Saharan Africa, and approximately two-thirds of newly diagnosed cases occur in this region. Since the beginning of the HIV/AIDS epidemic roughly 78 million individuals have contracted HIV, with about 33 million individuals dying as a result (WHO, 2020). Importantly, the prevalence of HIV-related mortalities has declined since 1999, largely due to the advent of effective antiretroviral therapy (ART) (GDB 2017 HIV collaborators, 2019).

In 2018, there were 96,142 individuals who were HIV+ and receiving care in the UK, with 4453 newly diagnosed PLWH. The median age of PLWH in the UK is currently 48 years, and this number is increasing (Public Health England, 2019).

1.1.3 Genetics

The HIV genome consists of two identical single-stranded viral RNA molecules enclosed within a viral capsid core (**Figure 1.1b**). Once inside of the target cell, the viral RNA is reverse transcribed into double-stranded proviral DNA (HIV provirus) where it integrates into the human genome.

The HIV genome is flanked on either side by long terminal repeat (LTR) sequences, in which the 5' LTR acts as the promoter for viral gene transcription (**Figure 1.1a**). Following down the reading frame in a 5' to 3' fashion, the first gene is the *gag* gene, which is responsible for encoding outer core membrane protein (MA/p17), capsid protein (CA/p24), nucleocapsid protein (NC/p7), and a nuclear acid stabilising protein (p6). The next gene on the reading frame is the *pol* gene, which encodes the protease (PR/p12), reverse transcriptase (RT/p51), RNAase H (p15) and integrase (IN/p31). Next, the *env* gene encodes the two envelope glycoproteins gp120 (SU) and gp41 (TM). In addition to these genes, the viral genome encodes various regulatory proteins. These include Tat and Rev, which are required for the initiation of replication, as well as Nef, Vif, Vpr and Vpu, which are required for viral replication, budding and pathogenesis respectively (Levy, 2007; Sauter *et al*., 2012).

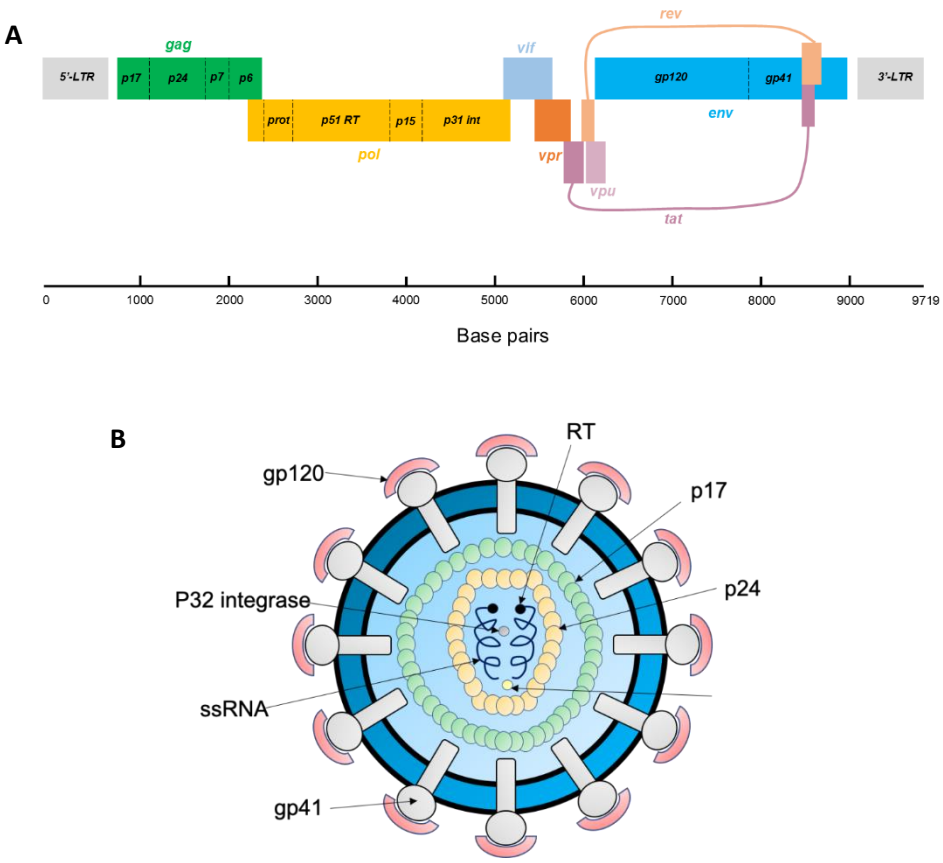

***Figure 1.1 - HIV genome and particle**. (**A**) The HIV genome is encoded on a single strand of RNA.* The *gag* gene encodes viral capsid proteins; *pol* encodes the viral reverse transcriptase (HIV-RT); *env* encodes the HIV envelope-associated proteins. *vif, vpr, tat* and *rev* encode the regulatory proteins. (**B**) Schematic of the HIV virus particle.

1.1.4 HIV pathogenesis

HIV is transmitted as a cell-free or cell-associated virus, most commonly in semen or at mucosal surfaces. Transmission can also occur via injection drug use, through the placenta to the foetus, or exposure to infected blood products (Moir *et al*., 2011).

Initially, HIV-1 particles interact with the CD4 receptor and either the CXCR4 co-receptor on the plasma membrane of T cells, or the CCR5 co-receptor on macrophages and some T lymphocytes (Naif, 2013) (**Figure 1.2**). Once within the cytoplasm, the viral RNA-encoded genome is reverse-transcribed into linear proviral DNA by HIV-1 reverse transcriptase (HIV-RT). The proviral DNA is then integrated into the host nuclear DNA by the viral integrase, which catalyses 3' end processing and viral DNA strand transfer (Sato *et al*., 2006). Proviral mRNA species are then transcribed following the integration of proviral DNA into the host cell's nuclear DNA. mRNA destined to encode regulatory proteins are spliced in the nucleus, while mRNA encoding structural proteins are transported into the cytoplasm where they are translated and packaged into new HIV particles along with unspliced proviral mRNA.

If there are no pre-existing immune pressures, the HIV virus will disseminate rapidly following transmission and will exponentially increase viremia (viral RNA) by infecting resting $CD4^+$ T cells. At this stage (1-2 days post infection) the virus can be detected in regional lymphatic tissue (Maher *et al*., 2005).

Shortly afterwards (5-6 days post infection), activated $CD4^+$ T cells are infected and the HIV virus rapidly migrates to gut-associated lymphoid tissue (GALT) via draining lymph nodes, where it induces the depletion of memory $CD4^+$ T cells (particularly the $CD4^+$, $CCR5^+$ subset) and acts as the major site for HIV replication (Guadalupe *et al*., 2003). After 3-6 weeks post infection the humoral response is activated, initiating the onset of clinical symptoms such as fever, malaise, fatigue, rash, acute neuropathy and gastrointestinal abnormalities (Levy, 2007; Burin des Roziers *et al*., 1995). This symptomatic phase then lasts roughly 2-6 weeks before the onset of an asymptomatic phase, where the viral load can drop from 10^5-10^{10} copies/ml down to as low as 10^2 copies/ml.

If left untreated, the pathogenesis of HIV infection progresses and CD4 count becomes gradually depleted until eventually a critical CD4 count threshold of 200 copies/μl is reached. At this point, the individual's immune system is severely weakened, and the individual has a significantly increased susceptibility to acquiring opportunistic infections and neoplasms. Here, the individual has progressed to AIDS. The progression from initial HIV infection to the development of AIDS is highly variable, and can range from 2-25 years (Mocroft *et al*., 1996; Iwuji *et al*., 2013).

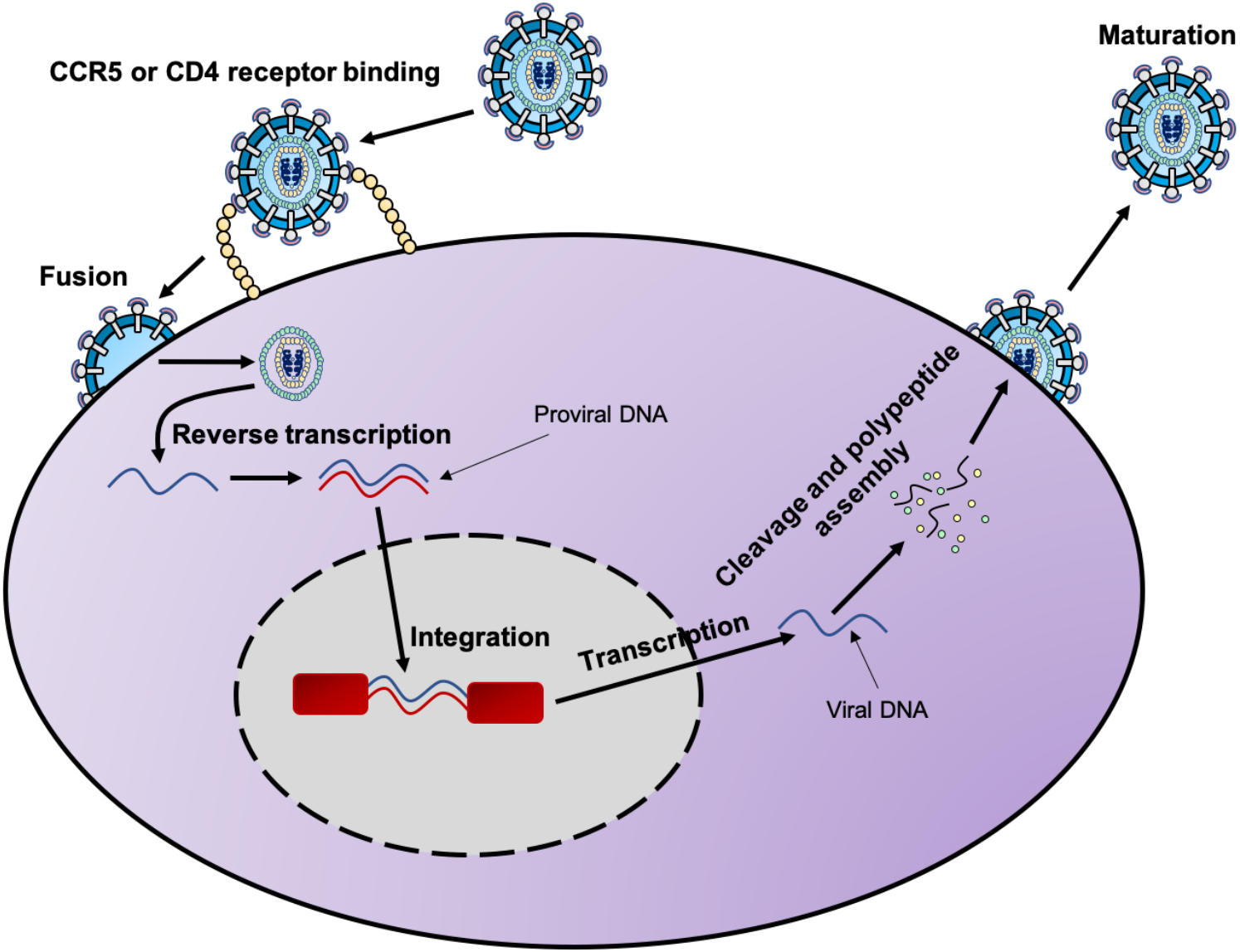

Figure 1.2 – Replicative life cycle of HIV infection. *Schematic depicting the various stages of the HIV infection lifecycle alongside the point of action of various antiretroviral classes.*

1.2 Antiretroviral therapy

At present, there is no available treatment that completely eradicates the HIV virus in an infected individual. As such, the most effective option for reducing morbidity and mortality in people living with HIV (PLWH) is through long-lasting viral suppression, which is achieved through ART.

1.2.1 History of ART

In 1987 the first antiretroviral (ARV) to be approved was zidovudine (AZT), which was prescribed as a monotherapy (FDA, 1987). Since then, more than 30 individual ARVs of various classes have been approved and rolled out for treatment, and one dual combination ARV has been approved for the prevention of HIV infection (Gulick, 2018; Clayden, 2018) (**Figure 1.3**). In addition, fixed-dose combination (FDC) tablets with a long half-life have reduced the burden of ART to once or twice daily dosing.

The early ARVs of the first half of the 90s were prescribed as mono- or dual-therapies. Many were overtly toxic whilst not being particularly potent. In response, highly active and better tolerated ARVs were developed and began to be prescribed as triple drug regimens, often with FDCs. Triple combination ART where ARVs from at least two different classes are used is termed 'combination antiretroviral therapy' (cART) or 'highly active antiretroviral therapy' (HAART) (WHO, 2016).

By the end of 2019, the global number of PLWH who are on ART is approximately 25.4 million, which is ~67% of the HIV+ population (WHO, 2020). The vast majority of untreated PLWH reside in less developed countries. Importantly, in the UK, 97% of diagnosed PLWH were on ART by the end of 2018 (Public Health England, 2019).

ARV dugs

1987 – Zidovudine (AZT)
1991 – Didanosine (ddI)*
1992 – Zalcitabine (ddC)*
1994 – Stavudine (d4T)*
1995 – Lamivudine (3TC), Saquinavir (SQV)*
1996 – Indinavir (IDV)*, Ritonavir (RTV), Nevirapine (NVP)
1997 – Nelfinavir (NFV)*, Delavirdine (DLV)*
1998 – Abacavir (ABC), Efavirenz (EFV)
1999 – Amprenavir (APV)*
2000 – Lopinavir (LVP)
2001 - Tenofovir disoproxil fumarate (TDF)
2003 – Atazanavir (ATV), Emtricitabine (FTC), Enfuvirtide (ENV)
2005 – Tipranavir (TPV)*
2006 – Darunavir (DRV)
2007 – Maraviroc (MVC)
2008 – Etravirine (ETR)
2011 – Rilpivirine (RIL)
2012 – Elvitegravir/cobicistat (EVG/COBI)
2013 – Dolutegravir (DTG)
2015 – Tenofovir alfenamide (TAF)
2018 – Bictegravir (BIC), Doravirine (DOR), Ibalizumab (IBZ)

Combination drugs

1997 – AZT/3TC
2000 – AZT/3TC/ABC
2002 - d4T/3TC*, d4T/3TC/NVP*
2004 – ABC/3TC, TDF/3TC, TDF/FTC
2005 – AZT/3TC/NVP
2006 – TDF/FTC/EFV
2011 – TDF/FTC/RIL
2012 – TDF/FTC/EGV/COBI
2014 – ABC/3TC/DTG
2015 – RAL/3TC, TAF/FTC/EVG/COBI
2016 – TAF/FTC, TAF/FTC/RIL
2017 – DTG/RIL, TDF/3TC/DTG, TDF/3TC/EFV
2018 – TAF/FTC/DRV/COBI, TAF/FTC/BIC, TDF/3TC/DOR

*** =** discontinued

Figure 1.3 – Evolution of ARV development.

1.2.2 Classes of ART and method of action

There are six main classes of ART drugs, each targeting different stages of the HIV-1 life cycle. These are: nucleoside reverse transcriptase inhibitors (NRTIs); protease inhibitors (PIs); non-nucleoside reverse transcriptase inhibitors (NNRTIs); integrase inhibitors (INIs); CCR5 antagonists, and fusion inhibitors (FIIs) (Arts & Hazuda, 2012).

NRTIs are prodrugs that exert their suppressive effects by inhibiting transcription of viral RNA via chain termination. Chain termination can occur during either RNA-dependant viral DNA synthesis or DNA-dependant viral DNA synthesis (Richman, 2011). In developed countries, abacavir (ABC), emtricitabine (FTC) and lamivudine (3TC) are the most commonly used NRTIs. Didanosine (ddI), stavudine (d4T), zalcitabine (ddC) and zidovudine (AZT) are older NRTIs that are no longer in use in developed countries due to their associated toxicity, although some are still in use in less developed countries and regions such as sub-Saharan Africa. Tenofovir disoproxil fumarate (TDF) and tenofovir alafenamide (TAF) are a nucleotide analogue rather than nucleosides, due to the phosphate group being located on the nitrous base. They are therefore sometimes referred to as NtRTIs, and both are in common use globally.

NNRTIs are another class of ARV that exert their suppressive effects by inhibiting HIV-RT. As opposed to NRTIs which inhibit polymerase activity by forming a hydrophobic pocket over the active site, NNRTIs are allosteric inhibitors and so induce the formation of a hydrophobic pocket proximal to the active site – indirectly reducing polymerase activity (Kohlstaedt *et al*., 1992; Tantillo *et* al., 1994). Currently used NNRTIs include efavirenz (EFV), etravirine (ETR), nevirapine (NVP), doravirine (DOR) and rilpivirine (RPV).

PIs are responsible for inhibiting the viral protease enzyme. The HIV-1 protease cleaves viral gag and gag-pol polyprotein precursors following transcription and during viral maturation (Park & Morrow, 1993). Therefore, inhibition of protease will result in a decrease in the formation of new HIV virus particles. Atazanavir (ATV) and darunavir (DRV) are the most commonly used PIs, but other PIs which were more commonly used in the past include amprenavir (APV), fosamprenavir (FPV), indinavir (IDV), lopinavir (LPV), nelfinavir (NFV), ritonavir (RTV), saquinavir (SQV) and tipranavir (TPV).

Integrase inhibitors are the newest and most mechanistically complex class of ARVs. They act by sequestering and inhibiting the viral integrase active site magnesiums, whilst simultaneously forming a hydrophobic group to block the proviral DNA binding to integrase (Grobler *et al*., 2002). Dolutegravir (DTG), elvitegravir (EVG), bictegravir (BIC) and raltegravir (RAL) are currently administered integrase inhibitors.

Enfuviritide (T20) is the only FII currently available. Fusion inhibitors block the fusion of HIV-1 particles with target cells by inhibiting the interaction between the two homologous domains of the viral gp41 protein, which are essential for HIV pathogenesis (Kahle *et al*., 2009). Unfortunately, T20 has a low antiviral activity and easily induces resistance. It can only be administered by subcutaneous injection.

CCR5 antagonists work by binding and inducing the stabilisation of a CCR5 receptor conformation that is not recognised by either HIV-1 CCR5 agonists. They do this by binding to hydrophobic pockets present in the transmembrane helices of CCR5 (Dragic *et al*., 2000; Tsamis *et al*., 2003). Maraviroc (MVC) and ibalizumab (IBZ) are the only currently licenced CCR5 antagonists.

1.2.3 Future perspectives of ART research

Since 2010 there have been three international conferences on ARV drug optimisation – CADO-1 in 2010, CADO-2 in 2013 and CADO-3 in 2017. At the most recent, CADO-3 conference, the goal was to better define the research necessary to optimise second- and third-line therapy (WHO, 2016). Whilst the general success of ART makes identifying improvements difficult, the top short (1-2 years) and medium term (2-5 years) priorities for the future of ART was identified as being the improvement and increased usage of TAF and DTG ARVs in cART globally. These are seen as being the current ARVs with the greatest potency and the lowest toxicity. The long term (>5 years) priorities were identified as being the improvement of long-acting formulations of new compounds, as well as the development of capsid and maturation inhibitors (Vitoria *et al*., 2018; WHO, 2016).

As of the beginning of 2019 there were six new ARVs in phase III studies. These include four entry blockers, a NNRTI and an integrase inhibitor (Vitoria *et al*., 2019).

1.3 Biology of ageing

Ageing is characterised by the progressive accumulation of molecular and cellular damage leading to a deterioration in replicative and regenerative processes in tissue, and an increased susceptibility to acquiring age-associated diseases such as cancer and diabetes (Kirkwood, 2005).

1.3.1 Evolutionary theories of ageing:

The mutation accumulation theory (Medwar, 1952) postulates that ageing is the result of random mutations which accumulate in the genome with increasing age, contributing to physical deterioration.

The antagonistic pleiotropy theory (Williams, 1957) suggests that organismal ageing is caused by pleiotrophic genes (genes with multiple phenotypic effects). These pleiotrophic genes provide a favourable advantage for reproduction early in life but become harmful and increase the rate of ageing later in life.

Thomas Kirkwood's Disposable Soma theory (Kirkwood, 1977), posits that ageing is caused by the physiological stand-off between somatic maintenance and investment in biological functions such as reproduction, with over commitment of resources to one resulting in decline of the other.

1.3.2 Molecular ageing and the mitochondrial theory of ageing

During the natural course of ageing, somatic (acquired) mutations accumulate in the mitochondrial genome. However, it is unknown whether these mutations are a consequence of the ageing process itself or a causative driver of ageing.

The mitochondrial free radical theory of ageing (MFRTA) (Harman, 1965) states that an increase in the production of reactive oxygen species (ROS) due to age-related mitochondrial dysfunction causes further mitochondrial deterioration and global cellular damage. At low levels, ROS are essential for intracellular signalling, but become toxic at increased levels as they damage many lipids, proteins and nucleic acids - increasing the rate of mutagenesis (Koopman *et al*., 2010).

According to the MFRTA, as organisms age, the accumulation of mitochondrial DNA (mtDNA) mutations increases, leading to respiratory chain abnormalities and an increase in ROS leakage. This in turn further increases the accumulation of mtDNA mutations, and so on in a 'vicious cycle' (Harman, 1972). However, if this were the case the propagation of mtDNA mutations would be exponential, which has been dismissed by more recent extensive studies (Tengan *et al*., 1997; Mott

et al., 2001; Kennedy *et al*., 2013; Itsara *et al*., 2014). In addition, *in vivo* and *in vitro* studies have demonstrated that manipulation of ROS has no effects on ageing or maximal lifespan (Ristow, 2011).

In 2004 Trifunovic and colleagues developed a knock-in mouse model deficient in the proof-reading domain of the mitochondrial polymerase *γ*. Subsequently, mice with this genotype experience an accumulation of age-related mtDNA point mutations and deletions, leading to the onset of a premature ageing phenotype. These mice exhibit a reduced lifespan, weight loss, osteoporosis, anaemia, reduced fertility, alopecia, loss of subcutaneous fat, kyphosis, and heart enlargement (Trifunovic *et al*., 2004). Taken together, the development of this mouse model has strengthened the causal link between mtDNA mutations, mitochondrial dysfunction and ageing, and has helped further understanding in this field.

More recently, López-Otín *et al.* (2013) characterised ageing into 9 cellular and molecular hallmarks: loss of proteolysis, telomere attrition, genomic instability, epigenetic alterations, altered intercellular communication, stem cell exhaustion, cellular senescence, deregulated nutrient signalling and mitochondrial dysfunction – further solidifying the significant role mitochondrial dysfunction plays in the multifactorial process of ageing (López-Otín *et al.,* 2013). This thesis primarily focuses on the impact of mitochondrial dysfunction in ageing.

1.4 Mitochondrial biology

1.4.1 Origins of mitochondria

Mitochondria are dynamic double-membraned organelles present in nearly every nucleated eukaryotic cell, and are significantly involved in a wide range of cellular processes such as energy production, haem synthesis, regulation of apoptosis and calcium handling, among others.

It is thought that mitochondria were once a prokaryotic species that become engulfed in eukaryotic cells as the result of an endosymbiotic relationship (Sagan, 1967). Whilst the exact mechanism behind this theory remains unknown, there are two prevalent mechanisms which have been proposed.

The first hypothesis is based on the small subunit ribosomal RNA (rRNA) phylogenetic tree and posits that a nucleated archezoa host phagocytosed an α-protobacterial endosymbiont, which was subsequently transformed into a mitochondrion (Yang *et al*., 1985; Cavalier-Smith *et al*., 1987). This hypothesis is commonly referred to as the 'archezoan hypothesis'. The second hypothesis, termed the 'symbiogenesis hypothesis' suggests that the endosymbiotic event entailing a physical and metabolic fusion occurred before the diversion of eukaryotes from prokaryotes, and this event then generated the ancestor of the eukaryotic cell. This was then followed by another divergence and development of a nucleus to form a eukaryotic cell (Martin & Muller, 1998).

Both hypotheses have plausible aspects, although it is the archezoan hypothesis which is considered the more plausible, due to the rRNA phylogenetic tree evidence (Roger *et al*., 2017).

1.4.2 Mitochondrial structure

As mentioned above, mitochondria are double-membrane structures that lie in the cytoplasm of most eukaryotic cells. The outer mitochondrial membrane (OMM) surrounds the inner mitochondrial membrane (IMM), which in turn encloses the mitochondrial matrix. The space between the OMM and IMM is termed the intermembrane space (IMS) (**Figure 1.4**).

The structure of the mitochondrion was first described by Palade (1953) through the utilisation of electron microscopy (EM). In this study, Palade noted the characteristic pattern of convoluted and pleomorphic IMM invaginations repeated in mitochondria in what was termed the 'baffle' model of cristae structure (Palade, 1953). The advancement of microscopy in later years has since disproved this theory by providing evidence that cristae are in fact connected to the IMS by tubular cristae junctions (Daems & Wisse, 1966; Perkins *et al*., 1997).

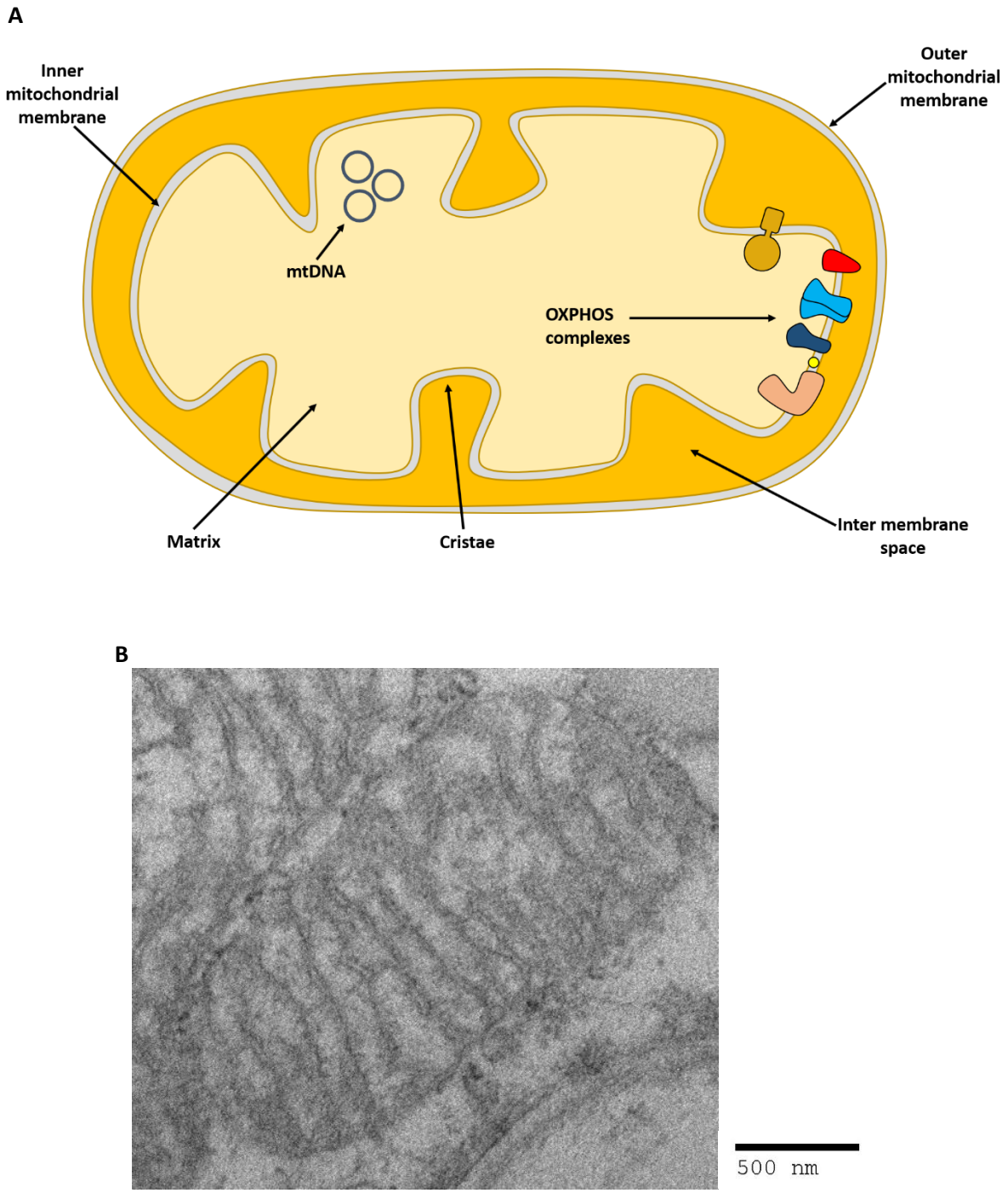

Figure 1.4 – Mitochondrial ultrastructure. *(**A**) Schematic depicting the OMM and IMM, as well as the IMS, cristae, matrix, mtDNA and OXPHOS complexes. (**B**) Electron micrograph (EM) image. (Scale bar = 500nm). EM image courtesy of Dr Amy Vincent.*

The double membrane of the mitochondrion is critical for the regulated transport of ions and metabolites into and out of the mitochondria. Here, due to the smooth porous structure of the OMM, ions and small uncharged molecules (up to ~5,000 Da) can diffuse into the IMS. Larger molecules such as proteins as well as hydrophilic molecules are able to pass into the IMS through protein channels such as the voltage-dependant anion channel (VDAC) or translocase of the outer mitochondrial membrane (TOMM) (Ponnalagu *et al.*, 2016). In addition to its role in molecule transport, the OMM is a platform for cell signalling convergence as well as being responsible for forming the interface with other subcellular organelles and compartments such as the endoplasmic reticulum (ER) and lysosomes.

In the immediate interior, the IMM encloses the matrix space, and can be divided into two distinct domains connected by cristae junctions – the inner boundary membrane (IMB) and the cristae membrane (CM). Importantly, the IMM houses the five complexes required for oxidative phosphorylation (OXPHOS) and so is the site of OXPHOS and protein synthesis (Vogel *et* al., 2006). Cristae organisation is modulated in order to maximise conditions for bioenergetic processes. This includes tightening of junctions prior to respiration (Demongeot *et al*., 2007; Hackenbrock *et al*., 1966; Mannella *et al*., 2001). In addition, during cell death cristae undergo morphological changes termed cristae remodelling, which promotes the redistribution and release of cytochrome *c* (Scorrano *et al*., 2002). Compared to the OMM, the IMM is far less permeable and so transport in and out of the IMM requires more stringent regulation. To highlight the difference in membrane permeability, even small solutes such as ions cannot pass through the IMM without the assistance of inner mitochondrial membrane translocases (TIMM) (Kulawiak *et al*., 2013).

The mitochondrial matrix is the site where many important biochemical processes such as the tricarboxylic acid cycle (TCA) and iron-sulphur (Fe-S) cluster formation occurs. In addition, the mitochondrial matrix contains many copies of the mitochondrial genome (mtDNA), which are packaged in the form of circular nucleoids, as well as the transcription and translation machinery required to undertake these processes.

1.4.3 Mitochondrial dynamics

The multifaceted and heterogenic involvement of mitochondria in a wide range of cellular processes is underscored by the vast morphological variability of the organelle. It has long been recognised that mitochondrial shape, size, length and organisation can vary between cells and in response to certain metabolic and cellular signals (Giacomello *et al*., 2020). In addition, mitochondria are known to constantly undergo fission and fusion processes in order to adapt to cellular and tissue demands (Bereiter-Hahn & Voth, 1994). The frequency of these fission and fusion processes is tightly regulated, as metabolic and cellular demands are constantly shifting. Mitochondrial fission is involved in the selective removal of damaged mitochondria (mitophagy), as well as distribution of the organelle, whereas fusion is essential for the stabilisation of mtDNA (Chen *et al*., 2010), adenosine triphosphate (ATP) production (Yao *et al*., 2019) and exchange of matrix components to mitigate mitochondrial stress (Legros *et al*., 2002).

Collectively, the processes that allow the alterations to mitochondria are known as mitochondrial dynamics. Disruptions of mitochondrial dynamics can lead to several human pathologies such as optic atrophy (Alexander *et al*., 2000; Delettre *et al*., 2000), Parkinson's Disease (Van Laar & Berman, 2009) and Charcot-Marie-Tooth disease (Palau *et al.,* 2009).

1.4.3.1 Fusion

Mitochondrial fusion is the process whereby two mitochondria fuse together to form a single mitochondrion. This process is a controlled, double membrane fusion event governed by several proteins of the dynamin-related (DRP) family of large GTPases. OMM fusion is performed by mitofusins 1 and 2 (MFN1 and MFN2) (Zuchner *et al*., 2004), whilst IMM fusion is undertaken by optic atrophy 1 (Opa1) (Meeusen *et al*., 2006) (**Figure 1.5**).

MFN1 and MFN2 have a high degree of structural homology, with both containing two 4,3 hydrophobic heptad repeats (HR1 and HR2) (Koshiba *et al*., 2004), and both being able to form homo- or heterodimers (Chen *et al*., 2005). However, genetic and biochemical studies have demonstrated that the two mitofusins have different functions and both are required for mitochondrial fusion. Whilst MFN1 is the core component of the fusion process together with Opa1, the exact role of MFN2 is unknown, although it has been shown to be associated with interactions with other organelles such as the endoplasmic reticulum (ER) (Cipolat *et al*., 2004; Ishihara *et al*., 2004; de Brito *et al*., 2008). During OMM fusion, MFN1 acts as a tether between the two fusing mitochondria, where adjacent HR2 domains dimerise in a GTP-dependant fashion to induce membrane clustering (Qi *et al*., 2016).

As mentioned above, Opa1 is the driver of IMM fission. Opa1 resides in the IMM as well as the IMS, and exists as one of two isoforms – L-Opa1, which is a membrane-bound protein that protrudes into the IMS in order to promote tethering to the IMM from the adjacent fusing mitochondria, and S-Opa1, which is thought to regulate cristae structure during fission (Mishra *et al*., 2014; DeVay *et al*., 2009; Lee *et al*., 2017). The balance between the two isoforms is required for effective fusion to occur.

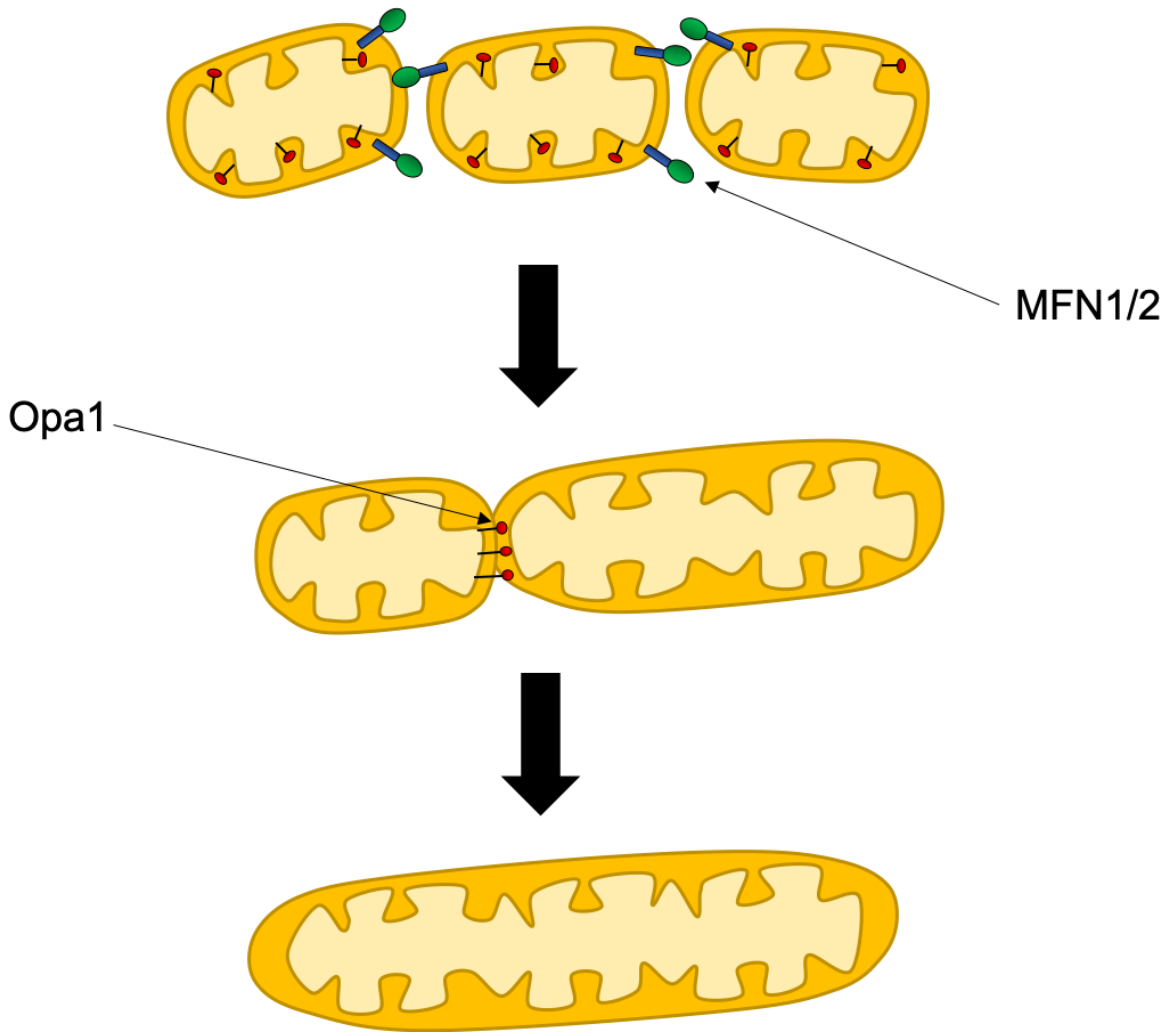

Figure 1.5 – Mitochondrial fusion*. Initially, the HR2 domain of MFN1/2 (green circle) docks to an adjacent HR2 domain of another MFN1/2, inducing a conformational change which drives the GTP-dependant hydrolysis of MFN1/2, leading to the fusion of the two OMMs. In the IMM, Opa1 interacts with cardiolipin in trans to fuse the IMMs from the adjacent mitochondria.*

1.4.3.2 Fission

Mitochondrial fission is the process by which a mitochondrion divides into two mitochondria. Fission is primarily carried out by the cytosolic Drp1 (Smirnova *et al*., 2001), which translocates to the mitochondria where it binds to OMM receptors: mitochondrial fission factor (MFF), mitochondrial fission protein 1 (FIS1) and mitochondrial dynamics protein of 49 kDa (MID49) (Otera *et al*., 2010; James *et al*., 2003; Loson *et al*., 2013). Next, GTP-mediated binding induces a conformational change and formation of linear polymers on the OMM. Through GTP hydrolysis, these polymers shorten to cause constriction of the mitochondrial membranes, ultimately leading to membrane scission (Mears *et al*., 2011; Kalia *et al*., 2018) (**Figure 1.6**).

In addition to the important role of the receptor proteins FIS1, MID49 and MFF, the ER has been shown to play an essential role in membrane constriction. Here, ER wraps around a mitochondrion to form mitochondria-ER tethers, initiating pre-recruitment mitochondrial constriction (Friedman & Nunnari, 2014). This ER-mediated constriction reduces the diameter of membranes to 30-70nm, which is not sufficient for membrane scission, and so Drp1 recruitment is required (Bohuszewicz & Low, 2018; Lee *et al*., 2016).

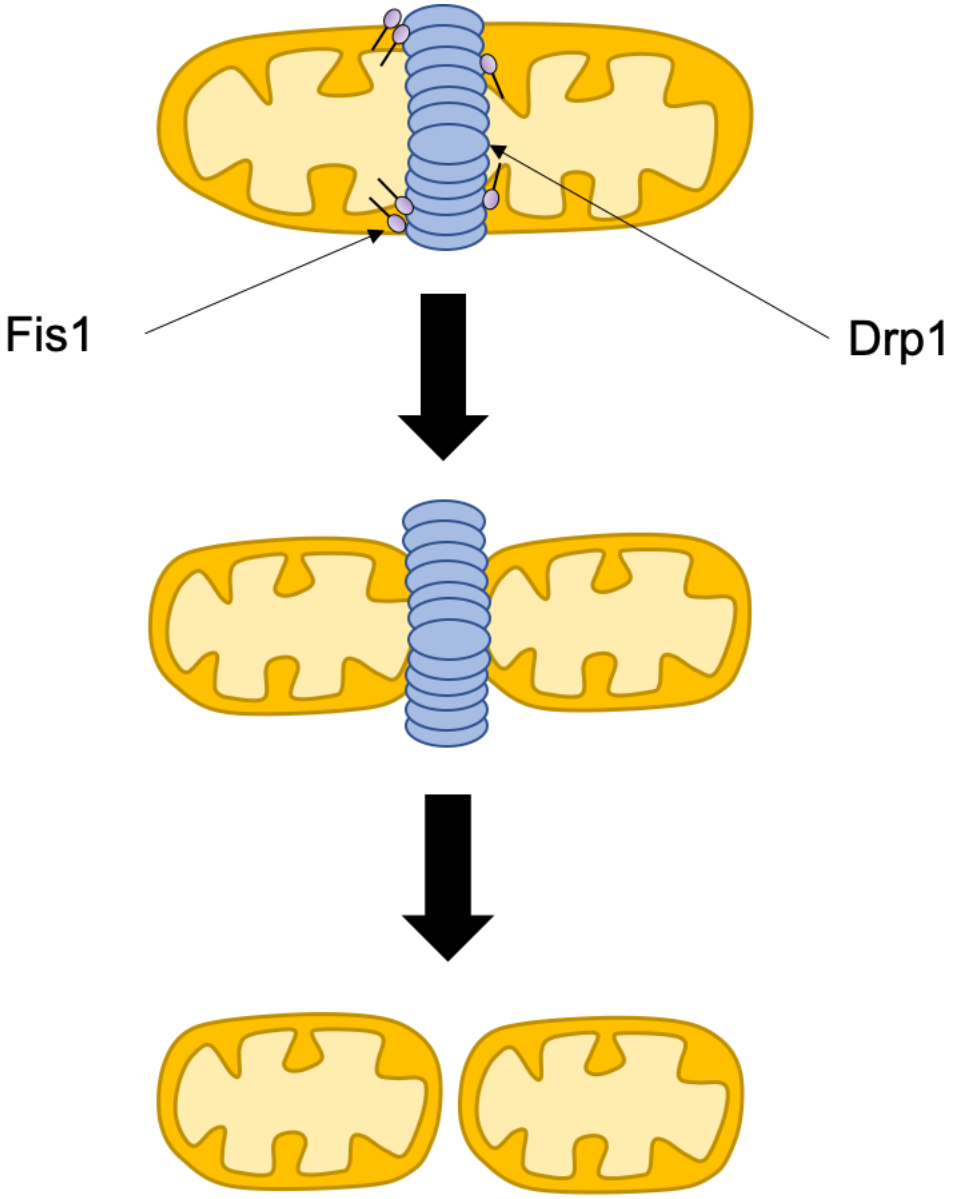

Figure 1.6 – Mitochondrial fission*. Upon Drp1 dephosphorylation by calcineurin, it is translocated to the mitochondria where it binds to its receptors (Fis1). Drp1 then oligomerises to induce GTP-hydrolysis dependant membrane constriction.*

1.4.4 Mitochondrial stress response

1.4.4.1 Biogenesis

Mitochondrial biogenesis is a tightly regulated mechanism whereby mitochondria increase their mass and mtDNA copy number in order to adapt to cell-specific bioenergetic requirements. The major regulator of mitochondrial biogenesis is the peroxisome proliferator-activated receptor-γ (PPARγ) coactivator-1α (PGC-1α). PGC1α is a co-transcriptional regulation factor that activates various transcription factors such as nuclear respiratory factor 1 and 2 (NRF-1/2), oestrogen related receptor α (ERRα), glucocorticoid, and PPARα. These transcription factors ultimately promote the expression of the mitochondrial transcription factor A (TFAM) (Wu *et al*., 1999), which is responsible for promoting the transcription and replication of mtDNA (Virbasius & Scarpulla, 1994).

As depicted in **Figure 1.7**, PGC-1α is activated by AMP-activated protein kinase (AMPK), which is the master regulator of intracellular bioenergetics in response to acute crises in energy requirement (Hardie, 2007). Here, an increased AMP:ATP and NAD^+:NADH ratio is detected by AMPK and Sirtuin 1 (SIRT1), which subsequently leads to PGC-1α phosphorylation and activation (Canto *et al*., 2009).

In addition to AMPK, nitric oxide (NO) (Nisoli *et al*., 2003), calcium-dependant protein kinase IV (CaMKIV) (Wu *et al*., 2000; Wu *et al*., 2002), Calcineurin (Chin *et al*., 1998; Ryder *et al*., 2003), and p38 mitogen-activated protein kinase (MAPK) (Boppart *et al*., 2000) have also been shown to be regulators of mitochondrial biogenesis in humans.

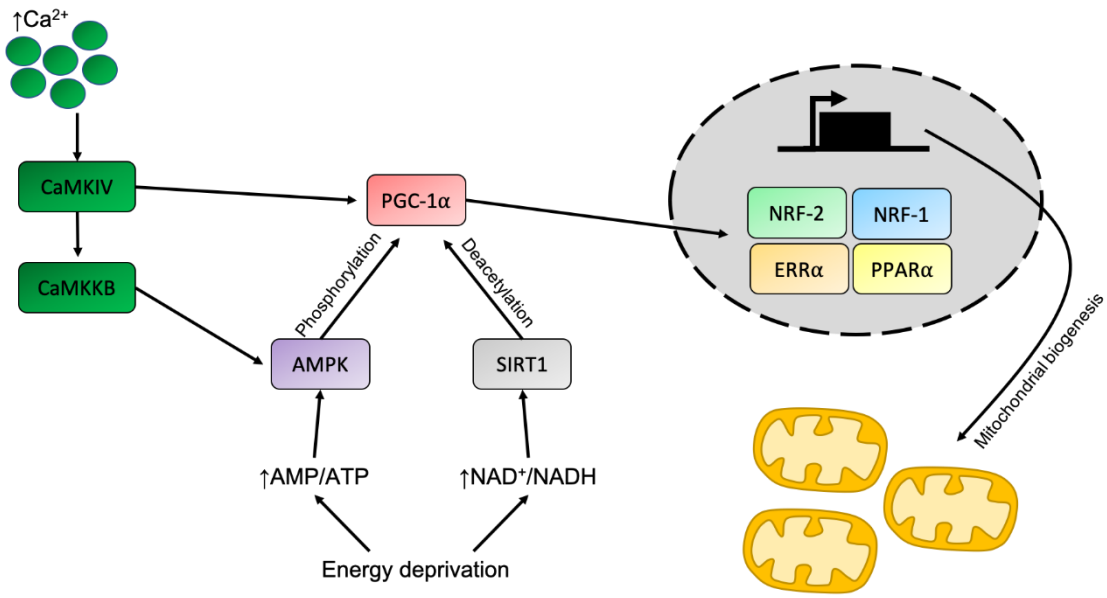

Figure 1.7 – Mitochondrial biogenesis signalling pathway*. PGC-1α is the master regulator of mitochondrial biogenesis by promoting the transcription of various nuclear transcription factors such as NRF-1/2, PPARα and ERRα. In the event of increased Ca^{2+} levels, CaMKIV is activated and then subsequently promotes the activation of PGC-1α.. In the event of energy deprivation (e.g. after exercise) AMP:ATP and NAD^+:NADH ratios are increased and detected by AMPK and SIRT1 respectively.*

1.4.4.2 Mitophagy

The selective degradation of irreparably damaged mitochondria, termed mitophagy, is an essential cellular quality control mechanism required to maintain bioenergetics. Impairment of mitophagy is associated with mitochondrial dysfunction, with consequences of cellular and tissue damage, and eventual manifestation of pathology. In particular, abnormalities in mitophagy are commonly age-related and so are associated with geriatric conditions such as Parkinson's Disease, cardiovascular problems, metabolic disorders and cancer (Palikaras *et al*., 2018).

Mitophagy is stimulated by several factors and can be classified as being either 'basal mitophagy', which is the continued process of mitophagy required for removal of old and damaged mitochondria (Palikaras *et al*., 2018), 'stress-induced mitophagy', which is induced by factors such as hypoxia or starvation (Liu *et al*., 2012; Kanki *et al*., 2009), or 'programmed mitophagy', which is required for development in several cell types (Sandoval *et al*., 2008; Schweers *et al*., 2007; Novak *et al*., 2010) or preventing paternal inheritance of mtDNA (Al Rawi *et al*., 2011; Rojansky *et al*., 2016).

There are several mechanisms of mitophagy that are utilised in different tissues, and the factors that regulate mitophagy can be classified as either 'ubiquitin-dependant' or 'ubiquitin-independent' (Khaminets *et al*., 2016).

Ubiquitin-dependant mitophagy progresses down the Parkin-PINK1 (phosphatase and tensin homologue (PTEN)-induced putative kinase 1) pathway (Pickles *et al*., 2018) (**Figure 1.8**). In basal conditions, PINK1 is imported into the IMS and rapidly cleaved and degraded by several proteases such as presenilin-associated rhomboid-like protein (PARL) (Jin *et al*., 2010). In the event of mitochondrial stress, membrane dissipation prevents the IMS translocation of truncated PINK1, and it is instead stabilised on the OMM where it is autophosphorylated (Harper *et al*., 2018; Sekine & Youle, 2018). PINK1 phosphorylation then initiates the recruitment of the E3 ubiquitin ligase Parkin, where it is subsequently phosphorylated and activated by PINK1 (Lazarou *et al*., 2012). In addition to phosphorylating Parkin, PINK1 also phosphorylates ubiquitin (Ub) and poly-Ub chains on several proteins on the OMM of mitochondria, thereby targeting them for degradation by the autophagosome (Chan *et al*., 2011; Sarraf *et al*, 2013). Additionally, PINK1 indirectly activates Drp1 activity to promote mitochondrial fission and enhance autophagic degradation of the mitochondria (Pryde *et al*., 2016), as well as targeting MFNs for proteasomal degradation, thus preventing mitochondrial fusion (Tanaka *et al*., 2010).

Aside from Parkin-mediated mitophagy, several other molecules can regulate ubiquitin-dependant mitophagy, such as Gp78, MUL1 and SMURF1 (Orvedahl *et al*., 2011). These molecules induce the

ubiquitination of OMM proteins in a similar way to Parkin ubiquitination, thereby anchoring the autophagosome to damaged mitochondria via their autophagosomal light chain (LC3).

In contrast to ubiquitin-dependant mitophagy, mitochondrial proteins themselves can induce mitophagy by acting as mitophagy receptors. Again, these molecules can attract and bind the autophagosome through LC3-interacting region (LIF) motifs (Gatica *et al*., 2018). Examples of these mitophagy-inducing OMM proteins include NIP3-like protein X (NIX) and BCL2 interacting protein 3 (BNIP3) (Quinsay *et al*., 2010; Zhang *et al*., 2016).

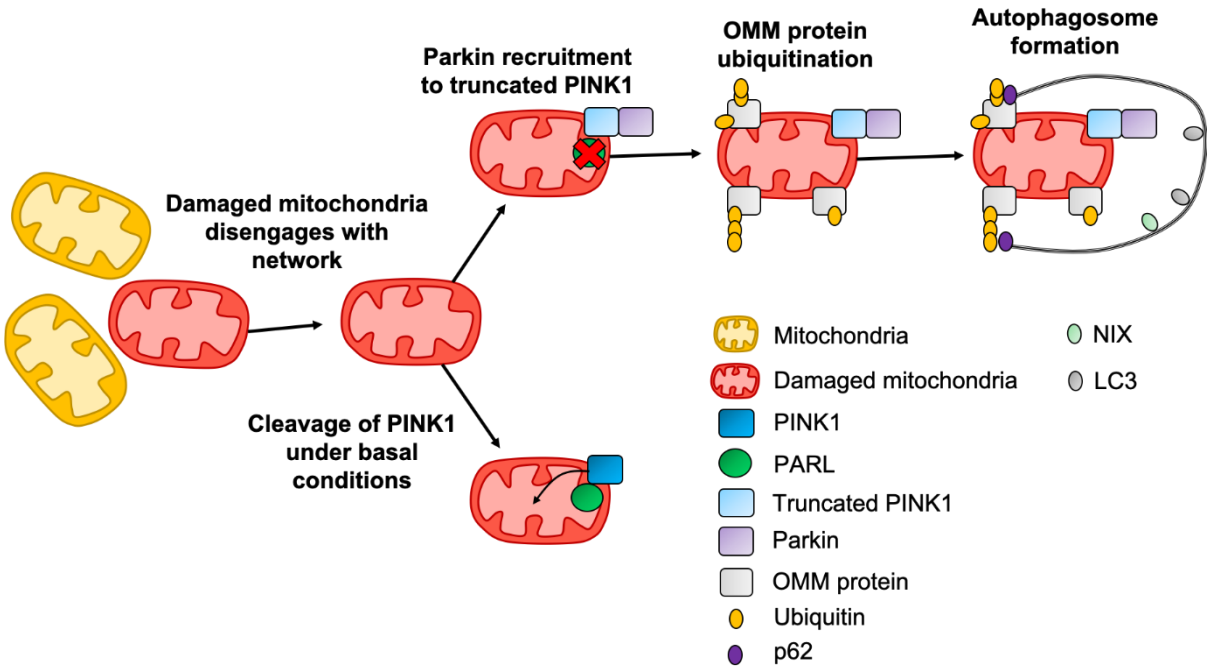

Figure 1.8 – PINK1-Parkin mitophagy pathway*. Damaged mitochondria have low membrane potential and are separated from the mitochondrial network. Under normal conditions, truncated PINK1 is cleaved and degradated by PARL and other proteases. During mitophagy, PARL protease activity is inhibited and truncated PINK1 localises on the OMM where it recruits and stabilises Parkin. Next, Parkin mediates the ubiquitination of OMM proteins, which subsequently initiates the recruitment of p62 and autophagosome formation.*

1.4.4.3 Mitochondrial protein homeostasis

Mitochondria contain their own genome, which encodes 37 essential genes (detailed further in **Section 1.4.7**) important for mitochondrial homeostasis. The other essential proteins and molecules required to maintain mitochondrial function, are encoded by the nucleus (nDNA), and are translocated into the mitochondria. The majority of these proteins arrive in a post-translational manner through TOM complexes on the OMM, and TIM complexes in the IMM. They then require post-transcriptional modifications and guidance to the right mitochondrial sub-compartment, which is commonly performed by Hsp70 (Sickmann *et al*., 2003; Young *et al*., 2003) (**Figure 1.9**).

The next step after nDNA-encoded protein importation and sorting is maturation, which is required for the assembly of the proteins into functional complexes. For the majority of these proteins the first step is proteolytic removal of the pre-sequence (Mossmann *et al*., 2012). This action is performed by the mitochondrial membrane protease (MPP), which cleaves the N-terminal pre-sequence, followed by additional cleavage by Icp55 and Oct1 (Vogtle *et al*., 2011). Another important processing event is undertaken on one of the subunits of the mitochondrial ribosome, MrpL32, performed by the m-AAA protease, which is part of the AAA+ family of proteases (Bonn *et al*., 2011).

Following maturation, the mitochondrial proteins require assembly into functional multimeric complexes. This process is performed by a range of chaperones and co-chaperones that reside in the mitochondrial matrix such as mtHsp70 and its co-chaperones, mtHsp60 and mtHsp10 (Lill *et al*., 2012). Whilst the exact process of protein assembly is unknown, it is suspected that protein folding requires disulphide bond formation (Banci *et al*., 2009; Weckbecker *et al*., 2012).

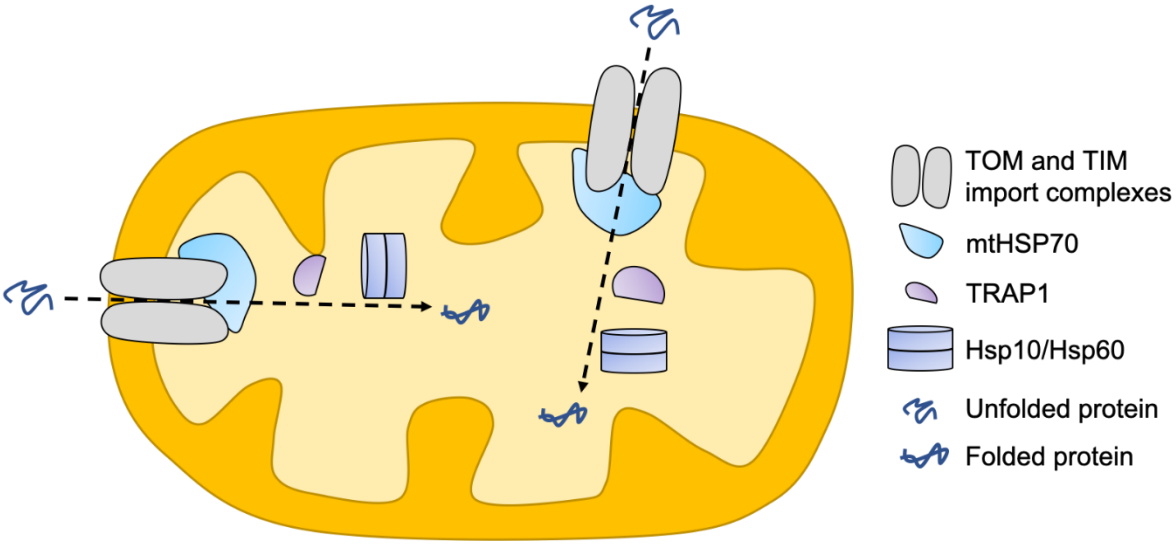

Figure 1.9 – Mitochondrial protein import and assembly*. Nuclear-encoded unfolded proteins are translocated to the mitochondria where they are imported via TOM and TIM complexes into the mitochondrial matrix. Once imported, the mitochondrial chaperone mtHsp70 mediates the assembly and folding of the proteins into functional complexes.*

1.4.4.4 Mitochondrial protein degradation and stress response

As with regular cellular homeostasis, misfolded, damaged, or non-assembled proteins in the mitochondria pose a serious threat to mitochondrial homeostasis and have been implicated in various pathologies such as Parkinson's and Alzheimer's disease (Kong *et al*., 2018). Protein damage can be induced by stressors such as reactive oxygen species (ROS), or alternatively by deleterious mtDNA mutations (Corral-Debrinski *et al*., 1991; Ahlqvist *et al*., 2012; Ross *et al*., 2013).

The mitochondrial proteome has an extremely high turnover rate, with an estimated 6-12% of the whole proteome being degraded during each generation (Augustin *et al*., 2005). As a result, mitochondria contain several quality control mechanisms in order to deal with the threat of proteotoxicity. The first of these processes is a highly conserved cross-membrane proteolytic system which removes and destroys abnormal proteins. Here, LonP and ClpX/P proteases reside in the matrix, whilst the m-AAA protease is localised on the IMM facing the matrix and the i-AAA protease resides on the IMM facing the IMS (**Figure 1.10**). The two AAA proteases are responsible for degradation of membrane proteins, but also contribute to cleavage of matrix proteins (Benedetti *et al*., 2006; Matsuda *et al*., 2010). Of these membrane proteins, the most significant proteins that are degradated by the AAA proteases belong to OXPHOS complexes, which are extremely susceptible to damage due to the amount of ROS produced during electron transfer.

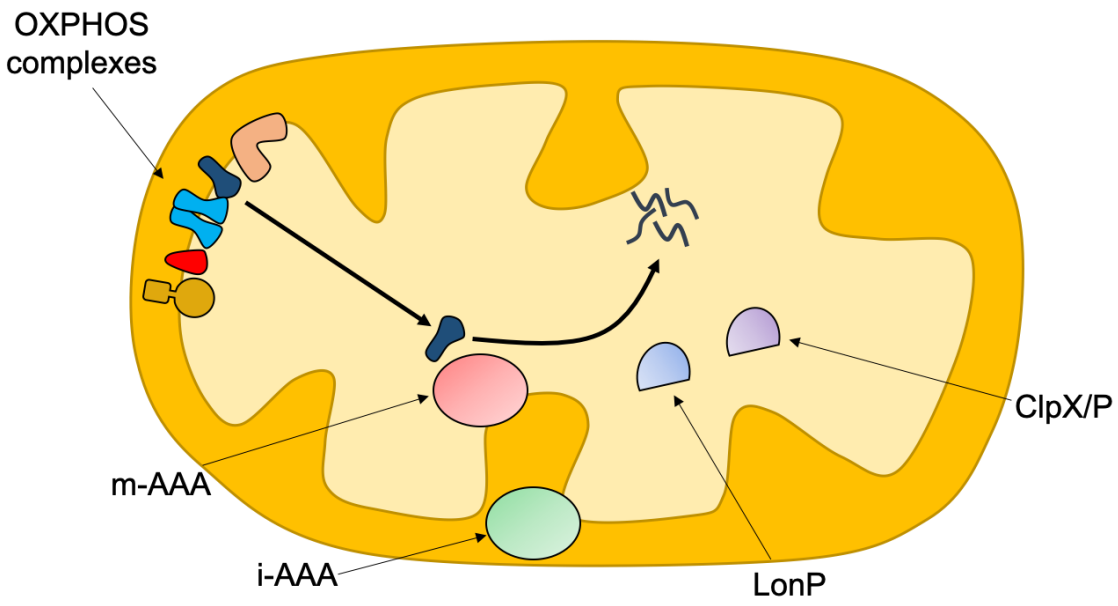

Figure 1.10 – Intramitochondrial proteolysis*. Mitochondria contain a highly conserved proteolytic system consisting of i-AAA proteases in the IMM facing the IMS, m-AAA proteases in the IMM facing the matrix, and LonP and ClpX/P proteases residing in the mitochondrial matrix. This system of proteases is responsible for proteolytically cleaving imported proteins as well as degradation of internal mitochondrial proteins such as OXPHOS complexes.*

The other conserved system of mitochondrial protein homeostasis is called the mitochondrial unfolded protein response (mtUPR). In the mtUPR, proteotoxic stress within the mitochondria is detected and triggers the activation of a nDNA-encoded gene expression program aimed at the proteolytic removal of the stress (**Figure 1.11**). An additional function of the mtUPR is to divert metabolism away from oxidative phosphorylation towards anaerobic cytoplasmic glycolysis in order to alleviate mitochondrial stress (Nargund *et al*., 2015).

Whilst the mechanisms by which misfolded or damaged proteins are recognised by the mtUPR are not fully understood, it is known that the mtUPR becomes activated in response to various stimuli, including: mtDNA depletion (Martinus *et al*., 1996); oxidative stress (Fiorese & Haynes, 2017); inhibition of mtDNA translation (Houtkooper *et al*., 2013); OXPHOS dysfunction (Duriex *et al*., 2011); or damage to mitochondrial chaperones (Haynes *et al*., 2007). To date, the strongest hypothesis is that oligopeptides generated in the matrix by ClpP proteases are detected by AFTS-1, which subsequently activates the mtUPR (Houtkooper *et al*., 2013). Here, ATFS-1 accumulates in the cytoplasm in response to declining membrane potential as a result of proteotoxicity, where its C-terminal nuclear localisation sequence has access to nuclear import machinery. Once in the nucleus, ATFS-1 promotes the activation of a range of genes involved in mitochondrial homeostasis, including genes involved in antioxidation, glycolytic factors, genes involved in regulating mitochondrial dynamics, such as NRF1, and mitochondrial chaperones such as mtHsp70 and Hsp60 (Narguud *et al*., 2015).

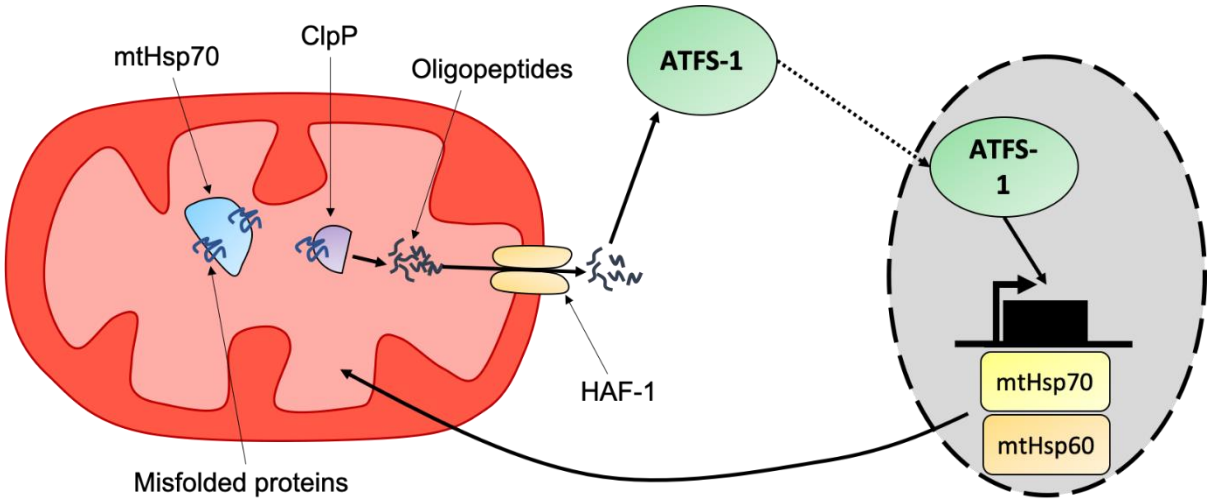

Figure 1.11 – The mtUPR*. Schematic depicting the mtUPR signalling pathway. Here, stressors are detected by the transcription factor ATFS-1 which becomes activated and subsequently translocated to the nucleus where it promotes the transcription of several genes involved in mitochondrial homeostasis.*

The final mechanism of mitochondrial protein homeostasis is the isolation and transportation of proteins for degradation away from the mitochondria. The most prominent mechanisms of this process are performed by mitochondria-derived vesicles (MDVs) and mitochondrial-derived compartments (MDCs) (Moehle *et al*., 2018).

MDVs have been shown to be strongly implicated in the early response to oxidative stress, preceding membrane depolarisation (Soubannier *et al*., 2012), by transporting oxidised proteins to the lysosome for degradation, as well as other mitochondrial proteins such as MAPL for degradation in the peroxisomes. Although MDV formation can occur independently of mitophagy, MDV trafficking relies on both PINK1 and Parkin (McLelland *et al*., 2014).

In contrast to MDV formation and trafficking, MDCs rely directly on mitochondrial fission and mitophagy machinery, and traffic mitochondrial cargo for degradation in the vacuole (Hughes *et al*., 2016).

1.4.5 Mitochondrial electron transport chain

One of the key functions of mitochondria is to regulate oxidative metabolism and provide cellular energy in the form of ATP. There are three respiratory pathways in which mitochondria produce ATP – anaerobic glycolysis, the tricarboxylic acid (TCA) cycle, and OXPHOS via the mitochondrial electron transport chain (ETC). In normal conditions, the generation of ATP is a multistep process that begins with glycolysis and leads to the TCA cycle in the mitochondrial matrix and finally OXPHOS.

1.4.5.1 Glycolysis and the TCA cycle

Glycolysis is an anaerobic process that occurs in the cell cytoplasm and produces two molecules of pyruvate and the net production of two molecules of ATP (**Equation 1.1**). The glycolysis pathway is composed of two stages: (1) initially, glucose is converted into fructose-1, 6-bisphosphate. Fructose-1, 6-bisphosphate is then further cleaved into three carbon fragments. (2) In the second stage, NAD^+ is converted to NADH through reduction reactions. NAD^+ levels are then regenerated back to baseline levels through the reduction of pyruvate into lactate (Berg *et al*., 2015a).

$$Glucose + 2(P_i) + 2(ADP) + 2(NAD^+) \rightarrow 2\,pyruvate + 2(H^+) + 2(ATP) + 2(NADH) + 2(H_2O)$$

Equation 1.1 – Glycolysis reaction *(Berg et al., 2015a).*

The next stage of respiration is the TCA (or Kreb's) cycle, which occurs in the mitochondrial matrix. The TCA cycle functions to harvest electrons for use in the ETC as well as aerobically processing glucose. The first stage is the generation of acetyl coenzyme A (acetyl CoA) from pyruvate, which is catalysed by pyruvate decarboxylase (**Equation 1.2**). This acetyl-CoA then feeds into the TCA cycle. Here, a series of oxidation and reduction reactions generate a single molecule of ATP, two molecules of CO_2, three NADH, and two $FADH_2$ electron carriers (**Equation 1.3**), all of which are required for oxidative phosphorylation via the ETC (Berg *et al*., 2015b).

$$Pyruvate + CoA + NAD^+ \rightarrow Acetyl\ CoA + NADH + H^+ + CO_2$$

Equation 1.2 Pyruvate decarboxylation reaction*. This reaction is catalysed by pyruvate dehydrogenase (Berg et al., 2015b).*

$$Acetyl\ CoA + 3[NAD^+ + FAD + ADP + P_i + 2(H_2O)] \rightarrow CoA + 3(NADH) + 2(H^+) + FADH_2 + ATP + 2(CO_2)$$

Equation 1.3 Net reaction of the TCA cycle *(Berg et al., 2015b).*

1.4.5.2 Oxidative phosphorylation

The final stage of respiration is OXPHOS, which comprises the mitochondrial respiratory chain complexes I-IV as well as ATP synthase/complex V, all of which are embedded into the IMM (**Figure 1.12**). Here, the transport of electrons along complexes I-IV, in combination with the translocation of protons across the IMM, produces a chemiosmotic gradient. This chemiosmotic gradient is then harnessed by complex V (CV) to allow the flow of electrons through the catalytic domain of ATP synthase, thus generating the energy required to drive ATP production.

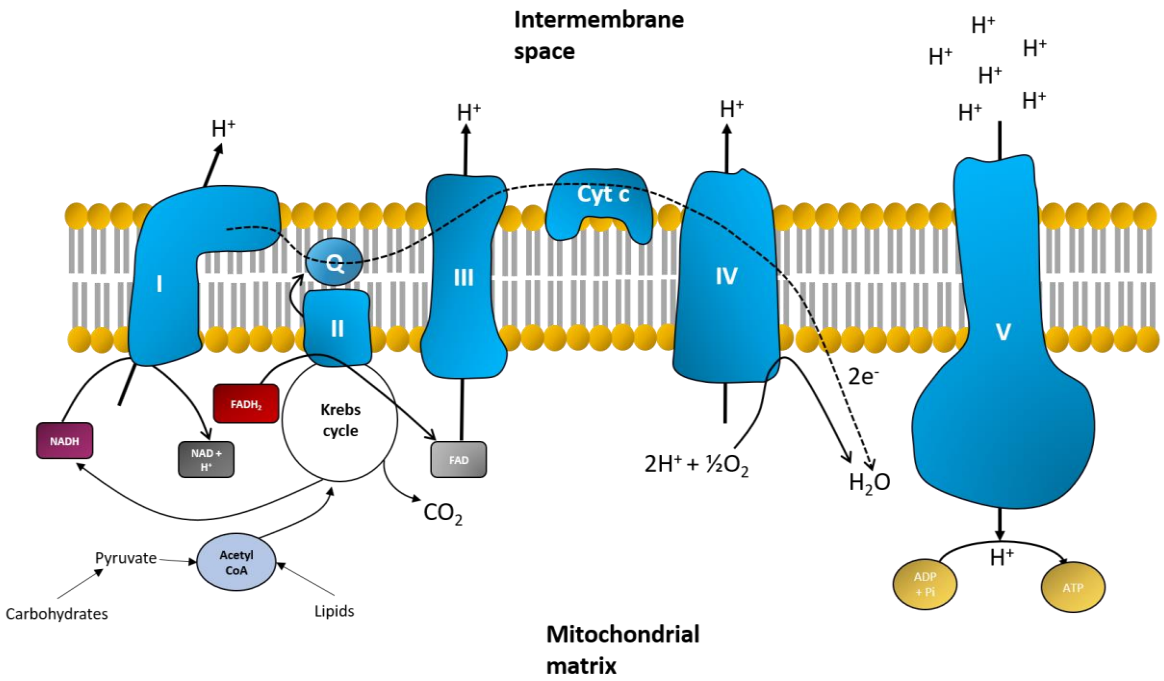

***Figure 1.12 – Oxidative phosphorylation**. Electron transport chain complexes I-IV are embedded into the IMM. Electrons (e^-) enter the electron transport chain at complexes I and II and are then shuttled to complex IV via Cytochrome c (Cyt c). This transfer of electrons generates the energy needed to translocate protons (H^+) across the IMM into the IMS. Finally, complex V harnesses the proton gradient to produce ATP from ADP + P_i.*

1.4.5.3 Oxidative phosphorylation complexes

As mentioned above, there are four complexes embedded into the IMM which make up the mitochondrial ETC, in addition to ATP synthase. Four of the five complexes have subunits encoded by mtDNA (CI, CIII, CIV and CV), whilst CII is the only complex that is entirely composed of nuclear-encoded subunits. In addition, it is the only complex that does not contribute to the electrochemical gradient (Chaban *et al*., 2014).

Complex I (NADH dehydrogenase), is the largest of the ETC complexes, with a molecular mass of ~1000kDa. It is composed of 45 subunits, seven of which are encoded by mtDNA whilst the other 38 are nDNA-encoded (Carrol *et al.,* 2006). CI has a characteristic L shape that is mainly embedded into the IMM lipid bilayer, with a small shoulder protruding into the matrix (Baradaran *et al*., 2013). The complex is made up of three functional modules: the P-module, Q-module and N-module.

CI binds NADH at the distal end of the N-module (in the matrix) and then transfers two electrons from NADH down seven Fe-S clusters to ubiquinone via flavin mononucleotide (FMN). Reduction of ubiquinone then induces a conformational change that triggers the translocation of four protons (H^+) into the IMS (Baradaran *et al*., 2013) (**Equation 1.4**).

$$NADH + Q + 5(H^+)_{matrix} \rightarrow NAD^+ + QH_2 + 4(H^+)_{cytoplasm}$$

Equation 1.4 – Complex I reaction *(Berg et al., 2015b).*

Complex II (succinate dehydrogenase) is the smallest complex of the ETC, being ~123kDa, and is composed of four nDNA-encoded subunits. In addition to its role in oxidising succinate, CII is responsible for the transfer of three electrons to ubiquinone via three Fe-S clusters, as described in **Equation 1.5** (Cecchine, 2003).

$$Succinate + FAD + 2(H^+) + Q \rightarrow Fumurate + FADH_2 + Q \rightarrow Fumerate + FAD + QH_2$$

Equation 1.5 – Complex II reaction *(Berg et al, 2015b).*

Complex III (cytochrome c oxioreductase) exists in the IMM as a dimer. It is composed of 11 subunits, of which only one is encoded by mtDNA (cytochrome b) (Benit *et al*., 2009). The first role of CIII is to oxidise ubiquinone into ubiquinol, which facilitates the translocation of two protons from

the matrix across the IMM into the IMS. Next, the electrons released from the newly formed ubiquinol are transferred to cytochrome c via cytochrome b (**Equation 1.6**) (Chaban *et al*., 2014).

$$2(QH_2) + Q + 2(Cyt\ c)_{ox} + 2(H^+)_{matrix} \rightarrow 2(Q) + QH_2 + 2(Cyt\ c)_{red} + (4H^+)_{cytoplasm}$$

Equation 1.6 – Complex III reaction *(Berg et al., 2015b).*

Complex IV (cytochrome c oxidase (COX)) is the third largest of the ETC complexes, being composed of 13 subunits, of which three are mtDNA-encoded. CIV accepts electrons from reduced cytochrome c and transfers it to molecular oxygen, forming two molecules of water (H_2O). This facilitates the pumping of four protons from the matrix into the IMS, thus contributing to the electrochemical gradient in the IMS (**Equation 1.7**) (Diaz *et al*., 2010).

$$4(Cyt\ c)_{red} + O_2 + 8(H^+)_{matrix} \rightarrow 4(Cyt\ c)_{ox} + 2(H_2O) + 4(H^+)_{cytoplasm}$$

Equation 1.7 – Complex IV reaction *(Berg et al., 2015).*

Complex V (ATP synthase) is the final complex of the OXPHOS system and is the site of ATP production. It is the second largest of the complexes, being composed of 15-18 subunits and weighing ~600kDa (Stock *et al*., 2000). The complex is composed of F_0 and F_1 domains. The F_0 domain resides in the IMM and contains subunits a, b, c, d, A6L, e, f, g, and OSCP, which form a ring-shaped barrel, whilst the F_1 domain is composed of subunits α, β, γ, and ε, which collectively form a central and peripheral stalk structure (Devenish *et al*., 2008; Jonckheere *et al*., 2012).

As alluded to above, the role of CV is to generate ATP from ADP. Here, the proton motive force generated by the electrochemical gradient is harnessed in order to drive the F_0 motor. This results in a conformational change in the catalytic F_1 domain that allows the phosphorylation of ADP and release of ATP (Chaban *et al*., 2014).

1.4.5.4 Supercomplexes

Several studies utilising the blue-native polyacrylamide gel electrophoresis (BN-PAGE) assay have demonstrated that ETC complexes are able to assemble into larger structures termed 'supercomplexes' (Schagger & Pfeiffer, 2000). These supercomplexes can be divided into four main groups. Here, complexes I, III_2 and IV were found to assemble into I + III_2, III_2 + IV_{1-2}, or I + III_2 + IV_{1-4} supercomplexes. In addition, CV is able to form dimers which resemble oligomeric cristae chains (Chaban *et al*., 2014). The abundance of these supercomplexes varies between species, and it has

been shown that in mammals the predominant supercomplex is the I + III_2 + IV_{1-4} complex (Schagger & Pfeiffer, 2000).

Whilst the structures of the supercomplexes has been elucidated, it is still unclear what the exact function of these macromolecules are. The overriding hypothesis of the function of supercomplexes is that they aid in maximising the flow of electrons across the ETC, thereby speeding up and increasing the efficiency of OXPHOS (Schagger & Pfeiffer, 2000). In addition, it is thought that the formation of supercomplexes reduces the leakage of electrons, and thus, the formation of ROS (Maranzana *et al*., 2013).

1.4.6 Other functions of mitochondria

1.4.6.1 Apoptosis signalling

Apoptosis is the coordinated process of controlled cell death required in multi-cellular organisms to maintain homeostatic balance between newly formed cells and irreparably damaged cells. In addition, apoptosis is necessary for the development of anatomical structures such as fingers and toes (Zakeri & Ahuja, 1997). Originally described by Kerr *et al*. (1972), apoptosis is regulated by a vast array of regulatory genes and proteins, and the event of apoptosis dysregulation can lead to uncontrolled cellular growth and cancer, as well as the accumulation of damaged cells and proteins which can cause diseases such as Alzheimer's Disease (D'Arcy, 2019).

Apoptosis can be divided into two major pathways: the intrinsic pathway (otherwise known as the mitochondrial pathway), where intracellular signals are detected by sensors in response to cellular damage such as hypoxia or DNA damage (Igney & Krammer, 2002); or the extrinsic pathway (otherwise known as the death receptor pathway), where a damaged cell is detected by the immune system and apoptosis is initiated by activation of receptors of the tumour necrosis factor (TNF) receptor family. The initiation of both pathways is dependent on the activation of a variety of cysteine-aspartic proteases termed caspases (Elmore, 2007).

As alluded to above, mitochondria play an essential role in the initiation of the intrinsic pathway (**Figure 1.13**). In response to factors such as DNA damage or the absence of cytokines or hormones, the mitochondrial permeability transition pore (MPTP) opens in conjunction with the loss of membrane potential. The opening of the MPTP facilitates the export of several pro-apoptotic molecules such as cytochrome *c*, Smac/Diablo, and HtrA2/Omi into the cytoplasm in order to initiate the apoptosis signalling cascade. Here, the initiator caspase, caspase-9, binds to the caspase recruitment (CARD) domain of the adapter protein apoptotic protease activating factor 1 (APAF1) to form the 'apoptosome', which then cleaves and activates caspases-3 and 7 to initiate apoptosis. (Cain *et al*., 2002). A second group of pro-apoptotic proteins are released from the mitochondria as a late stage event of apoptosis after the cell has already committed to die. These proteins include AIF, endonuclease G, and CAD, and they function in a caspase-independent manner to promote DNA and nuclear fragmentation (Joza *et al*., 2001).

Control and regulation of the intrinsic pathway of apoptosis is performed by members of the Bcl-2 family of proteins. There have been more than 25 members of the Bcl-2 family identified, of which some are pro-apoptotic, such as Bax, Bak, Bid, and Bad, and some are anti-apoptotic, including Bcl-2, BAG and Bcl-x (Cory & Adams, 2002; Riley *et al*., 2018).

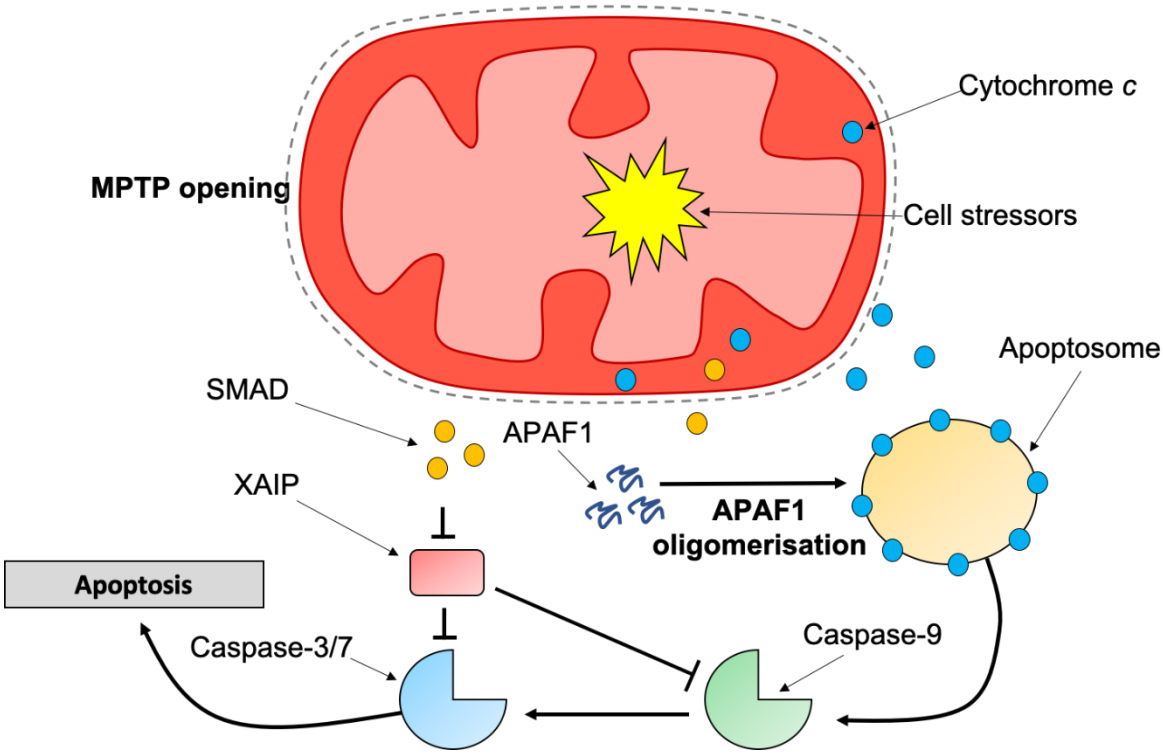

Figure 1.13 – Initiation of the intrinsic pathway of apoptosis.

1.4.6.2 Calcium handling

Calcium (Ca^{2+}) regulated signalling is a highly conserved mechanism that plays a vital role in several cellular and physiological processes such as muscle contraction, energy production and regulation of apoptosis.

Whilst ER are known to be the main site of calcium storage, various other organelles are involved in Ca^{2+} signalling such as lysosomes (Rodriguez *e al*., 1997), endosomes (Gerasimenko *et al*., 1998), Golgi apparatus (Pinton *et al*., 1998) and significantly, mitochondria (Contreras *et al*., 2010). Due to the vital role played by both the ER and mitochondria in regulating cellular Ca^{2+}, these organelles are commonly localised in close association with each other (Filippin *et al*., 2003).

With regards to the role of Ca^{2+} in mitochondrial biology, Ca^{2+} entry into the mitochondrial matrix is facilitated by the IMM mitochondrial Ca^{2+} uniporter (mCU), which is regulated by membrane potential (Kirichok *et al*., 2004). The function of several matrix proteins such as matrix dehydrogenases are regulated by Ca^{2+} levels (Denton, 2009). In addition, cytosolic Ca^{2+} has been shown to modulate several IMM enzymatic processes such as the malate-aspartate shuffle involved in respiration, or glutamate/malate respiration (Gellerich *et al*., 2009). Most importantly, increased import and overexpression of Ca^{2+} in mitochondria has been shown to induce mitochondrial membrane depolarisation and opening of the MPTP, leading to the initiation of the intrinsic pathway of apoptosis (Kroemer *et al*., 2007).

As mentioned above, regulation of intracellular Ca^{2+} levels is crucial for physiological processes such as muscle contraction. Here, action potentials arriving at the neuromuscular junction (NMJ) triggers the opening of Ca^{2+} channels, leading to the influx of extracellular Ca^{2+} into the neuron. This then triggers the release of acetylcholine (ACh) into the synaptic cleft, where it induces the opening of sodium (Na^{+}) and potassium (K^{+}) channels and subsequently depolarisation of the sarcolemal membrane. Depolarisation and opening of the sarcolemal membrane leads to Ca^{2+} release into the cytosol via L-type Ca^{2+} channels on the sarcoplasmic reticulum (SR). The cytosolic Ca^{2+} then binds to the actin filament regulatory protein troponin, which induces a conformational change in order to allow the formation of actin-myosin cross bridging and finally muscle contraction (Leiber, 2010). Muscle relaxation additionally requires the reuptake of Ca^{2+} by the SR via ATP-dependant Ca^{2+} pumps and sarcoplasmic/endoplasmic reticulum Ca^{2+} ATPases (SERCA) 1 and 2 (Brini & Carafoli, 2009).

1.4.6.3 Iron sulphur cluster formation

Individually, iron (Fe) and sulphur (S) are indispensable ubiquitous molecules in cells, but when overloaded induce cellular toxicity. To prevent this cellular toxicity, iron and sulphur elements are assembled into Fe-S clusters (Lill, 2009). These Fe-S clusters are essential co-factors for various proteins involved in cellular functions such as DNA replication and repair, gene expression regulation via tRNA modifications and importantly, OXPHOS (Lill *et al*., 2012).

In a regular eukaryotic cell, Fe-S cluster assembly machinery is found in both the cytosol and mitochondria. With regard to the mitochondrial Fe-S cluster assembly machinery, there are 18 proteins so far that have been identified in yeast, whilst 11 cytosolic proteins involved in Fe-S cluster formation have been identified (Braymer & Lill, 2017).

The process of Fe-S cluster formation can be divided into four stages: (1) *de novo* 2Fe-2S synthesis on Isu1 scaffolding proteins; (2) mtHsp70-mediated trafficking and export of 2Fe-2S clusters into the cytosol as well as insertion into mitochondrial apo-proteins; (3) conversion of 2Fe-2S clusters into 4Fe-4S clusters; (4) trafficking and import of the newly formed 4Fe-4S clusters back into the mitochondria (Rouault, 2012) (**Figure 1.14**).

As mentioned above, Fe-S clusters are essential in order for the TCA cycle and OXPHOS to function. They are found within complexes I-IV where they facilitate the transfer of electrons through continuous redox reactions (Beinert *et al*., 1997).

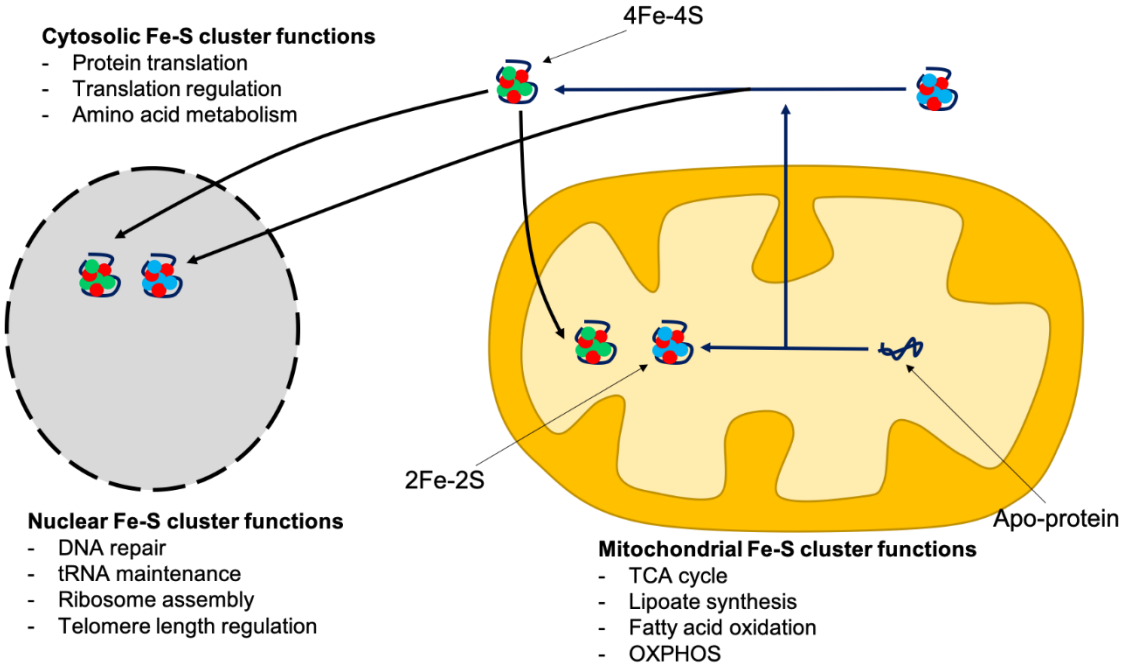

Figure 1.14 – Fe-S cluster formation and functions*. The formation and assembly of various Fe-S clusters is essential for several functions in eukaryotic cells.*

1.4.6.4 Reactive oxygen species (ROS) production

Reactive oxygen (ROS) and reactive nitrogen species (RNS) are a range of chemically active species that are involved in various intracellular signalling pathways, but can cause damage to various biomolecules such as proteins and DNA when levels are not controlled (Cui *et al*., 2012).

ROS are endogenously formed after the incomplete reduction of oxygen. The most commonly produced ROS is superoxide (O_2^-), which is formed after electrons leak from the mitochondrial respiratory chain and are accepted by molecular oxygen (Turrens, 2003). O_2^- can then be stabilised by superoxide dismutase to form hydrogen peroxide (H_2O_2), which is highly toxic and inflicts significant damage to macromolecules. H_2O_2 can subsequently be broken down into water and molecular oxygen through the actions of catalase (Ray *et al*., 2012). The other common ROS is the hydroxyl radical (HO•) (Ray *et al*., 2012).

As well as being the site of ROS production, mitochondria also contain a highly conserved defensive mechanism termed the antioxidant system. Oxidative stress is the physiological phenomenon caused by dysregulation of the antioxidant system, or when ROS levels themselves become too high and overwhelm the system. Oxidative stress results in the direct or indirect damage of macromolecules such as nucleic acids, proteins and lipids, and has been associated with the onset or progression of several pathologies (Sies, 2015) such as diabetes, atherosclerosis (Paravicini *et al*., 2006), neurodegeneration (Shukla *et al*., 2011; Kim *et al*., 2015), and cancer (Trachootham *et al*., 2009; Hayes *et al*., 2020).

Due to the close proximity of mitochondrial proteins and mtDNA nucleoids to the ROS-producing ETC, as well as the fact that these macromolecules have no protective histones or sufficient DNA repair machinery, they are highly susceptible to damage from these ROS (Turrens, 2003).

In contrast to the deleterious effects of ROS and RNS, these molecules play an essential role in a variety of intracellular signalling pathways such as autophagy (Scherz-Shouval *et al*., 2007), immunity (West *et al*., 2011), hypoxia (Chandel *et al*., 1998), mitochondrial dynamics (Bartz *et al*., 2015), and apoptosis (Pierce *et al*., 1991).

1.4.7 Mitochondrial genetics

1.4.7.1 mtDNA genome

Mitochondria are unique organelles in that they are the only organelle with its own genome. The mitochondrial genome is a circular double-stranded molecule roughly 16.6kb large (**Figure 1.15**). It encodes 37 genes: 13 OXPHOS complex subunits, as well as 22 transfer RNAs (tRNA), and two ribosomal RNAs (rRNA) required for the transcription and translation of the OXPHOS subunits (Anderson *et al*., 1981). The two strands of mtDNA differ in their composition with regard to guanine saturation, and so can be separated into heavy (H) and light (L) strands.

mtDNA is a very compact molecule and does not contain any non-coding introns. Instead, mtDNA possess a noncoding region (NCR) where the displacement loop (D-loop) is located. The NCR contains promoters of polycistronic transcription for both the H and L strands, appropriately termed the heavy strand promoter (HSP) and light strand promoter (LSP). Importantly, the NCR also harbours the origin for H strand replication (O_H) (Shadel & Clayton, 1997). The origin for light strand replication (O_L) is located in a tRNA cluster roughly 11,000bp downstream of the O_H (Falkenberg, 2018).

The mitochondrial genome exists in numerous copies per cell and can be found in the mitochondrial matrix in the form of circular nucleoids, localised within a close proximity to the IMM and OXPHOS complexes (Satoh & Kuroiwa, 1991). The number of mtDNA nucleoids per cell depends on the cell type and its energy requirement. For example, there are roughly 100,000 copies in mature oocytes, which require vast amounts of energy supply, whilst there are roughly 3600 copies in skeletal muscle fibres (Shoubridge & Wai, 2007; Miller *et al.,* 2003).

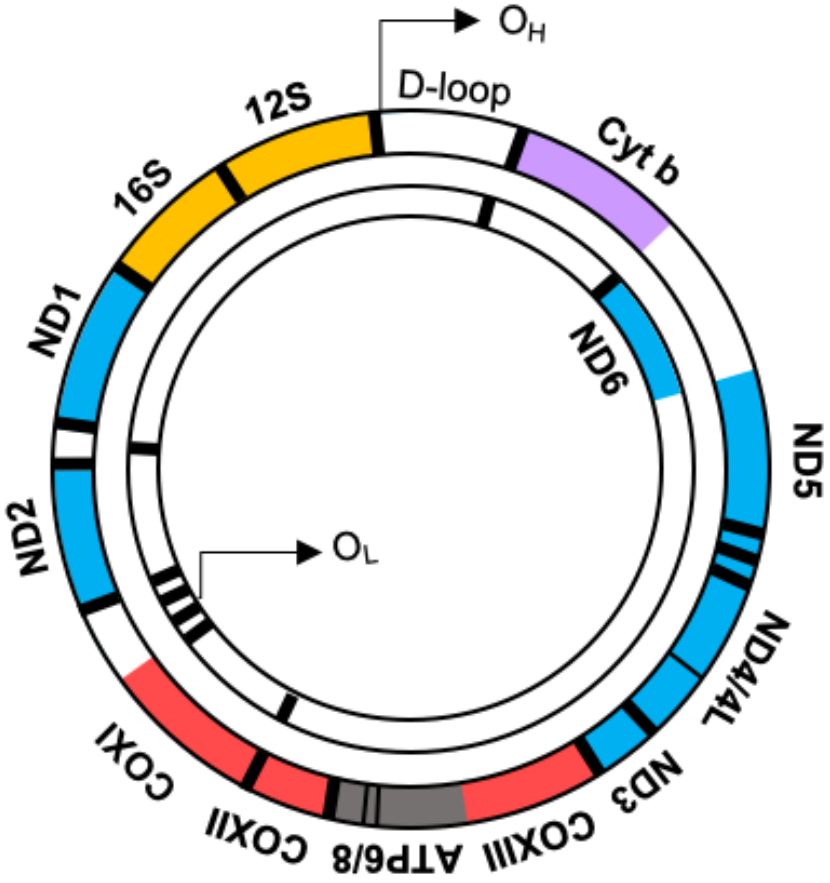

Figure 1.15 – Mitochondrial genome*. The mtDNA genome contains a noncoding region (D-Loop) and 37 genes – 13 OXPHOS subunits (CI = blue, CIII = purple, CIV = red and CV = dark grey), 22 tRNAs (black lines) and 2 rRNAs (yellow). In addition, the origins of heavy (O_H) and light (O_L) strand promotion are depicted.*

1.4.7.2 mtDNA replication

mtDNA replication occurs independently of the cell cycle and so is termed 'relaxed replication'. As a result, mtDNA replication requires its own distinct set of replication machinery. This machinery consists of: a mitochondrial polymerase, polymerase gamma (POLG); a helicase, Twinkle; a mitochondrial RNA polymerase (POLRMT); single-stranded binding protein (mtSSB); RNA ligase (RNaseH1), and topoisomerases (Milenkovic *et al*., 2013).

POLG is a heterotrimer that is composed of a catalytic subunit (POLGA) and two accessory subunits (POLGB), which are involved in replication fidelity (Gray & Wong, 1992; Fan *et al*., 2006). Whilst there are other known mtDNA polymerases, they are not essential for mtDNA replication (Sykora *et al*., 2017; Wisnovsky *et al*., 2016). The mtDNA helicase Twinkle is responsible for unwinding of mtDNA prior to transcription, whilst the function of mtSSB is to stabilise the unwound, single-stranded mtDNA. The POLRMT is responsible for initiating the synthesis of RNA stands, and finally, the topoisomerases are responsible for unwinding the mtDNA as it progresses through the replication fork (Young & Copeland, 2016).

There is still no consensus as to how mtDNA replication occurs in mammals, although extensive research over the last 20 years has demonstrated the presence of two distinct classes of mtDNA replication – 'synchronous' and 'asynchronous' (**Figure 1.16**).

In the 'synchronous' (or 'strand-coupled') model of mtDNA replication, initiation of the H and L strand occurs simultaneously at O_H in response to priming by oligonucleotide Okazaki fragments, and proceeds bidirectionally (Holt *et al*., 2000). This model of replication was first proposed by Robberson *et al*. (1972) and later developed by Holt *et al*. (2000), who discovered double-stranded replication intermediates through work using two-dimensional agarose gel electrophoresis (2D-AGE). Further progress to this model was demonstrated through the discovery of long stretches of DNA/RNA hybrids, in which whilst the leading H strand replicates as usual from O_H, the lagging strand replicates as short segments of RNA which subsequently hybridise with the leading strand to form mature DNA (Yang *et al*., 2002; Holt & Reyes, 2012). This model was called the RNA incorporation throughout the lagging strand (RITOLS) model of mtDNA replication.

In contrast to the two synchronous models of mtDNA replication, the asynchronous or 'stand-displacement model' (SDM) of replication suggests that replication of the H strand occurs within the D-loop at O_H and proceeds unidirectionally in a clockwise manner. After replication has progressed around two thirds of the H strand it reaches and exposes the O_L. This exposing of the O_L then initiates replication of the L strand, which proceeds in an anti-clockwise direction, lagging behind the H strand (the leading strand) (Brown *et al*., 2005; McKinney & Oliveria, 2013). The SDM of replication

was first proposed by Kasamatsu & Vinograd (1973), who observed the arrangement of replicating stands through electron microscopy work. This model was later refined by Clayton (1982).

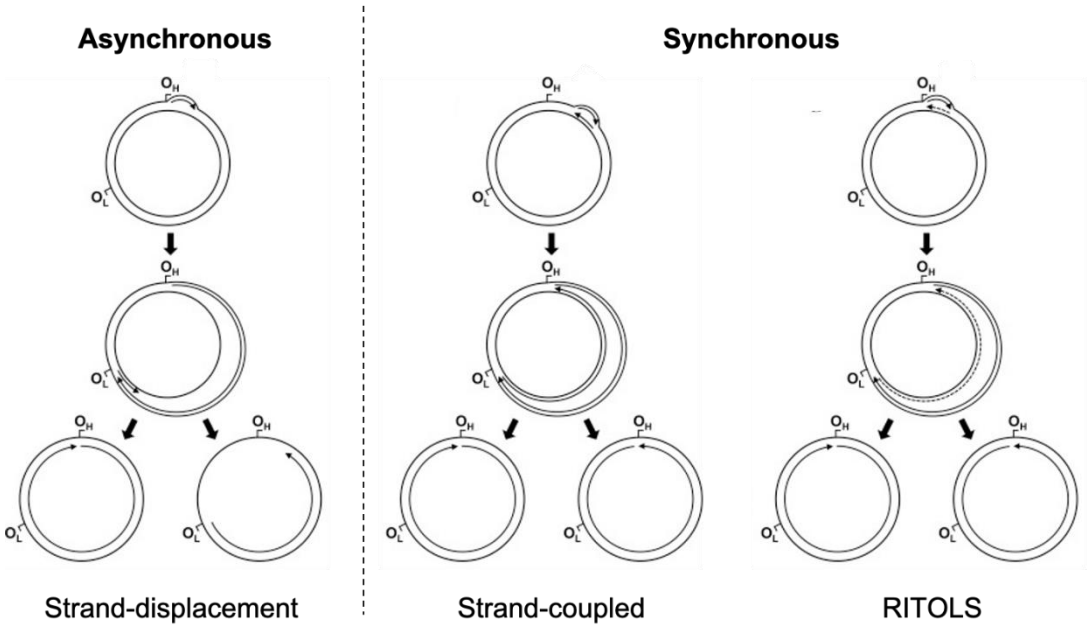

Figure 1.16 – Models of mtDNA replication*. The strand-displacement theory of mtDNA replication is an asynchronous model of replication, whilst the strand-coupled and RITOLS models propose a synchronous method of mtDNA replication. Adapted from McKinney & Oliveria (2013).*

1.4.7.3 Transcription

Transcription of mtDNA is a conserved process whereby genetic information encoded by mtDNA is copied onto messenger RNA (mRNA), which is then followed by its translation. Due to the fact that the mtDNA genome lacks non-coding introns, transcripts are generated as polycistronic mRNA that require cleavage. This cleavage occurs at the tRNA coding regions by RNA processing enzymes (MRPP1, 2 and 3), which is facilitated by folding of the mRNA (Ojala *et al*., 1981).

Transcription of both the H and L strands of mtDNA is initiated at the D-Loop of the mtDNA genome. In particular, H strand transcription is initiated at the HSP at two specific sites (HSP1 and HSP2). Here, initiation at HSP1 generates a transcript for the two mtDNA-encoded rRNAs, whilst initiation at HSP2 generates the transcript encoding the majority of the other mtDNA genes (Chang & Clayton, 1984; Zollo *et al*., 2012). Transcription of the L strand is initiated at the LSP. Importantly, transcription is a bidirectional process.

As with mtDNA replication, a range of nDNA-encoded regulatory proteins are required in order to undertake mtDNA transcription. The POLRMT is responsible for the actual transcription of mtDNA, but it cannot interact with the promoter DNA and initiate transcription without the assistance of mitochondrial transcription factor A (TFAM) and the mitochondrial transcription factor B2 (TFB2M) (Falkenberg *et al*., 2002; Barshad *et al*., 2018). Here, TFAM binds to a region 10-15bp upstream of the HSP and LSP, inducing a conformation change in the promoter region. This then allows the recruitment of POLMRT to the promoter region. Next, POLRMT binds to TFAM and then recruits TFB2M, forming the transcription competent initiation complex (Morozov *et al*., 2015) (**Figure 1.17**).

The next stage of transcription is the elongation process, before finally, the termination process. The termination stage is mediated by mitochondrial termination factor (mTERF), which induces the unwinding and base flipping of the DNA molecule by binding to the $tRNA^{leu(UUR)}$ gene (Yakubovskaya *et al*., 2010).

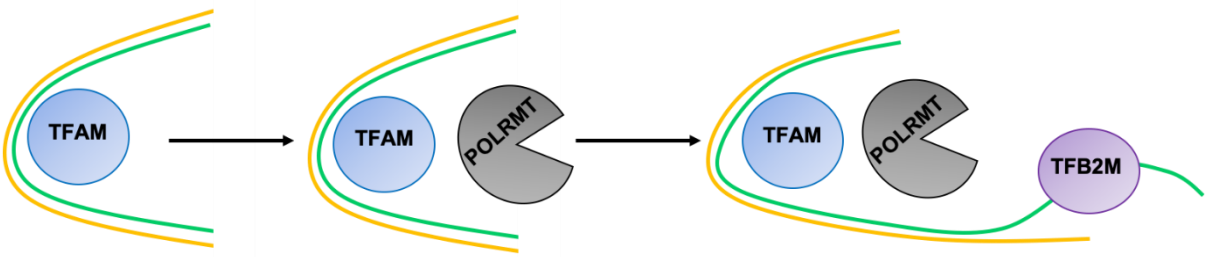

Figure 1.17 – Transcription initiation*. (1) TFAM binds to a region upstream of the HSP and LSP, (2) facilitating the binding of POLRMT and promoting its conformational change. (3) TFB2M binds to TFAM and POLRMT to form the transcription competent initiation complex.*

1.4.7.4 Translation

Translation of mitochondrial transcripts is a three-stage process that requires a range of nDNA-encoded regulatory proteins (**Figure 1.18**). The first stage of transcription is the initiation phase. Here, mt-mRNA is recruited to the mitochondrial small subunit (mtSSU) with the aid of the initiation factor 3 (IF3), which prevents the premature association with the large subunit (mtLSU) by competitively inhibiting its initiation codons (Bhargava & Spremulli, 2005). Next, initiation factor 2 (IF2) promotes the association of the P-binding site of mt-mRNA and $tRNA^{fmet}$ in a GTP-mediated fashion to form the 'mitochondrial monosome', which promotes the initiation of the elongation stage of translation (Ma & Spremulli, 1996; Kummer *et al*., 2018).

As mentioned above, the next step of mtDNA translation is the elongation stage, which requires the presence of three mitochondrial elongation factors (mtEF-Tu, mtEF-G1 and mtEF-Ts) (Di Notia *et al*., 2017). Firstly, the mt-mRNA, together with mtEF-Tu, charged mt-tRNA, and GTP, form a tertiary complex called the 'mitoribosome'. Following GTP hydrolysis, a mtEF-Tu/GDP complex is released for recycling by mtEF-T, allowing the tRNA to associate with the peptidyl (P) site of the mitoribosome, which promotes the formation of a peptide bond in the peptidyl transferase centre of mt-LSU (Cai *et al*., 2000). This results in the mitoribosome complex containing a deacetylated mt-tRNA and a de-peptidyl-tRNA at the A-site. Finally, the association of mtEF-G1 induces a conformational change in the mitoribosome that initiates the movement of the tRNA to the exit (E)-site and the di-peptidyl-tRNA to the A-site (Katunin *et al*., 2002). After rounds of cycling, the newly synthesised polypeptide is translocated into the mitochondrial matrix where it is folded via protein folding mechanisms described in **Section 1.4.4.3**.

The final stage of mtDNA translation is the termination step. Termination is initiated when the STOP codon enters the A-site of the mitoribosome, and several mitochondrial release factors (mtRFs) are associated with translation termination (Richter *et al*., 2010). Firstly, mtRF1a promotes the hydrolysis of the ester bond between the mt-tRNA at the P-site and the polypeptide chain, which is followed by the disassociation of the mitoribosome and release of mRNA and tRNA to be used in future translation. These steps are performed by the mitoribosome recycling factors mtRRF-1 and mtEF-G2 (Rorbach *et al*., 2008; Tsuboi *et al*., 2009).

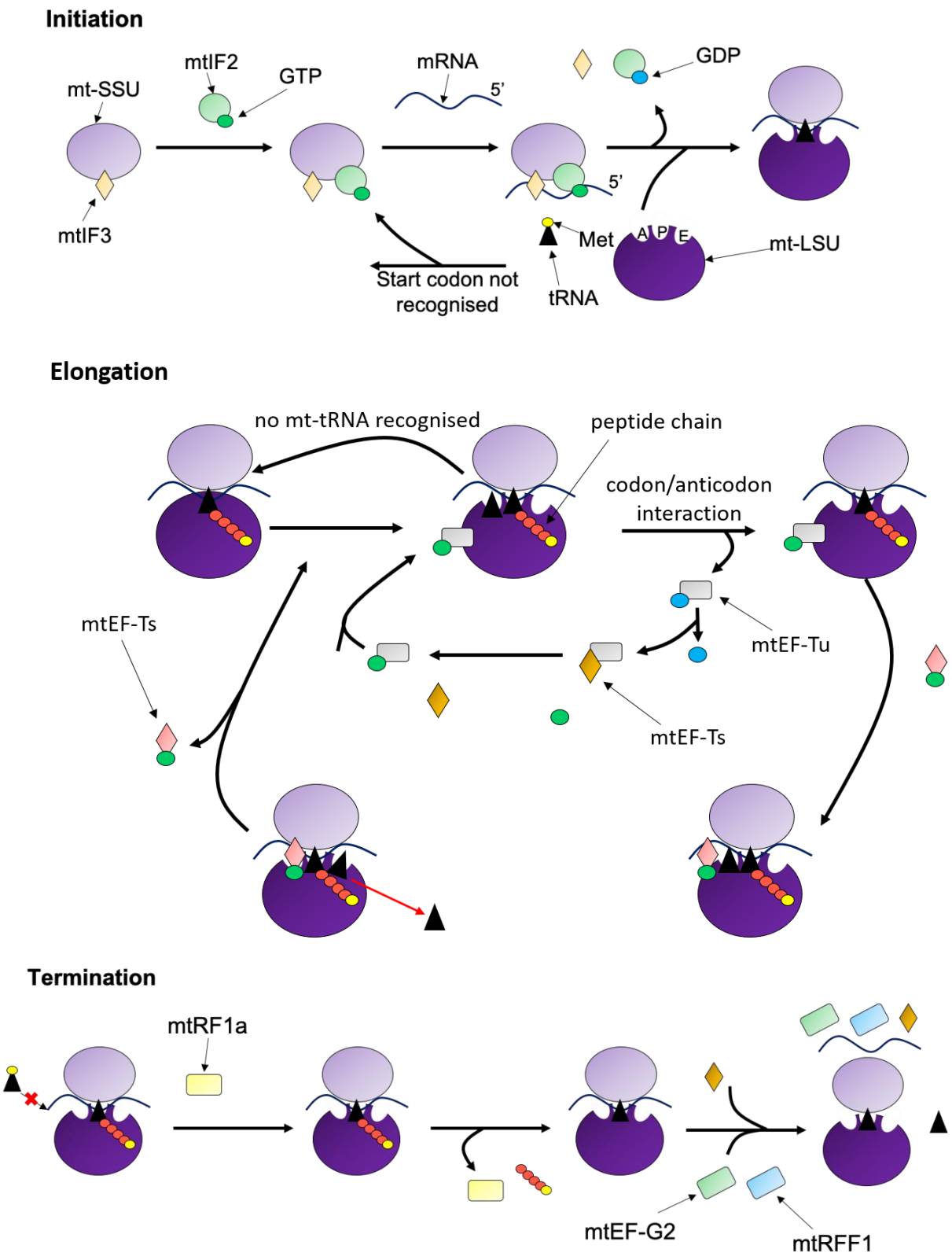

Figure 1.18 – Mitochondrial translation*. The process of mtDNA translation can be divided into the three phases of initiation, elongation and termination (with recycling). Adapted from Mia et al. (2017).*

1.4.7.5 Heteroplasmy and the threshold effect

As mtDNA exists in a highly polyploid state within cells it is possible for both wild-type and mutated mtDNA nucleoids to exist side-by-side in the same cell. This phenomenon is termed 'heteroplasmy', and if all the nucleoids in a cell are genetically identical it is said that the cell is homoplasmic.

Heteroplasmy is measured as a percentage of total mtDNA copy number and can vary greatly throughout adjacent cells of the same tissue. If the proportion of mutated mtDNA exceeds a certain threshold it can result in the phenotypic manifestation of the pathogenic mutational defect in what is known as the 'threshold effect' (Rossignol *et al*., 2003) (**Figure 1.19**). The threshold effect varies between the type of mtDNA mutation and the cell type themselves. For example, point mutations have been shown to have a threshold of around 90% heteroplasmy (Moslemi *et al*., 1999), whilst the threshold of mtDNA deletions is thought to range between 50-90% (Porteous *et al*., 1998; Sciacco *et al*., 1994). The large reported variation in threshold for deletions is thought to arise from the variation in size and location on the mtDNA genome (Rocha *et al*., 2018).

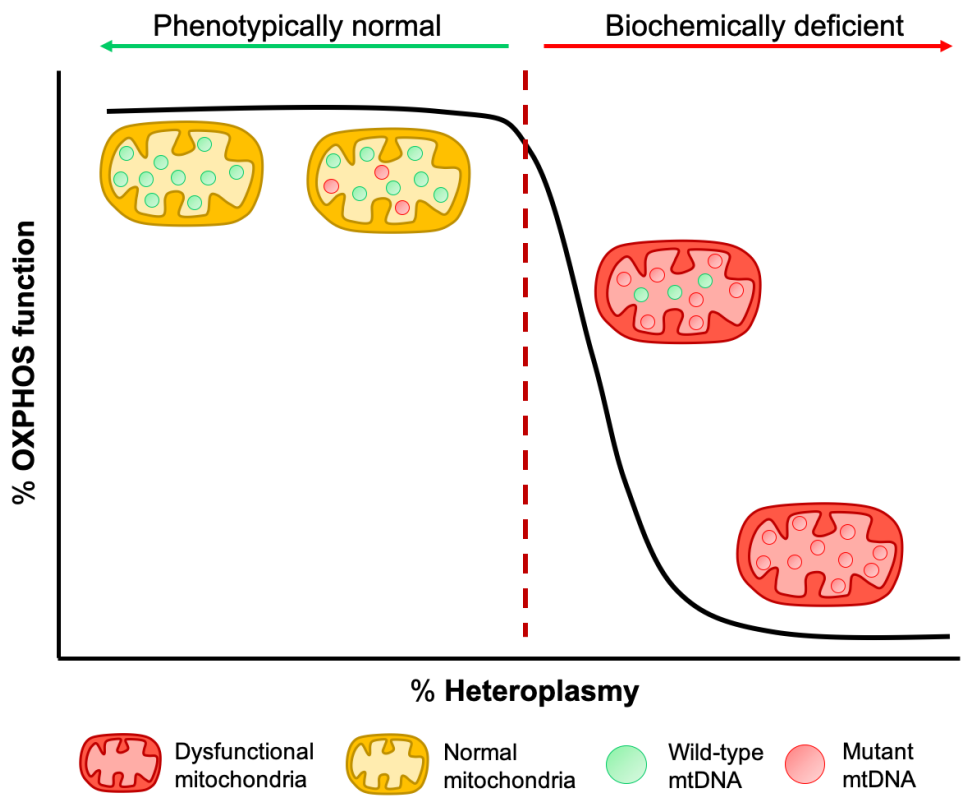

Figure 1.19 – mtDNA heteroplasmy and the threshold effect*. As heteroplasmy increases due to the increased proportion of mutant mtDNA compared to wild-type mtDNA, the function of OXPHOS (black line) decreases until a certain threshold is exceeded (red dotted line). Once exceeded, mitochondria become dysfunctional.*

1.4.7.6 Maternal inheritance and the bottleneck theory

A unique aspect of mtDNA is that it is exclusively inherited down the maternal line (Giles *et al*., 1980; Wallace, 2007). Whilst the mechanism behind this phenomenon is still not completely understood, it is thought to be the result of a combination of factors, one being that sperm contain ~1000 times less mtDNA than oocytes, in addition to the presence of a selective mechanism targeting sperm mtDNA for degradation (Sutovsky *et al*., 2000). The result of this exclusive maternal inheritance means that clinically asymptomatic women with low levels of mutated mtDNA may pass down their mutated mtDNA to their offspring. However, the proportion of mutated mtDNA variants can be highly variable between individual offspring, a phenomenon termed the 'mitochondrial bottleneck' (Howell *et al*., 2000; Taylor & Turnbull, 2005) (**Figure 1.20**). The cause of this phenomenon can be attributed to the initial reduction in compartmentalised mtDNA nucleoids followed by rapid replication of the remaining mtDNA following fertilisation (Cree *et al.,* 2008; Brown *et al*., 2001).

If the level of heteroplasmy exceeds the threshold, an individual may present with biochemical deficiency and clinical mitochondrial disease. For example, if the Leigh syndrome causing m.8993T > G mutation exceeds 30% then the child will likely present with clinical symptoms. The level of severity is increased in proportion to the level of heteroplasmy (White *et al*., 1999).

Interestingly, a recent study has questioned the theory of exclusively maternal mtDNA inheritance (Luo *et al*., 2018), although more work needs to be done in order to confirm this theory.

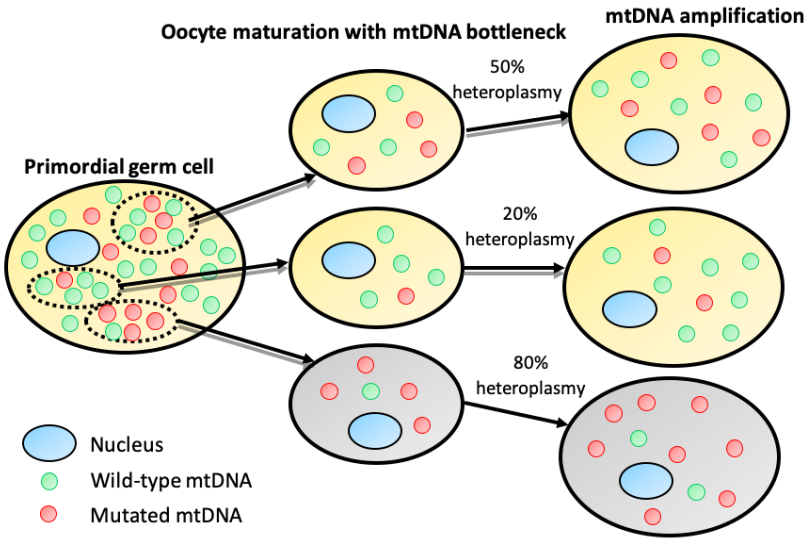

Figure 1.20 – Mitochondrial bottleneck*. Schematic depicting the inheritance of wild-type and mutated mtDNA variants and their amplification, which results in cells with varying levels of heteroplasmy.*

1.4.8 mtDNA mutations

mtDNA mutations can either be inherited or acquired throughout life as *de novo* mutations. Compared to nDNA, the mitochondrial genome is hyper-mutable, with a mutation rate roughly 10 times higher than that of nDNA (Brown *et al*., 1979). The hyper-mutable nature of mtDNA is caused by several factors. Firstly, mtDNA is damaged by high levels of ROS due to the fact that mtDNA nucleoids are localised in close proximity to the electron transport chain, where ROS is produced (Miquel *et al*., 1980). Secondly, as mtDNA is packaged as nucleoids and not as densely-packaged chromatin like nDNA, they are highly susceptible to damage from ROS and other factors. Importantly, the proof-reading exonuclease domain of the mtDNA polymerase POLG has a low fidelity, which in combination with the fact that the rate of mtDNA replication is very high, results in the increased susceptibility for mutation formation (Kunkel & Loeb, 1981; Bogenhagen & Clayton, 1977). In addition, mtDNA DNA repair machinery is not as comprehensive as that for nDNA, and so mutations are often not fully resolved (Fukui & Moraes, 2009).

The first mtDNA mutations were identified in 1989 (Holt *et al*., 1989; Wallace, 1989) and intense work in the field has since identified numerous other mtDNA mutations, with the estimated prevalence of mtDNA mutations in the North East of England being 20 for every 100,000 people (Gorman *et al*., 2015). The clinical pathology induced by mtDNA mutations, as well as the timing of onset, is extremely heterogeneous, with some mutations affecting isolated tissues and other causing multi-system pathologies (Campbell *et al*., 2014; Taylor *et al*., 2003).

1.4.8.1 Point mutations

mtDNA point mutations are a single base pair substitution. Point mutations are present in roughly 1 in 5000 of the adult population, and commonly occur in the 22 tRNA genes on the mtDNA genome (Gorman *et al*., 2015).

Point mutations are often caused by ROS-induced DNA damage, the most common of which are thymine glycol and 7,8-dihydro-8-oxo-2'-deoxyguanosine (8-oxo-dG) base lesions, of which 8-oxo-dG lesions are highly mutagenic (Bohr, 2002). For example, 8-oxo-dG lesions result in G:C to T:A transversions as a result of POLG mis-incorporating an A base opposite the oxidised G base.

The most common and well characterised mtDNA point mutations are the m.3243A>G and m.8344A>G mutations, which occur in the MT-TL1 and MT-TK tRNA genes, respectively (Gorman *et al*., 2015). There is large variability in the phenotypic spectrum caused by the m.3243A>G mutation, with 80% of patients presenting with the mitochondrial encephalopathy, lactic acidosis and stroke-like episodes (MELAS) phenotype. In contrast, some patients present with chronic progressive

external ophthalmoplegia (CPEO) or maternally-inherited diabetes and deafness (MIDD) (Nesbitt & McFarland, 2011; Nesbitt *et al*., 2013; Pickett *et al*., 2018; Urata *et al*., 2004). Similarly to the m.3242A>G mutation, the m8344A>G mutation has been reported to present as a wide range of phenotypes. First reported from patients with myoclonic epilepsy and ragged red fibres (MERRF) (Shoffner *et al*., 1989), the m.8344A>G mutation also presents as ataxia, diabetes mellitus, dementia, optic atrophy and hearing loss (Mancuso *et al*., 2013).

1.4.8.2 Single, large-scale deletions

mtDNA deletions are thought to arise sporadically during embryogenesis as the result of errors in mtDNA replication or repair of double-stranded breaks (DSBs) (Shoffner *et al*., 1989; Krishnan *et al*., 2008; Fukui & Moraes, 2009). Deletions can be characterised as either class I, II or III deletions depending on the mechanism of formation. Class I deletions have direct repeats, class II deletions have indirect repeats, whilst class III deletions have no repeats (Reeve *et al*., 2008).

Several models of mtDNA deletion formation have been proposed, the first of which assumes the asynchronous (or SDM) model of mtDNA replication. Here, during replication the L strand misaligns, resulting in the 3’ repeat annealing to the 5’ end of the H strand. This generates a single-strand loop that is susceptible to breakage and degeneration (Shoffner *et al*., 1989). Another model of deletion formation suggests that deletions are the result of DSB repair, where the homologous repeats generated from POLG exonuclease activity anneal together (Reeve *et al*., 2008, Krishnan *et al*., 2008). More recent work using mouse models has further supported the idea of deletion formation during the repair of DSBs. Here, micro-homology-mediated end joining or non-homologous end joining of DSBs resulted in class I deletions in neurons (Fukui & Moraes, 2009; Tadi *et al*., 2009; Lieber, 2010). The final model hypothesises that deletions are formed by copy-choice recombination during the mtDNA L-strand synthesis step of replication. Here, PolG can dissociate from a newly-synthesised DNA end following template H-stand replication. Next, the nascent L-stand unpairs from the DNA template and reanneals with a downstream repeat sequence. This model is attractive as it can account for class I, II and III deletions *in vitro*, as demonstrated following the recapitulation of deletions caused by nDNA-encoded maintenance genes (Persson *et al*., 2019, Nissanka *et al*., 2019).

Whilst there have been several reported mtDNA deletions of varying size, the most commonly reported deletion is the 4,977bp deletion between nucleotides 8482 and 13460. This mutation accounts for roughly 16% of adult mtDNA mutations and 12% of mitochondrial disease patients, and its prevalence has been shown to increase with age (Schon *et al*., 1989; Gorman *et al*., 2015; Williams *et al*., 2013). As with mtDNA point mutations, mtDNA deletions induce a range of clinical phenotypes. The three most common of these are Pearson syndrome, CPEO and Kearns-Sayre

syndrome (KSS) (Magner *et al*., 2015). In addition, deletions have been shown to induce non-syndromic disease symptoms such as ptosis, muscle weakness, and ophthalmoparesis (Mancuso *et al*., 2015).

In contrast to earlier reports, recent studies have demonstrated a relationship between mtDNA genotype and clinical phenotype. In addition, these factors have also been shown to be associated with the age of onset of clinical manifestation (Yamashita *et al*., 2008; Lopez-Gallardo *et al*., 2009; Grady *et al*., 2014). Interestingly, the pattern of OXPHOS biochemical deficiency was shown to be associated with the size and location of mtDNA deletion in skeletal muscle fibres (Rocha *et al*., 2018). In addition, fibres with greater levels of energy requirement harboured higher levels of mutation.

1.4.8.3 Clonal expansion of mtDNA mutations

'Clonal expansion' of mtDNA mutations is the dynamics process whereby a mutated mtDNA species accumulate in a cell and can eventually lead to onset and progression of several inherited and somatic mitochondrial diseases (Lawless *et al.,* 2020).

There are several alternative theories which explain the mechanism of clonal expansion, including 'random genetic drift' (Chinnery & Samuels, 1999; Elson *et al*., 2001), 'survival of the sickest' (de Grey, 1997; Yoneda *et al*., 1992), 'survival of the smallest' (Wallace, 1989), the 'negative feedback loop' theory (Kowald & Kirkwood, 2014; Kowald & Kirkwood, 2018) and the 'perinuclear niche' theory (Vincent *et al*., 2018) (**Figure 1.21**). Different theories appear to better explain the clonal expansion of certain forms of mtDNA mutations over the other. For example, the random genetic drift theory seems to explain the clonal expansion of point mutations, whilst not being appropriate to explain the clonal expansion of deletions.

The first theory mentioned is the random genetic drift theory. Unlike many of the other models, this theory proposes that there is no selective advantage for the replication of mutated mtDNA, and so commonly forms the null hypothesis for modelling clonal expansion. In this model, the clonal expansion and accumulation of mutated mtDNA occurs by chance due to the relaxed replication of mtDNA (Chinnery & Samuels, 1999; Elson *et al*., 2001; Kimura, 1968). This theory is supported by *in silico* models reported in Elson *et al.* (2001), which suggested that 4% of post-mitotic cells will present with biochemical COX deficiency by the age of 80 years.

The survival of the smallest theory was first proposed by Wallace (1989) and was the first theory to suggest a selection advantage for mutated mtDNA species. This theory suggests that due to the fact that mutated mtDNA species are smaller, they would be replicated quicker than wild-type mtDNA (Russell *et al*., 2018). Whilst this theory would seem to fit with the clonal expansion of deleted

mtDNA, it would not work for point mutations. Importantly, it was later demonstrated that smaller mtDNA species do not have a replication advantage in skeletal muscle fibres (Campbell *et al*., 2014).

Another alternative theory based on the selection advantage principle is the negative feedback theory. In this theory, mtDNA species which encompass deletions in genes encoding OXPHOS subunits have reduced respiratory function and subsequently reduced ROS production. As a result, replication of these species is upregulated in an attempt to compensate for biochemical reduction (de Grey, 1997; Kowald & Kirkwood, 2014). *MT-ND4, MT-ND5* and *MT-ND6* have been proposed as candidate genes in this hypothesis, as they lie on the major arc of the mtDNA genome and so are regularly deleted (Kowald & Kirkwood, 2018).

The most recent model of clonal expansion is the perinuclear niche theory proposed by Vincent *et al*. (2018). Through the investigation of how single mtDNA mutations expand over post-mitotic skeletal muscle fibres, this study demonstrated that genetic rearrangements can originate in a subsarcolemmal proliferative perinuclear niche and progressively expand. This theory suggests a selective advantage for mutated mtDNA species which results in the localised compensatory upregulation of mitochondrial biogenies. Importantly, this theory has only been examined in post-mitotic skeletal muscle tissue, and so its relevance to other tissues is unknown.

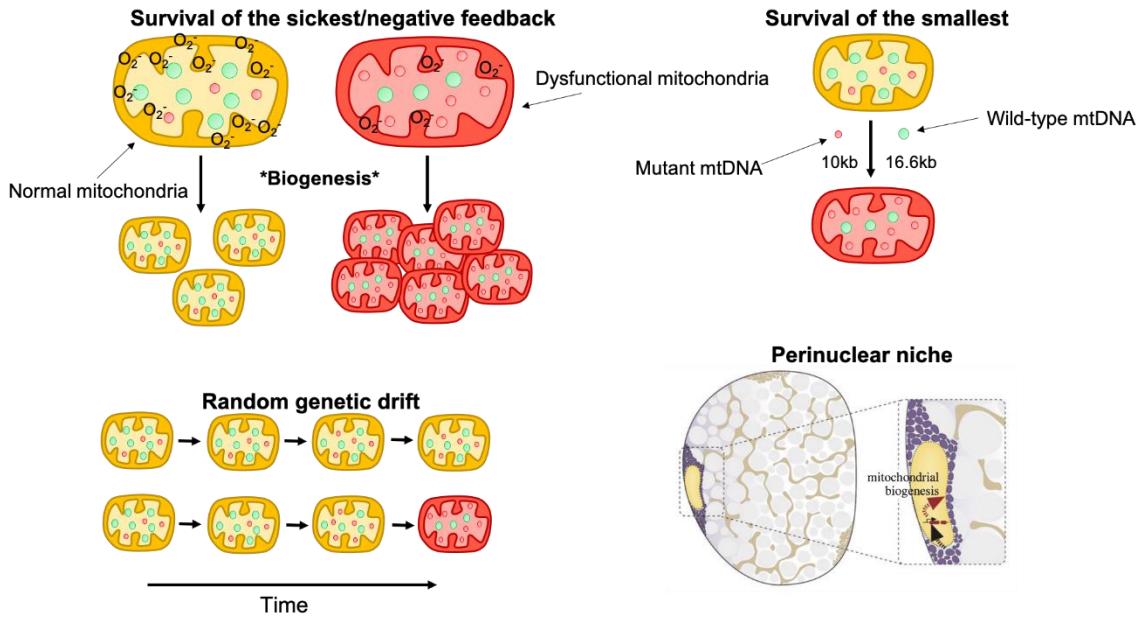

Figure 1.21 – Models of clonal expansion*. Several mechanisms have been proposed for the model of clonal expansion of mutated mtDNA species. Of these, the perinuclear niche, survival of the sickest, and survival of the smallest revolve around the idea of a selection advantage for mutated mtDNA, whilst the random genetic drift theory proposed that clonal expansion occurs by chance over a lifetime. The perinuclear niche figure was supplied by Lawless et al. (2020).*

1.4.8.4 Somatic mtDNA mutations and ageing

With support from various observational and experimental evidence, the accumulation and clonal expansion of acquired (somatic) mtDNA mutations with age has been implicated in several age-related diseases. The driving mechanism behind this pathology is widely hypothesised to be mtDNA-induced mitochondrial dysfunction (Trifunovic *et al*., 2008; Krishnan *et al*., 2007).

Aged humans present with increased levels of somatic mtDNA mutations compared to younger individuals. In contrast to germline inherited mtDNA mutations, somatic mtDNA mutations can be present in some cells but not in adjacent ones in tissues such as heart or skeletal muscle (Kang *et al*., 2016). This phenomenon subsequently presents as a mosaic pattern of respiratory chain deficiency.

In order to better understand the role of somatic mtDNA mutations in ageing, mouse models with various phenotypes have been developed and studied. In particular, the PolG mutator mouse, which carries a nDNA defect within the proofreading domain (D275A) of *PolG* and so induces increased mtDNA mutagenesis, has been extensively studied (Trifunovic *et al*., 2004; Kujoth *et al*., 2005). Due to this increased mutagenesis, the PolG mouse accumulates a high frequency of somatic mtDNA mutations during development and presents with premature ageing phenotypes such as anaemia, kyphosis, hearing loss and greying of the hair. Whilst both homozygous and heterozygous PolG mice develop mtDNA mutations, only the homozygous mouse presents with premature ageing phenotypes, suggesting that the accumulation of somatic mtDNA mutations is not solely responsible for the phenotypes. This is supported by a recent observation that increases in heteroplasmy levels of both germline and somatic mtDNA mutations was associated with the development of age-related phenotypes in the PolG mouse model (Ma *et al*., 2018).

1.5 Frailty in PLWH and the general population

Due to the virus-supressing effects of cART, PLWH are living longer. As a result, the average age and life expectancy of the roughly 36 million worldwide HIV-infected population is increasing. In addition to the fact that 20% of new seroconverts are older than 50, the mean age of PLWH is now 50 years or older, with an estimated 73% of PLWH expected to be over 50 years old by 2030 (Centers for Disease Control and Prevention, 2013; Smit *et al*., 2015). In the HIV ageing literature there has previously been a tendency to describe PLWH aged over 50 as 'old'. In the general population however, people aged over 65 years are considered 'old', whilst individuals aged 50-65 years are considered 'middle-aged'. It is now best practice to use the definitions for HIV+ individuals (Kooij *et al*., 2016). Hence, in this thesis both HIV+ and HIV- individuals between the ages of 50-65 are termed 'middle-aged', over 65 years are termed 'old', and collectively anyone over 50 years is considered 'older'.

Whilst cART has been effective in reducing the mortality rate and prevalence of HIV-associated comorbidities in PLWH, the increased age of these PLWH has resulted in an elevated burden of age-associated co-morbidities including neurodegenerative and cardiovascular diseases (Chow *et al*., 2012; Nightingale *et al*., 2014; Nou *et al*., 2016).

One of the most significant concerns arising from the rising age of the HIV-infected population is the increased prevalence of frailty (Leng & Margolick, 2015). Frailty is an age-related clinical syndrome characterised by a diminished physiological reserve alongside an increased susceptibility for comorbidities and mortality (Fried *et al*., 2001).

Frailty is known to be a multisystem condition involving the metabolic, musculoskeletal, neuroendocrine, immune, and cognitive systems (Clegg *et al*., 2013; Fried *et al*., 2001). Although the exact pathophysiological mechanisms underpinning frailty have yet to be fully elucidated, factors such as chronic inflammation (Franceschi *et al*., 2000; Roubenoff *et al*., 2003; Soysal *et al*., 2016; Leng *et al*., 2007), immunosenescence (Dihn *et al*., 2019), cell senescence (Lehman *et al*., 2018; Xu *et al*., 2018), decreased stem cell availability (Sousa-Victor *et al*., 2014; Sousa-Victor *et al*., 2016; Gonen & Toledana, 2014; Larrick & Mendelson, 2017), sarcopenia (Dodds & Sayer, 2015; Thompson & Dodds, 2020), insulin resistance (Chow *et al*., 2020; Perkisas & Vandewounde, 2016), neurocognitive decline (Puts *et al*., 2005; Boyle *et al*., 2010; Sugimoto *et al*., 2018), oxidative stress (Soysal *et al*., 2017; Vina *et al*., 2018; Liu *et al*., 2016; Namioka *et al*., 2017; Wu *et al*., 2009; Ingles *et al*., 2014; Serviddio *et al*., 2009; Ble *et al*., 2006), and mitochondrial dysfunction (Ferrucci & Zampino, 2020; Ashar *et al*., 2015; Andreux *et al*., 2018) have been implicated as causative factors (Ashar *et al*.,

2015; Andreux et *al*., 2018). In addition, declines in mitochondrial function are known to contribute to the pathogenesis and pathophysiology of each respective factor (Ferruci & Zampino, 2020).

Whilst there are several validated methods for determining frailty in the clinical setting, the most commonly used is the Fried's frailty phenotype (FFP), developed by Fried and colleagues (Fried *et al*., 2001).

1.5.1 Frieds frailty phenotype and alternative assessments of frailty

Developed and validated in 2001 using a cohort of men and woman over 65 in the Cardiovascular Health Study (CHS), the FFP is the most commonly used assessment method for characterising frailty in the clinical and research setting (Buta *et al*., 2015). FFP is based on the assumption that frailty is a clinical syndrome in which a cycle of age-related factors interplay with each other and that age-associated declines in lean body mass, balance, strength, endurance, walking performance and activity level collectively create a cycle of declining energetics and reserve (Fried *et al*., 2001) (**Figure 1.22**).

Importantly, the frailty phenotype can be used clinically to assess immune function decline and as a pre-operative evaluator for whether older individuals who undergo surgery are at risk of postoperative complications (Makary *et al*., 2010). In addition, the frailty phenotype can be used to independently predict several adverse health outcomes in older individuals such as cognitive decline, falls, disability, dependency, acute illness, and hospitalisation (Fried *et al*., 2001).

By using a set of five pre-defined criteria: self-reported weight loss, self-reported physical exhaustion, self-reported inactivity, slow gait speed and poor handgrip strength – the FFP can define individuals as frail, pre-frail or robust (non-frail) (**Table 1.1**).

FFP category	Eligibility
Robust	0 criteria
Pre-frail	1-2 criteria
Frail	3-5 criteria

Table 1.1 – Fried's frailty phenotype diagnostic scoring criteria.

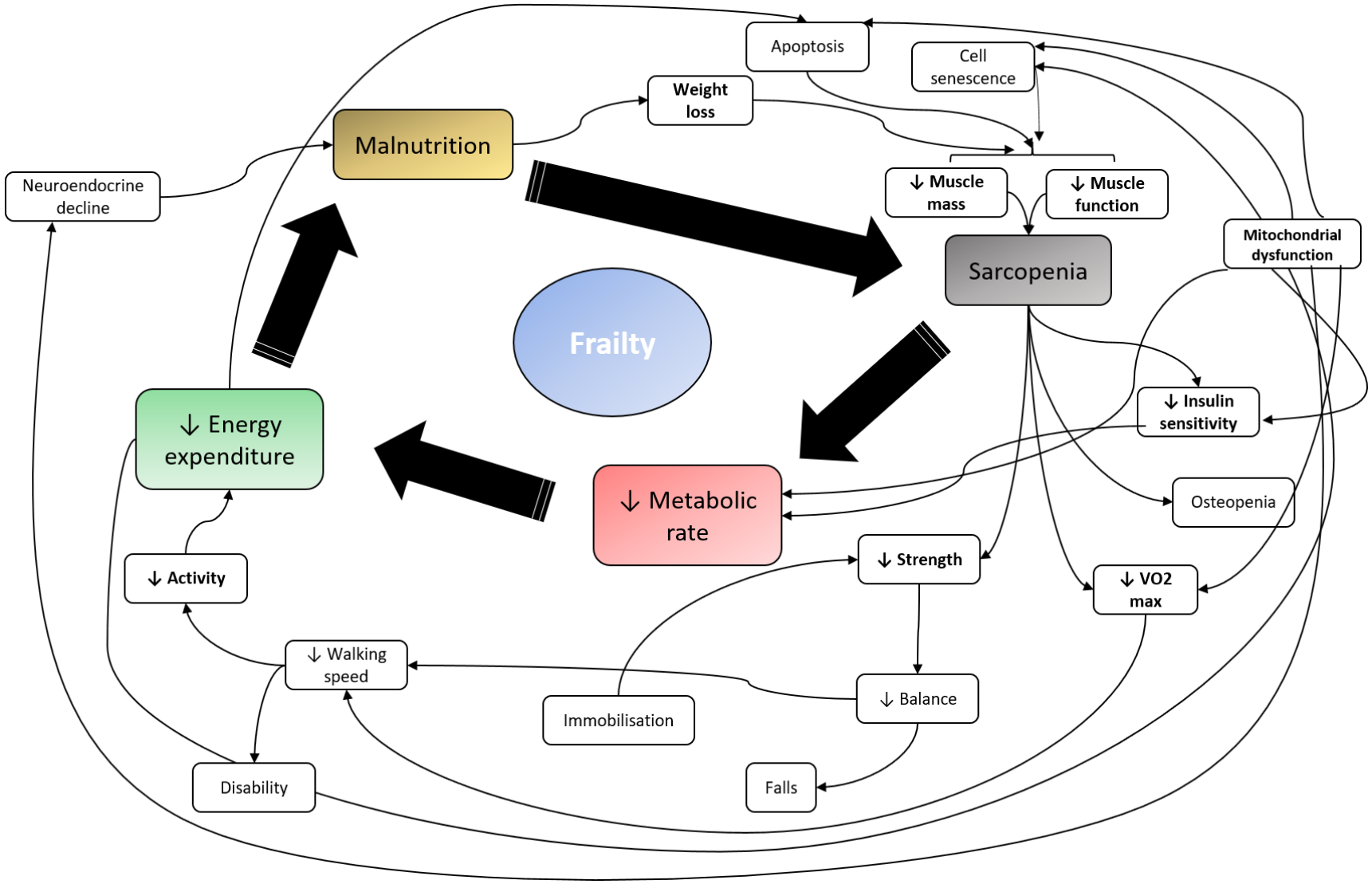

Figure 1.22 – Proposed cycle of frailty dynamics. *Adapted from Fried* et al. *(2001).*

The clinical validity of the prefrail category is not universally recognised, although a recent study demonstrated a reduction in oxidative capacity as well as protein levels of ETC complexes in skeletal muscle from prefrail individuals (defined through a modified three criteria FFP score) compared to age-matched individuals who had been classified as 'active' according to metabolic expenditure (MET) score, gait speed, skeletal muscle mass, and skeletal muscle strength results. These indicators of mitochondrial dysfunction at the cellular level were corroborated by the fact that gene sets related to mitochondrial function were also significantly downregulated in the old (> 61 years) prefrail individuals compared to 'active' individuals (Andreux *et al*., 2018). The fact that roughly half of the elderly population displays early signs of muscle decline indicates that the inclusion of the prefrail category is important for detecting potentially subtle differences between prefrail and frail individuals, which could aid in improving understanding of the pathogenesis of frailty and optimal opportunities for the potential intervention (Fernandez-Garrido *et al*., 2014).

The second most commonly used measure of frailty is the cumulative deficit model, or frailty index (FI). Based on the idea that frailty is an at-risk state caused by the age-related accumulation of deficits (Mitnitski *et al*., 2001), a frailty index can be developed from existing health data, as well as from information derived from a comprehensive geriatric assessment (FI-CGA) (Searle *et al*., 2008; Jones *et al*., 2004; Jones *et al*., 2005; Rockwood *et al*, 2010). Each deficit is translated into a binary tally and then expressed as the ratio of deficits considered, thus allowing for consistency across different studies (Rockwood & Mitnitski, 2011). The hypothesis behind the FI is that frailty is a multi-factorial state in which the quantity of deficits is more informative than the quality of deficits an individual has accumulated over the course of their adult life. Both the FI and FFP have been associated with the increased risk of an individual developing age-related comorbidities, albeit through alternate pathophysiological mechanisms (Clegg *et al*., 2013). An advantage of FI over the FFP is that the rate of deficit accumulation can be calculated and used to give an estimation of how quickly frailty will progress in an individual. Whilst the FI and FFP propose different pathophysiological mechanisms for frailty, both measurements appear to similarly predict frailty outcomes. Here, the convergent validity between outcome measures of both the FFP and FI were tested through both parametric and non-parametric correlation analyses (as described in Rockwood *et al*., 2007), and determined to be 0.65 in a study which utilised both. This indicates that there is considerable, but not complete, convergency between the assessments (Rockwood *et al*., 2007).

Aside from the FFP and FI, there are other alternative validated methods for measuring frailty. Briefly, these include the Study of Osteoporotic Fracture (SOF) Index, which assesses frailty using three characteristics in which only two need to be met for an individual to be classified as frail

(Ensrud *et al*., 2007); Edmonton Frailty Scale (EFS), which is commonly used in the hospital setting (Rolfson *et al*., 2006); Clinical Frailty Scale (CFS) which scores frailty on a scale of 1-7 based on clinical judgement of known markers of frailty (Rockwood *et* al., 2005a), and PRISMA-7, which is composed of seven self-reported characteristics (Raiche *et al*., 2008).

Importantly, in response to the development of various frailty assessments, a consensus between leading international frailty delegates agreed that criteria for successfully defining frailty includes having content validity (i.e. has multiple determinants and can be applied to numerous situations), criterion validity (i.e. can predict adverse outcomes), and construct validity (i.e. consistently predicts frailty in certain setting, such as in woman and in advanced age) (Rockwood *et al*., 2005b; Morley *et al*., 2013)

The geriatric field is currently looking to move towards more specific instruments and methods for assessing frailty in specific populations and settings. Two examples are the electronic Frailty Index (eFI) and the Hospital Frailty Risk Score (HFRS). These two methods of assessment can measure frailty through deficits solely using electronic heath records, and have both been validated to predict adverse health outcomes (Clegg *et al*., 2016; Ambagtsheer *et al*., 2019; Gilbert *et al*., 2018).

Although these different measurements of frailty are based on alternative pathophysiological hypotheses of frailty, there is a consensus that individuals with an increased accumulation of deficits are more vulnerable and so likely to be frail. There is also a consistency in the relationship between frailty and age, as well as frailty and female gender, within each alternative form of frailty measurement (Theou *et al.,* 2013).

1.5.2 Frailty in the general population

In the general population the process of ageing and complications which arise from adverse ageing are highly heterogeneous, with individuals of the same age experiencing vastly different health levels. As such, frailty was introduced as a universal term to describe this variability. Frailty is associated with age in the HIV-uninfected population (Althoff *et al.,* 2014; Hoogendijk *et al*., 2018), although the severity of frailty can be modified over time (Womack *et al*., 2013). In addition, the presence of frailty (as determined through the original FFP assessment) predicts outcomes such as falls, comorbidity, loss of independence and mortality in the general population (Fried *et al*., 2001; Fairhall *et al*., 2014; Li *et al*., 2014; Barbosa *et al*., 2017).

Due to the variability in study populations and methods of assessment, accurate figures on the epidemiology of frailty in the general population have proven difficult. A systematic review by Collard and colleagues pooled together results from over 61,000 community-dwelling residents of high-income countries aged 65 and over and assessed frailty using the FFP method. They demonstrated the weighted prevalence of frailty to be 11%, although there was vast variation in the prevalence of frailty between the different studies (4-59%) (Collard *et al*., 2012). A more recent systematic review and meta-analysis using data from more than 120,000 older individuals demonstrated that the incidence of frailty (as measured by various assessment criteria) was 43.4 new cases every 1000 person-years, and the incidence of prefrailty was 150.6 new cases every 1000 person-years (Ofori-Asenso *et al*., 2019). Other systematic reviews have demonstrated that the prevalence of frailty, as determined by the original FFP, among long-term care residents is 53% (Kojima, 2015), 37% in individuals with end-stage renal disease (Kojima, 2017), and 42% in patients with haematological malignancies, although in this study frailty was determined by a variety of validated methods (Handforth *et al.,* 2015).

There is still debate regarding the best method for assessing frailty in the clinical and hospital setting, mostly due to the large heterogeneity in pathogenesis and presentation of frailty in different individuals. Notably, a survey of 62 geriatricians conducted by Fried and Watson reported the characteristics that represent frailty. These included: malnourishment, functional dependence, pressure sores, prolonged bed rest, gait abnormalities, general muscle weakness, weight loss, being over 90 years old, fear of falling, anorexia, dementia, hip fractures, delirium, polypharmacy, and confusion (Fried & Watson, 1998).

Due to the large heterogeneity of frailty and lack of consensus that still exists, frailty is often used as an umbrella term for a syndrome that contains a vast array of symptoms, including loss of reserve and disability. Disability is related to frailty but is a distinct condition. A disability is defined as the

loss of functional ability and capacity to carry out tasks as an individual (Yoo *et al*., 2018). Disabilities may inversely affect an individual's quality of life (QOL) and cause an increased burden on health services, with QOL being inversely associated with frailty in community-dwelling adults (Kojima *et al*., 2016, Crocker *et al*., 2019). According to the WHO, 15% of people worldwide live with disabilities (United Nations, 2015), and up until 1996, the prevalence of disability among community-dwelling individuals above 70 years old was between 20-30%, and this number was forecast to keep increasing (Adams *et al.,* 1995). A more recent estimation put the prevalence of disability in this population at 66% (Virues-Ortega *et al*., 2011). As mentioned above, disabilities and frailty are distinct entities but can frequently coexist. Several studies have demonstrated that five criteria frailty phenotype characterised community-dwelling frail or prefrail individuals are more likely to develop disability (Makizako *et al*., 2015; Aguilar-Navarro *et al*., 2015).

An analysis of the SHARE study, which included data from more than 35,000 individuals over 50 years old, demonstrated that frailty, as measured by the FI, was lower in high-income countries compared to low-income countries. In addition, the mean FI score was inversely correlated with gross domestic product and health expenditure (Theou *et al*., 2013). Another study investigating the association of frailty with racial differences demonstrated that African-American men and woman had an adjusted higher prevalence of frailty compared to Caucasian men and women, and that African-American men were four times as likely to develop frailty compared to Caucasian men (Hirsch *et al*., 2006).

As the average age of the general population increases so too does the prevalence of frailty (defined by any validated assessment), and this increased prevalence is expected to pose significant problems with care of the elderly (Rodrigues-Laso *et al*., 2018). Indeed, data from various studies have indicated a pattern of increased healthcare costs in several sectors where there is an increased prevalence of frailty (Ensrud *et al*., 2018; Kim *et al*., 2019). Contextualising this issue, studies using the original FFP assessment of frailty have shown that greater than 60% of frail individuals are admitted to hospital within 3 years, placing strain on healthcare services (Fried *et al*., 2001; Chang *et al*., 2018). Importantly, as of 2017 England's National Health Service general practice contract states that identification of frailty is now a requirement (National Health Service England, 2017).

1.5.3 Progression to frailty

Frailty is a dynamic state in which individuals can progress through the different stages of robust, prefrail, and frail in both directions (Trevisan *et al*., 2017). There have been three distinct stages identified in the developmental process of frailty, starting from robustness and progressing to prefrailty, where reductions in physiological reserve lead to slight decreases in an individual's

capacity to respond to stressors and injury. Notably, exhaustion tends to be the first physical component of the FFP assessment that manifests in individuals developing frailty (Stenholm *et al*., 2019). The individual will then progress from prefrailty to frailty, where physiological reserves have fallen below the functional threshold and the individual can therefore no longer fully respond to stressors and/or injury, resulting in impaired or incomplete recovery (Lang *et al*., 2009). Finally, the individual will progress from frailty to the frail complications stage, where dramatic functional declines lead to disabilities, chronic and acute infections, as well as polypharmacy, increased hospitalisation, and mortality (Rodrigues-Laso *et al*., 2019; Ahmed *et al*., 2007) (**Figure 1.23**).

Longitudinal studies have suggested that frailty is reversible up to the frailty complications stage, where physiological reserves are exhausted. Indeed, up to 37% of individuals enrolled in longitudinal studies experience at least one transition between frailty states within 1-5 years of follow-up. This indicates the importance in developing a better understanding of intervention strategies aiming to slow or reverse the progression of frailty (Gill *et al*., 2006; Trevisan *et al*., 2017; Pollack *et al*., 2017).

The Survey of Health, Aging and Retirement in Europe (SHARE) study assessed the frailty status using the original FFP criteria, as well as several other factors of over 85,000 individuals aged 65 or older. It revealed that while 8.8% of the study population were classified as frail, 39.1% were prefrail. A two-year follow-up showed that without any intervention, 22.1% worsened, 61.8% did not change status and 16.6% improved their frailty status (Etman *et al*., 2012).

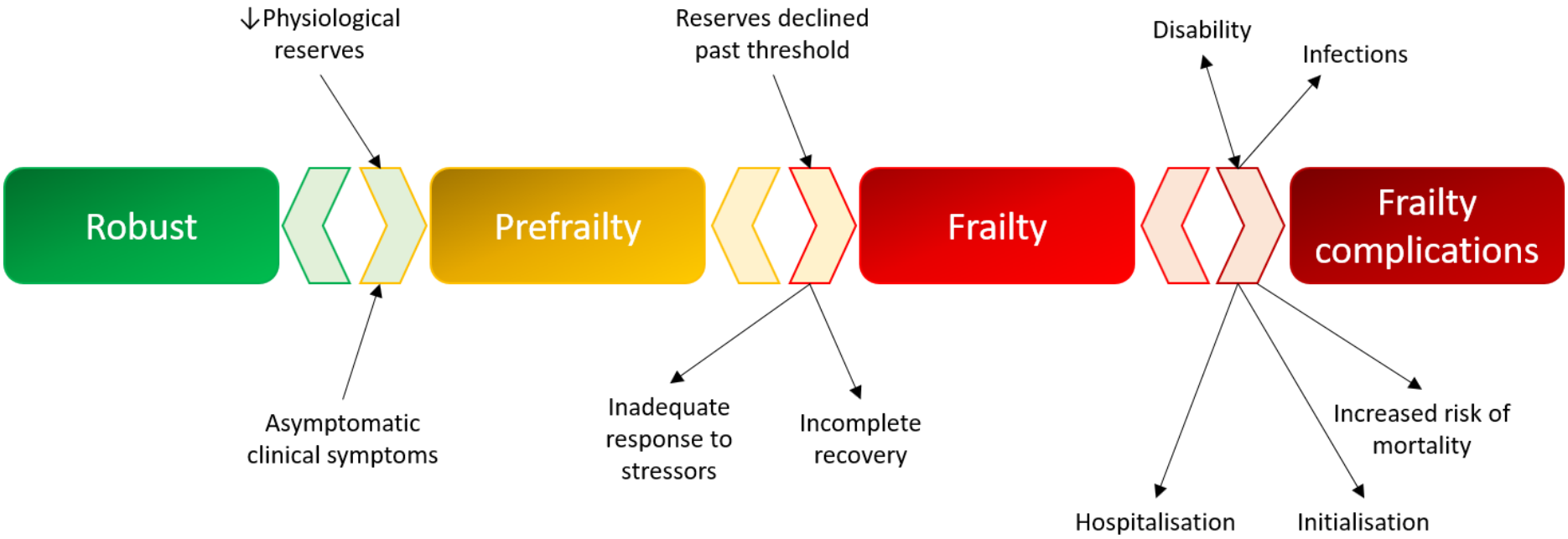

Figure 1.23 – Dynamics of the frailty syndrome

1.5.4 Risk factors of frailty

Over the past couple of decades studies have demonstrated a variety of risk factors directly implicated in the development and progression of frailty in the general population. These include old age, malnutrition, physical inactivity, cognitive decline, social isolation and being female (Fried *et al*., 2001; Nosraty *et al*., 2012; Luger *et al*., 2016; Feng *et al*., 2017; Martone *et al*., 2013) (**Figure 1.24**).

Of the risk factors noted above, physical inactivity appears to play one of the most significant roles. Physical inactivity can lead to loss of muscle mass and function, termed sarcopenia (Cruz-Jentoft *et al*., 2019). Sarcopenia will yield a reduced metabolic rate, a slower gait speed and reduced grip strength (Bortz, 2002; Walston, 2012; Cruz-Jentoft *et al*., 2019). Notably, these two factors are two of the five factors used in the FFP method of frailty assessment, indicating the significant role physical inactivity plays in the development of frailty (Fried *et* al., 2001). In support of this, a recent cohort study demonstrated an increased prevalence of frailty (as determined by a modified FFP criteria) in 60+ year old individuals with low physical activity levels and excessive time spent in a sitting position (da Silva *et al*., 2019). Highlighting the heterogeneic and multisystem nature of frailty, previous studies have suggested that comorbidities and injury can contribute to the development of frailty through the forced inhibition of physical activity (Blaum *et al.,* 2005).

Malnourishment has a similar contribution to the progression of frailty as does physical inactivity, and the two factors can often be interlinked, as hypothesised in the Fried definition of frailty (Fried *et al*., 2001). Nutritional deficiencies, particularly in protein and vitamin D and C intake, will result in unintentional weight loss and declines in bone mineral density (BMD), leading to an increased susceptibility to developing injuries (Fried *et al*., 2001; Lorenzo-Lopez *et al*., 2017). In support of this, it was shown that individuals with a low daily energy intake (< 21kcal/kg) have a 24% increased risk of developing frailty, as defined by the original FFP (Bartali *et al*., 2006). Additionally, low calorie intake will adversely impact an individual's energy producing capabilities, and therefore impact the individual's ability to perform daily tasks (Volkert *et al*., 2019; Landi *et al*., 2016; Martone *et al*., 2013). On the flip side, malnourishment in the form of excessive intake can lead to obesity, and obesity and excessive energy intake has been shown to significantly contribute to the pathogenesis of frailty (Volkert *et* al., 2019; Blaum *et al*., 2005), in particular, inter- and intra-muscular fat infiltration as a result of obesity is known to decrease muscle quality (Delmonico *et al*., 2009). Interestingly, a recent study has shown that the Mediterranean diet is linked to a decreased prevalence of frailty, defined by the frailty index (Kojima *et al*., 2018).

Multimorbidity is a known risk factor for frailty, and the prevalence of comorbid conditions is greater in frail individuals, defined through various frailty measurements, when compared to the normal

population (Vertano *et al*., 2019). A recent meta-analysis which included over 14,000 community-dwelling older individuals enrolled over nine studies demonstrated that 18% of individuals with multimorbidity (defined as having two or more comorbid diseases) were frail (regardless of frailty assessment) (Vertano *et al*., 2019), and this was further supported by a large UK study using a modified FFP assessment in 37-73 year olds which demonstrated that frailty was associated with multimorbidity (Hanlon *et al*., 2018). Importantly, the National Institute for Health and Care Excellence (NICE) in England now advise that the identification of frailty should be attempted in all encounters with elderly patients with multimorbidity (National Institute for Health and Care Excellence, 2016).

Another factor contributing to the pathogenesis of frailty is cognitive decline. Declines in cognitive function are often attributed to age-related diseases such as Alzheimer's Disease or other forms of dementia, as they can significantly impact an individual's ability to perform daily activities. In addition, cognitive decline can enhance physical function declines (Klein *et al*., 2005; Panza *et* al., 2018).

Social isolation is more prevalent in frail individuals compared to the general population (Gale *et al*., 2018). Consequently, social isolation can lead to a reduction in physical activity as well as weight loss (Schrempft *et al*., 2019). Together, these factors lead to a reduction in QOL and are directly associated with increased morbidity levels.

As mentioned previously, frailty, as defined by five criteria assessments, is more prevalent in females compared to age-matched males (Fried *et* al., 2001; Collard *et al*., 2012). Although not completely understood, this increased prevalence of frailty in females is suspected to be due to lower lean body mass and muscle function compared to males.

As mentioned above, the NICE now advise that frailty should be assessed in older individuals with the risk factor of multimorbidity (National Institute for Health and Care Excellence, 2016). Indeed, a recent report from the British Geriatrics Society has recommended that all older people who encounter health and social care should be assessed for frailty (through the PRISMA-7 questionnaire and assessments of gait speed and timed-up-and-go). As frailty is often not recognised in an older individual until they experience an adverse outcome such as a fall or delirium, the importance of better understanding the risk factors underpinning the pathogenesis of frailty are significant (Morely *et al*., 2013). Identifying frailty earlier through well-designed integrated pathways such as the Comprehensive Geriatric Assessment may therefore reduce the burden of frailty-related hospitalisations (British Geriatric Society, 2017). Indeed, the NHS is the first health system to

systematically identify individuals ≥65 years using a population-based stratification approach – the electronic Frailty Index (NHS, 2020).

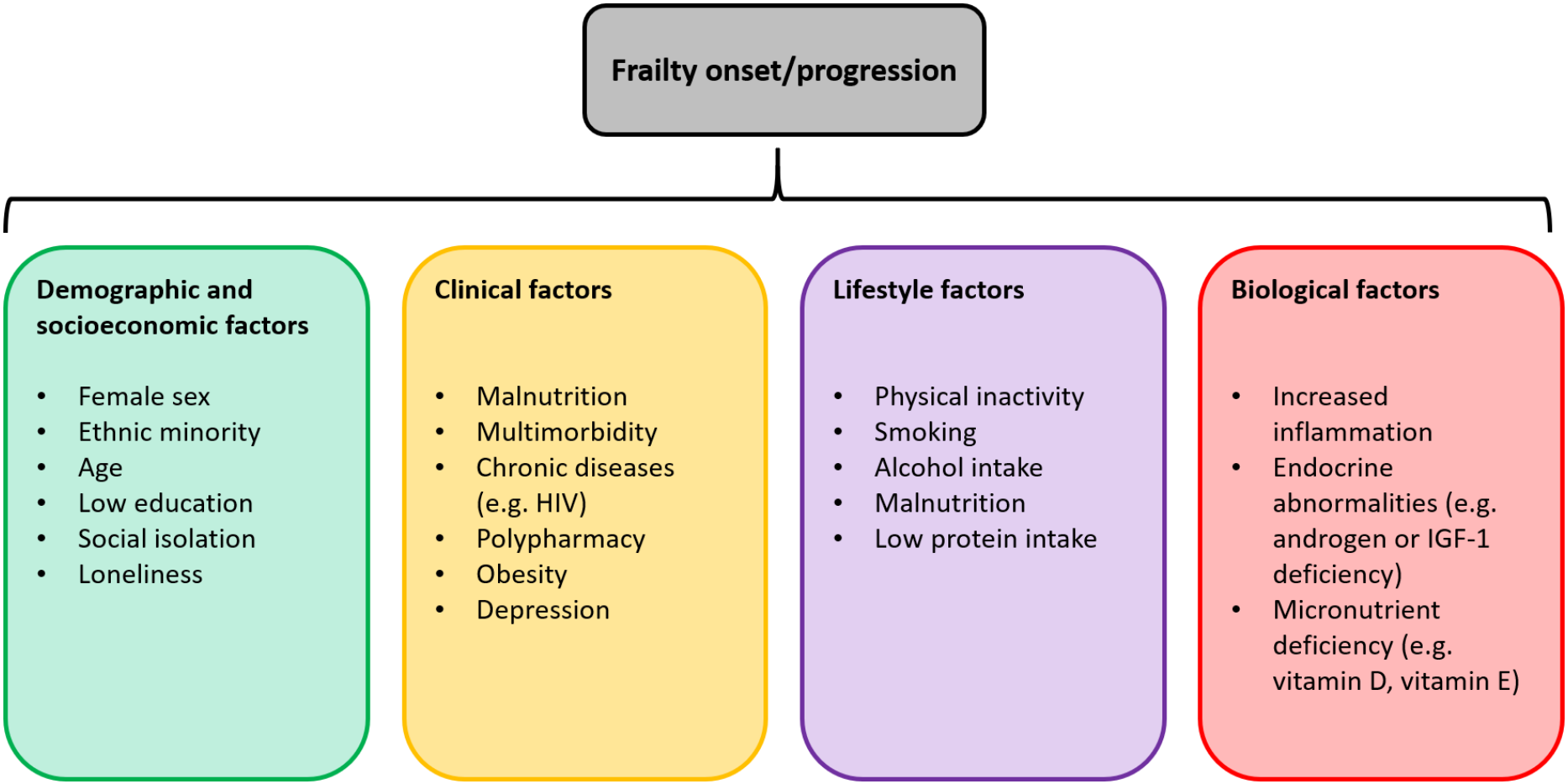

Figure 1.24 – Risk factors associated with the onset and progression of frailty

1.5.5 Pathophysiology of frailty

Frailty is known as a multisystem disorder (Fried *et al*., 2001; Thillainadesan *et al*., 2020; Dent *et al*., 2019; Fried *et al*., 2009), with involvements in the musculoskeletal system (Fried *et al*., 2001), neuroendocrine system (Clegg & Smith, 2018), inflammatory system (Kane *et al*., 2019), and haematological system (Alvarez-Rios *et al*., 2015), in which there is a nonlinear association between the number of abnormally functioning systems and frailty, as well as the number of comorbid diseases and frailty (Fried *et al*., 2009) (**Figure 1.25**). As such, increasing focus has been given to proposed subtypes of frailty, such as cognitive frailty, social frailty, and nutritional frailty (Panza *et al*., 2015).

1.5.5.1 Potential role of mitochondrial dysfunction in the pathophysiology of frailty

Although not confirmed, it is heavily suspected that dysregulated energetics may significantly underpin the pathogenesis and pathophysiology of frailty (Fried *et al*., 2001). It is well known that mitochondrial function and content declines with age, manifesting clinically as a reduction in OXPHOS and energy producing capacities (Short *et* al., 2005; Chistiakov *et al*. 2014). This reduction in energy production with age subsequently adversely affects the function of high energy-demanding tissues such as skeletal muscle and the brain, as discussed later. In support of this, it was recently demonstrated that frail animal models have a reduced mitochondrial content as well as increased lactate levels and abnormal cristae (Sayed *et* al., 2018). Further, mitochondrial function is also heavily implicated in the pathophysiology of frailty by affecting individual aspects of the frailty syndrome. For example, declining skeletal muscle oxidative capacity (as measured by phosphorus magnetic resonance spectroscopy, ^{31}P-MRS) is significantly associated with lower gait speed (Choi *et al*., 2016). Using novel immunofluorescence assays and ^{31}P-MRS to investigate OXPHOS complex activity was hence utilised in this study to investigate skeletal muscle oxidative capacity in ageing PLWH.

Aside from decreases in energy producing capacity, age-related mitochondrial dysfunction has several other adverse pathophysiological implications which can increase the risk of developing frailty. Briefly, these include: the dysregulation of redox signalling and an increase in ROS and therefore oxidative stress, which can damage important molecules such as DNA (Wu *et al*., 2009; Peterson *et al*., 2012). In support of this, studies have demonstrated elevated levels of circulating oxidative markers such as serum 8-hydroxy-2'-deoxyguanosine (8-OHdG) (Serviddio *et al*., 2009); inducing an increase in the release of inflammatory markers (Coen *et al*., 2013) and activation of the NLR family pyrin domain containing 3 (NLRP3) inflammasome, which both subsequently lead to inflammation in various tissues (Sayed *et al*., 2018; Volt *et al*., 2016); impairing calcium regulation,

which contributes to dysfunctional neurological system (Powers *et al*., 2011); and altering myofilament structure and function, which can progressively lead to declines in muscle quality and strength (Powers *et al*., 2011). In addition, several studies have implicated a role of mitochondrial genetics in frailty. For example, mtDNA copy number has been shown to be associated with frailty syndrome severity (Ashar *et al*., 2015), and there is evidence of mitochondrial haplogroup variation causing increased susceptibility to developing frailty (Moore *et al*., 2010).

1.5.5.2 Musculoskeletal and neuroendocrine decline in frailty pathophysiology

Several studies have demonstrated the significance of the musculoskeletal system in the onset and development of frailty. On average, sarcopenia begins in individuals around 40 years old and can lead to a 30-50% reduction in muscle mass and function by age 80 (Bortz, 2002; Cruz-Jentoft *et al*., 2019). Sarcopenia ultimately impairs strength and endurance and can adversely affect balance and gait, leaving the individual more susceptible to developing comorbidities and a reduction in QOL (Cruz-Jentoft *et al*., 2019). The pathogenesis and pathophysiology of sarcopenia is explained in more detail in **Section 1.6.4**. With regard to the multisystem nature of the pathophysiology of frailty, both hormonal deficiency and cytokine excess are involved in the pathogenesis of frailty (Morely *et al*., 2005; Fabbri *et al*., 2015; Swiecicka *et al*., 2018; Hanlon *et al*., 2018; Soysal *et al*., 2016), and both insulin resistance (IR) and diabetes are associated with excessive loss of lean body mass and muscle strength (Park *et al*., 2009), hence why I investigated body composition and intramyocellular lipid accumulation in this study. Furthermore, loss of lower leg muscle mass and strength is associated with elevated inflammation (Guralnik *et al*., 1994).

With regards to the impact of neuroendocrine decline in frailty, hormonal abnormalities, IR and increased level of inflammatory markers have been shown to contribute to the progression of frailty, irrespective of frailty assessment (Cappola *et al*., 2003; Swiecicka *et* al., 2018; Perez-Tasigchana *et al*., 2017; Ruan *et al*., 2017; Clegg *et al*., 2018). Underscoring the multisystem aspect of frailty, hormonal declines that result in an imbalance between catabolic and anabolic processes can adversely impact muscle mass and function and thus lead to sarcopenia (Bortz, 2002; Morley *et* al., 2013). The main driver of neuroendocrine decline in frail individuals has been attributed to impaired function of the hypothalamic-pituitary-gonadal/adrenal and growth hormone axis, which ultimately presents as declines in circulating oestrogen and androgen levels (Swiecicka *et al*., 2018). Declines in oestrogen and androgen levels subsequently increase the release of bone cytoclastic cytokines, which in turn lead to a reduction in BMD (Bortz, 2002). As mentioned above, a contributing factor to neuroendocrine decline in frail individuals is insulin resistance. It has been demonstrated that IR, as measured by the insulin resistance-homeostatic model assessment (IR-HOMA), is associated with

frailty prevalence frailty in women and men (determined by five criteria FFP) (Blaum *et al*., 2005) and a four times increased incidence of frailty (determined by five criteria FFP) (Kalyani *et al*., 2012).

1.5.5.3 Immunosenescence and inflammation in frailty pathophysiology

Ageing of the immune system eventually leads to a chronic low-grade systemic inflammatory state termed 'Inflamm-Aging', which is characterised by elevated levels of inflammatory molecules and an increased susceptibility to morbidity and mortality (De Martins *et al*., 2006; Piggott *et al*., 2015). Numerous studies have also demonstrated the elevated levels of inflammatory markers such as cortisol, interleukin-6 (IL-6), C reactive protein (CRP) and TNF-α, as well as declines in IGF-1, testosterone and growth hormone concentrations in frail individuals compared to the general population (Abbatecola & Paolisso, 2008; Soysal *et al*., 2016; Walston *et al*., 2002; Hubbard *et al*., 2009). As such, frailty is commonly recognised as a chronic inflammatory state (Vina *et al.,* 2016). One aspect of the adverse pathophysiological effects of inflammation is the specific impact on muscle strength, as studies have demonstrated an association between increased TNF-α levels and declines in muscle strength and mass over a 5-year period, as well as mortality (Bruunsgaard *et al.,* 2003). This is in part due to the TNF-α induced upregulation of NF-κB-dependant muscle catabolism and necrosis processes, which leads to a downregulation in regenerative processes (Concepcion-Huertas *et al*., 2013; Li *et al*., 2008). In addition, studies in both mice and humans have demonstrated the significant association between increased IL-6 levels with muscle atrophy and frailty (Baltgalvis *et al*., 2008; Ma *et al*., 2018; Marcos-Perez *et al*., 2018). There is also an indirect association between frailty and inflammation, as frailty determined by five criteria FFP in the Woman's Health and Aging studies is associated with an increasing number of inflammatory diseases (Chang *et al*., 2012). Interestingly, the degree to which inflammation contributes to the pathophysiology of frailty appears to be more significant in women compared to men. For example, higher baseline concentrations of CRP and fibrinogen were independently associated with frailty in woman but not men (Gale *et al*., 2013). In addition, elevated CRP levels were shown to be negatively associated with cognitive and skeletal muscle performance in women but not men (Canon & Crimmins, 2011).

Elevated inflammation may also be a consequence of diet. With regards to this, a recent study investigated the role of higher dietary inflammatory index (DII) in frailty and found that both male and female subjects (mean age 63) with a high DII score had an 37% increased risk of frailty, defined by SOF index (Shivappa *et al*., 2018). In support of the significant role which inflammation plays into the pathophysiology of frailty, molecular evidence from monocytes derived from frail individuals demonstrated an upregulation in the *ex vivo* expression of inflammatory pathways (Jia *et al*., 2001).

To compound the damaging effects of inflammation and ageing, with time, more cells develop the secretory phenotype associated with senescence (SASP). These cells are senescent and excrete additional inflammatory markers such as IL-1 and IL-6 (Coppe *et al*., 2008). Age-related immune system alterations which contribute to Inflamm-Aging are known to accelerate the loss of muscle mass and strength, as well as decreasing physical function capabilities (Dihn *et al*., 2019; Walston *et al*., 2006; Schlegal *et al*., 2006; Ferrucci *et al*., 2002; Visser *et al*., 2002; Cesari *et al*., 2004; Santos-Eggimann *et al*., 2009). In support of this, a recent study demonstrated a decreased $CD4^+/CD8^+$ T cell ratio (in favour of $CD8^+$ cells), and reduced proportion of $CD19^+$ B cells in frail individuals compared to robust individuals (Marcos-Perez *et al*., 2018). Frail individuals also appear to have higher proportions of $CD8^+CD28^-$, $CCR5^+CD8^+$ and $CCR5^+CD45^-$ T cells compared to robust individuals, indicating a diminished immune capability in these frail individuals (both men and very old women defined by original five criteria FFP) (De Fanis *et al*., 2008; Semba *et al*., 2005). In addition, it has also been shown that frailty score is inversely correlated to white blood cell (WBC) count (Fernandez-Garrdio *et al*., 2018). These age-related declines in immune function are likely to be somewhat caused by homeostatic pressure, which diminishes bone marrow production of B cells and limits their subsequent migration (Marttila *et al*., 2014).

Importantly, immune system changes are often compounded by increased inflammation in the form of a vicious cycle. For example, it has been shown that WBC count, in combination with IL-6 levels, were independently associated with frailty (Leng *et al*., 2007). An acute and dramatic increase in WBC count is recognised as an indicator of systemic inflammation, and this increase is associated with cardiovascular abnormalities and cancer mortality, as well as with all-cause mortality (Leng *et al*., 2005; Ruggiero *et al*., 2007).

1.5.5.4 Oxidative stress and molecular alterations in the pathophysiology of frailty

Studies have also demonstrated the involvement of oxidative damage and epigenetic modifications such as DNA methylation and telomere attrition in the pathophysiology of frailty (Breitling *et al,* 2016; Soysal *et al*., 2017; Vina *et al*., 2018; Liu *et al*., 2016; Namioka *et al*., 2017; Wu *et al*., 2009; Ingles *et al*., 2014; Serviddio *et al*., 2009; Ble *et al*., 2006). Several studies in the past decade have demonstrated that elevated levels of plasma markers of oxidative damage were related to frailty (defined through various methods), as opposed to the chronological age of the subject (Baptista *et al*., 2012; Liu *et al*., 2016; Saum *et al*., 2015; Wu *et al*., 2009), while additional studies have demonstrated the association between frailty and increased methylation of promoter CpG islands (Collerton *et al*., 2014). Of note, markers of oxidative stress such as malondialdehyde, oxidised glutathione, 4-hydroxy-2,3-nonenal, and protein carbonylation are elevated in frail individuals compared to robust individuals (Soysal *et al*., 2017; Ingles *et al*., 2014). In particular, several studies

have also shown that oxidative stress is associated with declines in grip strength and walking speed (Marcos-Perez *et* al. 2019; Soysal *et* al., 2017).

Oxidative damage is thought to contribute to frailty by upregulating inflammation through the activation of the NF-κB pathway, as well as directly impacting muscle quality and function (Baumann *et al*., 2016). Studies have also investigated the role of abhorrent genetic processes in the pathogenesis of frailty. As such, in a study investigating 620 single nucleotide polymorphisms (SNPs) involved in inflammation and hormone pathways, five were found to be associated with the Fried's frailty classification in men and women over 50 years (Mekli *et al*., 2015). In addition, variable number of tandem repeats (VNTR) polymorphisms in the genes for IL-1RN and IL-4 have been shown to be associated with higher FFP scores (Perez-Suarez *et al*., 2016).

Although the pathophysiology of frailty is extremely multifactorial, novel biomarkers remain highly desirable. MicroRNA (miRNA) are small RNA molecules involved in processing mRNA and are thus essential in the regulation of various intracellular signalling cascades and processes such as inflammation, response to muscle damage and mitochondrial function. The presence or absence of some circulating miRNA such as miR-21 can therefore be indicative of a pathophysiological process that is occurring, such as sarcopenia (Ameling *et* al., 2015; Fan *et al*., 2016; Weilner *et al*., 2015). A recent report showed that eight miRNAs were enriched in frail individuals (defined by the original FFP criteria) compared to young and age-matched robust individuals. These included miR-10a-3p, miR-92a-3p, miR-185-3p, miR-194-5p, miR-532-5p, MiR-326, miR-576-5p and miR-760 (Ipson *et al*., 2018), which are involved in insulin signalling as well as FoxO and AMPK signalling pathways (Martins *et al*., 2016). Additionally, there are several miRNAs that are involved in regulating mitochondrial functions and have been implicated in ageing. For example, miR-21 and miR-126a-3p promote the activation of Bcl-2 family members which regulate fission/fusion events as well as induce the activation of autophagy, and have been shown to be increased with age (Giuliani *et al*., 2018).

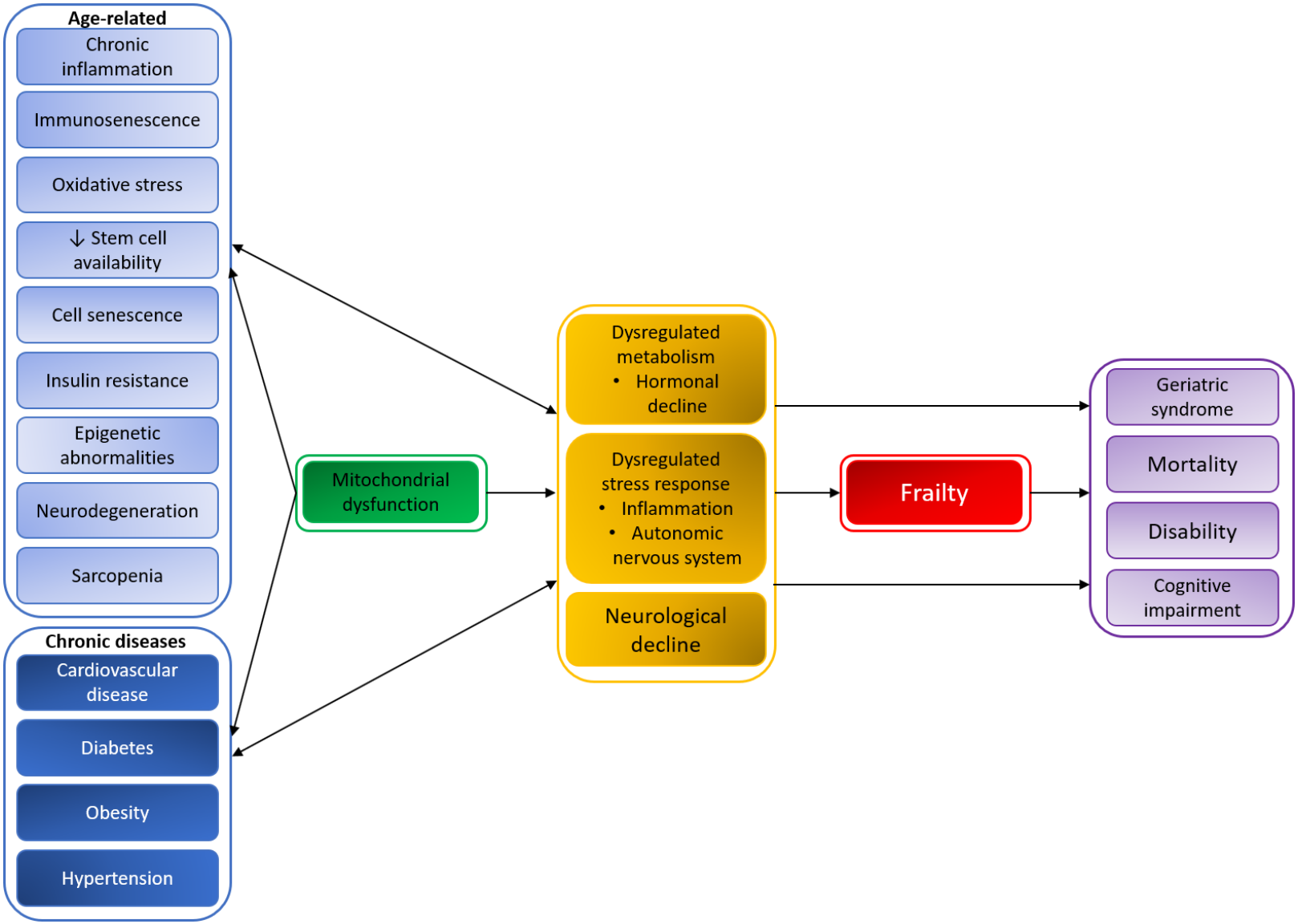

Figure 1.25 – Factors involved in the pathophysiology of frailty

1.5.6 Frailty in the HIV-infected population

Despite effective viral suppression and immune recovery in response to cART, PLWH experience an increased prevalence of age-related conditions compared to HIV- individuals of a similar age (Guaraldi *et al*., 2011; Smit *et al*., 2015; Chow *et al*., 2012; Althoff *et* al., 2014; Drummond *et al*., 2014; Kirk *et al*., 2013; Nou *et al*., 2016; Shiels *et al*., 2009; Sico *et al*., 2015; Desquilbet *et al*., 2007; Silverberg *et al*., 2015). These conditions include sensory dysfunction, falls, cardiovascular disease, kidney disease, lung disease, liver disease, cognitive decline, cancers, polypharmacy, and importantly, frailty (Greene *et al*., 2015; Chow *et al*., 2015; Drummond *et al*., 2014; Nou *e al*., 2016; Shiels *et al*., 2009; Sico *et al*., 2015; Silverberg *et al*., 2015).

As mentioned previously, studies utilising the original FFP criteria have shown that the prevalence of frailty in community-dwelling men and women over the age of 65 in the United States is between 7-12% (Fried *et al*., 2004). Whilst no studies have examined frailty in PLWH over 65s exclusively, the prevalence of frailty (as assessed by the original or modified five criteria frailty phenotype) in all ages of the HIV-infected population ranged between 9-19% (Altoff *et al*., 2014; Onen *et al*., 2009; Piggott *et al*., 2013; Pathai *et al*., 2012). However, when using a range of assessments, the prevalence of frailty in PLWH was found to range between 5-28.6% (Levett *et al*., 2016).

Although the underlying pathophysiologies of frailty are still not completely understood, similarities between ageing and HIV infection were observed prior to the extensive studies of the late 2000s which assessed frailty in the HIV-infected population. These pathologies included sarcopenia, lipodystrophy, anaemia, chronic renal disorders, immunosenescence, hepatic disorders, some cancers, and an increased susceptibility to acquired infections (Guaraldi *et al*., 2011; Deeks, 2011; Guaraldi *et al*., 2019a; Tate *et al*., 2013; Althoff *et al*., 2014). In addition, there are several shared etiologic factors of both frailty and HIV infection, such as oxidative stress, dysregulation of apoptosis and other mitochondrial functions, DNA alterations, telomere attrition, neuroendocrine decline and chronic inflammation (Bruunsgaard & Pedersen, 2003; Leng *et al*., 2007; Huang *et al*., 2005; Chavez *et al*., 2003; Erlandson *et* al., 2013; Margolick *et* al., 2017; Erlandson *et al*., 2017a; Zhang *et al*., 2015; Li *et al*., 2017; Guaraldi *et al*., 2019a; Branas *et al*., 2017). These observations suggest a potential overlap in the pathogenesis of frailty and HIV infection and indicate that PLWH are increasingly vulnerable to developing frailty and other age-related comorbidities (Margolick *et al*., 1992).

The most significant of these shared aetiologies would appear to be chronic inflammation and immune decline (Deeks, 2011; Margolick *et al*., 2017). Both of these factors have been shown to be strongly associated with the development of age-related diseases as well as geriatric syndromes such as frailty in the general population (Leng *et al*., 2007; Walston *et al*., 2002; Soysal *et al*., 2016).

Chronic inflammation and immune senescence are known play a significant role in multisystem physiological declines even in virally supressed PLWH (Deeks, 2011). In the HIV-infected population, increased levels of inflammation and immune activation were shown to be associated with poor Short Physical Performance Battery (SPPB) scores (Erlandson *et al*., 2014).

Although there are clearly links between HIV-infection and ageing phenotypes, controversy remains as to whether PLWH exhibit an **accelerated** ageing phenotype, whereby PLWH display an increased rate of age-related complications earlier than age-matched HIV- individuals, or instead experience **accentuated** ageing, whereby PLWH exhibit an enhanced frequency of age-related comorbidities in comparison to age-matched HIV- individuals (Pathai *et al*., 2014).

1.5.6.1 History of frailty research in the HIV setting

The first study to investigate frailty in the HIV-infected population was performed by Desquilbet and colleagues, who demonstrated that HIV infection was strongly associated with a frailty-related phenotype in men recruited to the Multicentre AIDS Cohort Study (MACS). Strikingly, this study indicated that a 55-year-old HIV+ man on cART was as likely to develop frailty as an ethnicity- and education-matched 65-year-old HIV- individual (Desquilbet *et al*., 2007). A follow-up study from the same group further demonstrated the link between frailty and HIV infection by demonstrating that CD4 count is an independent predictor of frailty in PLWH (Desquilbet *et al*., 2009), although future studies contradicted this observation (Onen *et al*., 2009, Althoff *et al*., 2014). Importantly, the latter study by Desquilbet and colleagues also indicated that the susceptibility of PLWH to developing frailty is decreased through cART, albeit not significantly.

In another study – the AIDS Linked to the IntraVenous Experience (ALIVE) study – a similar frailty phenotype as was used in the MACS study demonstrated that being HIV+ was associated with a three times increased risk of mortality, and being HIV+ as well as frail was associated with a seven times increased risk of mortality (Piggot *et al*., 2013).

Studies have also investigated the risks of frailty on adverse geriatric outcomes in PLWH using the original or modified FFP. Results from these studies include the increased risk of falls with increasing FFP score (Erlandson *et al*., 2012b), as well the increased prevalence of polypharmacy, multimorbidity and hospitalisation (Erlandson *et al*., 2012a) with frailty in PLWH. These studies also demonstrated that abnormalities in immune profiles are associated with declines in physical function and frailty. For example, individuals with lower physical function (as measured by the SPPB) had lower CD4/CD8 ratios, as well as higher proportions of $CD38^{+}HLA\text{-}DR^{+}$ T cells (a marker of T cell activation) compared to individuals with high physical function (Erlandson *et al*., 2012a). Further,

frailty was associated with higher levels of immune senescence and activation in PLWH (Erlandson *et al*., 2017a).

1.5.6.2 Assessments of frailty in PLWH

Early investigations into frailty in the HIV-infected population using individuals recruited into the MACS cohort utilised a frailty-related phenotype, similar to the original five criteria FFP (Fried *et al*., 2001; Desquilbet *et al*., 2007; Desquilbet *et al*., 2009).

The Veterans Aging Cohort Study (VACS) index is a FI-type prognostic tool specifically designed to measure frailty as a multisystem deterioration state in PLWH. Operationalised using HIV-infected men from the VACS study cohort, the VACS index is composed of deficits such as eGFR, hepatitis c co-infection, liver fibrosis and HIV-related factors such as CD4 count and viral load (Womack *et al*., 2013). Several cross-sectional studies have utilised the VACS index to measure frailty in PLWH and have demonstrated that inflammatory markers such as IL-6 and soluble CD14 are strongly correlated with VACS index score (Justice *et al*., 2014). Additionally, VACS index score was also significantly associated with cognitive impairment, physical function status and mortality (Justice *et al*., 2014).

The FI has also been adapted for the measurement of frailty in PLWH using PLWH in the Modena HIV Metabolic Clinic (MHMC). Here, Guaraldi and colleagues operationalised a 37-deficit index and found that the prevalence of frailty in virally supressed PLWH was 28% in 2015, and alarmingly, they predicted that in 2030, 50% of HIV+ patients will be frail at the age of 75 (Guaraldi *et al*., 2019b). Importantly, this deficit index did not include HIV-related factors (Akgun *et al*., 2014). The FI used in the MHMC study has been shown to more accurately predict 2-year mortality compared to the VACS index (Guaraldi *et al*., 2015). In addition, another study also demonstrated that the FI has a more significant association with age, co-morbidities, falls, and disability than the frailty phenotype measure used in the MACS studies (Guaraldi *et al*., 2017).

1.5.6.3 Risk factors for frailty development in PLWH

As demonstrated in **Table 1.2** there have been several cross-sectional studies involving ART-treated PLWH in which multiple factors have been shown to be associated with frailty in older PLWH (as assessed through a variety of validated frailty diagnostic methods in both men and women). These include age (Onen *et* al., 2009; Guaraldi *et* al., 2015) current CD4 count (Guaraldi *et* al., 2019a; Brothers *et* al., 2017; Branas *et* al., 2017; Ianas *et al*., 2013; Althoff *et al*., 2014; Pathai *et al*., 2012; Piggott *et al*., 2013; Terzian *et al*., 2009); nadir CD4 count (Onen *et al*., 2014; Guaraldi *et* al., 2017; Brothers *et* al., 2017; Erlandson *et al*., 2012a); detectable viral load (Althoff *et al*., 2014; Brothers *et al*., 2017; Piggott *et al*., 2013; Desquilbet *et al*., 2009); increased duration since HIV diagnosis (Onen *et al*., 2014; Brothers *et al*., 2017); use of PI-boosted regimens (Onen *et al*., 2009); BMI (Onen *et al*.,

2014; Pathai *et al*., 2012; Shah *et al*., 2012); hepatitis C co-infection (Ianas *et al*., 2013; Onen *et* al., 2014; Brothers *et al*., 2017); lipodystrophy (Shah *et al*., 2012); injection drug use (Brothers *et al*., 2017), and unemployment (Onen *et al*., 2014), amongst others. It is worth noting that the heterogeneity in study populations and frailty scales used, as well as the cross-sectional nature of many of these studies, undermine the clinical validity of some observations.

An important facet of frailty is its dynamic and plastic nature in both the general population and HIV-infected population (Althoff *et al*., 2014; Gill *et al*., 2006). In a longitudinal study of the MACS cohort, younger age was associated with a reversion from frailty to robust, whilst history of AIDS was associated with progression to frailty (defined by the original FFP criteria) (Althoff *et al*., 2014). In addition, a longer duration of HIV infection, smoking history and being female independently predicted advancement to frailty in the MHMC cohort (Erlandson *et al*., 2017a; Brothers *et al*., 2017).

As well as the beneficial effects on viral suppression and immune recovery, the advent of cART appeared to decrease the prevalence of frailty in PLWH (Desquilbet *et al*., 2009). HIV-infected men in the MACS study were found to be nine times more likely to be frail than HIV- individuals. Frailty was also positively associated with increasing age and increased duration of HIV infection, as well as CD4 count, viral load, and presence of AIDS (Desquilbet *et al*., 2007). Interestingly, the prevalence of frailty between 1994-1995, when cART usage was <0.1%, was 8%. This had decreased to 5% between 2000-2005, when the prevalence of cART usage was >70% (Desquilbet *et al*., 2009). Additionally, an FI based model has predicted that the prevalence of frailty in PLWH over 50 will decrease from 26% in 2015 to 7% in 2030, in part thanks to advances in cART effectiveness and availability (Guaraldi *et al*., 2019b).

	Factors related to frailty in PLWH	References
General factors	Age	Onen *et al*., 2009; Althoff *et al*., 2014; Desquilbet *et al*., 2007; Piggott *et al*., 2013; Ianas *et al*., 2012; Pathai *et al*., 2012; Guaraldi *et al.,* 2015
	Female gender	Zeballos *et* al., 2019; Bandeen-Roche *et* al., 2015; Womack *et al*., 2013; Mitniski *et al*., 2005; Brothers *et* al., 2017; Onen *et al*., 2014
	Smoking	Onen *et* al., 2014; Erlandson *et al*., 2017a; Brothers *et* al., 2017
Co-morbidities	Hepatitis C	Ianas *et al*., 2013; Brothers *et al.,* 2017; Onen *et al*., 2014
	BMI	Onen *et al*., 2009; Pathai *et al*., 2012; Shah *et al*., 2012
	Diabetes	Kelly *et* al., 2019; Piggott *et al*., 2013
	Hepatotoxicities	Piggott *et al*., 2013
	Lipodystrophy	Shah *et al*., 2012
	Inflammation	Justice *et al*., 2012; Erlandson *et al*., 2013; Leng *et al*., 2011; Margolick *et al*., 2013; Onen *et al*., 2014
	Cognitive decline	Onen *et al*., 2009; Marquine *et al*., 2014
	Low CD4:CD8 ratio	Guaraldi *et al*., 2019a; Erlandson *et al*., 2012a
	Fractures	Womack *et al*., 2013
HIV-related factors	Low CD4 count	Guaraldi *et al*., 2019a; Branas *et* al., 2017; Onen *et al*., 2014; Piggott *et al*., 2013; Althoff *et al*., 2014; Adeyemi *et al*., 2013; Brothers *et al.,* 2017
	Nadir CD4 count	Guaraldi *et* al., 2017; Onen *et al*., 2014; Erlandson *et al*., 2012a; Brothers *et al.,* 2017
	Viral load	Desquilbet *et* al., 2009; Piggott *et al*., 2013; Althoff *et al*., 2014; Brothers *et al.,* 2017
	History of AIDS	Desquilbet *et al*., 2009
	Time since diagnosis	Onen *et al*., 2014; Brothers *et al.,* 2017
	Duration of cART	Brothers *et* al., 2017; Althoff *et al*., 2014
	PI-containing ART regimen	Onen *et al*., 2014
	NNRTI-containing ART regimen	Erlandson *et al*., 2017a
Socio-economic factors	Unemployment	Onen *et al*., 2009; Erlandson *et al*., 2012a; Onen *et al*., 2014
	Poorer education	Erlandson *et al*., 2017a; Onen *et al*., 2009; Althoff *et al*., 2014; Piggott *et al*. 2013
	Low income	Onen *et al*., 2009

Table 1.2 – Factors associated with frailty among PLWH.

1.5.6.4 Comparisons to frailty in type 2 diabetes mellitus patients

Type 2 diabetes mellitus (T2DM) is chronic age-related disease, and similarly as in the context of HIV, T2DM patients appear to be more at risk of developing adverse ageing phenotypes such as frailty (Ottenbacher *et al*., 2009; Cacciatore *et al*., 2013; Hubbard *et al*., 2010). For example, frailty (as determined by the original five criteria FFP) was demonstrated to be 3-5 times higher in diabetic individuals over 65 compared to the age-matched general population (Saum *et al*., 2014). In addition, as in the HIV setting, the population of older T2DM patients is increasing, subsequently increasing the potential burden to the healthcare system (Won *et al*., 2018).

Of note, a recent systematic review demonstrated that the prevalence of frailty (as defined by several frailty measurements in a cohort of men and women with a mean age of 68) was approximately 24% in diabetics (Ida *et al*., 2019). This is slightly above the prevalence of frailty (as assessed by the original or modified five criteria frailty phenotype) estimated in all ages of the HIV-infected population, which ranged between 9-19% (Altoff *et al*., 2014; Onen *et al*., 2009; Piggott *et al*., 2013; Pathai *et al*., 2012). In addition, both are higher than the estimated prevalence of frailty (through various frailty assessments) in over 65s in the general population (Fried *et al*., 2004; Collard *et al*., 2012).

The underlying pathophysiological mechanisms of frailty in diabetic individuals is similar to that proposed in older PLWH, with long-term diabetic pathology accelerating the loss of skeletal muscle mass and function (Kalyani *et al*., 2014), as well as mitochondrial dysfunction as the result of insulin resistance (Krentz *et al*., 2013). Additionally, hyperglycaemia in T2DM is associated with increased chronic inflammation and oxidative stress (Morley *et al*., 2014). Importantly, frailty in older diabetic individuals is a multisystem disorder, as is the case in frailty in PLWH (Lee *et al*., 2017).

Whilst the risk factors and pathophysiology of frailty in T2DM individuals and older PLWH differ in some areas, there are important overlapping mechanisms. Hence, investigations into the mechanisms behind adverse ageing phenotypes such as frailty in older diabetic individuals may also help better understand frailty in older PLWH, and vice versa.

1.5.7 Frailty prevention and interventions

As mentioned above, frailty is a dynamic state and so 'treatment' for frailty can either be in the form of preventing prefrail individuals from progressing into frailty, or using interventions in order to reverse this progression.

In the case of frailty prevention, the success of care depends on how well-progressed frailty is in the individual. Primary care therefore provides the most significant opportunity for prevention. Here,

primary care providers who screen older individuals can identify the most at risk individuals, including middle-aged individuals with comorbidities such as diabetes and multiple sclerosis. In these individuals, frailty can be potentially prevented by first identifying specific factors that make that individual susceptible to developing frailty and then attempting to alter lifestyle factors which may be beneficial, such as dietary changes or increasing physical activity. As such, primary care interventions that promote physical activity have been shown to potentially limit the progression from prefrailty to frailty (Serra-Prat *et al*., 2017; Romera-Liebana *et al*., 2018). In further support, targeted primary care delivery through implementation of the Comprehensive Geriatric Assessment (CGA) has been shown to improve physical function, although it did not significantly affect emergency department readmission (Preston *et al*., 2018). In addition, studies have shown that interventions which address emergency department staffing and physical infrastructure reduce the amount of time a patient is in hospital, as well as the quality of care (Preston *et al*., 2018).

Due to the fact that the exact causes and outcomes of frailty in PLWH are yet to be fully determined, as well as the fact that there is no consensus in the best method of measuring frailty in PLWH, the optimal method of management of frail HIV-infected individuals remains controversial and as of yet, no effective pharmacological therapies are available (Calvani *et al*., 2013). In the general population, the gold standard approach to managing frailty is through specific intervention recommendations, such as, exercise, nutritional advice, pharmacological interventions, or cognitive therapy. In particular, exercise interventions seem the most effective (Walston *et al.*, 2018; Cameron *et al*., 2013; Cesari *et al*., 2015). Whilst studies in the general population have tested clinical interventions for individual components of the FFP, no studies have assessed interventions for frailty as a syndrome in the HIV+ population. A recently proposed method would be to routinely assess PLWH through a HIV-geriatric assessment (Erlandson *et al*., 2019). This would allow clinicians to comprehensively assess a patient's condition and evaluate the impact of potential interventions. Additionally, it is widely accepted that earlier diagnosis of HIV and subsequent earlier initiation of cART is beneficial (Molina *et al*., 2018).

Targeted clinical trials are evidently an important step in better understanding effective interventions for frailty in elderly individuals. However, clinical trials with elderly individuals are problematic as recruitment is complex and screening and assessments may be too invasive, especially in frail individuals. Other issues include the lack of focus on cost-effectiveness and on being patient centric as opposed to generic interventions.

Dent and colleagues recently published a review of the management of frailty in which they describe steps that need to be taken in order to improve the clinical care of frailty. Steps include the better

understanding of the pathophysiology of frailty; improving the methodology of clinical trials; identifying the best instruments and methods of frailty assessments; expanding knowledge on how to prevent the development of frailty; assess and improve screening tools for frailty; and developing pathologically-defined and targeted intervention guidelines (Dent *et al*., 2019). Hence, in this thesis I attempt to better understand the pathophysiology of frailty in older PLWH, with a special interest in the role mitochondrial dysfunction plays.

Importantly, frailty based screening services for PLWH are now ongoing, such as the Silver Clinic - a CGA based service - at Brighton and Sussex University Hospitals Trust, UK (Levett *et al*., 2020).

1.5.7.1 Physical activity as a potential intervention

With regards to interventions targeting physical function and sarcopenia, although there are several ongoing studies with promise, it is hoped that the ongoing Sarcopenia and Physical fRailty In older people multi-componenT Treatment strategies (SPRINTT) project will significantly increase our understanding of interventional benefits (Hopman *et al*., 2016). The SPRINTT project is a multi-centre project involving researchers and participants from 11 European countries and aims to specifically test the effect of multicomponent interventions in individuals with early stage frailty and sarcopenia.

Of the most up to date information derived from recent studies, the most promising interventions appear to be single-mode physical activity programmes (either resistance, aerobic or balance and coordination training programmes) which improve gait speed, mobility, muscle strength and ultimately physical function in older frail individuals (Landi *et al*., 2014; Zubala *et al*., 2017). Additionally, multicomponent activity programmes also improve muscle strength and balance (de Labra *et al*., 2015; Gine-Garriga *et al*., 2014; Cadore *et al*., 2013). Furthermore, physical activity interventions have been shown to contribute to the reversal of the adverse effects of chronic diseases and help maintain functional independence (Paulo *et al*., 2016; Virtuoso *et al*., 2012). Unfortunately, the effectiveness of the results from these studies are questionable, as they do not seem to re-test for frailty post-intervention (Gwyther *et al*., 2018). And so more work needs to be undertaken in order to better understand the optimal programme type for different severities of frailty.

Increasing physical activity has also been shown to have beneficial impacts on mitochondrial function in skeletal muscle. In particular, regular exercise in adulthood has been demonstrated to maintain the ultrastructure of mitochondria and other organelles involved in calcium handling, oxidative phosphorylation, and protein homeostasis (Zampieri *et al*., 2015). In addition, aerobic exercise has been shown to improve the energy producing capabilities of mitochondria by promoting

mitochondrial biogenesis through the activation of calcium-mediated signalling pathways, such as AMP-activated protein kinase (AMPK) and sirtuins (SIRT) (Marzetti *et al*., 2008; Rowe *et al*., 2014). Exercise induced ROS signalling also serve as beneficial signal mediators, by activating the PCG-1α and NF-κB pathways, which are responsible for regulating several mitochondrial functions such as biogenesis and autophagy (Marzetti *et al*., 2008). In contrast to the metabolic improvements seen in response to aerobic exercise, resistance exercise primarily improves muscle mass and strength (Suetta *et al*., 2008; Binder *et al*., 2005; Campbell *et al*., 2002; Benito *et al*., 2020). Mechanisms behind this phenomenon are underlined by improvements in endocrine signalling and subsequent insulin sensitivity, improved glucose utilisation and enhanced protein homeostasis (Kang & Krauss, 2010). Another beneficial mechanism of increased physical activity is the improvement in muscle stem cell regulation. Both endurance and strength training induce ultra-structural damage to skeletal muscle in combination with the release of growth factors such as IGF-1 and fibroblast growth factor (FGF), which ultimately results in the differentiation and proliferation of quiescent satellite cells (Kang & Krauss, 2010).

Finally, in PLWH, resistance exercise was also linked to increased CD4+ and CD8+ T cell counts (Zanetti *et al*., 2016; de Brito-Neto *et al*., 2019) and a decrease in levels of circulating pro-inflammatory cytokines (Zanetti *et al*., 2016) in two recent trials.

1.5.7.2 Dietary and hormonal interventions

Whilst various studies and clinical trials have attempted to elucidate the beneficial effects of hormone therapy, telehealth monitoring, or cognitive training, there is insufficient evidence to suggest these are effective therapy strategies (Frost *et al*., 2017; Apostolo *et al*., 2018). In particular, trials of monotherapies such as oestrogen or testosterone replacement in the late 90's and 00's improved muscle function but came with significant side effects (Snyder *et al*., 1999; Taaffe *et al*., 2005; Kenny *et al*., 2010). In contrast, a study by Friedlander and colleagues demonstrated that IGF-1 therapy improved BMD, muscle strength and ultimately physical function in elderly women who presented with no clinical IGF-1 deficiency (Friedlander *et al*., 2001).

Dietary changes have also been proposed as potential therapies for frailty and sarcopenia. For example, a consensus declared that protein intakes should be between 1.2-1.5 g/kg-bw/day in order to impede the loss of muscle mass and strength (Houston *et al*., 2008). In addition, previous studies have also shown that omega 3-fatty acid supplementation may enhance muscle protein synthesis and counteract muscle loss (Di Girolamo *et al*., 2014; Smith *et al*., 2011). Adherence to the Mediterranean diet, which is high in omega 3-fatty acids and antioxidants, has been shown to be associated with reduced odds for frailty (Ntanasi *et al*., 2018). Another study demonstrated that

magnesium levels are on average 6% lower in frail individuals compared to robust individuals, and a 12-week magnesium supplementation improved frail individual's performance in the chair stand, SPPB and 4m walk components of the FFP (Veronese *et al*., 2014). Finally, vitamin deficiency has also been associated with the age-related decline in muscle mass and strength (Chan *et al*., 2012).

1.6 Sarcopenia

In 2010 the European Working Group on Sarcopenia in Older People (EWGSOP) came to a consensus in defining sarcopenia as an age-related syndrome characterised by the progressive and generalised loss of skeletal muscle mass and strength, with adverse outcomes in physical function capabilities, disability, poor QOL and mortality (Cruz-Jentoft *et al*., 2010). Over the last decade considerable research into sarcopenia has been undertaken and sarcopenia is now recognised as a muscle disease with an ICD-10-MC Diagnosis Code (Vellas *et al*., 2018).

Improving the understanding of the causes of sarcopenia and optimal methods of care is essential due to the high social, personal and economic burden of the condition. As such, sarcopenia increases the risk of hospitalisation (Cawthon *et al*., 2017) and the cost of healthcare itself (Steffl *et al*., 2017). In addition, sarcopenia increases the risk of developing respiratory (Bone *et al*., 2017), cardiovascular (Bahat & Ilhan, 2016), and cognitive disease (Chang *et al*., 2016), the susceptibility for falls and fractures (Bischoff-Ferrari *et al*., 2015; Schaap *et al*., 2018), and mortality (De Buyser *et al*., 2016).

Systematic reviews using the EWGSOP definition have shown that the prevalence of sarcopenia is 1-29% in the community-dwelling population and 14-33% in long-term care populations (Cruz-Jentoft *et al*., 2014). Another, more recent meta-analysis demonstrated that PLWH have a 6.1 times higher odds ratio for developing sarcopenia compared to age, ethnicity, BMI and sex matched HIV-individuals (Oliveira *et al*., 2020)

In addition to defining sarcopenia, the EWGSOP made a distinction between primary sarcopenia (age-associated) and secondary sarcopenia (disease-associated) (Cruz-Jentoft *et al*., 2019). It is however often difficult to discriminate between the two as many individuals with sarcopenia are elderly and 90-95% also have a chronic morbidity (Hung *et al*., 2011). Other definitions that are used to describe adverse changes in muscle mass and function include dynapenia, which defines decreased contractility and loss of strength (Manini & Clark, 2012), disuse atrophy, which describes muscle loss due to inactivity (Biolo *et al*., 2005), and cachexia, which describes weakness and wasting due to chronic illness (Vanhoutte *et al*., 2016).

Both the loss of skeletal mass and strength has been associated with adverse health outcomes such as cognitive impairment, loss of physical independence, and an increased risk for hospitalisation and developing comorbidities. These include cardiac and respiratory disease, as well as mortality (Tolea & Galvin, 2015; Fielding *et al*., 2011; Morley *et al*., 2014).

Both sarcopenia and frailty are both acknowledged to be adverse age-related complications and have been shown to be interlinked with each other, although are not necessarily causative of each other (Studenski *et al*., 2014; Cruz-Jentoft *et al*., 2019). Underscoring the highly heterogenous and complex nature of age-related syndromes, it has been shown that declines in muscle mass and strength both contribute to poor health outcomes with age (Mitchell *et al*., 2012), and that obesity combined with loss of muscle strength but not muscle mass is predictive of the risk of falls (Scott *et al*., 2014). In addition, a more recent study demonstrated that the loss of muscle strength is more predictive of adverse age-related outcomes such as loss of independence rather than loss of muscle mass (dos Santos *et al*., 2017).

Muscle strength and muscle mass are associated with each other, although declines in either measure does not always equate to decline in the other. It has been demonstrated that the loss of muscle strength occurs at a rate five times higher than the loss of skeletal muscle mass in older adults, indicating that the loss of muscle strength is more significant to the pathophysiology of sarcopenia (Mitchell *et al*., 2012; Goodpaster *et al*., 2006; Venturelli *et al*., 2015). Loss of muscle strength is also now widely acknowledged as a better predictor of adverse health outcomes than the loss of muscle mass (Schaap *et al*., 2018, Ibrahim *et al*., 2016; Schaap *et al*., 2013). Finally, studies conducted within the Baltimore Longitudinal Study of Aging revealed that cognitive performance, visceral obesity and velocity of nerve conduction are the strongest predictors of muscle quality (Moore *et al*., 2014).

1.6.1 Skeletal muscle structure

Skeletal muscle is organised in a hierarchical formation whereby myofibres are bundled together into 'fascicles', which are held together by the perimysium. Myofibres contain repeating contractile units termed sarcomeres. Sarcomeres are in turn composed of thin and thick contractile myofilaments called actin and myosin (Lieber & Ward, 2011) (**Figure 1.26**).

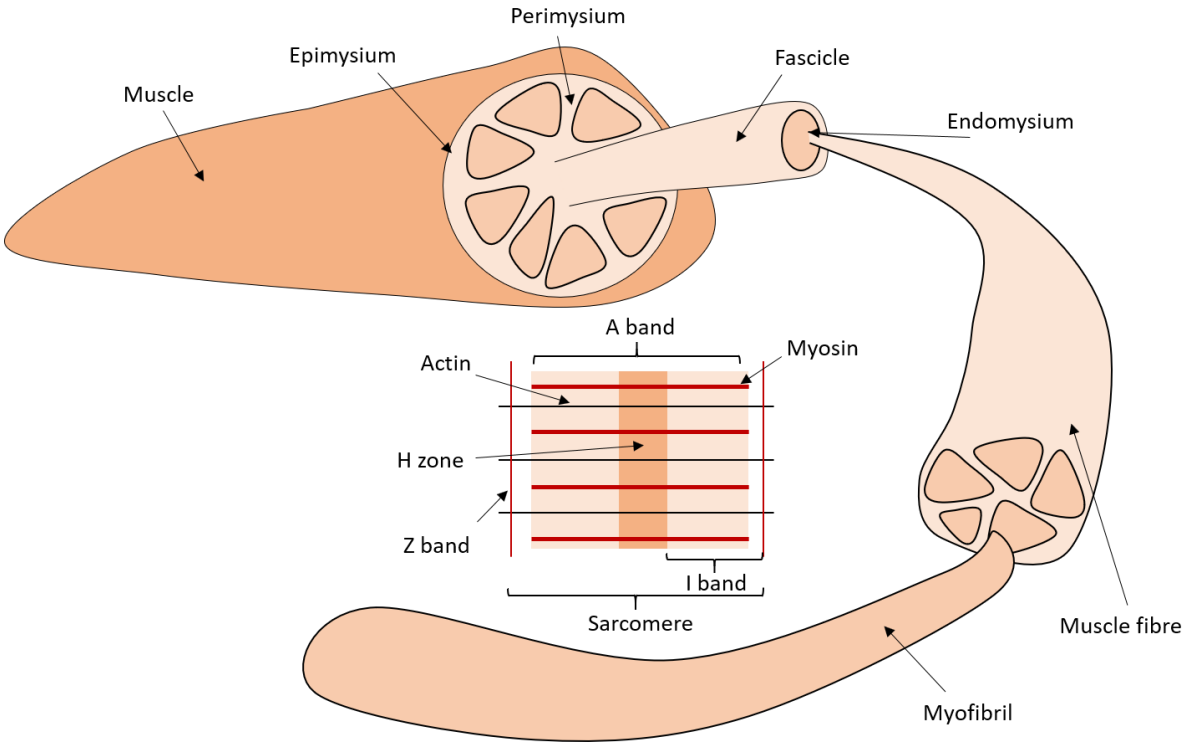

Figure 1.26 – Skeletal muscle structure.

1.6.2 Skeletal muscle mitochondria

Skeletal muscle mitochondria can either be intermyofibrillar (IMF) mitochondria or subsarcolemmal (SS) mitochondria, which are morphologically and biochemically distinct from each other (Glancy *et al*., 2015). Roughly 80% of skeletal muscle mitochondria are IMF, and they lie between myofibrils to form a rigid lattice like structure. SS mitochondria comprise the other ~20% of skeletal muscle mitochondria and have been shown to reside in small perinuclear clusters in the immediate interior of the sarcolemma (Cogswell *et al*., 1993).

As mentioned above, IMF and SS mitochondria have distinct morphology and biochemical functions. In particular, IMF mitochondria have a higher IMM and matrix enzyme activity, which is consistent with the fact that they provide energy required for muscle contraction (Ferreira *et al*., 2010). In comparison, SS mitochondria are thought to provide energy for the membrane and nucleus (Hood, 2001).

1.6.3 Skeletal muscle through the life course

Two of the parameters of sarcopenia – muscle mass and strength – are dynamic factors, and can vary significantly over the life course (Cruz-Jentoft *et al*., 2019).

In general, muscle mass and strength are higher in males compared to females, and maximal levels of both factors occur in young adulthood (≤ ~40 years) (Dodds *et al*., 2014). Subsequently, both muscle mass and strength decline beyond the age of 50, and the rate of loss also appears to accelerate with advancing age. Significantly, muscle mass in men and women is decreased by approximately 4.7% and 3.7% respectively in the seventh decade compared to the maximal, and the rate of muscle mass decrease accelerates to 0.64-0.7% and 0.8-0.9% each year in woman and men over 75 years old (Mitchell *et al*., 2012). Of note, loss of muscle mass predominantly occurs in the lower limbs (Narici & Maffulli, 2010).

Although the age-related declines in muscle mass and strength are multifactorial, it is acknowledged that genetic and lifestyle factors play a significant role (Bloom *et al*., 2018). In addition, the age-related decline in mitochondrial function is suspected to accelerate the decline in muscle mass and strength, primarily through declines in energy production. This was previously discussed in more detail in **Section 1.5.5.1**.

1.6.4 Identification and diagnosis of sarcopenia

According to the updated consensus of the EWGSOP(2), diagnosis of sarcopenia begins with identifying patients at risk of sarcopenia or with sarcopenia symptoms and then progressing the patients to further sarcopenia testing (Cruz-Jentoft *et al*., 2019). Here, individual sarcopenia parameters are tested (**Table 1.3**). Muscle strength is assessed through measurements of grip strength via a hand dynameter, as grip strength correlates with muscle strength in other parts of the body, and is a strong predictor of adverse patient outcomes (Ibrahim *et al*., 2016; Leong *et al*., 2015). The chair rise test can also be used to measure muscle strength in the legs. Importantly, the recent consensus is that grip strength as measured through a Jamar dynamometer is the best method of determining muscle strength (Cruz-Jentoft *et al*., 2019).

Muscle mass is also measured as part of the diagnosis of sarcopenia. Muscle mass can be quantified by several methods with adjustments for height or BMI (as described in Cruz-Jentoft *et al*., 2019). However, magnetic resonance imaging (MRI) and computed tomography (CT) are considered the gold standard for assessing muscle mass (Beaudart *et al*., 2016).

The final parameter tested is physical performance, which is defined as an objectively measured whole-body function related to locomotion, as it involves both the nervous system as well as the musculoskeletal system (Beaudart *et al*., 2018). A commonly used surrogate for physical performance is gait speed, which predicts adverse outcomes such as disability, falls, hospitalisation, and mortality (Studenski *et al*., 2011). Other commonly used surrogates include the SPPB and the Timed-Up and Go test (TUG), which also predict adverse health outcomes (Pavasini *et al*., 2016). Although several of the various methods are easily applied in the clinical setting, the most recent consensus recommends the use of gait speed to assess physical performance. This is primarily due to the convenience of undertaking the test (Cruz-Jentoft *et al*., 2019).

Several new methods for measuring sarcopenia at both the clinical and research level are currently being assessed. The majority of these tests aim to improve the measurement of muscle mass and quality, although some require expensive machinery. Some of these new methods include computed tomography (aimed at lumbar 3rd vertebra and psoas muscle) (Mourtzakis *et al*., 2008; Rutten *et al*., 2017), ultrasound assessment of muscle; d3 creatine A dilution tests (Shankaran *et al*., 2018), and specific biomarkers of sarcopenia. Of these, the d3 creatine A dilution tests appear to be the most promising, as higher levels are associated with DXA-derived lean body mass, physical performance and mobility (Shankaran *et al*., 2018; Cawthon *et al*., 2019).

Characterisation	↓ Muscle mass	↓ Muscle strength	↓ Physical performance
Robust	-	-	-
Pre-sarcopenia	X	-	-
Sarcopenia	X	X	-
Severe sarcopenia	X	X	X

Table 1.3 – Factors required for the diagnosis of sarcopenia (Cruz-Jentoft et al., 2010).

1.6.5 Pathophysiology of sarcopenia

Skeletal muscle is the largest organ is the human body, accounting for roughly 40-50% of body mass (Tieland *et al*., 2018). Skeletal muscle is involved in numerous physiological mechanisms including heat regulation, energy homeostasis, amino acid metabolism, and insulin sensitivity. With regards to the role skeletal muscle plays in insulin sensitivity and other neuroendocrine functions such as the release of myokines and anabolic and catabolic peptides, immune function and inflammation, skeletal muscle is now considered an endocrine organ (Aversa *et al*., 2012; Bonetto *et al*., 2013).

The most significant factors involved in the pathogenesis of sarcopenia include inflammation (Curcio *et al*., 2016, Cruz-Jentoft *et al*., 2019), physical inactivity (Mijnarends *et al*., 2016), malnourishment (Muscaritoli *et* al., 2010; Cederholm *et* al., 2017; Cederholm *et* al., 2019), and other age-related factors, as described in **Figure 1.27**.

1.6.5.1 Chronic inflammation in the pathophysiology of sarcopenia

As described in previous sections, systemic inflammation plays a hugely significant role in the pathophysiology of several adverse age-related pathologies, including frailty. Individuals with sarcopenia have higher levels of circulating IL-6, and levels of inflammatory markers such as TNF-α, CRP and IL-6 are inversely correlated with skeletal muscle protein synthesis rates (Standley *et al*., 2013). These observations suggest that chronic inflammation impedes skeletal muscle anabolic functions (Toth *et al*., 2005; Mayot *et al*., 2007). Additionally, in skeletal muscle, systemic inflammation, in particular increased TNF-α levels, can upregulate mTOR-associated protein degradation pathways such as the ubiquitin-proteasome pathway, which can lead to increased skeletal muscle autophagy and simultaneously inhibit the production of peptides essential for muscle growth (Xia *et al*., 2017). In addition, TNF-α destabilises MyoD and myogenin to subsequently impair skeletal muscle regenerative capacity (Langen *et al*., 2004). Eventually, these factors can lead to increased skeletal muscle senescence and apoptosis, which ultimately results in decreased muscle mass and function (Brocca *et al*., 2012). To highlight the multifactorial nature of sarcopenia, previous studies have revealed that the protein intake sufficiently needed to maintain muscle mass and

quality is dramatically increased in the presence of high levels of IL-6 (Bartali *et al*., 2013). The use of alcohol and tobacco is also associated with a higher risk of developing sarcopenia (Maddalozzo *et al*., 2009; Lee *et al*., 2007).

1.6.5.2 Neuroendocrine function and sarcopenia

Skeletal muscle is responsible for a range of various endocrine functions including the insulin-stimulated uptake of glucose from blood, fatty acid metabolism, and glycogen synthesis (Otto-Buckzkowska, 2003). In addition, skeletal muscle derived myokines are involved in regulating functions in several tissues including the liver, bone, and adipose tissue (Schnyder & Handschin, 2015). In resting conditions, skeletal muscle metabolism accounts for roughly 20% of whole-body metabolic activities (Muller *et al*., 2013). Declines in oestrogen in post-menopausal women and testosterone in men are responsible for declines in muscle mass and muscle strength, and circulating levels of IGF-1, cortisol and vitamin D are lower in frail individuals compared to robust individuals (Puts *et al*., 2005; Leng *et al*., 2009; Beaudart *et* al., 2014; Muir *et* al., 2011). As mentioned previously, these observations indicate that dysregulation in the GH-IGF-1 somatotropic axis as well as the hypothalamic-pituitary-adrenal axis are implicated in the pathogenesis and pathophysiology of sarcopenia and frailty. Dysregulated endocrine signalling has also been implicated in the disruption of protein homeostasis through anabolic insensitivity, contributing to loss of muscle mass and strength (Koopman & van Loon, 2009). In addition, as circulating IGF-1 is involved in protein synthesis via activation of the Akt-mTOR pathway (Glass, 2010), the reduced levels of IGF-1 with age will adversely contribute to protein homeostasis.

The reduction in muscle insulin sensitivity occurs rapidly after physical inactivity and has been shown to directly contribute to an increased susceptibility of developing cardiovascular abnormalities, through the induction of dyslipidaemia (Mazzucco *et al*., 2010).

1.6.5.3 Physical inactivity and sarcopenia

Numerous studies have demonstrated the age-related decline in skeletal muscle perfusion capabilities. This age-related decrease in maximal oxidative capacity is known to adversely impact muscle mass and strength by promoting a more oxidative and pro-inflammatory microenvironment, in which autophagy and protein homeostasis becomes dysregulated, leading to the upregulation of apoptosis and cell senescence (Choi *et al*., 2016; Zane *et al*., 2017; Adelnia *et al*., 2019). Aside from age-related mitochondrial decline, the reduction in perfusion capabilities is thought to be explained in part by muscle ultrastructure abnormalities such as reduction in capillary number (Bigler *et al*., 2016) and impairment of endothelial and other arterial functions (Das *et al*., 2018; Ward *et al*.,

2018). In support of this, Prior and colleagues previously demonstrated the significant association between VO_2 max and muscle capillary-to-fibre ratio (Prior *et al*., 2016).

The loss of muscle mass with age occurs exponentially, and is dictated by the level of physical activity. Extended bed rest itself can lead to a 3-5% decline in lean body mass in healthy volunteers, and this impact can be accentuated when combined with other risk factors such as chronic disease (Genton *et al*., 2011). In further support, a 6-week bed rest study demonstrated that muscle atrophy was associated with a 6% decrease in resting energy expenditure (Ritz *et al*., 1998). Pathophysiologically, physical inactivity is associated with an increased rate of fat deposition (Olsen *et al*., 2008), which can propagate the increase in systemic inflammation and reduced insulin sensitivity (Guillet *et al*., 2012; Masgrau *et al*., 2012). Altogether, these factors accentuate muscle catabolic functions and so lead to reduced muscle mass and strength. This biological phenomenon is commonly seen in cancer patients and in other chronic diseases associated with a sedentary lifestyle (Manini, 2010). Physical inactivity is also associated with decreased antioxidant activity. With regard to this, increased exercise training results in the elevated activities of glutathione peroxidase, and physical inactivity leads to redox imbalance (Agostini *et al*., 2010).

Reduced levels of lean body mass in combination with excess adiposity is a condition termed sarcopenic obesity, and is common in older individuals (Johnson Stoklossa *et al*., 2017). The increased adiposity exacerbates the adverse pathophysiological functions present in sarcopenia by increasing the fatty infiltration into muscle, which further increases inflammation, and adversely impacts the individual's physical performance capabilities (Kalinkovich & Livshits, 2017; Barbat-Artigas *et al*., 2014).

Dynapenia has been shown to be associated with fatigue, disability and falls, as well as reduced bone stimulation leading to osteoporosis (Manini & Clark, 2012; Binkley *et al*., 2013). Dynapenia is therefore a predictor of loss of independence in chronically ill patients and elderly.

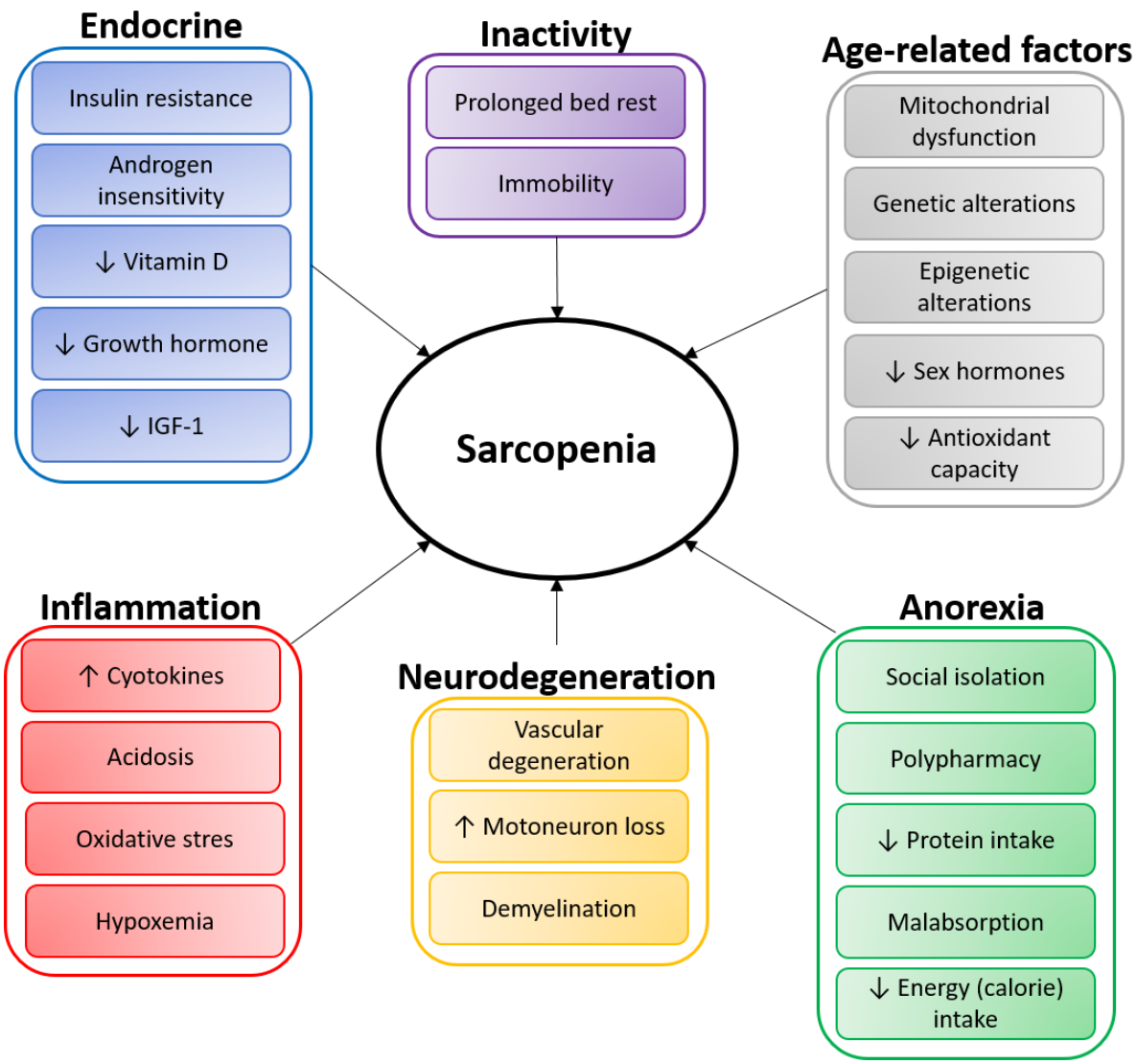

Figure 1.27 – Factors involved in the pathophysiology of sarcopenia.

1.6.6 Epidemiology of sarcopenia in PLWH

In a recent study of 1720 majority male, virally-supressed PLWH (median age 52), the prevalence of sarcopenia was determined to be 25.7%. However, the majority of sarcopenic PLWH were female, and only 8.8% of men over 50 were classified as sarcopenic (Echeverria *et al*., 2018). In addition, results from this study also demonstrated a close association between sarcopenia and presarcopenia.

The prevalence of sarcopenia in this cohort was similar to previous studies in similarly age, gender, and BMI matched PLWH (Pinto Neto *et al*., 2016; Wasserman *et al*., 2014; Oliveira *et al*., 2020). As was the association of presarcopenia with sarcopenia (Pinto Neto *et al*., 2016). Importantly, these studies demonstrate that sarcopenia appears to be more prevalent in PLWH compared to matched HIV-uninfected individuals. However, differences in the method used to classify sarcopenia appears to affect the prevalence of sarcopenia (Echeverria *et al*., 2018).

Notably, results from these studies demonstrated that risk factors for sarcopenia in PLWH are similar to that seen in the general population. These include old age, low BMI and malnutrition (Echeverria *et al*., 2018; Pinto Neto *et al*., 2016; Wasserman *et al*., 2014; Oliveira *et al*., 2020). In addition, these studies demonstrate that HIV-related factors such as duration with HIV infection increase the susceptibility to developing sarcopenia, most likely through increased inflammation, although CD4 count and viral load appeared not to have an effect (Echeverria *et al*., 2018).

1.7 Skeletal muscle mitochondrial dysfunction in PLWH

ART is extremely effective at reducing HIV viremia, and the advent of ART has dramatically reduced HIV and AIDS-related morbidity and mortality (GBD HIV collaborators, 2019). In addition, ART restores CD4 counts to near normal levels in the majority of individuals, although factors such as CD4 count at ART initiation and being male (Maman *et al*., 2012), as well as older age (Fatti *et al*., 2014; Simms *et al*., 2018), duration on ART (He *et al*., 2016), hepatitis C (HCV) coinfection (Laskus *et* al., 1998; Laskus *et* al., 2000) and other genetic and environmental factors like polymorphisms in TNF-α (Haas *et al*., 2006) prevent immune recovery in roughly 15-30% of ART-treated PLWH (Autran *et* al., 1999).

However, use of ARVs in monotherapy or in combination (cART) has been associated with various toxicities (**Table 1.4**). Although the exact mechanisms underpinning these toxicities has yet to be completely understood, it is widely regarded that ARV-induced mitochondrial dysfunction is significantly implicated in its pathogenesis (Lim & Copeland, 2001).

The association between mitochondrial dysfunction and ART-related toxicities was first described in patients treated with the nucleoside reverse transcriptase inhibitor (NRTI) zidovudine (AZT), who presented with myopathy (Dalakas *et al*., 1990). *Ex vivo* histology work on tissue from AZT-treated myopathy patients subsequently demonstrated ragged-red fibres and abnormal mitochondria with loss of cristae - features characteristic of mitochondrial myopathy observed in some mitochondrial disease patients (Margolis *et al*., 2014; Gorman *et al*., 2015). This was shown to be due to the depletion of mtDNA content through the inhibition of the mtDNA PolG (Dalakas *et* al., 1990; Arnaudo *et al*., 1991). Further studies then demonstrated that other ARVs in the NRTI class (albeit it with different affinities) induce mitochondrial toxicities in various tissues, such as peripheral neuropathy, lactic acidosis and hepatotoxicity (Selvaraj *et al*., 2014). As a result, newer NRTIs with a reduced PolG-inhibiting capacity were developed and stavudine (d4T) (2018) has been discontinued. Additionally, whilst AZT is now only used in the prevention of neonatal HIV acquisition, either as a pre-exposure prophylaxis, or as a post-exposure prophylaxis (Kourtis & Bulterys, 2010), as it has consistently been shown to effectively prevent neonatal transmission of HIV compared to other ARVs such as nevirapine (NVP), in which resistance is more common (Eshleman *et al*., 2001). Whilst other ARVs such as tenofovir disoproxil fumarate (TDF) would appear to be safer whilst still being effective, AZTs continued use in preventing neonatal transmission is down to the accumulated demonstration of its efficiency (Shaffer *et al*., 1999*;* Hurst *et al*., 2016). However, previous studies around the effects of AZT on neonatal mitochondrial function are controversial, with some studies suggesting there is limited adverse effect, and conversely an upregulation in mtDNA content (Cote *et*

al., 2008; Desai *et* al., 2008). The discrepancy between the adverse effects of AZT on neonatal and adult mitochondrial function could be due to the short-term in which neonatal AZT is administered.

In more recent years studies have demonstrated the presence of mitochondrial toxicities induced by other NRTIs, such as TDF-induced renal abnormalities (Kohler *et al*., 2009; Samuels *et al*., 2017), as well as toxicities induced by different classes of ARV, such as protease inhibitor (PI)-induced lipodystrophy (Domingo *et al*., 2014; Dragovic *et al*., 2014; Alikhani *et al*., 2019). This suggested that ARVs can induce mitochondrial dysfunction independent of PolG-inhibiting mechanisms, such as changes in mitochondrial membrane potential (ΔΨm), abnormal mitochondrial morphology, and increased oxidative stress.

Clinical toxicity	Tissue affected	NRTIs implicated	Reference
Myopathy	Skeletal muscle	AZT	Dalkas *et al*., 1990
Peripheral neuropathy	Peripheral nervous system	ddI, ddC, d4T	Dalkas, 2001; Fichtenbaum *et al*., 1995; Sacktor *et al*., 2009
Lipoatrophy	Subcutaneous fat	d4T, AZT	van Vonderen *et al*., 2009; Joly *et al*., 2002
Pancreatitis	Pancreas	ddI	Sarner *et al*., 2002
Lactic acidosis	Liver, skeletal muscle	d4T, ddI	Boubaker *et al*., 2001
Renal tubular toxicity	Renal proximal convoluted tubules	TDF	Kohler *et al*., 2009; Samuels *et al*., 2017

Table 1.4 – Mitochondrial toxicities associated with NRTIs. *AZT = zidovudine; ddI = didanosine; ddC = zalcitabine; d4T = stavudine; TDF = tenofovir disoproxil fumarate.*

1.7.1 NRTI-induced skeletal muscle mitochondrial dysfunction in PLWH – the 'PolG hypothesis'

As mentioned previously, early *in vitro* studies demonstrated that NRTIs inhibit PolG, which leads to the depletion of mtDNA, and subsequently mitochondrial dysfunction. This mechanism was dubbed the 'PolG hypothesis' (Brinkman *et al*., 1999).

NRTI triphosphates competitively bind to the polymerase subunit of PolG (Lewis *et al*., 1996), responsible for DNA replication, but as they lack the 3' hydroxyl group (3'OH) they induce chain termination and subsequently inhibit replication of nascent mtDNA, leading to a reduction in mtDNA content (Lewis & Dalkas 1995). This depletion of mtDNA leads to diminished energy production capabilities, namely through declines in the rate of oxidative phosphorylation and by undermining ETC complex formation, as well as increasing ROS production. Diminished energy production then leads to clinical toxicities (Arnaudo *et al*., 1991; Lewis *et al*., 1992; Wallace, 1992). This effect is similar to that seen in mitochondrial toxicities present in some hereditable mitochondrial disease patients, where reduced levels of mtDNA depletion become pathogenic (Moraes *et al*., 1991; Gorman *et al*., 2015).

The various NRTIs have different steric conformations (**Figure 1.28**) and so inhibit PolG with different affinities. *In vitro* studies have demonstrated that zalcitabine (ddC), didanosine (ddI), and d4T have the strongest PolG inhibiting capacities, while AZT inhibits PolG weakly: ddC ≥ ddI ≥ d4T > lamivudine (3TC) > TDF > emtricitabine (FTC) > AZT > abacavir (ABC) (Hoschele *et al*., 2006; Kakuda *et al*., 2000). Conversely, though monophosphorylated AZT (AZT-MP) is inefficiently excised from the exonuclease domain of PolG, which could explain how AZT induces mtDNA depletion without strongly inhibiting the polymerase domain (Lim & Copeland, 2001).

Although there are many factors and key unknowns about the exact mechanisms underpinning NRTI-induced skeletal muscle mitochondrial dysfunction, largely due in part to the vast heterogeneity in HIV+ populations as well as mitochondrial dysfunction itself, a study by Hendrickson and colleagues (2009) demonstrated that the risk of developing mitochondrial toxicities may be modified by mtDNA haplogroup. In particular, having the mtDNA haplogroup H appears to increase the risk of developing ART-induced lipoatrophy (Hendrickson *et al*., 2009). In addition, studies have highlighted the risk that the presence of chronic diseases, which are highly prevalent in older PLWH, may predispose certain PLWH to increased mitochondrial dysfunction. For example, a large body of literature has demonstrated mitochondrial dysfunction in various tissues in type 2 diabetes mellitus (T2DM), such as heart (Ruegsegger *et* al., 2018; Montaigne *et al.,* 2014; Mackenzie *et al*., 2013; Croston *et al*., 2014; Marciniak *et al*., 2014; Yan *et al*., 2013; Vazquez *et al*., 2015) and skeletal muscle (Meex *et al*., 2010;

Johnson *et al*., 2016; Rabol *et al*., 2009). Results from both human and mouse studies have demonstrated decreased oxidative metabolism and mitochondrial biogenesis in T2DM, leading to impaired lipid metabolism (Szendroedi *et al*., 2014). It is therefore likely that the presence of a chronic condition may predispose an ART-treated HIV+ individual to developing mitochondrial dysfunction in various tissues.

The mechanisms of the PolG hypothesis suggest that NRTI toxicity is cumulative and the toxic manifestations increase with the duration of exposure (Chawla *et al*., 2018). As such, mitochondrial toxicities occurring in ART-treated patients often results in the temporary termination of treatment, as treatment termination of the culprit NRTI is suspected to reverse to mitochondrially-toxic effect (McComsey *et al*., 2005). In addition, switching to two-drug ART regimens as opposed to three or four-drug regimens has been shown to reduce the susceptibility to developing adverse events such as toxicities. However, these regimens may not be as effective at supressing the virus (Llibre *et al*., 2018; Mondi *et al*., 2015; Perez-Molina *et al*., 2017 Margolis *et al*., 2017). However, there is limited data as to whether resumption of a potentially toxic ARV reinstates the toxicity. It would depend on the particular ARV, tissue effected, and how cumulative the toxicity itself is. For example, it has been suggested that myopathy may arise several years after cessation of treatment (Payne *et al*., 2011).

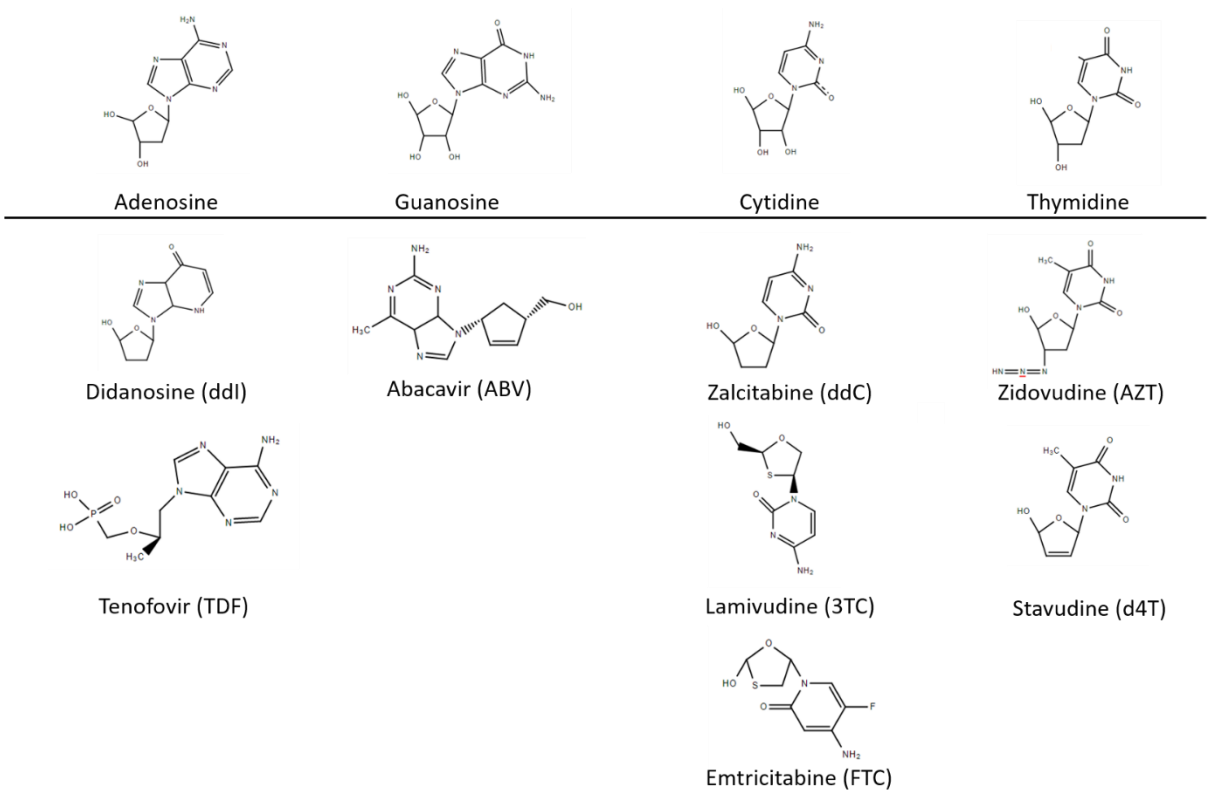

Figure 1.28 – Chemical structures of the commonly used NRTIs.

1.7.2 NRTI-induced mitochondrial dysfunction beyond the PolG hypothesis

The discrepancy between the poor PolG-inhibiting capabilities and severe clinical toxicities caused by AZT, as well as the fact that newer NRTIs that have weaker PolG inhibitory effect have been shown to induce mitochondrial toxicities, led to the questioning of the robustness of the PolG hypothesis. In addition, more recent *in vitro* studies have demonstrated mitochondrial dysfunction in the absence of mtDNA depletion, for example AZT-induced reduction of ATP production and simultaneous ROS increase in rat heart tissue (Enomoto *et al*., 2011), impaired fatty acid oxidation in d4T-treated cultured rat hepatocytes (Igoudjil *et al*., 2006), reduced ATP production in AZT-treated murine brown adipocytes (Viengchareun *et al*., 2007) and inhibition of mitochondrial respiration and ATP production in ABC-treated Hep3B cells (Blas-Garcia *et al*., 2010). The robustness of the PolG hypothesis has also been questioned by *in vivo* studies, whereby PBMCs from patients experiencing NRTI-induced mitochondrial toxicities had normal mtDNA levels (Lewis & Dalkas 1995; McComsey *et al*., 2002), as well as normal mtDNA levels in PBMCs from d4T-, AZT- and ddI-treated PLWH with lipodystrophy (McComsey *et al*., 2008). Some studies have in fact reported an increase in mtDNA content in patients treated with NRTIs (Oldfors *et al*., 1995). Moreover, PIs and NNRTIs, which do not directly inhibit PolG, are also associated with mitochondrial dysfunction (Deng *et al*., 2010; Blas-Garcia *et al*., 2010; Apostolova *et al*., 2010).

Another caveat to the questioning of the PolG hypothesis is the fact that PLWH who have been exposed to some of the early NRTIs have an excess of skeletal muscle mtDNA mutations, which can lead to declines in mitochondrial function at the individual myofibre level. Importantly, these defects are still seen years after cessation of treatment (Payne *et al*., 2011). This not only dismisses the hypothesis of mtDNA depletion as a result of PolG inhibition, preferring instead large-scale mtDNA deletions, but provides a basis for the hypothesis that there is a legacy effect of historical NRTI exposure, and PLWH who were exposed to these NRTIs are at a higher risk for developing mitochondrial dysfunction (Payne *et* al., 2011; Hunt & Payne, 2020). As such, the prevalence of mtDNA deletions in various tissues from PLWH exposed to various ARVs was investigated using quantitative real-time PCR in **Chapter 4** and **Chapter 8**.

Indeed, alternative mechanisms of NRTI-induced mitochondrial dysfunction beyond PolG inhibition have been proposed, including the formation of mtDNA deletions, depletion in ribonucleotide (RN) and deoxyribonucleotide (dRN) pools (Jordheim & Dumonet, 2007), and dysregulation of ETC complex formation (Lund & Wallace 2008) (**Figure 1.29**).

1.7.2.1 Perturbations in endogenous nucleotide pools

As most NRTIs are administered as prodrugs, they need to be metabolised intracellularly into their active moieties (triphosphates) in order to exert their effects (Peter, 2004). This occurs via either the *de novo* or salvage pathways, similarly to how deoxynucleotide triphosphates (dNTPs) are produced from endogenous RNs and dRNs (Van Rompay *et al*., 2000). Due to the similarities in conformation and metabolism, unphosphorylated NRTIs compete with endogenous RNs for phosphorylation, which can reduce the size of RN and dRN pools (Jordheim & Dumonet, 2007; Selvaraj *et* al., 2014). NRTI-triphosphates (NRTI-TPs) also compete with endogenous dNTPs for incorporation into elongating DNA, in which the former induce chain termination (Jordheim & Dumonet, 2007). Both of these processes ultimately lead to impaired mtDNA replication and reduced mtDNA content (McComsey *et al*., 2002). Tissue-specific differences in the ratios of intracellular kinases (e.g. thymidine kinase 1 and 2 (TK1 and TK2 respectively)) could explain the discrepancy between mtDNA depletion levels in different tissues and in response to different NRTIs. For example, TK1 is predominantly expressed in the cytosol of active cells, while TK2 is expressed more in the mitochondria and in quiescent cells (Lemmon & Schlessinger, 2010). AZT has been shown to have a higher affinity to phosphorylation by TK1 rather than TK2, whilst ddI and ddC are the opposite (Feeney & Mallon, 2010). This suggests that AZT is more likely to deplete RN and dRN pools in more active cells, while ddC and ddI are more likely to deplete the pools in quiescent cells such as skeletal muscle fibres, although this is not necessarily reflected in clinical observations (Arnaudo *et al*., 1991; Lewis *et al*., 1992).

1.7.2.2 ART and mitochondrial genomic alterations

Another proposed alternative mechanism of NRTI-induced mitochondrial dysfunction is the formation and propagation of mtDNA mutations. As well as its polymerase functions, PolG contains a 3'-5' exonuclease domain which is responsible for proofreading activities (Stumpf & Copeland, 2013). *In vitro* studies have shown that monophosphorylated NRTIs (NRTI-MP), particularly AZT-MP, have a high affinity to the exonuclease domain of PolG (Maagaard & Kvale 2009) and inhibit the proofreading capabilities once bound, subsequently lowering the fidelity of mtDNA replication and increasing the susceptibility of mtDNA mutation formation (Wang *et* al., 1996). Further studies from our lab have shown that large-scale mtDNA deletions induced by NRTIs clonally expand with age in skeletal muscle fibres, causing mitochondrial dysfunction (Payne *et al*., 2011).

As well as the depletion of mtDNA content, NRTIs have also been shown to deplete mtRNA content. Although the mechanisms of mtRNA depletion are yet to be fully understood, a study by McComsey *et* al. (2008) demonstrated the reduction of mtRNA content in lipodystrophy affected PLWH and suggested the mechanism could be through limitations in the availability of cofactors needed for

mtRNA synthesis as well as through PolG inhibition. mtRNA and mtDNA depletion may be intertwined, as mtDNA synthesis requires RNA-primed DNA replication (Young & Copeland, 2016).

1.7.2.3 Other proposed mechanisms of ART-induced mitochondrial dysfunction

NRTIs, in particular AZT, have been shown to directly affect CI of the ETC and subsequently cause defects in oxidative phosphorylation capabilities. A study by Lund & Wallace (2004) demonstrated AZT-induced decoupling of CI (Lund & Wallace 2004), while other studies have suggested AZT disrupts electron flow through CI (Pereira *et al*., 2002), and both AZT and ddC cause disruptions in NADH linked respiration (Szabados *et al*., 1999). Although controversial, the likely mechanism behind this phenomenon is NRTI-induced inhibition of cyclic adenosine monophosphate (cAMP)-mediated phosphorylation events responsible for ETC complex formation (Lund & Wallace 2008). To investigate this further, in this thesis I utilised a novel immunofluorescence assay that allows the quantification of CI proteins in individual myofibres in PLWH.

Another proposed alternative theory which has gained more traction in recent years is the idea of increased ROS and oxidative stress being responsible for diminished oxidative capacity (Cote *et al*., 2005; Schieber & Chandel, 2014). *In vitro* studies on various human cell lines have demonstrated that short-term exposure to NRTIs such as AZT + 3TC, d4T + 3TC (Ciccosanti *et al*., 2010) and AZT + d4T (Lagathu *et al.,* 2007) has a direct effect on ROS production. A recent study using liver autopsies from AIDS patients and mice exposed to ARVs demonstrated a significantly higher proportion of 8-oxo-G positive mtDNA in ART-treated cells (Liang *et* al., 2018). Although yet to be fully elucidated, the mechanisms underpinning this theory centre around the idea of oxidative damage to macromolecules involved in oxidative phosphorylation, such as PolG and mtDNA, which are highly susceptible to oxidative damage (Richter *et al*., 1988). This is supported by *ex vivo* studies on AZT-treated mouse tissue (Nerurkar *et al*., 2001). In addition, ROS signalling is implicated in several physiological processes such as lipid metabolism and apoptosis, and an imbalance in redox potential has adverse effects on these processes. One of the key signalling pathways involved is thought to be that of PPAR-γ. Expression of the PGC-1α as well as PPAR-γ itself is reduced in ART-treated patients (Caron *et al*., 2009; Feeney & Mallon, 2010), as well as in *in vitro* studies (Viengchareun *et al*., 2007). A study by Kohler and colleagues, (2009) demonstrated that mitochondrial superoxide dismutase and mitochondrially-targeted catalase dismutase were reduced in AZT-induced cardiomyopathy tissue in a transgenic mouse model (Kohler *et al*., 2009).

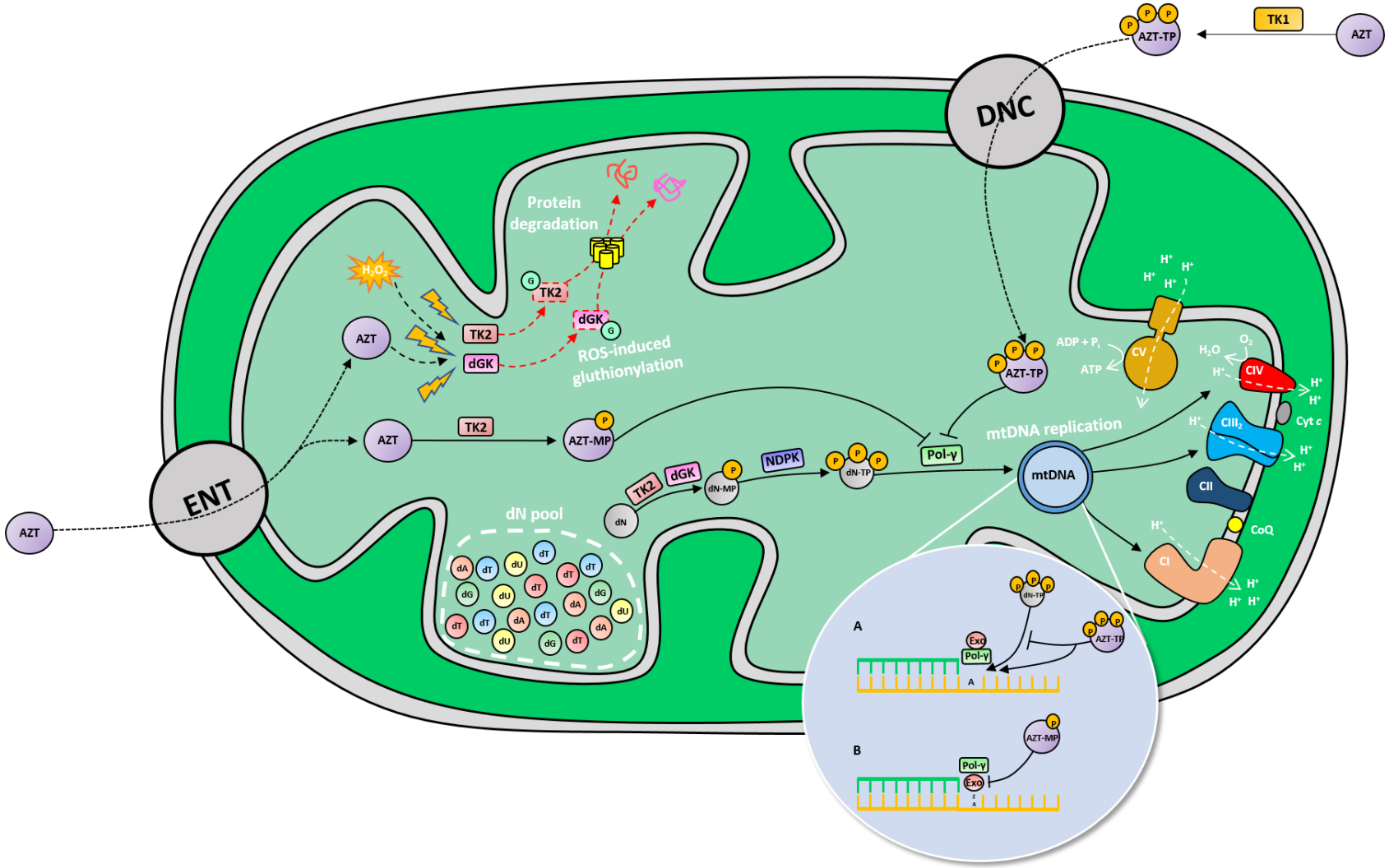

Figure 1.29 – Intramitochondrial actions of 'mitochondrially toxic' NRTIs. (***A***) *Triphosphorylated AZT (AZT-TP) competitively binds to the polymerase domain of PolG and induces chain termination of mtDNA replication as it lacks the '3 OH group.* (***B***) *Monophosphorylated AZT (AZT-MP) accumulates in the mitochondrial matrix and has a high affinity towards the exonuclease domain of PolG, where it inhibits exonuclease activities, subsequently reducing the fidelity of mtDNA replication. Unphosphorylated AZT and AZT-MP also increase the rate of ROS production, causing oxidative stress and oxidative damage to cellular kinases such as TK2. This then leads to the reduction in the rate of RN and dRN phosphorylation.*

1.7.3 PI and NNRTI induced mitochondrial dysfunction

Similarly to NRTIs, some PIs and NNRTIs have been shown to induce a range of adverse pathophysiological factors that are linked to mitochondrial dysfunction (**Table 1.5**). Unlike NRTIs, PIs and NNRTIs do not directly inhibit PolG and therefore do not induce mtDNA depletion via the mechanisms described in the PolG hypothesis (Deng *et al*., 2010; Blas-Garcia *et al*., 2010; Apostolova *et al*., 2010). Instead, the proposed mechanisms underpinning this mitochondrial dysfunction centre around alterations in the regulation of mitochondrial bioenergetics and apoptosis (Apostolova *et al*., 2010).

Due to the event of cART, where a PI or NNRTI is administered alongside a backbone of two NRTIs, it has become difficult to dissect the exact contributions of ARVs from these classes of drugs on ART-induced mitochondrial toxicities seen in PLWH. As a result, most of the work on PI and NNRTI-induced mitochondrial dysfunction has been done through *in vitro* studies.

Clinical reports from PLWH treated with PIs described occurrences of lipodystrophy, insulin resistance (IR) and cardiovascular abnormalities (Bongiovanni *et* al., 2004; Koster *et* al., 2003). As mentioned above, PIs do not inhibit PolG, and so PI-induced mitochondrial defects are related to disturbances in redox regulation, mitochondrial membrane potential (ΔΨm) and energy production. Indinavir (IDV) and nelfinavir (NFV) have been shown to inhibit the glucose transporter isoform 4 (GLUT4) *in vitro* (Kumar *et al*., 2010) and IDV was also found to reduce respiration and ATP production in brown and white murine adipocytes (Viengchareun *et al*., 2007). Both these effects are thought to contribute to PI-induced insulin resistance. In support of this, increased β cell apoptosis followed ΔΨm reduction and increased cytochrome *c* release in PI-treated INS-1 cells (Zhang *et al*., 2009). Both ritonavir (RTV) (HPAEC cells) (Wang *et al*., 2009), and IDV (HPAEC and HUVEC cells) (Wang *et al*., 2009) increased ROS production in the respective cell lines, leading to increased apoptosis. PIs have also been shown to induce cell senescence in PLWH-derived fibroblasts and fat tissue as a result of elevated ROS levels (Caron *et al*., 2007). Saquinavir (SQV), RTV and NFV all induced mitochondrial fragmentation and disruption of the mitochondrial network in the same patient-derived cell lines (Roumier *et al*., 2006). Although the exact pathophysiological mechanisms remain controversial, it is thought that PI-induced inhibition of the MPP plays a key role (Mukhopadhyay *et al*., 2002). As with studies with NRTIs, PI-induced mitochondrial defects appear to be cell type-specific. In non-adipocyte related cell lines NFV, RTV, SQV, IDV and lopinavir (LPV) have all been found to exert anti-apoptotic effects (Badley, 2005), and NFV upregulated anti-apoptotic Bcl-2 family proteins in leukaemia cells (Bruning *et al*., 2010).

The NNRTI efavirenz (EFV) has been associated with lipodystrophy in clinical studies (Zaera *et al*., 2001). NNRTI-induced lipodystrophy is thought to be caused by inhibition of adipocyte differentiation and reduced lipogenesis (Jemsek *et al*., 2006; Moyle *et al*., 2012). Several *in vitro* studies have reported disruption of the ΔΨm in EFV-treated cell lines, which lead to increased rates of apoptosis (Pilon *et al*., 2002). Another study demonstrated the EFV dose-dependent increase in ROS production and decrease in ΔΨm *in vitro*, again leading to increased apoptosis (Jamaluddin *et al*., 2010). EFV also caused increased ROS production and decreased ΔΨm as a result of CI inhibition in patient-derived hepatic cells (Blas-Garcia *et al*., 2010; Apostolova *et al*., 2010). Treatment with EFV also increased the rate of mitophagy in hepatic cells (Apostolova *et al*., 2011). Finally, EFV treatment has also been shown to induce ER stress in brain endothelial cells, leading to thinning of the blood-brain barrier (Bertrand *et al.*, 2016). This mechanism is thought to underpin the pathophysiology of cerebrovascular pathology in EFV-treated PLWH (Bertrand *et al*., 2016).

ART class	Drug	Adverse effects
PI	Saquinavir (SQV)	CVR; Insulin resistance; Lipohypertrophy
	Ritonavir (RTV)	CVR; Insulin resistance; Lipohypertrophy; Dyslipidemia
	Indinavir (IDV)	CVR; Nephrotoxicity; HB; Insulin resistance; Lipohypertrophy; Dyslipidemia
	Nelfinavir (NFV)	CVR; CRs; Insulin resistance; Lipohypertrophy; Dyslipidemia
	Atazanavir (ATV)	CVR; Nephrotoxicity; HB; Lipohypertrophy
	Darunavir (DRV)	Hepatoxicity; CRs; Lipohypertrophy
NNRTI	Nevirapine (NVP)	Hepatotoxicity; CRs; Dyslipidemia
	Etravirine (EFV)	Hepatotoxicity; CRs; CNS toxicity; Insulin resistance; Dyslipidemia; Lipodystrophy; Stroke
	Delavirdine (DLV)	CRs
	Etravirine (ETR)	CRs

Table 1.5 – Pathologies associated with NNRTI and PI use. *CVR = cardiovascular disease risk; HB = hyperbilirubinemia; CRs = cutaneous reactions.*

1.7.4 Mitochondrial dysfunction in ART-naïve PLWH

Although the majority of mitochondrial defects and subsequent toxicities in PLWH are associated with ART, numerous reports have described mitochondrial abnormalities in ART-naïve PLWH. Maagaard and colleagues demonstrated mtDNA depletion in T and B lymphocytes in ART-naive PLWH (Maagaard *et al*., 2005). Although the mechanisms underpinning this mtDNA depletion are not fully understood, it is suggested that the pro-apoptotic effects of HIV proteins were heavily implicated either directly or indirectly (Fevrier *et al*., 2011; Rumlova *et al*., 2014).

The HIV Env glycoprotein (gp120) is expressed on ER and has been shown to cause ER stress when misfolded Env accumulates (Fields *et al*., 2016). ER stress can then lead to mitochondrial membrane ($\Delta\Psi m$) depolarisation and increased apoptosis as a result of BAX translocation to mitochondria (Ferri *et al*., 2000). The gp120 glycoprotein also increased MFN1 and DRP1 levels *in vitro* (Fields *et al*., 2016) and induced cristae remodelling and mitochondrial swelling (Avdoshina *et al*., 2016).

The viral protein Nef has also been shown to trigger apoptosis *in vitro*, either through decreasing the expression of Bcl-2 or by decreasing $\Delta\Psi m$ (Lenassi *et al*., 2010). Tat protein also induces apoptosis in Jurkat cells by decreasing the levels of Bcl-2 proteins, as well as increasing oxidative stress by downregulating the levels of superoxide dismutase 2 (SOD2) (Giacca, 2005). In addition, Tat proteins were also shown to trigger changes in mitochondrial structure and induce mitochondrial fragmentation, leading to disruptions in $\Delta\Psi m$ and accumulations of damaged mitochondria (Rozzi *et al*., 2018). Finally, Vpr proteins have also been shown *in vitro* to increase mitochondrially-mediated apoptosis by reducing levels of Bcl-2 and Bcl-XL (Deniaud *et al*., 2004; Huang *et al*., 2012).

1.7.5 Impact of genetic and environmental factors

The HIV+ population is extremely diverse genetically, demographically and in lifestyle factors. It is therefore difficult to determine the exact impact any potential confounding factors, such as smoking or alcohol intake, have on the development of mitochondrial defects. In addition, diversity in study protocols used in many of the current cohort studies make it difficult to extrapolate the exact impact many genetic or lifestyle factors have on increasing the susceptibility of developing mitochondrial dysfunction in PLWH. For example, there are potential confounding factors such as smoking, body composition, and levels of exercise activity which are either not routinely assessed, or assessment methods vary (Nansseu *et al*., 2020).

However, it has been shown that chronic exposure to ethanol can increase the level of ROS production (Kukielka *et al*., 1994) whilst simultaneously decreasing the levels of the antioxidant

glutathione (Fernandez-Checa *et al*., 1998). This can lead to increased oxidative stress with consequences for mitochondrial function (Blas-Garcia *et al*., 2010).

Finally, studies investigating mitochondrial haplogroups of PLWH in the AIDS clinical trials (ACTG) group have shown associations between the European haplogroup T and peripheral neuropathy (Hulgan *et al*., 2005), whilst having a mtDNA haplogroup H was associated with increased risk of lipoatrophy (Henrickson *et al*., 2009).

1.8 Kidney function in the HIV setting

As the average age of PLWH increases, kidney diseases are becoming more prevalent. In addition to HIV-associated kidney disease (HIVAN), kidney disease in PLWH can manifest as various pathologies, such as acute kidney injury (AKI), chronic kidney disease (CKD) and end-stage renal disease (ESRD). In particular, whilst the advent of ART has reduced the prevalence of HIVAN in PLWH, AKI, CKD, and ESRD pose now significant issues (Swanepoel *et al*., 2018). CKD is therefore seen as one of the most important age-associated comorbidities in older PLWH.

1.8.1 Kidney structure and function

Kidneys are responsible for the control of the body's fluid levels, filtration of blood, removal of waste, and electrolyte regulation. As a result of blood filtration, urine is created and ultimately drained into the bladder via the pelvis (Smith, 1952).

The kidney is composed of a fibrous outer layer termed the renal capsule, a peripheral layer called the cortex, and an interior layer called the medulla. The medulla is arranged into pyramidal structures which, in combination with the cortex, form the renal lobe (**Figure 1.30**). Nephrons are structures that span the cortex and medulla and are where the majority of kidney processes occur. In particular, nephrons contain a glomerular blood filter composed of podocytes and tubular epithelium, which can be further subdivided into proximal, intermediate, and distal segments (Smith, 1952; Davidson, 2009).

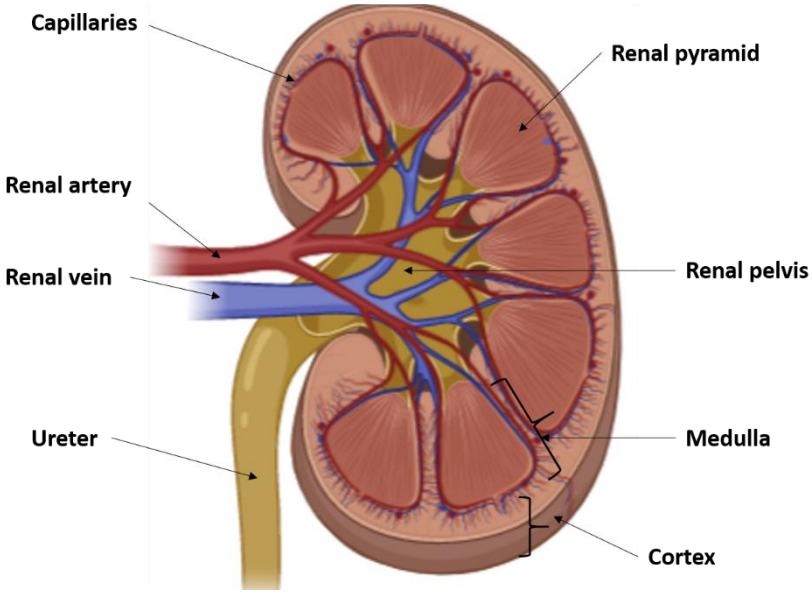

Figure 1.30 – Kidney structure.

1.8.2 Kidney disease and HIV infection

1.8.2.1 Renal diseases in PLWH

AKI is a broad clinical condition describing acute kidney failure, often resulting in electrolyte imbalance and a significant decrease or elimination of urine, with the sufferer then requiring haemodialysis (Okusa & Davenport, 2014). Histologically, AKI is characterised by focal or diffuse tubular luminal dilation, loss of proximal tubule brush border, simplification of lining epithelium, and loss of nuclei (Gaut & Liapis, 2020). Although the prevalence of AKI in PLWH has fallen since the advent of ART, the prevalence still remains high, and these virally-supressed PLWH appear to experience higher rates of more severe AKI (Li *et al*., 2012; Nadkarni *et al*., 2015). Indeed, although the burden of AKI is not as significant as that of CKD in PLWH, AKI is recognised as being a risk factor for the initiation and progression of CKD (Chawla *et al*., 2014; Pannu, 2013; Coca *et al*., 2011).

Similarly to AKI, the prevalence of CKD in virally-supressed PLWH remains high. The decline in eGFR (estimated glomerular filtration rate) with age is known to be enhanced in both virally-supressed and non-virally suppressed PLWH compared to the HIV-uninfected population (Wetzels *et al*., 2007; Choi *et* al., 2009; Scherezer *et al*., 2012). This increased prevalence of pathology appears to be down to the high prevalence of risk factors that are found in PLWH, as discussed below (Medapalli *et al*., 2012).

HIVAN was the first renal disease to be described in HIV+ individuals, and unlike AKI and CKD, the prevalence of HIVAN has significantly fallen since the advent of ART. HIVAN is now only commonly seen in newly-diagnosed PLWH with late-stage HIV infection, or those who have discontinued ART (Wyatt, 2017).

1.8.2.2 Risk factors for renal disease in PLWH

Risk factors for CKD include: black race, hypertension, age, recreational drug use, HCV as well as HBV coinfection, and diabetes. In particular, diabetes appears to increase the susceptibility for CKD onset and progression, primarily due to increased inflammation seen in diabetic individuals (Medapalli *et al*., 2012; Mallipattu *et al*., 2013). Notably, HBV and HCV coinfection with HIV is associated with a 2- to 3- fold increased risk of CKD (Lucas *et al*., 2013; Mocroft *et al*., 2012).

Among the common risk factors for kidney disease, sepsis appears to increase the severity of AKI in PLWH (Nadkarni *et al*., 2015).

Another major risk factor for renal disease is African ancestry (Kopp & Winkler, 2003). This is primarily due to pathogenic polymorphisms in the *APOL1* gene, which encodes apolipoprotein 1 (Lucas *et al*., 2014, Kasembeli *et al*., 2015). Although the mechanisms behind *APOL1* mediated

kidney pathology are unknown, increased *APOL1* expression is thought to cause podocyte injury by inducing apoptosis or autophagy in renal epithelium as a result of increased cellular and mitochondrial membrane permeability (Fu *et al*., 2017; Kruzel-Davila *et al*., 2017; Me *et al*., 2017).

1.8.2.3 ART and renal disease in HIV

Exposure to the nucleoside reverse transcriptase inhibitor tenofovir disoproxil fumarate (TDF) increases the susceptibility of developing renal disease (Woodward *et al*., 2009; Bonjoch *et al*., 2014; Flandre *et al*., 2011; Hall *et al*., 2011; Winston *et al*., 2006; Goicoechea *et al*., 2008).

In addition, increased age, immunodeficiency, and concomitant use of didanosine or ritonavir-boosted protease inhibitors are risk factors for AKI in PLWH (Hamzah *et al*., 2017). Finally, the incidence of CKD was increased 16% with every year of TDF exposure, 21% with every year of atazanavir (ATV) exposure, and 8% with every year of ritonavir-boosted lopinavir (LPV) in the EuroSIDA study of HIV+ individuals (Mocroft *et al*., 2010).

1.8.2.4 Mitochondrial dysfunction in chronic kidney disease

As mitochondria are responsible for various cellular processes essential for kidney function, as well as the fact that kidneys are second only to the heart in oxygen consumption and mitochondrial abundance (Wirthensohn & Guder, 1986), mitochondrial dysfunction has serious implications for kidney function and therefore kidney disease.

Although the link between mitochondrial function and CKD is heavily suspected, the underlying mechanisms remain elusive. Various *in vitro* studies have sought to assess alterations in mitochondrial function in CKD disease models. This includes the demonstration of increased mitochondrial fragmentation in kidney tubules (Galloway *et al*., 2012; Zhan *et al*., 2015). In addition, studies have demonstrated increased phosphorylation of Drp1 and therefore increased mitochondrial fission in podocytes (Ayanga *et al*., 2016; Han *et al*., 2008). MtDNA mutations, and defective mitophagy have also been linked to CKD (Hartleben *et al*., 2010).

Additionally, alterations in mitochondrial biogenesis have also been implicated in renal abnormalities (Tran *et al*., 2016; Hershberger *et al*., 2017; Yuan *et al*., 2012; Perico *et al*., 2016). Of note, deacetylation of PGC-1α was demonstrated to reduce aldosterone-induced podocyte injury, whist an activator of SIRT1 – Resveratrol – increased mitochondrial biogenesis and protected mitochondrial induced podocyte injury (Yuan *et al*., 2012).

Importantly, the link between kidney mitochondrial dysfunction and diabetes gives insights into how mitochondrial dysfunction may induce CKD. In this instance, oxidative stress as the result of mitochondrial dysfunction is a common pathway behind CKD in in diabetic individuals (Brownlee,

2005). Here, the free radical theory of diabetic microvascular complications hypothesises that increased ROS production results in damage to renal epithelial cells and accelerates the progression of kidney disease (Brownlee, 2005). In support of this, both *in vitro* and *in vivo* studies have demonstrated increased ROS in diabetic mouse models displaying kidney abnormalities, including podocyte apoptosis and elimination (Brownlee, 2005; Wang *et al*., 2012; Dieter *et al*., 2015). Finally, several studies have demonstrated that administration of the mitochondrial-targeted antioxidant mitoTEMPO reduced the prevalence of pathological diabetic neuropathy features (Chen *et al*., 2015; Sims *et al*., 2014).

Perturbations in mitochondrial dynamics are also thought to be associated with diabetic kidney abnormalities. For example, PGC-1α was significantly downregulated in streptozotocin-induced diabetic rat tubules, as well as in OVE26, Akt2 and *db/db* mice (Morigi *et al*., 2015; Dugan *et al*., 2013; Nakatani & Ingani, 2016; Hasegawa *et al*., 2013; Platt & Coward, 2017). In addition, knockout of SIRT1 in non-diabetic mice resulted in albuminuria (Hasegawa *et al*., 2013).

Given the importance of kidney disease as an age-associated comorbidity in PLWH, we therefore performed a pilot study of mitochondrial dysfunction in HIV/ART associated kidney disease.

Chapter 2 – Thesis Aims and objectives

Due to the successful virus-supressing effects of ART, PLWH now experience a lower prevalence of HIV-related morbidity and mortality. As a result, PLWH are now on average living longer, and the average age of the HIV+ population is increasing (GDB 2017 HIV collaborators, 2019; Public Health England, 2019).

Some older PLWH exhibit features of unsuccessful ageing, such as frailty and sarcopenia (Desquilibet *et al*., 2007; Brothers *et* al., 2017; Erlandson *et* al., 2015; Echeverria *et al*., 2018; Pinto Neto *et al*., 2016; Wasserman *et al*., 2014). This phenomenon has serious implications with regard to the effects a population experiencing adverse ageing phenotypes has on healthcare systems, and so focus has shifted towards trying to better understand the causes of this adverse ageing in virally-supressed PLWH (Kojima *et al*., 2019).

Mitochondrial dysfunction is one of the best characterised pathways of human ageing (Lopez-Otin *et al*., 2013). Therefore, given the established role mitochondrial dysfunction plays in ART-mediated toxicities and other HIV-related comorbidities (Hunt & Payne, 2020), recent interest has been shown towards the potential role of mitochondrial dysfunction as a driver of unsuccessful ageing in older PLWH. However, few studies have investigated mitochondrial function in skeletal muscle of older PLWH and in particular, how age-related skeletal muscle mitochondrial dysfunction is linked to adverse ageing phenotypes and their underlying pathophysiological decline.

The over-arching hypothesis of this thesis is therefore that:

'*Mitochondrial dysfunction is an important driver of adverse ageing phenotypes in PLWH*'.

The primary aims of this thesis were therefore to:

1. Better understand skeletal muscle mitochondrial dysfunction in PLWH in the contemporary cART era.
2. Compare the prevalence of adverse ageing phenotypes and clinical factors between older PLWH and age-matched HIV- individuals.
3. Determine whether older PLWH have greater levels of skeletal muscle mitochondrial dysfunction compared to age-matched HIV- individuals, and whether skeletal muscle mitochondrial dysfunction is associated with adverse ageing phenotypes in older PLWH.
4. Investigate the levels of various other skeletal muscle pathophysiological factors in older PLWH, and subsequently compare whether any of these factors are more prevalent than in age-matched HIV- individuals.

In addition, aside from skeletal muscle mitochondrial dysfunction and the adverse implications that has on the older PLWH, a growing concern in the field of mitochondrial dysfunction in the contemporary cART era is TDF-induced renal pathology (Guaraldi *et* al., 2011; Lucas *et* al., 2008; Samuels *et al.,* 2017; Swanepoel *et al*., 2018). Due to the difficulty in obtaining renal biopsies from TDF-treated PLWH with renal pathology, in combination with the lack of validated techniques to investigate mitochondrial dysfunction at the individual cellular level in these individuals, the secondary aims of this thesis was to:

1. Assess whether mitochondrial dysfunction can be investigated in renal tissue from TDF-treated PLWH at the cellular and molecular level using novel experimental techniques.
2. Compare mechanisms of ART-induced mitochondrial dysfunction in renal tissue with that seen in skeletal muscle tissue.

Chapter 3 – Methods

3.1 Ethical guidelines

All participant samples were collected with informed written consent. All human tissue was stored in compliance with the Human Tissue Act (HTA licence number – 12534), on HTA licenced premises.

Control skeletal muscle tissue was acquired with prior informed consent from the distal part of the hamstring of people undergoing anterior cruciate ligament (ACL) surgery. Approval for this was given by Newcastle biobank (NAHPB reference: 042). More detailed patient and control information is given in the relevant chapters and sections.

Specific research ethics and NHS research governance arrangements are detailed in the following sections.

3.2 Patient cohorts

Data from the work presented in this thesis is derived from patients recruited as part of three studies. Two studies were set up with the aim of investigating mitochondrial function in skeletal muscle from HIV+ and HIV- people in various settings (MAGMA study and SMMFA study), whilst the other study aimed to investigate mitochondrial function in renal tissue from PLWH and HIV- individuals. This section describes the various cohorts.

3.2.1 MAGMA study

All research activity was conducted with permission from local research ethics committee (REC) and HRA (Health Research Authority), ref. 17/NE/0015.

30 HIV+ and 15 HIV- males were recruited as part of the MAGMA study, with patients giving prior written permission. 38 patients were recruited at the Royal Victoria Infirmary (RVI) in Newcastle upon Tyne, UK, whilst 7 patients were recruited at St Marys Hospital in London, UK. All patients were 50 years or older. HIV+ individuals were able to participate if they had been on ART and had a low or undetectable HIV-1 viral load (<200 copies/ml). Exclusion criteria included: being female, inability to give informed consent, life expectancy <6 months, known coagulation disorder or taking anti-coagulant medication, known or suspected neuromuscular disorder of a genetic basis, and being unable to walk 4 meters (including with a walking aid). Further study details are in the MAGMA study protocol (**Appendix 1**).

Patient details for the MAGMA study subjects are described in **Table 3.1**, with delineation as to whether individuals were recruited as part of the MAGMA study or as part of the SMMFA study described in the following section.

All participants completed a standardised interview and any missing clinical information as well as $CD4^+$ lymphocyte count, HIV diagnosis, ART history and viral load were identified and confirmed through patient medical records where available. Laboratory results were the most recent values available. The presence or absence of the following comorbidities was self-reported and subsequently confirmed through medical records: stroke and CVD, neuropathy, diabetes, dementia, cancer, renal disease, fractures, hepatitis, peripheral vascular disease, joint disease or replacements, osteoporosis, and falls. Medications were self-reported and confirmed through medical records. In addition, patients underwent a dual-energy X-ray absorptiometry (DXA) scan in order to assess body composition and muscle mass . Patients were also asked to undertake a range of tests such as walking, grip strength, standing/sitting, and stair climb in order to assess frailty, sarcopenia and physical capabilities. In addition, percutaneous muscle biopsies were acquired from all 45 patients for research purposes and stored at -80°C.

3.2.2 Skeletal muscle mitochondrial function and ART (SMMFA) study

Samples were obtained from the Newcastle Academic Health Partners Biobank. Samples had previously been collected under REC and HRA approved research protocols and subsequently stored in the Biobank under REC approval 12/NE/0395 and 17/NE/0361. Donors had given prior consent for retention of residual tissue for the purposes of future research. Research activity on these samples was approved by the Biobank oversight committee and was conducted under REC approval 17/NE/0015 (**Appendix 5**).

Skeletal muscle samples were taken by tibialis anterior (TA) biopsy from adult PLWH (n = 37) for research purposes and obtained through the Newcastle Academic Health Partners Bioresource, with patients giving prior written consent. TA biopsies were stored at -80°C. **Table 3.1** describes the patient cohort, with delineation as to whether patients were recruited as part of the SMMFA study or MAGMA study described above.

Subjects were classified into three groups depending on whether they had been treated with ART and if so, further grouped depending on whether they had previous or current exposure to certain NRTIs: group 1 (‘naïve’) had no previous exposure to any ART; group 2 (‘contemporary’) had only ever received contemporary NRTIs – tenofovir (TDF), abacavir (ABC), lamivudine (3TC) or emtricitabine (FTC); group 3 (‘historical’) were currently being treated with contemporary NRTIs, but

had previously been exposed to one or more of the older NRTIs known to be associated with mitochondrial toxicity – zidovudine (AZT), zalcitabine (ddC), didanosine (ddI) or stavudine (d4T).

3.2.3 Skeletal muscle biopsies

Skeletal muscle samples were taken by tibialis anterior (TA) biopsy from adult PLWH (n = 37) and obtained through the Newcastle Academic Health Partners Bioresource as part of the SMMFA study, with patients giving prior written consent. In addition, percutaneous biopsies were obtained from PLWH (n = 30) and HIV- individuals (n = 15) as part of the MAGMA study. **Table 3.1** delineates whether an individual was recruited as part of the MAGMA study or SMMFA study.

Control skeletal muscle tissue required for the calibration of the multiplex immunofluorescence for CI, CIV and mitochondrial mass assay was acquired with prior informed consent from the distal part of the hamstring of HIV-uninfected individuals undergoing anterior cruciate ligament (ACL) surgery. Age and gender details for these individuals (n = 3) is described in **Table 3.1**. Approval for this was given by Newcastle biobank (NAHPB reference: 042).

Group	Age	Sex	Ethnicity	Months since diagnosis	Months on ART	Months with untreated HIV	CD4+ (cells/µl)	Nadir CD4+ (cells/µl)	Viral load (copies/ml)	Current treatments	All treatments	^{31}P-MRS	MAGMA	SMMFA
ART naïve	37	M	WB	64	0	64	1165	1033	4300	N/A	N/A	N	N	Y
	45	F	BA	99	0	99	214	214	1050	N/A	N/A	N	N	Y
	49	M	WB	227	0	227	223	199	18900	N/A	N/A	N	N	Y
	46	M	BA	110	0	110	387	328	17000	N/A	N/A	N	N	Y
	27	M	WB	45	0	45	391	283	34300	N/A	N/A	N	N	Y
	50	F	WB	120	0	120	1358	541	40	N/A	N/A	N	N	Y
	32	F	BA	27	0	27	380	380	13900	N/A	N/A	N	N	Y
	53	F	WB	//	0	//	1439	//	40	N/A	N/A	N	N	Y
	34	M	WB	31	0	31	422	389	4700	N/A	N/A	N	N	Y
	32	F	WB	44	0	44	626	522	41600	N/A	N/A	N	N	Y
	24	M	WB	31	0	31	217	197	1250	N/A	N/A	N	N	Y
	27	M	WB	37	0	37	633	438	12700	N/A	N/A	N	N	Y
	23	M	WB	50	0	50	796	451	150	N/A	N/A	N	N	Y
Contemporary NRTI	55	M	WB	96	48	48	503	117	<40	TDF/FTC/ATV/r	TDF/FTC/ATV/r	Y	N	Y
	39	M	WB	40	12	28	417	187	<40	TDF/FTC/EFV	TDF/FTC/EFV	N	N	Y
	39	M	WB	//	//	//	687	405	//	TDF/FTC/EFV	TDF/FTC/EFV	N	N	Y
	62	M	WB	63	62	1	190	56	<40	TDF/FTC/NVP	TDF/FTC/NVP	Y	N	Y
	25	M	WB	311	33	278	729	270	<40	TDF/FTC/ATV/r	TDF/FTC/ATV/r/ABC/3TC	N	N	Y
	66	M	WB	71	26	45	455	287	<40	TDF/FTC/EFV	TDF/FTC/EFV	Y	N	Y

54	M	WB	79	38	41	638	244	<40	TDF/FTC/DRV/r	TDF/FTC/EFV/DRV/r	Y	N	Y
53	M	WB	73	48	25	804	301	<40	TDF/FTC/EFV	TDF/FTC/EFV	Y	N	Y
34	F	BA	21	18	3	265	//	<40	TDF/FTC/EFV	TDF/FTC/EFV	N	N	Y
57	M	WB	145	21	124	432	379	<40	TDF/FTC/EFV	TDF/FTC/EFV	Y	N	Y
61	M	WB	181	95	86	1049	200-350	<20	TDF/FTC/EFV	TDF/FTC/EFV/LPV/r	N	Y	Y
57	M	WB	269	151	118	259	100-200	<20	ABC/3TC/DRV/r	ABC/3TC/DRV/r/EFV/TDF/FTC	N	Y	Y
71	M	WB	87	86	1	549	100-200	31	TDF/FTC/EFV/ABC /3TC/DTG	TDF/FTC/EFV/ABC/3TC/DTG/RPV	N	Y	Y
52	M	WB	96	82	14	//	>350	//	TDF/FTC/RPV	TDF/FTC/RPV/EFV	N	Y	Y
60	M	WB	266	99	167	584	0-100	52	ABC/3TC/DTG	ABC/3TC/DTG/TDF/FTC/ATV/r	N	Y	Y
62	M	WB	28	28	0	773	>350	63	TDF/FTC/DRV/c	TDF/FTC/DRV/c/r	N	Y	Y
54	M	WB	155	155	0	744	100-200	355	ABC/3TC/DTG	ABC/3TC/DTG/TDF/FTC/RAL/MVC/NVP	N	Y	Y
51	M	WB	99	//	99	598	200-350	118	TDF/FTC/EFV	TDF/FTC/EFV	N	Y	Y
54	M	WB	81	22	59	1111	>350	<20	TDF/FTC/RAL	TDF/FTC/RAL	N	Y	Y
53	M	WB	152	83	69	669	200-350	<20	TDF/FTC/RPV	ABC/3TC/TDF/FTC/RPV	N	Y	Y
68	M	WB	373	65	308	878	0-100	<20	ABC/3TC/DTG/TP V/DTG/r	ABC/3TC/DTG/TPV/TDF/FTC/r	N	Y	Y
50	M	WB	33	32	1	746	0-100	188	TDF/FTC/DRV/r	TDF/FTC/DRV/r	N	Y	Y
56	M	WB	135	134	1	388	0-100	350	TDF/FTC/EFV	TDF/FTC/EFV	N	Y	Y
54	M	WB	283	160	123	624	0-100	<20	ATV/c	TDF/IDV/ATV/c	N	Y	Y
65	M	WB	297	120	157	781	>350	<20	TDF/FTC/DTG	TDF/FTC/DTG/EFV	N	Y	Y
60	M	WB	176	99	77	//	200-350	<20	TDF/FTC/DRV/c	TDF/FTC/DRV/c	N	Y	Y
53	M	WB	141	126	15	568	200-350	74	TDF/FTC/NVP	TDF/FTC/NVP	N	Y	Y

	51	M	WB	64	60	4	446	200-350	63	TDF/FTC/RAL	TDF/FTC/RAL	N	Y	Y
	65	M	WB	162	6	156	737	>350	105	ABC/3TC/DTG	ABC/3TC/DTG	N	Y	Y
Historical NRTI	71	M	WB	130	130	0	530	//	<40	TDF/FTC/EFV	DDI/AZT/3TC/EFV/TDF/FTC	Y	N	Y
	62	M	WB	299	248	51	370	//	<40	DRV/r/MVC/RAL	AZT/DDC/3TC/SQV/IDV/DDI/D4T/ABC/EFV/APV/NFV/HU/LPV/r/TDF/T20/FTC/NVP/DRV/r/MVC/RAL	N	N	Y
	63	M	WB	238	221	17	438	//	<40	ABC/3TC/NVP	AZT/DDI/D4T/3TC/DDC/IDV/NVP/ABC	Y	N	Y
	49	M	WB	193	193	0	762	120	<40	TDF/FTC/ATV/r	AZT/DDI/D4T/3TC/SQV/NVP/IDV/NFV/ABC/TDF/LPV/FTC/ATV/r	Y	N	Y
	48	M	WB	158	151	7	872	10	<40	TDF/ABC/NVP	AZT/DDI/D4T/3TC/RTV/NVP/IDV/DDC/ABC/ATV/r/TDF	Y	N	Y
	54	M	WB	96	96	0	//	//	//	DDI/3TC/NVP	AZT/3TC/EFV/DDI/NVP	N	N	Y
	62	M	WB	284	202	82	422	//	<40	ABC/NVP/LPV/r	SQV/AZT/DDC/3TC/D4T/DDI/IDV/ABC/NVP/NFV/LPV/r	Y	N	Y
	50	M	WB	140	138	2	669	0	<40	TDF/FTC/NVP	AZT/D4T/IDV/NFV/SQV/3TC/NVP/DDI/TDF/FTC	N	N	Y
	56	M	BA	240	224	16	401	150	97	TDF/FTC/ETR/DRV/r	AZT/DDC/SQV/3TC/IDV/D4T/NVP/DDI/ABC/LPV/r/TDF/ATV/r/FPV/r/DRV/r/MVC/FTC	Y	N	Y
	45	M	WB	165	146	19	592	305	<40	RAL/ABC/ATV/r	D4T/3TC/NVP/DDI/IDV/ABC/ATV/r/RAL	Y	N	Y
	51	M	WB	236	164	72	559	327	<40	TDF/FTC/EFV	AZT/DDI/RTV/NFV/TDF/FTC/EFV	Y	N	Y
	74	F	WB	200	182	18	825	//	<40	TDF/FTC/EFV	AZT/DDI/D4T/SQV/TDF/3TC/EFV/FTC	Y	N	Y
	60	F	WB	145	144	1	666	96	<40	ABC/3TC/EFV	D4T/ABC/EFV/3TC	Y	N	Y
	63	F	WB	182	153	29	865	300	<40	TDF/FTC/EFV	D4T/3TC/NVP/NFV/EFV/AZT/TDF/FTC	Y	N	Y
	54	M	WB	246	241	5	659	100-200	<20	TDF/FTC/EFV	AZT/3TC/ddI/SQV/TDF/FTC/EFV	N	Y	Y
	58	M	WB	252	240	12	994	200-350	<20	TDF/FTC	AZT/3TC/TDF/FTC	N	Y	Y
	62	M	WB	265	33	232	247	100-200	<20	ABC/3TC/DTG	AZT/ABC/3TC/DTG/TDF/LPV/r	N	Y	Y
	61	M	WB	444	163	281	571	0-100	<20	TDF/FTC/DRV/EFV/RAL/r	ddC/TDF/FTC/DRV/EFV/RAL/NVP/NFV/ATV/TAF/r	N	Y	Y

	55	M	WB	314	85	229	650	>350	<20	TDF/FTC/NFV	AZT/3TC/TDF/FTC/NFV	N	Y	Y
	56	M	WB	227	156	71	589	0-100	83	TDF/FTC/ATV/r	AZT/3TC/TDF/FTC/ATV/NFV/EFV/ddI/FPV/ATV/r	N	Y	Y
	85	M	WB	306	253	53	451	100-200	30	ABC/3TC/DTG	AZT/ddI/d4T/IDV/TDF/ABC/3TC/DTG	N	Y	Y
	70	M	WB	200	184	16	357	0-100	<20	TDF/FTC/NVP	AZT/3TC/TDF/FTC/NVP	N	Y	Y
	70	M	WB	355	236	119	738	//	<20	DRV/r	AZT/ddC/3TC/SQV/ DRV/r	N	Y	Y
	67	M	WB	124	123	1	486	0-100	84	TDF/FTC/NVP	AZT/3TC/EFV/ddC/DRV/r/ TDF/FTC/NVP	N	Y	Y
	54	M	WB	196	97	99	1118	200-350	<20	TDF/FTC	AZT/3TC/TDF/FTC	N	Y	Y
HIV-	50	M	WB	//	//	//	//	//	//	//	//	N	Y	N
	70	M	WB	//	//	//	//	//	//	//	//	N	Y	N
	51	M	MR	//	//	//	//	//	//	//	//	N	Y	N
	70	M	WB	//	//	//	//	//	//	//	//	N	Y	N
	52	M	WB	//	//	//	//	//	//	//	//	N	Y	N
	58	M	WB	//	//	//	//	//	//	//	//	N	Y	N
	69	M	WB	//	//	//	//	//	//	//	//	N	Y	N
	51	M	WB	//	//	//	//	//	//	//	//	N	Y	N
	59	M	WB	//	//	//	//	//	//	//	//	N	Y	N
	57	M	WB	//	//	//	//	//	//	//	//	N	Y	N
	62	M	WB	//	//	//	//	//	//	//	//	N	Y	N
	60	M	WB	//	//	//	//	//	//	//	//	N	Y	N
	63	M	WB	//	//	//	//	//	//	//	//	N	Y	N
	54	M	BA	//	//	//	//	//	//	//	//	N	Y	N
	69	M	WB	//	//	//	//	//	//	//	//	N	Y	N

Control ACL	24	M	//	//	//	//	//	//	//	//	//	N	Y	Y
	20	M	//	//	//	//	//	//	//	//	//	N	Y	Y
	22	M	//	//	//	//	//	//	//	//	//	N	Y	Y

Table 3.1 – Cohort characteristics. *WB (white British); BA (black African); N/A (not applicable); TDF (tenofovir disoproxil fumarate); FTC (emtricitabine); /r (ritonavir boosted); ATV (atazanavir); EFV (efavirenz); NVP (nevirapine); ABC (abacavir); 3TC (lamivudine); DRV (darunavir); ddI (didanosine); AZT (zidovudine); MVC (maraviroc); RAL (raltegravir); ddC (zalcitabine); SQV (saquinavir); IDV (indinavir); d4T (stavudine); APV (amprenavir); NFV (nelfinavir); HU (hydroxyurea); LPV (lopinavir); T20 (enfuvirtide); RTV (ritonavir); ETR (etravirine); Y = yes; N = no; // = missing value.*

3.2.4 Mitochondrial disease patients

In order to qualitatively contextualise the level of skeletal muscle mitochondrial dysfunction in the HIV+ and HIV- individuals of the MAGMA study, post-mortem percutaneous muscle biopsies were acquired from mitochondrial disease patients (**Table 3.2**) from the Newcastle Mitochondrial Research Biobank (REC - 16/NE/0267) and stored at -80°C until use.

Patient	Age	Gender	Genotype	Phenotype
1	80	Male	p.T251I/p.P587L and p.A467T ***POLG***	CPEO
2	52	Male	Homozygous p.(Ala467Thr) ***POLG***	Neuropathy; CPEO; progressive sensory ataxia

Table 3.2 – Mitochondrial disease patient characteristics*. Both patients had confirmed mitochondrial disease, with varying mutations in the nDNA-encoded maintenance gene POLG. Both patients were decease. CPEO = chronic progressive external ophthalmoplegia.*

3.2.5 Renal mitochondrial function study

Renal biopsies were collected as diagnostic procedures, with additional consent obtained for subsequent research use of the tissue. These samples were supplied in anonymised form by the Cellular Pathology department of the Royal Free Hospital, London. The research performed on these samples as part of this thesis was conducted under REC permission 17/NE/0015.

Percutaneous biopsies were taken from PLWH (n = 6) (supplied as residual diagnostic tissue from Royal Free Hospital London (RFH) Cellular Pathology Department) and open renal biopsies were taken from HIV- individuals (n = 5) (supplied by Dr Ashwin Sachdeva and Manchester University NHS Biobank as residual diagnostic tissue). All biopsies were formalin-fixed and paraffin-embedded.

Of the PLWH, four were being treated with an ART regimen including TDF at the time of biopsy, while one had never been exposed to TDF, and clinical information was missing for one subject (**Table 8.1**). Of the four TDF-treated PLWH, only patient 3 had discontinued TDF treatment.

Aside from their age, race and gender, little information was given to us about the HIV- control subjects. Biopsies came from 'normal' tissue adjacent to explanted renal masses, however, I did not know whether these individuals had been diagnosed with any renal pathologies and I have no information about potential co-morbidities or other adverse factors such as certain medications.

3.3 MAGMA study protocol and assessment of adverse ageing phenotypes

3.3.1 Clinical interview

All participants (n = 45), recruited in both Newcastle (n = 38) and London (n = 7), were asked to complete a health questionnaire during the sole study visit (**Appendix 2**). This was carried out by a clinical researcher and data was made available for examination alongside biological samples.

This health questionnaire included: general questions about age, country of birth, ethnicity and sexual orientation; lifestyle questions about smoker status, whether they drink alcohol, and how many units a week, as well as whether they had used recreational drugs in the last 6 months, and which ones.

Participants where then asked to list whether they suffered from any medical conditions including: heart disease, peripheral vascular disease, stroke, liver disease, diabetes, cancer, joint disease, fractures, osteoporosis, and falls. In addition, participants were asked to list what medications they were currently prescribed or buying over-the-counter.

Finally, HIV+ participants (n = 30) were asked to list what HIV treatments they were currently or have previously been on, as well as when they started and finished the respective treatments. In addition, HIV+ participants were asked when they were first diagnosed with HIV, when they think they first became HIV positive, and what their lowest CD4 count was (either: 0-100; 100-200; 200-350, or more than 350 copies/µl). This information was subsequently confirmed through medical records where available.

3.3.2 Determination of frailty

A frailty phenotype was assessed using a modified five FFP criteria as previously described by Onen and colleagues (2009). Cut-offs for weakness and slow walking time are described in **Table 3.3**.

For the self-reported unintentional weight loss, participants were asked (1) whether their weight had increased, decreased, or stayed the same in the last 12 months?; (2) if 'decreased', was the weight loss intentional?; (3) if 'yes', how much weight did they lose, in kg or lbs? Note, answers in lbs were covered to kg (1lbs = 0.45kg).

For self-reported low physical activity, participants were asked whether their health limited their ability to do vigorous activities such as running or lifting heavy objects (**Table 3.3**).

For self-reported exhaustion, participants were asked to confirm whether 'rarely or none of the time (<1 day)', 'some or a little of the time (1-2 days)', 'occasionally or a moderate amount of time (3-4 days)', or 'most or all of the time (5-7 days)' was most appropriate for the following two questions: (1) everything I did was an effort; (2) I could not get going (**Table 3.3; Appendix 2**).

Missing clinical and HIV-related information were later identified and confirmed through patient medical records where available. Laboratory results were the most recent values available.

	FFP criteria	Definition
Self-reported	Low physical activity	When subjects answer 3 to questions regarding whether their health limits their ability to conduct vigorous activities: 1 = not at all; 2 = yes, limited a little; 3 = yes, limited a lot
	Exhaustion	When subjects answer 2 or 3 to either statement: How often have you felt that: (1) Everything you did was an effort (2) I could not get going 0 = rarely (<1 day); 1 = some of the time (1-2 days); 2 = occasionally (3-4 days); 3 = most of the time (5-7 days)
	Unintentional weight loss	>4.5kg/10 lbs weight loss in the past 12 months or <5% of previous year's body weight
Clinical assessment	Weak grip strength	Male BMI (kg/m^2) / Kg ≤24 / ≤29 24.1-26.0 / ≤30 26.1-28.0 / ≤30 >28 / ≤32
	Slow walking time	Male height (cm) / seconds ≤173 / ≥7 >173 / ≥6

Table 3.3 – Diagnostic criteria for assessing frailty.

3.3.3 Short Physical Performance Battery (SPPB)

Assessment of physical function was done by a SPPB, which consisted of a repeat chair stand (recorded as the time taken in seconds to complete 5 and 10 stands without using their arms); standing balance test (recorded as the time - up to 30 seconds – that the participant can hold a side-by-side, semi-tandem, tandem and single-leg stands) (**Figure 3.1**); hand grip assessment (the average of three dominant hand grip measurements using a hand dynamometer, measured in kilograms (kg)) and 4m walk (recorded as the time taken, in seconds, for the participant to walk 4 meters in a straight line. Results were derived from the average of 3 repeats). SPPB was scored using a binary tally and scored out of 12 (**Table 3.4**), with 0 points indicating the individual's inability to complete a task and 4 points demonstrating the optimal performance in the task (Guralnik *et al*., 1994) (**Appendix 3**).

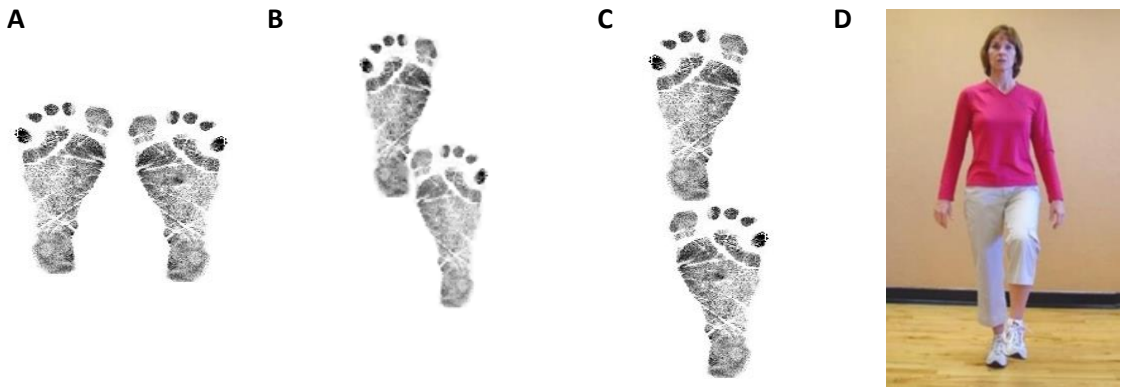

Figure 3.1 – Foot positions in the standing balance test component of the SPPB*. (**A**) side-by-side, (**B**) semi-tandem, (**C**) tandem and (**D**) single-leg stand.*

Characterisation	Score
Robust	**> 11**
Intermediate physical performance	**9-11**
Low physical performance	**< 9**

Table 3.4 – SPPB scoring classification.

3.3.4 MET score

Metabolic equivalent (MET) expenditure per week was calculated as an additional surrogate for physical performance assessment. Patients were asked to answer how many days, hours and minutes a week they performed vigorous physical activities such as heavy lifting, aerobics or fast cycling; moderate physical activities such as carrying light loads, cycling at a moderate pace or doubles tennis etc; walking; and sitting (**Appendix 4**). Results were calculated as described in Ainsworth *et al*. (1993) and Ainsworth *et al*. (2000).

3.3.5 Classification of sarcopenia

According to the EWGSOP, sarcopenia can be classified in the clinical and research setting based on analyses of muscle mass, muscle strength and physical performance (Cruz-Jentoft *et al.* 2019).

In our study, (1) muscle mass was quantified as appendicular skeletal muscle mass by dual-energy X-ray absorptiometry (DXA). The cut-off point for this variable was having an appendicular skeletal muscle mass/height^2 index (ASMI) of 7.26kg/m^2. Subjects with an AMSI below the cut-off point were defined as having abnormal muscle mass; (2) muscle strength was assessed using a Jamar handheld dynamometer, with cut-off points described in **Table 3.3**, and (3) physical performance was assessed through the SPPB, as described in **Section 3.3.3**.

Patients were classified as having presarcopenia if they had abnormal results for muscle mass; sarcopenia if they had abnormal results for muscle mass as well as either muscle strength or physical performance, and severe sarcopenia if they had abnormal results from all three criteria (**Table 3.5**).

Status	Decreased muscle mass	Decreased muscle strength	Physical function decline
Presarcopenia	X	-	-
Sarcopenia	X	X	-
Severe sarcopenia	X	X	X

Table 3.5 – Variables used to characterise the presence of presarcopenia, sarcopenia and severe sarcopenia, as defined by the EWGSOP. *(Cruz-Jentoft et al*., 2019).

3.4 Immunofluorescence and fluorescence histochemistry

3.4.1 Cryosectioning and microtome sectioning

Snap-frozen skeletal muscle biopsies were cut into sections of various thicknesses onto glass slides using the Cryo-star HM 560 cryostat (Lecia), which was maintained at -20˚C. Sections were then left to air-dry at room temperature for one hour and then stored at -80˚C until required for use. After use, sections were stored at -20˚C.

Formalin-fixed paraffin-embedded (FFPE) renal biopsies were sectioned at 4µm, 10µm and 15µm onto glass slides using a microtome and left to settle for 24 hours at 37˚C before being stored at 4˚C.

3.4.2 Multiplex immunofluorescence for quantification of mitochondrial protein level in human skeletal muscle

Multiplex immunofluorescence using antibodies for subunits of mitochondrial OXPHOS complexes and a mitochondrial outer membrane protein was carried out on frozen muscle sections (10µm) in order to quantify the levels of ETC complexes I and IV as well as mitochondrial mass in individual myofibres. Complex I was detected by an antibody against the NDUFB8 subunit and complex IV was detected with an antibody against MTCO1. An antibody against Porin (VDAC1) was used to quantify mitochondrial mass and the basement membrane glycoprotein laminin was used to label myofibril boundaries (**Table 3.6**). Firstly, the sections were air-dried at room temperature (RT) before fixation in cold 4% paraformaldehyde (PFA) (Sigma) in phosphate buffered saline (PBS) (ChemCruz) for 3 minutes. After washes for 3 x 5 minutes in tris-buffered saline with Tween 20 (TBST), the antigenic sites were exposed through a graded methanol series (Fisher Chemical): 10 minutes 70% methanol, 10 minutes 95% methanol, 20 minutes 100% methanol, 10 minutes 95% methanol, 10 minutes 75% methanol, then washed 3 x 5 minutes in TBST. Sections were then incubated in 10% normal goat serum (NGS) to prevent non-specific protein binding before another 3 x 5 minute wash cycle. Next, endogenous biotin was blocked by incubating the sections for 15 minutes in avidin, followed by 2 x 5 minute washes, then 15 minutes in biotin from the Avidin/Biotin blocking kit (Vector Laboratories). Sections were then incubated in the primary antibody cocktail diluted in 10% NGS overnight in a 4°C humidified chamber (**Table 3.6**). Initially on day 2 the sections were washed in TBST for 3 x 5 minute wash cycles before being incubated in the secondary antibody cocktail for two hours in a humidified chamber at 4°C. All secondary antibodies were diluted in 10% NGS. Sections were then incubated in streptavidin-conjugated Alexa 647 (Thermo Fisher Scientific) at 1:100 diluted in 10% NGS for two hours in at 4°C in a dark humidified chamber (**Table 3.7**). After a final round of 3 x 5 minute TBST

washes, the sections were mounted in Prolong Gold Antifade Mountant (Thermo Fisher Scientific) and stored at -20°C until required for imaging.

3.4.3 Multiplex immunofluorescence for quantification of mitochondrial protein level in human renal tissue

A novel multiplex immunofluorescence assay was used to quantify levels of complexes I, III, IV and V of the ETC as well as mitochondrial mass in proximal tubules.

Serial 4um renal sections were cut and allowed to air dry for an hour at RT, deparaffinised in 2 changes of Histoclear then taken to water for 5 minutes. Next, the sections were rehydrated in a graded ethanol (EtOH) series (10 minutes 100% EtOH, 5 minutes 95% EtOH, 5 minutes 70% EtOH) then taken to water for 5 minutes. Antigen retrieval of the sections was performed with 1mM EDTA pH8.0 buffer for 40 minutes. Sections were incubated in 10% NGS for 1 hour to block endogenous protein activity and then covered in the primary antibody cocktail (**see Table 3.6**) overnight at 4°C.

Following washes in TBST, sections were incubated in a secondary antibody cocktail for 2 hours at RT (**Table 3.7**). Sections were then washed again in TBST, and for the CI and CIV assay, were incubated in the tertiary antibody cocktail for 2 hours at room temperature then washed in TBST. All sections were then subjected to incubation in 0.1% Sudan Black B (BDH) for 25 minutes in order to minimise autofluorescence, then washed in deionised water (dH_2O) for 10 minutes. Sections were then mounted in ProLong Gold Antifade Mountant (Thermo Fisher Scientific) and stored at -20°C until imaged. Separate panels were used to analyse mitochondrial OXPHOS complexes I/IV (CI, CIV) and complexes III/V (CIII, CV) as described in tables below.

Assay	Antibody	Target	Host	Isotype	Manufacturer	Product #	Dilution
CI + CIV	NDUFB8	Mitochondrial complex I subunit	Mouse	IgG1	Abcam	ab110242	1:100
CI + CIV	MTCO1	Mitochondrial complex IV subunit	Mouse	IgG2a	Abcam	ab14705	1:200
CIII + CV	UQCRFS1	Mitochondrial complex III subunit	Mouse	IgG2b	Abcam	ab14746	1:200
CIII + CV	ATPB	Mitochondrial complex V subunit	Mouse	IgG1	Abcam	ab14730	1:200
Both	VDAC1	Mitochondrial mass marker - Porin	Mouse	IgG2b	Abcam	ab14734	1:200
Both (Skeletal muscle)	Laminin	Myofibre boundary	Rabbit	IgG	Sigma	Sigma L9393	1:50

Table 3.6 – Antibodies used in the primary antibody cocktail for multiplex immunofluorescence staining of human skeletal muscle (CI/CIV assay) and human renal tissue (CI/CIV and CIII/CV assays).

Assay	Antibody	Conjugate	Target	Host	Isotype	Specificity	Manufacturer	Dilution
CI + CIV	Anti-IgG1-biotin	-	NDUFB8	Goat	IgG1	Mouse	Jackson ImmunoResearch Laboratories 115-065-205	1:100
CI + CIV	AlexaFluor 647	Streptavidin	Biotin	Goat	IgG1	Mouse	ThermoFisher Scientific S-32357	1:200
CI + CIV	AlexaFluor 488	-	MTCO1	Goat	IgG2a	Mouse	ThermoFisher Scientific A-21131	1:200
CIII + CV	AlexaFluor 647	-	UQCRFS1	Goat	IgG2b	Mouse	ThermoFisher Scientific A-21121	1:200
CIII + CV	AlexaFluor 488	-	ATPB	Goat	IgG1	Mouse	ThermoFisher Scientific A-21242	1:200
Both	AlexaFluor 546	-	VDAC1	Goat	IgG2b	Mouse	ThermoFisher Scientific A-21143	1:200
Both (Skeletal muscle)	AlexaFluor 405	-	Laminin	Goat	IgG	Rabbit	ThermoFisher Scientific A-31556	1:100

Table 3.7 – Antibodies used in the secondary and tertiary antibody cocktail for multiplex immunofluorescence staining of human skeletal muscle (CI/CIV assay) and human renal tissue (CI/CIV and CIII/CV assays).

3.4.4 Image acquisition and determination of ETC complex activity in skeletal muscle

Fluorescent images were acquired using a Zeiss Axio Imager M1 and Zen 2011 (blue edition) software with a Monochrome Digital Camera (AxioCam MRm) at 20x magnification. Filter cubes for Alexa Fluor dyes at wavelengths 405nm, 488nm, 546nm and 647nm were used for laminin, MTCO1, VDAC1 and NDUFB8 respectively. Exposure time was set for the four channels and maintained between cases in order to avoid pixel saturation. Images were tiled and then processed at 16-bit czi files and exported as Tagged-Image File Format (TIFF) files. The tiled images were then processed by Zen 2011 (blue edition) software using the stitching function.

Stitched images were analysed with the Quadruple Immunofluorescence Analyser developed in our lab (Rocha *et al*., 2015). Briefly, the raw intensity values for MTCO1, VDAC1 and NDUFB8 in individual myofibres were corrected for background signal by subtracting the mean optical density (OD) from the no primary control (NPC) for each fluorophore, respectively.

An in-house R Shiny script software was then used to generate z-scores indicating how many standard deviations a fibre deviated from the control population, and was initially used to assess mitochondrial mass in the patient myofibres. Individual myofibres were classified into mitochondrial mass groups depending on their z-score: ‘very low’ (VDAC1_z < -3); ‘low’ (-3 < VDAC1_z < -2); ‘normal’ (-2 < VDAC1_z < +2); ‘high’ (+2 < VDAC1_z < +3) and ‘very high’ (3 < VDAC1_z). Individual myofibres were then classified into groups based on their z-scores for MTCO1 and NDUFB8: ‘positive’ (z > -3); ‘intermediate positive (+)’ (-3 > z > -4.5); ‘intermediate negative (-)’ (-4.5 > z > -6) and ‘deficient’ (z < -6).

3.4.5 Image acquisition and determination of ETC complex activity in renal tissue

Fluorescent images were acquired using a Zeiss Axio Imager M1 and Zen 2011 (blue edition) software with a Monochrome Digital Camera (AxioCam MRm) at 20x magnification. Filter cubes for Alexa Fluor dyes at wavelengths 405nm, 488nm, 546nm and 647nm were used for DAPI, MTCO1 or ATPB, VDAC1 and NDUFB8 or UQCRSF1, respectively. Exposure time was established from a case with the putatively highest signalling intensity for the four channels and maintained between cases. As the renal tissue from HIV+ subjects was taken by needle biopsy, the sections were small enough to tile, whereas the open biopsy sections taken from HIV- subjects were much larger and so were imaged as snaps. 40 PCTs were randomly manually identified per subject, except for patient 6 where a maximum of 23 PCTs were present. Each PCT was marked in order to prevent multiple imaging of the same PCT.

Stitched images were analysed with the Quadruple Immunofluorescence Analyser developed in the Wellcome Centre for Mitochondrial Research (Rocha *et al*., 2015). Briefly, the raw intensity values for MTCO1, ATPB, VDAC1, UQCRFS1 and NDUFB8 in individual PCTs was corrected for background signal by subtracting the mean OD from the NPC for each fluorophore, respectively.

An in-house R Shiny based web application was then used to generate z-scores indicating how many standard deviations a PCT deviated from the control population. This was initially used to assess mitochondrial mass in the patient PCTs. Individual PCTs were then classified into mitochondrial mass groups depending on their z-score: 'very low' (VDAC1_z < -3); 'low' (-3 < VDAC1_z < -2); 'normal' (-2 < VDAC1_z < +2); 'high' (+2 < VDAC1_z < +3) and 'very high' (3 < VDAC1_z). Individual PCTs were then classified into groups based on their z-scores for MTCO1, NDUFB8, UQCRFS1 and ATPB. Respective z-scores were calculated after normalisation to VDAC1 staining intensity: 'positive' (z > -3); 'intermediate positive (+)' (-3 > z > -4.5); 'intermediate negative (-)' (-4.5 > z > -6) and 'deficient' (z < -6). Subsequently, the 'deficient', 'intermediate -' and 'intermediate +' groups were pooled together to create the 'deficient' group (i.e. z < -3 = deficient).

3.4.6 Duplex fluorescence histochemistry for the quantification of intramyocellular lipid accumulation

Fluorescence histochemistry was carried out on 10µm frozen transverse muscle sections in order to detect and quantify intramyocellular lipid droplets in skeletal muscle fibres. BODIPY (493/503) (ThermoFisher) is a lipid-soluble fluorescent dye used to detect and measure intramyocellular lipid droplets, and was diluted in DMSO to create a stock at a concentration of 1mg/mL. Cryosections were air-dried at RT for 30 minutes and then fixed by incubation in 3.7% formaldehyde (ChemCruz) in PBS for 30 minutes at RT. Sections underwent a wash cycle of PBS for 5 minutes, followed by 5 minutes in 0.25% Triton x-100 (ThermoFisher) diluted in PBS. Next, the sections were incubated in IgG Goat-anti-rabbit Laminin antibody (Sigma) diluted at 1:100 in 0.05% Tween 20/PBS, for 60 minutes in a humidified chamber. Sections then underwent another wash cycle followed by incubation in the secondary cocktail (**Table 3.8**) for 90 minutes in a dark humidified chamber at RT. Following a final wash cycle sections were mounted in Molwiol 4-88 (Sigma) and stored at -20˚C.

Primary antibody	Isotype	Product #	Dilution	Secondary antibody/dye	Isotype	Product #	Dilution
Laminin	IgG	Sigma L9393	1:100	AlexaFluor 405	IgG	ThermoFisher Scientific A-31556	1:200
-	-	-	-	BODIPY (493/503)	-	ThermoFisher Scientific D3822	1:100

Table 3.8 – Antibodies and dyes used in the duplex fluorescence histochemistry assay for the quantification of intramyocellular lipid accumulation.

3.4.7 Image acquisition and analysis for quantification of intramyocellular lipid accumulation

Fluorescent images were acquired using a Zeiss Axio Imager M1 and Zen 2011 (blue edition) software with a Monochrome Digital Camera (AxioCam MRm) at 20x magnification. Filter cubes at wavelengths 405nm and 488nm were used for laminin and BODIPY (493/503) respectively. Exposure time for the two channels was set and maintained between cases in order to remove pixel saturation. Images were then tiled and processed at 16-bit czi files and exported as TIFF files and then processed by Zen 2011 (blue edition) software using the stitch function.

Stitched images were then analysed on the Zen 2011 (blue edition) software. Briefly, each individual fibre was qualitatively classified into one of four categories depending on the extent of BODIPY staining coverage and staining intensity – BODIPY+++; BODIPY++; BODIPY+ and BODIPY-.

3.4.8 Duplex immunofluorescence for quantification of Pax7^{+} satellite cells

Duplex immunofluorescence was carried out on 10µm transverse muscle cryosections in order to quantify the frequency of quiescent Pax7^{+} muscle satellite cells. Cryosections were air-dried for 1 hour at RT before fixation in cold 4% PFA for 4 minutes. Sections were then washed in a cycle of three, 5 minute washes in PBST before endogenous protein was blocked by incubation in 5% NGS/0.2% Triton-x100 diluted in PBST for 1 hour at RT. Sections were then washed for 5 minutes in PBST before the Pax7 primary antibody (DSHB) was applied and sections were incubated overnight at 4˚C in a dark humidified chamber (**Table 3.9**). After incubation with Pax7 primary antibody, the sections went through a washing cycle before the secondary antibody cocktail (diluted in 10% NGS) was applied for 2 hours at RT in a humidified chamber. Sections were then washed again in PBST and

incubated with Hoerst for 15 minutes in a dark humidified chamber in order to counter stain for nuclei. Finally, the sections went through another wash cycle, mounted using ProLong Gold Antifade Mountant (Thermo Fisher Scientific) and then stored at -20˚C.

Primary antibody	Isotype	Product #	Concentration	Secondary antibody	Isotype	Product #	Dilution
Pax7	IgG1	DSHB	8.5µg/ml	AlexaFluor 488	IgG1	ThermoFisher Scientific A-21242	1:200
-	-	-	-	Hoerst	-	-	1:1200

Table 3.9 – Antibodies used in the duplex immunofluorescence assay to quantify Pax7⁺ satellite cells.

3.4.9 Image acquisition and analysis for quantification of Pax7⁺ satellite cells

Fluorescent images were acquired using a Zeiss Axio Imager M1 and Zen 2011 (blue edition) software with a Monochrome Digital Camera (AxioCam MRm) at 20x magnification. Filter cubes at wavelengths 405nm and 488nm were used for Hoerst and Pax7, respectively. Exposure time for the two channels was set and maintained between cases in order to remove pixel saturation. Images were then tiled and processed as 16-bit czi files and exported as TIFF files and then processed by Zen 2011 (blue edition) software using the stitch function.

Stitched images were then analysed on Zen 2011 (blue edition) software. Here, a Pax7⁺ satellite cell was confirmed by co-localised staining of Pax7 and nuclei identified Hoerst. The number of Pax7⁺ satellite cells was then quantified and expressed as the proportion of Pax7⁺ satellite cells per 100 fibres. These values were then $\log_{10}$ transformed in order to normalise the data sets.

3.4.10 Multiplex immunofluorescence for fibre type quantification

A multiplex immunofluorescence assay to quantify the proportions of fibre types I, IIa and IIx, as well as their cross-sectional area, was performed on patients biopsies. 10µm transverse cryosections were removed from -80˚C and air-dried for 1 hour at room temperature before fixation with cold 4% PFA for 3 minutes. Sections underwent a 3 x 5 minute washing cycle in TBST and then incubated in 10% NGS for 1 hour at room temperature in order to block non-specific protein binding. Following another cycle of washes, the sections were incubated overnight at 4˚C in the primary antibody cocktail (**Table 3.10**), diluted in 5% NGS. Following another cycle of washes the sections were

incubated in the secondary antibody cocktail (**Table 3.10**) for 90 minutes at RT in a dark humidified chamber. Finally, sections were subjected to a washing cycle and mounted in ProLong Gold Antifade Mountant (Thermo Fisher Scientific) and stored at -20˚C.

Primary antibody	Target	Dilution	Product code	Secondary antibody	Dilution	Product code
BA-F8	Type I	1:100	DSHB 10572253	Anti-IgG2b-488	1:200	Invitrogen A31141
SC-71	Type IIa	1:100	DSHB 2147165	Anti-IgG1-546	1:200	Invitrogen A21123
6H1	Type IIx	1:15	DSHB 2314830	Anti-IgM-647	1:200	Invitrogen A21238
Laminin	Myofibre boundary	1:100	Sigma L9393	Anti-rabbit-405	1:200	Invitrogen A31556

Table 3.10 – Antibodies used in the primary and secondary cocktails for the detection and quantification of fibre types I, IIa and IIx.

3.4.11 Image acquisition and analysis of fibre type quantification

Fluorescent images were acquired using a Zeiss Axio Imager M1 and Zen 2011 (blue edition) software with a Monochrome Digital Camera (AxioCam MRm) at 20x magnification. Filter cubes at wavelengths 405nm, 488nm, 546nm and 647nm were used for laminin, BE-F8, SC-71 and 6H1 antibodies, respectively. Exposure time for the four channels was set and maintained between cases in order to remove pixel saturation. Images were then tiled and processed as 16-bit czi files and exported as TIFF files, then processed by Zen 2011 (blue edition) software using the stitch function.

Stitched images were then analysed on the in-house R script Quadruple Immunofluorescence Analyser developed in our lab (Rocha *et al*., 2015). Briefly, each individual fibre was qualitatively characterised as one of the three fibre types (I, IIa and IIx) based on staining pattern. In addition, the cross-sectional area (CSA) (μm^2) of each fibre was quantified using the in-house drawing tool.

3.4.12 Preparation of slides for lipofuscin quantification, and image acquisition and analysis

In order to quantify the frequency of, and area (μm^2) covered by lipofuscin granules, 10µm transverse cryo-sections were removed from -80°C storage and air-dried for 1 hour. Sections were then immediately cover-slipped with Prolong gold and stored at -20°C until imaged.

Fluorescent images were acquired using a Zeiss Axio Imager M1 and Zen 2011 (blue edition) software with a Monochrome Digital Camera (AxioCam MRm) at 20x magnification. Filter cubes at wavelengths 546nm and 647nm were used for the identification of autofluorescent lipofuscin granules. Exposure time for the four channels was set and maintained between cases in order to remove pixel saturation. Images were then tiled and processed as 16-bit czi files and exported as TIFF files and then processed by Zen 2011 (blue edition) software using the stitch function.

Stitched images were then analysed on Columbus Image Data Storage and Analysis System software. Briefly, thresholds for the positive identification of lipofuscin granules were set for both 546nm and 647nm channels, and lipofuscin granules were confirmed by co-localisation in both respective channels. Lipofuscin is identifiable by its auto fluorescence across multiple wavelengths. The frequency, as well as CSA (μm^2) covered by co-localised lipofuscin granules was then automatically quantified.

3.5 Histochemistry

3.5.1 Haematoxylin & Eosin histochemistry staining and imaging for renal tissue

FFPE sections (4µm) were dewaxed at 60°C for 1 hour and then immediately deparaffinised in two changes of Histoclear. Next, sections were dehydrated in a graded ethanol series (10 minutes 100% EtOH, 5 minutes 95% EtOH, 5 minutes 70% EtOH) before being taken to water for 10 minutes. Sections were then stained with haematoxylin for 10 minutes then rinsed clear in dH_2O followed by staining with Scott's tap water for one minute in order to blue the nuclei. Sections were then stained with Eosin for one minute for cytoplasmic staining. Finally, sections were rinsed clear in dH_2O then rehydrated through a graded ethanol series (10 dips 70% EtOH, 10 dips 95% EtOH, 20 dips 100% EtOH) followed by two changes of 20 dips in Histoclear, then mounted in DPX. Sections were stored at RT until imaged.

For imaging, sections were imaged using Zeiss Axio Scope A1 (brightfield) at 10x magnification. Sections were tiled and then stitched using the 'stitch' function in Zeiss Zen blue edition to acquire an image of the full section.

3.5.2 Haematoxylin & Eosin histochemistry staining and imaging for skeletal muscle tissue

Haematoxylin & Eosin histochemistry was undertaken in order to identify and quantify the proportions of degenerated and regenerated fibres. Here, 10µm cryosections were removed from -80˚C and air-dried for 1 hour at room temperature. Sections were then initially fixed with cold 4% PFA for 3 minutes and before being rinsed clear in dH_2O. Next, sections were stained with Haematoxylin for 10 minutes in order to stain nuclei and then rinsed clear in dH_2O. Next, sections were washed in Scott's tap water for 1 minute to blue the nuclei and then rinsed clear in dH_2O. Sections were then stained with Eosin for 1 minute in order to stain the cytoplasm. Finally, sections were rinsed clear in dH_2O then rehydrated through an ethanol gradient (10 dips 70% EtOH, 10 dips 95% EtOH, 20 dips 100% EtOH) followed by 2 changes of 20 dips in Histoclear and mounted in DPX. Sections were stored at RT until imaged.

3.5.3 Masson's trichrome histochemistry for skeletal muscle fibrosis

Masson's trichrome histochemistry was undertaken in order to quantify skeletal muscle fibrosis. 10µm cryosections were removed from -80˚C and air-dried for 1 hour at room temperature. Sections were then initially fixed with cold 4% PFA for 3 minutes and then further fixed in Bouin's Fluid (Sigma), heated to 60˚C for 30 minutes, before being rinsed clear in dH_2O. Next, sections were

stained with Weigert's Iron Haematoxylin (Abcam) for 5 minutes in order to stain nuclei and then rinsed clear in dH_2O. Next, sections were stained for 15 minutes in acid fuscin (Abcam) in order to stain cytoplasm and then differentiated in phoshotunsic acid solution (Abcam) for 10 minutes following a rinse in dH_2O. Sections were then rinsed and incubated in alanine blue (Abcam) for 7 minutes in order to stain collagenous tissue, before being rinsed clear in dH_2O and subsequently differentiated in acetic acid (Abcam) for 3 minutes. Finally, sections were rehydrated through an ethanol gradient (10 dips 70% EtOH, 10 dips 95% EtOH, 20 dips 100% EtOH) followed by 2 changes of 20 dips in Histoclear and mounted in DPX. Sections were stored at RT until imaged.

3.5.4 Succinate dehydrogenase histochemistry

Tissue was subjected to succinate dehydrogenase histochemistry in order to prepare tissue for laser capture microdissection. 15µm serial skeletal muscle cryo-sections were removed from -80°C and left to air dry for one hour. Sections were then rinsed in 1M PBS whilst the succinate dehydrogenase (SDH) reaction medium was prepared: 100µl sodium succinate, 100µl PBS, 10µl sodium azide and 800µl NBT. SDH reaction medium reagents were defrosted in at 55°C. Once prepared, sections were covered with SDH reaction medium and incubated for 40 minutes at 37°C. Sections were then washed in a cycle of three, 5 minute rinses with 1M PBS then dehydrated in an ethanol gradient of 10 minutes in 70%, then 90% then two 10 minute incubations in 100%, followed by two changes in Histoclear and stored at 4°C.

3.5.5 Brightfield microscopy

Brightfield images were acquired using a Zeiss Axio Imager M1 and Zen 2011 (blue edition) software with a chromatic digital camera (AxioCam MRm) at 10x magnification. Exposure time was set and maintained between cases in order to avoid pixel saturation. Images were processed as 16-bit czi files and exported as TIFF files. The tiled images were then processed by Zen 2011 (blue edition) software using the stitching function.

3.6 Laser capture microdissection of single cells

In order to isolate tissue for subsequent quantitative PCR analysis, laser capture microdissection was performed, followed by amplification of isolated tissue lysate.

3.6.1 Single cell lysis buffer and lysate amplification

Lysis buffer (0.5M Tris-HCl, 0.5% Tween 20 and 1% Proteinase K) was made fresh into autoclaved 1.5ml Eppendorf tubes and kept on ice.

Cells were captured into 15µl of lysis buffer and kept on ice. Immediately before amplification, cells were centrifuged on a short cycle and then amplified at 55˚C for 16 hours followed by a 10 minute incubation at 95˚C.

3.6.2 Laser capture microdissection

Cells were isolated from histochemically stained tissue sections by laser capture microdissection using a Ziess Laser Capture Microdissection microscope with Palm Robo v4.6 using either the Closecut + AutoLPC function for glass slides and RoboLPC for membrane slides (Zeiss).

15µl of lysis buffer was added into the cap of two 0.2ml Eppendorf tubes, which were then inserted into the TubeCollector prior to cell isolation.

3.7 Quantitative PCR for the detection of mtDNA mutations

In order to detect and quantify mtDNA mutations in human homogenate tissue, a qualitative real-time PCR (qPCR) assay was utilised. The mitochondrially encoded NADH-dehydrogenase core subunit 1 gene (*MT-ND1*, Genbank accession ID: NC_012920.1) and NADH-dehydrogenase core subunit 4 gene(*MT-ND4,* Genebank accession ID: NC_012920.1) were used respectively as mtDNA targets.

3.7.1 Preparation of PCR reagents

Stock probes (IDT) and primers to be used in qPCR assays were resuspended using Ambion nuclease-free water (ThermoFischer Scientific) under a UV sterilizing PCR cabinet (UVP) to the working concentration of 10µM and the stored at -20˚C.

3.7.2 Generation of qPCR standard templates

Quantitative standards of qPCR assays were prepared by PCR generated templates.

MT-ND1 and *MT-ND4* standards were generated using a control DNA sample. Primer sequences are described in **Table 3.11**.

PCR reactions were performed in a mastermix containing:- 1X MyTaq Reaction Buffer, one unit of MyTaq HS DNA Polymerase (Bioline), 400nM of each respective forward and reverse primer and dH_2O. Approximately 30ng of DNA was loaded into each reaction well of 8-strip PCR tubes (StarLab) and ran on an Applied Biosystems Veriti 96 well thermal cycler (ThermoFischer Scientific). Run conditions were: initial denaturation at 95˚C for one minute followed by 30 cycles of denaturation at 95˚C for 15 seconds and finally annealing at 61˚C for 15 seconds and extension at 72˚C for 10 seconds.

Gene	Amplicon size (BP)	Forward primer sequence (5'-3')	Reverse primer sequence (5'-3')	Annealing temp
MT-ND1	1040	CAGCCGCTATTAAAGGTTCG	AGAGTGCGTCATATGTTGTTX	61
MT-ND4	1072	ATCGCTCACACCTCATATCC	TAGGTCTGTTTGTCGTAGGC	61

Table 3.11 – Primers used to generate the standard templates for the respective genes.

3.7.3 Agarose gel electrophoresis

Amplified template PCR products were pooled together and mixed with Orange G loading buffer (50% glycerol, Orange G powder (Sigma) and 50% water) and loaded into a 1% agarose gel (1g agarose (Bioline) in 100ml 1X TAE buffer and 0.4mg/µl UltraPure ethidium bromide (Invitrogen)). As a ladder, I used a GeneRuler 1kb Plus DNA Ladder (ThermoFischer Scientific) as well as a negative PCR product, both mixed with Orange G dye. Agarose gels were electrophoresed at 75V for one hour in 1X TAE buffer.

3.7.4 Purification and quantification of standards

Agarose gels were imaged with the UVP GelDoc-It imaging system (UVP) and the gel-extracted fragment was extracted with a QIAquick gel extraction kit (Qiagen). Concentrations of the templates were measured using a Nanodrop ND-1000 Spectrophotometer and template DNA copy number concentrations were calculated using **Equation 3.1**. Template DNA was then multiplexed together to obtain a single copy number of 10^{10}ng/µl, then diluted by a factor of 10 to achieve a starting copy number stock of 10^{9}ng/µl. Stock template were then stored at -20˚C.

$$Copy\ number = \left[\frac{C}{(L\ x\ 2\ x\ 300)}\right] x\ A$$

Equation 3.1 – Formula used to calculate the starting copy number stocks (copies/µl)*. C is the DNA concentration in nanolitres, L is the amplicon length in base pairs and A is Avogadro's constant (6.023 x 10^{23}).*

3.7.5 Quantitative PCR for the detection and quantification of large-scale mtDNA mutations

All qPCR reaction plates were set up in a UV hood to minimise DNA contamination. qPCR was performed on a CFX96 Touch Real-Time PCR Detection System (Bio-Rad). mtDNA from the single-cell lysate was quantified using a probe-based multiplex assay targeting mitochondrial *MT-ND1* and *MT-ND4* genes. *MT-ND4* is in the major arc of the mtDNA genome and is usually lost through large-scale mtDNA mutations. In contrast, *MT-ND1* lies on the minor arc as is rarely deleted. Primers for both *MT-ND1* and *MT-ND4* are described in **Table 3.12**. 2µl of DNA lysate from individual muscle fibers were amplified separately in triplicate using the ND1/ND4 combination, mixed with 18µl mastermix: 10µl iTaq (Bio-Rad, catalog #172-5134); 75nM ND1 forward primer; 75nM ND1 reverse primer; 75nM ND4 forward primer; 75nM ND4 reverse primer; 200nM HEX probe; 200nM Cy5 probe; 5.8µl deionised water. Amplification conditions were: three minutes at 95°C (for activation of iTaq), then

39 cycles of 10 seconds at 95°C followed by one minute at 62°C (for probe/primer hybridization and DNA synthesis). We screened for mtDNA deletions in individual myofibres by determining the ratio of *MT-ND1 to MT-ND4* relative to a calibrator sample ($\delta\delta C_t$), as previously described (He *et al*., 2002; Bury *et al*., 2017). We screened for mtDNA depletion in individual cells by considering the calculated starting quantity (SQ) of mtDNA relative to the 5th centile of SQ in CI-normal cells from the same individuals.

Gene	Amplicon size (BP)	Forward primer sequence (5'-3')	Reverse primer sequence (5'-3')	Fluorophore
MT-ND1	111	ACGCCATAAAACTCTTCACCAAAG	GGGTTCATAGTAGAAGAGCGATGG	HEX
MT-ND4	107	ACGCCATAAAACTCTTCACCAAAG	GGGTTCATAGTAGAAGAGCGATGG	Cy5

Table 3.12 – Primers for the qPCR amplification of mitochondrial and nuclear genes used in the large-scale mtDNA deletion assay. *All primers were from Integrated DNA Technologies.*

3.8 Phosphorus magnetic resonance spectroscopy (^{31}P-MRS)

^{31}P-MRS analysis was performed by Dr Brendan Payne (Newcastle University) in a previous study (Payne *et al*., 2014) in order to quantify skeletal muscle oxidative potential *in vivo* in response to short bouts of exercise. Briefly, MR studies were performed on calf muscle using a 3T Intera Achieva magnet (Philips). ^{31}P-MRS measurements were obtained using a calf coil with a voxel within soleus muscle throughout a cycle of: a 1 minute baseline resting period; a 3 minute period of calf flexion exercise at 25% of maximal voluntary contractile force; and a 6 minute recovery period (Trenall *et al*., 2006, Hollingworth *et al*., 2008), which was designed to keep metabolism within the aerobic phase. Analysis was performed in jMRUI v3.0 (Java Magnetic Resonance User Interface) using AMARES with appropriate prior knowledge parameters for skeletal muscle (Naressi *et al*., 2001) and metabolite levels were calculated as previously described (Hollingworth *et al*., 2008). Phosphorylation potential was calculated from the concentration of ATP, buffered at 8.2 mM, and the empirically calculated concentrations of adenosine diphosphate (ADP) and inorganic phosphate (Pi) (**Equation 3.2**) (Harris *et al*., 1974).

$$Phosporylation\ potential = \frac{[ATP]}{[ADP\ x\ Pi]}$$

Equation 3.2 – Formula used to calculate the phosphorylation potential of calm muscle from ^{31}P-MRS analysis.

3.9 Statistical analyses

Statistical analysis was performed in Prism v5.04, IBM SPSS Statistics v23 and Microsoft Excel 2016. Graphs were produced in Prism v5.04.

The chosen sample size for the MAGMA study was well-powered to detect a mean difference of 0.33 $\log_{10}$ between groups (α 0.05, 1-β 0.8) based on past experience of SD for this measure. The sample size was also chosen in order to detect a moderate correlation (r = 0.5) (α 0.05, 1-β 0.8) between treatment parameters and mitochondrial dysfunction (Lachin, 1981).

Normality was determined by Shapiro-Wilk tests. Unpaired t tests were performed to assess differences in means between parametric data from two experimental groups. Mann-Whitney tests assessed differences between non-parametric data from two experimental groups. One-way ANOVA was used to determine differences between the means of three or more groups, with Tukey's multiple comparison post hoc test used to determine differences between respective individual groups. Fisher's exact test or chi-squared tests determined differences between nominal data.

Linear regression analysis was performed in order to determine the associations between factors. Pearson's correlation was performed on parametric data, while Spearman's correlation was performed on non-parametric data sets. Multivariate linear regression was used to determine associations between factors after adjustment for other variables. Of note, unstandardised regression coefficients and their significance were reported, as well as the fit of the models and how much variance (adjusted r^2) they accounted for. Multivariate linear regression models and their components are described in more detail in the relevant sections.

Statistical significance was set at $p \leq 0.05$.

Finally, description of the specific tests used to handle specific data sets relevant to the respective experiments are described in the methods section of each respective chapter.

Chapter 4 – Skeletal muscle mitochondrial dysfunction in PLWH in the contemporary ART setting

4.1 Introduction

As discussed in **Section 1.7**, whilst the advent of antiretroviral therapy (ART) has been successful at suppressing HIV viral loads and restoring immune function in the majority of treated PLWH, several clinical reports and cohort studies have demonstrated the presence of ART-related mitochondrial toxicities in different tissues (Dalakas *et al*., 1990; Dalakas *et al*., 2001; Arnaudo *et al*., 1991; Lewis *et* al., 2003; Kakuda *et al*., 1999).

The first of these studies demonstrated the presence of myopathy in PLWH treated with the nucleotide reverse transcriptase inhibitor (NRTI) zidovudine (AZT), in a monotherapy. This toxicity appeared to be underpinned by mtDNA depletion caused by the inhibition of the mitochondrial polymerase - PolG (Dalakas *et al*., 1990). In the following years, numerous reports surfaced of NRTI-treated PLWH presenting with various other toxicities in several tissues, all of which were linked to mechanisms involving PolG, leading to mitochondrial dysfunction (Brinkman *et* al., 1999; Lim & Copeland, 2001; Dalakas *et al*., 2001; Arnaudo *et al*., 1991). As such, several of the older NRTIs associated with these toxicities were either discontinued or phased out of HIV treatments, and replaced with newer NRTIs that had a safer profile and lower binding affinity to PolG (Venter *et al*., 2019; Venhoff *et al*., 2007).

Aside from the PolG hypothesis, several other proposed mechanisms underpinning ART-induced mitochondrial dysfunction have been hypothesised (Selvaraj *et al*., 2014; Apostolova *et al*., 2011), including depletion of the endogenous dRN and RN pools (Jordhiem & Dumonet, 2007), and increased oxidative stress (Cote *et al*., 2005; Schieber & Chandel, 2014; Apostolova *et al*., 2010).

Additionally, in recent years, reports of mitochondrial toxicities have surfaced in PLWH treated with these newer NRTIs (Payne *et al.,* 2014; Samuels *et al*., 2017; Fields *et al*., 2019), PLWH treated with protease inhibitors (PIs) (Deng *et* al., 2010; Apostolova *et* al., 2011; Domingo *et al*., 2014; Dragovic *et al*., 2014; Alikhani *et al*., 2019; Carr *et al*., 1999), and non-nucleoside reverse transcriptase inhibitors (NNRTIs) (Zaera *et al*., 2001). In addition, mitochondrial dysfunction has been demonstrated in tissue from ART-naïve PLWH (Maagaard *et al*., 2005).

However, due to the fact that the vast majority of PLWH are now on one of numerous variations of combination ART (cART), in combination with the large heterogeneity of the HIV+ population, it has

become difficult to determine the exact effect certain ARVs have on mitochondrial function. In addition, the demonstration from our group of the presence of clonally expanded mtDNA deletions in PLWH who were previously treated with the older, supposedly 'mitochondrially-toxic' NRTIs has led to the questioning of whether there is a 'legacy effect' in HIV+ individuals who were treated with these ARVs (Payne *et al*., 2011), further complicating the understand in the field.

As the average age of the HIV+ population is steadily increasing, in combination with the fact that older PLWH exhibit a higher prevalence of age-related phenotypes such as frailty (Guaraldi *et* al., 2011; Piggott *et* al., 2016; Kooij *et al*., 2016), and age-related pathologies (Guaraldi *et al*., 2011), the better understanding of mitochondrial dysfunction in the contemporary ART era is vital.

As such, by examining mitochondrial dysfunction in skeletal muscle tissue from PLWH treated with various ART regimens through novel techniques, I sought to better understand ART-associated mitochondrial function in a clinically relevant tissue in the contemporary ART era.

4.2 Experimental aims

Various studies have demonstrated a 'mitochondrially toxic' effect of several of the early NRTIs in a range of tissues, including skeletal muscle (Dalakas *et al*., 1990; Arnaudo *et al*., 1991; Payne *et al*., 2011). In contrast, few studies have sought to investigate whether PLWH who have only been exposed to newer NRTIs with a lower PolG-binding affinity develop skeletal muscle mitochondrial dysfunction. In addition, it is not fully understood whether previous treatment with older NRTIs leads to an excess of mitochondrial defects in a 'legacy effect'. Therefore, in this study I aimed to:

- Determine whether ART-treated PLWH have cellular defects of mitochondrial complex I and IV in skeletal muscle.
- Determine the nature of mtDNA defects responsible for mitochondrial CI and CIV deficiency in skeletal muscle of PLWH at the single cell level.
- Determine the proportion of myofibres showing deficiency of mitochondrial CI and CIV in the skeletal muscle of PLWH who have been exposed only to those NRTIs in contemporary usage, and to compare this with those PLWH who have also been exposed to older NRTIs.
- Assess whether previous exposure to older NRTIs is responsible for a 'legacy effect', whereby PLWH previously treated with 'mitochondrially-toxic' NRTIs have an excess of mtDNA mutations in skeletal muscle and subsequent mitochondrial defects in individual myofibres.

4.3 Methods

4.3.1 Patient cohort

Skeletal muscle biopsies obtained from 67 HIV+ individuals from both the MAGMA and SMMFA studies were included in this study cohort, with subject clinical and HIV-related characteristics described fully in **Table 3.1**. Subjects were combined from both MAGMA and SMMFA cohorts in order to increase the power to detect inter- and intra-group differences. Specifically, 30 subjects were derived from the MAGMA study, whilst 37 were derived from the SMMFA study.

Control skeletal muscle tissue (for calibration of the multiplex immunofluorescence assay) was acquired with prior informed consent from the distal part of the hamstring of people undergoing anterior cruciate ligament (ACL) surgery. Approval for this was given by Newcastle biobank (NAHPB reference: 042), as described in **Section 3.2.3**.

4.3.2 Multiplex immunofluorescence for quantification of skeletal muscle mitochondrial complex I and IV activity and mitochondrial mass

10µm cryosections were subjected to multiplex immunofluorescence staining for the quantification of mitochondrial CI and CIV activity as well as mitochondrial mass in skeletal muscle, as described in **Section 3.4.2**.

4.3.3 Image acquisition and analysis of mitochondrial complex I and IV activity and mitochondrial mass

Fluorescent images were acquired using a Zeiss Axio Imager M1 and Zen 2011 (blue edition) software with a Monochrome Digital Camera (AxioCam MRm) at 20x magnification, as described in **Section 3.4.4**. The 'intermediate –', 'intermediate +' groups were pulled together to create a 'intermediate' group ($-3 > z > -6$).

4.3.4 Succinate dehydrogenase histochemistry

Prior to laser capture microdissection of individual myofibres, 15µm cryosections were subjected to succinate dehydrogenase histochemistry in order to improve visualisation of tissue, as described in **Section 3.5.4**.

4.3.5 Laser capture microdissection of individual myofibres

Laser capture microdissection of tissue of interest was undertaken in order to acquire tissue for downstream qPCR analysis. Serial 15µm cryo-sections were cut onto membrane slides (as described in **Section 3.4.1**) from the skeletal muscle biopsies of interest and before SDH histochemistry (as described in **Section 3.5.4** and above). CI positive, intermediate and deficient myofibres from patients in both the 'contemporary' and 'historical' groups were laser microdissected as described in **Section 3.6.2** and captured into 15µm lysis buffer, as described in **Section 3.6.1**.

4.3.6 Quantitative PCR for the detection and quantification of mtDNA mutations

A duplex quantitative real-time PCR assay targeting the mitochondrial genes *MT-ND1* and *MT-ND4* was used to detect and quantify deletions in the mitochondrial genome, as described in **Section 3.7.5**. By assuming that *MT-ND1* was not deleted through mutations I was also able to calculate mtDNA copy number. Details of all primers and standards used, as well as their preparation, are described in **Section 3.7**.

4.3.7 Phosphorus magnetic resonance spectroscopy (^{31}P-MRS)

^{31}P-MRS analysis was performed by Dr Brendan Payne (Newcastle University) in a previous study (Payne *et al*., 2014) in order to quantify skeletal muscle oxidative potential *in vivo* in response to short bouts of exercise, as described in **Section 3.8**.

4.3.8 Statistical analyses

Statistical tests were performed in Prism v5.04 and IBM SPSS Statistics v23. Graphs were also made in Prism v5.04.

Shapiro-Wilk tests were performed in order to determine normality of data sets. The percentage of myofibres classified as either deficient, intermediate, or positive for both CI and CIV was quantified and subsequently log-transformed in order to normalise the data. The average VDAC1 z-score for each subject was also quantified, although not log-transformed. Differences in the proportion of myofibres with CI and CIV deficiency was compared between NRTI patient groups using a one-way ANOVA with Tukey's multiple comparison post hoc test to compare differences between groups. In addition, unpaired t tests were used to determine differences in proportional CI and CIV deficiency between PI and NNRTI groups. Fisher's exact test was used to determine differences between the prevalence of current PI and NNRTI treatment between the two ART-treated groups. Finally, chi-squared test was performed in order to determine if there was significant differences in sex between the treatment groups.

Unadjusted linear regression analysis between CI deficiency and clinical as well as HIV-related factors was done using Pearson's correlation analyses in order to assess the relationship between mitochondrial dysfunction in the form of CI deficiency and the respective factors. Multivariate linear regression analysis was also undertaken, with models including factors determined to be significant from univariate analysis as independent variables and CI deficiency as the dependant variable. Unstandardised regression coefficients and their significance were reported, as well as the fit of the models and how much variance (adjusted r^2) they accounted for.

Statistical significance was set at $p \leq 0.05$.

mtDNA deletions in individual myofibres were determined by the ratio of *MT-ND1 to MT-ND4* relative to a calibrator sample ($\delta\delta C_t$ method). We screened for mtDNA depletion in individual cells by considering the calculated starting quantity (SQ) of mtDNA relative to the 5th centile of SQ in CI-normal cells from the same individuals.

4.4 Results

4.4.1 Cohort clinical characteristics

The full clinical characteristics of the subjects (n = 67) are described in **Table 3.1** in **Section 3.2.3**. All subjects were HIV+ and the mean age of the cohort was 53.1 (range 23-85) years. 13% were female and 92.5% of participants were white British (**Table 4.1**). Subjects were derived from both the MAGMA and SMMFA study cohorts.

The subjects were divided into three groups depending on the form of ART they have been exposed to. Subjects in the 'naïve' group (n = 13) had no previous exposure to any form of ART, while subjects in the 'contemporary' group (n = 29) had only been exposed to those NRTIs which are currently in common use in the UK (abacavir (ABC), lamivudine (3TC), emtricitabine (FTC) and tenofovir disoproxil fumarate (TDF)), and subjects in the 'historical' group (n = 25) were currently being treated with these contemporary ARVs, but had previous exposure to those older NRTIs which are generally considered as being mitochondrially-toxic (zidovudine (AZT), zalcitabine (ddC), didanosine (ddI) and stavudine (d4T)).

The mean age of the naïve group was 36.8 years (range 23-53), contemporary group was 54.5 years (range 25-71) and historical group 60 years (45-85). As expected, patients in the historical group had a higher mean duration on ART compared to the contemporary group. In addition, patients in the historical group also had a significantly higher duration since diagnosis and duration with untreated HIV infection compared to the naïve and contemporary groups. The vast majority of individuals in the two ART treated groups had suppressed plasma HIV viral load (<200 copies/mL). In the untreated group, the mean HIV viral load was about 11,000 copies/mL (**Table 4.1**).

	Naïve (n = 13)	Contemporary (n = 29)	Historical (n = 25)	*P*
Age[+]	38.6 (23-53)	54.5 (25-71)	60.0 (45-85)	<0.0001
Female sex^	5 (38%)	1 (3%)	3 (12%)	0.009
Months since diagnosis[*]	74 (58)	142 (96)	225 (80)	<0.0001
Months on ART[*]	0	71 (47)	168 (57)	<0.0001
Months untreated[*]	74 (58)	73 (82)	57 (80)	0.72
CD4 count (copies/µl)[*]	635 (431)	616 (223)	618 (213)	0.98
Nadir CD4 (copies/µl)[*]	415 (228)	221 (111)	162 (112)	<0.0001
Viral load (copies/ml)[*]	11533 (13607)	71 (89)	37 (20)	<0.0001
Current treatment with PIs^	0	9 (31%)	7 (24%)	0.98
Current treatment with NNRTIs^	0	14 (48%)	15 (60%)	0.42

Table 4.1 – Cohort clinical and HIV-related characteristics. *[+] = values are given as the mean (with range). [*] = values are given as the mean (± SD). ^ = nominal value (%). P values calculated by one-way ANOVA, or chi-squared for nominal values. Differences in the prevalence of current treatment with PIs and NNRTIs was determined by Fisher's exact test between the contemporary and historical groups.*

4.4.2 Mitochondrial respiratory chain complex I and IV dysfunction in ART-treated PLWH

Previous studies using COX/SDH histochemistry have demonstrated possible persistent mitochondrial defects in skeletal muscle of PLWH who have been treated with older, supposedly mitochondrially-toxic NRTIs (Payne *et al*., 2011). To further investigate whether these NRTIs produce a legacy effect whereby skeletal muscle mitochondrial dysfunction, underpinned by clonally expanded mtDNA deletions, persists even after the cessation of treatment with those NRTIs, I subjected skeletal muscle sections (10µm) to a multiplex immunofluorescence assay (**Figure 4.1a**). As well as being more objective and quantitative than COX/SDH histochemistry, this validated assay has the advantage of simultaneously quantifying CI protein levels and mitochondrial mass in addition to CIV protein levels.

A mean of 1229 myofibres were examined per subject. Initially, I compared the proportions of CI and CIV deficient myofibres between ART treatment groups. The data was skewed and so subsequently log-transformed in order to normalise the data. The proportion of myofibres with CI deficiency was significantly different between the three groups (p = 0.017, **one-way ANOVA**) (**Figure 4.1c**), with both the historical (p = 0.0061, **Tukey's multiple comparisons**) and contemporary (p = 0.046) groups having a significantly higher proportion than the naïve group. Whilst there was no significant difference in the proportion of myofibres with CIV deficiency across the three groups (p = 0.12 **one-way ANOVA**), patients in the contemporary group had a significantly higher proportion of CIV deficiency compared to the naïve group (p = 0.025, **Tukey's multiple comparisons**) (**Figure 4.1d**).

Next, I assessed mitochondrial mass by VDAC1 staining intensity in individual myofibres. Here, there was no significant difference in the average myofibre mitochondrial mass between the three groups (**Figure 4.1e**).

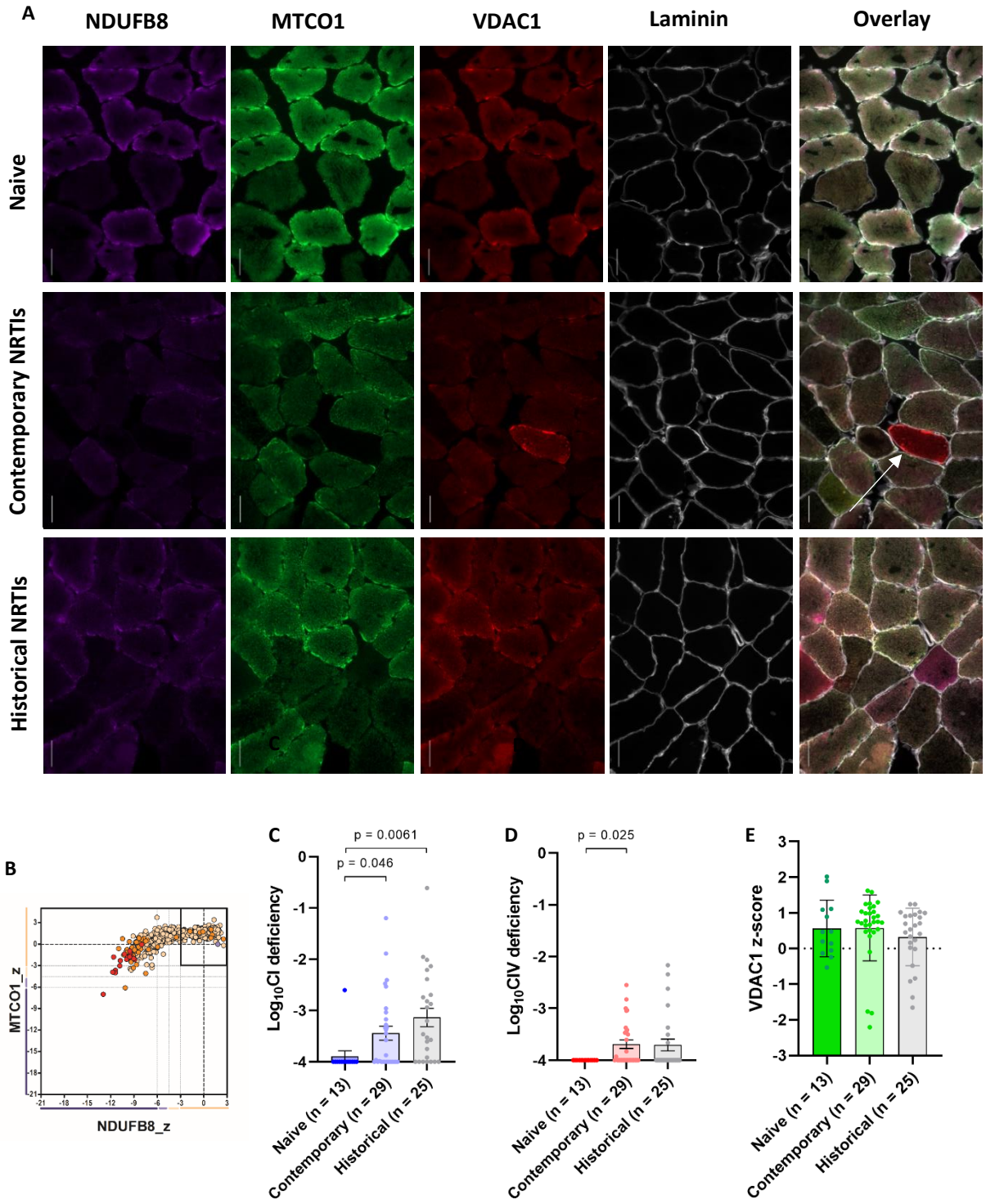

Figure 4.1 – Skeletal muscle mitochondrial function in various NRTI regimens. *(**A**) Example of multiplex immunofluorescence for CI (NDUFB8), CIV (MTCO1), mitochondrial mass (VDAC1) and laminin in ART-naïve, contemporary NRTI, and historical NRTI-treated PLWH. The bright red fibre (arrow in the overlay channel) is deficient in CI and CIV but shows VDAC1 hyperintensity, indicating compensatory mitochondrial proliferation. Scale bar = 100µm. (**B**) Dot plots depicting the fibre z-scores for example plot of quantitative CI (x-axis) and CIV (y-axis) deficiency in a participant exposed to historical NRTIs. Each dot represents an individual myofibre plotted by NDUFB8 and MTCO1 z-score. Dots are coloured according to mitochondrial mass: cream ('normal'), orange ('high') and red ('very high'). Dotted lines indicate the cut off points of -1.5SD, -3SD, -4.5SD and -6SD. Each dot represents an individual fibre. (**C-E**) Proportional levels of (**C**) CI-deficient, and (**D**) CIV-deficient myofibres by ART exposure group (mean ± SEM). Each dot represents an individual subject and is plotted by the (log_{10}) proportion of myofibres with the respective mitochondrial defects. (**E**) Mitochondrial mass (expressed as mean VDAC1 z-score) (mean ± SEM). Each dot represents the mean of all fibres examined in an individual subject.*

Finally, I performed unadjusted linear regression analysis in order to determine whether CI and CIV skeletal muscle mitochondrial deficiency was synergistic. I found that CI deficiency was significantly associated with CIV deficiency when investigated in all participants (n = 67; r = 0.68; $p < 0.0001$, **Pearson's correlation**) (**Figure 4.2**).

As the proportion of myofibres with CI defects was higher than those with CIV defects, I focussed subsequent analyses on CI deficient myofibres. This finding is also significant as it is the first time that CI defects have been shown to be more predominant than CIV defects in skeletal muscle of older PLWH.

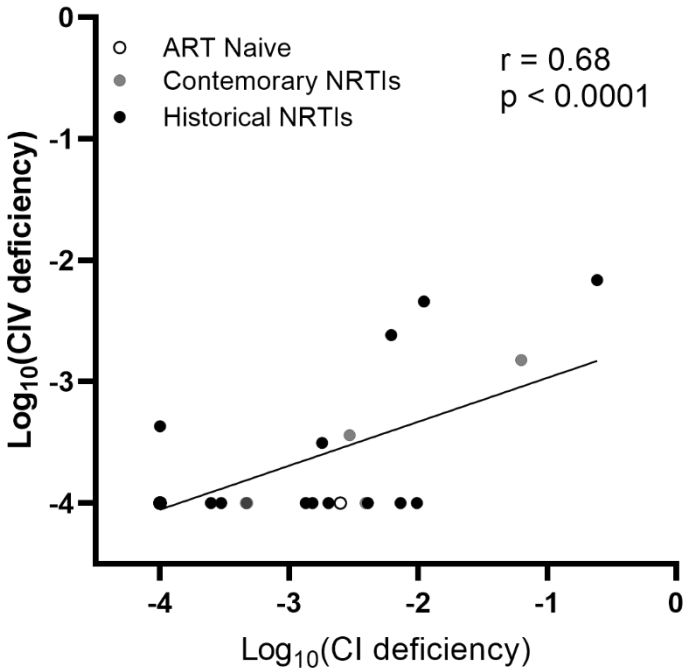

Figure 4.2 – Correlation between CI and CIV skeletal muscle deficiency in PLWH. *Dot plot demonstrating the significant positive association (r = 0.68; p < 0.0001) between the proportion of CI- and CIV-deficient myofibres in our cohort of PLWH (n = 67) (Pearson's correlation and linear regression for line). Each dot represents an individual subject in either the ART naïve (n = 13, white), contemporary NRTI (n = 29, grey) or historical NRTI (n = 25, black) groups.*

4.4.3 Mitochondrial function in PI or NNRTI-treated PLWH

As previous *in vitro* studies have demonstrated a potential mitochondrially-toxic effect induced by various protease inhibitors (PIs) and non-nucleoside reverse transcriptase inhibitors (NNRTIs), I wanted to investigate whether there was evidence of skeletal muscle mitochondrial dysfunction in PLWH currently treated with ARVs from either of these classes.

Here, there was no significant difference in the proportion of myofibres with either CI or CIV deficiency (**unpaired t test**) between PLWH who were treated with PIs (n = 16) and those who were treated with an ART regimen that did not include a PI (n = 38) (**Figure 4.3a, b**). In addition, there was also no significant difference in the proportion of myofibres with CI and CIV deficiency between PLWH who were treated with NNRTIs (n = 29) and those who were not (n = 25) (**Figure 4.3d, e**). Finally, there was no significant difference in myofibre mitochondrial mass between PI and non-PI-treated PLWH or NNRTI and non-NNRTI-treated PLWH (**Figure 4.3c, f**).

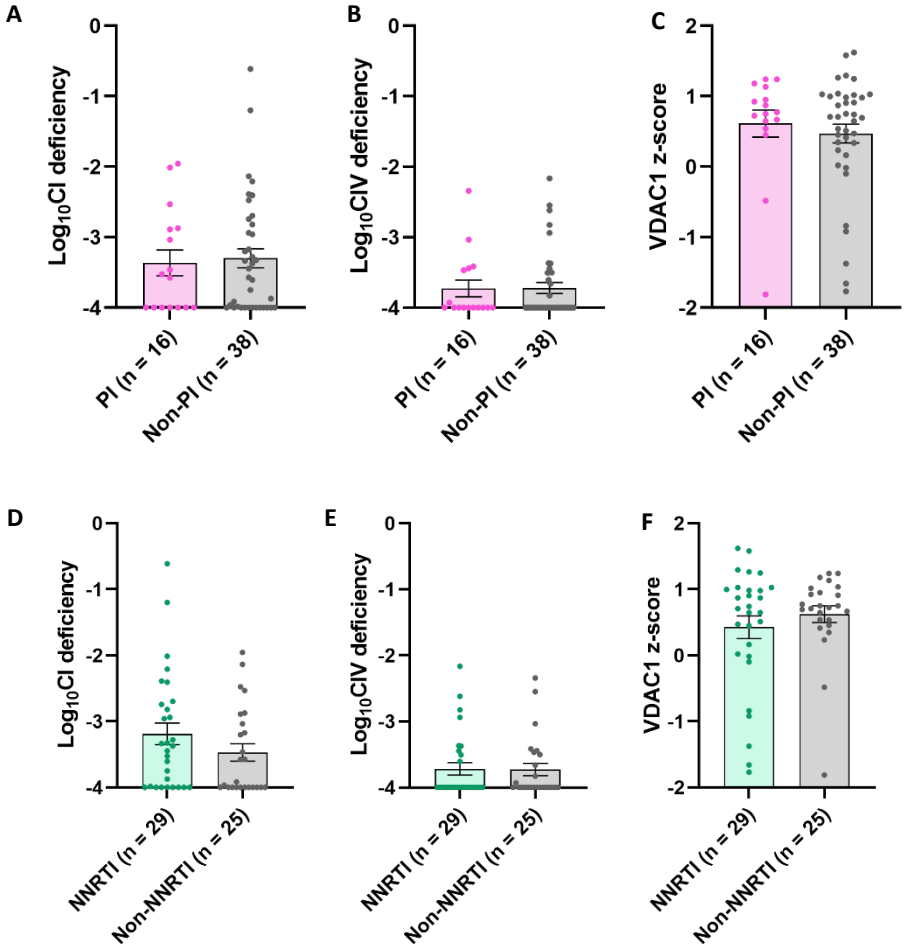

Figure 4.3 – Skeletal muscle mitochondrial dysfunction in PI and NNRTI-treated PLWH. *Dot plots (mean ± SEM) showing proportional (**A**) CI, or (**B**) CIV deficiency, and (**C**) average myofibre mitochondrial mass in PLWH who were on PI treatment and those who were not. (**D**) proportional CI, (**E**) proportional CIV deficiency, and (**F**) average mitochondrial mass in NNRTI-treated and non-NNRTI-treated PLWH. Each dot represents an individual patient.*

4.4.4 Comparison of mitochondrial defects in PLWH quantification methods

COX/SDH histochemistry has long been the gold standard for assessing mitochondrial dysfunction in skeletal muscle fibres, through quantification of the percentage of mtDNA-encoded COX deficient fibres. It has also been a powerful tool for assessing mitochondrial dysfunction in skeletal muscle from PLWH (Payne *et al*., 2011). Here, I wanted to assess whether the results from multiplex immunofluorescence (**Section 3.4.2**) agreed with COX/SDH histochemistry results.

Unadjusted linear regression analysis using data from COX/SDH histochemistry (previously performed by Dr Brendan Payne, Newcastle University) and multiplex immunofluorescence (**Section 4.4.2**), both performed on skeletal muscle serial sections cut from the same SMMFA patient samples (n = 37), showed that proportional CI (r = 0.70; $p < 0.0001$, **Pearson's correlation**) and CIV (r = 0.56; $p = 0.0003$) deficiency both had a statistically significant positive correlation with the percentage COX defect (**Figure 4.4**).

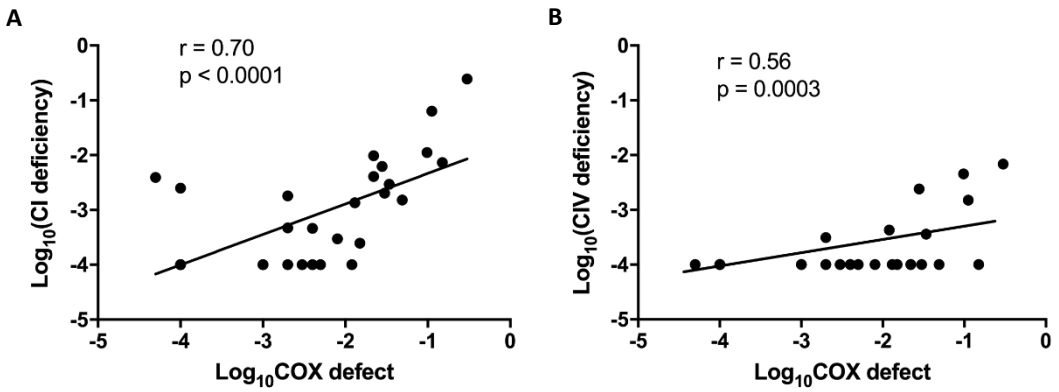

Figure 4.4 – NDUFB8 and MTCO1 deficiency correlates with COX defect level*. The log-transformed proportion of COX defect level was significantly associated with the log-transformed proportion of (**A**) NDUFB8-deficient fibres (r = 0.70; p < 0.0001) and (**B**) MTCO1-deficient fibres (r = 0.56; p = 0.0003) (Pearson's correlation and linear regression for line).*

4.4.5 ^{31}P-MRS quantification of skeletal muscle respiratory capacity

For 17 of the subjects in this study (listed in **Table 3.1**), data on *in vivo* mitochondrial function was available from ^{31}P-MRS. These measurements had been taken as part of a previous study conducted in our lab (Payne *et al*., 2014), and reanalysed by me. These 17 PLWH included individuals from the contemporary NRTI (n = 6) and historical NRTI (n = 11) groups, along with 23 age-matched HIV-controls. ^{31}P-MRS data were therefore compared with cellular skeletal muscle mitochondrial defects measured by multiplex immunofluorescence.

There was a statistically significant difference in resting-state ADP/ATP ratio across the three groups (p = 0.0015, **one-way ANOVA**), with both the historical NRTI (p = 0.0077, **Tukey's multiple comparison**) and contemporary NRTI (p = 0.011, **Tukey's multiple comparison**) exposed HIV+ groups having a higher resting ADP/ATP ratio than the HIV-uninfected group (**Figure 4.5a**). There was no significant difference between the NRTI exposure groups.

In order to assess whether higher levels of skeletal muscle mitochondrial dysfunction at the cellular level translated to mitochondrial dysfunction at the physiological level, I performed unadjusted linear regression analysis between the proportion of CI-deficient myofibres and the resting-state ADP/ATP ratio in the paired HIV+ subjects (n = 17). Surprisingly, I found that proportional CI-deficiency did not significantly predict diminished mitochondrial respiratory capacity in the form of ADP/ATP ratio (r = 0.35; p = 0.17, **Pearson's correlation**) (**Figure 4.5b**), suggesting that cellular OXPHOS deficiency does not necessarily predict declines in physiological respiratory capacity.

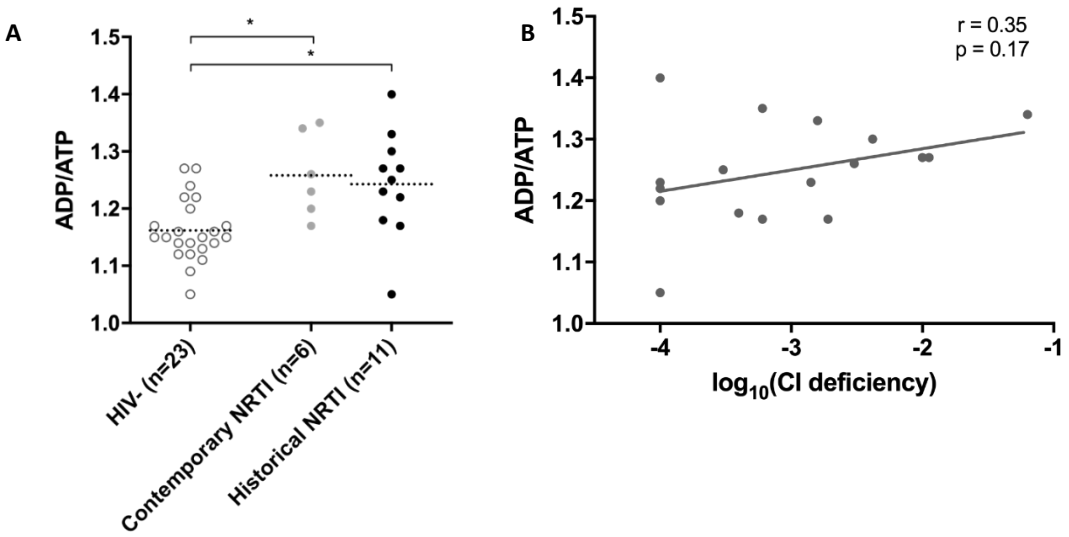

Figure 4.5 – Skeletal muscle mitochondrial respiratory capacity. (***A***) *ADP/ATP ratio in skeletal muscle through ^{31}P-MRS analysis. Each dot represents an individual subject in either the contemporary NRTI (n = 6), historical NRTI (n = 11), or HIV-uninfected control (n = 23) group. Dotted lines indicate the mean.* (***B***) *Correlation of proportional CI deficiency in skeletal muscle biopsies and ADP/ATP ratio in calf muscle (Pearson's correlation and linear regression for line). Each dot represents and individual subject with available data for both histological analyses and in vivo mitochondrial function assessment (n = 17).*

4.4.6 Clinical and HIV-related predictors of skeletal muscle mitochondrial dysfunction,

After demonstrating that mitochondrial dysfunction is present in skeletal muscle fibres from PLWH with exposure to contemporary ART, I next assessed whether HIV-related clinical factors or general clinical characteristics predicted myofibre mitochondrial CI defects (**Table 4.2**). These clinical parameters included age (**Figure 4.6a**), current (**Figure 4.6b**) as well as nadir CD4 count (copies/µl) (**Figure 4.6c**), viral load (copies/ml) (**Figure 4.6d**), time since HIV diagnosis (**Figure 4.6e**), duration on ART (**Figure 4.6f**), and duration with untreated HIV infection (**Figure 4.6g**).

Through univariate linear regression analysis, I found that duration on ART significantly predicted proportional CI deficient myofibres (r = 0.29; *p* = 0.017, **Pearson's correlation**) (**Figure 4.6d**).

The association between CI deficiency and age did not quite reach statistical significance (*p* = 0.056) (**Pearson's correlation**). Further, as the age of both the historical and contemporary groups was higher than the ART-naïve group, I performed linear regression analysis between age and proportional CI deficiency within each of the individual groups in order to better understand the predictive significance of age on mitochondrial function in ART-treated PLWH. Importantly, age did not significantly predict proportional CI deficiency in either the historical (n = 25; r = -0.33; *p* = 0.11, **Pearson's correlation**), or contemporary (n = 29; r = 0.25; *p* = 0.19) ART groups. In addition, age did not significantly predict CI deficiency when the two groups were combined (n = 54; r = 0.02; *p* = 0.88).

There was no significant correlation between CD4 count and proportional CI deficiency, suggesting that CD4 count is not a reliable predictor of mitochondrial defects in skeletal muscle of the general PLWH population. In addition, there was no significant association between proportional CI deficiency and age, months since diagnosis, months with untreated HIV infection, nadir CD4 count, or viral load.

As this was an observational study, factors such as age and duration on ART were highly dependent of treatment group. This is inevitable, as choices of NRTIs used in ART have changed over time as new agents became available. Hence, I then performed multivariate linear regression to see if the effect of duration of ART treatment was independent of the effect of age. Here, both variables were positively associated with CI deficiency (unstandardised regression coefficients, age = 0.011; duration on ART = 0.02) but neither was independently statistically significant (*p* = 0.24 and *p* = 0.23 respectively, **multivariate linear regression**). Overall model fit was statistically significant (*p* = 0.04), but only predictive of a small amount of the variation in proportional CI deficiency (r^2 = 0.1).

	CI deficiency	
	r	***p***
Age	0.23	0.056
CD4 count (copies/µl)	-0.012	0.93
Nadir CD4 count (copies/µl)	-0.11	0.43
Viral load (copies/ml)	-0.24	0.061
Months since diagnosis	0.073	0.56
Months on ART	**0.29**	**0.017**
Months untreated	-0.24	0.051

Table 4.2 – HIV-related clinical predictors of proportional myofibre CI deficiency*. Table depicting the unadjusted linear regression analysis (Pearson's correlation) between proportional log_{10}(CI deficiency) and HIV-related clinical parameters. Statistically significant results are in bold.*

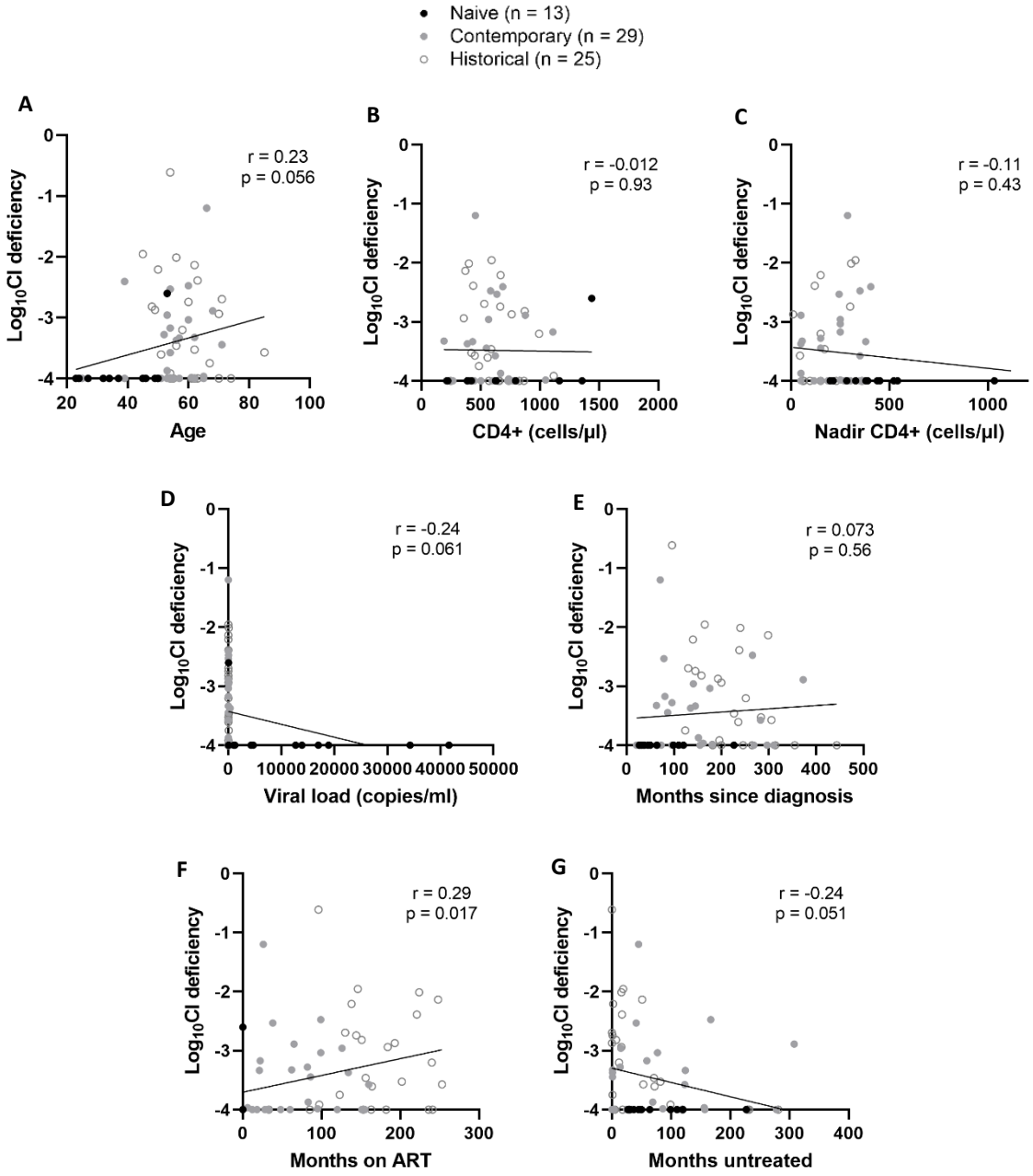

Figure 4.6 – Correlations between proportional CI deficiency and clinical parameters*. Scatter plots depicting linear regression analysis (Pearson's correlation) between proportional CI deficiency and (**A**) age, (**B**) CD4 T cell count (cells/µl), (**C**) nadir CD4 T cell count (cells/µl), (**D**) viral load (copies/ml), (**E**) time since HIV diagnosis (months), (**F**) duration on ART (r = 0.29; p = 0.0017), and (**F**) months untreated. Pearson's correlation and linear regression for the correlation and line. Black dots = ART naïve PLWH (n = 13), grey dots = contemporary NRTI (n = 29), and white dots = historical NRTI (n = 25).*

4.4.7 Molecular basis of skeletal muscle mitochondrial dysfunction in ART-treated PLWH

Finally, to better understand the molecular mechanisms underpinning the skeletal muscle mitochondrial dysfunction demonstrated in ART-treated PLWH, I subjected individual myofibres to laser capture microdissection (n = 90) and qPCR analyses (described in **Section 3.5.5**). In particular, CI-deficient (n = 24), CI-intermediate (n = 27) and CI-positive (n = 39) myofibres were dissected from subjects in both the historical (n = 5) and contemporary (n = 4) groups.

Initially, I excluded mtDNA depletion as a cause of CI deficiency in myofibres. In keeping with our VDAC1 data for mitochondrial mass at the myofibre level, there was no evidence of reduced mtDNA content in individual CI deficient fibres (**Figure 4.7**).

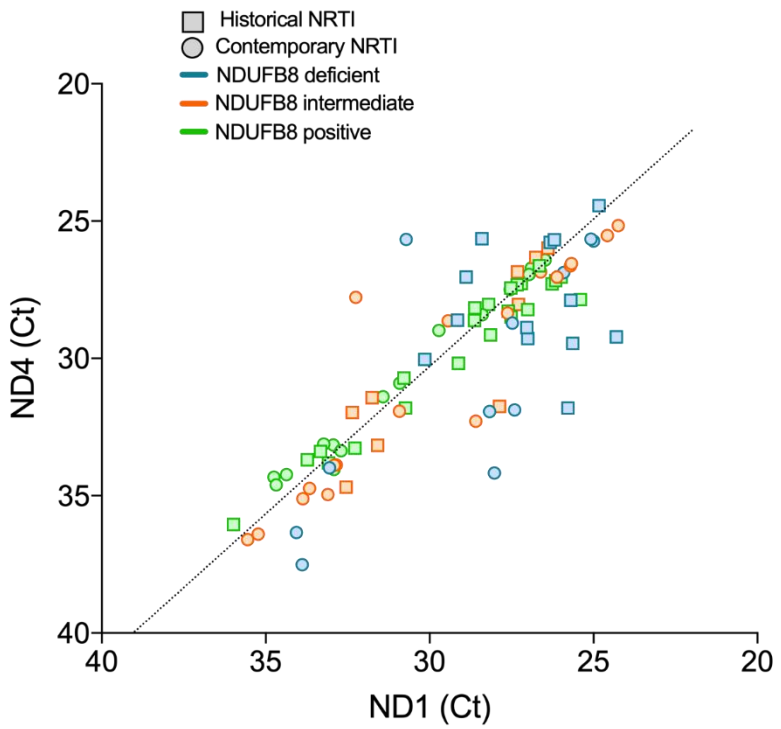

Figure 4.7 – mtDNA copy number in individual myofibres*. Dot plot demonstrating no significant levels of mtDNA depletion in individual CI-deficient (n = 24, blue), CI-intermediate (n = 27, orange) and CI-positive (n = 39, green) myofibres from PLWH exposed to only contemporary NRTIs (circle) or contemporary NRTIs but previously historical NRTIs (square). Dots are plotted by MT-ND1 and MT-ND4 copy number (Ct). Dotted line indicates the mean MT-ND1 and MT-ND4 copy number of the CI-positive myofibre population which was used as the control.*

MT-ND1 lies on the minor arc of the mitochondrial genome and so is rarely deleted in large-scale mtDNA deletions. I therefore used *MT-ND1* copy number as a measure of whole mtDNA copy number using the standard curve method and compared *MT-ND1* and *MT-ND4* copy number to determine the presence of mtDNA deletions.

Published data in the HIV and ageing field has previously demonstrated the presence of large-scale mtDNA deletions in skeletal muscle from PLWH (Payne *et al*., 2011). Here, by quantifying the copy number of the two mitochondrially-encoded genes *MT-ND1* and *MT-ND4,* expressed relative to a control, I found that 64% of CI-deficient myofibres contained large-scale mtDNA deletions. In addition, 22% of CI-intermediate fibres had mtDNA deletions as well as 8% of CI-positive fibres (**Figure 4.8a**).

Interestingly, mtDNA deletions in the minor arc (*MT-ND1*) of the mitochondrial genome were present in all three groups of myofibres, albeit at a significantly less prevalent frequency than major arc deletions (*MT-ND4*). Briefly, 79% of deletions in CI-deficient fibres were in the major arc, while 21% were in the minor arc. 67% of deletions in both CI-intermediate and CI-positive fibres were in the major arc while 33% were in the minor arc. Interestingly, I found that there was a significant difference in the mtDNA deletion heteroplasmy (as measured by ddCt) across the three groups of fibres ($p < 0.0001$, **one-way ANOVA**) (**Figure 4.8a**), with mtDNA deletion heteroplasmy in CI-deficient fibres being significantly greater than mtDNA deletion heteroplasmy seen in both the CI-intermediate ($p = 0.0089$, **Tukey's multiple comparison**), and CI-positive fibres (p , 0.0001, **Tukey's multiple comparison**). Further studies should look to map the exact locations and sizes of the mtDNA deletions.

I next wanted to assess whether there were any differences in the patterns of mtDNA deletions occurring in CI-deficient and CI-intermediate myofibres isolated from PLWH in the historical (n = 45) and contemporary (n = 45) ART treatment groups. I subsequently found that there was no significant difference in the pattern of mtDNA deletion locations (**unpaired t test**) (**Figure 4.8b**). This suggests that the type of ARV or exposure to a particular NRTI has no discernible implication with regards to the size or location of mtDNA deletions underpinning mitochondrial defects in skeletal muscle.

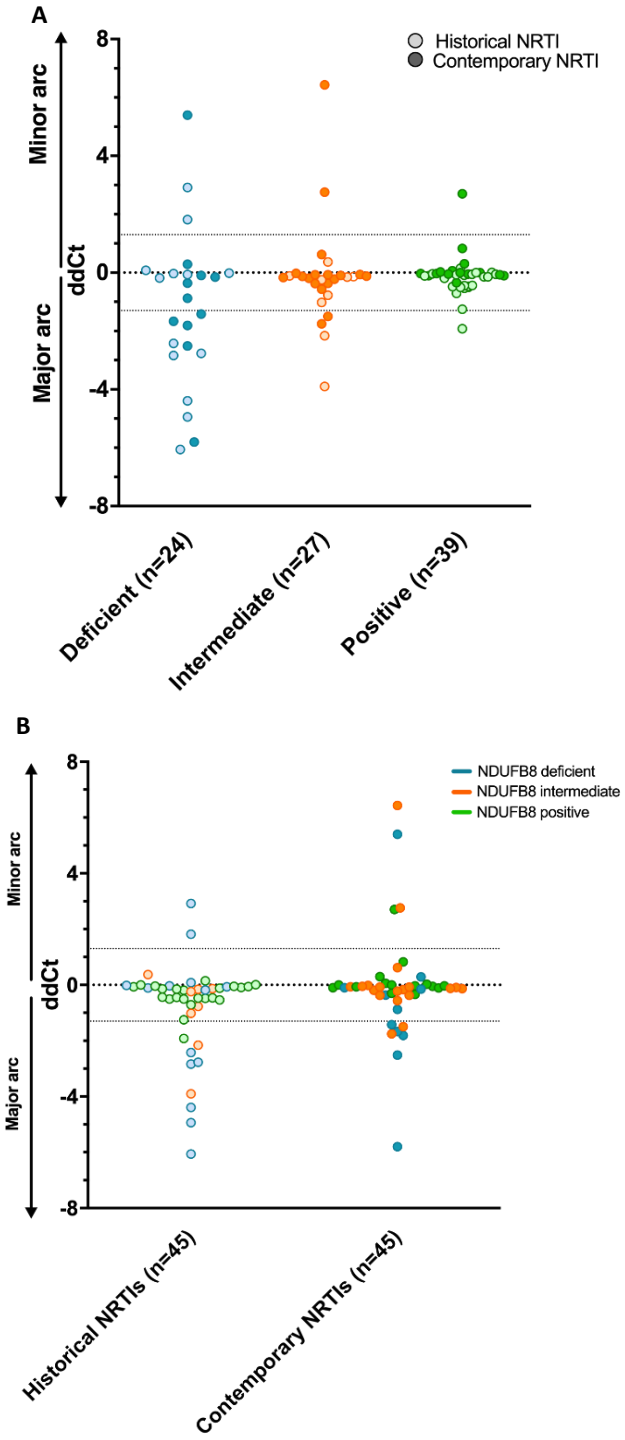

Figure 4.8 – mtDNA deletions detected by qPCR in single myofibres. *(**A**) Distribution of mtDNA deletion levels in CI-deficient (n = 24), CI-intermediate (n = 27) and CI-positive (n = 39) single myofibres. Lightly shaded dots represent myofibres from historical NRTI-treated PLWH and darkly shaded dots represent fibres form contemporary NRTI-treated PLWH. (**B**) Distribution of mtDNA deletions in all fibres from PLWH exposed to historical NRTIs (n = 45) and contemporary NRTIs (n = 45). For both (**A**) and (**B**) each dot represents an individual myofibre and deletion sizes are expressed as $\delta\delta C_t$ (difference in MT-ND1 and MT-ND4 C_t values relative to control). Myofibres with a $\delta\delta C_t$ above 2 standard deviations (thin dotted line) from the control were classified as having minor arc deletions, and myofibres with a $\delta\delta C_t$ below 2 standard deviations (thin dotted line) were determined to have a major arc deletion.*

4.5 Discussion

4.5.1 Conclusions

Whilst early clinical reports and subsequent cohort studies have demonstrated a mitochondrially-toxic effect of various NRTIs used in the monotherapy era of ART (Dalakas *et al*., 1990; Arnaudo *et al*., 1991), few studies have investigated whether newer NRTIs developed to overcome the toxic profile of these NRTIs similarly induce mitochondrial dysfunction, particularly in skeletal muscle. This is primarily due to the fact that clinical trials and *in vitro* studies demonstrated that these newer NRTIs have a low PolG-binding affinity and few clinical reports of associated toxicities have surfaced (Venter *et al*., 2019; Venhoff *et al*., 2007). With regards to the growing interest in adverse ageing in older PLWH and the strong association between mitochondrial dysfunction and ageing (Lopez-Otin *et* al., 2013), this study sought to better characterise mitochondrial function in a functionally relevant tissue in PLWH in the contemporary ART era. These included PLWH who have never been on ART, PLWH who have been exposed to older, mitochondrially-toxic NRTIs but are now on 'safer' NRTIs, and PLWH who have only ever been exposed to the NRTIs that remain in contemporary use.

4.5.1.1 ART-treated PLWH have greater cellular, molecular and physiological mitochondrial dysfunction than ART-naive PLWH

This is the first study to demonstrate a defect of cellular mitochondrial function in skeletal muscle of PLWH who have only ever been exposed to contemporary ART regimens, despite the perception that contemporary NRTIs are free from mitochondrial toxicity (Venhoff *et al*., 2007). This statement is supported by both cellular and molecular findings from skeletal muscle tissue biopsies, as well as *in vivo* functional evidence from ^{31}P-MRS.

I demonstrate that PLWH who have been exposed to only contemporary NRTIs as well as PLWH who are currently on contemporary NRTIs but have previously been exposed to older NRTIs both displayed a significantly higher proportion of myofibres with CI deficiency compared to ART-naïve PLWH. PLWH who have been exposed to contemporary NRTIs also had a significantly higher proportion of myofibres with CIV deficiency compared to ART-naïve PLWH. In addition, there was no significant difference in proportional CI or CIV deficiency between age-matched patients in the historical or contemporary groups, suggesting that the levels of CI and CIV deficiency are similar in both ART-treated groups. Finally, as none of the HIV-related or clinical parameters significantly predicted greater CI deficiency through adjusted multivariate linear regression analyses, these findings indicate that ARVs themselves play a significant role in mitochondrial dysfunction (Dalakas *et al*., 1990, Arnaudo *et al*., 1991; Payne *et al*., 2011; Lim *et al*., 2001).

Another aim of this study was to better understand the molecular mechanisms underpinning mitochondrial dysfunction at the cellular level. qPCR analysis demonstrated the presence of large-scale mtDNA deletions, primarily in the major arc portion of the mtDNA genome, in the majority of CI-deficient myofibres. This supports previous data which demonstrated mtDNA deletions in skeletal muscle fibres with mitochondrial dysfunction, as determined by COX/SDH histochemistry, in ART-treated PLWH (Payne *et al*., 2011). mtDNA deletions were also found in the minor arc of the mitochondrial genome. As these findings have not previously been described in skeletal muscle from ART-treated PLWH, this merits future research.

qPCR analysis also failed to identify alterations in mtDNA content. This finding is supported by immunofluorescence analysis whereby no increase or decline in average myofibre mitochondrial mass was observed. Together, these findings suggest the absence of a compensatory upregulation in mitochondrial mass in response to OXPHOS defects.

Additionally, through ^{31}P-MRS analysis previously performed by Dr Brendan Payne on subjects included in the SMMFA cohort (Payne *et* al., 2014) and further analysed by me, it was demonstrated that contemporary and historical NRTI-treated PLWH had a significantly diminished resting-state ADP/ATP level when compared to age-matched HIV- individuals. This observation provides an important validation of our cellular and molecular findings, as well as pointing to a possible non-invasive read-out for future studies. However, ADP/ATP ratio was not significantly predicted by proportional CI deficiency. This is most likely due to the small number of subjects with paired ^{31}P-MRS measurements, thereby limiting the power to detect an association with CI deficiency. These findings support previous observations of decreased phosphocreatine concentrations in skeletal muscle from AZT-treated PLWH (Sinwell *et al*., 1995).

4.5.1.2 Potential causes of mitochondrial dysfunction in ART-treated PLWH

These novel findings raise a number of mechanistic questions. In both the historical and contemporary NRTI exposure groups I observed that the mitochondrial ETC complex defects seen in individual myofibres were predominantly explained by mtDNA deletions. This is surprising as most *in vitro* data suggest that contemporary NRTIs have a low PolG-binding affinity (Venhoff *et al*., 2007) and do not inhibit mtDNA replication (Birkus *et al*., 2002). Nevertheless, it is conceivable that very prolonged exposure to a contemporary NRTI *in vivo,* and/or cell-type specific effect could be sufficient to promote mtDNA deletions, potentially via chronic oxidative stress. These mtDNA deletions would subsequently clonally expand after an extended period of time, even after cessation of treatment (Payne *et al*., 2011). For example, work from our group has recently demonstrated the presence of mtDNA deletions in the renal tract in the setting of TDF exposure (Samuels *et al*., 2017).

Another possibility is that other ART classes such as protease inhibitors (PIs) or non-nucleoside reverse transcriptase inhibitors (NNRTIs) might contribute to mitochondrial dysfunction in contemporary cART treatment. For example, limited *in vitro* data suggests that the NNRTI efavirenz may impair mitochondrial function (Funes *et al*., 2014). I therefore stratified PLWH in both the contemporary and historical NRTI groups into whether they were on an ART regimen that included a PI or NNRTI, but subsequently found no difference in skeletal muscle CI or CIV deficiency. In addition, there was no difference in average myofibre mitochondrial mass. Additionally, it is possible that long-term treated HIV infection itself might be having a detrimental effect on mitochondrial function. However, the lack of any mitochondrial defects in the ART-naïve group argues against this being a major effect.

Finally, as mitochondrial dysfunction is known to increase with age (Barazzoni *et al*., 2000; Welle *et al*., 2003; Short *et al*., 2005; Lopez-Otin *et al*., 2013), another hypothesis could be that the skeletal muscle mitochondrial defects seen in the ART-treated groups could be due to increased age and age-related effects such as chronic inflammation, immunosenescence, and oxidative stress, which could be propagating the formation of mtDNA mutations, among other damaging effects (Melov *et al*., 1999; Zorov *et al*., 2014; Rao *et al*., 2014; Massaad & Klann, 2011). Indeed, CI defects have been reported in different tissues from Parkinson's Disease patients (Franco-Iborra *et al*., 2016; Kraytsberg *et al*., 2006; Balaban *et al*., 2005). However, adjusted linear regression analysis demonstrated that the mitochondrial defects were not explained by age itself. It would therefore be interesting to investigate the effect of these other age-related factors such as chronic inflammation or immunosenescence.

4.5.1.3 Is there a legacy effect in PLWH treated with historical NRTIs?

The final objective of this study was to assess whether there is a 'legacy effect' induced by exposure to older NRTIs. Although this theory needs to be tested in a larger, ideally longitudinal cohort of PLWH and HIV- individuals, this study suggests against the presence of a legacy effect. This is due to the fact that PLWH in the historical NRTI group did not have an excess of cellular mitochondrial defects compared to age-matched PLWH in the contemporary group. In addition, isolated CI-deficient myofibres from patients in both groups were seen to have a similar prevalence and pattern of mtDNA deletions underpinning the cellular defects. However, the levels of ART-induced mitochondrial dysfunction can vary between tissue types, and so whilst these findings suggest against a legacy effect in skeletal muscle, this may not be the case in other relevant tissue such as the liver or PBMCs.

4.5.1.4 Significance of predominant CI deficiency

An important strength of this study was that I employed techniques that can objectively quantify mitochondrial deficiency with single-fibre resolution. Given the stochastic nature of somatic (acquired) mtDNA defects within postmitotic tissues such as skeletal muscle, studies of homogenised tissue may miss these defects (Murphy *et al*., 2012). As opposed to the current gold-standard in histologically detecting cellular mitochondrial defects, sequential COX/SDH histochemistry, our assay allows for the objective quantification of CI defects and mitochondrial mass, as well as CIV defects. This is a significant advantage as genes encoding CI subunits form the greatest proportion of the mtDNA genome and are therefore the most commonly deleted genes in the event of large-scale mtDNA deletions. Our observation that CI defects, as opposed to CIV defects, predominate in skeletal muscle of PLWH could be of potential therapeutic relevance. Interestingly, CI deficiency is the most commonly observed biochemical defect in child-onset mitochondrial disease (Fassone & Rahman, 2012), and can result in a range of clinical phenotypes, such as leigh syndrome, lactic acidosis, hypertrophic cardiomyopathy and significantly, myopathy (Distelmaier *et al*., 2009).

Unfortunately though, treatment strategies for isolated CI deficiency in mitochondrial disease are limited due to poor understanding of the underlying pathophysiology, and are therefore restricted to symptomatic treatment (Rodenburg, 2016). However, limited *in vitro* data demonstrate that targeting ROS production may alleviate some of the detrimental consequences of CI deficiency, such as mitochondrial membrane (ΨΔ) depolarisation (Distelmaier *et al*., 2009). In addition, the hypothesis that impaired calcium homeostasis as the result of CI deficiency is a significant pathophysiological mechanism underpinning CI-related pathology is being explored (Rodenburg, 2016; Valsecchi *et al*., 2009).

4.5.2 Summary of experimental findings

	Naïve ART	Contemporary ART	Historical ART	Conclusions
Physiological mitochondrial dysfunction	• Not investigated	• Lower oxidative capacity than HIV-uninfected individuals • Comparable levels to historical NRTI group	• Lower oxidative capacity than HIV-uninfected individuals • Comparable levels to contemporary NRTI group	• ART treated PLWH have lower physiological skeletal muscle oxidative capacity compared to age-matched HIV-uninfected individuals
Cellular mitochondrial dysfunction	• Low levels of CI deficiency compared to contemporary and historical NRTI groups • Lower CIV deficiency compared to contemporary NRTI group • Normal levels of mitochondrial mass	• Higher levels of CI deficiency than naïve patients • Comparable levels of CI deficiency with historical NRTI group • Higher levels of CIV deficiency compared to naïve group • Normal levels of mitochondrial mass	• Higher levels of l CI deficiency than ART-naïve patients • Comparable levels of CI and CIV deficiency compared to contemporary NRTI group • Normal levels of mitochondrial mass	• Skeletal muscle mitochondrial dysfunction in contemporary and historical ART groups is comparable • No compensatory upregulation in mitochondrial mass
Molecular mitochondrial dysfunction	• Not investigated as cellular mitochondrial deficiency not observed	• mtDNA deletions present in CI-deficient and intermediate fibres • No difference in mtDNA pattern compared to historical NRTI patients	• mtDNA deletions present in CI-deficient and intermediate fibres • No difference in mtDNA pattern compared to contemporary NRTI patients	• Majority of CI-deficient and intermediate fibres contained mtDNA deletions • No evidence of mtDNA depletion
Cellular mitochondrial dysfunction in PI-treated PLWH	• Not investigated	• PLWH currently treated with a PI had no difference in proportional CI or CIV deficiency compared to ART-treated PLWH not currently treated with a PI		• No evidence of increased mitochondrial dysfunction in PI-treated PLWH
Cellular mitochondrial dysfunction in NNRTI-treated PLWH	• Not investigated	• PLWH currently treated with a NNRTI had no difference in proportional CI or CIV deficiency compared to ART-treated PLWH not currently treated with a NNRTI		• No evidence of increased mitochondrial dysfunction in NNRTI-treated PLWH

Table 4.3 – Summary of experimental findings.

4.5.3 Limitations

The work presented in this chapter demonstrates an array of novel findings and a convincing hypothesis that ART leads to an accelerated onset of skeletal muscle mitochondrial defects in ART-treated PLWH compared to ART-naïve PLWH. However, as mentioned previously, there were a number of limitations to our study.

Our study was limited to only 67 subjects who participated in only one study visit. Although this sample size provided enough materials and data in order to demonstrate novel findings, it does limit the scope of investigations. A larger, longitudinal study group recruited based on exposure to particular combinations of ARVs (e.g. two NRTIs + PI vs two NRTIs + NNRTI, or subdividing the contemporary group into patients with and without exposure to tenofovir disoproxil fumarate (TDF), or subdividing the historical group into patients with and without exposure to zidovudine (AZT)) would give us greater power to detect differences in mitochondrial defects over a period of time.

As both age and NRTI exposure type are difficult to control due to the strong correlation between these factors, studies like those mentioned above would also allow us to better understand the exact effects of particular NRTIs *in vivo* (Venhoff *et al*., 2007). Indeed, the limitation regarding being unable to extract the specific effects of factors such as age from individual groups promoted the recruitment of the MAGMA study, discussed in the following chapters, whereby older age-matched HIV+ and HIV-uninfected males were recruited in an observational study.

As mentioned above, the significantly lower age of the ART-naïve group compared to both ART-treated groups is a limitation. However, as the majority of ART-naive PLWH are younger, this would be very difficult to control. Indeed, a major strength of this study is that it included an ART-naïve comparator group, due to the fact that the majority of newly-diagnosed PLWH begin ART soon after diagnosis and so ART-naive individuals are difficult to recruit.

Of particular note, the ^{31}P-MRS study was limited by the fact that not enough ART-naïve PLWH participated, and although contemporary ART and historical ART-treated PLWH participated, numbers were low.

Whilst the multiplex immunofluorescence assay that was used to quantify mitochondrial protein levels in individual skeletal muscle fibres has many advantages over other assays such as COX/SDH histochemistry, it too has some disadvantages. Primarily, as the assay measures protein levels of subunits of the ETC complexes I and IV, it cannot measure the actual activity of the electron transport chain, which is instead inferred by antibody level. The qPCR analysis is also limited by issues in detecting very small mtDNA deletions.

4.5.4 Future work

As mentioned above, this study was limited by the size of the patient cohort and that fact that it was an observational study. Future work should look to perform these analyses on a larger group of PLWH and ideally at numerous time points (perhaps every 2-5 years).

Another potential aspect of future work should be to investigate the power of individual NRTIs to induce mitochondrial dysfunction through mtDNA deletion mutation formation. In the current study I have demonstrated the presence of defects in oxidative phosphorylation in skeletal muscle fibres from PLWH exposed to both historical and contemporary NRTIs, predominantly underpinned by mtDNA deletions. It is impossible to extract the effects of individual NRTIs from our cohort, and so *in vitro* assessments using fibroblasts, myofibre-derived cell lines or induced pluripotent stem cells treated with individual NRTIs, as well as combinations of NRTIs over various periods of time, should be performed. In addition, some previous studies have performed similar investigations, but none have looked specifically at the effect of various ARVs on myofibre-derived cell lines. Another alternative would be to perform similar work to that mentioned previously but in mouse models treated with various ARVs.

In order to further investigate the cellular and molecular mechanisms underpinning skeletal muscle fibre mitochondrial defects, future studies should look to directly quantify and map the size and locations of mtDNA deletions. This could potentially be performed through long-range PCR or southern blot studies or if available, next-generation sequencing analysis (Taylor *et al*., 2014). As the mitochondrial defects were not explained by mtDNA depletions via the PolG hypothesis, future work should look to explore the viability of other mechanisms of mitochondrial dysfunction and induction of mtDNA mutations. One potential aspect could be to investigate the frequency of oxidatively damaged macromolecules, either histochemically or through molecular assessments (Liang *et al*., 2018).

Finally, as it was difficult to extract the specific effects of factors such as age and HIV-related parameters on skeletal muscle mitochondrial dysfunction, further work was undertaken on the MAGMA cohort of older HIV+ and HIV- individuals in the following chapters.

Chapter 5 – Ageing phenotypes in older PLWH

5.1 Introduction

Due to the success of antiretroviral therapy (ART), the average age of the HIV+ population in developed countries is increasing, with the proportion of PLWH over the age of 50 expected to be an estimated 73% by 2030 (Centres for Disease Control and Prevention, 2013; Smit *et al*., 2015).

In combination with the fact that virally-supressed PLWH appear to have an excess of risk factors for adverse ageing (Brothers *et al*., 2017; Onen *et al*., 2014; Desquilbet *et al*., 2007) and chronic conditions such as elevated chronic inflammation (Deeks, 2011; Justice *et al*., 2012; Erlandson *et al*., 2013; Erlandson *et al*., 2017a; Leng *et al*., 2011; Margolick *et al*., 2013; Onen *et al*., 2014), this population of ageing PLWH appear to be undergoing accelerated ageing (Pathai *et al*., 2014). A result of this phenomenon is that the HIV+ population exhibit declining physical function and a higher prevalence of adverse ageing phenotypes such as frailty and sarcopenia (Guaraldi *et* al., 2011; Kooij *et al*., 2016; Desquilbet *et al*., 2007; Desquilbet et *al.,* 2009; Brothers *et* al., 2017; Echeverria *et al*., 2018; Pinto Neto *et al*., 2016; Wasserman *et al*., 2014; Oliveira *et al*., 2020). This may have serious adverse implications for both the healthcare system and PLWH themselves (Kim *et al*., 2019; Smit *et al*., 2015).

As such, a better understanding of the risk factors and causes underpinning this biological phenomenon are needed in order to develop optimal intervention and preventative strategies for PLWH with adverse ageing phenotypes.

As a result, the MAGMA study was set up with the aim of developing pathologically-defined subgroups for stratified interventional trials. This study includes 45 males over the age of 50, both HIV+ and HIV-uninfected, and sought to better understand the underlying pathophysiological mechanisms behind accelerated ageing in PLWH, with a special interest in the role of age-related mitochondrial dysfunction.

In this chapter, I quantified physical function as well as the prevalence of frailty and sarcopenia in older (≥ 50 years) PLWH and age-matched HIV- individuals using a range of clinically-validated assessments, and sought to identify potential links with both clinical parameters and body composition factors.

5.2 Experimental aims

The significant medical, functional, and socioeconomic consequences of adverse ageing phenotypes such as frailty in HIV-infected individuals (Kim *et al*., 2019; Smit *et al*., 2015) means that a better understanding of the causes and consequences of these conditions in PLWH is imperative.

By utilising an array of clinical assessments that measure physical functional capabilities, as well as assessments of frailty, sarcopenia and body composition, in addition to data obtained from health records detailing general and HIV-related clinical data, in this study I sought to:

- Quantify the prevalence of frailty and sarcopenia in older PLWH and age-matched HIV-individuals.
- Determine whether any HIV-related or general clinical parameters are predictive of reduced physical function and adverse ageing phenotypes in older PLWH.
- Determine whether body composition changes and physical activity levels are predictive of adverse ageing phenotypes in older PLWH.

5.3 Methods

5.3.1 Patient cohort and ethical guidelines

This study was approved by the research ethics committee (Newcastle and North Tyneside 2 (17-NE-0015)), as detailed in **Section 3.1**.

30 HIV+ and 15 HIV- males were recruited as part of the MAGMA study, with patients giving prior written permission. All patients were 50 years or older and therefore classed as 'older'. Full inclusion criteria and study visit details are described in **Section 3.2.1** and **Section 3.3**.

5.3.2 Clinical interview

In order to assess clinical parameters and undertake physical performance assessments, all participants (n = 45), recruited in both Newcastle (n = 37) and London (n = 8), were asked to complete a health questionnaire during the sole study visit, as described in **Section 3.3.1** (further described in **Appendix 2**).

5.3.2 Determination of frailty

A frailty phenotype was assessed as previously described using a modified five FFP criteria (Onen *et al*., 2009), as described in **Section 3.3.2**.

5.3.3 Short Physical Performance Battery (SPPB) assessment

Assessment of physical function was done through a short physical performance battery (SPPB) test, as described in **Section 3.3.3**.

5.3.4 MET score

Metabolic equivalent (MET) expenditure per week was calculated as a surrogate for physical activity assessment. Criteria and cut-offs are described in **Section 3.3.4**.

5.3.5 Classification of sarcopenia

According to the EWGSOP, sarcopenia can be classified in the clinical and research setting based on analyses of muscle mass, muscle strength, and physical performance (Cruz-Jentoft *et al.* 2019), as described in **Section 3.3.5**.

5.3.6 Statistical analysis

Statistical analysis was performed in Prism v5.04, IBM SPSS Statistics v23 and Microsoft Excel 2016. Graphs were produced in Prism v5.04.

Normality was assessed through Shapiro-Wilk tests. Statistical differences between the HIV+ and HIV- individuals were determined by Fisher's exact test for nominal data and unpaired t tests for ordinal data. One-way ANOVA was performed to assess differences between factors with three or more variables, such as smoker category or SPPB category.

Unadjusted linear regression analysis between clinical factors, body composition factors and HIV-related factors was performed using Pearson's correlation for normally distributed data, or Spearman correlation for non-normally distributed data. Multivariate linear regression analysis with adjustment for age was also conducted, with models described in more detail in the relevant sections. As outcomes of multivariate linear regression analysis, unstandardised regression coefficients and their statistical significance were reported, as well as the fit of the models and how much variance (adjusted r^2) they accounted for.

Initially, differences in the various clinical, HIV-related, and body composition parameters between frail, prefrail, and robust, as well as sarcopenic, presarcopenic, and non-sarcopenic PLWH was determined through one-way ANOVA analysis. However, as the size of some groups was small, the prefrail HIV+ group was combined with the frail HIV+ group to create the frail/prefrail HIV+ group and the presarcopenia HIV+ group was combined with the sarcopenia HV+ group to form the sarcopenic/presarcopenic HIV+ group, as done in a recent study (Kooij *et al*., 2016). Differences between the frail/prefrail and robust groups, as well as the sarcopenic/presarcopenic and non-sarcopenic groups were determined by unpaired t tests for normally-distributed data and Mann-Whitney tests for non-parametric data. Statistical significance was set at $p \leq 0.05$.

5.4 Results

5.4.1 MAGMA study cohort characteristics

Table 5.1 summarises the general clinical characteristics of both the HIV+ (n = 30) and HIV- (n = 15) groups. The median age of the HIV+ group was 58 (range 50-85) compared to 59 (range 50-70) years in the HIV- group, confirming excellent age-matching, as expected from the study design.

As described in **Table 5.2**, individuals in the HIV+ group were virally-supressed and had good immune function. 11 (37%) individuals had previously been exposed to older, supposedly mitochondrially-toxic NRTIs (stavudine (d4T), didanosine (ddI), zalcitabine (ddC), zidovudine (AZT)). 9 (30%) were being treated with protease inhibitors (PI), and 11 (37%) were being treated with non-nucleoside reverse transcriptase inhibitors (NNRTI) at time of study visit.

Aside from waist circumference (p = 0.0043) and BMI (p = 0.0003) (**unpaired t test**) (**Figure 5.1b, c**), the HIV+ and HIV- groups were well matched for body composition factors as well as prevalence of various comorbidities (**Table 5.1/Figure 5.1**).

	HIV+ (n = 30)	HIV- (n = 15)	*p*
Age (years)	58 (54-65)	59 (52-69)	0.99
Race (white)	30 (100%)	13 (87%)	0.11
Alcohol consumption (current)	16 (53%)	13 (87%)	**0.046**
Tobacco use:			0.14
Current	11 (37%)	2 (13%)	
Former	11 (37%)	5 (33%)	
Never	8 (27%)	8 (53%)	
Recreational drugs:			
Cannabis	4 (13%)	1 (7%)	0.65
Other	2 (7%)	1 (7%)	1
HBV or HCV infection	5 (17%)	2 (13%)	0.98
Diabetes mellitus (Type 2)	3 (10%)	3 (20%)	0.38
Chronic kidney disease	3 (10%)	0 (0%)	0.54
Number of Comorbidities*	1.2 (1.1)	1.1 (0.8)	0.67
Number of medications*	3.7 (3.0)	2.5 (2.1)	0.18
Polypharmacy	18 (60%)	7 (47%)	0.53
BMI (kg/m^2)*	27.2 (3.3)	32.8 (6.3)	**0.0003**
Body composition:			
Waist circumference (cm)*	97 (9.9)	108 (14.3)	**0.0043**
% Fat mass+	30 (7.8)	34 (7.9)	0.15
% Muscle mass+	70 (7.8)	66 (7.9)	0.15

***Table 5.1 – Clinical characteristics**. Nominal data expressed as the number (%). Ordinal data expressed as the median (± interquartile range). * Expressed as mean (SD). + = Missing information from two HIV- patients who were unable to undertake a DXA scan. P values were determined by Fisher's exact test for nominal data, unpaired t test for ordinal data, and ANOVA for categories such as tobacco use. Statistically significant results were in bold.*

	HIV+ (n = 30)
CD4 count (copies/µl)	656 (231)
Nadir CD4 count (copies/µl)	72 (86)
Viral load (copies/ml)	66 (91)
Historical NRTI exposure (AZT, ddI, d4T, ddC)	11 (37%)
PI treated	9 (30%)
NNRTI treated	11 (37%)
Months since diagnosis	200 (105)
Months on ART	118 (69)
Months untreated	86 (89)

Table 5.2 – Cohort HIV-related characteristics. *Data presented as mean (SD) or number (%).*

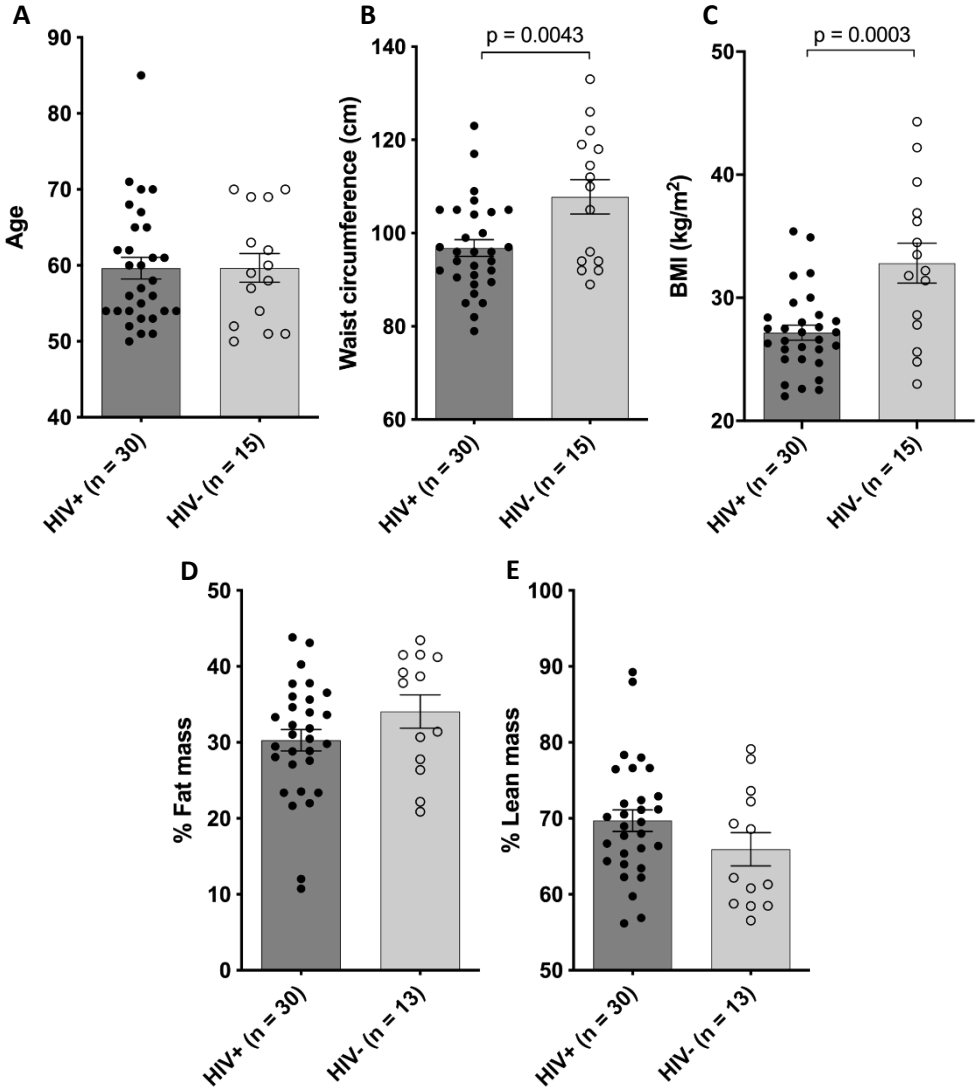

Figure 5.1 – Clinical characteristics by HIV status. *Dot plot graphs (mean ± SEM) depicting the differences between the HIV+ and HIV- groups with regard to (**A**) age, (**B**) waist circumference (cm) (p = 0.0043, unpaired t test), (**C**) BMI (kg/m²) (p = 0.0003), (**D**) percentage fat mass, and (**E**) percentage lean mass. Each dot represents an individual subject.*

5.4.2 Physical performance capabilities, frailty, and sarcopenia in older HIV+ and HIV- individuals

4 (13%) individuals from the HIV+ group (n = 30) were classified as frail according to the modified FFP assessment, while 15 (50%) were classified as prefrail. None of the HIV- group (n = 15) were classified as frail and 7 (53%) HIV- individuals were classified as prefrail (**Table 5.3**). Excess of frailty and sarcopenia in the HIV+ group did not reach statistical significance (**Fisher's exact test**), nor was there a statistically significant difference in FFP score between the two groups (**Figure 5.2a**).

In the HIV+ group, 5 (17%) individuals were defined as being sarcopenic and 6 (20%) as presarcopenic according to the EWGSOP classification (Cruz-Jentoft *et al*., 2019), whilst no individuals in the HIV- group were classified as either sarcopenic or presarcopenic. There was a significantly higher prevalence of combined sarcopenic and presarcopenic (n = 11) individuals in the HIV+ group compared to the HIV- group (n = 0; $p = 0.0093$, **Fisher's exact test**) (**Table 5.3**). 15 (100%) individuals from the HIV- group were non-sarcopenic, which was significantly higher compared to the HIV+ group ($p = 0.008$, **Fisher's exact test**). Although the HIV+ group had a slightly lower mean grip strength (35.3 ± 8.91 kg) compared to the HIV- group (37.5 ± 6.60 kg), this difference was not statistically significant ($p = 0.39$, **unpaired t test**) (**Figure 5.2d**). In addition, the percentage of individuals with pathologically low grip strength (as defined in the FFP assessment) was not significantly different between the two groups (**Fisher's exact test**).

The two groups were well matched for physical performance results in the form of SPPB score (**Fisher's exact test**) (**Figure 5.2b**) and physical activity levels in the form of MET score (**Figure 5.2e**).

	HIV+ (n = 30)	HIV- (n = 15)	*p*
Frailty status:			0.61
Frail	4 (13%)	0 (0%)	
Pre-frail	15 (50%)	8 (53%)	
Robust	11 (37%)	7 (47%)	
FFP Score^	1 (0-2)	0 (0-1)	0.12
Physical performance (SPPB):			0.87
Low	1 (3%)	0 (0%)	
Intermediate	10 (34%)	4 (27%)	
High	19 (63%)	11 (73%)	
SPPB Score^	10 (9-11)	10 (9-12)	0.53
MET score^*	1446 (497-4100)	1446 (630-5172)	0.44
Muscle function:			
Sarcopenia*+	5 (17%)	0 (0%)	**0.0093**
Pre-sarcopenia*+	6 (20%)	0 (0%)	
Non-sarcopenic*+	18 (60%)	13 (100%)	**0.008**
Grip strength (kg)*	35.3 (8.9)	37.5 (6.6)	0.39
Low grip strength*	11 (37%)	3 (20%)	0.25
ASMI (kg/m^2)+	8.1 (1.4)	8.6 (1.0)	0.21

Table 5.3 – Cohort physical function, frailty, and sarcopenia results*. Nominal data expressed as the number (%). * Expressed as mean (SD) for parametric data and median (IQR) for non-parametric tests (denoted by ^). + Missing information from two HIV- patients who were unable to undertake a DXA scan. P values were determined by Fisher's exact test for nominal data, unpaired t test for ordinal data, and ANOVA for categories such as SPPB category. Statistically significant results are in bold.*

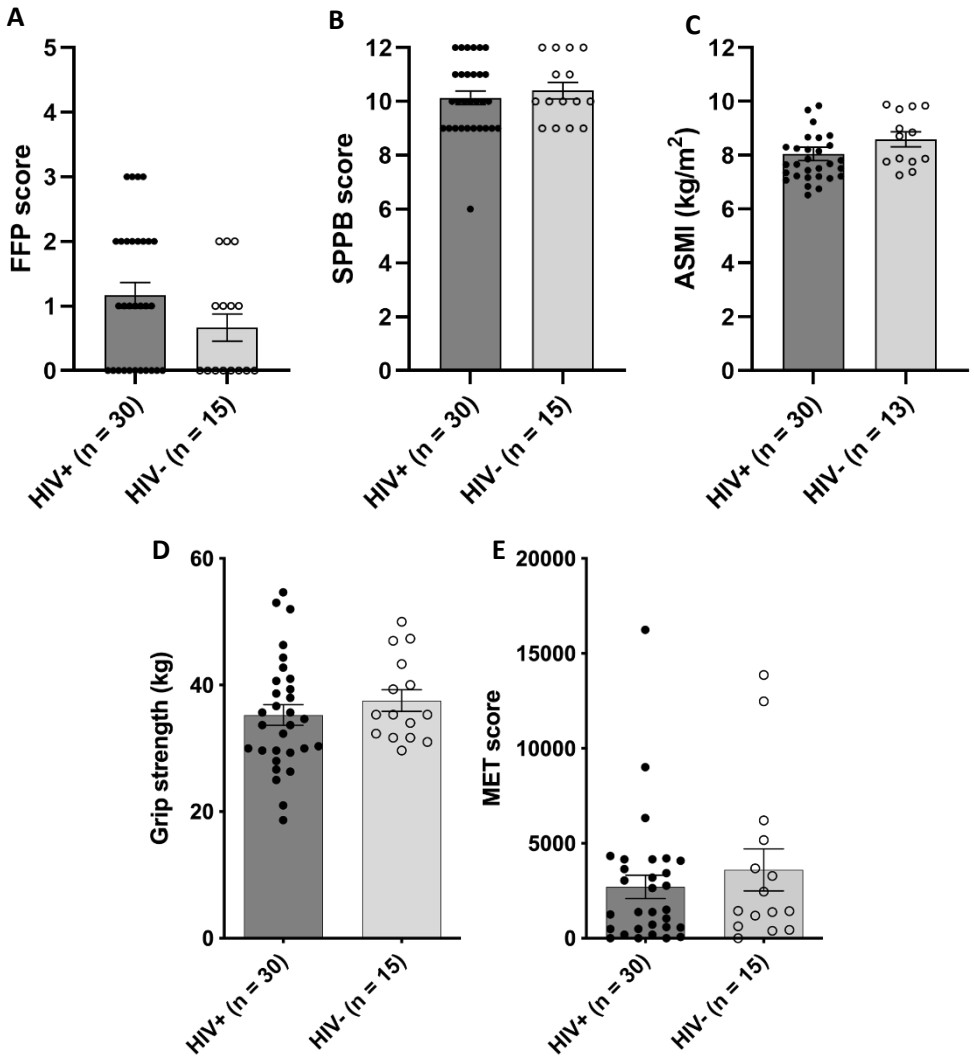

Figure 5.2 – Physical assessment characteristics by HIV status. *Dot plot graphs (mean ± SEM) depicting the differences between the HIV+ and HIV- groups with regard to (**A**) FFP score, (**B**) SPPB score, (**C**) ASMI (kg/m^2), (**D**) grip strength (kg), and (**E**) MET score. Each dot represents an individual subject.*

5.4.3 Determinants of physical function in older PLWH

Initially, I wanted to investigate whether HIV-related factors such as CD4 count and months since diagnosis predicted abnormalities in clinical characteristics and physical function such as comorbidities, FFP score, MET score, SPPB score, and body composition factors in the HIV+ group (n = 30) (**Table 5.4**). In addition, as age is a well-known risk factor for adverse physical outcomes, I additionally sought to determine whether age predicted these outcomes.

Interestingly, unadjusted linear regression analysis demonstrated that a greater duration of untreated HIV infection significantly predicted poorer grip strength (r = -0.41; *p* = 0.023, **Pearson's correlation**) (**Figure 5.3a**). As such, in order to investigate the effect of greater months with untreated HIV infection after adjustment for age, I developed a multivariate linear regression model with grip strength as the dependant variable and age, as well as months untreated, as the independent variables. Here, multivariate linear regression confirmed that the association between grip strength and duration of untreated infection was independent of age (unstandardised regression coefficient = -0.039; *p* = 0.037, **multivariate linear regression**) (**Table 5.4**). The overall model fit was significant (*p* = 0.037), but only predictive of a small amount of variation (r^2 = 0.22).

In addition, a greater CD4 count significantly predicted a higher appendicular skeletal muscle mass index (ASMI) (r = 0.40; *p* = 0.035, **Pearson's correlation**) (**Figure 5.3b**). This was then adjusted for age in a multivariate linear regression model. Here, multivariate linear regression confirmed that the significant association between CD4 count and ASMI was independent of age (unstandardised regression coefficient = 0.002; *p* = 0.046, **multivariate linear regression**) (**Table 7.4**). However, the overall model fit was not significant (*p* = 0.11) and was only predictive of a small amount of variation (r^2 = 0.094).

Finally, there were no other significant associations between physiological factors mentioned above and HIV-related factors such as duration of HIV and ART, or exposure to mitochondrially-toxic NRTIs (ddC, ddI, d4T and AZT) (**Table 5.4**).

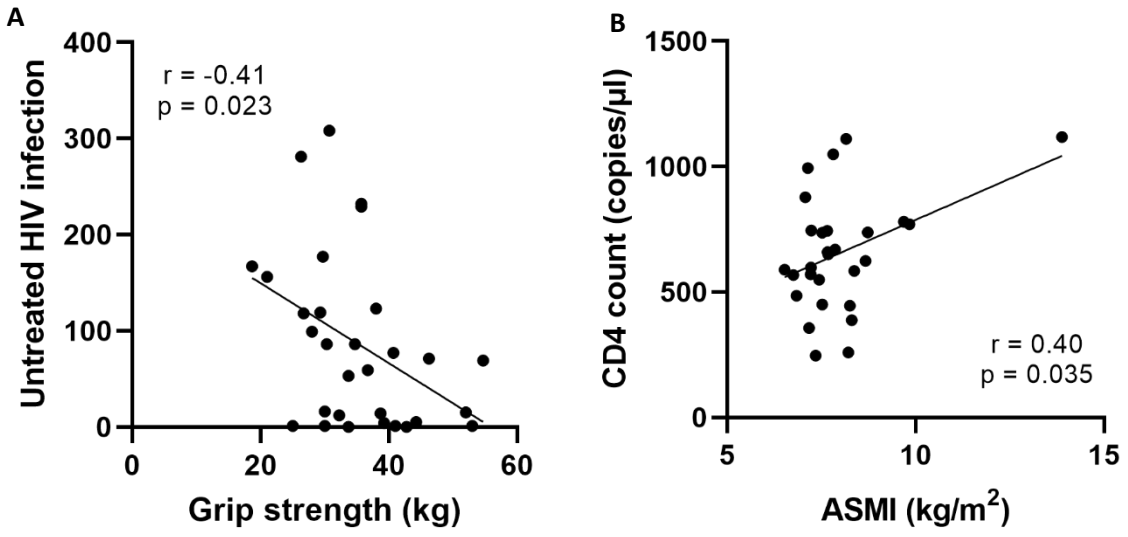

Figure 5.3 – Linear regression analysis of physical determinants in older PLWH*. Scatter plots representing the linear regression analysis (Pearson's correlation) between (**A**) months with untreated HIV infection and grip strength (kg), and (**B**) CD4 count (copies/µl) and ASMI (kg/m^2).*

	Age		Months since diagnosis		Months on ART		Months untreated			CD4 count (copies/µl)			Mitochondrially toxic NRTI	
	r	*p*	r	*p*	r	*p*	r	*p*	MV *p*	r	*p*	MV *p*	r	*p*
Age	-	-	0.34	0.065	0.29	0.12	0.17	0.37	-	-0.18	0.35	-	-	0.082
BMI (kg/m²)	0.038	0.84	-0.11	0.57	-0.29	0.13	0.072	0.70	-	0.33	0.09	-	-	0.10
Waist circumference (cm)	0.01	0.96	-0.12	0.52	-0.072	0.71	-0.11	0.57	-	-0.014	0.95	-	-	0.34
Number of comorbidities	0.10	0.58	0.078	0.68	0.10	0.61	0.018	0.92	-	0.14	0.47	-	-	0.78
Number of medications	-0.11	0.58	0.25	0.19	0.12	0.53	0.21	0.28	-	0.12	0.54	-	-	0.68
Polypharmacy	-	0.17	-	0.48	-	0.60	-	0.20	-	-	0.32	-	-	-
Grip strength (kg)	-0.27	0.15	-0.34	0.064	0.038	0.84	**-0.41**	**0.020**	**0.037**	-0.14	0.50	-	-	0.50
ASMI (kg/m²)	-0.14	0.47	-0.095	0.62	-0.14	0.45	-0.01	0.96	-	**0.40**	**0.035**	**0.046**	-	0.81
% Fat mass	-0.25	0.18	-0.29	0.16	-0.15	0.43	-0.23	0.23	-	0.15	0.46	-	-	0.59
% Lean mass	0.25	0.18	0.29	0.16	0.15	0.43	0.23	0.23	-	-0.15	0.46	-	-	0.59
FFP score^	-0.007	0.97	0.19	0.32	-0.15	0.44	0.34	0.065	-	0.10	0.61	-	-	0.86
MET score^	0.26	0.89	-0.13	0.48	-0.006	0.98	-0.15	0.44	-	-0.19	0.35	-	-	0.44
SPPB score^	-0.082	0.67	-0.22	0.24	0.097	0.61	-0.16	0.40	-	-0.014	0.95	-	-	0.49

Table 5.4 – Predictors of physical function*. Table depicting associations between clinical and HIV-related parameters in older HIV+ (n = 30) individuals. Linear regression and correlation analysis was determined by Pearson's correlation for normal data and Spearman's correlation for non-normal data (denoted by ^). Individuals were grouped into mitochondrially-toxic NRTI (n = 11) and non-mitochondrially toxic NRTI (n = 19), and statistical differences determined were by unpaired t test (parametric) and Mann-Whitney test (non-parametric). Statistically significant values are in bold. MV = multivariate.*

5.4.4 Determinants of ageing phenotypes in older PLWH

To better understand the associations between the various clinical factors, body composition factors, and HIV-related factors with frailty and sarcopenia in older PLWH, I stratified the HIV+ group (n = 30) into frail (n = 4), prefrail (n = 15) and robust (n = 11) HIV+ groups, as well as sarcopenic (n = 5), presarcopenic (n = 6) and non-sarcopenic (n = 19) HIV+ groups.

There was no significant difference in any of the clinical, HIV-related, body composition, physical performance, or lifestyle factors between the frail, prefrail, and robust PLWH (**one-way ANOVA**) (**Figure 5.4**). Nor was there any significant difference in any these factors between the sarcopenia, presarcopenia, and non-sarcopenia HIV+ groups (**Figure 5.5**).

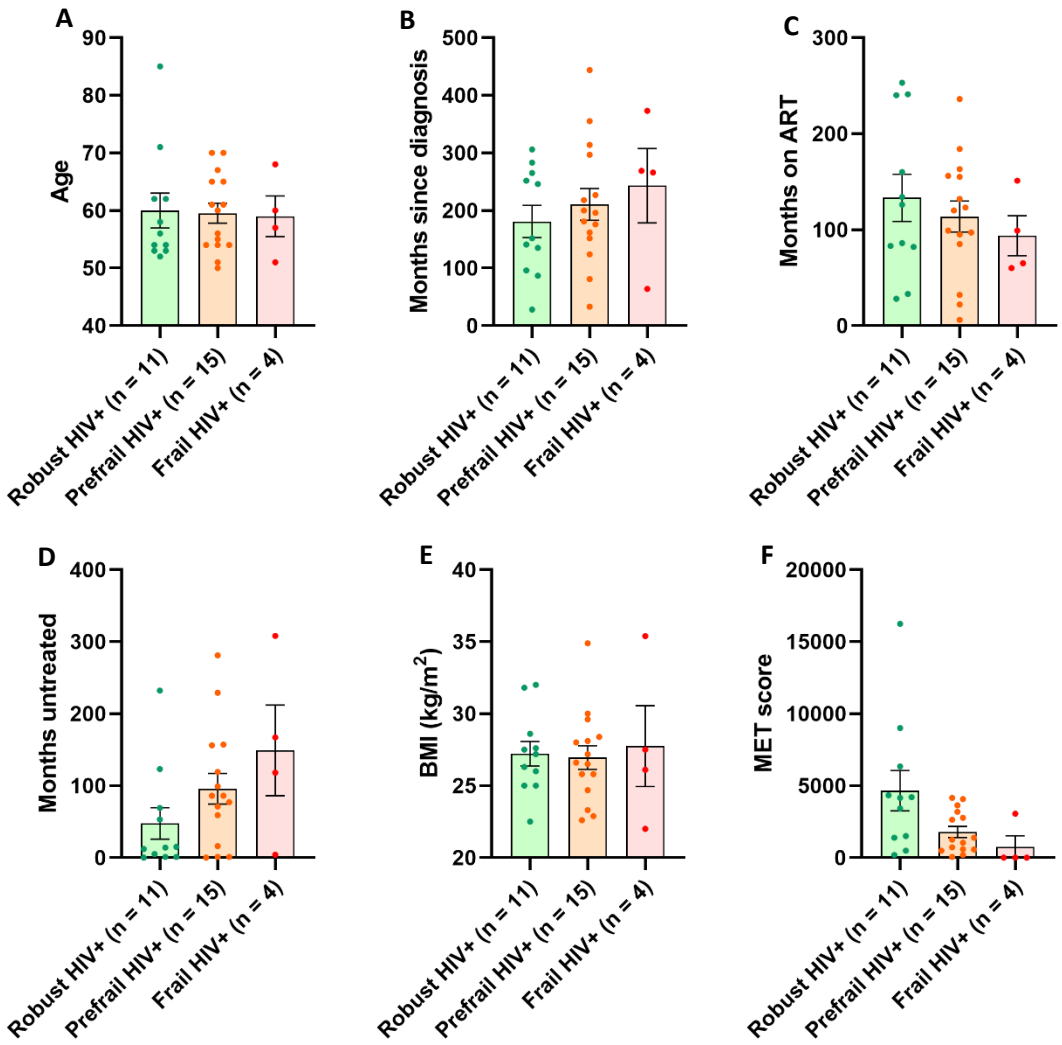

Figure 5.4 – Clinical parameters in frail PLWH. *Dot plots (mean ± SEM) showing (**A**) age, (**B**) months since diagnosis, (**C**) months on ART, (**D**) months untreated, (**E**) BMI (kg/m^2), and (**F**) MET score in frail PLWH (n = 4), prefrail PLWH (n = 15) and robust PLWH (n = 11). Each dot represents an individual subject.*

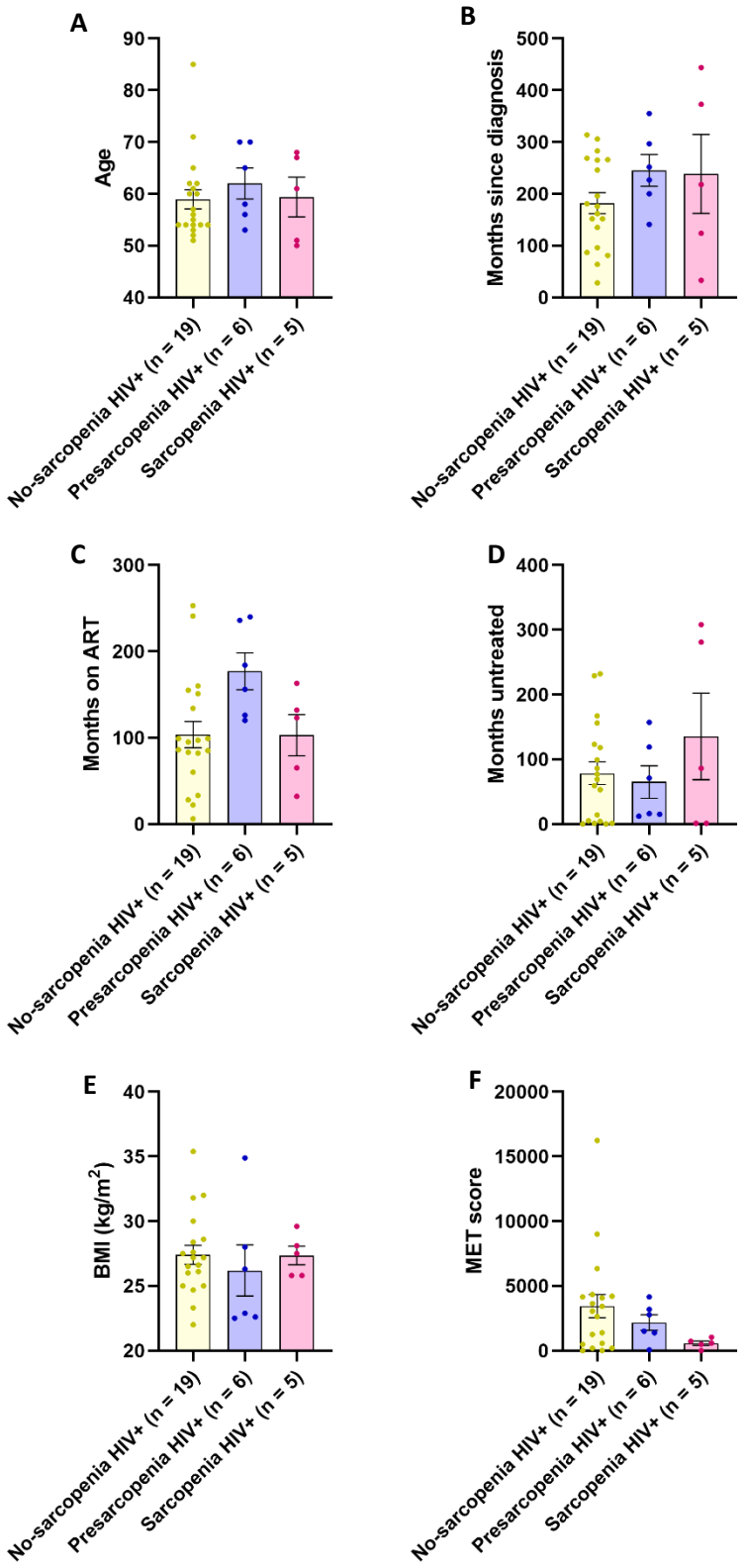

Figure 5.5 – Clinical parameters in sarcopenic PLWH. *Dot plots (mean ± SEM) showing (**A**) age, (**B**) months since diagnosis, (**C**) months on ART, (**D**) months untreated, (**E**) BMI (kg/m²), and (**F**) MET score in sarcopenic PLWH (n = 5), presarcopenic PLWH (n = 6) and non-sarcopenic PLWH (n = 19). Each dot represents an individual subject.*

Although frailty and sarcopenia were only seen in the HIV+ group, they were nevertheless uncommon. Therefore, in order to increase the power to detect differences between PLWH with normal ageing phenotypes and those with adverse ageing phenotypes, I grouped the HIV+ group (n = 30) into frail/prefrail HIV+ (n = 19) and sarcopenic/presarcopenic HIV+ (n = 11) groups, as has been done in previous studies (Kooij *et al*., 2016). The frail/prefrail HIV+ group was then compared to the robust HIV+ group (n = 11) (**Table 5.5**), whilst the sarcopenia/presarcopenia HIV+ group was compared to the non-sarcopenic HIV+ group (n = 19) (**Table 5.6**). Of note, measurements of grip strength were not included as part of these assessments as they are important components of both frailty and sarcopenia classification criteria. In addition, measurements of fat and lean mass were not included in the assessments in sarcopenic/presarcopenic PLWH as they are also important components of the sarcopenia diagnostic criteria.

Interestingly, MET score was significantly lower in the frail/prefrail group (n = 19) compared to the robust group (n = 11; $p = 0.0097$, **Mann-Whitney test**) (**Figure 5.6f**).

Notably, there was no significant difference in any other factor tested between the frail/prefrail HIV+ and robust HIV+ groups, or the sarcopenia/presarcopenia HIV+ (n = 11) and non-sarcopenia HIV+ groups (n = 19) (**Figure 5.7**). Importantly, age was not a predictor of frailty or sarcopenia.

	Frail/Pre-frail HIV+ (n = 19)	Robust HIV+ (n = 11)	*P*
Age	59 (6.6)	60 (10.0)	0.85
Months since diagnosis	218 (108.3)	181 (92.9)	0.36
Months on ART	110 (58.3)	133 (81.6)	0.36
Months untreated	107 (92.1)	48 (72.2)	0.077
CD4 count (copies/µl)	691 (240.9)	592 (207.6)	0.28
MET score^	1040 (198-3050)	4158 (1386-6336)	**0.0097**
SPPB score^	10 (9-11)	10 (9-11)	0.84
BMI (kg/m^2)	27 (3.6)	27 (2.8)	0.94
Waist circumference (cm)	96 (11.3)	98 (7.2)	0.54
% Fat mass$^+$	30 (9.2)	30 (4.5)	0.85
% Lean mass$^+$	70 (9.2)	70 (4.5)	0.85
Number of comorbidities	1 (1.1)	1 (1)	0.26
Number of medications	4 (3.4)	3 (2)	0.27

Table 5.5 – Clinical characteristics in frail/prefrail PLWH*. Expressed as mean (SD) for parametric data, and median (IQR) for non-parametric data (denoted by ^). + = Missing information from two HIV- patients who were unable to undertake a DXA scan. P values were determined by unpaired t test for normalised data and Mann-Whitney test for non-normalised data. Statistically significant values are in bold.*

	Sarcopenic/Pre-sarcopenic HIV+ (n = 11)	Non-sarcopenic HIV+ (n = 19)	*P*
Age	61 (7.6)	59 (8.1)	0.54
Months since diagnosis	242 (120.1)	182 (87.4)	0.12
Months on ART	134 (63.3)	104 (67)	0.12
Months untreated	97 (110.5)	79 (76.3)	0.59
CD4 count (copies/µl)	664 (182.9)	650 (262.5)	0.88
MET score^	1040 (495-2772)	3050 (498-4212)	0.18
FFP score^	1 (1-2)	1 (0-2)	0.59
BMI (kg/m^2)	27 (3.6)	27 (3.2)	0.59
Waist circumference (cm)	97 (11.4)	97 (9.3)	0.91
Number of comorbidities	1 (0.7)	1 (1.2)	0.79
Number of medications	3 (2.7)	4 (3.1)	0.40

Table 5.6 – Clinical characteristics in sarcopenic/presarcopenic PLWH*. Expressed as mean (SD) and median (IQR) for non-parametric data (denoted by ^). P values were determined by unpaired t test for normalised data and Mann-Whitney test for non-normalised data. There were no statistically significant results*

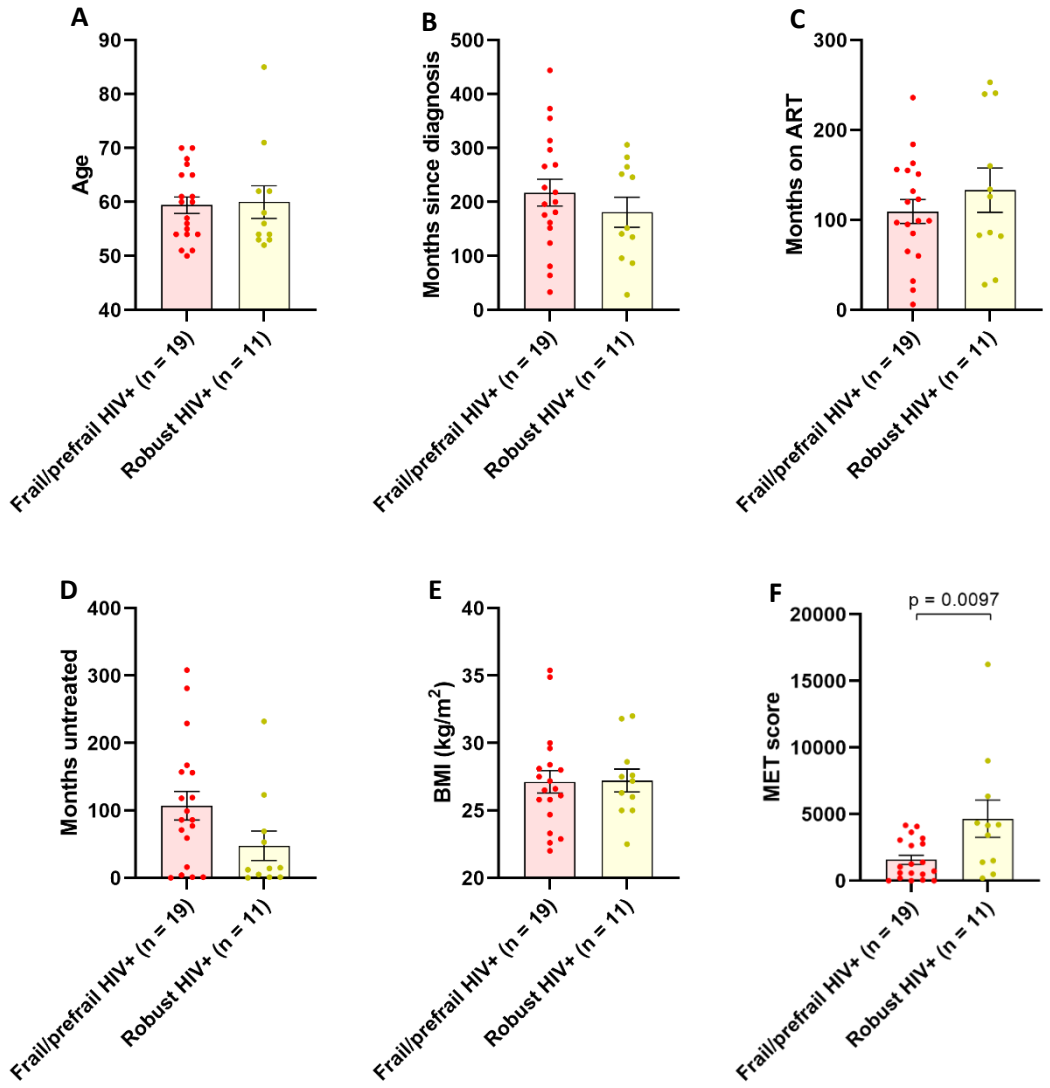

Figure 5.6 – Clinical characteristics in frail/prefrail PLWH. *Dot plots (mean ± SEM) showing (**A**) age, (**B**) months since diagnosis, (**C**) months on ART, (**D**) months untreated, (**E**) BMI (kg/m^2), and (**F**) MET score in frail/prefrail PLWH (n = 19) and robust PLWH (n = 11). Each dot represents an individual subject.*

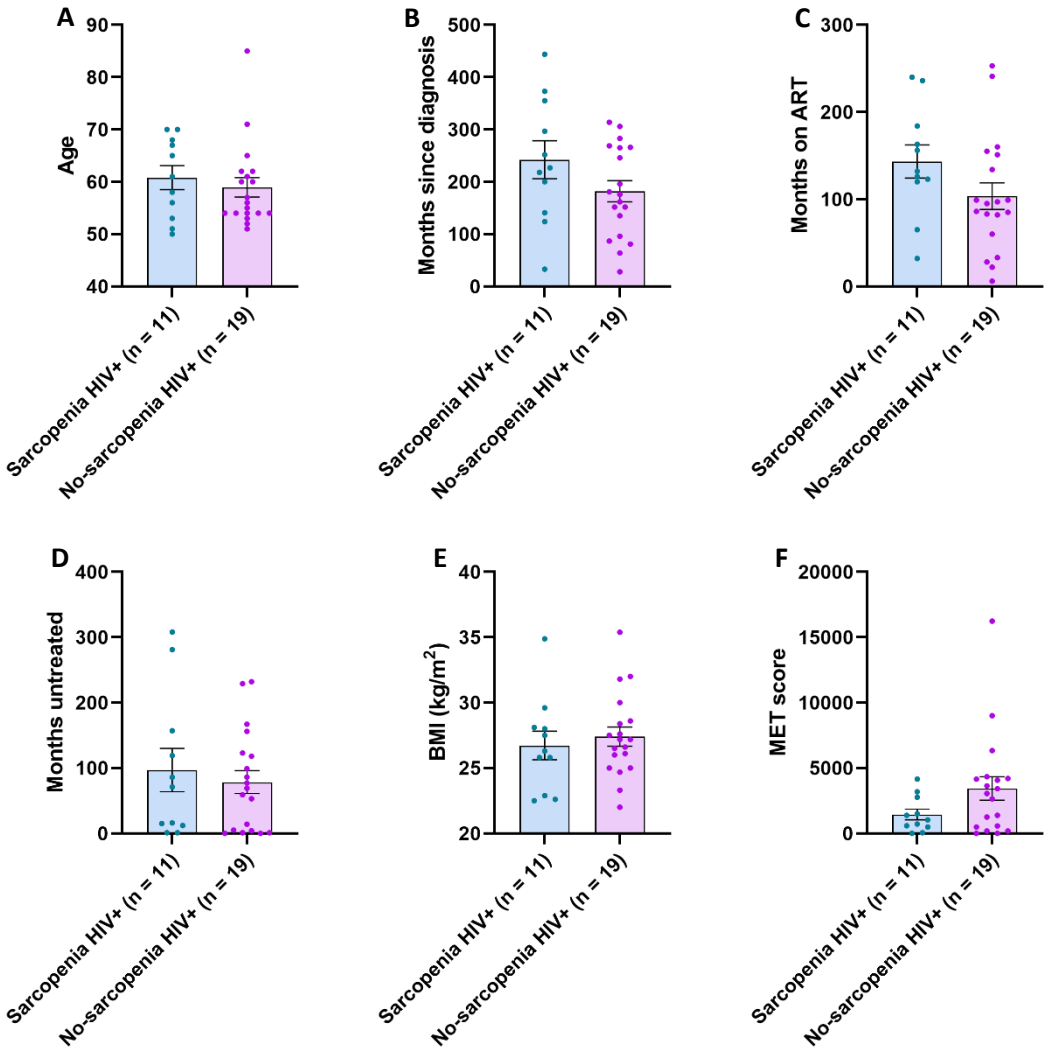

Figure 5.7 – Clinical characteristics in sarcopenic/presarcopenic PLWH. *Dot plots (mean ± SEM) showing (**A**) age, (**B**) months since diagnosis, (**C**) months on ART, (**D**) months untreated, (**E**) BMI (kg/m^2), and (**F**) MET score in sarcopenic/presarcopenic PLWH (n = 19) and non-sarcopenic PLWH (n = 19). Each dot represents an individual subject.*

5.5 Discussion

In this chapter, as well as in later chapters of this thesis (**Chapters 6** and **Chapter 7**), data collected and analysed as part of the MAGMA study is presented for the first time.

Here, using a range of validated clinical assessments such as the assessment of sarcopenia using the EWGSOP diagnostic criteria, modified FFP assessment (Onen *et al*., 2009), SPPB, and MET score, I demonstrated that our cohort of older PLWH have a higher prevalence of frailty, sarcopenia, and pre-sarcopenia compared to the age-matched HIV- individuals. Although due to the small cohort size and therefore limitation in the statistical power, this was not statistically significant. However, the prevalence of combined sarcopenic and presarcopenic HIV+ individuals compared to sarcopenic/presarcopenic HIV- individuals was significantly higher. These data support various previous observations of a higher prevalence of frailty (Desquilbet *et al*., 2007; Kooij *et* al., 2016; Brothers *et* al., 2017) and sarcopenia (Echeverria *et al*., 2018; Pinto Neto *et al*., 2016; Wasserman *et al*., 2014; Oliveira *et al*., 2020) in PLWH compared to age-matched HIV- individuals, as well as a decline in physical performance capabilities in this group (Onen *et al*., 2009; Erlandson *et al*., 2014).

One of the experimental aims of this study was to investigate the links between adverse ageing phenotypes such as frailty and sarcopenia, and clinical, HIV-related, as well as body composition factors in older PLWH. As HIV-related clinical parameters such as low CD4 count (Guaraldi *et al*., 2019a; Erlandson *et al*., 2012; Onen *et al*., 2014), months on ART (Brothers *et al*., 2017; Althoff *et al*., 2014), and exposure to particular ARVs (Onen *et al*., 2014; Erlandson *et al*., 2017a) are known risk factors for frailty in PLWH, through linear regression analyses I sought to identify whether these factors predicted adverse outcomes in the physiological factors mentioned above. Interestingly, of these factors, a longer duration of untreated HIV infection significantly predicted poorer grip strength. This was confirmed in a multivariate linear regression model after adjustment for age. In addition, a lower CD4 count was significantly associated with lower adjusted muscle mass, as assessed through ASMI. However, this association was not independent of the effect of age, and was driven mainly by one outlier. Together, these findings suggest that a longer duration of untreated HIV infection may lead to a decline in physical strength, which may subsequently produce an increased susceptibility to developing adverse ageing phenotypes, supporting previous data (Brothers *et al*., 2017; Althoff *et al*., 2014; Desquilbet *et al*., 2009; Guaraldi *et al*., 2019a; Erlandson *et al*., 2012a; Branas *et al*., 2017; Erlandson *et al*., 2017b). Indeed, as the majority of these HIV+ patients have been virally-supressed as the result of cART, this physiological phenomenon is likely to be due to a 'legacy effect' of untreated HIV infection, whereby incomplete immune recovery may induce residual chronic inflammation and immune activation that may predispose the individual to

complications and morbidity (Wilson & Sereti, 2013; Guaraldi *et al*., 2011). These findings may also have clinical significance when determining whether PLWH are more at risk of developing frailty or whether they will progress through the frailty phenotypes faster. However, more work, including longitudinal study, needs to be undertaken in order to better understand these associations.

Finally, by initially stratifying the HIV+ group by whether they are frail, prefrail, or robust, as well as whether they were sarcopenic, presarcopenic, or non-sarcopenic, I assessed whether any of the clinical, HIV-related, or body composition factors were significantly altered in PLWH with adverse ageing phenotypes. Notably, there were no statistically significant associations, and so in order to increase the power to detect differences in these factors, I next stratified the HIV+ individuals into frail/prefrail or sarcopenic/presarcopenic groups, as done recently in a study by Kooij and colleagues (Kooij *et* al., 2016). Here, I investigated whether any of the clinical, HIV-related, or body composition factors were significantly altered in frail and sarcopenic older PLWH compared to age-matched robust PLWH. Interestingly, MET score was significantly higher in robust PLWH compared to frail/prefrail PLWH. Importantly, although the relationship between frailty/prefrailty and physical activity is complex and bidirectional, this novel finding supports previous observations regarding the potential therapeutic advantages of exercise training programmes in preventing the onset of frailty (Walston *et al.*, 2018; Cameron *et al*., 2013; Silva *et al*., 2017). Notably, there was no significant difference in any of the factors mentioned above when comparing sarcopenic/presarcopenic older PLWH and age-matched non-sarcopenic PLWH.

An important advantage of this study compared to other cohort studies conducted in this field is the large array of clinical tests performed in order to assess not only frailty and sarcopenia in older PLWH and age-matched HIV- individuals, but also body composition factors and numerous surrogates for physical function capability. This allowed for a more comprehensive analysis of the relationships between these factors in older PLWH.

5.5.1 Summary of experimental findings

	Conclusions
Cohort characteristics	• Well matched for age, comorbidities, and most lifestyle factors. • HIV- group had higher BMI and waist circumference • HIV+ group had higher alcohol consumption
Prevalence of adverse ageing phenotypes and physical function parameters	• Higher prevalence of frailty and sarcopenia in HIV+ group compared to HIV- group, although not statistically significant. • Prevalence of combined sarcopenic and presarcopenic HIV+ individuals significantly higher compared to sarcopenic/presarcopenic HIV- individuals. • Well matched for physical performance results.
Prediction of HIV parameters on clinical factors	• Months untreated HIV infection predicted poor grip strength, after adjustment for age. CD4 count predicted higher adjusted muscle mass, after further adjustment for age.
Determinants of factors associated with ageing phenotypes in PLWH	• MET score was significantly lower in frail/prefrail PLWH compared to robust PLWH.

Table 5.7 – Summary of experimental findings.

5.5.2 Limitations

Whilst this study has advantageous aspects, it is limited by the fact that it is not a longitudinal study. As frailty is a dynamic state, the frailty status of our cohort could change over time, and this phenomenon is therefore not accounted for in this study.

Another limitation lies in the fact that our cohort is composed solely of males. This was a deliberate aspect of the study protocol design, as older HIV+ women are more heterogeneic than older HIV+ men, owing to the effects of menopause. Furthermore, the majority of the older HIV+ population in England is male. Finally, body composition and skeletal muscle changes in ageing differ between men and women. This ultimately means that the findings are not generalisable to older HIV+ women, and a separate study should be conducted in this group.

5.5.3 Future work

As mentioned above, any future studies should aim to be longitudinal cohort studies. In addition, the cohort size should be increased to increase the in which power to investigate effects within groups. Comparable studies should ideally also be undertaken in older HIV+ and HIV- females.

In the next chapter I go on to examine the effect of mitochondrial dysfunction in these ageing phenotypes in PLWH.

Chapter 6 – Skeletal muscle mitochondrial dysfunction in older PLWH and adverse ageing phenotypes

6.1 Introduction

The link between mammalian mitochondrial dysfunction and ageing in several tissues is well acknowledged. This link appears, in part, to be underpinned by an accumulation of mtDNA mutations with age, with resultant age-related decreases in oxidative capacity amongst other mitochondrial functions, ultimately leading to a decline in cellular function (Kujoth *et al.,* 2005; Nooteboom *et al*., 2010; Lopez-Otin *et* al., 2013; Park & Larsson, 2011; Kauppila *et al*., 2017; Lawless *et al*., 2020). Indeed, mitochondrial dysfunction was noted as one of the nine cellular and molecular hallmarks of ageing (Lopez-Otin *et al*., 2013). Importantly, recent data also appear to suggest a causal link between age-related mitochondrial dysfunction and frailty, as well as sarcopenia (Alway *et al*., 2017; Andreux *et* al., 2018; Brierley *et* al., 1998).

Mitochondrial dysfunction is well described in PLWH. In particular, early studies demonstrated a reduction in mtDNA content in PLWH who were exposed to certain older NRTIs that inhibited the mitochondrial polymerase – PolG (Dalakas *et* al., 1990; Arnaudo *et* al., 1991; Lim & Copeland, 2001). In addition, later studies by our group demonstrated an excess of mtDNA deletions in PLWH exposed to those ARVs, even after they have switched to supposedly less harmful, newer, ARVs (Payne *et al*., 2011). In further support, data presented in **Chapter 4** indicated that skeletal muscle from PLWH treated with both newer and older ARVs also had an excess of mitochondrial dysfunction.

Taken together, there is a strong hypothesis that the increased prevalence of adverse ageing phenotypes experienced by older (≥50 years) PLWH compared to the age-matched general population (Desquilbet *et* al., 2007; Kooij *et al*., 2016; Curcio *et al*., 2016; Echeverria *et al*., 2018) may be underpinned by both age-related and HIV-related mitochondrial dysfunction. Due to the increasing age of the HIV+ population and the adverse impact this will have on healthcare, attempts to better understand the underlying pathophysiological mechanisms of adverse ageing in this population is imperative (Steffl *et al*., 2017; Kim *et al*., 2019).

6.2 Experimental aims

Mitochondrial dysfunction is widely recognised as one of the key hallmarks of the ageing process in the general population (Lopez-Otin *et al*., 2013). In addition, the established role of mitochondrial dysfunction in toxicities experienced by PLWH exposed to older nucleoside reverse transcriptase inhibitors suggests that mitochondrial dysfunction may be a driver of adverse ageing seen in older PLWH (Dalakas *et* al., 1990; Arnaudo *et* al., 1991; Dalakas *et* al., 2001; Ashar *et* al., 2015; Hunt & Payne, 2020).

Researchers in the field of ageing with HIV are now giving more attention to the hypothesis that mitochondrial dysfunction plays a causative role in adverse ageing phenotypes in PLWH. However, few studies have investigated mitochondrial function at the cellular level in tissues heavily implicated in the ageing process, such as skeletal muscle. As such, using clinical data and tissue collected as part of the MAGMA study, in this chapter I aimed to:

- Determine if there is mitochondrial CI and CIV deficiency at the individual myofibre level in older PLWH compared with age-matched HIV- controls.
- Determine if there is an alteration in mitochondrial mass at the individual myofibre level in older PLWH compared with age-matched HIV- controls.
- Determine whether skeletal muscle mitochondrial CI and CIV deficiency is associated with adverse ageing phenotypes such as frailty and sarcopenia.
- Determine whether skeletal muscle mitochondrial CI and CIV deficiency is predicted by any physical, clinical, or lifestyle factors in older PLWH.

6.3 Methods

6.3.1 Patient cohort

This study was approved by the research ethics committee (Newcastle and North Tyneside 2 (17-NE-0015)). Skeletal muscle samples were taken by percutaneous biopsy from HIV-infected males (n = 30) as well as HIV-uninfected males (n = 15) as part of the MAGMA study (**Table 3.1**), with patients giving prior written permission.

Control skeletal muscle tissue (for calibration of the multiplex immunofluorescence assay) was acquired with prior informed consent from the distal part of the hamstring of people undergoing anterior cruciate ligament (ACL) surgery. Approval for this was given by Newcastle biobank (NAHPB reference: 042) (described in **Section 3.2.3**).

In addition, percutaneous skeletal muscle biopsies from the two mitochondrial disease patients described in **Section 3.2.4** were also subjected to the multiplex immunofluorescence assay for quantification of Complex I (CI) and IV (CIV) deficiency as a positive control group, in order to provide additional context to the levels of CI/CIV deficiency observed.

6.3.2 Multiplex immunofluorescence for the quantification of mitochondrial protein level in human skeletal muscle

Transverse cryo-sections (10µm) were subjected to a validated multiplex immunofluorescence assay in order to objectively quantify the abundance of mitochondrial ETC complexes I and IV as well as mitochondrial mass within individual myofibres, using the CI + CIV assay described in **Section 3.4.2** (Rocha *et al*., 2015).

6.3.3 Image acquisition and analysis for mitochondrial protein level

Fluorescent images were acquired using a Zeiss Axio Imager M1 and Zen 2011 (blue edition) software with a Monochrome Digital Camera (AxioCam MRm) at 20x magnification, as described in **Section 3.4.4**. The 'intermediate –', 'intermediate +' and 'deficient' groups were pooled together to create the 'abnormal' group (z > -3).

6.3.4 Statistical analysis

Statistical analysis was performed in Prism v5.04, IBM SPSS Statistics v23 and Microsoft Excel 2016. Graphs were produced in Prism v5.04.

Normality was assessed by Shapiro-Wilk tests. Statistical differences in mitochondrial function between the HIV+ and HIV- individuals as well as PLWH stratified by frailty/prefrailty and sarcopenia/presarcopenia were determined by unpaired t tests for normalised data and Mann-Whitney tests for non-normal data sets. One-Way ANOVA was used to determine differences in mitochondrial parameters between frail, prefrail, and robust PLWH, as well as sarcopenic, presarcopenic, and non-sarcopenic PLWH. Fisher's exact test was performed in order to determine differences in mitochondrial deficiency in nominal data sets such as stratification by smoker status.

Linear regression analysis between mitochondrial dysfunction and clinical as well as body composition factors was performed using Pearson's correlation for normal data, or Spearman's correlation for non-normal data. Finally, multivariate linear regression analysis was undertaken with factors of interest. Here, these multivariate models included (1) average myofibre mitochondrial mass as the dependant variable, and age, percentage fat mass and proportional CI deficiency as the independent variables; (2) proportional CI deficiency as the dependant variable and age as well as number of medications as the independent variables. Unstandardised regression coefficients and their statistical significance were reported, as well as the fit of the models and how much variance (adjusted r^2) they accounted for.

Statistical significance was set at $p \leq 0.05$.

6.4 Results

6.4.1 Cohort characteristics

Patient characteristics for both the HIV+ (n = 30) and HIV- (n = 15) groups are described in **Table 5.1** in **Chapter 5**. Briefly, the median age of the HIV+ group was 58 years (range 50-85) compared to 59 years (range 50-70) in the HIV- group. 4 (13%) individuals from the HIV+ group were classified as frail according to the FFP assessment, while 15 (50%) were classified as prefrail. None of the HIV- group were classified as frail and 7 (53%) HIV- individuals were classified as prefrail. In the HIV+ group, 5 (17%) individuals were defined as being sarcopenic and 6 (20%) as presarcopenic, whilst 15 (100%) were classified as non-sarcopenic in the HIV- group

In addition, the HIV-related characteristics of the HIV+ individuals are described in **Table 5.2** in **Chapter 5**. Briefly, individuals in the HIV+ group were virally-supressed and had restored CD4 counts. 11 (37%) individuals had previously been exposed to older, supposedly mitochondrially-toxic NRTIs (stavudine (d4T), didanosine (ddI), zalcitabine (ddC), zidovudine (AZT)). 9 (30%) were being treated with protease inhibitors (PIs) and 11 (37%) were being treated with non-nucleoside reverse transcriptase inhibitors (NNRTIs) at time of study visit.

Skeletal muscle biopsies from two post-mortem mitochondrial disease patients (described in **Section 3.2.4**) were included in the multiplex immunofluorescence quantification of mitochondrial function in order to add qualitative contextualisation.

6.4.2 Skeletal muscle mitochondrial dysfunction in older PLWH

The HIV+ group (n = 30) had a significantly higher proportion of myofibres with mitochondrial dysfunction in the form of CI (*p* = 0.049, **unpaired t test**) and CIV (*p* = 0.001) deficiency compared to the HIV- group (n = 15) (**Figure 6.1b, c**). For a contextual comparison, I also included results from two individuals with diagnosed mitochondrial disease (**Table 3.2, Section 3.2.4**). In general, proportional levels of both CI and CIV deficiency were higher in the mitochondrial disease patients than both the HIV+ and HIV- groups, although the cases with the highest levels of proportional CI and CIV deficiency were comparable with these disease controls (**Figure 6.1b, c**).

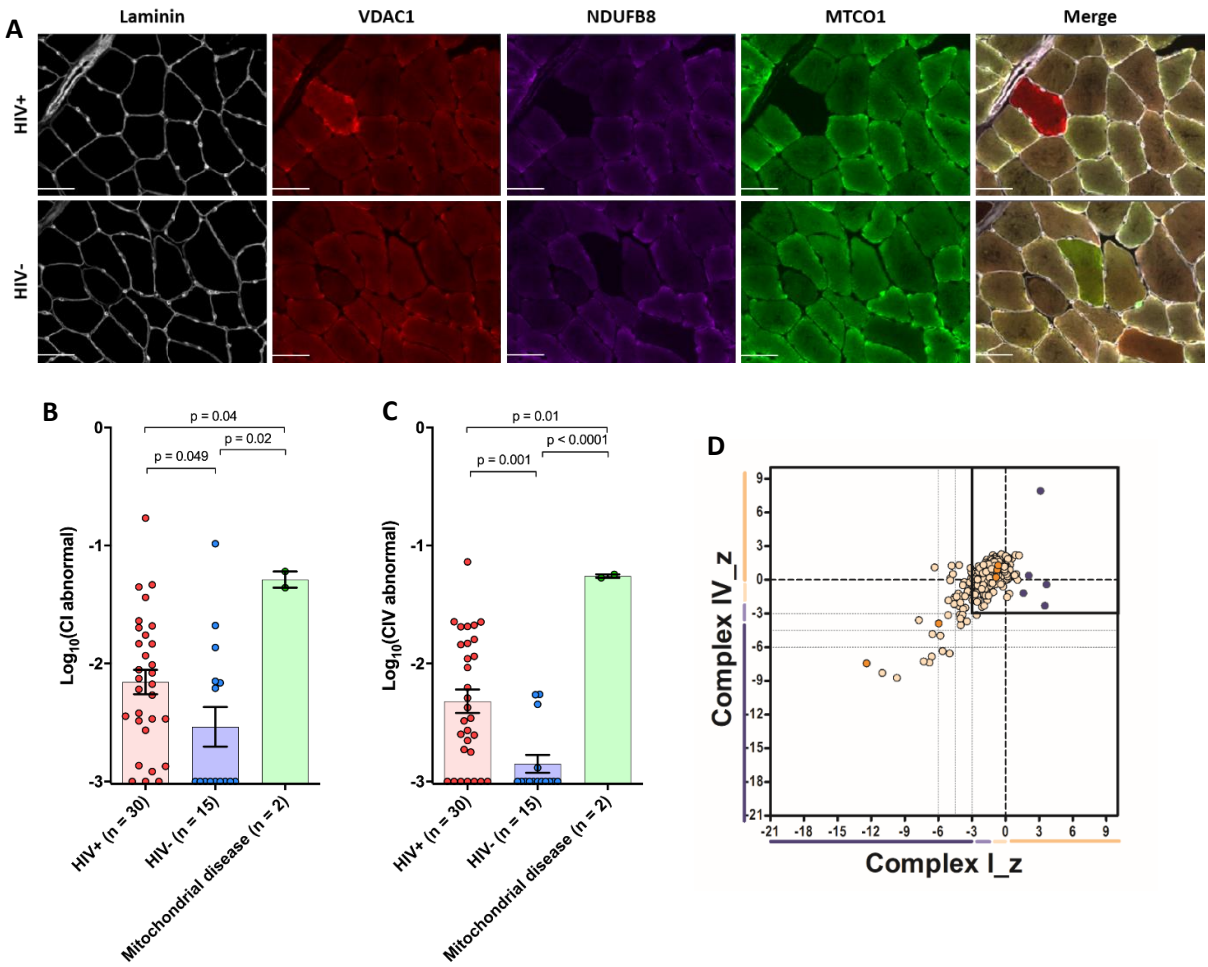

Figure 6.1 – Skeletal muscle mitochondrial dysfunction. *(**A**) Representative images of multiplex immunofluorescence staining on 10µm skeletal muscle sections from a HIV+ and HIV- individual. Markers include laminin, VDAC1 (mitochondrial mass marker), NDUFB8 (CI subunit) and MTCO1 (CIV subunit). Scale bar = 100µm. (**B**) Dot plot (mean ± SEM) showing significantly higher proportion of muscle fibre CI defects in the HIV+ group (n = 30) compared to the HIV- group (n = 15; p = 0.049). The mitochondrial disease group (n = 2) had a significantly higher proportion of CI defects compared to both the HIV+ group (p = 0.04) and HIV- group (p = 0.02). Each dot represents an individual patient. (**C**) Dot plot (mean ± SEM) showing a significantly higher proportion of fibres with CIV deficiency in the HIV+ group compared to the HIV- group (p = 0.001). The mitochondrial disease group also had a significantly higher proportion of fibres with CIV deficiency compared to both the HIV+ (p = 0.01) and HIV- groups (p < 0.0001). (**D**) Example dot plot of a HIV+ individual depicting the CI and CIV z-score of each individual fibre. Fibres with a z < -3 were classified as abnormal and z > -3 were classified as normal. Dots are coloured depending on mitochondrial mass status: dark blue = very low; light blue = low; pale yellow = normal; orange = high and red = very high.*

Using a marker for voltage-dependant anion channel 1 (VDAC1) in our multiplex immunofluorescence assay allowed for the quantification of the average mitochondrial mass in individual myofibres. Here, there was no significant difference in the average skeletal muscle mitochondrial mass between the HIV+ and HIV- groups (**unpaired t test**) (**Figure 6.2**).

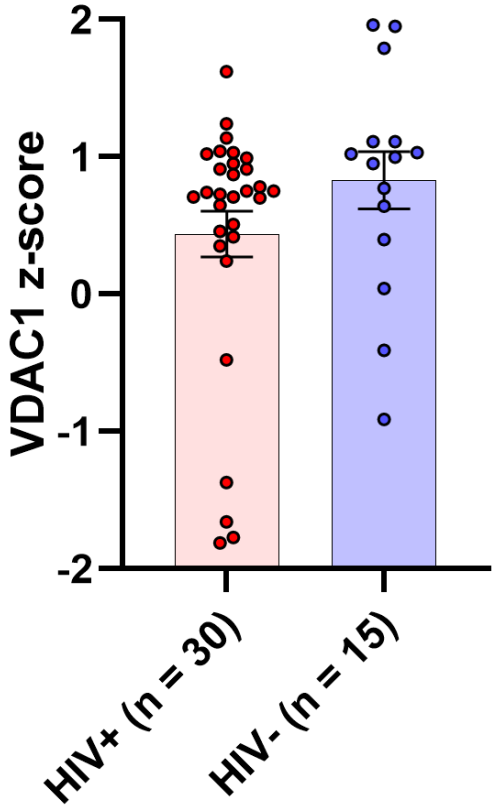

Figure 6.2 – Skeletal muscle mitochondrial mass*. Dot plot (mean ± SEM) representing average mitochondrial mass for each subject. Z-scores were calculated for each individual fibre and the mean score was calculated for each patient. There was no significant difference in mitochondrial mass between the HIV+ (n = 30) and HIV- (n = 15) groups (p = 0.16,* ***unpaired t test****). Each dot represents an individual patient.*

Finally, unadjusted linear regression analysis was undertaken in both the HIV+ and HIV- groups in order to determine if proportional CI and CIV deficiency was significantly associated with each other.

Here, proportional CI deficiency was highly significantly associated with proportional CIV deficiency in both the HIV+ (n = 30; r = 0.61; $p < 0.0001$) (**Pearson's correlation**) and HIV- groups (n = 15; r = 0.79; $p = 0.001$) (**Figure 6.3a**).

Additionally, there was a strong association between proportional CI deficiency and mitochondrial mass in the HIV+ group, although this was not statistically significant (n = 30; r = 0.33; $p = 0.074$) (**Pearson's correlation**). The association between proportional CI deficiency and mitochondrial mass was also not statistically significant in the HIV- group (n = 15; r = 0.30; $p = 0.28$) (**Figure 6.3b**). Nor was proportional CIV deficiency significantly associated with mitochondrial mass in either the HIV+ (n = 30; r = 0.17; $p = 0.37$) or HIV- groups (n = 15; r = 0.18; $p = 0.51$) (**Figure 6.3c**).

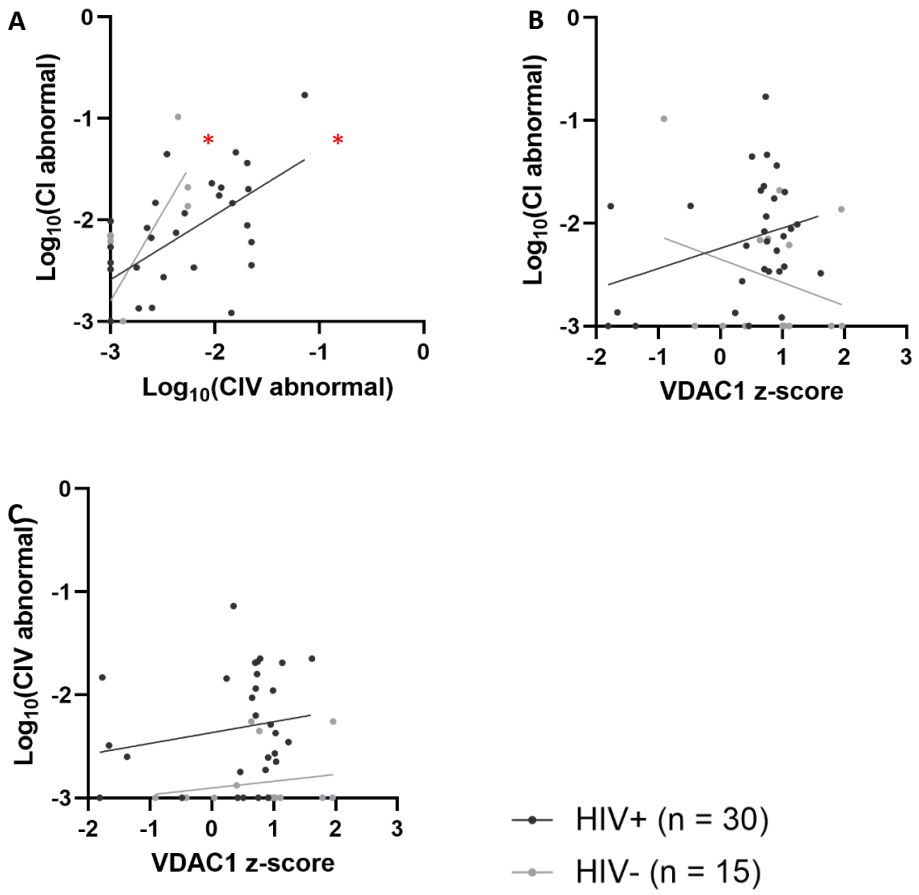

Figure 6.3 – Associations between mitochondrial parameters*. Scatter plots depicting the linear regression (Pearson's correlation) between log_{10}(CI abnormal) and (**A**) log_{10}(CIV abnormal) and (**B**) VDAC1 z-score; and between log_{10}(CIV abnormal) and (**C**) VDAC1 z-score. Each dot represents an individual patient. Black dots represent HIV+ individuals, and grey dots represent HIV- individuals. * = statistical significance.*

6.4.3 Clinical factors predicting skeletal muscle mitochondrial dysfunction in older PLWH

In order to better understand whether clinical factors (such as age and number of medications), body composition, or environmental factors (such as smoker status) predicted the greater skeletal muscle mitochondrial dysfunction seen in older PLWH, linear regression analyses were undertaken in the HIV+ group (n = 30).

Results from the various unadjusted linear regression analyses are described in **Table 6.1**. Of these analyses, proportional CI deficiency was significantly predicted by a lower number of medications (n = 30; r = -0.42; *p* = 0.02, **Pearson's correlation**) (**Figure 6.4e**). However, multivariate linear regression demonstrated that the association between proportional CI deficiency and number of medications was not independent of age (unstandardised regression coefficient = 0.38; *p* = 0.28, **multivariate linear regression**) (**Table 6.1**). Indeed, the model fit was not significant (*p* = 0.10), and subsequently only predictive of a small amount of variation in proportional CI deficiency (r^2 = 0.094).

Additionally, average mitochondrial mass in individual myofibres (determined by VDAC1 z-score) was significantly predicted by a higher percentage lean mass (r = 0.43; *p* = 0.0018, **Pearson's correlation**) (**Figure 6.6d**), and subsequently a lower percentage fat mass (r = -0.43; *p* = 0.0018) (**Figure 6.6c**).

Mitochondrial mass is known to be linked with both age and OXPHOS deficiency. Hence, in order to determine if average myofibre mitochondrial mass was predicted by lower percentage fat mass independently of the effect of both age and proportional CI deficiency, a multivariate linear regression model was developed with VDAC1 z-score as the dependant variable and age, percentage fat mass, and proportional CI deficiency as the independent variables. Here, multivariate linear regression confirmed that the association of mitochondrial mass and percentage fat mass was independent of both age and proportional CI deficiency (unstandardised regression coefficient = -0.044; *p* = 0.043, **multivariate linear regression**) (**Table 6.2**). Model fit was marginally above statistical significance (*p* = 0.053), and only predictive of a small amount of variance in VDAC1 z-score (r^2 = 0.17).

There were no significant clinical predictors of proportional CIV deficiency in the HIV+ group (**Figure 6.5**).

Finally, supporting previous work in this thesis (**Section 4.4.6**), unadjusted linear regression analyses demonstrated that none of the HIV-related clinical parameters significantly predicted proportional CI or CIV deficiency, or mitochondrial mass (**Table 6.1**).

	HIV+ (n = 30)						
	CI abnormal			CIV abnormal		VDAC1 z-score	
	r	*p*	adjusted *p*	r	*p*	r	*p*
Age	0.18	0.33	-	0.33	0.077	0.22	0.25
BMI (kg/m^2)	0.18	0.35	-	-0.066	0.73	-0.085	0.66
Waist circumference (cm)	0.077	0.69	-	-0.17	0.37	-0.14	0.45
# Comorbidities	-0.24	0.20	-	0.31	0.093	-0.18	0.35
# Medications	**-0.42**	**0.020**	**0.28**	0.29	0.12	-0.19	0.31
Polypharmacy*	-	0.98	-	-	0.66	-	0.49
% Fat mass$^+$	-0.34	0.064	-	-0.31	0.094	**-0.43**	**0.018**
% Lean mass$^+$	0.34	0.064	-	0.31	0.094	**0.43**	**0.018**
Smokers*	-	0.45	-	-	0.75	-	0.45
Alcohol drinkers*	-	0.91	-	-	0.60	-	0.41
Recreational drug use*	-	0.54	-	-	0.32	-	0.47
Months since diagnosis	0.27	0.15	-	0.19	0.31	-0.16	0.40
Months on ART	0.24	0.21	-	0.20	0.30	0.011	0.96
Months untreated	0.13	0.48	-	0.08	0.67	-0.20	0.30
CD4 count (copies/µl)	-0.17	0.39	-	-0.034	0.87	-0.21	0.29
Mitochondrially-toxic NRTIs*	-	0.98	-	-	0.51	-	0.38

Table 6.1 – Mitochondrial dysfunction and clinical characteristics linear correlation. *Table depicting the associations between proportional skeletal muscle CI and CIV deficiency in older HIV+ (n = 30) and age-matched HIV- (n = 15) individuals. Linear regression and correlation analysis was determined by Pearson's correlation for normal data and Spearman's correlation for non-normal data (denoted by ^). * = ordinal data in which individuals were stratified by yes/no, and differences determined by unpaired t test. + = DXA data missing from 2 HIV- individuals. Statistically significant values are in bold.*

Dependant variable	Independent variables	Unstandardised regression coefficients			*p*		
		Age	CI deficiency	% fat mass	Age	CI deficiency	% fat mass
VDAC1 z-score	Age, CI deficiency, % fat mass	-0.004	0.41	**-0.044**	0. 85	0.18	**0.043**

Table 6.2 – Multivariate linear regression models. *Table depicting the dependant and independent variables, as well as the corrected coefficients and p value outputs from a multivariate linear regression model to determine predictive factors of VDAC1 z-score. Statistically significant results are bold.*

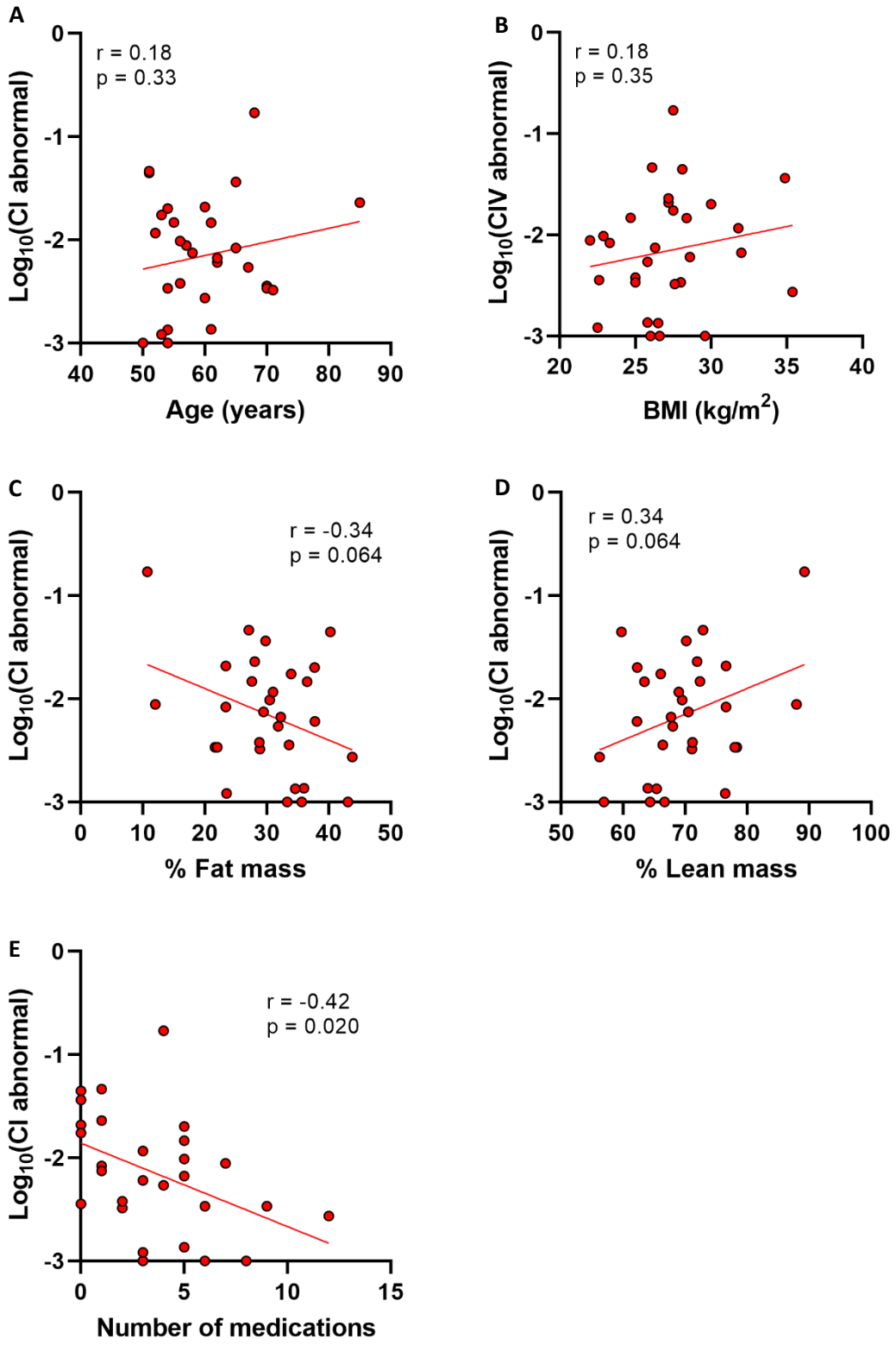

Figure 6.4 - Clinical predictors of proportional CI deficiency*. Scatter plots showing linear correlation analysis (Pearson's correlation) between proportional CI deficiency and (**A**) age, (**B**) BMI (kg/m²), (**C**) percentage fat mass, (**D**) percentage lean mass;, and (**E**) number of medications. Each dot represents an individual patient.*

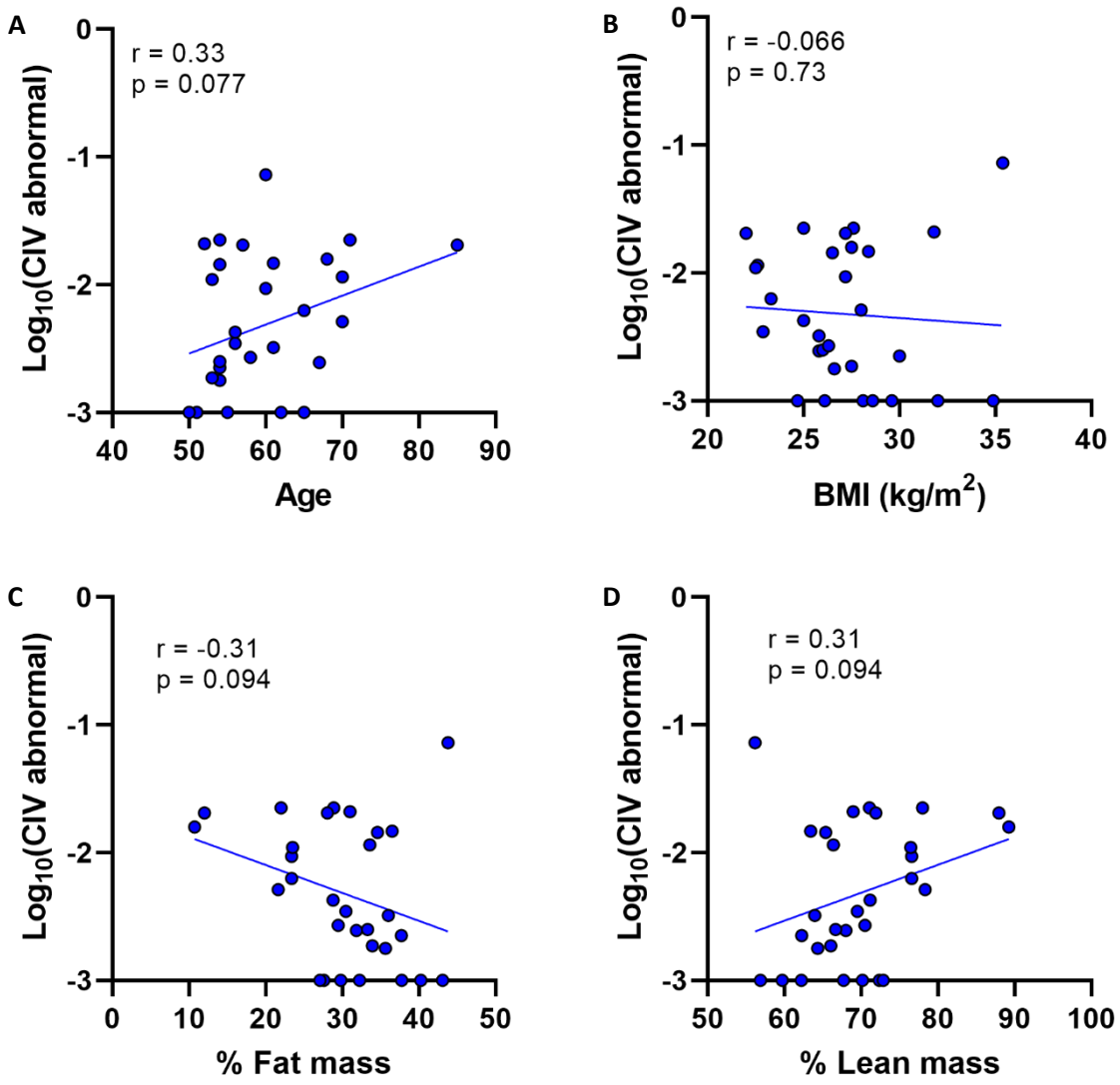

Figure 6.5 - Clinical predictors of proportional CIV deficiency. *Scatter plots showing linear correlation analysis (Pearson's correlation) between proportional CIV deficiency (**A**) age, (**B**) BMI (kg/m²), (**C**) percentage fat mass, and (**D**) percentage lean mass. Each dot represents an individual patient.*

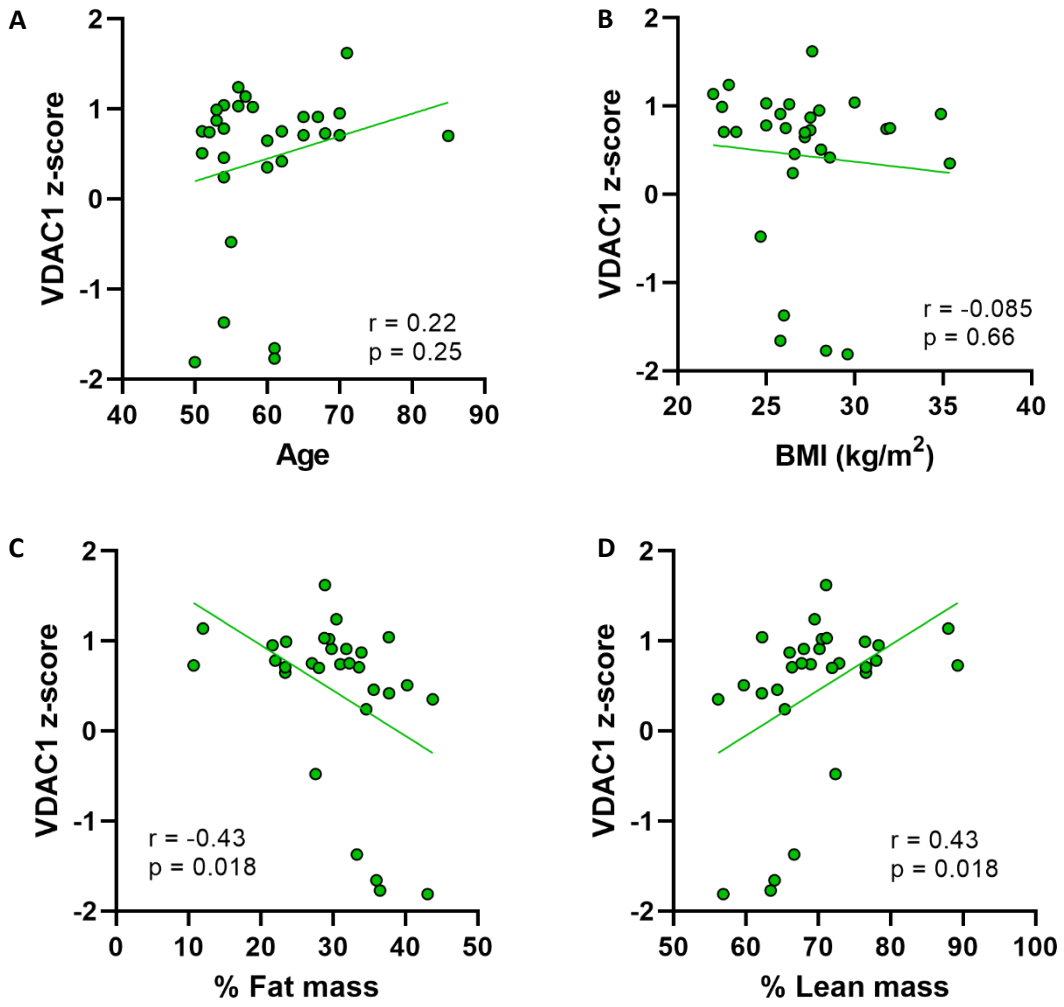

Figure 6.6 - Clinical predictors of VDAC1 z-score*. Scatter plots showing linear regression analysis (Pearson's correlation) between average VDAC1 z-score and (**A**) age, (**B**) BMI (kg/m^2), (**C**) percentage fat mass, and (**D**) percentage lean mass. Each dot represents an individual patient.*

6.4.4 Physical function outcomes of skeletal muscle mitochondrial dysfunction

Next, I sought to investigate the relationship between skeletal muscle mitochondrial dysfunction and outcomes of the physical function and ageing phenotype assessments (**Table 6.3**).

Here, through unadjusted linear regression analyses it was found that proportional CI deficiency did not significantly predict any of the respective physical outcomes such as MET score (**Figure 6.7a**), SPPB score (**Figure 6.7b**), FFP score (**Figure 6.7c**), grip strength (**Figure 6.7d**) or ASMI (**Figure 6.7e**) (**Pearson's correlation**).

In addition, proportional CIV deficiency did not significantly predict any of the respective physical factors (**Figure 6.8a-e**).

Finally, it was also found that mean myofibre mitochondrial mass (determined by VDAC1 z-score) did not significantly predict any of the respective physical factors (**Figure 6.9a-e**).

	HIV+ (n = 30)					
	CI abnormal		**CIV abnormal**		**VDAC1 z-score**	
	r	***p***	**r**	***p***	**r**	***p***
MET score^	0.014	0.94	0.22	0.24	0.26	0.16
SPPB score^	0.17	0.38	-0.037	0.84	0.22	0.25
FFP score^	0.11	0.094	0.11	0.99	-0.17	0.38
Grip strength (kg)	0.015	0.94	-0.17	0.36	0.21	0.20
ASMI (kg/m^2)	-0.29	0.12	0.14	0.46	0.056	0.77

Table 6.3 – Mitochondrial dysfunction and physical function parameters*. Table depicting the correlation between proportional CI and CIV deficiency as well as average VDAC1 z-score and physical function and adverse ageing phenotype parameters. ^ indicate non-parametric data. Pearson's correlation performed on parametric data and Spearman's correlation performed on non-parametric data.*

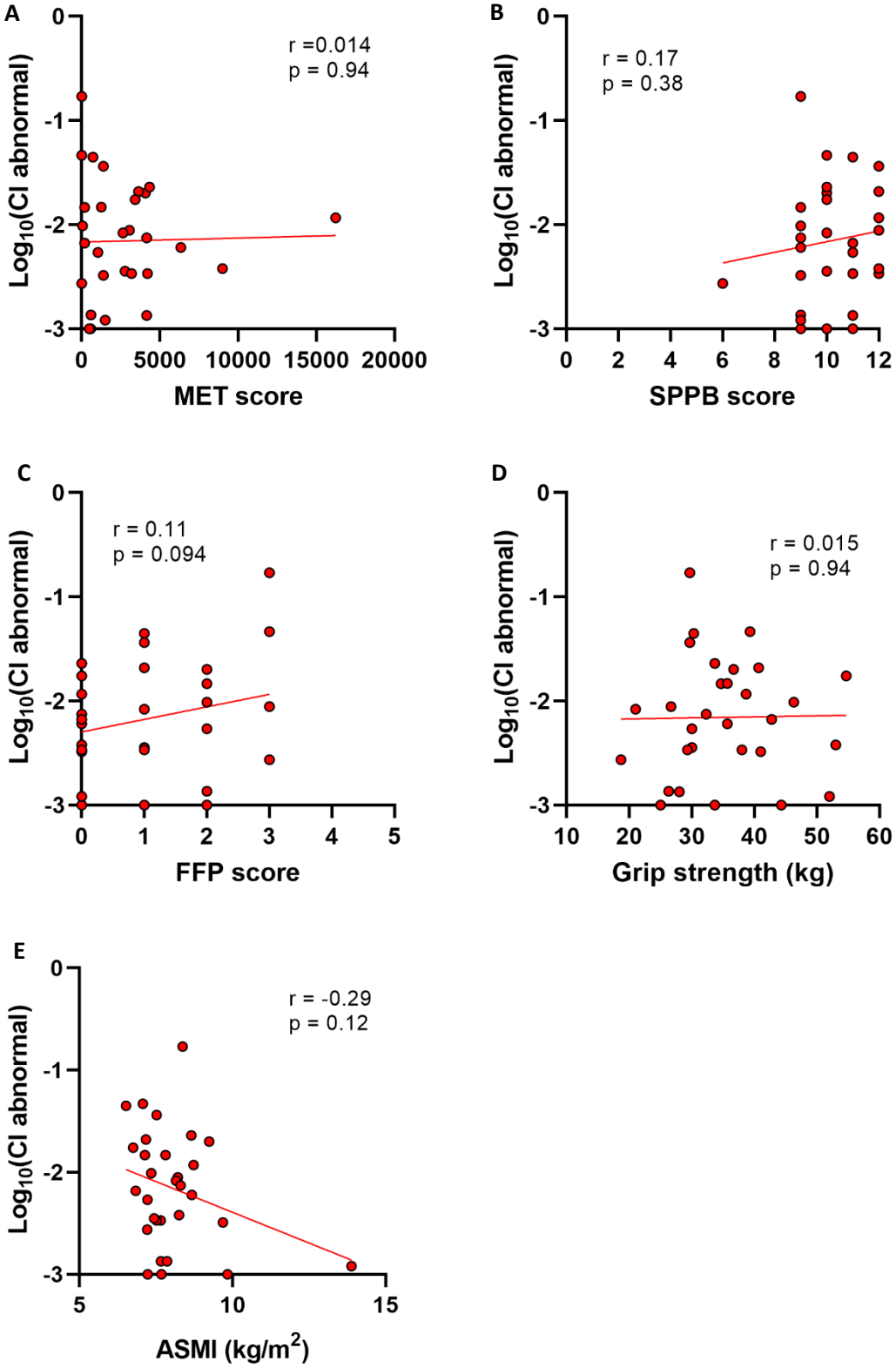

Figure 6.7 – Physical performance predictors of proportional CI deficiency. *Scatter plots showing linear correlation analysis between proportional CI deficiency and (**A**) MET score^, (**B**) SPPB score^, (**C**) FFP score^, (**D**) grip strength (kg), and ASMI (kg/m²). ^ indicates non-parametric data. Correlation for parametric data determined by Pearson's correlation, and non-parametric data determined by Spearman's correlation. Each dot represents an individual patient.*

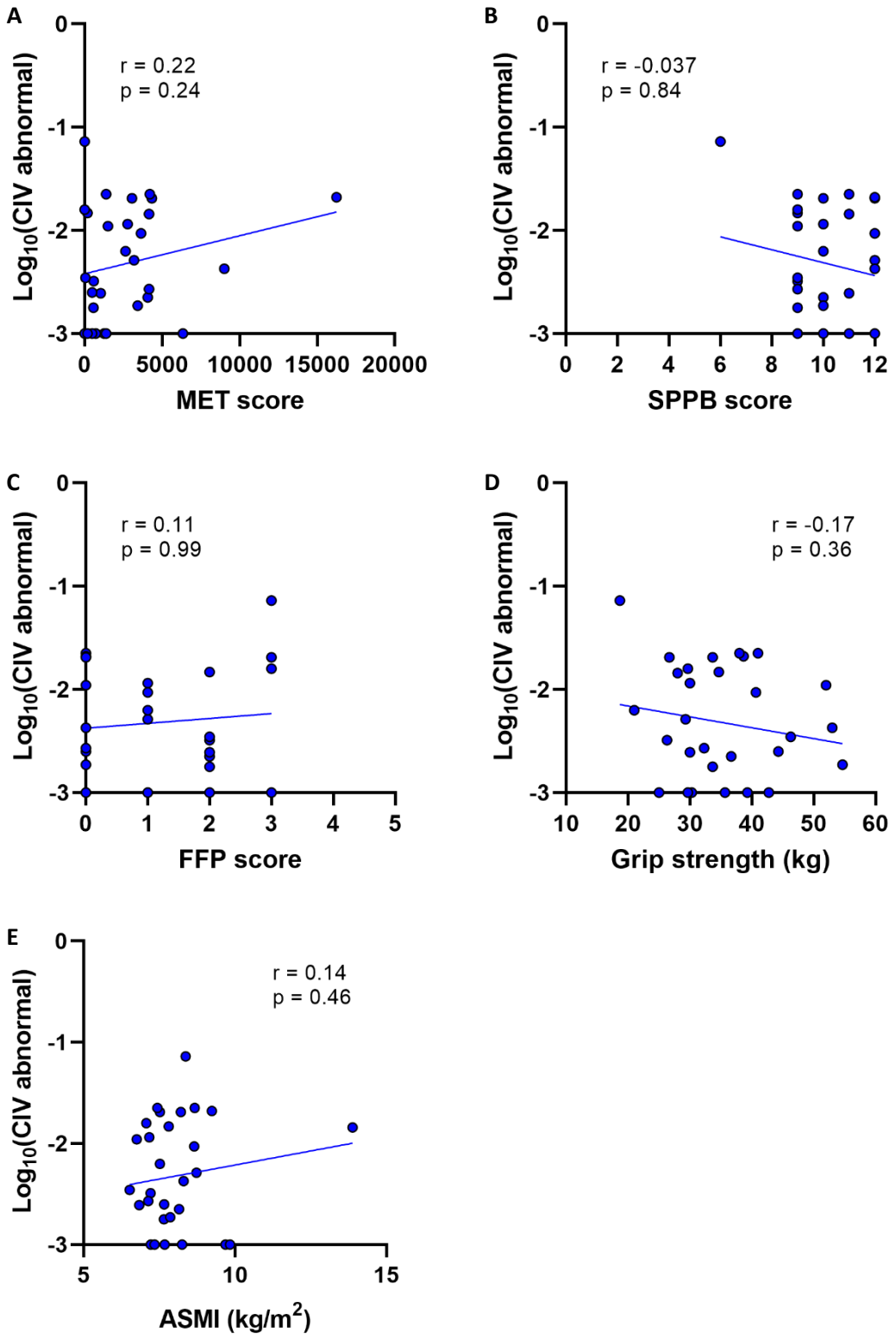

Figure 6.8 – Physical performance predictors of proportional CIV deficiency*. Scatter plots showing linear correlation analysis between proportional CI deficiency and (**A**) MET score^, (**B**) SPPB score^, (**C**) FFP score^, (**D**) grip strength (kg), and ASMI (kg/m²). ^ indicates non-parametric data. Correlation for parametric data determined by Pearson's correlation, and non-parametric data determined by Spearman's correlation. Each dot represents an individual patient.*

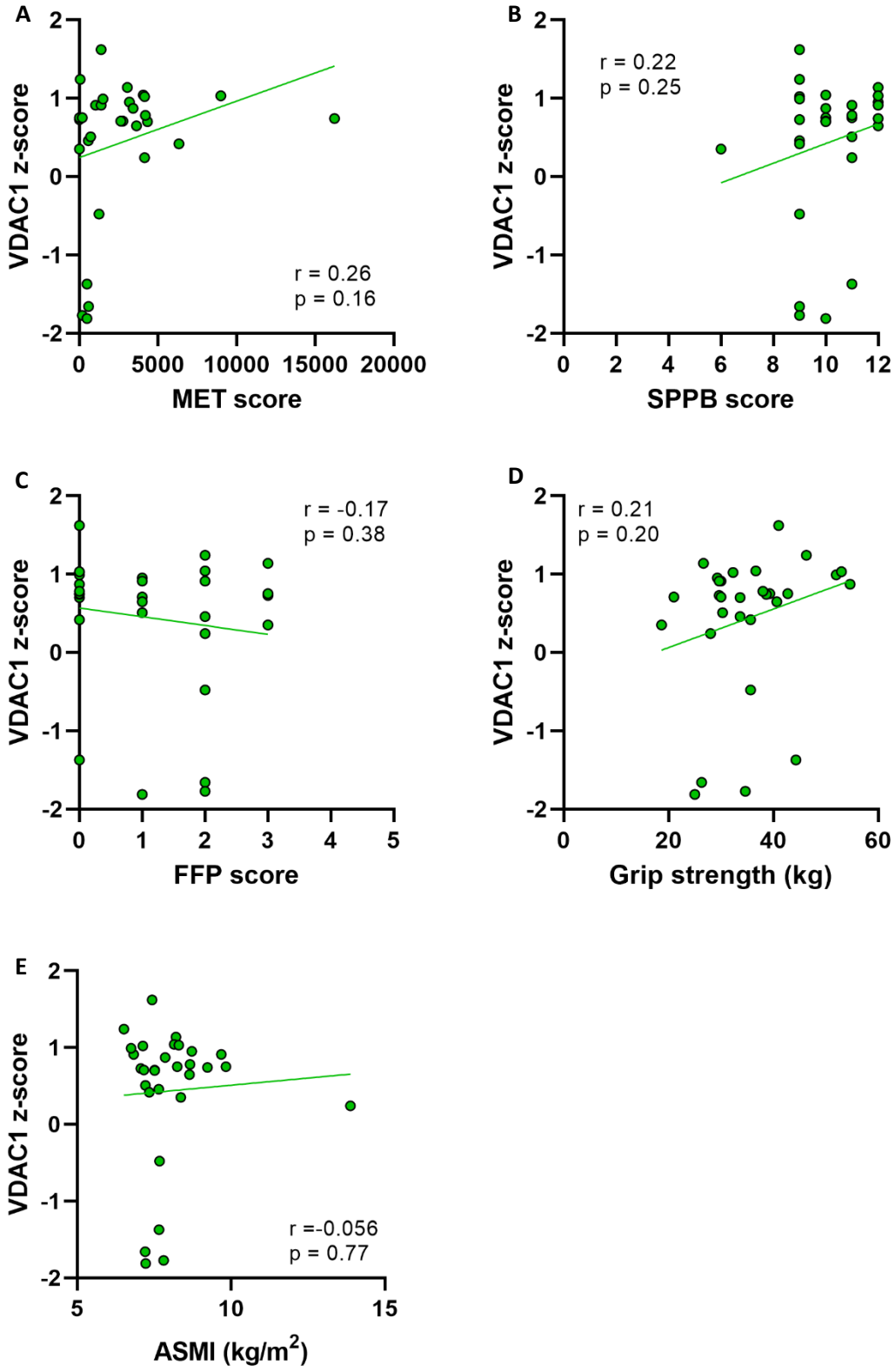

Figure 6.9 – Physical performance predictors of myofibre mitochondrial mass*. Scatter plots showing linear correlation analysis between average VDAC1 z-score and (**A**) MET score^, (**B**) SPPB score^, (**C**) FFP score^, (**D**) grip strength (kg), and ASMI (kg/m²). ^ indicates non-parametric data. Correlation for parametric data determined by Pearson's correlation, and non-parametric data determined by Spearman's correlation. Each dot represents an individual patient.*

6.4.5 Skeletal muscle mitochondrial function in frail and sarcopenic PLWH

I next investigated whether skeletal muscle mitochondrial dysfunction was higher in PLWH with the adverse ageing phenotypes of frailty and sarcopenia.

Therefore, I stratified the HIV+ group (n = 30) into frail (n = 4), prefrail (n = 15), and robust (n = 11), as well as into sarcopenic (n = 5), presarcopenic, (n = 6), and non-sarcopenic (n = 19), and compared mitochondrial parameters between the respective groups.

There was no significant difference in proportional CI deficiency between frail, prefrail, and robust HIV+ individuals (p = 0.15, **one-way ANOVA**) (**Figure 6.10a**). Although the frail HIV+ individuals had numerically higher proportional CI deficiency compared to robust and prefrail PLWH, this was not statistically significant, most likely due to the small number in the group. There was also no significant difference in proportional CI deficiency between sarcopenic, presarcopenic, and non-sarcopenic HIV+ individuals (p = 0.32) (**Figure 6.10b**).

In addition, there was also no significant difference in proportional CIV deficiency between the frail, prefrail and robust HIV+ groups (p = 0.17, **one-way ANOVA**) (**Figure 6.10c**). Again, the levels of proportional CIV deficiency were higher in the frail group compared to both the prefrail and robust groups, but due to the small size of the group, this difference was not statistically significant. There was also no significant difference in proportional CIV deficiency between the sarcopenic, presarcopenic, and non-sarcopenic HIV+ groups (p = 0.46) (**Figure 6.10d**).

Finally, there was also no significant difference in average myofibre mitochondrial mass between the frail, prefrail, and robust HIV+ individuals (p = 0.29, **one-way ANOVA**) (**Figure 6.10e**), or between the sarcopenic, presarcopenic, and non-sarcopenic HIV+ individuals (p = 0.076) (**Figure 6.10f**).

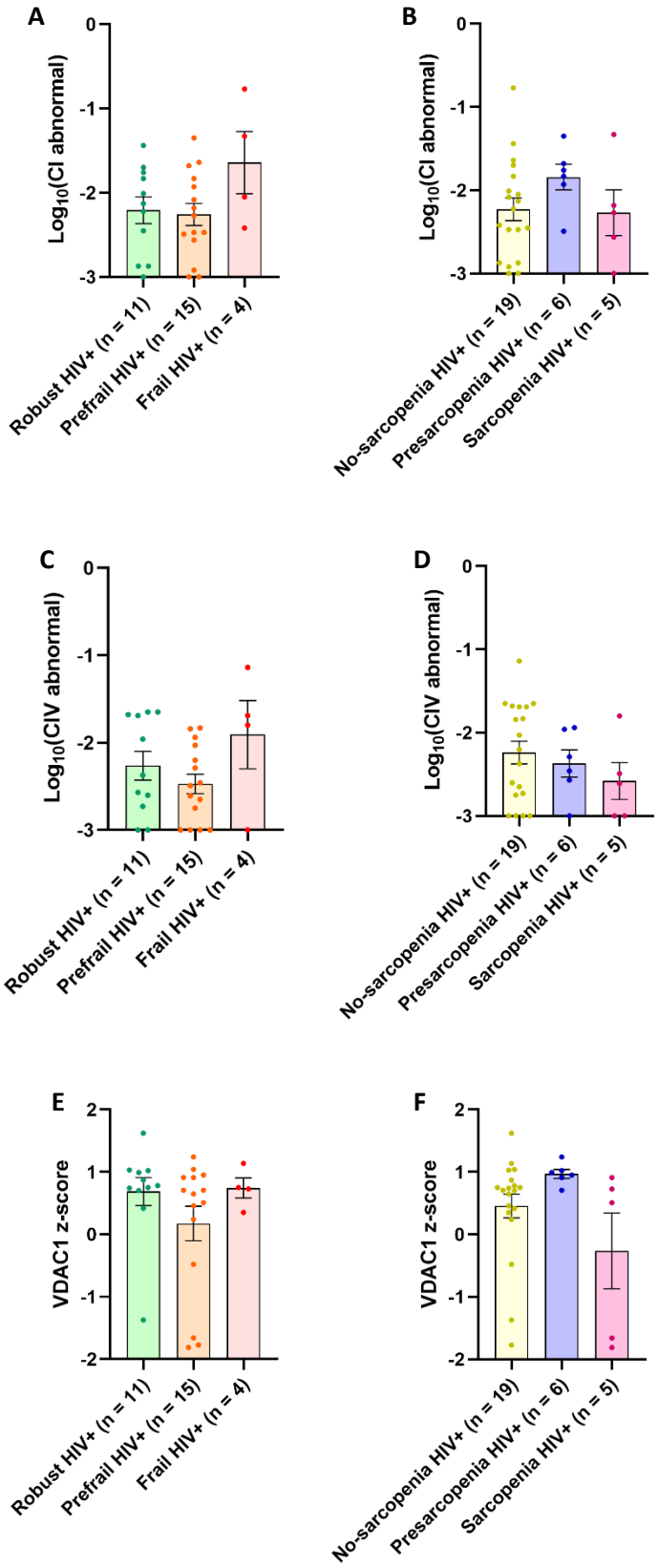

Figure 6.10 – Mitochondrial function in adverse ageing phenotypes in older PLWH. *Dot plots (mean ± SEM) showing no significant difference in log_{10}(CI abnormal) between (**A**) frail (n = 4), prefrail (n = 15) and robust (n = 11) PLWH, or (**B**) sarcopenic (n = 5), presarcopenic (n = 6) or non-sarcopenic (n = 19) PLWH. log_{10}(CIV abnormal) between (**C**) frail, prefrail and robust PLWH or (**D**) sarcopenic, presarcopenic and non-sarcopenic PLWH; average VDAC1 z-score between (**E**) frail, prefrail and robust PLWH, or between (**F**) sarcopenic, presarcopenic and non-sarcopenic PLWH.*

Similarly to analyses performed in **Section 5.4.4**, in order to increase the power to detect differences between the groups, in combination with the fact that prefrailty and presarcopenia are more physiologically related to frailty and sarcopenia than being robust, HIV+ patients classified as prefrail (n = 15) were grouped with the HIV+ frail individuals (n = 4) to form the frailty/prefrailty HIV+ group (n = 19), and HIV+ subjects classified as presarcopenic (n = 6) were grouped with sarcopenic PLWH (n = 5) to form the sarcopenia/presarcopenia HIV+ group (n = 11).

Interestingly, frail/prefrail HIV+ individuals (n = 19) did not have a significantly higher proportion of myofibres with CI (p = 0.72, **unpaired t test**) or CIV deficiency (p = 0.67) (**Figure 6.11a, b**) compared to robust HIV+ individuals (n = 11). Nor was there a significant difference in average myofibre mitochondrial mass, as measured by VDAC1 z-score (p = 0.19) (**Figure 6.11c**).

In addition, there was no difference in proportional CI deficiency (p = 0.38, **unpaired t test**), CIV deficiency (p = 0.27), or average myofibre mitochondrial mass (p = 0.50) between sarcopenic/presarcopenic PLWH (n = 11) and non-sarcopenic PLWH (n = 19) (**Figure 6.11d, e, f**).

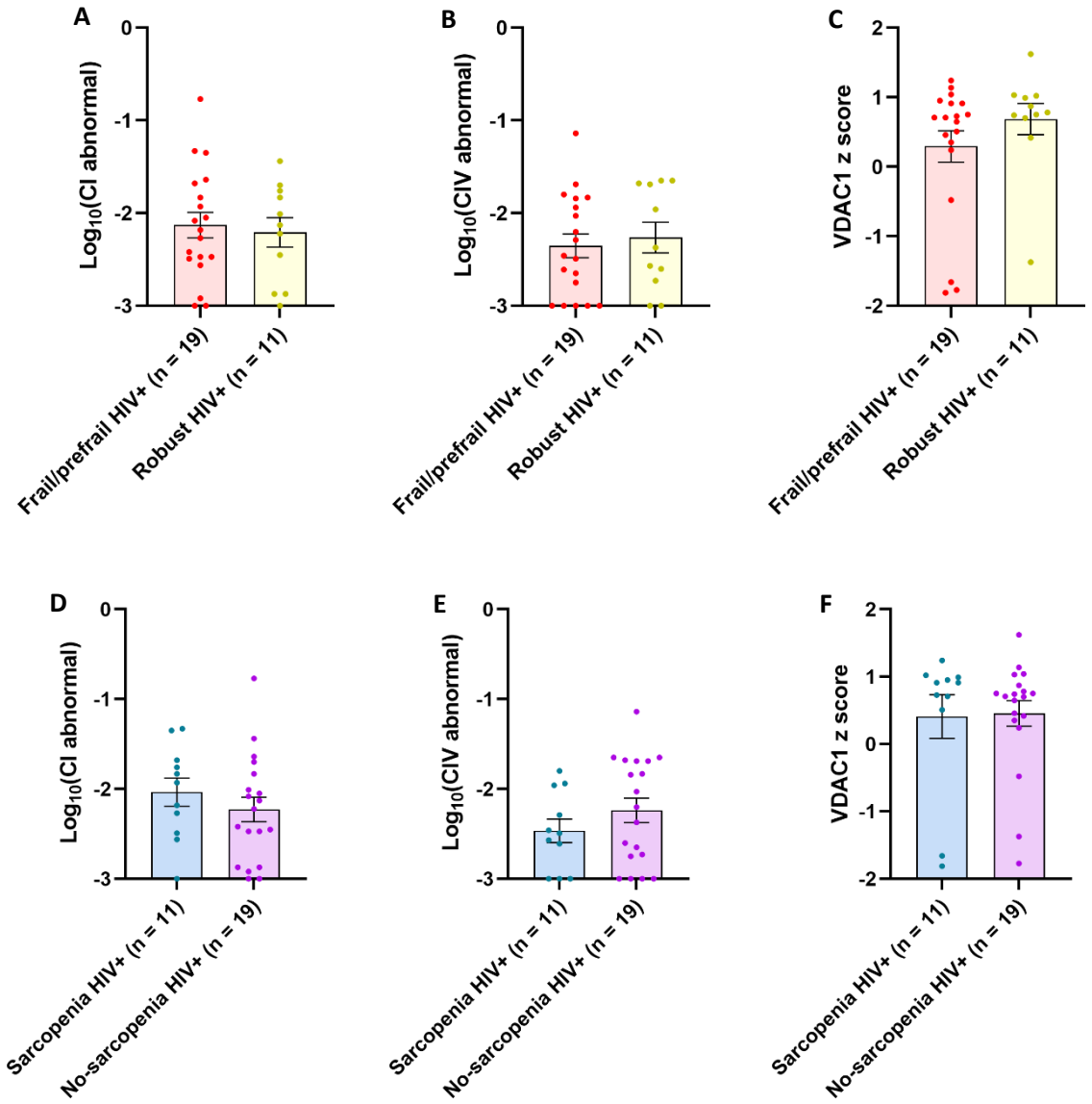

Figure 6.11 – Mitochondrial dysfunction in frail/prefrail and sarcopenic/presarcopenic older PLWH*. Dot plots (mean ± SEM) showing mitochondrial dysfunction in frail/prefrail HIV+ (n = 19) and robust HIV+ (n = 11) in the form of (**A**) proportional CI and (**B**) CIV deficiency, in addition to (**C**) mitochondrial mass (VDAC1 z score). Proportional (**D**) CI and (**E**) CIV deficiency and (**F**) mitochondrial mass (VDAC1 z score) in sarcopenia/presarcopenia HIV+ (n = 11) and no-sarcopenia HIV+ (n = 19) individuals. Each dot represents an individual patient.*

6.5 Discussion

Here, I presented data regarding skeletal muscle mitochondrial dysfunction in adverse ageing phenotypes in older HIV+ and HIV- individuals recruited to the MAGMA study. This study is the first study to comprehensively investigate skeletal muscle mitochondrial dysfunction (in the form of OXPHOS subunit protein deficiency and mitochondrial mass) in the context of the highly heterogenous pathophysiology of frailty, sarcopenia, and physical function decline in older PLWH.

6.5.1 Conclusions

6.5.1.1 Older PLWH have higher skeletal muscle mitochondrial mass compared to age-matched HIV- individuals

Importantly, this cohort study demonstrated that older (≥ 50 years) PLWH have higher levels of skeletal muscle mitochondrial dysfunction compared to age-matched HIV- individuals. Notably, this increase in CI and CIV deficiency in older PLWH did not seem to be compensated by an upregulation in mitochondrial mass. Interestingly, whilst other studies have found higher levels of skeletal muscle mitochondrial dysfunction in PLWH compared to HIV-uninfected individuals, this study demonstrated mitochondrial defects at the individual myofibre level, in contrast to the tissue homogenate level (Jankowski *et al*., 2019). In addition, as a result of utilising a novel multiplex immunofluorescence assay developed in our lab (Rocha *et al*., 2015), this study is the first to objectively quantify and subsequently demonstrate significantly higher levels of CI deficiency as well as CIV deficiency in older PLWH compared to age-matched HIV- individuals. Previous studies have been limited by only being able to qualitatively quantify cytochrome oxidase (COX) activity at the myofibre level through COX/succinate dehydrogenase (SDH) histochemistry (Payne *et al*., 2011).

6.5.1.2 Determinants of skeletal muscle mitochondrial dysfunction in older PLWH

An important aim of this study following the quantification of skeletal muscle mitochondrial (dys)function was to investigate whether this mitochondrial dysfunction was predicted by clinical or environmental factors in older PLWH, as several of these factors are thought to impair mitochondrial function through potential mechanisms such as chronic inflammation and oxidative stress (Hollensworth *et al*., 2000; Voets *et al*., 2012; Castro Mdel *et al*., 2012; Andreazza *et al*., 2010; Sun *et al*., 2016; Harman, 1972). As such, through unadjusted linear regression analyses I demonstrated that a greater average myofibre mitochondrial mass was significantly associated with a higher percentage of lean body mass and simultaneously associated with a lower percentage of fat body mass. As percentage lean and fat body mass are inverses of each other, and the fact that fat mass is more detrimental to age-related physiology than lean body mass in PLWH (Erlandson *et al*., 2017a;

Onen *et al*., 2009), I assessed the association between myofibre mitochondrial mass and percentage fat mass after adjustment for skeletal muscle CI deficiency and age. Here, this association remained significant after adjustment for these factors, suggesting that a lower proportion of fat tissue promotes a more efficient regulation of mitochondrial content in older PLWH, even in the event of OXPHOS decline. As increased physical activity is associated with both decreased fat mass and enhanced mitochondrial function in the general population (Menshikova *et al*., 2006; Distefano *et al*., 2018), it could be that greater levels of physical activity were promoting the upregulation of skeletal muscle mitochondrial mass. However, the lack of significant association between MET score and either CI and CIV deficiency, or mitochondrial mass in the older PLWH suggests that this is not the case. Altogether, these findings support previous work demonstrating the harmful effects excess fat tissue has on mitochondrial function in the general population (Shetty *et* al., 2009; Winalawansa, 2019; Li *et* al., 2017; Slawik & Vidal-Puig, 2006).

In addition, in older PLWH, proportional CI deficiency was surprisingly significantly predicted by a lower number of medications through unadjusted linear regression analysis. However, through multivariate linear regression analysis it was demonstrated that this significant association was dependant on age. As older people are generally prescribed with more medications and generally have a higher prevalence of comorbidities (Divo *et al*., 2016), this result makes sense.

6.5.1.3 Potential other underlying pathophysiological mechanisms underpinning skeletal muscle mitochondrial dysfunction in older PLWH in the contemporary ART era

Importantly, data from a previously discussed chapter of this thesis (**Chapter 4**) demonstrated that there was no difference in skeletal muscle mitochondrial dysfunction between ART-treated PLWH who have been exposed to mitochondrially-toxic NRTIs and those who have not, as well as PLWH who are on protease inhibitors (PIs) or non-nucleoside reverse transcriptase inhibitors (NNRTIs) compared to those who were not. In addition, adjusted multivariate linear regression analysis conducted in that chapter demonstrated that there was no significant associations between skeletal muscle mitochondrial dysfunction and HIV-related factors (**Section 4.4.6**). However, a key strength of the MAGMA study was that it recruited age-matched HIV+ and HIV- individuals, and so allowed for the better understanding of the effect of age on mitochondrial function in older PLWH. Therefore, linear regression analyses was again performed in order to assess the predictive effect of HIV-related clinical parameters on skeletal muscle mitochondrial function. Importantly, none of the HIV-related factors significantly predicted either proportional CI and CIV deficiency, or mitochondrial mass. Additionally, previous exposure to older NRTIs that have been shown to induce mitochondrial toxicities, or current exposure to PIs or NNRTIs, also did not significantly predict skeletal muscle mitochondrial defects. These are important findings, as together with the data presented in a larger

cohort in **Chapter 4**, they comprehensively demonstrate that ART-treated PLWH have higher levels of skeletal muscle mitochondrial dysfunction compared to age-matched HIV- individuals, although there is no direct effect of previous exposure to older, supposedly mitochondrially-toxic NRTIs on skeletal muscle function. Indeed, they suggest that the underlying pathophysiological mechanisms behind age-related physiological decline are more likely to be indirect effects of HIV infection, such as chronic inflammation, immunosenescence, or oxidative stress (Melov *et al*., 1999; Zorov *et al*., 2014; Rao *et al*., 2014; Massaad & Klann, 2011; Deeks, 2011; Erlandson *et al*., 2017a).

6.1.5.4 Frail and sarcopenic PLWH do not have significantly greater levels of skeletal muscle mitochondrial dysfunction than robust and non-sarcopenic PLWH

Finally, another important experimental aim was to determine whether PLWH with adverse ageing phenotypes such as frailty and sarcopenia have excess skeletal muscle mitochondrial dysfunction compared to age-matched PLWH who did not have these phenotypes. To do this, I firstly stratified the HIV+ group into frail, prefrail and robust groups, as well as sarcopenic, presarcopenic and non-sarcopenic groups and assessed differences in proportional CI and CIV levels, as well as mitochondrial mass. Here, although the frail HIV+ group appeared to have higher levels of proportional CI deficiency, this was not statistically significant. This is most likely due to the small size of the group meaning analysis was underpowered to detect group differences. Hence, I further classified the HIV+ individuals into whether they were defined as frail and prefrail as well as those defined as sarcopenic and presarcopenic, as similarly done in a previous study (Kooij *et al*., 2016), and compared proportional CI, CIV levels and mitochondrial mass against robust and non-sarcopenic PLWH. Again, I found that there was no significant differences in skeletal muscle mitochondrial dysfunction between the experimental groups. These findings indicate that although older PLWH have greater levels of skeletal muscle mitochondrial dysfunction compared to age-matched HIV- individuals, this mitochondrial dysfunction is not a significant direct causative factor of the greater risk of frailty and sarcopenia in PLWH (Onen *et al*., 2012; Desquilbet *et al*., 2009; Brothers *et al*., 2017; Echeverria *et al*., 2018).

6.5.2 Summary of experimental findings

	Older PLWH	Older HIV- individuals	Conclusions
Proportional CI and CIV deficiency	• Higher proportional CI and CIV deficiency than HIV- individuals • Highest levels of deficiency comparable with levels seen in mitochondrial disease patients	• Lower proportional CI and CIV deficiency than HIV+ individuals • Highest levels of deficiency comparable with levels seen in mitochondrial disease patients	• Older PLWH have significantly higher CI and CIV deficiency compared to age-matched HIV- individuals.
Mitochondrial mass	• Comparable to HIV- individuals	• Comparable to HIV+ individuals	• No difference in average myofibre mitochondrial mass between older HIV+ and HIV- individuals
Associations with clinical factors in older PLWH	• Higher prevalence of medications predicted unadjusted CI deficiency, but not after adjustment for age • Higher percentage lean mass predicted higher mitochondrial mass independently of age and CI deficiency • Lower percentage of fat mass predicted higher mitochondrial mass independently of age and CI deficiency		
Associations of mitochondrial deficiency with physical factors in older PLWH	• No significant associations		
Mitochondrial dysfunction in adverse ageing phenotypes in older PLWH	• No difference in mitochondrial dysfunction between frail and robust, or sarcopenic and presarcopenic PLWH		

Table 6.4 – Summary of experimental findings.

6.5.3 Limitations

As discussed in **Section 5.5**, the MAGMA study was an observational study. Due to the fact that frailty is dynamic, a longitudinal cohort study in which the participants undertake several study visits would allow for a better understanding of the role of skeletal muscle mitochondrial dysfunction in the pathophysiology of adverse ageing phenotypes such as frailty or sarcopenia. In addition, both the HIV+ and HIV- participants were male, limiting our capabilities to understand the role of skeletal muscle mitochondrial dysfunction in adverse ageing phenotypes in older HIV+ women.

6.5.4 Future work

As mentioned above, this study was limited by the cohort size and the fact that it was not a longitudinal study. Therefore, future work should look to perform these analyses on a larger cohort with both older male and female PLWH and ideally at numerous time points. In addition, as the prevalence of individuals over 65 years old was small, future studies should look to include more of these patients.

Whilst this study utilised a novel multiplex immunofluorescence assay which allowed the objective quantification of CI and CIV deficiency at the individual myofibre level (Rocha *et al*., 2015), skeletal muscle mitochondrial function could also be assessed with other assays (Fraizer *et al*., 2020; Hunt & Payne, 2020). In light of the fact that greater skeletal muscle mitochondrial mass was associated with lean body mass, these studies could include homogenate tissue studies which quantify levels of enzymes involved in mitochondrial biogenesis, such as PGC-1α, or markers of other mitochondrial dynamics such as fission and fusion molecules. Additionally, investigating the levels of other OXPHOS complexes III and V, or levels of proteins and enzymes involved in other forms of mitochondrial metabolism such as citrate would be of interest.

As mitochondrial dysfunction was not significantly predictive of adverse ageing phenotypes in older PLWH, I subsequently went on to investigate other aspects of age-associated skeletal muscle pathology and their potential role in adverse ageing phenotypes in older PLWH in the following chapter.

Chapter 7 – Assessment of age-related skeletal muscle pathophysiological mechanisms in older PLWH

7.1 Introduction

The average age of the HIV-infected population is increasing, and the prevalence of adverse ageing phenotypes such as frailty and sarcopenia is also greater in the HIV+ population compared to the age-matched general population (Centers for Disease Control and Prevention, 2013; Desquilibet *et al*., 2007; Piggott *et* al., 2016; Kooij *et al*.,2016; Echeverria *et al*., 2018).

Both frailty and sarcopenia are known to be a multisystem conditions involving the metabolic, musculoskeletal, neuroendocrine, immune, and cognitive systems (Clegg *et al*., 2013; Fried *et al*., 2001). Although the exact pathophysiological mechanisms underpinning frailty have yet to be fully elucidated, factors such as chronic inflammation (Soysal *et al*., 2016; Leng *et al*., 2007), immunosenescence (Dihn *et al*., 2019), cell senescence (Lehman *et al*., 2018; Xu *et al*., 2018), decreased stem cell availability (Sousa-Victor *et al*., 2016; Fry *et al*., 2015; Gonen & Toledana, 2014; Larrick & Mendelson, 2017), insulin resistance (Cacciatore *et al*., 2013; Hubbard *et al*., 2010; Perez-Tasigchana *et al*., 2017), and mitochondrial dysfunction (Ferrucci & Zampino, 2020; Ashar *et al*., 2015; Andreux et *al*., 2018) have been implicated as causative factors. In addition, declines in mitochondrial function are known to contribute to the pathogenesis and pathophysiology of each respective factor (Ferruci & Zampino, 2020).

Age-related declines in skeletal muscle function is widely acknowledged to be a significant causative factor in both frailty and sarcopenia (Mitchell *et al*., 2012; Cruz-Jentoft *et* al., 2019). Whilst many of the pathophysiological factors are known, such as changes in fibre type composition (Murgia *et al*., 2017; Ubaida-Mohien *et al*., 2019), intramyocellular lipid accumulation (St-John-Pelletier *et al*., 2017, lipofuscin accumulation (Reeg & Grune, 2015), or decreased stem cell prevalence (Fry *et al*., 2015; Lopez-Otin *et* al., 2013), no previous studies have investigated the specific link between these factors and the potential role they play in the context of frailty and sarcopenia in the older HIV+ population.

Whilst the preceding chapters have investigated adverse ageing phenotypes in older PLWH (**Chapter 5**) and the impact of skeletal muscle mitochondrial dysfunction in these individuals (**Chapter 6**), this chapter aims to better understand the role of several other potential pathophysiological processes affecting skeletal muscle, and the role that these factors may play in adverse ageing phenotypes in older PLWH.

7.1.1 Fibre type composition

Skeletal muscle fibres are multinucleated single cells, and in human skeletal muscle there are three types of fibres – one 'slow twitch' (type I) and two 'fast twitch' (type IIa and IIx). Each respective fibre type is composed of specific isoforms of myosin heavy chain (MHC), and this determines the fibre type functions, contractile capabilities and metabolic profile (Scott *et al*., 2001).

Type I fibres are slow twitch due to their oxidative metabolism, while type IIa fibres are composed of a mix of slow and fast twitch MHCs, and type IIx are fast twitch and so completely glycolytic (Burke *et al*., 1971; Berchtold *et al*., 2000). Due to their oxidative metabolism, type I fibres have a higher abundance of mitochondria, mtDNA, mtrRNA, and mtmRNA compared to both type IIa and type IIx fibres, and thus have a higher oxidative capacity (Howald *et al*., 1985; Picard *et* al., 2012; Picard *et* al., 2008). As expected, there is a higher activity of PGC-1a in type I fibres, and it has been suggested that PGC-1a expression could drive the conversion of the fast twitch fibres into type I fibres through upregulation of various transcription factors (calcineurin signalling; Mef2; MAPK signalling) (Lin *et al*., 2002; Olson *et al*., 2008; Murgia *et al*., 2017). Adult skeletal muscle displays impressive plasticity, and as well as in response to degeneration from ageing, fibre type conversion and increase in mitochondrial content can occur in response to endurance training and mechanical overload (Chin, 1998; Olson, 2008; Nielsen *et al*., 2010).

Importantly, the selected atrophy of certain fibres and fibre type switching occurs with ageing (Larsson *et al*., 2019). The proportion of type I fibres increases with age, whilst the proportion of type IIa and IIx decrease with age (Brunner *et al*., 2007; Grimby, 1995; Murgia *et al*., 2017; Ubaida-Mohien *et al*., 2019; Roberts *et al*., 2018; Verdijk *et al*., 2009; 2010; 2012; 2014; McKay *et al*., 2012; 2013), and this is suspected to contribute to frailty and prefrailty (St-Jean Pelletier *et* al., 2017; Sonjak *et al*., 2019). Whilst the exact mechanisms are unknown, it has previously been demonstrated that there is a general upregulation in the expression of ribosomal proteins in type I fibres, and a simultaneous downregulation in their expression in both type IIa and IIx fibres (Rose *et al*., 2009), as well as increased denervation with age (Rowan *et al*., 2012). This suggests a decline in sarcomere quality control in both type IIa and IIx fibres. Another alternative mechanism could be the declining fuel sources available to fast twitch fibres with age. As such, fast twitch fibres contain a higher concentration of glycogen (required for glycolysis) than slow twitch fibres, and muscle glycogen contents are known to decrease with age (Nielsen *et al*., 2011).

As mentioned previously, skeletal muscle mass and strength decline with age. At the cellular level, larger fibres are commonly the more glycolytic type IIa and IIx fibres, indicating an inverse relationship between VO_{2max} and fibre size (Van Der laarse *et al*., 1998). Muscle fibre size has also

been shown to decrease with age, although this decrease primarily occurs in both type II fibres compared to type I fibres (St-Jean Pelletier *et al*., 2017; Sonjak *et al*., 2019). This could be due to the fact that the fast twitch fibre types are generally smaller (Dreyer *et al*., 2006; Van Der Laarse *et al*., 1998). As type II fibres are primarily glycolytic and heavily involved in resistance activities, this age-related decrease in fibre size has been suggested to contribute to the decline in muscle function with age (Miljkovic *et al*., 2015). In addition to the decrease in average fibre size with age, the total number of muscle fibres also decreases with age, suggesting an age-related increase in fibre atrophy (Lexell *et al*., 1983).

A recent investigation into the proteomics of the fibres type in both old and young individuals demonstrated a reduction in the expression of OXPHOS complexes in both slow and fast twitch fibres with age, although this was more pronounced in the fast twitch fibres (Murgia *et al*., 2017). In addition, the expression of proteins involved in regulating mitochondrial dynamics such as MFN2 and OPA1 (involved in mitochondrial fusion) is decreased in older fibres, whilst the expression of proteins involved in proteolysis and autophagy are increased. Finally, enzymes involved in the TCA cycle were also elevated in older fibres. This coincided with the age-related increase in the expression of proteins involved in glycolytic metabolism in type I fibres, indicating a general decline in skeletal muscle mitochondrial homeostasis with age (Murgia *et al*., 2017; Murgia *et al*., 2019). As a result, both skeletal muscle oxidative function in the form of OXPHOS complex prevalence, as well as fibre type proportions, were investigated in a cohort of older PLWH in this study.

Type I fibres are more likely to undergo hypertrophy compared to type II fibres. One reason for this is due to the fact that the highly oxidative type I fibres contain more myonuclei per mm of fibre length than the glycolytic fibres, and hypertrophy is dependent on newly formed myonuclei (Sayegh & Lajtha, 1989). In addition, a higher proportion of type I MHC mRNA compared to type IIa MHC mRNA, as seen in type I fibres, is associated with a faster rate of protein synthesis and better regulated protein homeostasis (Toth & Tchernof, 2006). Interestingly, type I fibres have a higher rate of transcription and translation than type IIa or IIx fibres (Habets *et al*., 1999).

7.1.2 Skeletal muscle satellite cell decline with age

Declines in tissue homeostatic and regenerative capacity are a common characteristic of ageing, which is driven at the cellular level by the reduction in functioning stem cell capacity (Jones & Rando, 2011; Dorshkind *et* al., 2009). Tissue repair and regular homeostasis in adults requires a functioning population of undifferentiated pluripotent stem cells within fully differentiated tissue. These stem cells are contained in a systemically controlled microenvironment termed the 'niche', where various trophic and growth factors, as well as cytokines, regulate and maintain the stem cells (Jasper & Kennedy, 2012).

In skeletal muscle, stem cells are termed satellite cells (SCs) and are located beneath the basal lamina of mature myofibres (Mauro, 1961). SC niches are established in early development and remain in a quiescent state, characterised by expression of the paired-box protein (Pax7), until induced by injury or stress (Yin *et al*., 2013; Dell'Orso *et al*., 2019). In response to injury or stress, these $Pax7^+$ SCs become activated and begin to proliferate, before committing to one of three pathways: (a) exiting the cell cycle; (b) differentiation and fusion in order to repair damaged myofibres or form new myofibres, or (c) self-renewal in order to replenish and maintain the SC pool (Weissman, 2000). In addition, the myogenic regulatory factors Myf5 and MyoD, which are involved in embryonic muscle development, are required for skeletal muscle regeneration in adults (Yamamota *et al*., 2018). In the past few years single cell RNA sequencing and proteomics have confirmed the heterogeneity of SCs within SC pools in normal resting adult muscle, and has confirmed the presence of the core cell types - quiescent SCs, activated SCs, primary myoblasts and committed progenitors (Porpiglia *et al*., 2017; Rubenstein *et al*., 2020; Dell'Orso *et al*., 2019; Barruet *et al*., 2020).

With regards to pathway (b), quiescent $Pax7^+$ SCs become activated, enter the cell cycle and acquire MyoD expression, which facilitates their expansion. Next, activated SCs will then either commit to differentiation, and in doing so downregulate Pax7 expression, or alternatively return to quiescence in the niche by losing MyoD expression and undertake MyoD-induced Myogenin activation (pathway (c)). Differentiating SCs then further proliferate and express Myogenin, which in combination with other myogenic differentiation factors such as myocyte enhancer factor 2 (Mef2), activates downstream genes. This allows differentiated myoblasts to fuse with either an existing fibre or contribute to the development of new and growing myotubes (Almada & Wagers, 2016) (**Figure 7.1**).

As mentioned above, ageing is characterised by the decline in stem cell function (Lopez-Otin *et al*., 2013). The regenerative potential of SCs has been shown to decline with age, and this decline is particularly pronounced in sarcopenic muscle, where there is an increased formation of fibrotic

tissue (Zwetsloot *et al*., 2013; Sousa-Victor *et* al., 2014; Fry *et al*., 2015). The consequences of dysfunctional SC dynamics will reduce the individual's capacity to respond to hypertrophic stimuli such as exercise, or respond to stressors and injury (Blau *et al*., 2015; Cartee *et al*., 2016). Interestingly, work from *in vitro* studies has demonstrated that Pax7 null muscles are smaller, contain less nuclei, have a narrower diameter compared to normal Pax7$^+$ SCs, and have an earlier mortality (Oustanina *et al*., 2004; Kuang *et al*., 2006).

7.1.2.1 Mechanisms of age-related Pax$^+$ SC decrease

Whilst the exact mechanism for the age-related decline in skeletal muscle SCs is yet to be fully elucidated, several mechanisms have been proposed. These include changes in the niche leading to poor trophic signalling response, or declines in the systemic signalling modulation (Conboy *et al*., 2005; Brack *et al*., 2007; Rando & Chang *et al*., 2012; Carlson *et al*, 2009). The underlying genetic mechanisms for these phenomena are the increased expression of genes associated with FOXO regulation, which is responsible for atrophy. In addition, aged SCs have abhorrently altered genes associated with mitochondrial function and protein homeostasis (Pietrangelo *et al*., 2009; Bortoli *et al*., 2003). Herein, a recent *in vitro* study demonstrated that SCs with a higher burden of somatic mutations proliferate and differentiate slower than SCs with a lower mutational burden (Franco *et al*., 2018). Alternatively, aged SCs display declines in Notch signalling. This is due to the age-associated downregulation of Notch ligands, which are responsible for regulating the proliferation of activated SCs (Conboy *et al*., 2003). These age-related changes have been shown to decrease the activation, proliferative and differentiation potential of SCs (Shadrach & Wagers, 2001; Roth *et al*., 2000; Shefer *et al*., 2006; Day *et al*., 2010; Charge *et al.,* 2002).

Additionally, the proportion of Pax7$^+$ SCs in skeletal muscle is roughly 30% at birth but falls to roughly 5% in adults and 2% in older mice (Gopinath & Rando, 2008).

Age-related increases in cell senescence and apoptosis are also known to affect SC populations. Age-associated decline in the proliferation potential and function of stem cells has been shown to be associated with increased senescence (Sousa-Victor *et* al., 2014) and subsequently attenuated by ablation of p16INK4a (Janzen *et al*., 2006), whilst telomere shortening has been reported in several stem cell compartments (Flores *et al*., 2008). In addition, age-related DNA damage accumulation impairs several mechanisms of SC function such as quiescence, self-renewal, and regeneration (Rossi *et al*., 2007; Sousa-Victor *et al*., 2014). Interestingly, SCs have been shown to enter alternative differentiation programmes such as those towards adipogenic or fibrogenic fates, with increasing frequency with age, thereby reducing the functional capacity of the niche whilst simultaneously

increasing adiposity and fibrosis in skeletal muscle, both of which significantly contribute to sarcopenia and frailty (Taylor-Jones *et al*., 2002).

The final set of factors that affect SC function with age are changes in extrinsic signals from the SC microenvironment. In particular, age-related declines in transforming growth factor β inhibit SC proliferation by altering Notch signalling (Baltgalvis *et al*., 2008), whilst declines in Wnt, responsible for differentiation following Notch-dependant proliferation, and Transforming Growth Factor (TGF-β) signalling have also been demonstrated in aged individuals (Brack *et al*., 2007; Conboy *et* al., 2003; Conboy *et al*., 2005; Carlson *et al*., 2009).

Adult SC niches are often under hypoxic conditions and so utilise glycolysis as a metabolic pathway when quiescent (Suda *et al*., 2011; Escribese *et al*., 2012; Chandel *et al*., 2016). When undergoing proliferation and differentiation, myoblasts switch from glycolysis to OXPHOS. This metabolic switch is mediated by high levels of mitophagy (Domenech *et al*., 2015; Esteban-Martinez *et al*., 2017; Rajasekaran *et al*., 2020). Differentiation can also be impaired by the age-associated dysregulation of redox status and oxidative stress (Rajasekaran *et* al., 2020). Collectively, these factors suggest that the age-related dysregulation of mitochondrial dynamics could have an adverse effect on SC function in adult skeletal muscle, hence why I investigated pax7^{+} SC prevalence and skeletal muscle mitochondrial dysfunction in the form of OXPHOS complex deficiency in older PLWH.

Finally, SCs require a tightly coordinated regulation of epigenetic modifications, such as DNA methylation (Carrio *et al*., 2015; Carrio *et al*., 2016), histone modifications (Asp *et al*., 2011), and transcription factor activation of MRFs via specific muscle miRNA (myomiRs) (Chen *et al*., 2006; Chen *et al*., 2010; Rao *et al*., 2006) in order retain SC niche dynamics and function. Therefore, the age-related decline in epigenetic regulation contributes to the dysregulation of SC niches with age.

Altogether, previous research in the field of muscle stem cells and ageing has demonstrated that there are various factors that contribute to the age-related decline of Pax7^{+} SCs. However, in this study I will be focusing on whether age-related declines in skeletal muscle mitochondrial function contribute to muscle stem cell declines, and whether these factors predict physiological decline and adverse ageing phenotypes in older PLWH.

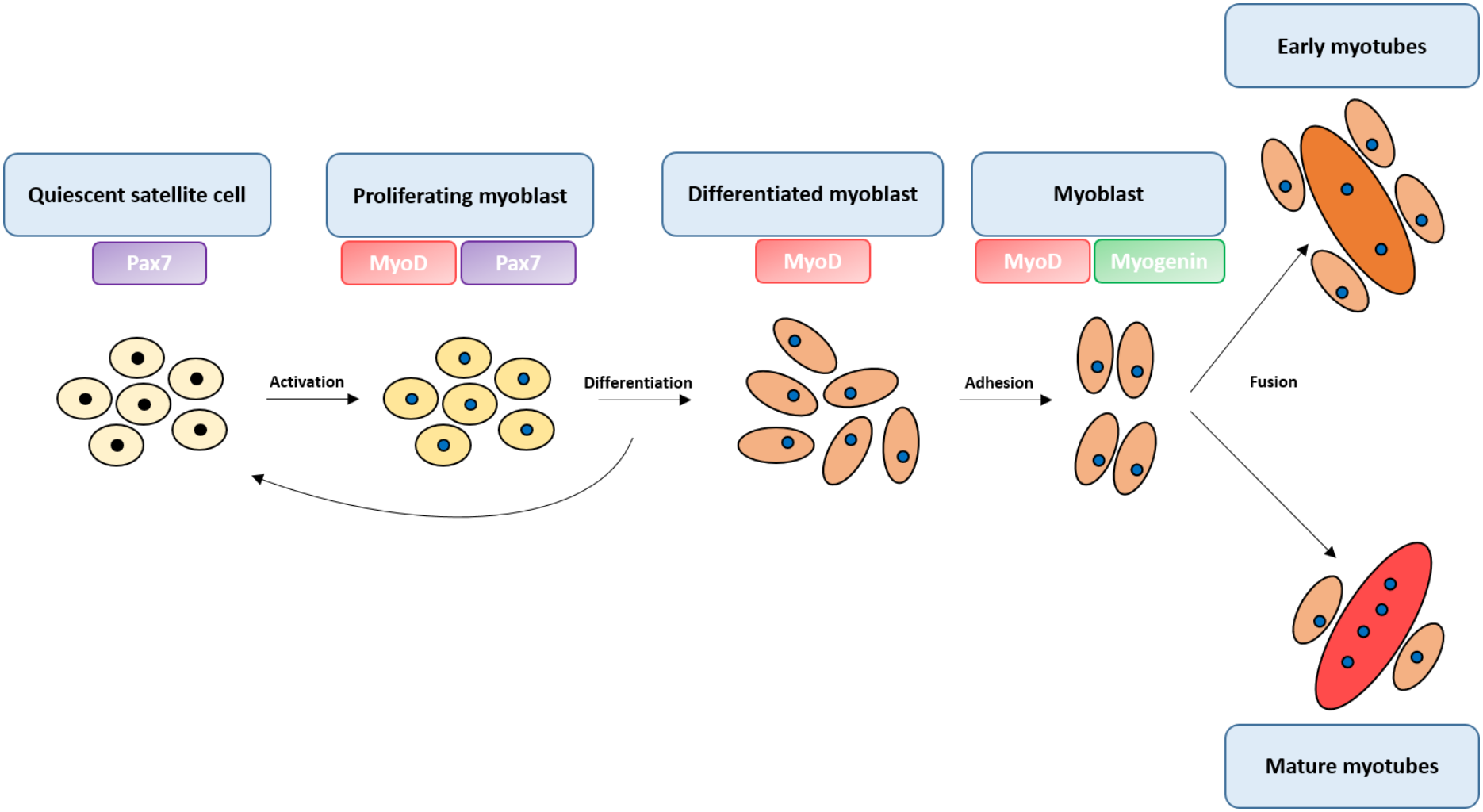

Figure 7.1 – Lineage progression of muscle fibre formation.

7.1.3 Neuromuscular junction decline with age

Age is associated with a decline in neurophysiological functions, and this decline is implicated in the progressive loss of muscle mass and strength with age.

Autopsy and clinical studies have demonstrated that ageing skeletal muscle undergo greater levels of denervation, which leads to a loss of muscle mass and function (Hepple & Rice, 2016; Mosole *et al*., 2014; Messi *et al*., 2016; Rowan *et al*., 2012). Denervation is regularly compensated by a re-innervation programme which aims to replace the damage from denervation in a continuous cycle. As individuals age the rate of reinnervation deteriorates and denervated fibres thus become apoptotic. This leads to muscle atrophy and contractile dysfunction (Rowan et al., 2012; Gonzalez-Freire et al., 2014). This ageing phenomenon has been supported by studies showing the age-dependant increase in muscle fibres positive for denervation-responsive sodium channels (Rowan et al., 2012) (**Figure 7.2**). The denervation-reinnervation cycle is also an important process as it can alter fibre type conformations and remodels the spatial domain of motor units (Hepple & Rice, 2016).

Mitochondria play important roles in the NMJ, as they provide energy and act as the buffer for the large calcium ion loads needed to conduct an action potential (Barrett *et al*., 2011). Mitochondrial abnormalities have been identified in the pre-synaptic region of the NMJ. These abnormalities include cristae swelling and fragmentation, formation of megamitochondria in aged rats, and reduction in mitochondrial respiratory capacity. Importantly, these factors appear to correlate with denervation (Garcia *et al*., 2013; Spendiff *et al*., 2016). In axon terminals that contain abnormal mitochondria there is a reduction in ETC efficiency, an increase in ROS and an increased susceptibility to permeability transition (Garcia *et al*., 2013; Trounce *et al*., 1989; Hepple & Rice, 2016). Whilst it is well understood how age-related mitochondrial abnormalities may contribute to NMJ denervation, the extent of which it actually contributes to the physiology of age-related declines remain controversial. Hence, a study of aged human limb segments found that 95% of muscle fibre segments with high levels of pathogenic mtDNA mutations did not exhibit atrophy (Bua *et* al., 2006). In contrast, an alternative study of post-mortem spinal cord motoneurons of elderly individuals found evidence of mtDNA depletion, but not mtDNA deletions (Rygiel *et* al., 2014).

As it has been difficult to study the dynamics of the NMJ in humans, several mouse models originally developed to study neurodegenerative diseases have been increasingly utilised. One of the foremost mouse models is one with a homozygous deletion of the Cu/Zn superoxide dismutase (Cu/Zn SOD), which develops age-related muscle atrophy as a result of mitochondrial dysfunction, a switch to type I fibres, increased ROS, and exaggerated alternations in the NMJ (Sakellariou *et al*., 2011).

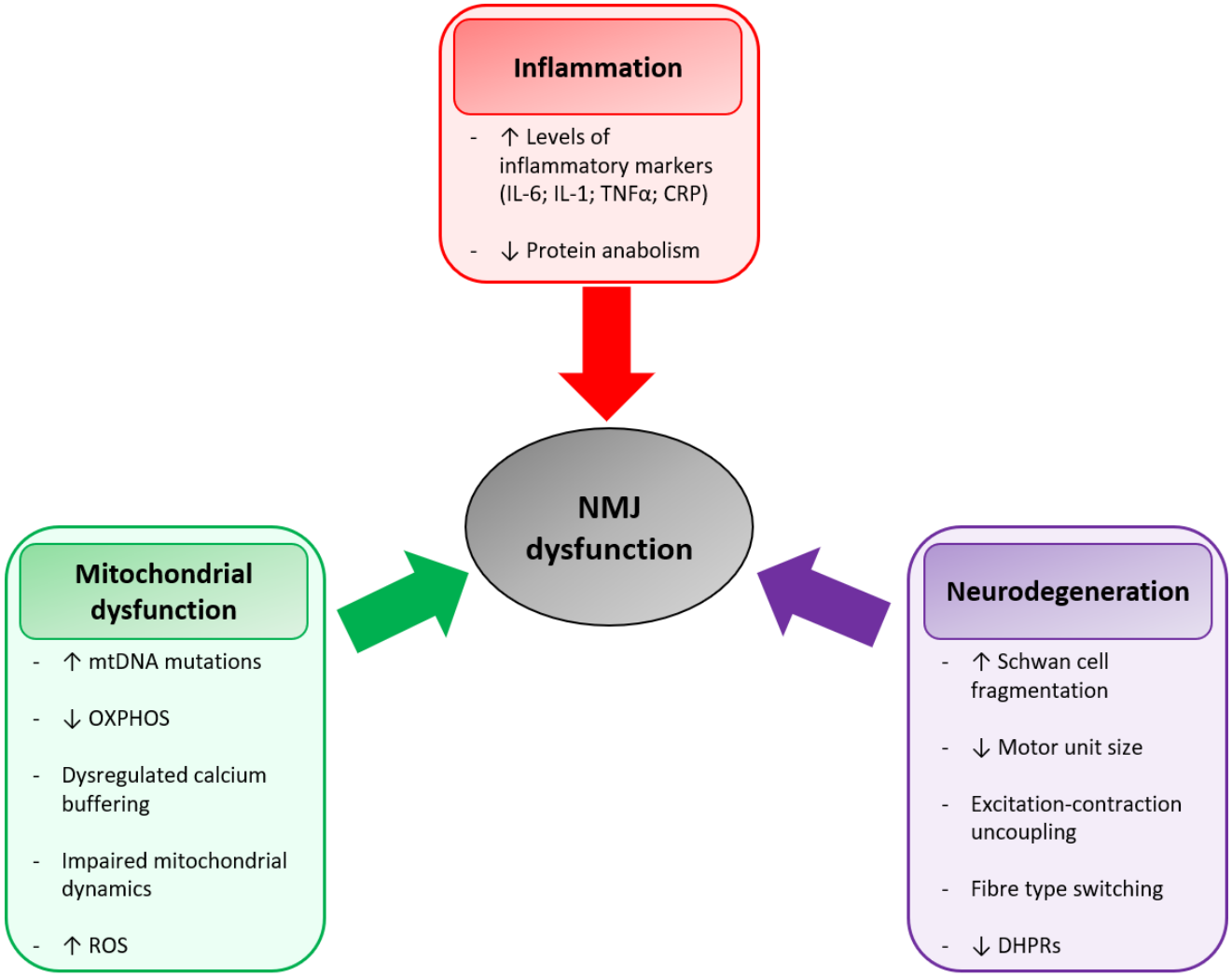

Figure 7.2 – Primary factors involved in neuromuscular junction decline with age. *Factors can be broadly defined into the three categories of mitochondrial dysfunction, neurodegenerative, and inflammatory factors.*

7.1.4 Skeletal muscle insulin resistance

Under basal conditions, skeletal muscle is responsible for approximately 80% of insulin-stimulated glucose uptake as well as regulation of several metabolic functions (Petersen *et al*., 2002; Petersen *et al*., 2007). Insulin resistance (IR) is defined as the decline in the ability of insulin to stimulate glucose uptake from peripheral tissues, such as skeletal muscle and the liver.

In physiological conditions, insulin promotes glucose uptake via the canonical IRS-PI3K-Akt pathway as well as stimulating glucose transported type (GLUT) 4 translocation to the membrane by inactivating the Akt substrate 160 (AS160). This in turn promotes GLUT4 fusion with the plasma membrane and subsequent uptake of glucose (Sakamoto & Holman, 2008) (**Figure 7.3**).

Skeletal muscle IR is primarily caused by the prolonged exposure to high levels of fatty acids such as palmitic and stearic acids (Hirabara *et al*., 2010; Yuzefovych *et al*., 2010). In brief, this leads to oxidative stress, alterations in gene transcription, as well as increases in inflammation and mitochondrial dysfunction (Hirabara *et al*., 2007; Griffin *et al*., 1999; Randle *et al*., 1963; Calvalho-Filho *et al*., 2005).

The first proposed mechanism for the pathogenesis of skeletal muscle IR was from Randle and colleagues, who demonstrated that elevated fatty acid oxidation increased acetyl-CoA production. Elevated levels of acetyl-CoA then inhibited pyruvate dehydrogenase activity and increased citrate levels. Next, citrate in combination with a higher ATP:ADP ratio inhibited phosphofructokinase, which subsequently reduced glucose flux and resulted in hexokinase II inhibition, increased cellular glucose content, and therefore a reduction in glucose uptake (Randle *et al*., 1963; Randle, 1998; Dresner *et al*., 1999). This finding has been further supported by several *in vivo* and *in vitro* studies (Jenkins *et al*., 1988; Boden & Chen, 1995; Griffin *et al*., 1999; Roden *et al*., 1996; Rothman *et al*., 1992).

Several studies have additionally demonstrated the ability of saturated fatty acids to alter insulin signalling (Hirabara *et al*., 2010; Roden *et al*., 1996; Hawley *et al*., 2000; Savage *et al*., 2007). As such, elevated levels of saturated fatty acids have been shown to reduce the activation of PI3-kinase, JNK, mTOR, and Akt signalling pathway activation due to decreased Insulin Receptor Substrate 1 (IRS-1) phosphorylation (Yu *et al*., 2002, Kim *et al*., 2000). These signalling pathways are involved in growth and glucose sensitivity and so decreased activation of these signalling pathways subsequently contribute to declines in insulin sensitivity and tissue dysfunction (Zisman *et al*., 2000).

Another pathophysiological mechanism underpinning fatty acid-induced IR is the induction of lipotoxicity. This occurs as a result of levels of circulating fatty acids exceeding uptake and storage

capabilities in white adipose tissue (Consitt *et al*., 2009). This lipotoxicity and increased levels of circulating fatty acids and fatty acid derivatives such as diacylglycerol, ceramides, triacylglycerol and sphingosines are associated with glucose intolerance and therefore IR (Chavez *et al*., 2003; Holland & Summers, 2008; Lipina & Hundal, 2011).

Increased levels of circulating fatty acids also increase the activation of inflammatory pathways through the interaction with members of the Toll-like receptor (TLR) family, in addition to increasing the production and secretion of cytokines such as IL-6, IL-1 and TNF-α (Haversen *et al*., 2009; Wen *et al*., 2011; Dali-Yousef *et al*., 2013). One example is the increased activation of the NF-κB pathway in skeletal muscle via JNK and IKK complex activation, which indirectly promotes IRS-1 inhibition (Hotamisiligil *et al*., 1993). Importantly, increased macrophage and T cells levels have also been demonstrated in skeletal muscle of type 2 diabetes mellitus (T2DM) and obese-induced IR patients (Khan *et al*., 2015; Varma *et al*., 2009; Patsouris *et al*., 2014; Fink *et al*., 2014), and a mice fed with a high-fat diet to induce IR also exhibited increased accumulation of skeletal muscle immune cells, indicating increased inflammation in IR (Olefsky & Glass, 2010; Patsouris *et al*., 2014; Nguyen *et al*., 2007; Fink *et al*., 2013; Hong *et al*., 2009; Lee *et al*., 2011). Importantly, immune cell accumulation and increased TNF-α signalling have both been shown to adversely impact IR by contributing to the inhibition of IRS-1 signalling (Khan *et al*., 2015; Austin *et al*., 2008; Schmitz-Peiffer & Biden, 2008).

7.1.4.1 Links between age-related mitochondrial dysfunction and insulin resistance

One of the most significant responses to increased saturated fatty acid levels is the alteration in gene expression. Examples include alterations to enzymes involved in the glycolysis pathway such as pyruvate dehydrogenase kinase isozyme 1 (PDK-1) and lactate dehydrogenase (LDHA) (Xu *et al*., 2006; Lopez *et al*., 2004). Additionally, the downregulation of PCG-1α expression, as well as downregulation of mtDNA genes encoding OXPHOS complexes (Sparks *et al*., 2005; Heilbronn *et al*., 2007) and other genes involved in regulating mitochondrial function, such as NRF-1 and NRF-2, also occurs (Scarpulla, 2008). Taken together, these findings indicate that altered gene expression in response to increased levels of saturated fatty acids results in the dysregulation of normal mitochondrial and metabolic function, resulting in decreased insulin sensitivity and therefore IR. As a result, in this study I investigated intramyocellular lipid accumulation and ETC CI and CIV prevalence in the context of adverse ageing phenotypes in older PLWH.

Another important pathogenic factor is increased ROS production and oxidative stress. ROS are involved in several signalling pathways implicated in modulating insulin sensitivity and other metabolic functions, and so significantly elevated ROS levels are associated with impaired IRS-1 activation and therefore decreased GLUT4 transcription and function (Bloch-Damti & Bashan, 2005;

Anderson *et al*., 2009). In addition, oxidative stress causes molecular damage to proteins and DNA, which will lead to the abhorrent processes described above. Taken together, imbalances to the redox potential will result in impaired glucose tolerance (Rains & Jain, 2011). This theory has been supported by *in vitro* studies which demonstrated the reduction in insulin-stimulated glucose uptake in response to elevated H_2O_2 levels (Maddux *et al*., 2001). This is also supported by the demonstration of elevated ROS levels in cellular models for IR (Houstis *et* al., 2006), and the fact that overexpression of the antioxidant mitochondrial superoxide dismutase (MnSOD) in rodent models improved insulin sensitivity and glucose uptake (Hoehn *et al*., 2009; Boden *et al*., 2012). Importantly, T2DM, metabolic syndrome and obesity are all associated with increased ROS in skeletal muscle (Abdul-Ghani *et al*., 2008; Bonnard *et al*., 2008; Kumashiro *et al*., 2008).

Significantly, several studies have demonstrated a decline in mitochondrial content and function in T2DM and insulin-resistant obese individuals (Holloway *et al*., 2007; Schrauwen-Hinderling *et al*., 2007). Decreased mitochondrial fatty acid oxidative capacity was also demonstrated in primary myocytes derived from T2DM patients (Kim *et al*., 2000; Hulver *et al*., 2003; Ukropcova *et al*., 2005), and humans and rats supplemented with a high-fat diet displayed decreases in PGC-1 signalling, oxygen consumption and ATP synthesis (Brehm *et al*., 2006; Sparks *et al*., 2005; Desco *et al*., 2002; Erdei *et al*., 2006; Szendroedi *et al*., 2009). One of the pathogenic mechanisms underpinning these abnormalities is the increased prevalence of mtDNA mutations in T2DM and insulin-resistant obese individuals (Lim *et al*., 2001; Guo *et al*., 2005; Juo *et al*., 2010). These could cause alterations in mitochondrial homeostasis and ultimately lead to increased inflammation and oxidative stress, as mentioned above. As such, fatty acid induced mitochondrial fission has been shown to be associated with reduced insulin-stimulated glucose uptake. Finally, a recent study demonstrated lower mitochondrial oxidative capacity (as measured by ^{31}P-MRS) was associated with a more severe HOME-IR score, as well as decreased insulin sensitivity (Fabrri *et al*., 2017). This finding is supported by other patient-based studies which have shown the positive correlation between mitochondrial activity and insulin sensitivity (Szendroedi *et al*., 2009; Szendroedi *et al*., 2014).

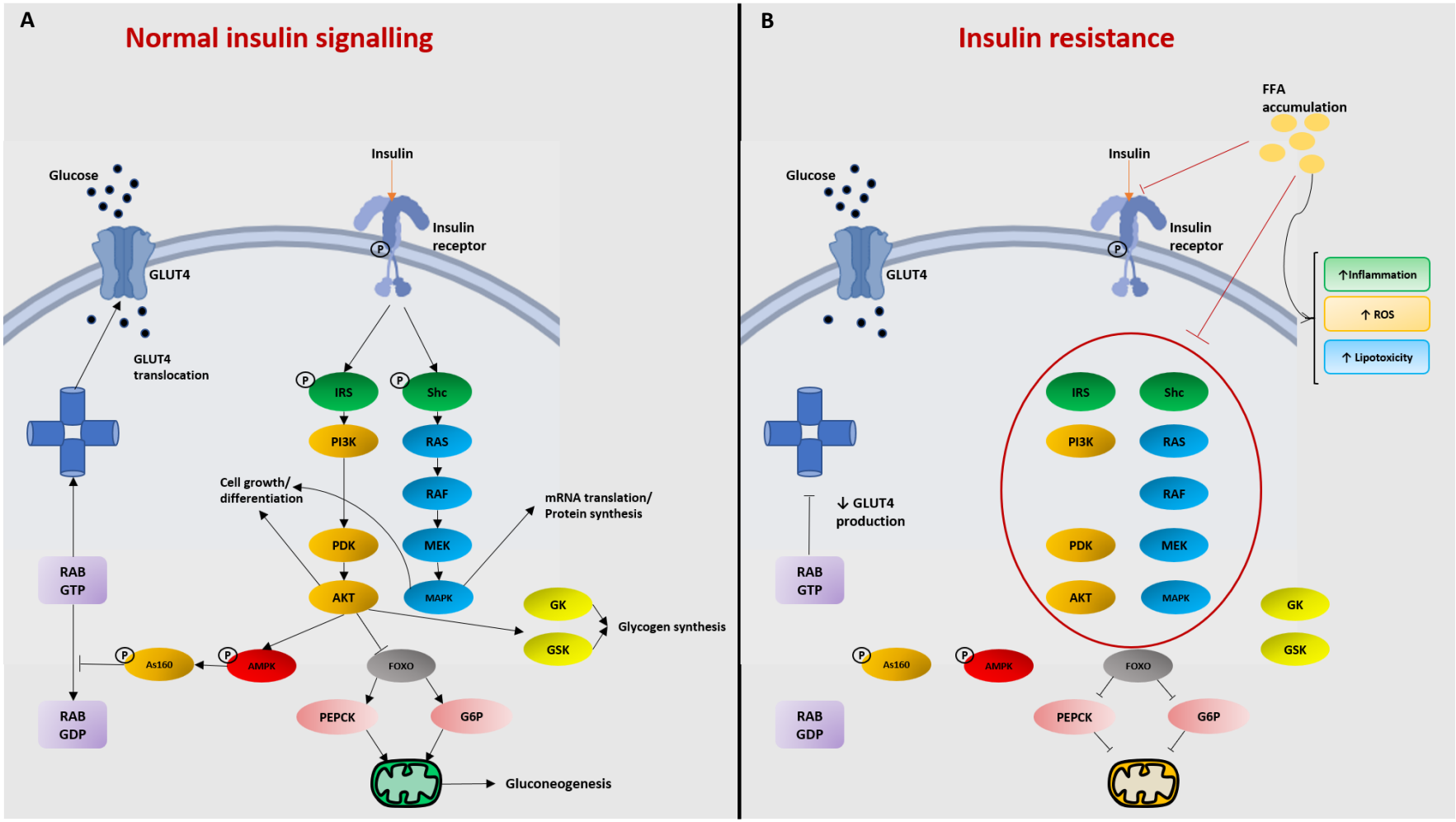

Figure 7.3 – Normal insulin signalling and insulin signalling in IR muscle. *(**A**) Insulin binds to the insulin receptor, which subsequently induces its conformational change and phosphorylation, leading to the recruitment and phosphorylation of insulin receptor substrate (IRS) and Shc proteins. Shc then activates the RAS/RAF/MAPK pathway which leads to the upregulation in mRNA translation and protein synthesis. IRS activates the PI3K/AKT signalling pathway which leads to mitochondrial-induced gluconeogenesis as well as cell growth and differentiation, and glycogen synthesis. In addition, this pathway induces the production of GLUT4 transporters and increased GLUT4 signalling. (**B**) In the presence of increased free fatty acids there is a decline in baseline insulin signalling due to increased competition for the insulin receptor. This prevents the signalling pathways activated in normal insulin signalling and thus prevents the downstream effects of insulin signalling. In addition, accumulation of FFAs leads to increased inflammation, ROS production and lipids involved in lipotoxicity.*

7.1.5 Lipofuscin accumulation

Lipofuscin granules are autofluorescent pigments composed of highly oxidised, cross-linked lipids and misfolded proteins (Hohn *et al*., 2010; Konig *et al*., 2017; Rodolfo *et al*., 2018). Due to the highly-oxidised nature of lipofuscin granules, they cannot be degraded and so accumulate with age in lysosomes and cytoplasm in post-mitotic tissues such as neurons, cardiac and skeletal muscle (Brunk & Terman 2002, Hohn & Grune 2013, Moreno-Garcia 2018).

Previous studies have indicated that lipofuscin accumulation accentuates age-related pathophysiological factors by inhibiting the proteasome, and therefore proteolytic removal of damaged proteins - leading to an increase in ROS production, cytotoxicity and inflammation (Reeg & Grune, 2015). Lipofuscin accumulation in lysosomes also adversely impacts protein homeostasis and decreases the efficiency of autophagy, which can lead to the inefficient clearance of damaged mitochondria (Terman & Bunk 2004; Ryhanen *et al*., 2009; Hohn *et al*., 2011; Reeg & Grune, 2015; Terman *et al*., 2010). Both these mechanisms lead to further oxidation of proteins and lipids, increasing the formation and accumulation of lipofuscin pigments, and subsequent dysregulation of lysosomal activities. In addition, previous studies have demonstrated that the accelerated accumulation of lipofuscin is linked to the pathogenesis of Parkinson's disease (Ulfig, 1989) and Alzheimer's Disease (Mountjoy *et al*., 2005).

Although not extensively proven, Terman and Brunk postulated the 'mitochondrial-lysosomal axis theory of aging', which states that the incomplete degradation of mitochondria through mitophagy is the primary cause of lipofuscin accumulation (Brunk & Terman, 2002; Terman *et* al., 2010; Konig *et al*., 2017).

7.2 Experimental aims

Age-related decline in skeletal muscle function is recognised as one of the significant causative factors in adverse ageing phenotypes seen in the general population and PLWH (Mitchell *et al*., 2012; Cruz-Jentoft *et al*., 2019).

Whilst numerous observational and longitudinal cohort studies have identified several risk factors that contribute to the age-related decline in skeletal muscle function, such as mitochondrial dysfunction and intramyocellular lipid accumulation (IMCL), the underlying pathophysiological mechanisms remain not fully understood. In addition, few studies have investigated the level and role of several of these skeletal muscle pathophysiological factors in the ageing with HIV setting. Therefore, in this study I sought to:

- Determine the prevalence of several age-related skeletal muscle pathophysiological factors including IMCL, quiescent stem cell prevalence, fibre type composition, fibrosis, lipofuscin accumulation, and the proportion of regenerated and degenerated fibres, in older PLWH compared with age-matched HIV- individuals.
- Determine whether skeletal muscle CI and CIV deficiency as well as mitochondrial mass is predictive of these age-related skeletal muscle pathophysiological factors in older PLWH.
- Determine the associations between these pathophysiological skeletal muscle factors, and whether they are predicted by any of the clinical, HIV-related, physical, or lifestyle parameters.
- Determine whether any of these pathophysiological factors are associated with adverse ageing phenotypes in older PLWH.

7.3 Methods

7.3.1 Patient cohort

This study was approved by the research ethics committee (Newcastle and North Tyneside 2 (17-NE-0015)). Skeletal muscle samples were taken by percutaneous biopsy from older (≥ 50 years) HIV-infected males (n = 30) as well as HIV-uninfected males (n = 15) as part of the MAGMA study (**Table 3.1**), with patients giving prior written permission.

7.3.2 Immunofluorescence and fluorescence histochemistry

7.3.2.1 Duplex fluorescence histochemistry for the quantification of intramyocellular lipid accumulation

Fluorescence histochemistry was carried out on 10µm frozen transverse muscle sections in order to detect and quantify intramyocellular lipid droplets in skeletal muscle fibres, as described in **Section 3.4.6**.

7.3.2.2 Image acquisition and analysis of intramyocellular lipid accumulation

Fluorescent images were acquired using a Zeiss Axio Imager M1 and Zen 2011 (blue edition) software with a Monochrome Digital Camera (AxioCam MRm) at 20x magnification, and analysed as described in **Section 3.4.7**.

7.3.2.3 Duplex immunofluorescence for the quantification of Pax7$^+$ satellite cells

10µm cryosections were subjected to a duplex immunofluorescence staining assay, as described in **Section 3.4.8** in order to quantify the prevalence of quiescent Pax7$^+$ satellite cells.

7.3.2.4 Image acquisition and analysis for quantification of Pax7$^+$ satellite cells

Fluorescent images were acquired and the prevalence of Pax$^+$ satellite cells was quantified as described in **Section 3.4.9**. Briefly, the number of myofibres per biopsy as well as the prevalence of Pax7$^+$ cells (characterised by colocalised staining in the DAPI and Pax7 channels) was quantified in each subject in order to determine the proportion of Pax7$^+$ satellite cells per 100 fibres.

7.3.2.5 Multiplex immunofluorescence for fibre type quantification

Multiplex immunofluorescence for the quantification of fibre types I, IIa, and IIx as well as fibre cross-sectional area (µm^2) was performed as described in **Section 3.4.10**.

7.3.2.6 Image acquisition and analysis of fibre type quantification

Fluorescent images were acquired using a Zeiss Axio Imager M1 and Zen 2011 (blue edition) software with a Monochrome Digital Camera (AxioCam MRm) at 20x magnification, as described in **Section 3.4.11**.

7.3.2.7 Preparation of slides for lipofuscin quantification, image acquisition and analysis

For the quantification of skeletal muscle lipofuscin accumulation, 10µm transverse cryo-sections were removed from -80°C storage and air-dried for 1 hour. Sections were then immediately cover-slipped with Prolong gold and stored at -20°C until imaged. Image acquisition and analysis was performed using Columbus Image Data Storage and Analysis System software as described in **Section 3.4.12**.

7.3.3 Histochemistry

7.3.3.1 Haematoxylin & Eosin histochemistry staining and imaging for the quantification of regenerated and degenerated skeletal muscle fibres

10µm cryosections were subjected to haematoxylin & eosin histochemistry in order to quantify to proportion of regenerated and degenerated myofibres, as described in **Section 3.5.2**.

7.3.3.2 Masson's trichrome histochemistry for skeletal muscle fibrosis

Masson's trichrome histochemistry was performed on 10µm cryosections in order to quantify skeletal muscle fibrosis, as described in **Section 3.5.3**.

7.3.3.3 Brightfield microscopy

Brightfield images were acquired using a Zeiss Axio Imager M1 and Zen 2011 (blue edition) software with a chromatic digital camera (AxioCam MRm) at 10x magnification, as described in **Section 3.5.5**.

7.3.4 Statistical analysis

Statistical analysis was performed in Prism v5.04, IBM SPSS Statistics v23 and Microsoft Excel 2016. Graphs were produced in Prism v5.04.

Normality was assessed by Shapiro-Wilk tests. Statistical differences in the various pathogenic muscle parameters between the HIV+ and HIV- individuals as well as PLWH stratified by frailty/prefrailty and sarcopenia/presarcopenia was determined by unpaired t tests for normalised data and Mann-Whitney tests for non-normally distributed data sets. Differences in skeletal muscle pathogenic factors between frail, prefrail, and robust PLWH as well as between sarcopenic, presarcopenic, and non-sarcopenic PLWH were determined by one-way ANOVA with Tukey's multiple comparisons test to investigate differences between the comparator groups. Fisher's exact

test was performed in order to determine differences in the various pathogenic muscle parameters in nominal data sets such as stratification by smoker status.

Unadjusted linear regression analysis between pathophysiological skeletal muscle factors and clinical as well as physical factors was performed using linear regression and Pearson's correlation for normally distributed data, or Spearman correlation for non-normally distributed data. Adjusted linear multivariate regression analysis was also undertaken, with respective models including age and factors determined to be significant from univariate analysis as independent variables and predicted factors as the dependant variable. Reported outcomes of multivariate linear regression analysis included unstandardised regression coefficients and their significance, as well as the fit of the models and how much variance (adjusted r^2) they accounted for. This is described further in the relevant results sections.

Statistical significance was set at $p \leq 0.05$.

7.4 Results

7.4.1 No difference in intramyocellular lipid accumulation between older HIV+ and HIV- individuals

In order to investigate intramyocellular lipid accumulation (IMCL), I initially qualitatively classified individual muscle fibres into one of four groups depending on expression of Bodipy: Bodipy+++ for fibres with very high expression of punctate bodipy-stained granules, then Bodipy++, Bodipy+ and Bodipy- respectively (**Figure 7.4**).

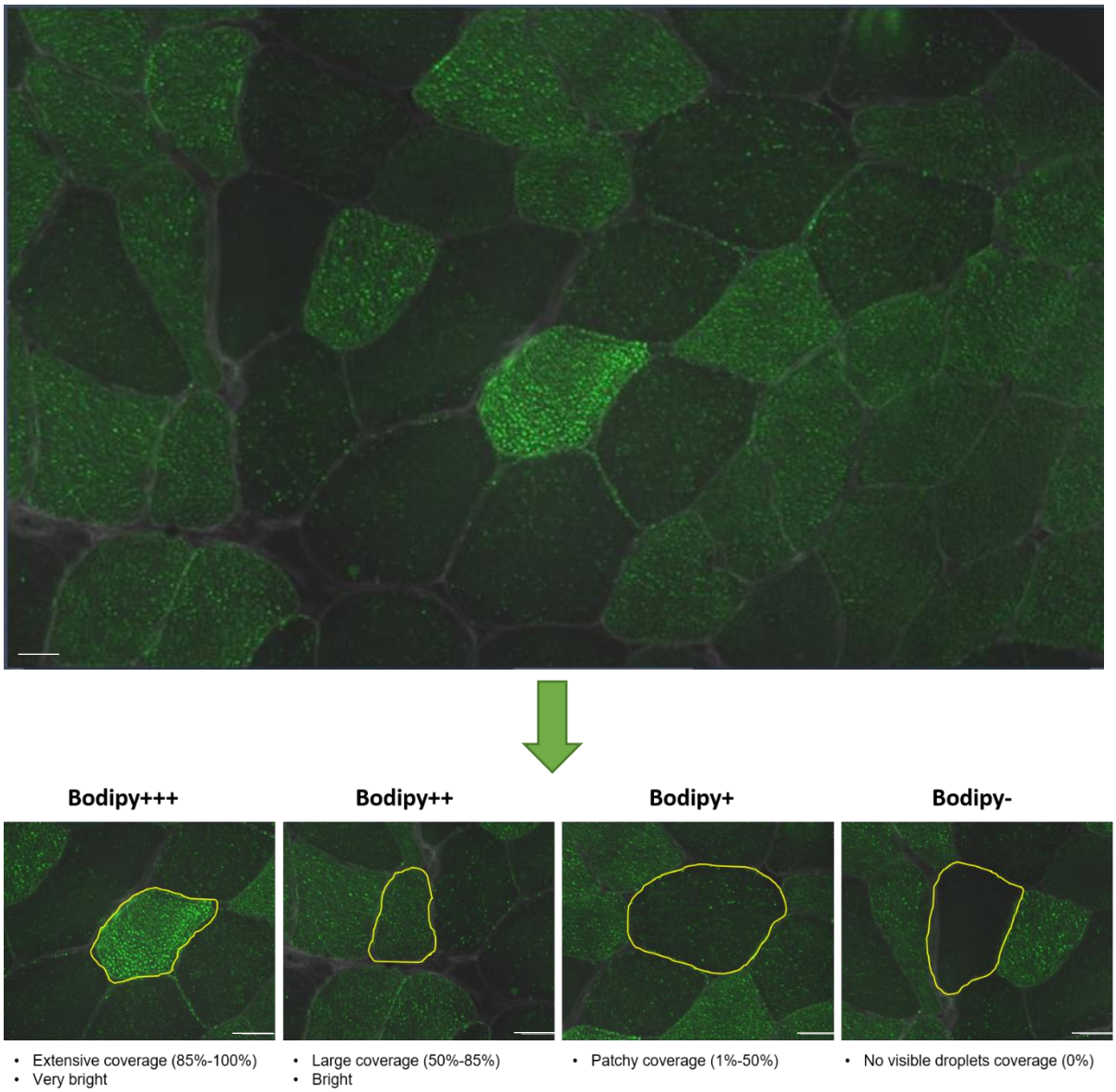

Figure 7.4 – Example fluorescence image depicting the qualitative classification system used to quantify IMCL*. Bodipy+++ fibres display extensive and bright Bodipy staining coverage; Bodipy++ fibres display slightly less coverage with less intense staining; Bodipy+ fibres display patchy coverage with weak staining intensity, and Bodipy- fibres display no Bodipy granules. Scale bars = 50µm.*

The percentage of fibres in each respective Bodipy class was quantified for the individual subjects (n = 45). This data was then subsequently log transformed and normalised to allow the use of parametric tests (**Figure 7.5**).

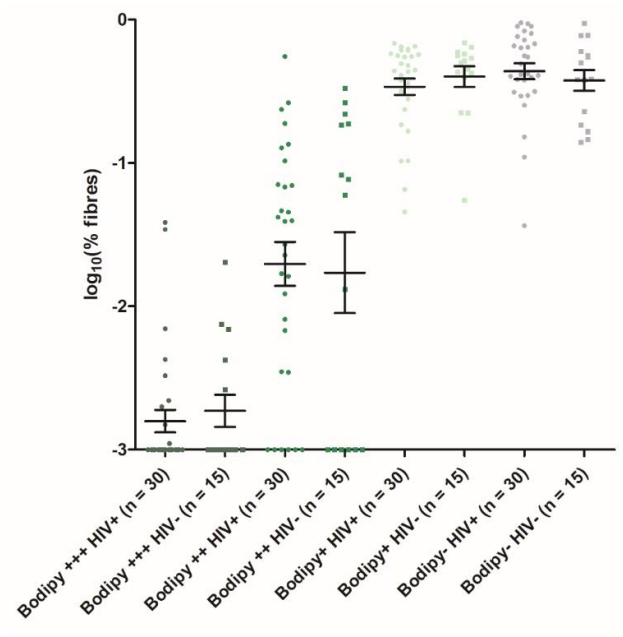

Figure 7.5 – Proportion of fibres with IMCL. *Dot plot (mean ± SEM) representing Log_{10} percentage of Bodipy+++, Bodipy++, Bodipy+ and Bodipy- fibres for both the HIV+ (n = 30) and HIV- (n = 15) individuals. Each dot represents an individual patient.*

There were no significant differences in expression of any of the bodipy categories between the HIV+ and HIV- groups (**unpaired t tests**).

I next grouped the Bodipy+++ and Bodipy++ categories together to generate a classification of abnormal bodipy expression. This was the used as the primary group for compassions – the 'Bodipy abnormal (BodipyAbn)' group.

Here, there was no significant difference in the proportion of BodipyAbn fibres between the HIV+ or HIV- groups (**unpaired t test**) (**Figure 7.6b**), nor the proportion of Bodipy- fibres between the experimental groups (**Figure 7.6c**).

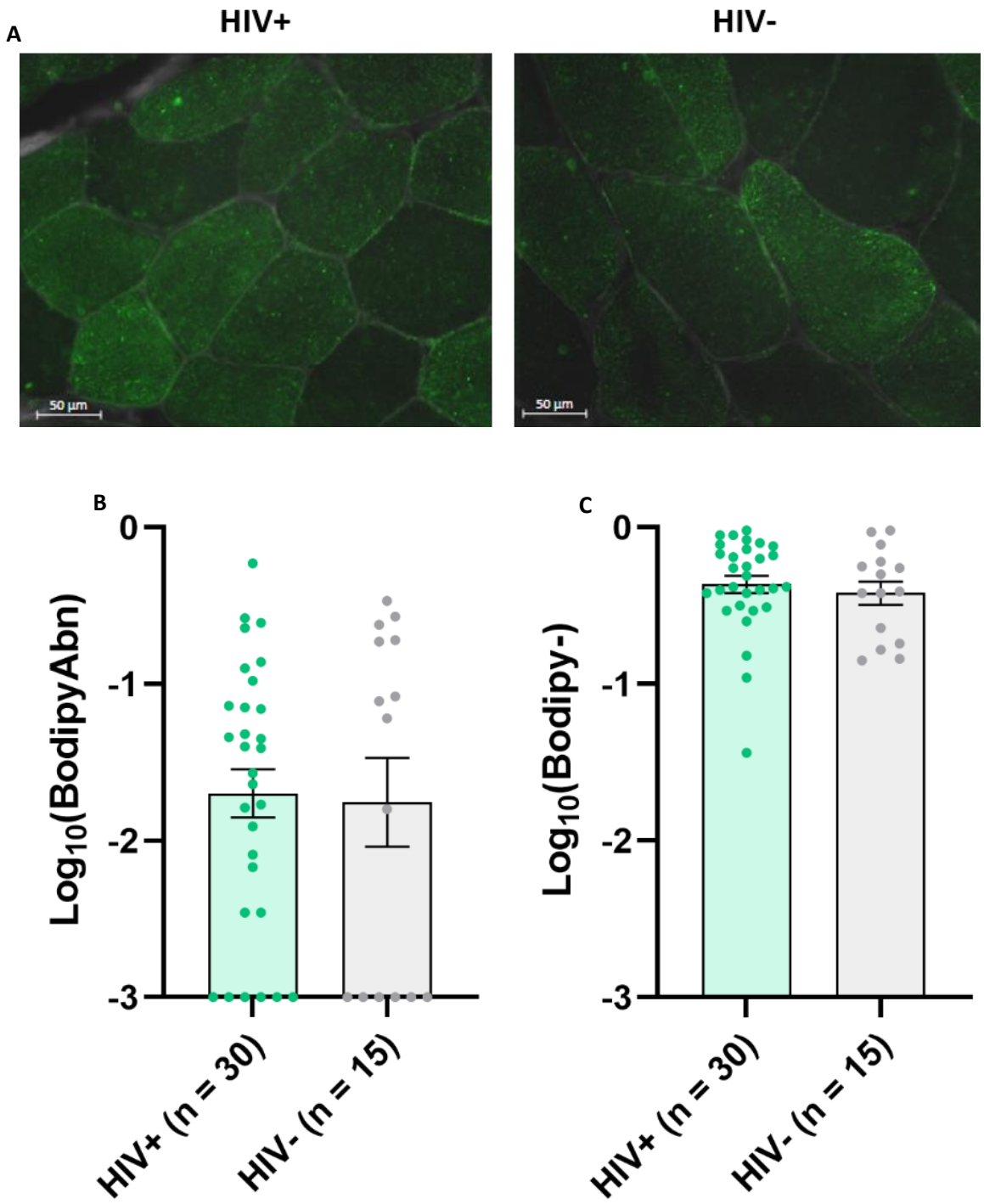

Figure 7.6 – Proportion of BodipyAbn and Bodipy- fibres. (***A***) *Representative images of skeletal muscle sections from a HIV+ and HIV- individual depicting Bodipy (493/503) staining. Scale bar = 50µm; Dot plots (mean ± SEM) depicting (**B**) the log_{10} proportion of BodipyAbn fibres for HIV+ (n = 30) and HIV- (n = 15) individuals, and (**C**) the log_{10} proportion of Bodipy- fibres for HIV+ and HIV- individuals. Each dot represents an individual patient.*

7.4.2 Impact of NRTI and PI use on IMCL in older PLWH

I wanted to investigate whether IMCL was predicted by current exposure to particular ARVs, such as nucleoside reverse transcriptase inhibitors (NRTIs) or protease inhibitors (PIs), as previous studies have demonstrated a link between these classes of ARV and lipodystrophy (Glidden *et al*., 2018; Carr *et al*., 1999; Dragovic *et al*., 2014; Miller *et al.*, 2003; McComsey *et al*., 2016). Herein, HIV+ individuals who had been exposed to mitochondrially toxic NRTIs (didanosine (ddI), zalcitabine (ddC), stavudine (d4T), and zidovudine (AZT)) (n = 11) had a significantly lower proportion of IMCL (defined as BodipyAbn, see above) compared to HIV+ individuals who had not been exposed to those respective NRTIs (n = 19, p = 0.024, **unpaired t-test**) (**Figure 7.7a**). There was no significant difference in IMCL between HIV+ individuals who had been exposed to PIs (n = 9) and those who had not (n = 21) (**Figure 7.7b**).

Of the mitochondrially-toxic NRTIs, AZT and d4T have in particular been shown to be associated with fat redistribution elsewhere in the body (Moyle *et al*., 2006; Jones *et al*., 2005; Domingo *et al*., 2014; Dragovic *et al*., 2014; de Waal *et al*., 2013). I therefore tested the association between current/previous exposure to AZT and/or d4T and IMCL. Interestingly, I found that HIV+ subjects exposed to AZT/d4T (n = 10) had a significantly lower proportion of BodipyAbn fibres than the HIV+ subjects not exposed to AZT/d4T (n = 20; p = 0.027, **unpaired t test**) (**Figure 7.7c**).

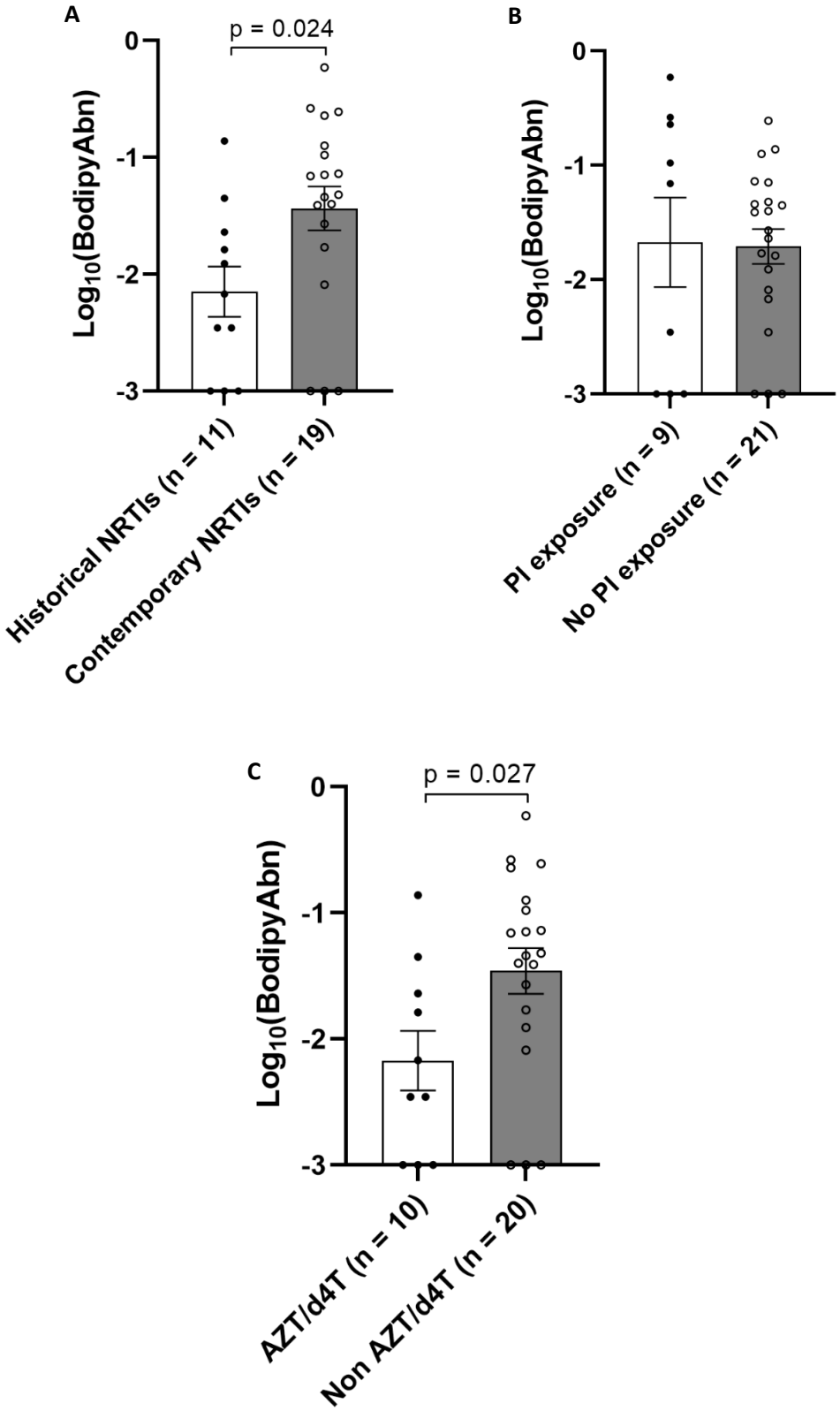

Figure 7.7 – Proportion of BodipyAbn fibres and ART regimens. *Dot plots (mean ± SEM) depicting the log_{10} proportion of BodipyAbn fibres in (**A**) HIV+ individuals who have been exposed to mitochondrially-toxic NNRTIs (n = 11) and those who have not (n = 19), (**B**) HIV+ individuals who have been exposed to PIs (n = 9) and those who have not (n = 21), and (**C**) HIV+ individuals who have been exposed to either AZT or d4T (n = 10) against those who have not (n = 20). Each dot represents an individual patient.*

7.4.3 Predictors of intramyocellular lipid accumulation in older PLWH

Next, I wanted to investigate whether IMCL was significantly predicted by any of the clinical, HIV-related, body composition, or lifestyle factors assessed as part of the MAGMA study, in older HIV+ individuals (n = 30).

7.4.3.1 Clinical predictors of IMCL

Here, I performed unadjusted bivariate linear regression analysis and Fisher's exact tests in order to assess whether any clinical, HIV-related, or lifestyle factors significantly predicted increased IMCL, with results depicted in **Table 7.1**.

Notably, greater IMCL was not significantly predicted by any of the clinical, lifestyle or body composition factors such as age (**Figure 7.8a**), BMI (**Figure 7.8b**), percentage lean mass (**Figure 7.8c**), or percentage fat mass (**Figure 7.8d**) in older PLWH (n = 30) (**Pearson's correlation and Fisher's exact test**) (**Table 7.1**).

Interestingly, none of the HIV-related factors such as CD4 count or duration on ART significantly predicted increased IMCL.

	IMCL HIV+ (n = 30)	
	r	***p***
Age	0.017	0.93
BMI (kg/m^2)	0.19	0.31
Waist circumference (cm)	-0.026	0.89
# Comorbidities	0.30	0.11
# Medications	0.12	0.52
Polypharmacy*	-	0.67
% Fat mass	-0.23	0.22
% Lean mass	0.23	0.22
Months since diagnosis	0.090	0.64
Months on ART	-0.043	0.82
Months untreated	0.13	0.50
CD4 count (copies/µl)	0.21	0.28
Smokers*	-	0.93
Alcohol drinkers*	-	0.77
Recreational drug use*	-	0.80

Table 7.1 – Clinical predictors of IMCL in older PLWH. *Table depicting the associations between proportional Log_{10}(BodipyAbn) and various clinical factors. Linear regression and correlation analysis was performed by Pearson's correlation. * = ordinal data in which individuals were stratified by yes/no and differences determined by Fisher's exact test.*

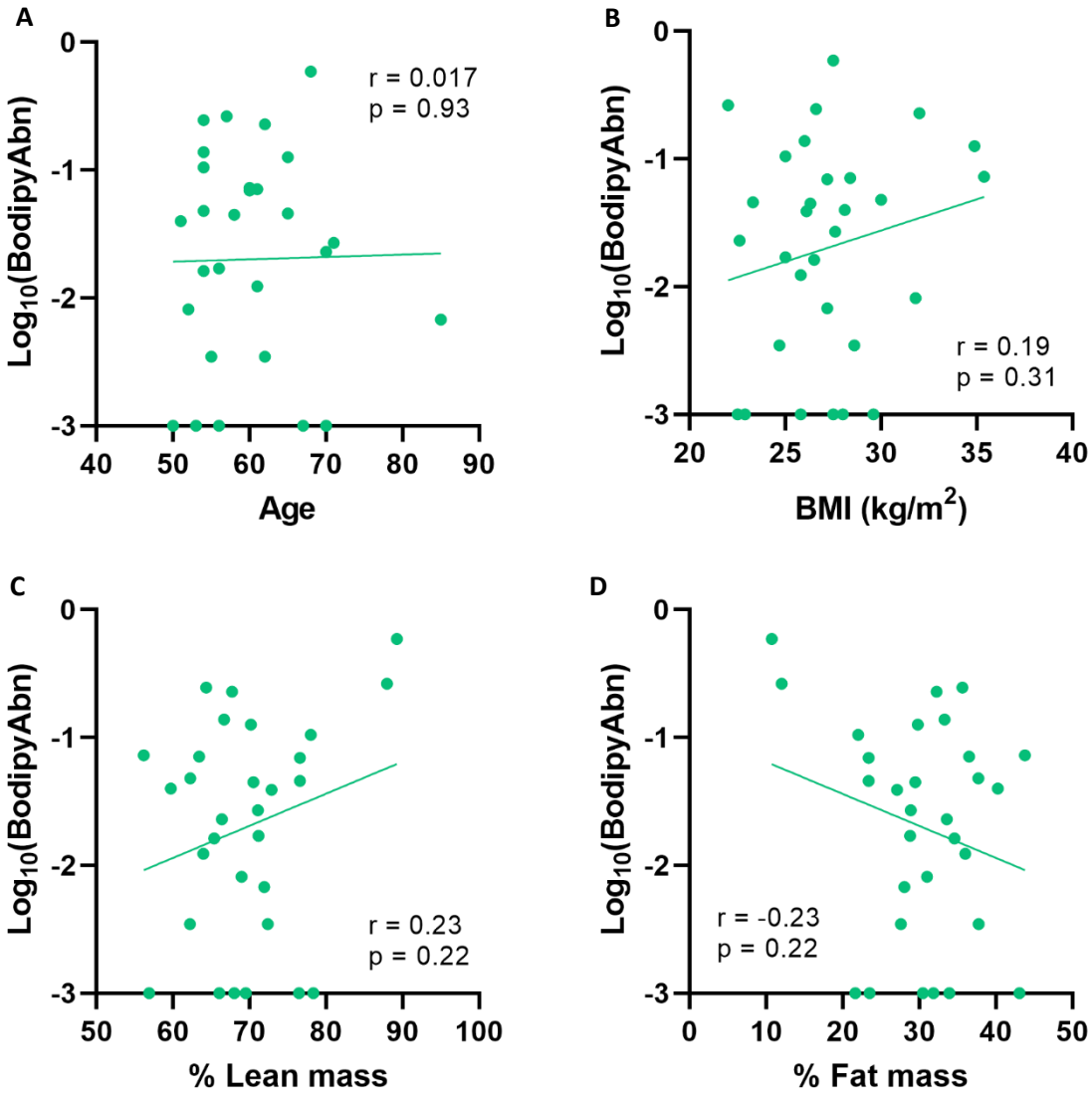

Figure 7.8 – Clinical determinants of IMCL in older PLWH. *Scatter plots depicting the linear regression analysis (Pearson's correlation) between log_{10}(BodipyAbn) and (**A**) age, (**B**) BMI (kg/m^2), (**C**) percentage lean mass, and (**D**) percentage fat mass in older PLWH (n = 30).*

7.4.3.2 Physical determents of IMCL

Next, I performed linear regression analysis to determine if any of the physical parameters such as FFP score or grip strength predicted IMCL in older PLWH (**Table 7.2**).

As such, there were no statistically significant associations between IMCL and any of the respective factors (**Pearson's and Spearman's correlation**) (**Figure 7.9a-e**).

	IMCL	
	HIV+ (n = 30)	
	r	***p***
FFP score^	0.23	0.22
SPPB score^	0.085	0.65
MET score^	-0.25	0.19
Grip strength (kg)	-0.24	0.21
ASMI (kg/m^2)	0.21	0.26

Table 7.2 – Physical factors predicting IMCL in older PLWH. *Table depicting the associations between proportional Log_{10}(BodipyAbn) and various factors. Linear regression and correlation analysis was determined by Pearson's correlation for normally distributed data and Spearman's correlation for non-normally distributed data (denoted by ^).*

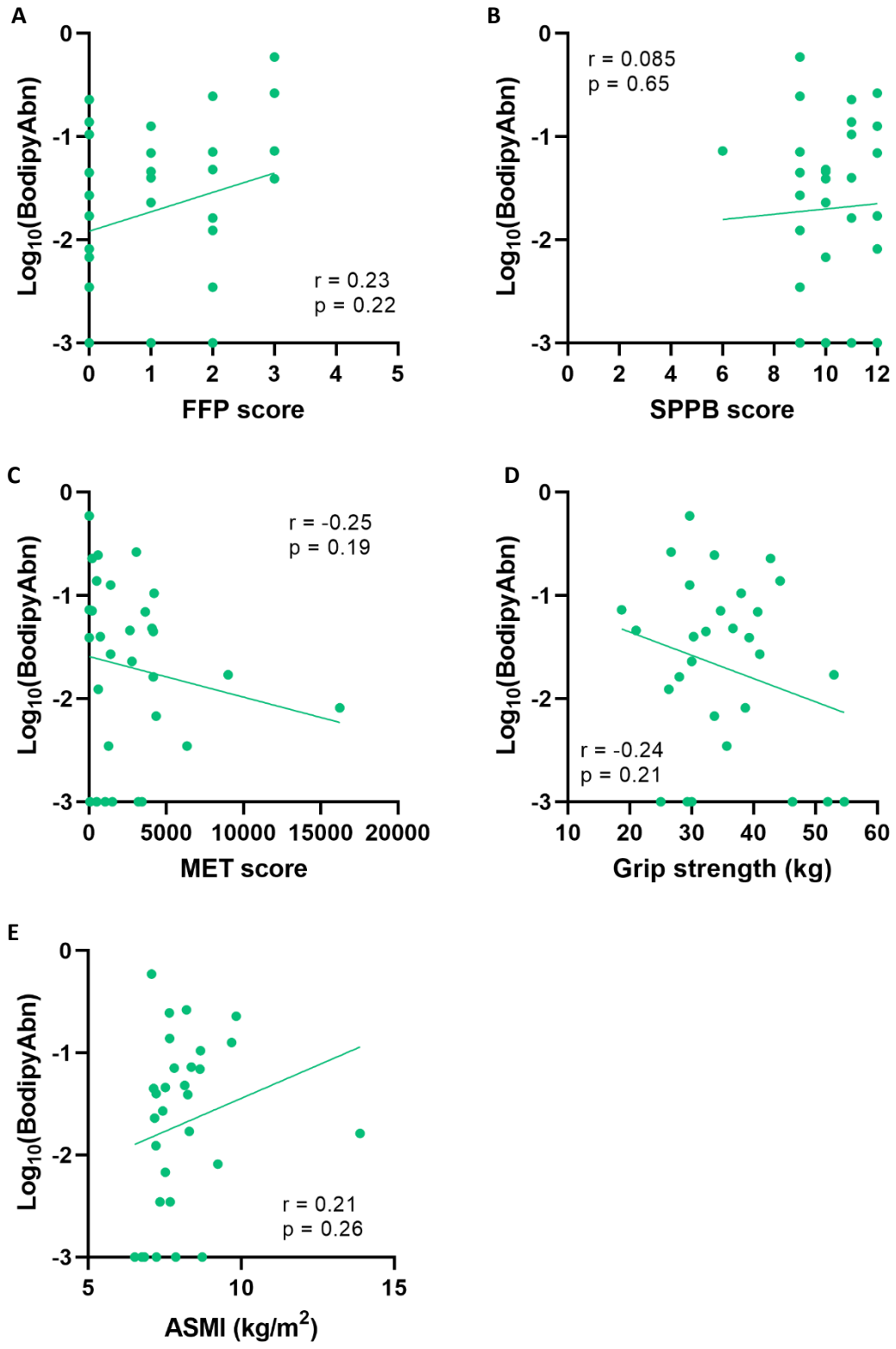

Figure 7.9 – Physical determinants of IMCL. *Scatter plots depicting the linear regression between log_{10}(BodipyAbn) and (**A**) FFP score, (**B**) SPPB score, (**C**) MET score, (**D**) grip strength (kg), and (**E**) ASMI (kg/m^2) in older PLWH (n = 30). Pearson's correlation was performed for parametric data (**D** and **E**), and spearman's correlation was performed on non-parametric data (**A**, **B**, **C**).*

7.4.3.3 Pathophysiological skeletal muscle determinants of IMCL in older PLWH

Finally, unadjusted linear regression analysis between IMCL and results from the various other muscle pathophysiology assessments such as Pax7$^+$ SC prevalence and fibrosis was undertaken in order to investigate pathophysiological determinants of IMCL in older PLWH (full data for these parameters are presented later in this chapter).

Again, there was no statistically significant associations between these factors in the HIV+ individuals (n = 30 (**Pearson's correlation**) (**Table 7.3**).

	IMCL	
	HIV+ (n = 30)	
	r	***p***
Type I %	0.040	0.83
Type IIa %	-0.27	0.15
Type IIx %	0.35	0.059
Fibre CSA (µm^2)	0.046	0.81
Log$_{10}$(Pax7$^+$ SC)	-0.026	0.89
Log$_{10}$(% Fibrosis)	-0.13	0.49
Log$_{10}$(Lipofuscin CSA)$^+$	-0.008	0.97
Log$_{10}$(Lipofuscin frequency)$^+$	0.10	0.62
Regenerated fibres	0.060	0.76
Degenerated fibres	-0.067	0.73

Table 7.3 – Pathophysiological skeletal muscle determinants of IMCL*. Table depicting the associations between proportional Log$_{10}$(BodipyAbn) and various skeletal muscle pathophysiological factors. Linear regression and correlation analysis was determined by Pearson's correlation. + = data missing from 1 patient.*

7.4.4 IMCL in older frail and sarcopenic PLWH

After demonstrating that there was no significant difference in IMCL between older HIV+ and HIV- individuals, I stratified the HIV+ group into whether they were frail (n = 4), prefrail (n = 15), or robust (n = 11), as well as whether they were classified as sarcopenic (n = 5), presarcopenic (n = 6), or non-sarcopenic (n = 19) and compared IMCL between the respective groups.

Here, although IMCL was numerically higher in frail PLWH, there was no significant difference in IMCL between the frail, prefrail and robust HIV+ groups (p = 0.090, **one-way ANOVA**) (**Figure 7.10a**), or between the sarcopenic, presarcopenic and non-sarcopenic groups (p = 0.22) (**Figure 7.10b**).

However, to increase the power to detect differences, the robust and prefrail groups were pooled together (n = 26), and IMCL was compared against frail individuals (n = 4). Here, it was demonstrated that frail PLWH had significantly higher IMCL compared to robust/prefrail PLWH (p = 0.027, **unpaired t test**) (**Figure 7.10c**).

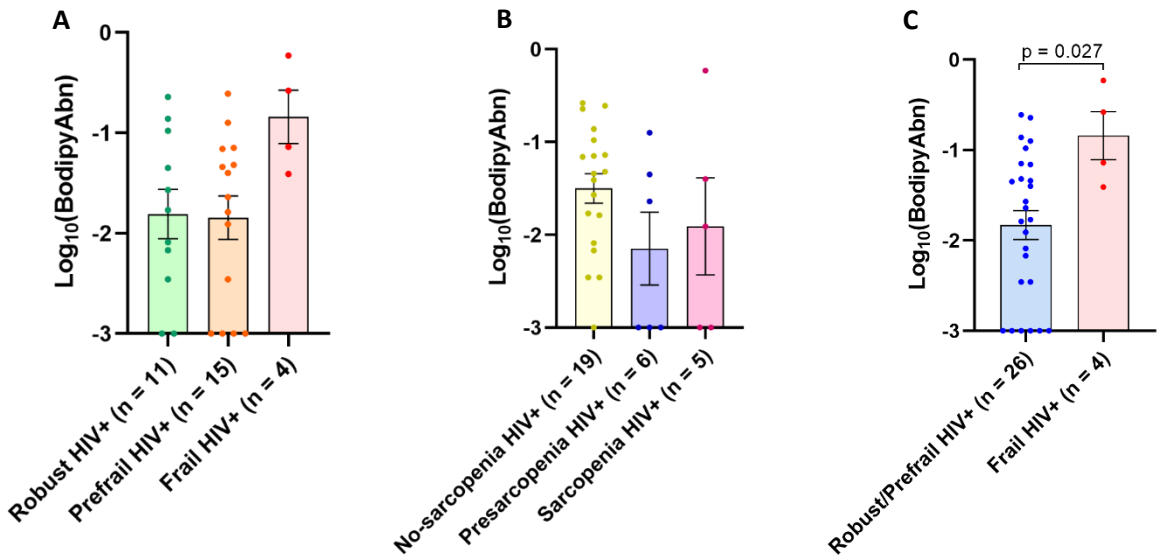

Figure 7.10 – IMCL differences in frailty and sarcopenia classification. *Dot plots (mean ± SEM) depicting proportional Log_{10}(BodipyAbn) differences between (**A**) frail (n = 4), prefrail (n = 15), and robust PLWH (n = 11) and (**B**) sarcopenic (n = 5), presarcopenic (n = 6), and non-sarcopenic (n = 19) PLWH. (**C**) Frail PLWH (n = 4) had a statistically significant greater level of IMCL compared to robust/prefrail PLWH (n = 26). Each dot represents an individual patient.*

Next, in order to overcome limitations regarding the small prevalence of frail and sarcopenic HIV+, in combination with the fact that prefrailty and presarcopenia is more physiologically related to frailty and sarcopenia than being robust or non-sarcopenic, HIV+ patients classified as prefrail (n = 15) were grouped with the frail HIV+ individuals (n = 4), and HIV+ patients classified as presarcopenic (n = 6) were grouped with sarcopenic PLWH (n = 5). Here, I determined if there were differences in IMCL between the respective groups and robust HIV+ (n = 11) and non-sarcopenic HIV+ individuals (n = 19).

Notably, there was no significant difference in IMCL between frail/prefrail PLWH (n = 19) and robust PLWH (n = 11) (p = 0.60, **unpaired t test**) (**Figure 7.11a**) or between sarcopenic/presarcopenic PLWH (n = 11) and non-sarcopenic PLWH (n = 19) (p = 0.093) (**Figure 7.11b**).

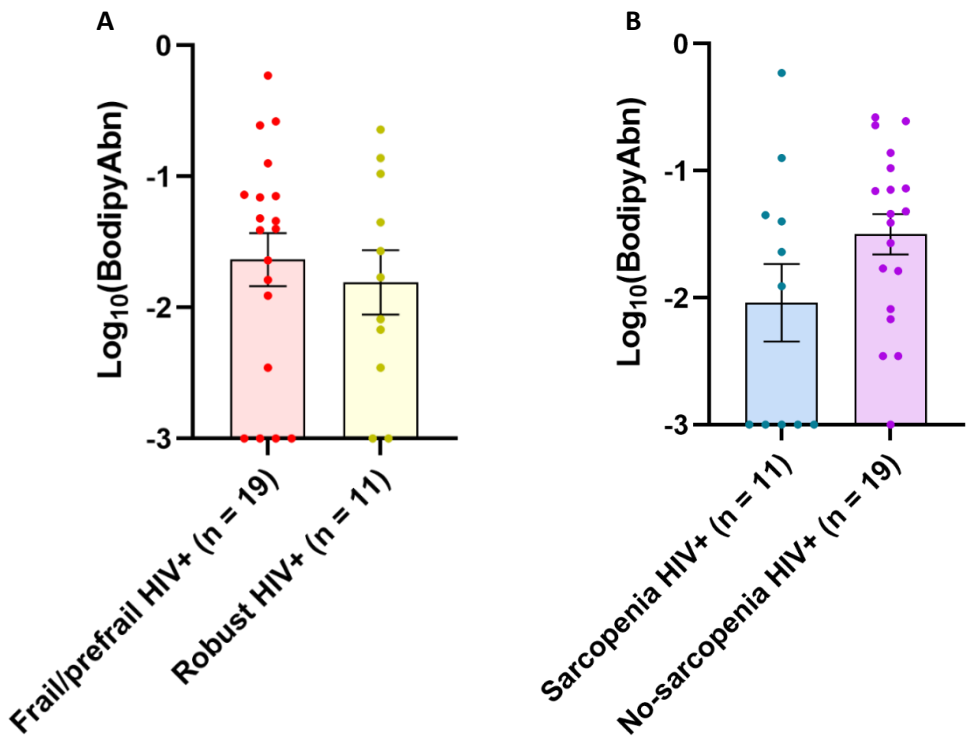

Figure 7.11 – IMCL in frail/prefrail older PLWH and sarcopenic/presarcopenic PLWH*. Dot plots (mean ± SEM) depicting proportional Log$_{10}$(BodipyAbn) in (**A**) frail/prefrail HIV+ (n = 19) and robust HIV+ (n = 11), as well as (**B**) sarcopenic/presarcopenic HIV+ (n = 11) and non-sarcopenic HIV+ (n = 19). There were no significant differences between any of the respective experimental groups, determined by unpaired t tests. Each dot represents an individual patient.*

7.4.5 No difference in Pax7⁺ satellite cell prevalence between older PLWH and HIV- individuals

In order to quantify the frequency of undifferentiated satellite cells (SCs) in skeletal muscle of our subjects, and subsequently investigate the role of SCs in the pathophysiology of frailty and sarcopenia in older PLWH, I stained the 10µm skeletal muscle sections with a duplex immunofluorescence assay with a nuclei marker (DAPI) and SC marker (Pax7) (**Figure 7.12**).

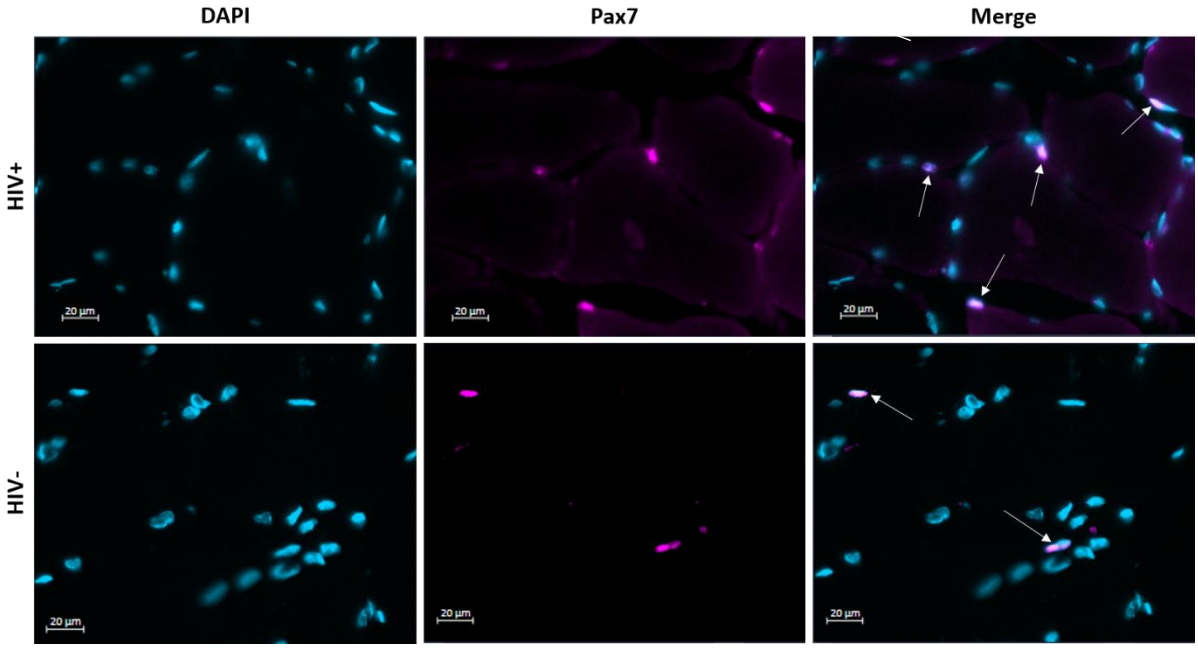

Figure 7.12 – Example fluorescence image of Pax7⁺ satellite cells*. 10µm skeletal muscle sections from HIV+ and HIV- individuals were stained with immunofluorescence markers for nuclei (DAPI) and quiescent SCs (Pax7). Pax7⁺ SCs were confirmed by co-localisation with a nuclei (e.g. white arrows). Scale bar = 20µm.*

A Pax7⁺ SC was determined by the strong staining intensity in the Pax7 channel and co-localisation with the nuclear marker DAPI (white arrows in **Figure 7.12**).

The number of Pax7⁺ SCs and the total number of fibres were quantified, allowing us to determine the frequency of Pax7⁺ SCs per 100 fibres. In order to normalise the distribution of the data these values were then log transformed.

Notably, there was no significant difference in the frequency of Pax7⁺ SCs per 100 fibres between the HIV+ (n = 30) and HIV- (n = 15) groups (**unpaired t test**) (**Figure 7.13**).

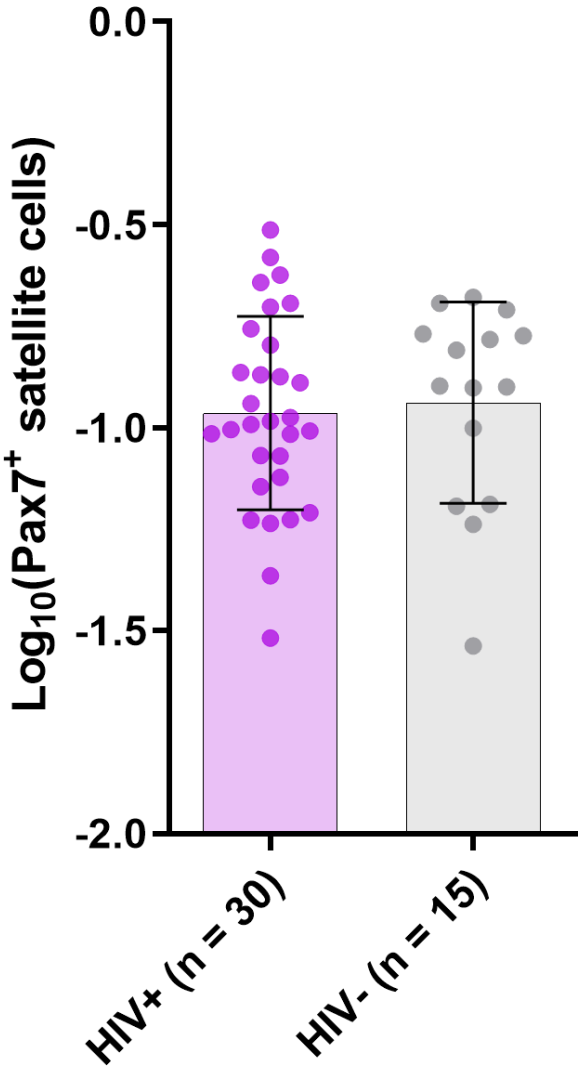

Figure 7.13 – No difference in Pax7⁺ satellite cell frequency per 100 fibres between the HIV+ and HIV- groups. *Dot plot (mean ± SEM) depicting the log_{10}(frequency of Pax7⁺ satellite cells per 100 fibres) for both the HIV+ (n = 30) and HIV- (n = 15) groups. Each dot represents an individual patient.*

7.4.6 Predictors of Pax7$^+$ satellite cell abundance

Next, I wanted to investigate whether the frequency of Pax7$^+$ SCs was significantly predicted by any HIV-related or clinical factors, as well as body composition, environmental factors, and other skeletal muscle pathophysiological factors. To do this I performed linear regression analyses and unpaired t test analysis between the $\log_{10}$-transformed frequency of Pax7$^+$ SCs per 100 fibres and the respective comparator factors. Pearson's correlation was performed on normally distributed data sets whilst Spearman's correlation was performed on non-normally distributed data sets.

7.4.6.1 Clinical predictors of Pax7$^+$ SC prevalence in older PLWH

Notably, Pax7$^+$ SC prevalence was not significantly predicted by any clinical, body composition, HIV-related, or environmental factors (**Table 7.4**). This included age (**Figure 7.14a**), BMI (**Figure 7.14b**), percentage lean mass (**Figure 7.14c**) or percentage fat mass (**Figure 7.14d**) (**Pearson's correlation**).

	Pax7 SC prevalence HIV+ (n = 30)	
	r	***p***
Age	0.15	0.43
BMI (kg/m^2)	0.30	0.88
Waist circumference (cm)	0.087	0.65
# Comorbidities	0.022	0.91
# Medications	0.067	0.73
Polypharmacy*	-	0.90
% Fat mass	-0.07	0.72
% Lean mass	0.07	0.72
Months since diagnosis	0.24	0.20
Months on ART	0.15	0.43
Months untreated	0.15	0.42
CD4 count (copies/µl)	0.08	0.69
Smokers*	-	0.27
Alcohol drinkers*	-	0.23
Recreational drug use*	-	0.80

Table 7.4 – Clinical predictors of Pax7$^+$ SC prevalence in older PLWH. *Table depicting the associations between Log_{10}(Pax7$^+$ SCs per 100 fibres) and various clinical factors. Linear regression and correlation analysis was determined by Pearson's correlation. * = ordinal data in which individuals were stratified by yes/no and differences determined by unpaired t tests.*

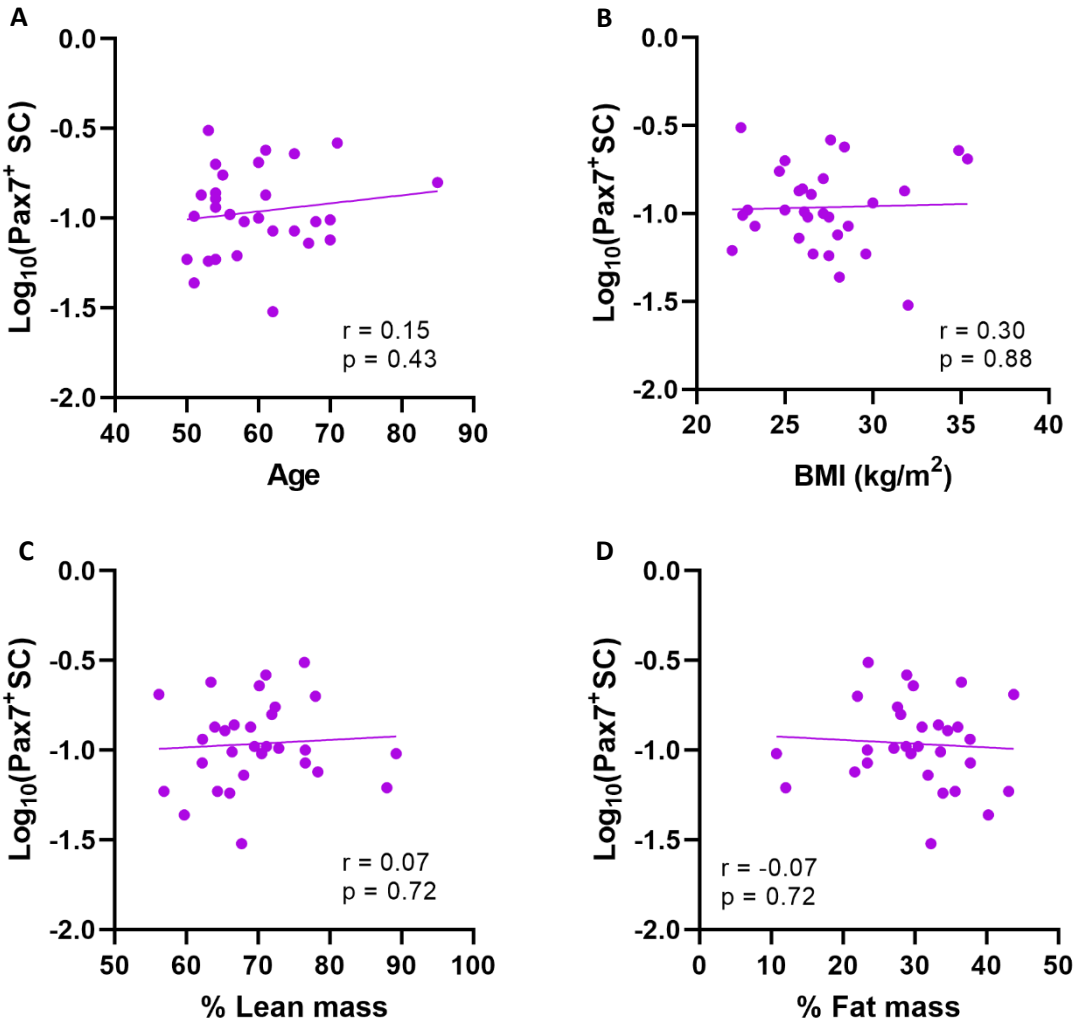

Figure 7.14 – Clinical determinants of Pax7⁺ SC prevalence. *Scatter plots depicting the linear regression (Pearson's correlation) between proportional Log_{10}(Pax7⁺ SCs per 100 fibres) and (**A**) age, (**B**) BMI (kg/m²), (**C**) percentage lean mass, and (**D**) percentage fat mass in older PLWH (n = 30).*

7.4.6.2 Physical determinants of Pax7⁺ SCs in older PLWH

Next, in order to determine whether there were any physical determinants of the prevalence of Pax7⁺ SCs, I performed unadjusted linear regression analyses between Pax7⁺ SC prevalence and physical parameters. Again, there was no significant associations between these factors and Pax7⁺ SC prevalence (**Table 7.5/Figure 7.15**).

	Pax7 SC prevalence	
	HIV+ (n = 30)	
	r	***p***
FFP score^	-0.066	0.73
SPPB score^	-0.25	0.19
MET score^	0.059	0.76
Grip strength (kg)	0.076	0.69
ASMI (kg/m^2)	0.019	0.92

Table 7.5 – Physical factors predicting Pax7⁺ SC prevalence in older PLWH. *Table depicting the associations between proportional Log_{10}(Pax7⁺ SCs per 100 fibres) and various factors. Linear regression and correlation was determined by Pearson's correlation for normalised data and Spearman's correlation for non-normalised data (denoted by ^).*

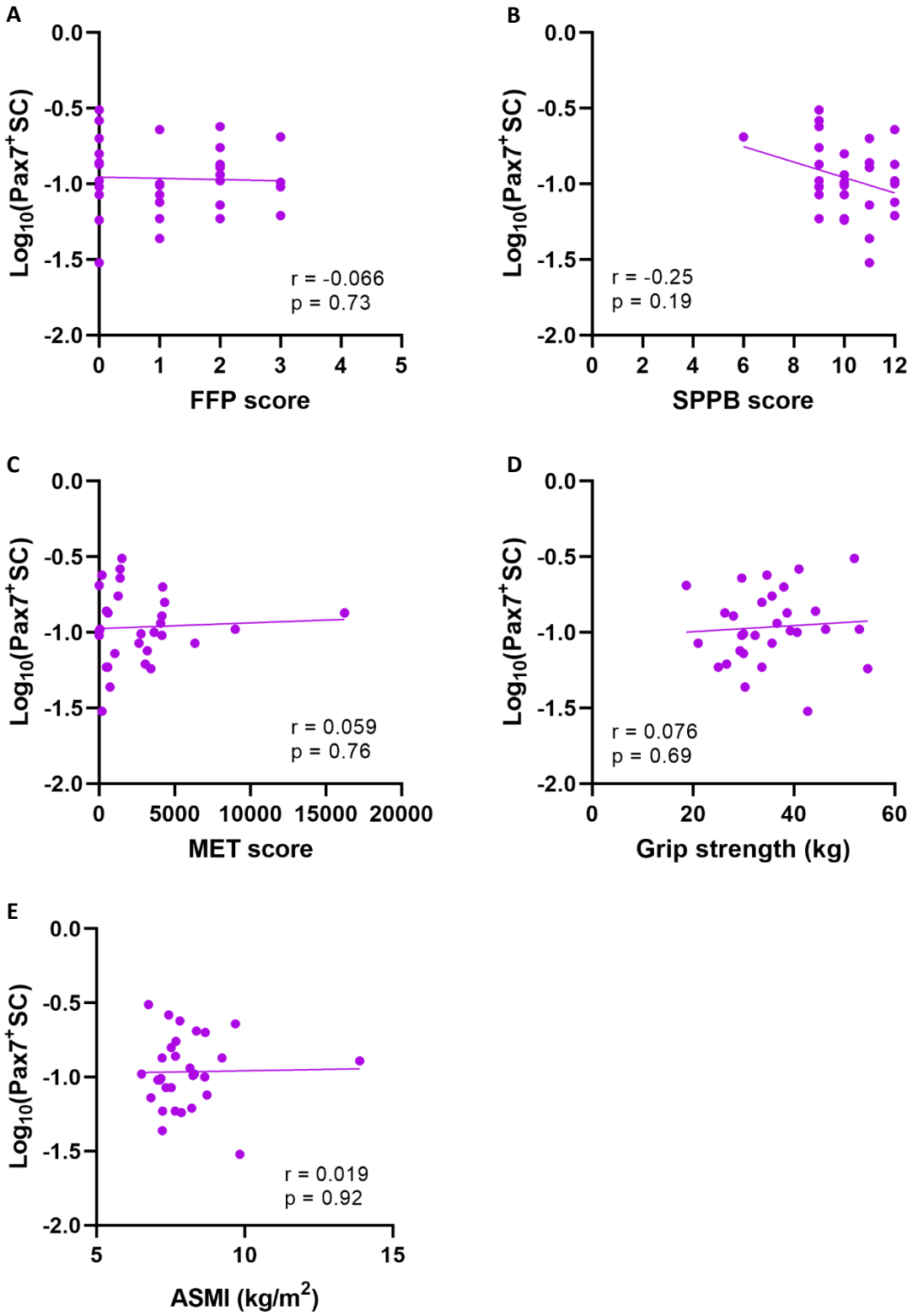

Figure 7.15 – Physical determinants of Pax7⁺ SC prevalence. *Scatter plots depicting the linear regression between Log_{10}(Pax7⁺ SCs per 100 fibres) and (**A**) FFP score, (**B**) SPPB score, (**C**) MET score, (**D**) grip strength (kg), and (**E**) ASMI (kg/m²) in older PLWH (n = 30). Pearson's correlation was performed for parametric data (**D** and **E**), and spearman's correlation was performed on non-parametric data (**A**, **B**, **C**).*

7.4.6.3 Pathophysiological skeletal muscle determinants of Pax7$^+$ SC prevalence in older PLWH

Finally, linear regression analyses was performed in order to determine whether Pax7$^+$ SC prevalence was predicted by other pathophysiological skeletal muscle factors (full data for these parameters are presented later in this chapter) (**Table 7.6**).

Interestingly, Pax7$^+$ SC prevalence was significantly predicted by skeletal muscle fibrosis (r = 0.57; *p* = 0.001, **Pearson's correlation**) (**Figure 7.16a**) and a greater proportion of regenerated fibres (r = 0.52; *p* = 0.003) (**Figure 7.16b**) in older PLWH (n = 30).

As the prevalence of Pax7$^+$ SCs is linked with age, multivariate linear regression models were developed with Pax7$^+$ SCs as the dependant variable, and age as well as either fibrosis or percentage of regenerated fibres as the independent variables.

Here, multivariate linear regression confirmed that the association between Pax7$^+$ SC prevalence and fibrosis was independent of the effect of age (unstandardised regression coefficient = 0.62; *p* = 0.002, **multivariate linear regression**) (**Table 7.6**). Indeed, the overall model fit was statistically significant (*p* = 0.005), and was predictive of roughly a third of the variation in Pax7$^+$ SC prevalence (r^2 = 0.32).

In addition, multivariable linear regression analysis also confirmed that the association between Pax7$^+$ SC prevalence and the proportion of regenerated fibres was independent of the effect of age (unstandardised regression coefficient = 0.013; *p* = 0.005, **multivariate linear regression**) (**Table 7.6**). The overall model fit was statistically significant (*p* = 0.012), although only predictive of a small amount of variation in Pax7$^+$ SC prevalence (r^2 = 0.28).

	Pax7 SC prevalence		
	HIV+ (n = 30)		
	r	*p*	Age-adjusted *p*
Type I %	-0.072	0.71	-
Type IIa %	-0.017	0.93	-
Type IIx %	0.19	0.32	-
Fibre CSA (μm^2)	0.18	0.34	-
Log_{10}(BodipyAbn)	-0.026	0.89	-
Log_{10}(% Fibrosis)	**0.57**	**0.001**	**0.002**
Log_{10}(Lipofuscin CSA)$^+$	0.052	0.79	-
Log_{10}(Lipofuscin frequency)$^+$	0.10	0.60	-
Regenerated fibres	**0.52**	**0.003**	**0.005**
Degenerated fibres	0.031	0.87	-

Table 7.6 – Skeletal muscle determinants of Pax7$^+$ SC prevalence. *Table depicting the associations between proportional Log_{10}(Pax7$^+$ SC per 100 fibres) and various skeletal muscle pathophysiological factors. Linear regression and correlation analysis was determined by Pearson's correlation. Multivariate linear regression with adjustment for age was performed for determinants significantly associated with Pax7$^+$ SC prevalence through univariate regression analyses. Statistically significant associations are bold. + = data missing from 1 patient.*

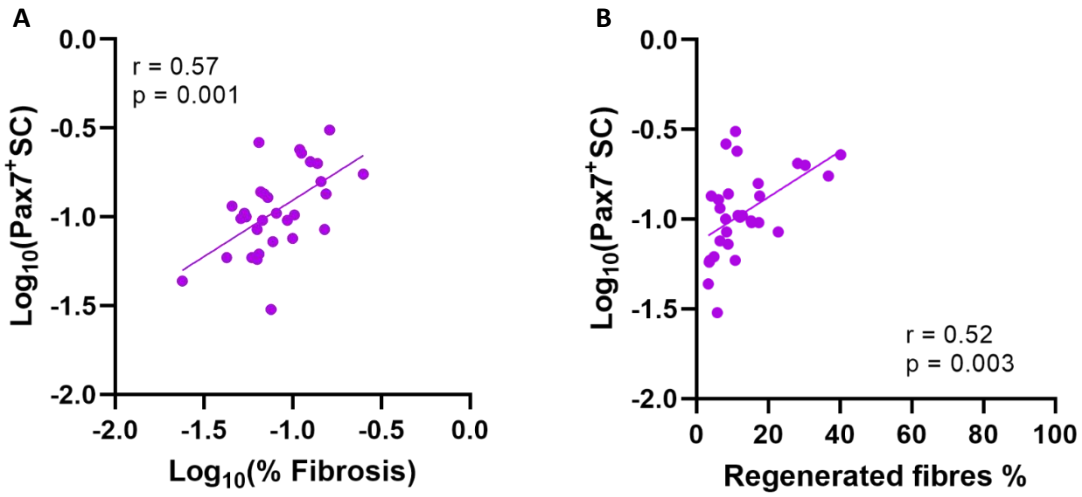

Figure 7.16 – Pathophysiological determinants of Pax7$^+$ SC prevalence. *Scatter plots depicting linear regression analysis (Pearson's correlation) between proportional Log_{10}(Pax7$^+$ SCs per 100 fibres) and (**A**) Log10(% fibrosis), and (**B**) percentage regenerated fibres. Each dot represents an individual patient.*

7.4.7 Pax7⁺ satellite cell prevalence in frail and sarcopenic older PLWH

To investigate differences in quiescent Pax7⁺ SC prevalence between PLWH in the respective frailty and sarcopenic classification groups, the HIV+ individuals (n = 30) were stratified into frail (n = 4), prefrail (n = 15), and robust (n = 11) groups, as well as sarcopenic (n = 5), presarcopenic (n = 6), and non-sarcopenic (n = 19) groups, and the prevalence of $\log_{10}$(Pax7⁺ SCs per 100 fibres) was compared.

Here, there was no significant difference in the prevalence of Pax7⁺ SCs between the frail, prefrail and robust HIV+ groups (p = 0.78, **one-way ANOVA**) (**Figure 7.17a**). In addition, there was also no significant difference between the sarcopenia, presarcopenic and no-sarcopenia HIV+ groups (p = 0.22) (**Figure 7.17b**).

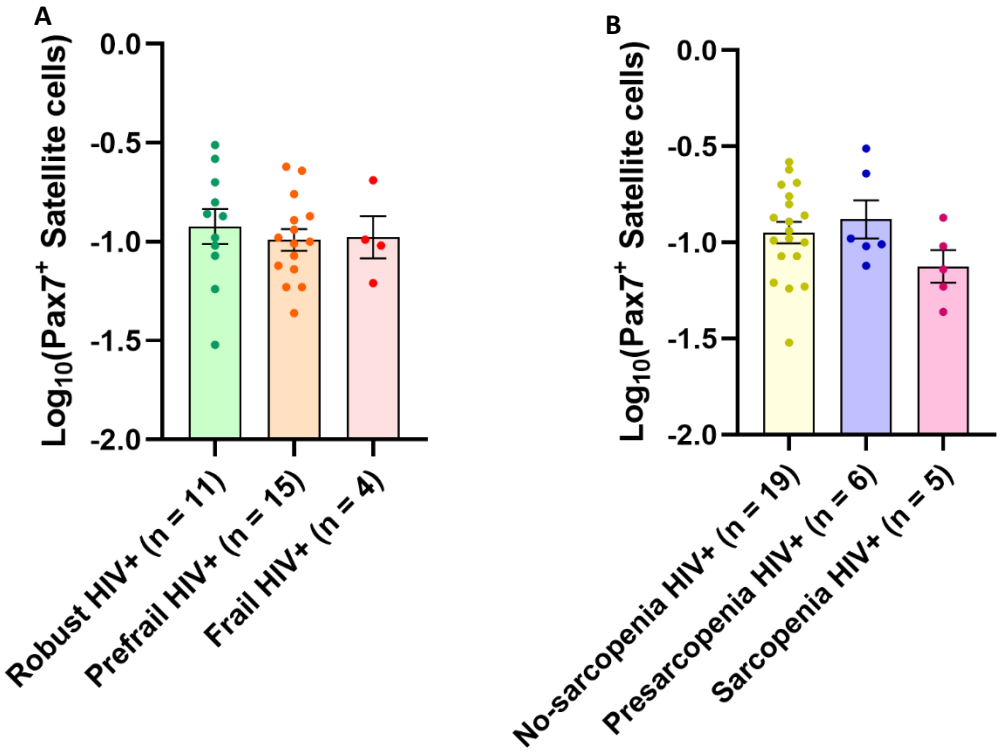

Figure 7.17 – Quiescent Pax7⁺ SC prevalence in frail and sarcopenic PLWH*. Dot plots (mean ± SEM) showing no significant difference in $\log_{10}$(Pax7⁺ SCs per 100 fibres) between HIV+ (**A**) frail (n = 4), prefrail (n = 15) and robust (n = 11) individuals, or (**B**) sarcopenic (n = 5), presarcopenic (n = 6) and non-sarcopenic (n = 19) individuals. Each dot represents an individual patient.*

Next, the HIV+ group (n = 30) was stratified into frail/prefrail HIV+ (n = 19) and sarcopenic/presarcopenic HIV+ (n = 11) groups in order to assess whether quiescent satellite cell prevalence was altered in these groups compared to robust HIV+ (n = 11) and non-sarcopenic PLWH (n = 19) respectively.

Importantly, there was no statistically significant difference in the proportion of Pax7$^+$ SCs between frail/prefrail PLWH and robust PLWH (p = 0.48, **unpaired t test**) (**Figure 7.18a**). In addition, there was also no significant difference in proportional Pax7$^+$ SC prevalence between sarcopenic/presarcopenic PLWH and non-sarcopenic PLWH (p = 0.65) (**Figure 7.18b**).

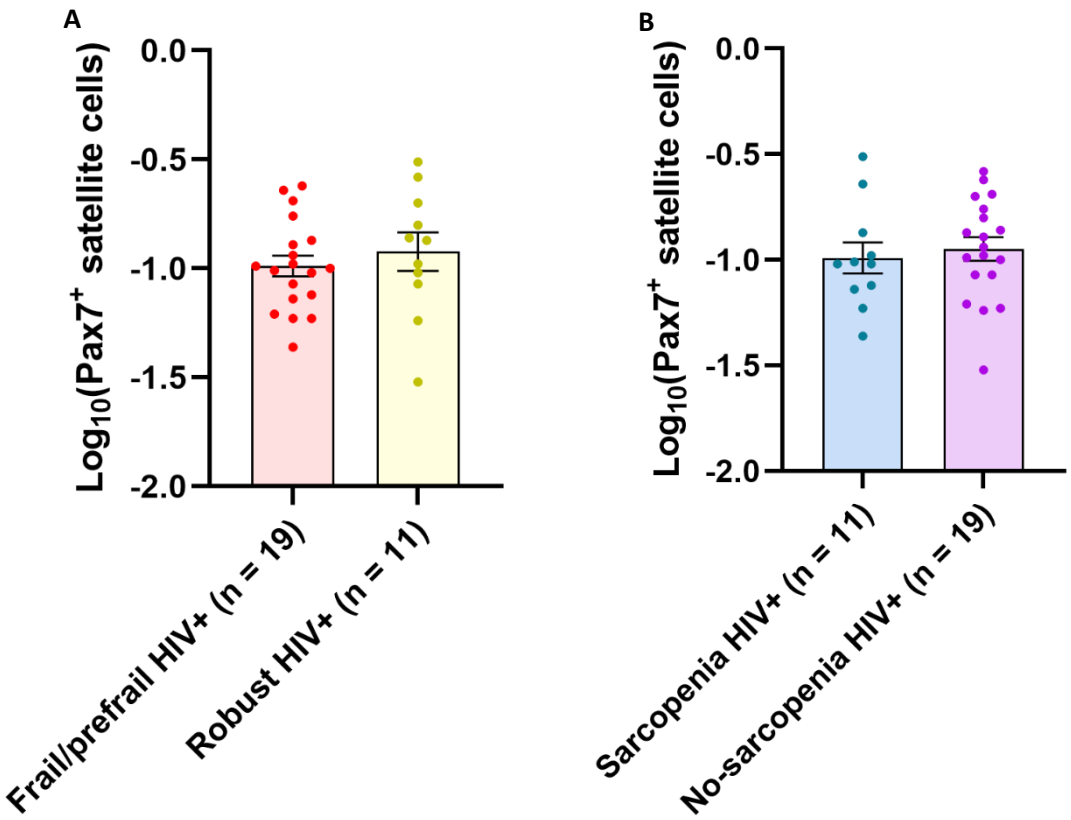

Figure 7.18 – Pax7$^+$ SC prevalence in adverse ageing phenotypes in older PLWH. *Dot plots (mean ± SEM) depicting no significant difference in log_{10}(Pax7$^+$ SCs) between (**A**) frail/prefrail PLWH (n = 19) and robust PLWH (n = 11), and between (**B**) sarcopenic/presarcopenic PLWH (n = 11) and non-sarcopenic PLWH (n = 19). Each dot represents an individual patient.*

7.4.8 No difference in fibre type proportions or fibre CSA between older HIV+ and HIV- individuals

Using a multiplex immunofluorescence assay I quantified the proportions of fibre types I, IIa, and IIx, as well as the average fibre CSA (μm^2) of the respective fibre types in 10µm cryo-sections (n = 45) (**Figure 7.19**).

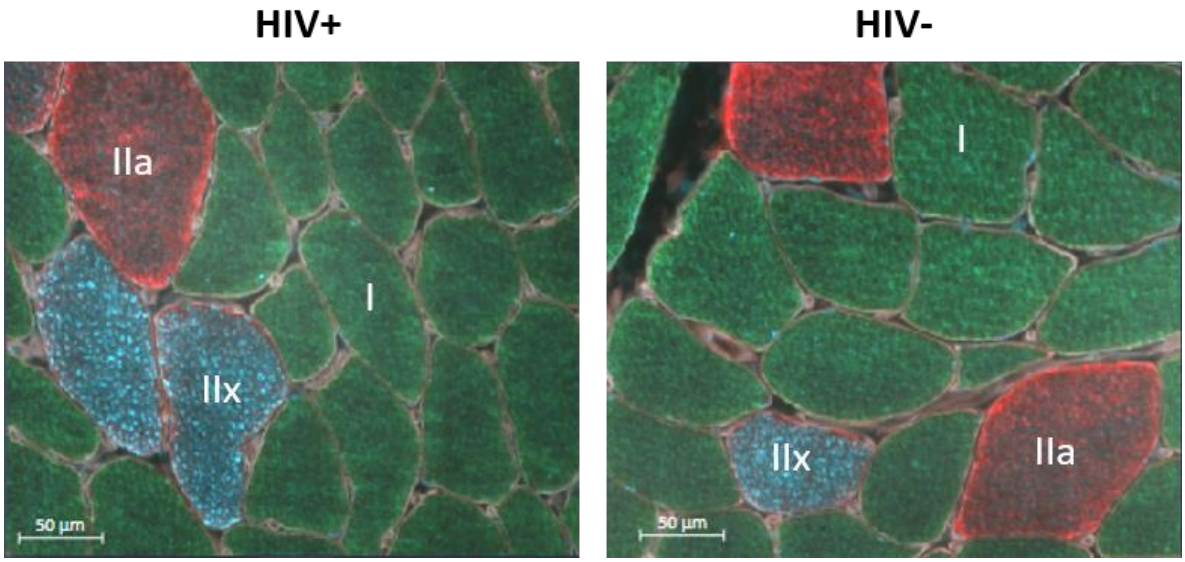

Figure 7.19 – Example fluorescence image of cryosections stained with fibre type markers. *Representative images of skeletal muscle sections from HIV+ and HIV- individuals stained with fibre type markers. Each skeletal muscle section was stained with markers to distinguish type I (BA-F8), type IIa (SC-71), type IIx (6H1) as well as a myofibre boundary marker (laminin). As depicted in the figure, type I fibres are green, type IIa are red, and type IIx are blue. Scale bar = 50µm.*

Here, the percentage of the three fibre types was significantly different in HIV+ individuals (n = 30; $p < 0.0001$, **one-way ANOVA**), with the percentage of type I fibres being significantly greater than that of both type IIa ($p = 0.0001$, **Tukey's multiple comparison**) and type IIx fibres ($p < 0.0001$), as well as the percentage of type IIa fibres being significantly greater than the percentage of type IIx fibres ($p < 0.0006$). However, there was no significant difference in the proportions of any of the respective fibre types between HIV+ and HIV- individuals (**unpaired t tests**) (**Figure 7.20a**).

In addition, the average fibre CSA was significantly different between the three fibres types in HIV+ individuals (n = 30; $p < 0.0001$, **one-way ANOVA**), with the fibre CSA of type IIa fibres being significantly greater than type I fibres ($p = 0.0006$, **Tukey's multiple comparison**). However, there was no significant difference in the average fibre CSA of the three fibre types individually, or when grouped together, between the HIV+ and HIV- individuals (**unpaired t tests**) (**Figure 7.20b**).

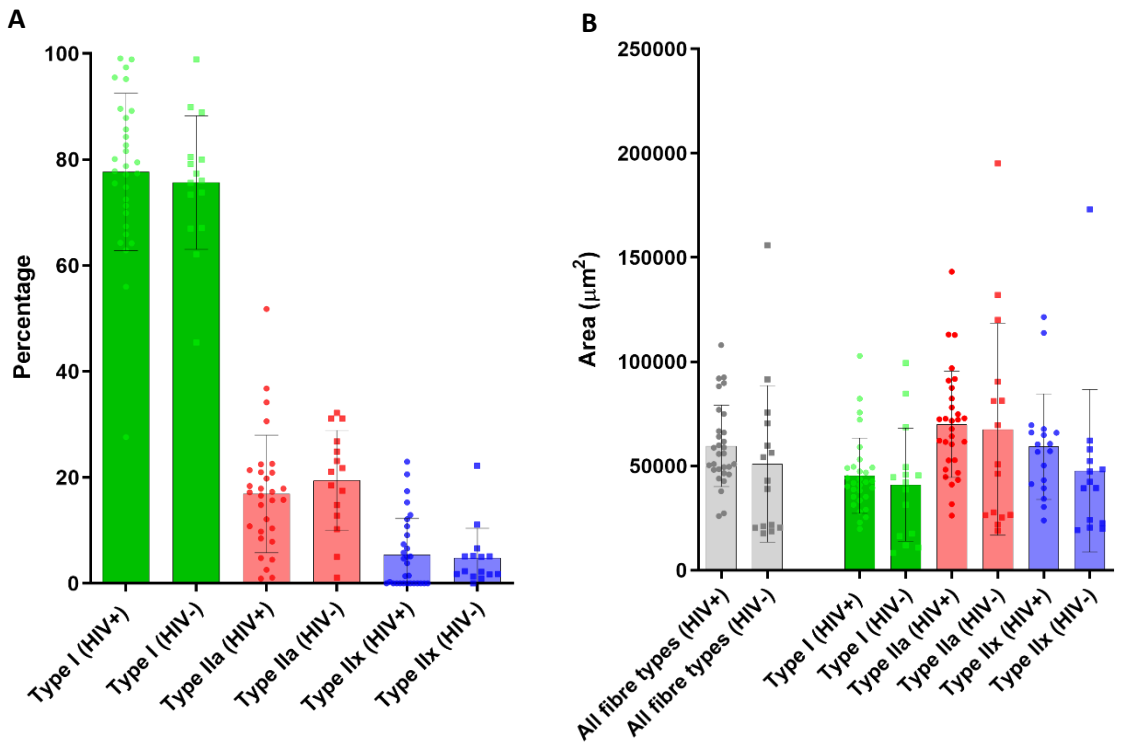

Figure 7.20 – No difference in fibre type proportions or fibre CSA between the HIV+ and HIV- groups*. Dot plots (mean ± SEM) representing (**A**) the proportion of type I, IIa, and IIx fibres for the HIV+ (n = 30) and HIV- (n = 15) patients. There was no significant difference in the proportion of the respective fibre types between the two groups, although there was a significantly higher proportion of type I fibres in both the HIV+ and HIV- groups compared to type IIa and type IIx fibres. (**B**) The average CSA (µm²) of each fibre type for both the HIV+ and HIV- groups, as well as the average CSA of all fibre types combined for each individual (grey bars). Dots represent induvial patients.*

7.4.9 Determinants of fibre type proportions and average fibre CSA

Here, I wanted to investigate whether the prevalence of fibre types I, IIa, IIx and average fibre CSA (μm^2) was predicted by any clinical, HIV-related, environmental, or body composition factors, as well as other skeletal muscle pathophysiological factors such as fibrosis or IMCL.

7.4.9.1 Clinical determinants of fibre type proportions and fibre CSA in older PLWH

Of the clinical factors and HIV-related parameters, an increased percentage of type IIx fibres was significantly predicted by a greater number of comorbidities in older PLWH (n = 30; r = 0.52; *p* = 0.003, **Pearson's correlation**) (**Figure 7.23e**). In addition, a greater number of medications also significantly predicted a higher proportion of type IIx fibres (r = 0.46; *p* = 0.011) (**Figure 7.23f**).

The percentage of type I fibres was also significantly lower in HIV+ individuals with polypharmacy (n = 19; *p* = 0.038, **unpaired t test**) (**Table 7.7**).

Hence, as the proportion of fibre type IIx is known to decline with age, and the prevalence of prescribed medications and comorbidities generally increases with age, I generated multivariate linear regression models with the percentage fibre type IIx as the dependant variable, and age as well as either number of medications, or number of comorbidities as the independent variables. Here, multivariate linear regression confirmed that the association between the proportion of type IIx fibres and number of comorbidities was independent of the effect of age (unstandardised regression coefficient = 3.33; *p* = 0.004, **multivariate linear regression**) (**Table 7.7**). The model fit was significant (*p* = 0.014), although it only explained a reasonably small amount of variation in the proportion of type IIx fibres (r^2 = 0.27).

Similarly, multivariate linear regression confirmed that the association between the proportion of type IIx fibres and number of medications was independent of age (unstandardised regression coefficient = 1.07; *p* = 0.011, **multivariate linear regression**) (**Table 7.7**). Again, the model fit was statistically significant (*p* = 0.035), although it only predicted a small amount of variation in the proportion of type IIx fibres (r^2 = 0.22).

There were no significant associations between clinical determinants and fibre type IIa proportions (**Figure 7.22**), or fibre CSA (**Figure 7.24**).

	Type I		Type IIa		Type IIx			Fibre CSA	
	HIV+ (n = 30)		HIV+ (n = 30)		HIV+ (n = 30)			HIV+ (n = 30)	
	r	*p*	*r*	*p*	r	*p*	Age-adjusted *p*	r	*p*
Age	0.055	0.77	-0.11	0.55	0.065	0.74	-	0.052	0.79
BMI (kg/m²)	-0.20	0.30	0.11	0.57	0.26	0.17	-	0.06	0.75
Waist circumference (cm)	-0.25	0.18	0.24	0.21	0.16	0.39	-	0.096	0.61
# Comorbidities	-0.29	0.12	0.070	0.71	**0.52**	**0.003**	**0.004**	-0.022	0.91
# Medications	-0.31	0.094	0.14	0.47	**0.46**	**0.011**	**0.011**	-0.24	0.20
Polypharmacy*	-	**0.038**	-	0.10	-	0.070	-	-	0.19
% Fat mass	-0.055	0.77	0.13	0.50	-0.085	0.66	-	-0.031	0.87
% Lean mass	0.055	0.77	-0.13	0.50	0.085	0.66	-	0.031	0.87
Months since diagnosis	-0.21	0.26	0.083	0.66	0.33	0.076	-	0.071	0.71
Months on ART	-0.041	0.83	0	0.99	0.092	0.63	-	0.001	0.99
Months untreated	-0.21	0.26	0.095	0.62	0.30	0.10	-	0.069	0.72
CD4 count (copies/µl)	-0.047	0.81	-0.007	0.97	0.12	0.56	-	-0.15	0.44
Smokers*	-	0.45	-	0.77	-	0.77	-	-	0.24
Alcohol drinkers*	-	0.76	-	0.91	-	0.91	-	-	0.62
Recreational drug use*	-	0.98	-	0.90	-	0.90	-	-	0.90

Table 7.7 – Clinical predictors of fibre type proportion and fibre CSA in older PLWH. *Table depicting the associations between proportional fibre types as well as average fibre CSA (µm²) and various clinical factors. Linear regression and correlation analysis was determined by Pearson's correlation. * = ordinal data in which individuals were stratified by yes/no and differences determined by unpaired t tests.*

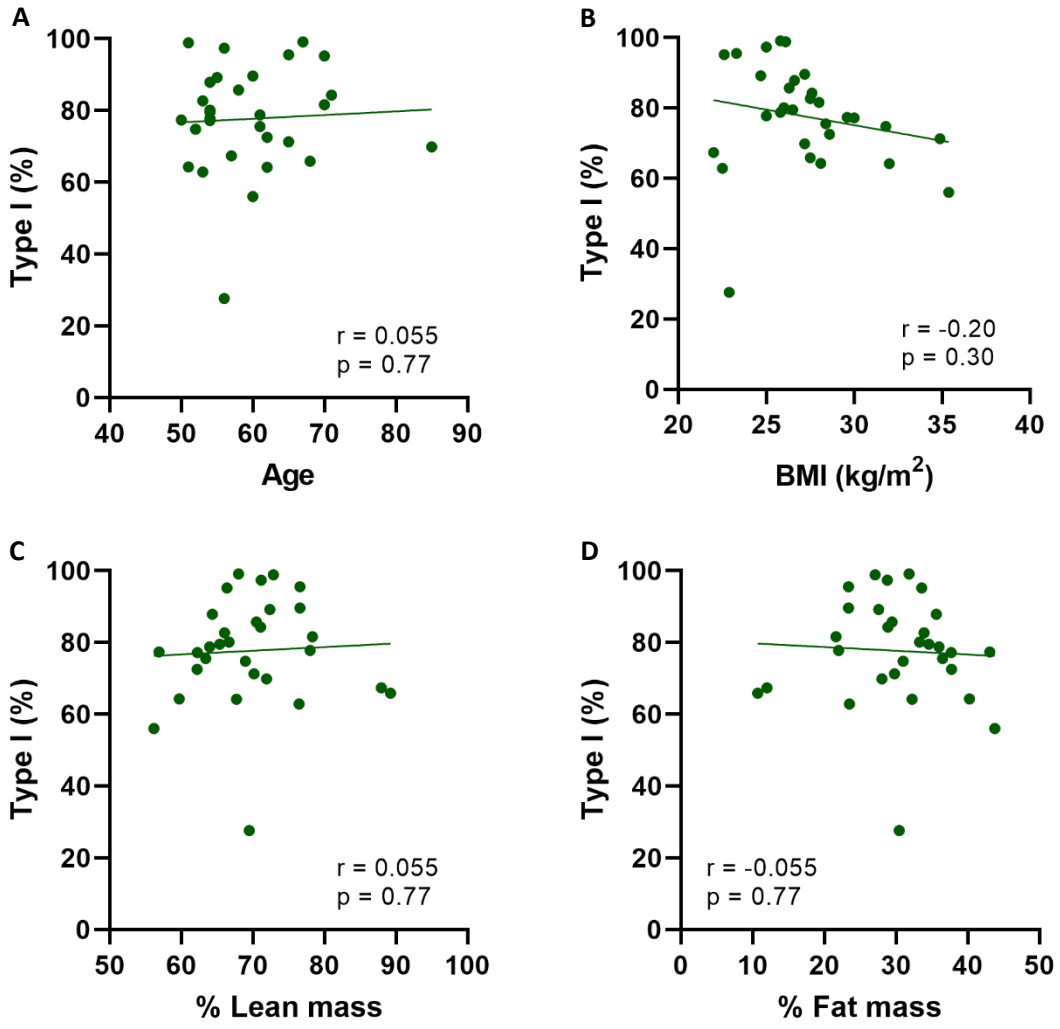

Figure 7.21 – Clinical determinants of fibre type I prevalence*. Scatter plots depicting the linear regression (Pearson's correlation) between the percentage of type I fibres and (**A**) age, (**B**) BMI (kg/m^2), (**C**) percentage lean mass, and (**D**) percentage fat mass in older PLWH (n = 30).*

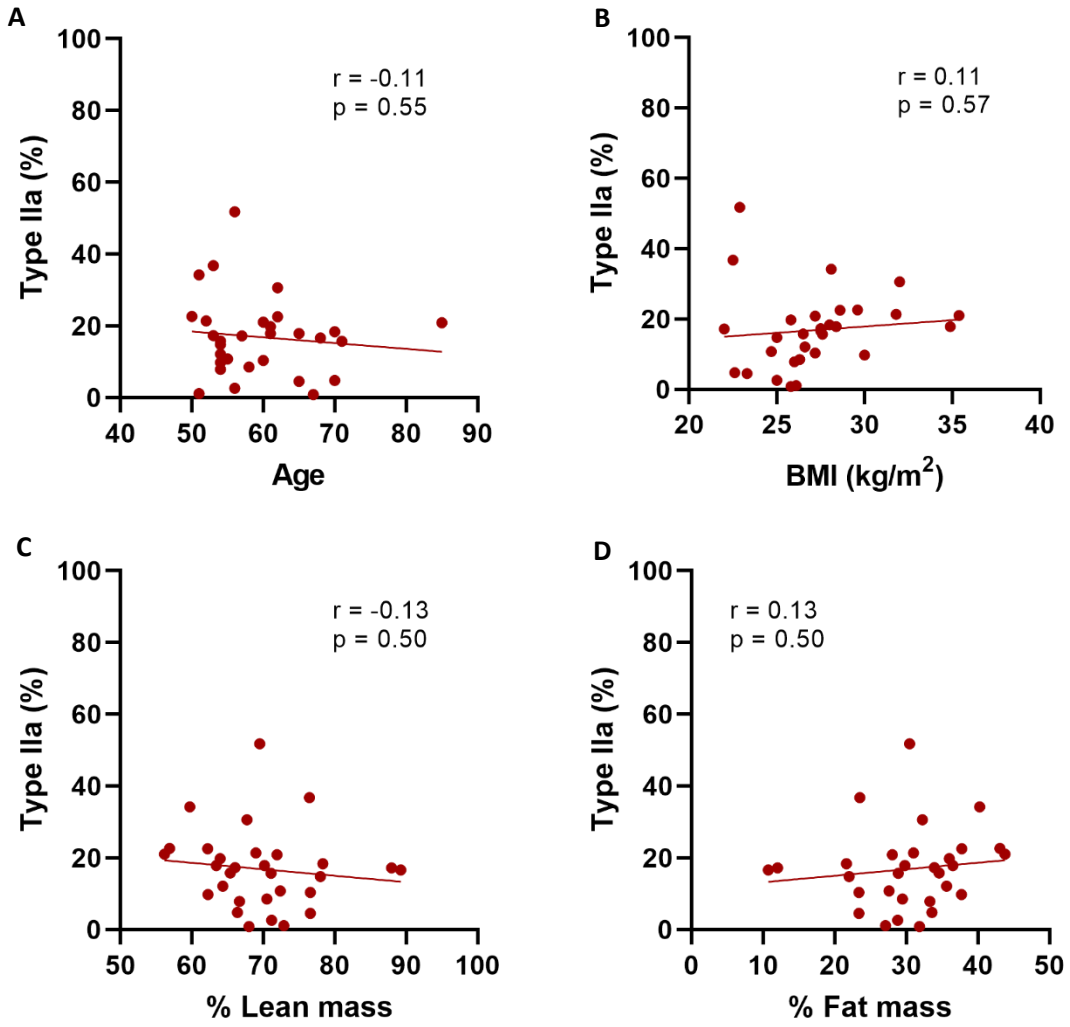

Figure 7.22 – Clinical determinants of fibre type IIa prevalence. *Scatter plots depicting the linear regression (Pearson's correlation) between the percentage of type IIa fibres and (**A**) age, (**B**) BMI (kg/m²), (**C**) percentage lean mass, and (**D**) percentage fat mass in older PLWH (n = 30).*

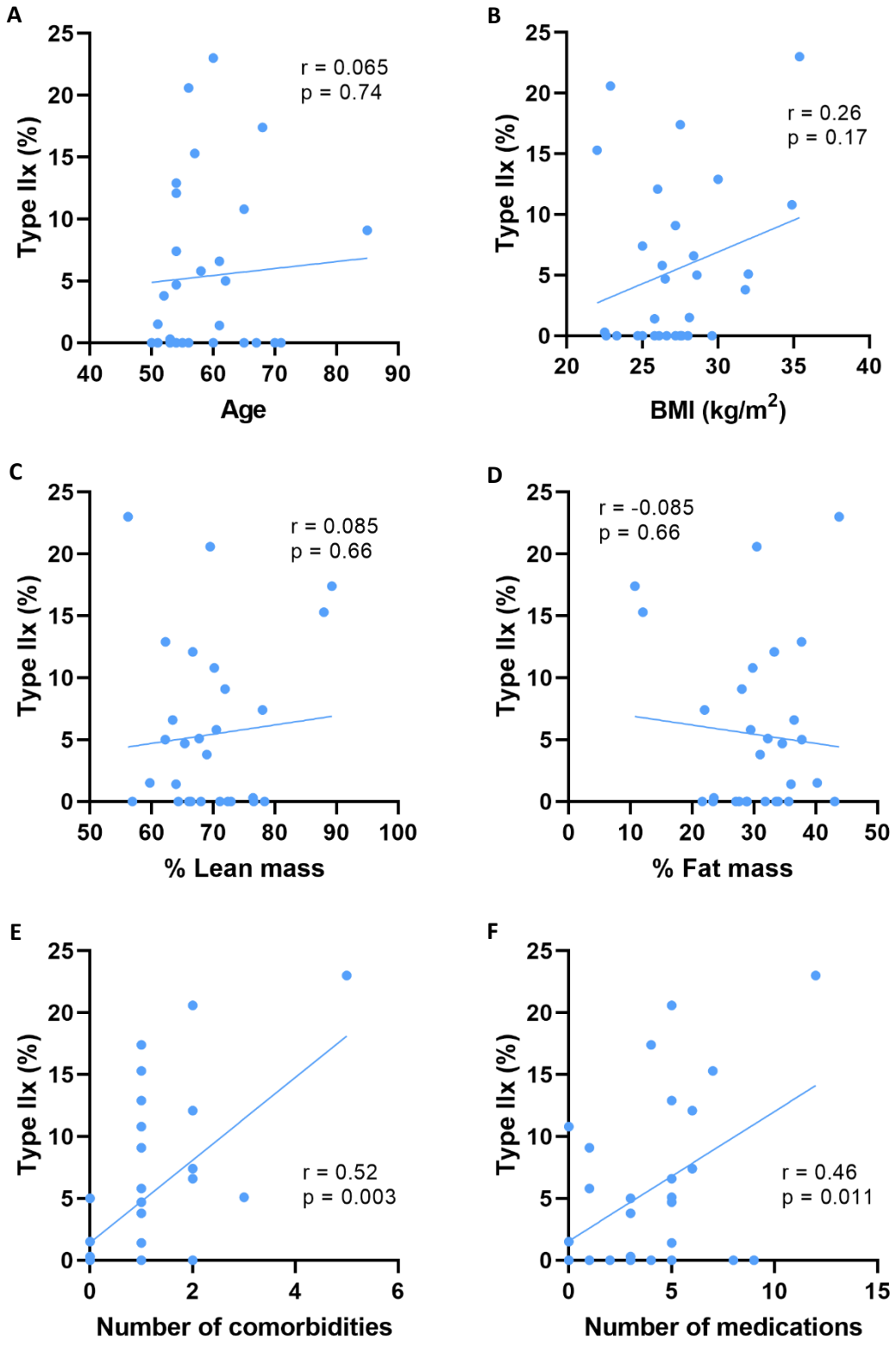

Figure 7.23 – Clinical determinants of fibre type IIx prevalence. *Scatter plots depicting the linear regression (Pearson's correlation) between the percentage of type IIx fibres and (**A**) age, (**B**) BMI (kg/m²), (**C**) percentage lean mass, (**D**) percentage fat mass, (**E**) number of comorbidities, (**F**) number of medications in older PLWH (n = 30).*

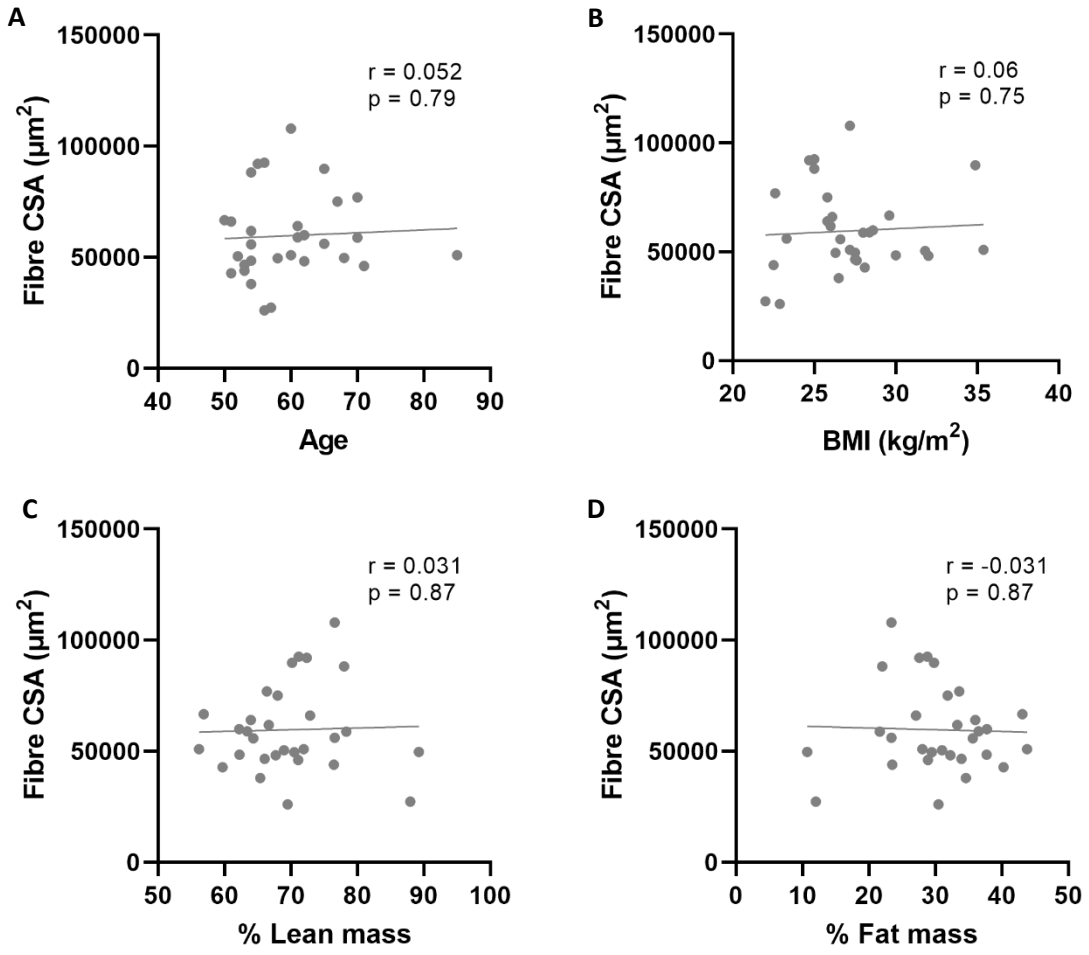

Figure 7.24 – Clinical determinants of average fibre CSA*. Scatter plots depicting the linear regression (Pearson's correlation) between the average fibre CSA (µm²) and (**A**) age, (**B**) BMI (kg/m²), (**C**) percentage lean mass, and (**D**) percentage fat mass in older PLWH (n = 30).*

7.4.9.2 Physical determinants of fibre type proportions and fibre CSA in older PLWH

Next, I sought to determine whether physical parameters predicted the proportions of the respective fibre types or average fibre CSA (**Table 7.8**).

Notably, there were no significant associations between physical factors and proportions of either fibre type I (**Figure 7.25**), type IIa (**Figure 7.26**) or type IIx (**Figure 7.27**), as well as average fibre CSA (**Figure 7.28**) (**Table 7.8**).

	Type I		**Type IIa**		**Type IIx**		**Fibre CSA**	
	HIV+ (n = 30)		**HIV+ (n = 30)**		**HIV+ (n = 30)**		**HIV+ (n = 30)**	
	r	***p***	***r***	***p***	**r**	***p***	**r**	***p***
FFP score^	-0.027	0.89	-0.14	0.48	0.19	0.35	-0.034	0.86
SPPB score^	0.18	0.35	-0.17	0.36	-0.13	0.50	0.21	0.28
MET score^	0.21	0.27	-0.13	0.50	-0.14	0.47	0.065	0.73
Grip strength (kg)	-0.043	0.82	0.17	0.36	-0.19	0.33	0.050	0.79
ASMI (kg/m^2)	0.062	0.74	-0.09	0.64	0.009	0.96	0.006	0.98

Table 7.8 – Physical factors predicting fibre type proportions and fibre CSA in older PLWH. *Table depicting the associations between proportional fibre types and average fibre CSA (µm^2) and various factors. Linear regression and correlation was determined by Pearson's correlation for normally distributed data and Spearman's correlation for non-normally distributed data (denoted by ^).*

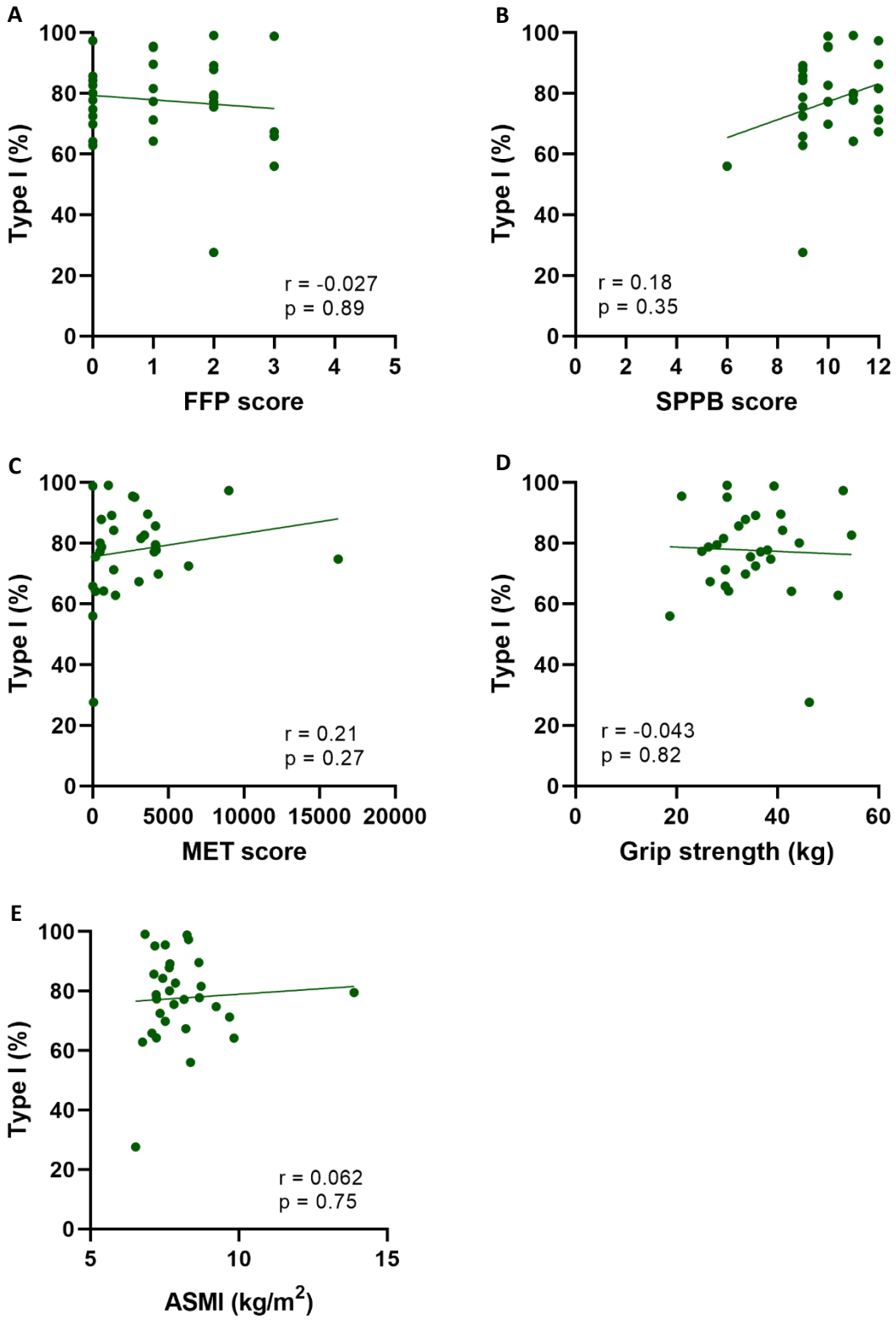

Figure 7.25 – Physical determinants of type I percentage. *Scatter plots depicting the linear regression between the percentage of type I fibres and (**A**) FFP score, (**B**) SPPB score, (**C**) MET score, (**D**) grip strength (kg), and (**E**) ASMI (kg/m²) in older PLWH (n = 30). Pearson's correlation was performed for parametric data (**D** and **E**), and spearman's correlation was performed on non-parametric data (**A, B, C**).*

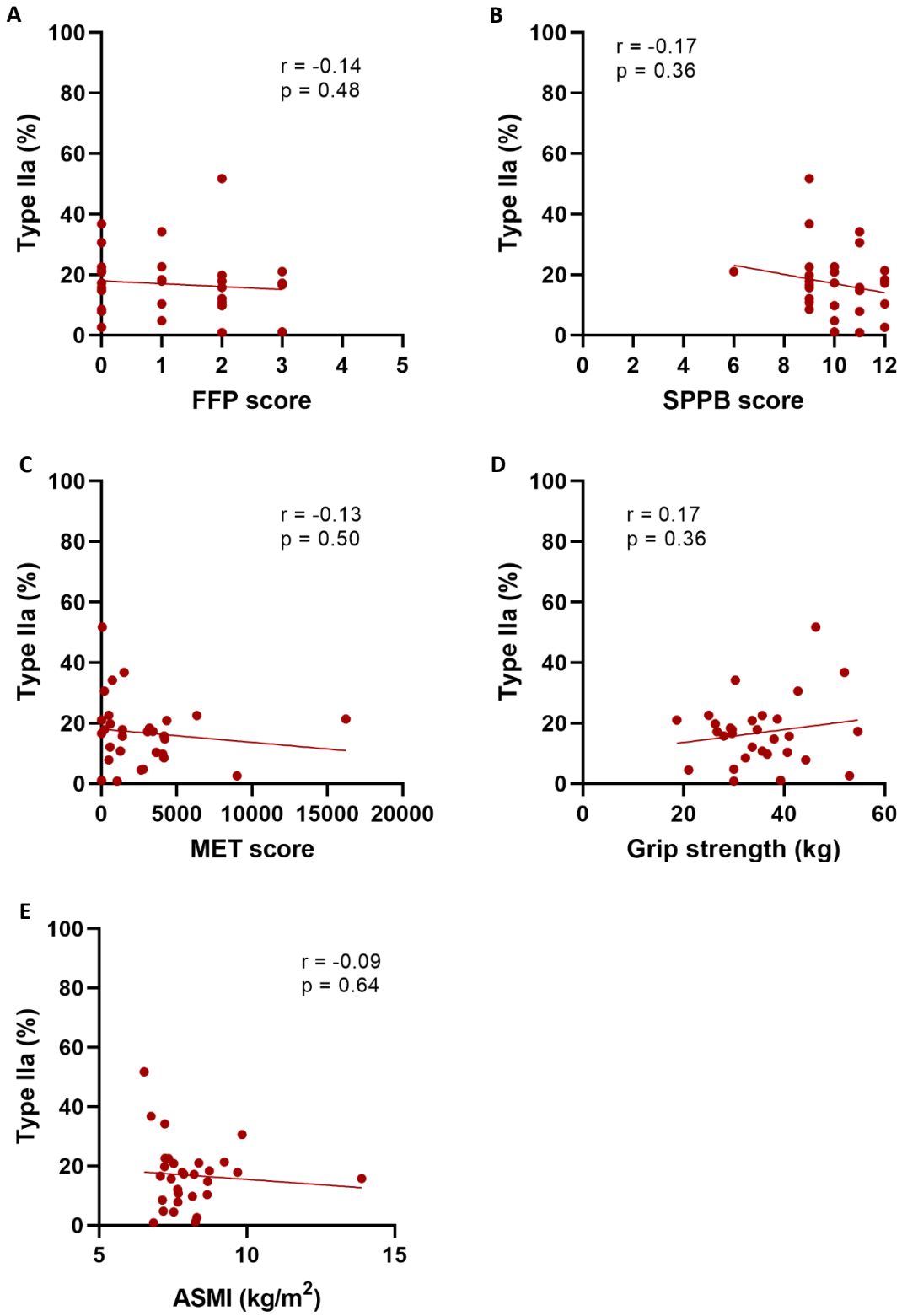

Figure 7.26 – Physical determinants of type IIa percentage. *Scatter plots depicting the linear regression between the percentage of type IIa fibres and (**A**) FFP score, (**B**) SPPB score, (**C**) MET score, (**D**) grip strength (kg), and (**E**) ASMI (kg/m²) in older PLWH (n = 30). Pearson's correlation was performed for parametric data (**D** and **E**), and spearman's correlation was performed on non-parametric data (**A**, **B**, **C**).*

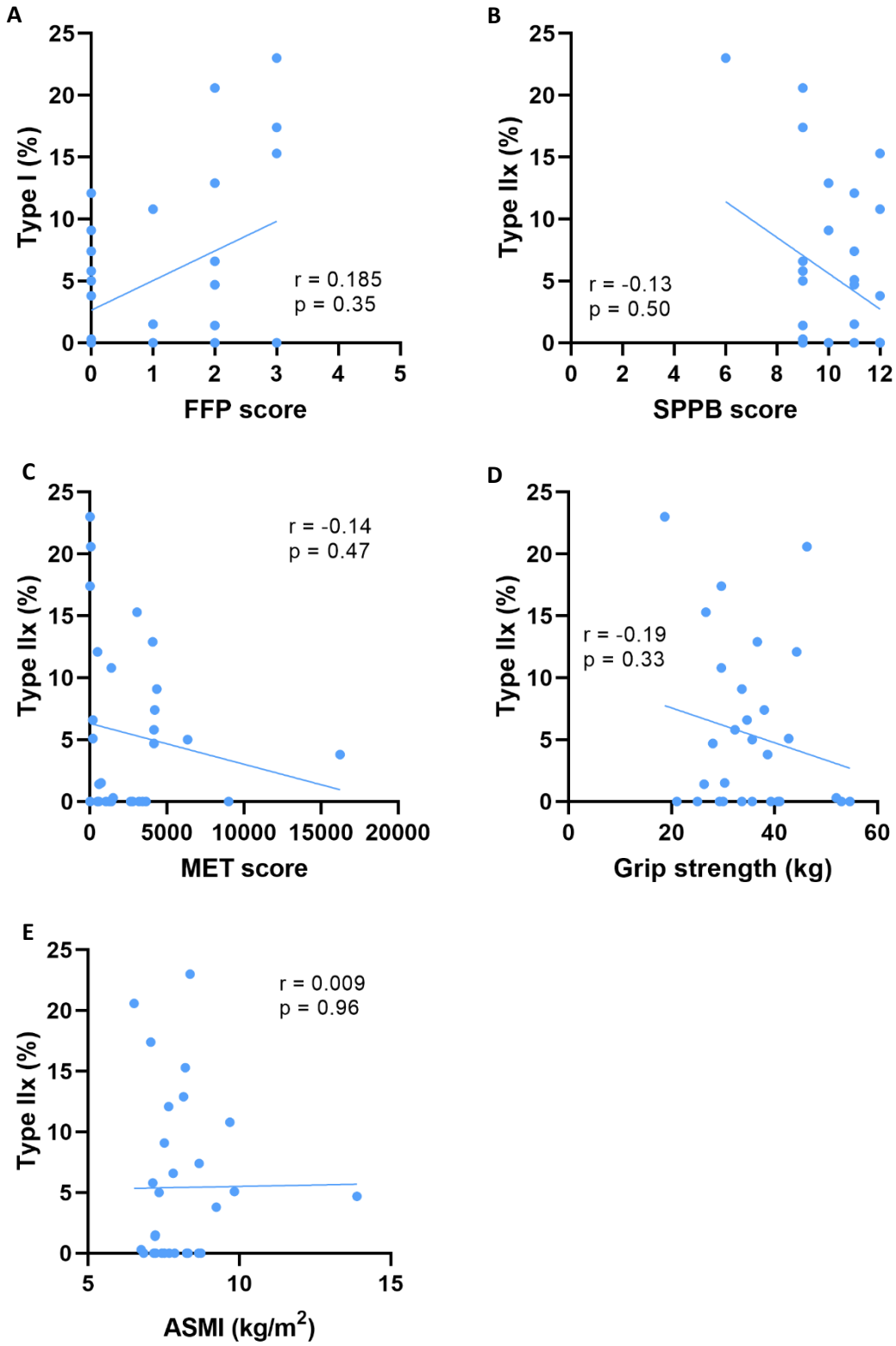

Figure 7.27 – Physical determinants of type IIx percentage. *Scatter plots depicting the linear regression between the percentage of type IIx fibres and (**A**) FFP score, (**B**) SPPB score, (**C**) MET score, (**D**) grip strength (kg), and (**E**) ASMI (kg/m²) in older PLWH (n = 30). Pearson's correlation was performed for parametric data (**D** and **E**), and spearman's correlation was performed on non-parametric data (**A**, **B**, **C**).*

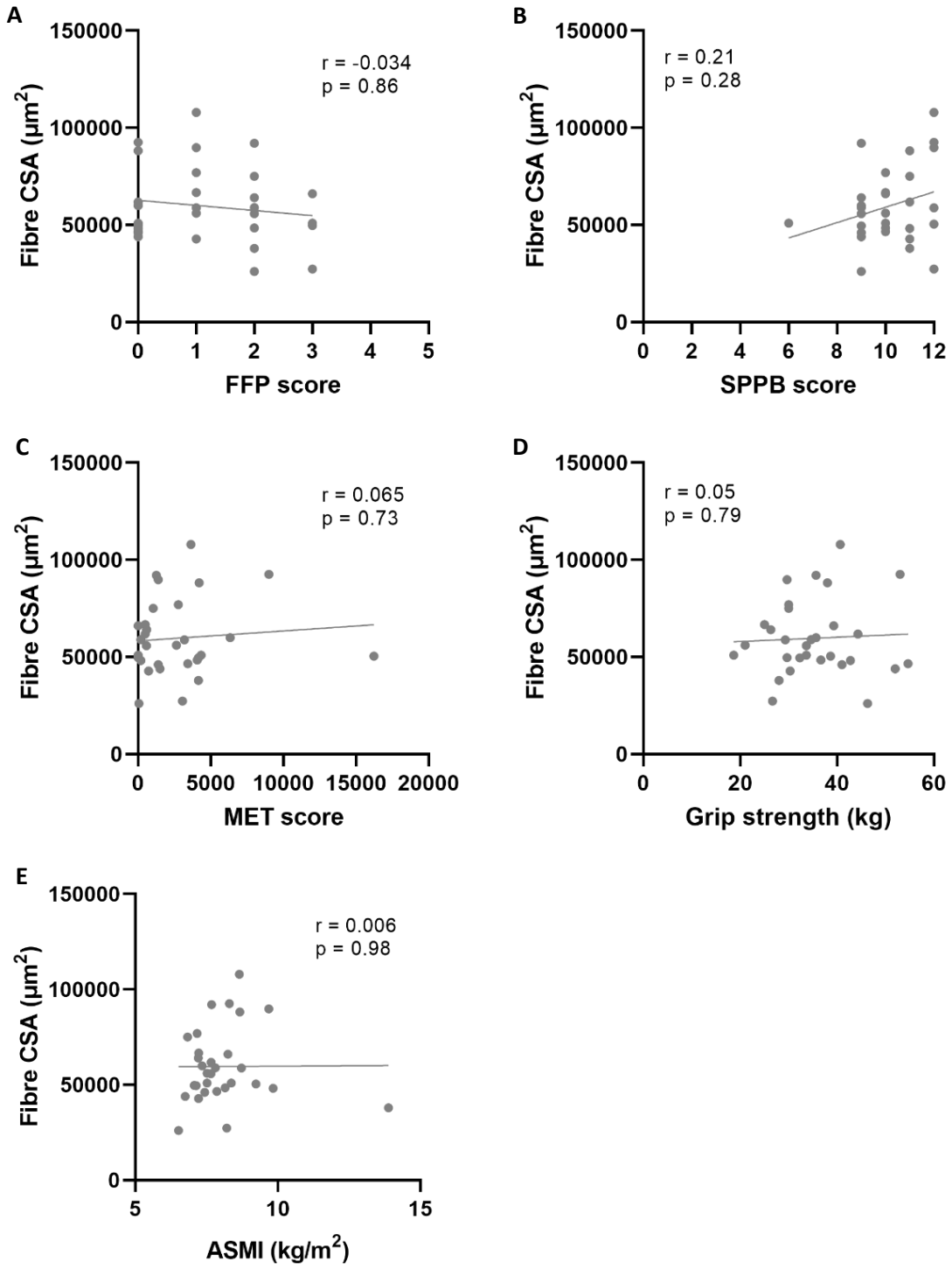

Figure 7.28 – Physical determinants of fibre CSA*. Scatter plots depicting the linear regression between the average fibre CSA (µm²) and (**A**) FFP score, (**B**) SPPB score, (**C**) MET score, (**D**) grip strength (kg), and (**E**) ASMI (kg/m²) in older PLWH (n = 30). Pearson's correlation was performed for parametric data (**D** and **E**), and spearman's correlation was performed on non-parametric data (**A**, **B**, **C**).*

7.4.9.3 Pathophysiological skeletal muscle determinants of fibre type proportions and fibre CSA in older PLWH

Finally, linear regression analyses was performed in order to determine whether pathophysiological skeletal muscle factors assessed as part of the MAGMA study (full data presented later in the chapter) predicted the proportions of the respective fibre types or average fibre CSA (**Table 7.9**).

Here, fibre CSA was significantly associated with percentage regenerated fibres in older PLWH (n = 30; r = 0.45; *p* = 0.014) (**Pearson's correlation**) (**Figure 7.29**).

Subsequently, as fibre CSA is known to decline with age, a multivariate linear regression model was developed with average fibre CSA as the dependant variable, and age and the proportion of regenerated fibres as the independent variables. Here, this multivariate linear regression model confirmed that the association between fibre CSA and the proportion of regenerated fibres was independent of age (unstandardised regression coefficient = 0.45; *p* = 0.016, **multivariate linear regression**) (**Table 7.9**). However, the model fit was marginally not statistically significant (*p* = 0.051), and subsequently only predicted a small amount of variation in fibre CSA (r^2 = 0.20).

	Type I		**Type IIa**		**Type IIx**		**Fibre CSA**		
	HIV+ (n = 30)		**HIV+ (n = 30)**		**HIV+ (n = 30)**		**HIV+ (n = 30)**		
	r	***p***	***r***	***p***	**r**	***p***	**r**	***p***	**Age-adjusted *p***
Log_{10}(Pax7⁺ SC)	-0.072	0.71	-0.017	0.93	0.19	0.32	0.18	0.34	-
Log_{10}(BodipyAbn)	0.040	0.83	-0.27	0.15	0.35	0.059	0.046	0.81	-
Log_{10}(% Fibrosis)	0.072	0.71	-0.12	0.54	0.02	0.92	0.23	0.22	-
Log_{10}(Lipofuscin CSA)⁺	-0.025	0.90	0.11	0.59	-0.12	0.54	-0.001	0.99	-
Log_{10}(Lipofuscin frequency)⁺	0.017	0.93	0.023	0.91	-0.076	0.69	0.14	0.46	-
Regenerated fibres	-0.11	0.55	-0.028	0.88	0.29	0.12	**0.45**	**0.014**	**0.016**
Degenerated fibres	0.32	0.087	-0.31	0.098	-0.19	0.31	0.34	0.064	-

Table 7.9 – Skeletal muscle determinants of fibre type proportions and average fibre CSA*. Table depicting the associations between fibre type proportions and average fibre CSA (μm²) and various skeletal muscle pathological factors. Linear regression and correlation analysis was determined by Pearson's correlation. Multivariate linear regression with adjustment for age was performed for determinants significantly associated through univariate regression analyses. Statistically significant associations are bold. + = data missing from 1 patient.*

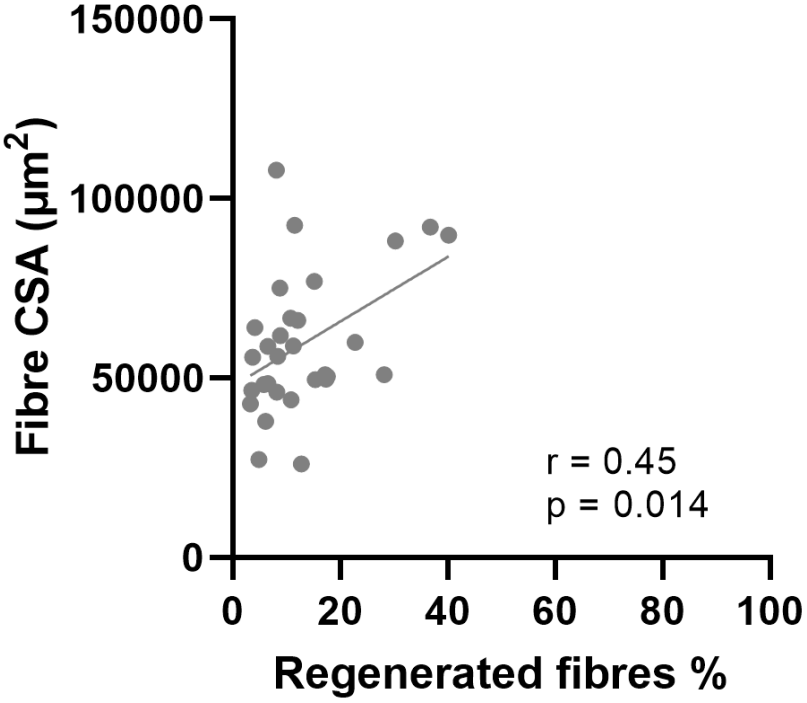

Figure 7.29 – Pathophysiological determinants of fibre CSA*. Scatter plots depicting linear regression analysis (Pearson's correlation) between average fibre CSA (µm²) and percentage degenerated fibres. Each dot represents an individual patient.*

7.4.10 Fibre type proportions and fibre CSA in frail and sarcopenic older PLWH

Next, in order to better understand fibre type proportions and fibre CSA specifically in frailty and sarcopenia in older PLWH, I stratified the HIV+ group (n = 30) into frail (n = 4), prefrail (n = 15), and robust (n = 11) groups, as well as sarcopenic (n = 5), presarcopenic (n = 6), and non-sarcopenic (n = 19) groups.

With regards to the frail, prefrail, and robust HIV+ groups, there was no significant differences between the proportion of type I (p = 0.70, **one-way ANOVA**) (**Figure 7.30a**) and type IIa fibres (p = 0.83) (**Figure 7.30c**), as well as average fibre CSA (p = 0.37) (**Figure 7.30g**). However, there was a statistically significant difference in the proportion of type IIx fibres between the three groups (p = 0.021) (**Figure 7.30e**). In particular, frail PLWH had a significantly higher proportion of type IIx fibres compared to both the prefrail (p = 0.033, **Tukey's multiple comparison**) and robust (p = 0.019) groups (**Figure 7.30e**).

There was no significant difference in the proportions of fibre type I (p = 0.42, **one-way ANOVA**) (**Figure 7.30b**), type IIa (p = 0.24) (**Figure 7.30d**) and type IIx fibres (p = 0.87) (**Figure 7.30f**), or average fibre CSA (p = 0.96) (**Figure 7.30h**) between the sarcopenic, presarcopenic, and non-sarcopenic groups.

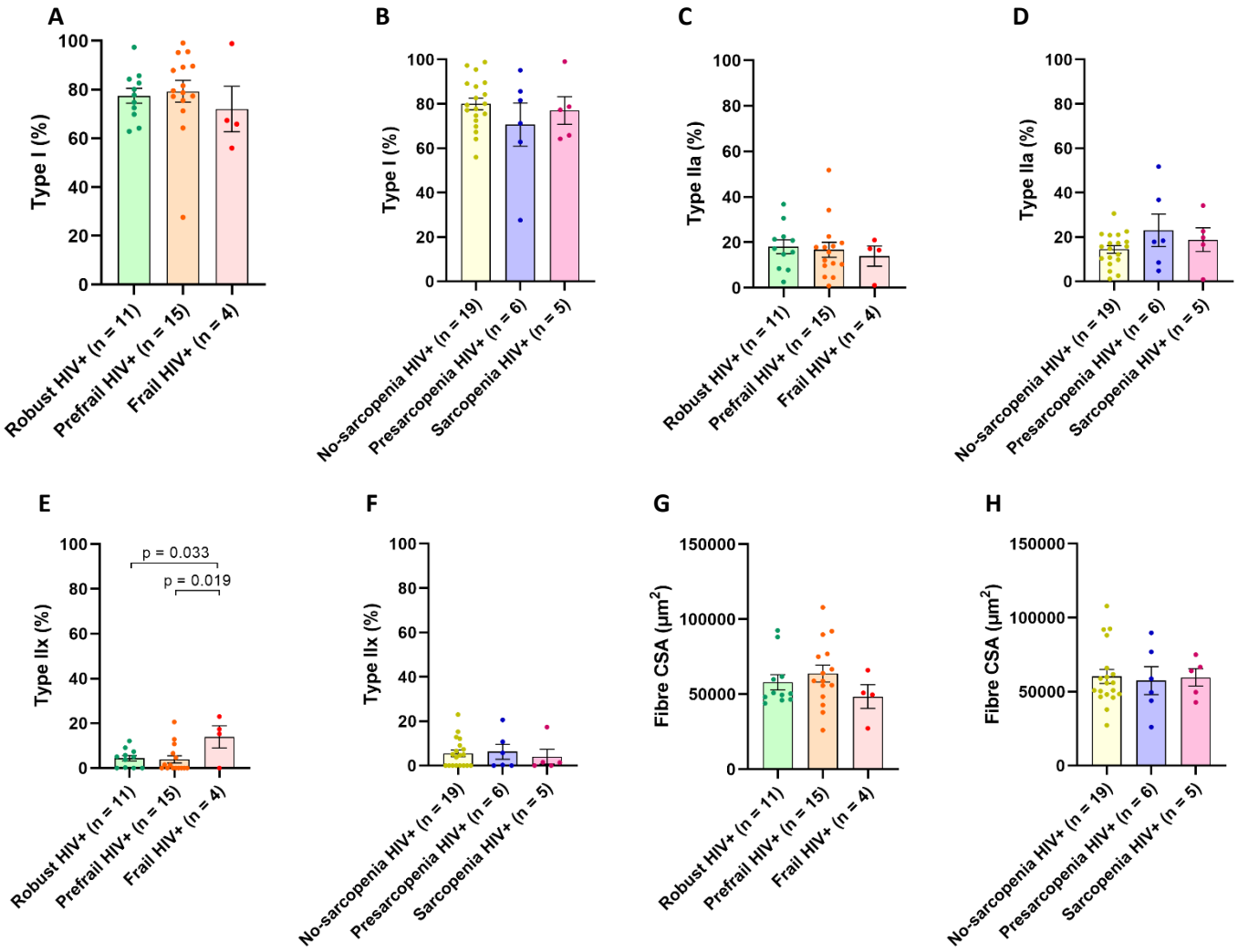

Figure 7.30 – Fibre type proportions and fibre CSA in frail and sarcopenic PLWH. *Dot plots (mean ± SEM) showing the differences between frail (n = 4), prefrail (n = 15) and robust (n = 11) PLWH in the proportions of (**A**) % fibre type I, (**C**) % fibre type IIa, (**E**) % fibre type IIx and (**G**) fibre CSA (µm²). No differences between sarcopenic (n = 5), presarcopenic (n = 6) and non-sarcopenic (n = 19) PLWH in the proportions of (**B**) % fibre type I, (**D**) % fibre type IIa, (**F**) % fibre type IIx and (**H**) fibre CSA (µm²). Each dot represent an individual patient.*

Next, the HIV+ group (n = 30) was stratified into frail/prefrail HIV+ (n = 19) and sarcopenic/presarcopenic HIV+ (n = 11) groups. Here, I determined whether there were differences in the proportion of fibre types I, IIa, and IIx, as well as average fibre CSA between the respective groups and robust HIV+ (n = 11) and non-sarcopenic HIV+ individuals (n = 19).

Again, there was no significant difference in the proportion of type I fibres between frail/prefrail PLWH and robust PLWH (p = 0.96, **unpaired t test**) (**Figure 7.31a**), nor was there a significant difference between sarcopenic/presarcopenic PLWH and non-sarcopenic PLWH (p = 0.26) (**Figure 7.31e**). In addition, there was no significant difference in the proportion of type IIa fibres between frail/prefrail PLWH and robust PLWH (p = 0.66) (**Figure 7.31b**) or between sarcopenic/presarcopenic PLWH and non-sarcopenic PLWH (p = 0.11) (**Figure 7.31f**).

There was also no statistically significant difference in the proportion of type IIx fibres between frail/prefrail PLWH and robust PLWH (p = 0.55, **unpaired t test**) (**Figure 7.31c**) or between sarcopenic/presarcopenic PLWH and non-sarcopenic PLWH (p = 0.92) (**Figure 7.31g**). Finally, there was also no significant difference in average fibre CSA between frail/prefrail PLWH and robust PLWH (p = 0.96) (**Figure 7.31d**), or between sarcopenic/presarcopenic PLWH and non-sarcopenic PLWH (p = 0.81) (**Figure 7.31h**).

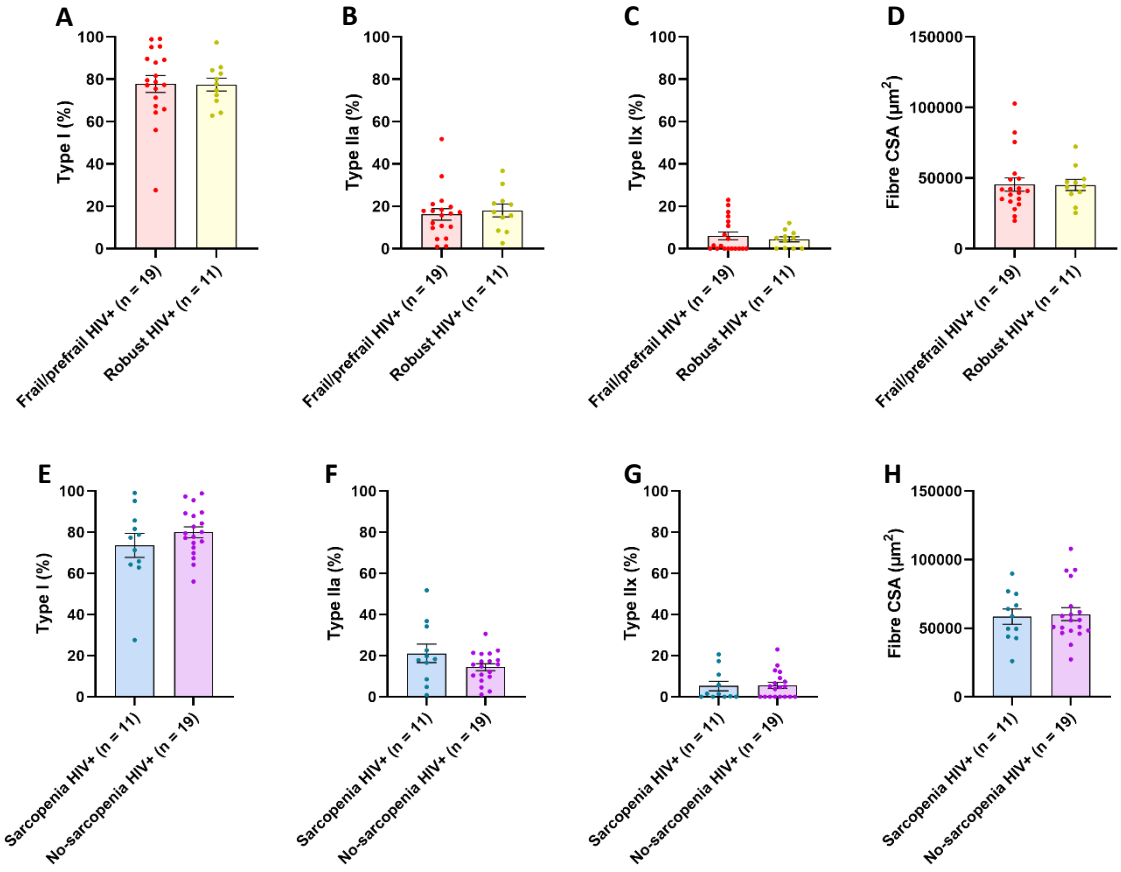

Figure 7.31 – Fibre type proportions and fibre CSA in adverse ageing phenotypes in older PLWH. *Dot plots (mean ± SEM) depicting the differences between frail/prefrail HIV+ individuals (n = 19) and robust HIV+ individuals (n = 11) in (**A**) fibre type I proportion, (**B**) fibre type IIa proportion, (**C**) fibre type IIx proportion, or (**D**) average fibre CSA (µm²). And between sarcopenic/presarcopenic HIV+ individuals (n = 11) and non-sarcopenic HIV+ individuals (n = 19) in (**E**) fibre type I proportion, (**F**) fibre type IIa proportion, (**G**) fibre type IIx proportion, or (**H**) average fibre CSA (µm²). Each dot represents an individual patient.*

7.4.11 Greater skeletal muscle fibrosis in older PLWH compared to age-matched HIV- individuals

10µm skeletal muscle sections (n = 45) were subjected to Masson's trichrome histochemistry (**Figure 7.32a**) in order to quantify the levels of tissue fibrosis and to subsequently investigate whether increased levels of fibrosis were contributing to declines in physical and muscle specific function.

The CSA (μm^2) of each section was measured, as well as the area of fibrotic tissue (μm^2), allowing for the quantification of the proportion of fibrotic tissue for each subject. In order to normalise the distribution of the results, the data was log transformed.

Interestingly, the HIV+ group (n = 30) had a significantly higher proportion of fibrotic tissue compared to the HIV- group (n = 15) ($p < 0.0001$, **unpaired t test**) (**Figure 7.32b**).

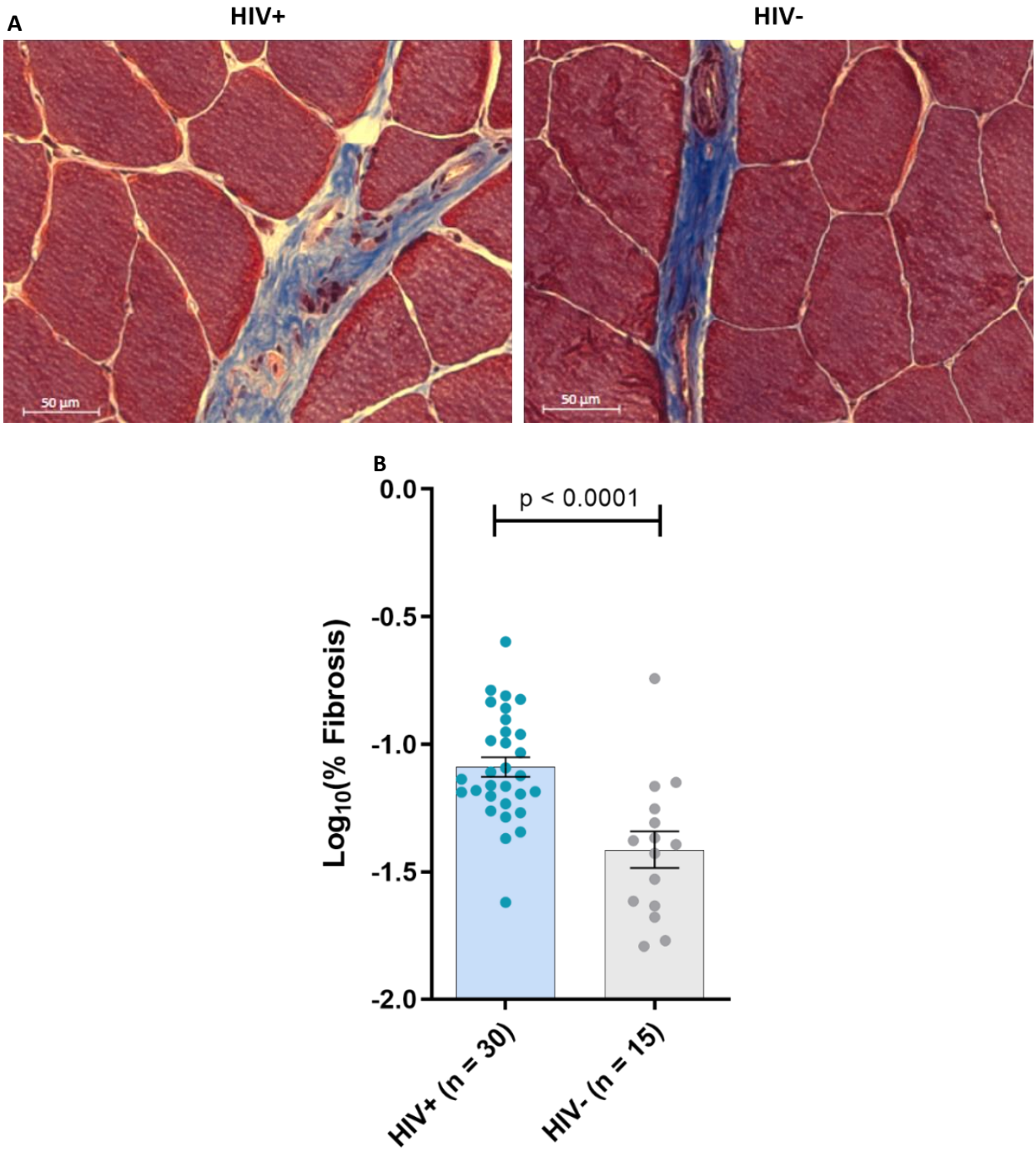

Figure 7.32 – Elevated skeletal muscle fibrosis in PLWH. (***A***) *Example brightfield image of a skeletal muscle section from a HIV+ and HIV- individual stained with Masson's trichrome histochemistry. Fibrotic tissue appears blue. Scale bar = 50µm.* (***B***) *Dot plot (mean ± SEM) showing the significantly higher levels of fibrosis in skeletal muscle from HIV+ individuals (n = 30) compared to HIV- individuals (n = 15; p < 0.0001, unpaired t test).*

7.4.12 Determinants of skeletal muscle fibrosis

Following this result, I next wanted to investigate whether the elevated levels of tissue fibrosis was predicted by any of the various clinical, lifestyle, or body composition factors, as well as any of the pathophysiologic skeletal muscle factors such as IMCL or quiescent satellite cell prevalence.

7.4.12.1 Clinical predictors of skeletal muscle fibrosis in older PLWH

Notably, increased skeletal muscle fibrosis was not significantly predicted by any of the clinical, body composition, or lifestyle factors (**Pearson's correlation**) (**Table 7.10/Figure 7.33**). In addition, skeletal muscle fibrosis was not significantly predicted by any of the HIV-related factors, although it was marginally associated with both percentage lean and fat mass.

	Log_{10}(%Fibrosis) HIV+ (n = 30)	
	r	***p***
Age	0.20	0.30
BMI (kg/m^2)	0.03	0.87
Waist circumference (cm)	0.012	0.95
# Comorbidities	0.11	0.57
# Medications	0.14	0.46
Polypharmacy*	-	0.45
% Fat mass	-0.35	0.059
% Lean mass	0.35	0.059
Months since diagnosis	0.19	0.31
Months on ART	-0.044	0.82
Months untreated	0.25	0.19
CD4 count (copies/µl)	-0.013	0.95
Smokers*	-	0.059
Alcohol drinkers*	-	0.57
Recreational drug use*	-	0.45

Table 7.10 – Clinical predictors of skeletal muscle fibrosis in older PLWH. *Table depicting the associations between Log_{10}(%Fibrosis) and various clinical factors. Linear regression and correlation analysis was determined by Pearson's correlation. * = ordinal data in which individuals were stratified by yes/no and differences determined by unpaired t tests.*

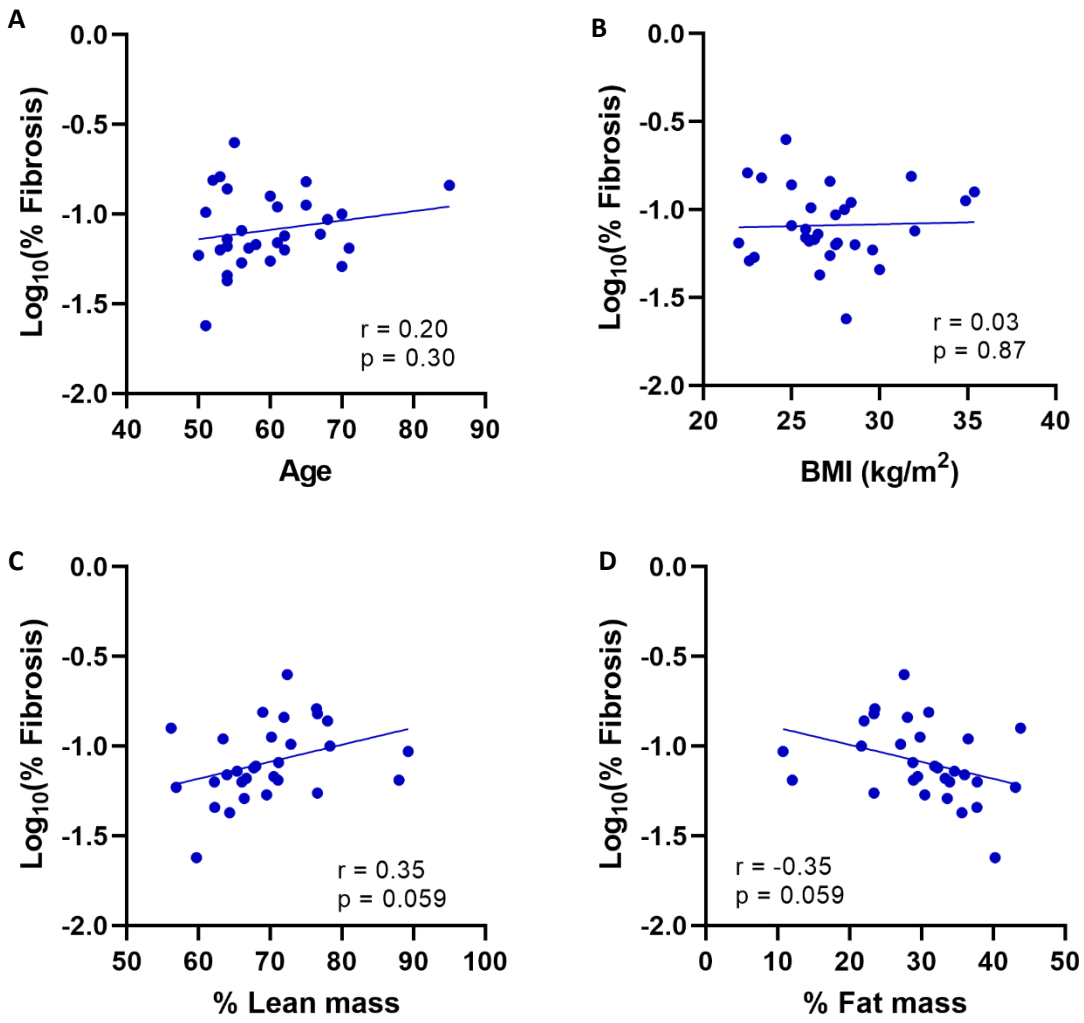

Figure 7.33 – Clinical determinants of fibrosis. *Scatter plots depicting the linear regression (Pearson's correlation) between log_{10}(% fibrosis) and (**A**) age, (**B**) BMI (kg/m^2), (**C**) percentage lean mass, and (**D**) percentage fat mass in older PLWH (n = 30). Each dot represents an individual patient.*

7.4.12.2 Physical determinants of skeletal muscle fibrosis in older PLWH

Next, I investigated whether parameters of physical function predicted skeletal muscle fibrosis in older PLWH through unadjusted linear regression analysis (**Table 7.11**).

Here, there were no significant associations between the proportion of skeletal muscle fibrosis and any of the physical parameters (**Pearson's and Spearman's correlation**) (**Figure 7.34**).

	Log_{10}(%Fibrosis) HIV+ (n = 30)	
	r	***p***
FFP score^	-0.083	0.66
SPPB score^	-0.003	0.99
MET score^	0.07	0.71
Grip strength (kg)	-0.022	0.91
ASMI (kg/m^2)	0.11	0.58

Table 7.11 – Physical factors predicting skeletal muscle fibrosis in older PLWH. *Table depicting the associations between Log_{10}(%Fibrosis) and various factors. Linear regression and correlation analysis was determined by Pearson's correlation for normally distributed data and Spearman's correlation for non-normally distributed data (denoted by ^).*

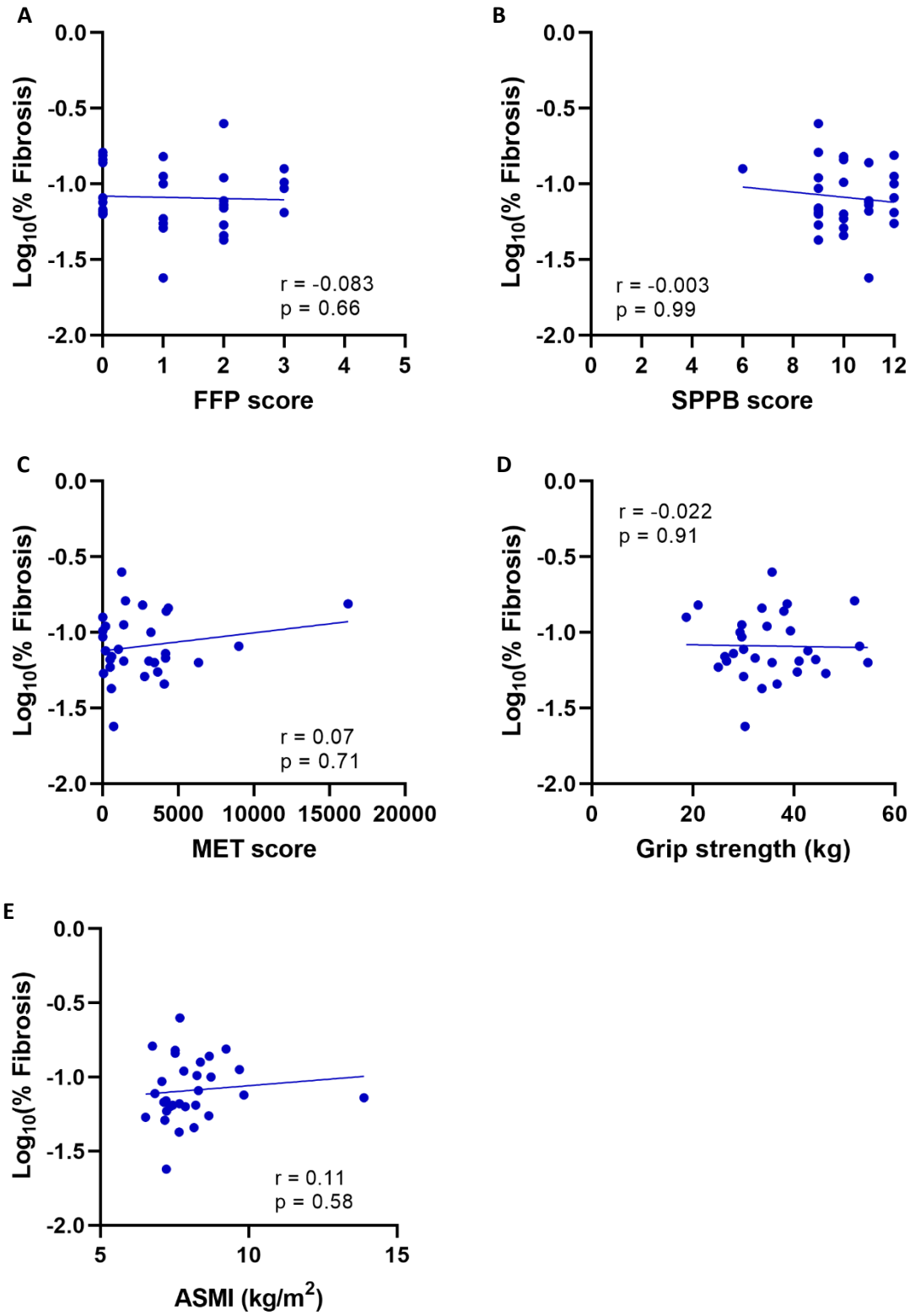

Figure 7.34 – Physical factors predicting skeletal muscle fibrosis. *Scatter plots depicting the linear regression between log_{10}(% fibrosis) and (**A**) FFP score, (**B**) SPPB score, (**C**) MET score, (**D**) grip strength (kg), and (**E**) ASMI (kg/m^2) in older PLWH (n = 30). Pearson's correlation was performed for parametric data (**D** and **E**), and Spearman's correlation was performed on non-parametric data (**A**, **B**, **C**). Each dot represents an individual patient.*

7.4.12.3 Pathophysiological determinants of skeletal muscle fibrosis in older PLWH

Finally, linear regression analysis was performed in order to determine if any pathophysiological skeletal muscle parameters significantly predicted skeletal muscle fibrosis (**Table 7.12**).

As demonstrated previously in **Section 7.4.6.3**, through univariate linear regression analysis it was found that greater skeletal muscle fibrosis was significantly associated with the prevalence of $Pax7^+$ SCs (r = 0.57; *p* = 0.001, **Pearson's correlation**) (**Figure 7.35a**). In addition, fibrosis was significantly associated with and the percentage of regenerated fibres (r = 0.59; *p* = 0.001) (**Figure 7.35b**).

Next, multivariate linear regression models were developed with fibrosis as the dependant variable, and age, as well as either $pax7^+$ SC prevalence, or the percentage of regenerated fibres as the independent variables.

Here, multivariate linear regression analysis confirmed that the association between skeletal muscle fibrosis and $Pax7^+$ SC prevalence was independent of the effect of age (unstandardised regression coefficient = 0.49; *p* = 0.002, **multivariate linear regression**) (**Table 7.12**). Overall model fit was statistically significant (*p* = 0.004), and the model was predictive of a third of the variation in fibrosis (r^2 = 0.33).

In addition, the association between fibrosis and the proportion of regenerated fibres was also independent of age (unstandardised regression coefficient = 0.013; *p* = 0.001, **multivariate linear regression**) (**Table 7.12**). Again, the overall model fit was significant (*p* = 0.02) and predictive of a modest amount of variation in fibrosis (r^2 = 0.36).

	Log$_{10}$(%Fibrosis) HIV+ (n = 30)		
	r	***p***	**Age-adjusted *p***
Type I %	0.078	0.68	-
Type IIa %	-0.12	0.54	-
Type IIx %	0.020	0.92	-
Fibre CSA (µm^2)	0.23	0.22	-
Log$_{10}$(Pax7$^+$ SC)	**0.57**	**0.001**	**0.002**
Log$_{10}$(% BodipyAbn)	-0.13	0.49	-
Log$_{10}$(Lipofuscin CSA)$^+$	0.037	0.85	-
Log$_{10}$(Lipofuscin frequency)$^+$	-0.097	0.62	-
Regenerated fibres	**0.59**	**0.001**	**0.001**
Degenerated fibres	0.07	0.71	-

Table 7.12 – Skeletal muscle pathophysiological determinants of fibrosis*. Table depicting the associations between log$_{10}$(%Fibrosis) and various skeletal muscle pathophysiological factors. Linear regression and correlation analysis was determined by Pearson's correlation. Multivariate linear regression with adjustment for age was performed for determinants significantly associated through univariate regression analyses. Statistically significant associations are bold. + = data missing from 1 patient.*

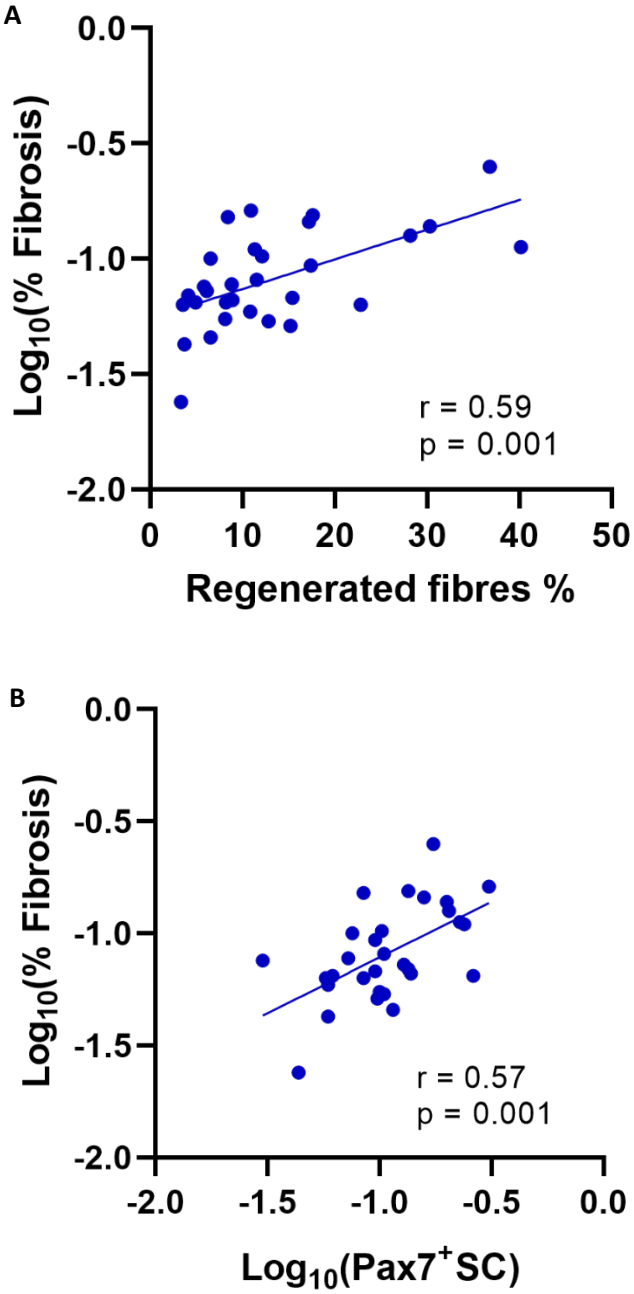

Figure 7.35 – Pathophysiological determinants of skeletal muscle fibrosis*. Scatter plots depicting linear regression analysis (Pearson's correlation) between log_{10}(%Fibrosis) and (**A**) percentage regenerated fibres and (**B**) log_{10}($Pax7^+$ SCs per 100 fibres). Each dot represents an individual patient.*

7.4.13 Skeletal muscle fibrosis in frail and sarcopenic older PLWH

Next, I sought to determine whether there were differences in skeletal muscle fibrosis between frail (n = 4), prefrail (n = 15), and robust (n = 11) PLWH, as well as sarcopenic (n = 5), presarcopenic (n = 6), and non-sarcopenic PLWH (n = 19).

Here, there was no significant difference in the proportion of fibrotic skeletal muscle tissue between the frail, prefrail, and robust HIV+ individuals (*p* = 0.42, **one-way ANOVA**) (**Figure 7.36a**). In addition, there was also no significant difference in skeletal muscle fibrosis between the sarcopenic, presarcopenic, and non-sarcopenic HIV+ individuals (*p* = 0.27) (**Figure 7.36b**).

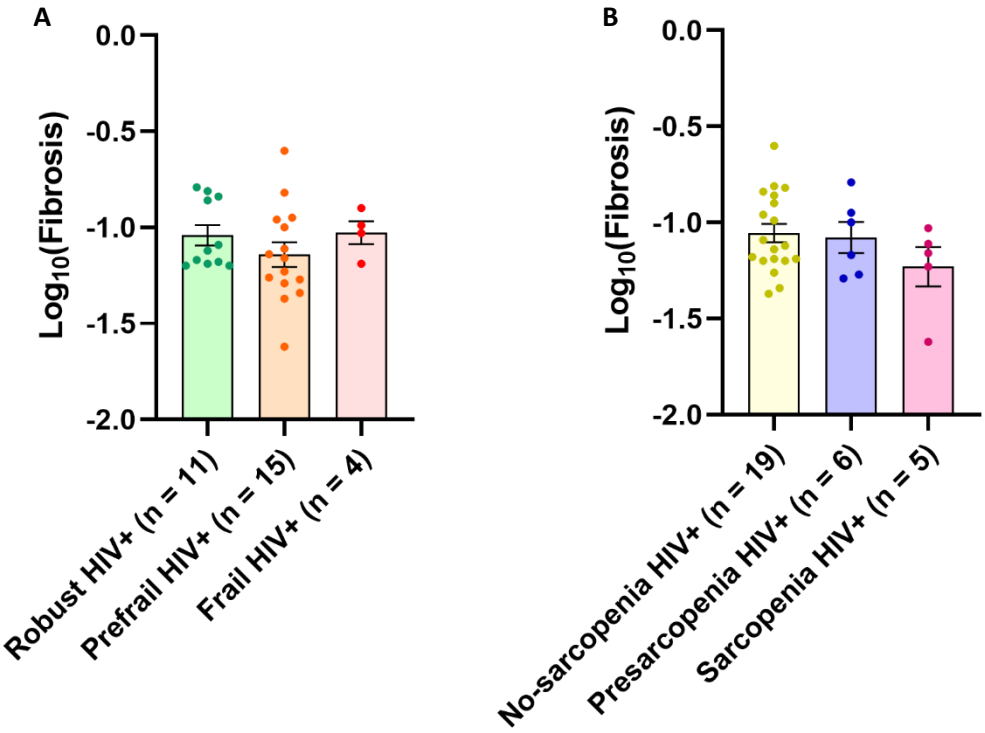

Figure 7.36 – Skeletal muscle fibrosis differences across the frailty and sarcopenic spectrum. *Dot plots (mean ± SEM) showing no significant differences in log_{10}(fibrosis) between (**A**) frail (n = 4), prefrail (n = 15), and robust (n = 11) PLWH, or between (**B**) sarcopenic (n = 5), presarcopenic (n = 6), and non-sarcopenic PLWH (n = 19). Dots represent individual patients.*

As performed previously, I next stratified the HIV+ group (n = 30) into frail/prefrail HIV+ (n = 19) and sarcopenic/presarcopenic HIV+ (n = 11) groups and compared the proportion of skeletal muscle fibrosis in the respective groups against robust HIV+ (n = 11) and non-sarcopenic HIV+ individuals (n = 19).

Notably, there was no significant difference in the level of skeletal muscle fibrosis between older frail/prefrail PLWH (n = 19) and age-matched robust PLWH (n = 11; $p = 0.35$, **unpaired t test**) (**Figure 7.37a**). Similarly, there was also no significant difference in skeletal muscle fibrosis between sarcopenic/presarcopenic PLWH (n = 11) and non-sarcopenic PLWH (n = 19; $p = 0.26$) (**Figure 7.37b**).

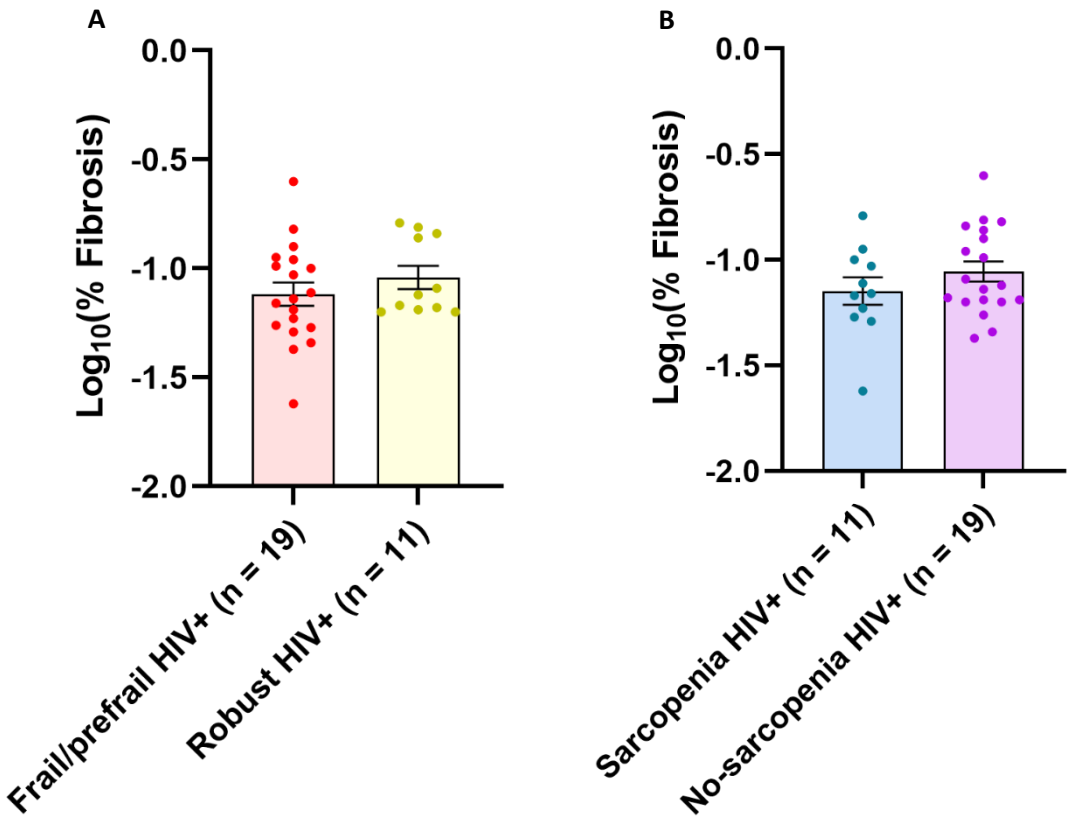

Figure 7.37 – Skeletal muscle fibrosis in adverse ageing phenotypes in older PLWH*. Dot plots (mean ± SEM) depicting no significant difference in log_{10}(% fibrosis) between (**A**) frail/prefrail PLWH (n = 19) and robust PLWH (n = 11), as well as (**B**) sarcopenia/presarcopenia PLWH (n = 11) and non-sarcopenic PLWH (n = 19). Each dot represents an individual patient.*

7.4.14 H&E histochemistry for assessment of regenerated and degenerated myofibres

H&E histochemistry was performed on 10µm cryo-sections (n = 45) in order to quantify the proportion of muscle fibres with central nuclei, indicative of regenerated fibres, and the proportion of degenerated fibres (**Figure 7.38**).

Interestingly, the HIV- group (n = 15) had a significantly higher proportion of regenerated fibres compared to the HIV+ group (n = 30; p = 0.02, **unpaired t test**) (**Figure 7.39a**). Whilst there was no significant difference in the proportion of degenerated fibres between the two groups (**Figure 7.39b**).

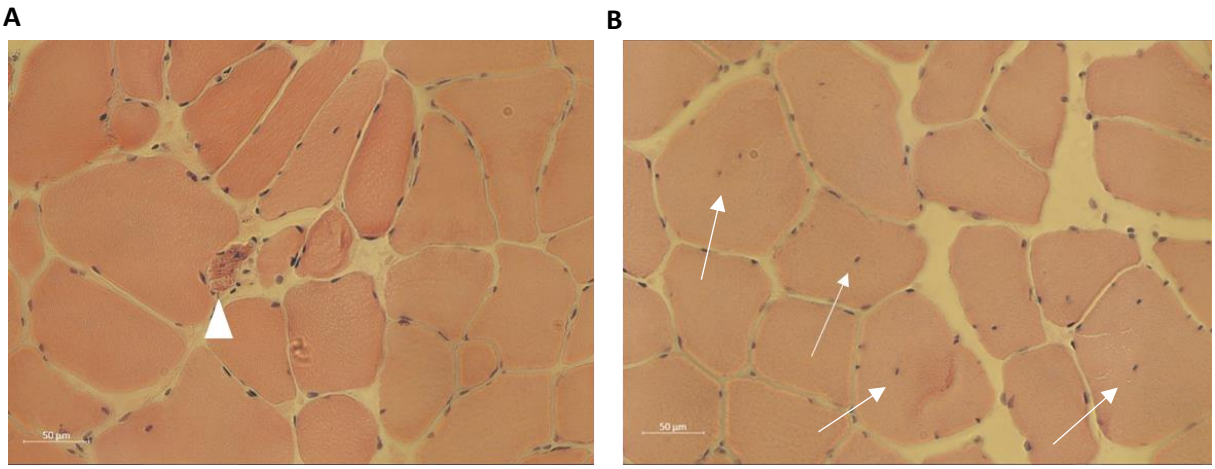

Figure 7.38 – Example H&E histochemistry for degenerated and regenerated fibres. *(**A**) Degenerated fibres (indicated by thick white arrow). (**B**) Regenerated fibre characterised by central nuclei (indicated by thin white arrows). Scale bar = 50µm.*

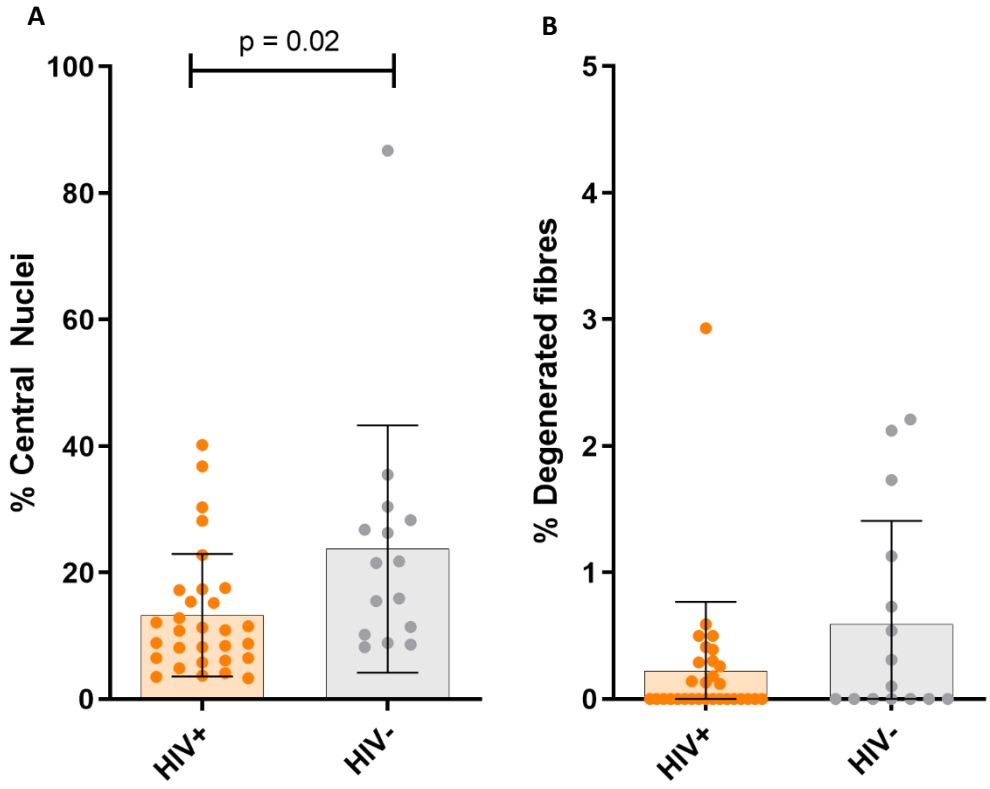

Figure 7.39 – Greater proportion of regenerated fibres in HIV- individuals*. Dot plots (mean ± SEM) showing (**A**) a significantly higher level of proportional regenerated fibres in the HIV- group (n = 15) compared to the HIV+ group (n = 30; p = 0.02), and (**B**) no significant difference in the proportion of degenerated fibres between the HIV+ and HIV- groups. Each dot represents an individual patient.*

7.4.15 Predictors of the proportion of regenerated and degenerated fibres in older PLWH

I next sought to investigate whether the proportion of regenerated fibres and degenerated fibres was predicted by any of the clinical, HIV-related, lifestyle, body composition, or pathogenic skeletal muscle factors in older PLWH. To this end, I performed linear regression analysis and unpaired t tests between these factors.

7.4.15.1 Clinical predictors of regenerated and degenerated fibres in older PLWH

With regards to the HIV-related factors, the proportion of regenerated fibres was significantly predicted by a greater duration of untreated HIV infection (n = 30; r = 0.39; *p* = 0.035) (**Figure 7.40e**). As such, through a multivariate linear regression model which included the proportion of regenerated fibres as the dependant variable and age as well as months untreated as the independent variables, the association between regenerated fibres and months of untreated HIV infection was confirmed to be independent of age (unstandardised regression coefficient = 0.041; *p* = 0.045, **multivariate linear regression**) (**Table 7.13**). However, the overall model fit was not statistically significant (*p* = 0.11) and was subsequently predictive of only a small amount of variation in the percentage of regenerated fibres (r^2 = 0.15).

Of the lifestyle factors, smokers had a significantly lower proportion of regenerated fibres compared to non-smokers (*p* = 0.039, **unpaired t test**) (**Table 7.13**).

None of the clinical parameters significantly predicted the proportion of degenerated fibres (**Figure 7.41/Table 7.13**).

	% Regenerated fibres HIV+ (n = 30)			% Degenerated fibres HIV+ (n = 30)	
	r	*p*	Age-adjusted *p*	r	*p*
Age	0.11	0.55	-	0.033	0.86
BMI (kg/m²)	0.31	0.92	-	-0.14	0.45
Waist circumference (cm)	0.52	0.056	-	-0.091	0.63
# Comorbidities	0.21	0.26	-	-0.15	0.42
# Medications	0.032	0.87	-	-0.093	0.63
Polypharmacy*	-	0.92	-	-	0.32
% Fat mass	-0.10	0.78	-	-0.028	0.93
% Lean mass	0.10	0.78	-	0.028	0.93
Months since diagnosis	0.35	0.061	-	-0.10	0.60
Months on ART	-0.012	0.95	-	0.12	0.53
Months untreated	**0.39**	**0.035**	**0.045**	-0.20	0.28
CD4 count (copies/µl)	-0.085	0.67	-	-0.22	0.27
Smokers*	-	**0.039**	-	-	0.28
Alcohol drinkers*	-	0.83	-	-	0.48
Recreational drug use*	-	0.44	-	-	0.93

Table 7.13 – Clinical predictors of regenerated and degenerated fibre prevalence in older PLWH. *Table depicting the associations between the percentage of regenerated and degenerated fibres and various clinical factors. Linear regression and correlation analysis was determined by Pearson's correlation. * = ordinal data in which individuals were stratified by yes/no and differences determined by unpaired t tests. Statistically significant associations are bold.*

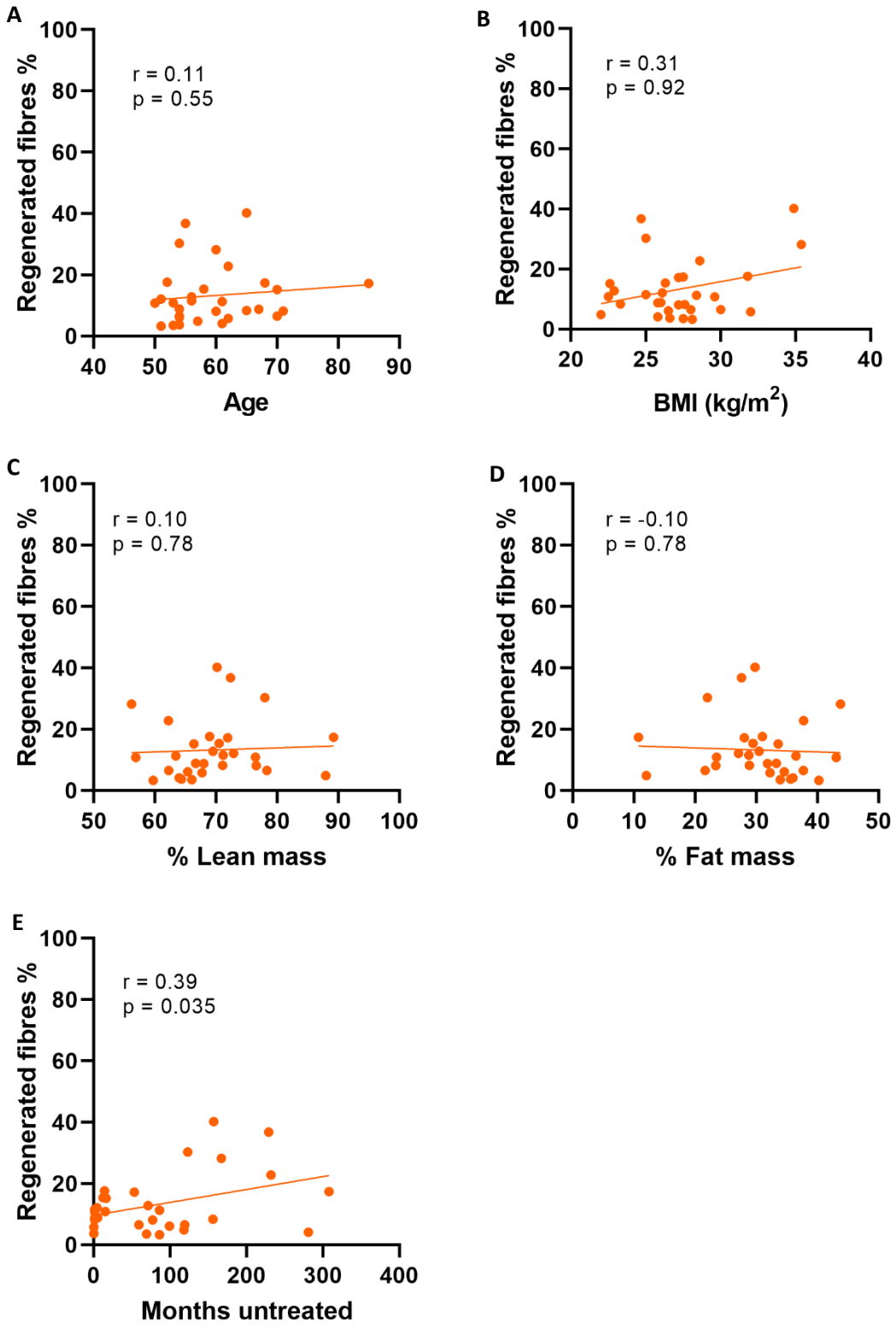

Figure 7.40 - Clinical determinants of percentage regenerated fibres. *Scatter plots depicting the linear regression (Pearson's correlation) between the percentage of regenerated fibres and (**A**) age, (**B**) BMI (kg/m²), (**C**) percentage lean mass, (**D**) percentage fat mass, and (**E**) months untreated HIV infection in older PLWH (n = 30). Each dot represents an individual patient.*

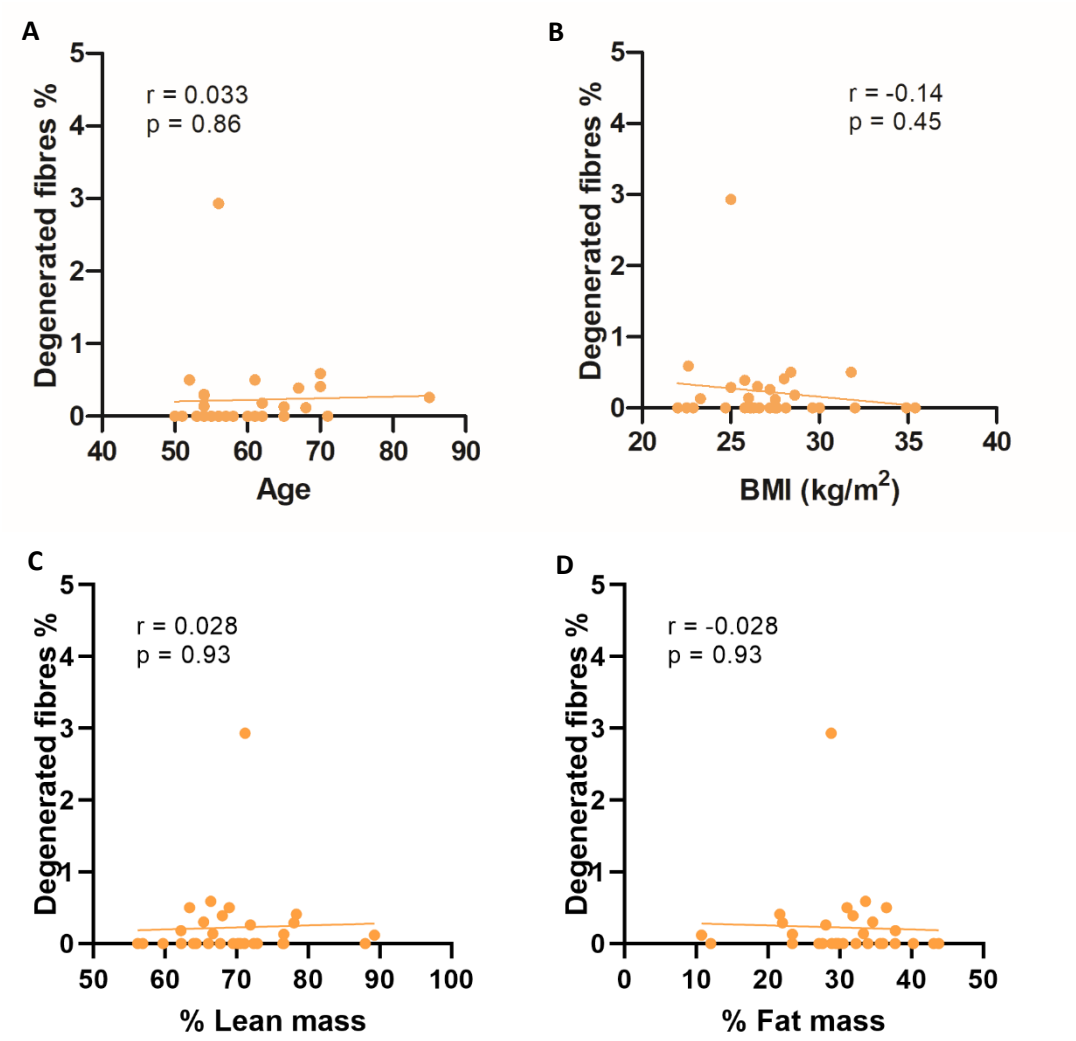

Figure 7.41 – Clinical determinants of percentage degenerated fibres*. Scatter plots depicting the linear regression (Pearson's correlation) between the percentage of degenerated fibres and (**A**) age, (**B**) BMI (kg/m^2), (**C**) percentage lean mass, and (**D**) percentage fat mass in older PLWH (n = 30). Each dot represents an individual patient.*

7.4.15.2 Physical determinants of regenerated and degenerated fibre percentages in older PLWH

Through linear regression analysis, I next determined whether physical parameters significantly predicted the percentage of regenerated and degenerated fibres in older PLWH.

As described in **Table 7.14**, MET score was significantly associated with the proportion of degenerated fibres in the older PLWH (n = 30; r = 0.41; *p* = 0.025, **Spearmans's correlation**) (**Figure 7.43c**). Subsequently, in a multivariate linear regression model where the predictive value of MET score for the proportion of degenerated fibres was adjusted for age, the association between degenerated fibre proportion and MET score was demonstrated to be independent of the effect of age (unstandardised regression coefficient = 0.000078; *p* = 0.009, **multivariate linear regression**) (**Table 7.14**). Indeed, the overall model fit was statistically significant (*p* = 0.030) but was only predictive of a modest amount of variance in the percentage of degenerated fibres (r^2 = 0.29).

There were no other significant associations between physical parameters and either the percentage of regenerated (**Figure 7.42**) or degenerated fibres (**Figure 7.43**).

	% Regenerated fibres HIV+ (n = 30)		**% Degenerated fibres HIV+ (n = 30)**		
	r	***p***	**r**	***p***	**Age-adjusted *p***
FFP score^	-0.083	0.66	-0.21	0.26	-
SPPB score^	-0.19	0.31	0.32	0.081	-
MET score^	0.081	0.67	**0.41**	**0.025**	**0.009**
Grip strength (kg)	-0.20	0.47	0.30	0.10	-
ASMI (kg/m^2)	0.38	0.84	0.087	0.65	-

Table 7.14 – Physical factors predicting percentage regenerated and degenerated fibres in older PLWH. *Table depicting the associations between the percentage of regenerated and degenerated fibres, and various physical factors. Linear regression and correlation analysis was determined by Pearson's correlation for normally distributed data and Spearman's correlation for non-normally distributed data (denoted by ^).*

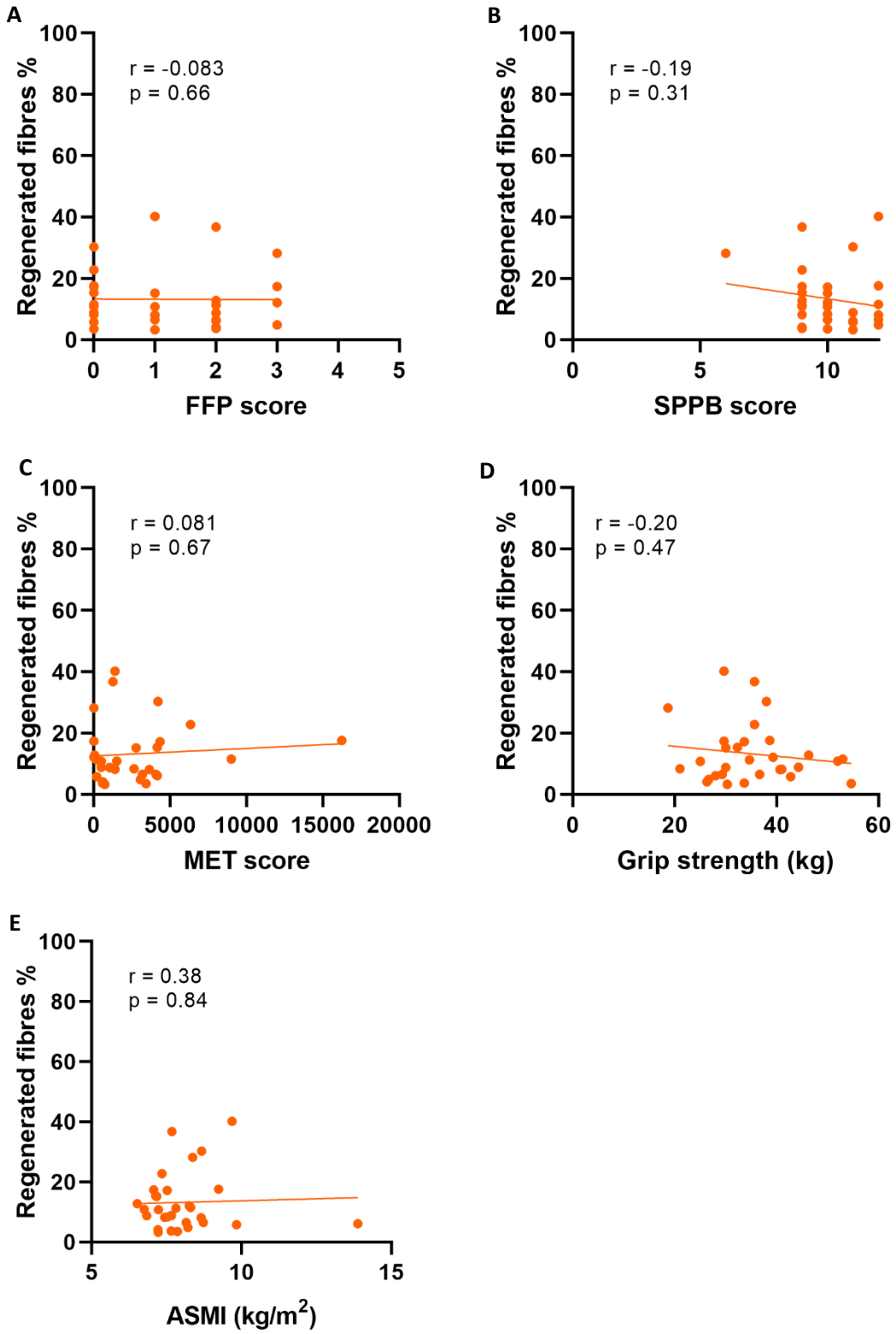

Figure 7.42 – Physical factors predicting percentage regenerated fibres. *Scatter plots depicting the linear regression between percentage regenerated fibres and (**A**) FFP score, (**B**) SPPB score, (**C**) MET score, (**D**) grip strength (kg), and (**E**) ASMI (kg/m²) in older PLWH (n = 30). Pearson's correlation was performed for parametric data (**D** and **E**), and Spearman's correlation was performed on non-parametric data (**A**, **B**, **C**). Each dot represents an individual patient.*

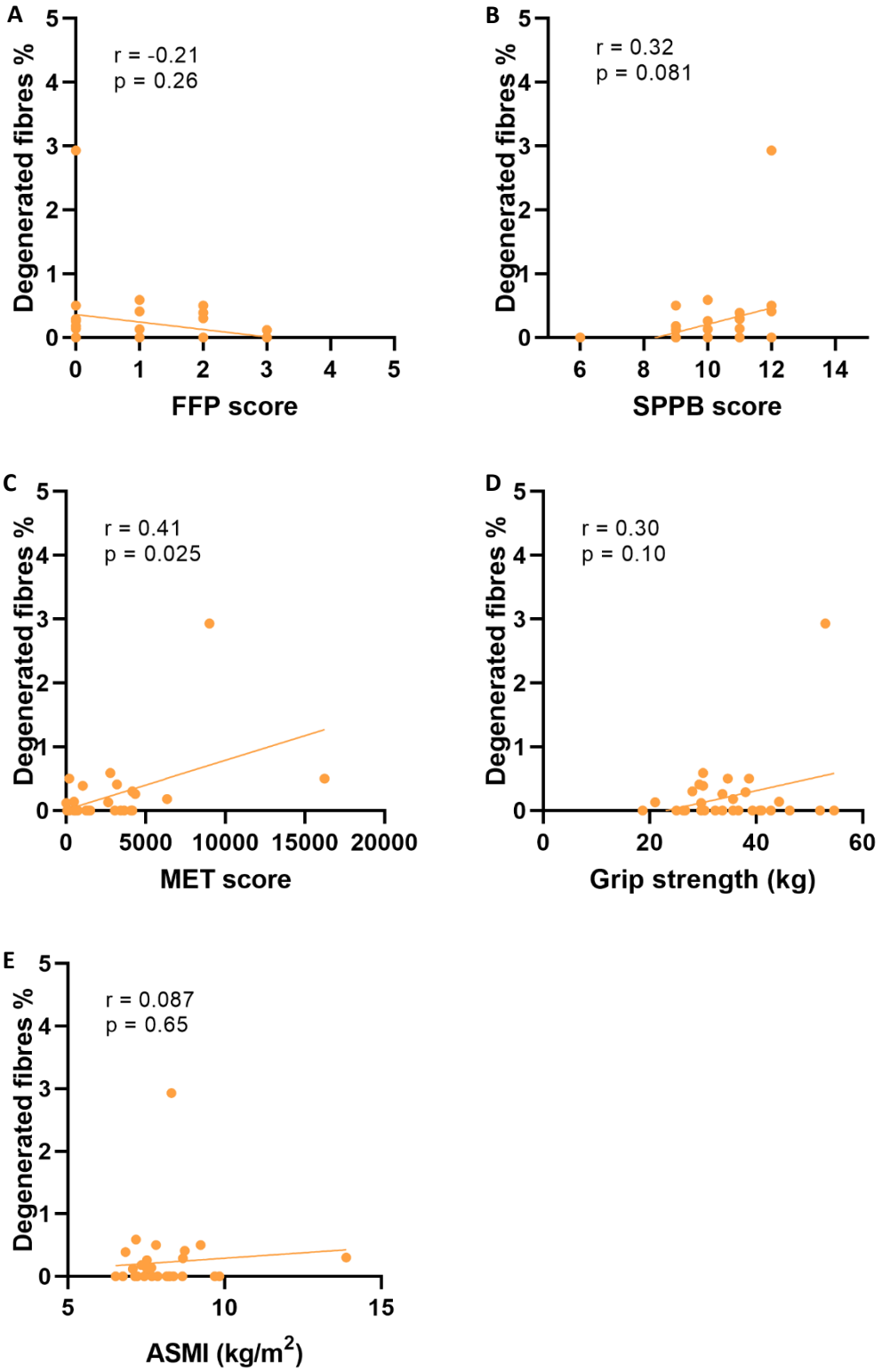

Figure 7.43 – Physical factors predicting percentage degenerated fibres. *Scatter plots depicting the linear regression between percentage degenerated fibres and (**A**) FFP score, (**B**) SPPB score, (**C**) MET score, (**D**) grip strength (kg), and (**E**) ASMI (kg/m²) in older PLWH (n = 30). Pearson's correlation was performed for parametric data (**D** and **E**), and Spearman's correlation was performed on non-parametric data (**A**, **B**, **C**). Each dot represents an individual patient.*

7.4.15.3 Pathophysiological skeletal muscle determinants of the percentage regenerated and degenerated fibres in older PLWH

Finally, linear regression analyses was performed in order to determine whether pathophysiological skeletal muscle factors significantly predicted the proportion of regenerated and degenerated fibres in older PLWH (**Table 7.15**).

Here, unadjusted linear regression analysis demonstrated that the proportion of regenerated fibres was significantly associated with average fibre CSA (r = 0.45, *p* = 0.014, **Pearson's correlation**) (**Figure 7.44a**), and predicted by the prevalence of Pax7$^+$ SCs (r = 0.52; *p* = 0.003) (**Figure 7.44b**), and skeletal muscle fibrosis (r = 0.59; *p* = 0.001) (**Figure 7.44c**).

Next, as these pathophysiological factors are linked with age, multivariate linear regression models were developed with the percentage regenerated fibres as the dependant variable, and age as well as either Pax7$^+$ SC prevalence, fibre CSA, or fibrosis percentage as the independent variables.

Firstly, multivariate linear regression analysis confirmed that the association between the percentage of regenerated fibres and fibre CSA was independent of the effect of age (unstandardised regression coefficient = 0.01; *p* = 0.016, **multivariate linear regression**) (**Table 7.15**), and that the overall model fit was statistically significant (*p* = 0.044). However, the model was predictive of a small amount of variation in the percentage of regenerated fibres (r^2 = 0.21).

Additionally, the association between the percentage of regenerated fibres and fibrosis was also independent of the effect of age in a model with fibrosis and age as the independent variables (unstandardised regression coefficient = 26.9; *p* = 0.001) (**Table 7.15**). The overall model fit was statistically significant (*p* = 0.003) and predictive of a modest amount of variation in the percentage of regenerated fibres (r^2 = 0.35).

Next, in a multivariate linear regression model with Pax7$^+$ SC prevalence and age as the independent variables, the association between the percentage of regenerated fibres and the prevalence of Pax7$^+$ SC was also independent of the effect of age (unstandardised regression coefficient = 20.87; *p* = 0.005) (**Table 7.15**). Again, the overall model fit was significant (*p* = 0.014), although predictive of only a small amount of variation in the percentage of regenerated fibres (r^2 = 0.27).

In univariate linear regression analysis, the proportion of degenerated fibres was significantly associated with the area covered by lipofuscin granules (r = -0.60; *p* = 0.001, **Pearson's correlation**) (**Figure 7.44d**). Next, a multivariate linear regression model with the percentage of degenerated fibres as the dependant variable and age as well as lipofuscin CSA as the independent variables, the significant association between degenerated fibres and lipofuscin CSA was independent of the effect

of age (unstandardised regression coefficient = -0.28; *p* = 0.001, **multivariate linear regression**) (**Table 7.15**). Again, the overall model fit was statistically significant (*p* = 0.003) and was predictive of a reasonably small amount of variation in the percentage of degenerated fibres (r^2 = 0.37).

	HIV+ (n = 30)					
	% Regenerated fibres			% Degenerated fibres		
	r	*p*	Age-adjusted *p*	r	*p*	Age-adjusted *p*
Type I %	-0.11	0.55	-	0.32	0.087	-
Type IIa %	-0.028	0.88	-	-0.31	0.098	-
Type IIx %	0.29	0.12	-	-0.19	0.30	-
Fibre CSA (μm^2)	**0.45**	**0.014**	**0.016**	0.34	0.064	**-**
Log_{10}(Pax7$^+$ SC)	**0.52**	**0.003**	**0.001**	0.031	0.87	**-**
Log_{10}(% BodipyAbn)	0.059	0.76	-	-0.067	0.73	-
Log_{10}(Lipofuscin CSA)$^+$	0.097	0.62	-	**-0.60**	**0.001**	**0.001**
Log_{10}(Lipofuscin frequency)$^+$	-0.006	0.93	-	-0.096	0.62	-
Log_{10}(% Fibrosis)	**0.59**	**0.001**	**0.005**	0.07	0.71	**-**

Table 7.15 – Skeletal muscle determinants of regenerated and degenerated fibre proportions*. Table depicting the associations between the percentage of regenerated and degenerated fibres and various skeletal muscle pathological factors. Linear regression and correlation analysis was determined by Pearson's correlation. Multivariate linear regression with adjustment for age was performed for determinant significantly associated through univariate regression analyses.+ = data missing from 1 patient. Statistically significant associations are bold.*

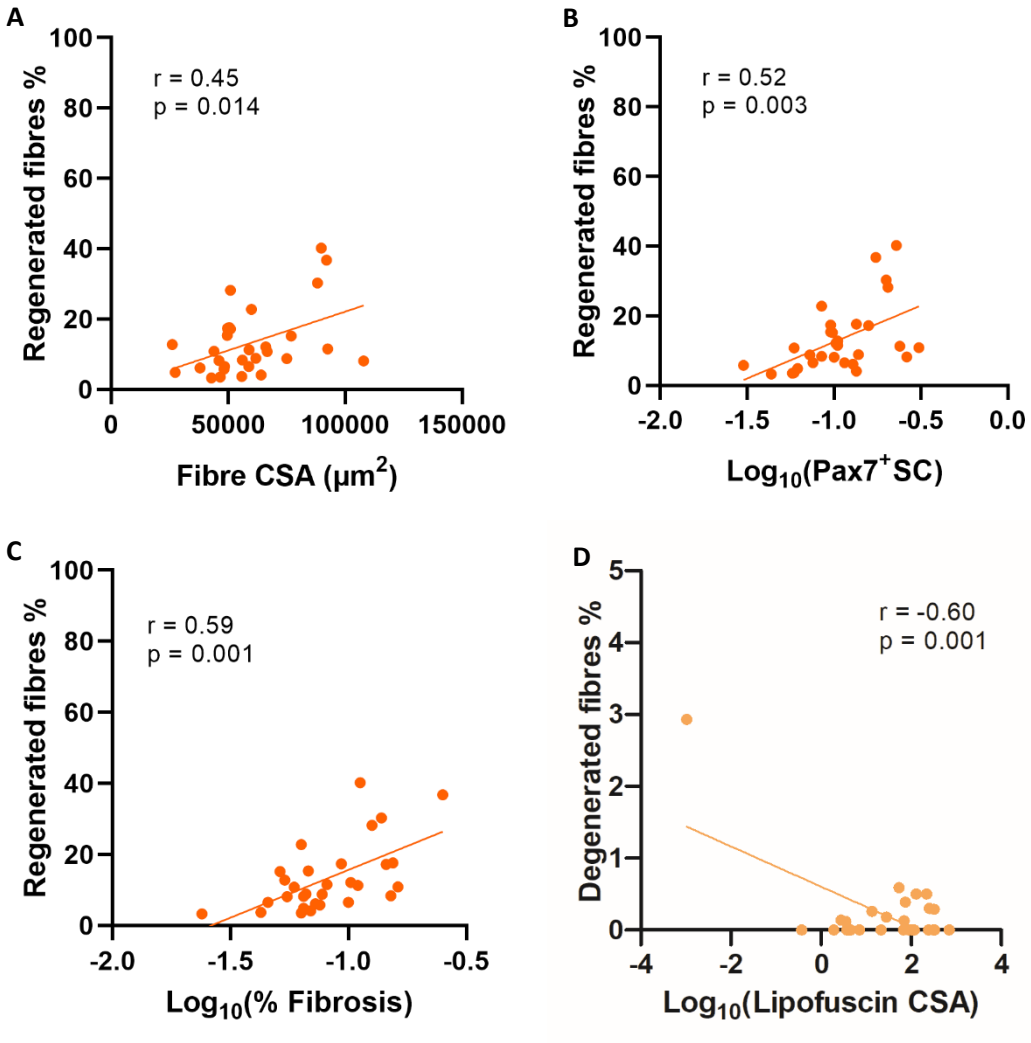

Figure 7.44 – Pathophysiological determinants of regenerated and degenerated fibres*. Scatter plots depicting linear regression analysis (Pearson's correlation) between the percentage of regenerated fibres and (**A**) fibre CSA (µm²), (**B**) log_{10}(Pax7⁺ SCs per 100 fibres), and (**C**) log_{10}(% fibrosis); percentage of degenerated fibres and (**D**) log_{10}(lipofuscin CSA (µm²)). Each dot represents an individual patient.*

7.4.16 Regenerated and degenerated fibre proportions in frail and sarcopenic older PLWH

Here, in order to better understand proportions of regenerated and degenerated fibres in frailty and sarcopenia in older PLWH, I grouped the HIV+ group (n = 30) into frail (n = 4), prefrail (n = 15), and robust PLWH (n = 11), as well as sarcopenic (n = 5), presarcopenic (n = 6), and non-sarcopenic PLWH (n = 19).

There was no significant difference in the proportion of either regenerated (p = 0.80, **one-way ANOVA**) (**Figure 7.45a**) or degenerated fibres (p = 0.42) between the frail, prefrail and robust groups (**Figure 7.45c**). There was also no significant difference in the proportion of either regenerated (p = 0.41) (**Figure 7.45b**) or degenerated fibres (p = 0.80) between the sarcopenia, presarcopenia or no-sarcopenia groups (**Figure 7.45d**).

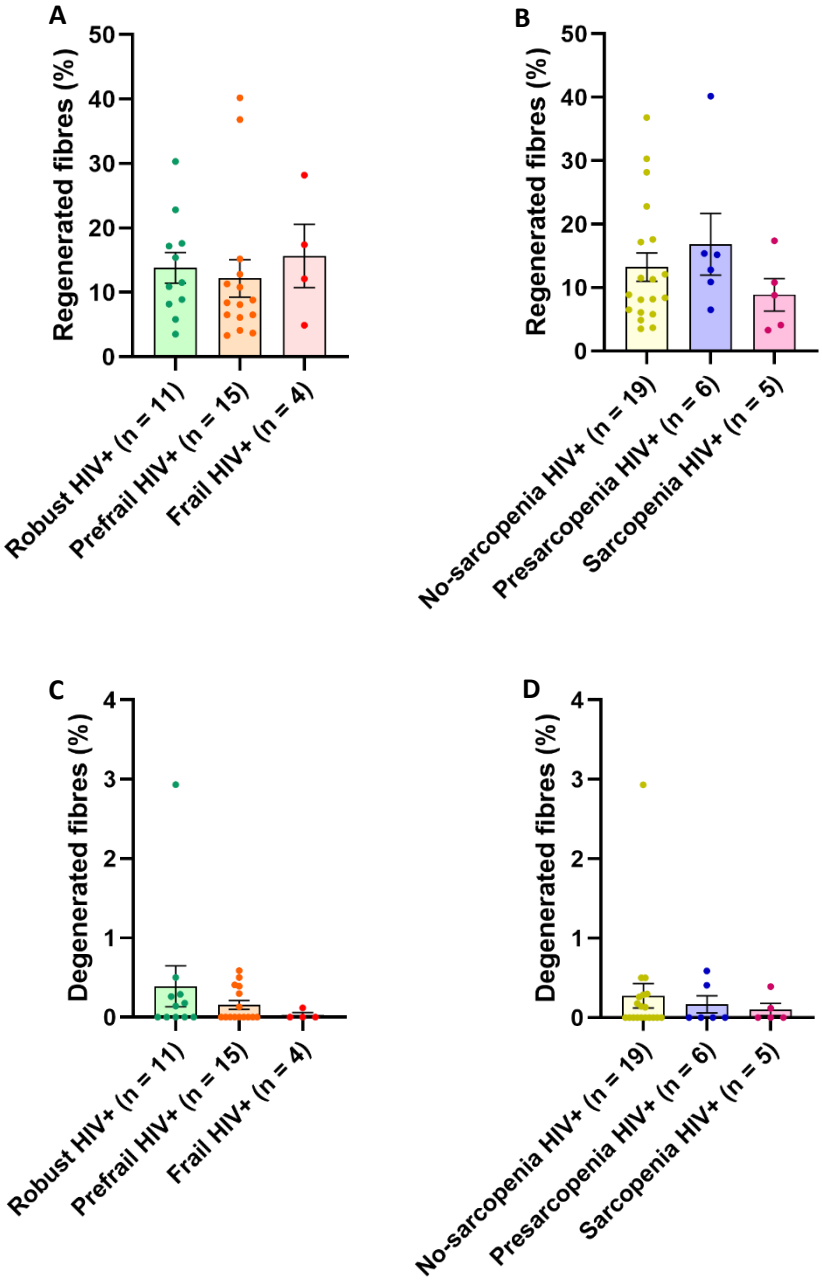

Figure 7.45 – Differences in the proportion of regenerated and degenerated fibres across the frailty and sarcopenia spectrum. *Dot plots (mean ± SEM) depicting no significant differences in the proportion of regenerated fibres between (**A**) frail (n = 4), prefrail (n = 15) and robust (n = 11) PLWH, or (**B**) sarcopenic (n = 5), presarcopenic (n = 6) and non-sarcopenic (n = 19) PLWH; no significant differences in the proportion of degenerated fibres between (**C**) frail, prefrail and robust PLWH, or (**D**) sarcopenic, presarcopenic and non-sarcopenic PLWH. Each dot represent an individual patient.*

Next, in an attempt to improve the power to detect differences between PLWH characterised by the adverse ageing phenotypes, I stratified the HIV+ group (n = 30) into frail/prefrail HIV+ (n = 19) and sarcopenic/presarcopenic HIV+ (n = 11) groups, as done in previous sections and studies (Kooij *et al*., 2016). I then determined if there were differences in the proportion of regenerated and degenerated fibres between the respective groups and robust HIV+ (n = 11) and non-sarcopenic HIV+ individuals (n = 19).

Here, there was no significant difference in the proportion of regenerated fibres between the frail/prefrail HIV+ group and the robust HIV+ group (p = 0.81, **unpaired t test**) (**Figure 7.46a**), or between the sarcopenia/presarcopenia HIV+ group and the no-sarcopenia HIV+ group (p = 0.99) (**Figure 7.46b**).

Additionally, there was also no significant difference in the proportion of degenerated fibres between the frail/prefrail HIV+ group (n = 19) and the robust HIV+ group (n = 11; p = 0.21, **unpaired t test**) (**Figure 7.46c**), or between the sarcopenia/presarcopenia HIV+ group (n = 11) and the no-sarcopenia HIV+ group (n = 19; p = 0.51) (**Figure 7.46d**).

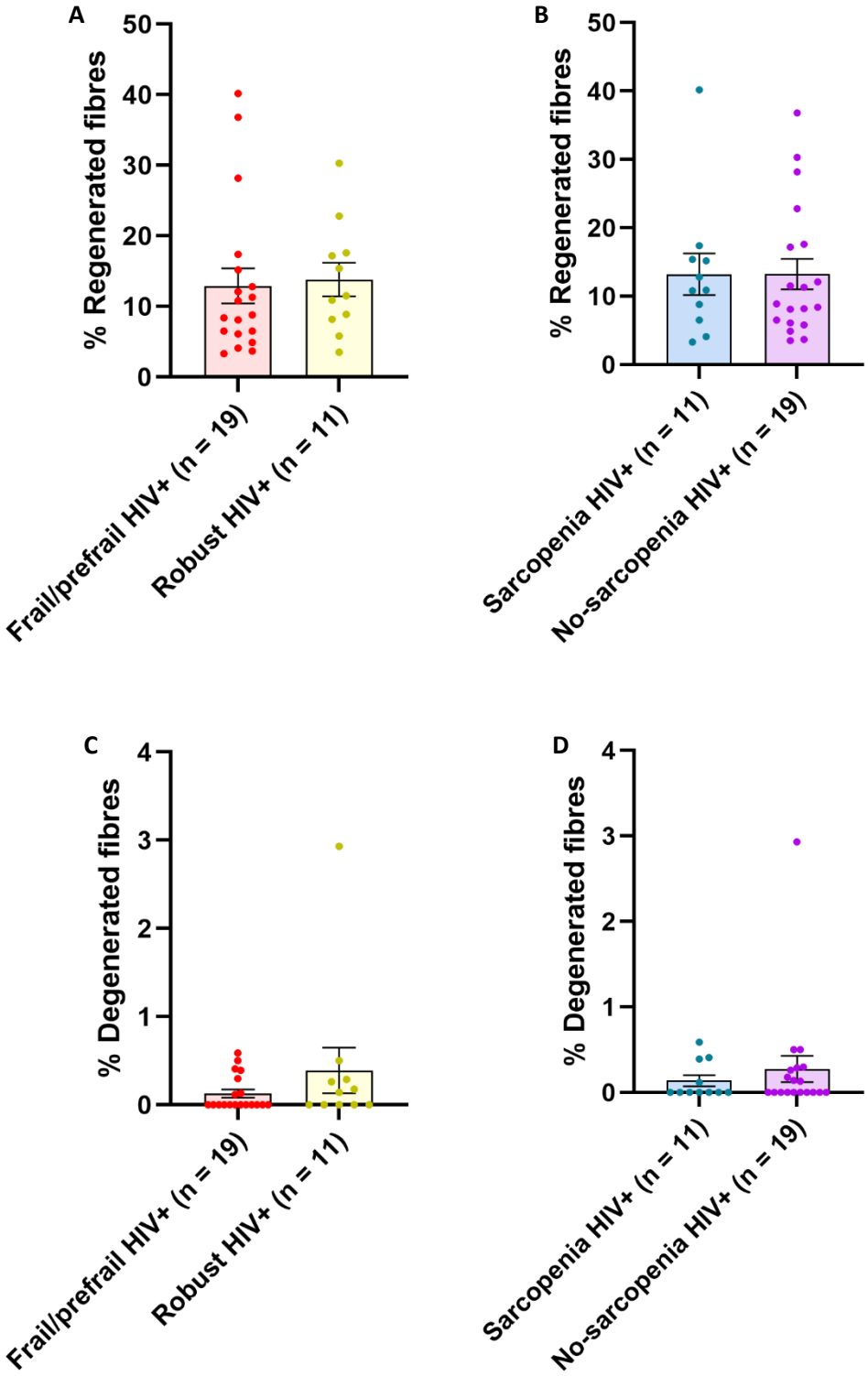

Figure 7.46 – Regenerated and degenerated fibres in adverse ageing phenotypes in older PLWH. *Dot plots (mean ± SEM) showing no significant difference in the proportion of regenerated fibres between (**A**) frail/prefrail PLWH (n = 19) and robust PLWH (n = 11), or (**B**) sarcopenic/presarcopenic PLWH (n = 11) and non-sarcopenic PLWH (n = 19); degenerated fibre proportion between (**C**) frail/prefrail PLWH (n = 19) and robust PLWH (n = 11), or (**D**) sarcopenic/presarcopenic PLWH (n = 11) and non-sarcopenic PLWH (n = 19).*

7.4.17 No difference in lipofuscin accumulation between older PLWH and HIV- individuals

Due to the autofluorescent nature of lipofuscin granules I was able to observe and quantify granules in 10µm skeletal muscle sections simply by air-drying, fixing, cover-slipping, and imaging the sections at two different wavelengths (546nm and 647nm). Unlike with antibody-targeting immunofluorescence in which a no primary control (NPC) can be used, the autofluorescence aspect of lipofuscin imaging means all imaged sections contain lipofuscin granules and so there are no NPCs. Therefore, lipofuscin granules were confirmed by co-localisation in both the 546 and 647 channels (**Figure 7.47**). Once imaged, I subsequently quantified the CSA (μm^2) covered by the lipofuscin granules as well as the frequency of granules per μm^2 for HIV+ (n = 29) and HIV- (n = 13) individuals. One subject from the HIV+ group and two from the HIV- group were excluded due to poor tissue quality.

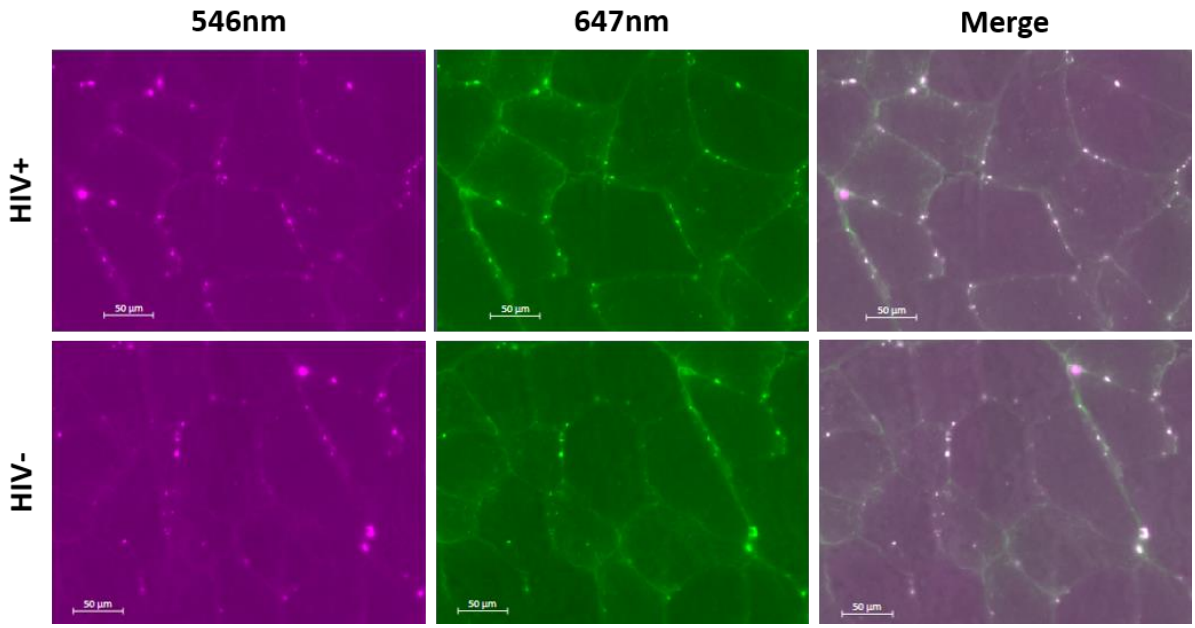

Figure 7.47 – Example fluorescence image of lipofuscin granules*. 10µm skeletal muscle sections from HIV+ and HIV- individuals were imaged at 546nm and 647nm channels and merged. Lipofuscin granules were confirmed by localisation in both channels. Scale bar = 50µm.*

For both the frequency and area of lipofuscin granules, data was normalised through log transformation.

Notably, neither the frequency (**Figure 7.48a**) nor area covered by lipofuscin granules (**Figure 7.48b**) was significantly different between the HIV+ and HIV- groups (**unpaired t tests**).

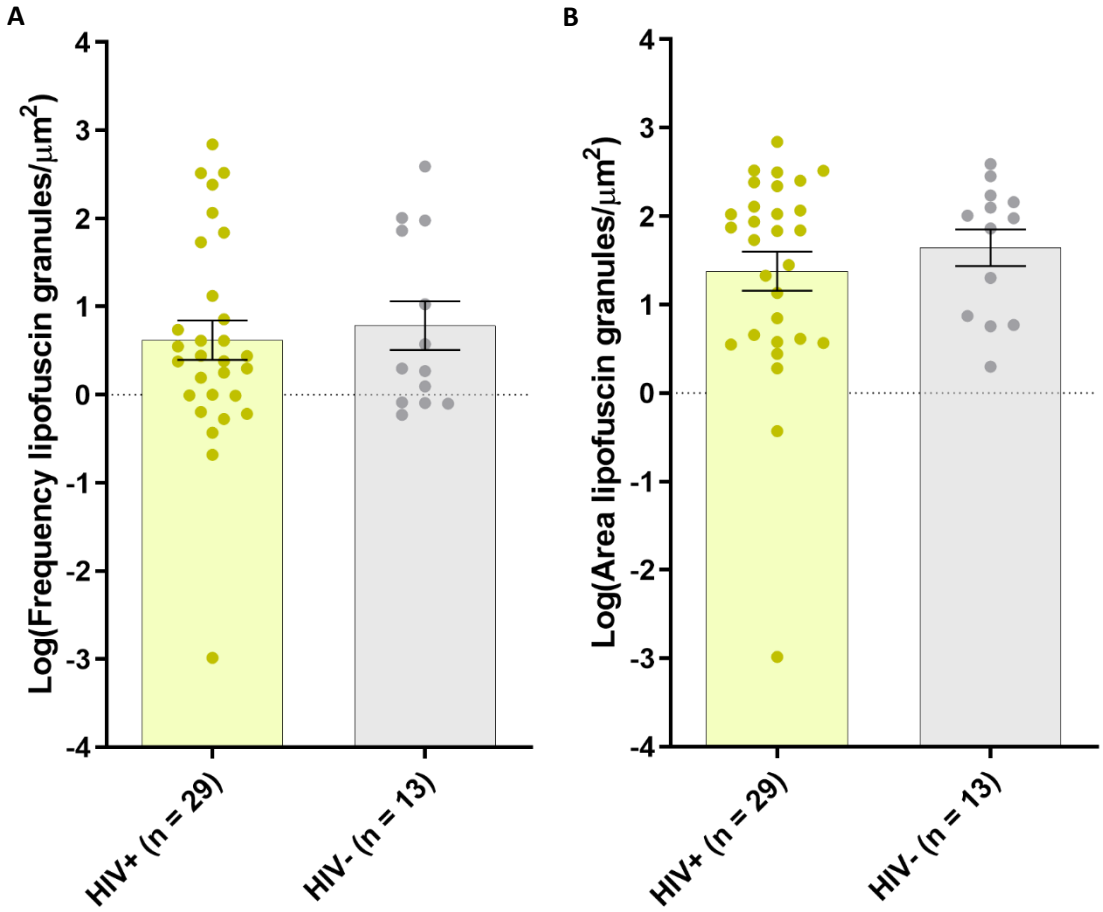

Figure 7.48 – No difference in proportional frequency of lipofuscin granules or proportional area covered by lipofuscin granules*. Dot plots (mean ± SEM) showing (**A**) no significant difference in the proportional frequency of lipofuscin granules between the HIV+ (n = 29) and HIV- (n = 13) groups; (**B**) no significant difference in proportional CSA (μm²) covered by lipofuscin granules. Each dot represents an individual patient.*

7.4.18 Determinants of lipofuscin accumulation

7.4.18.1 Clinical determinants of lipofuscin coverage in older PLWH

I next sought to assess whether the area covered by of lipofuscin granules was predicted by clinical parameters collected as part of the MAGMA study, such as HIV-related and clinical characteristics, body composition, and lifestyle factors (**Table 7.16**).

Here, in unadjusted regression analysis, the area covered by lipofuscin granules was significantly greater in PLWH with higher CD4 counts (r = 0.48; *p* = 0.012, **Pearson's correlation**) (**Figure 7.49e**). As lipofuscin accumulation is linked with age, a multivariate linear regression model was developed with lipofuscin CSA as the dependant variable, and age as well as CD4 count as the independent variables. Thus, multivariate linear regression confirmed that the significant association between lipofuscin area and CD4 count was independent of age (regression coefficient = 0.003; *p* = 0.012, **multivariate linear regression**) (**Table 7.16**). The overall fit of this model was statistically significant (*p* = 0.039) and was predictive of a small amount of the variation in lipofuscin CSA (r^2 = 0.24).

In addition, PLWH with polypharmacy had a significantly higher lipofuscin area than those who do not have polypharmacy (*p* = 0.044, **unpaired t test**) (**Table 7.16**). Finally, HIV+ smokers had a significantly higher area covered by lipofuscin granules compared to older PLWH who do not smoke (*p* = 0.012, **unpaired t test**) (**Table 7.16**).

	Log_{10}(Lipofuscin CSA (μm^2)) HIV+ (n = 29)		
	r	***p***	**Age-adjusted *p***
Age	-0.21	0.88	-
BMI (kg/m^2)	0.24	0.21	-
Waist circumference (cm)	0.21	0.28	-
# Comorbidities	0.13	0.51	-
# Medications	-0.092	0.64	-
Polypharmacy*	-	**0.044**	**-**
% Fat mass	0.18	0.36	-
% Lean mass	-0.18	0.36	-
Months since diagnosis	-0.076	0.69	-
Months on ART	-0.19	0.32	-
Months untreated	0.047	0.81	-
CD4 count (copies/µl)	**0.48**	**0.012**	**0.012**
Smokers*	-	**0.012**	-
Alcohol drinkers*	-	0.30	-
Recreational drug use*	-	0.37	-

Table 7.16 – Clinical predictors of lipofuscin accumulation in older PLWH. *Table depicting the associations between log_{10}(lipofuscin CSA) and various clinical factors. Linear regression and correlation analysis was determined by Pearson's correlation. * = ordinal data in which individuals were stratified by yes/no and differences determined by unpaired t test. Statistically significant associations are bold.*

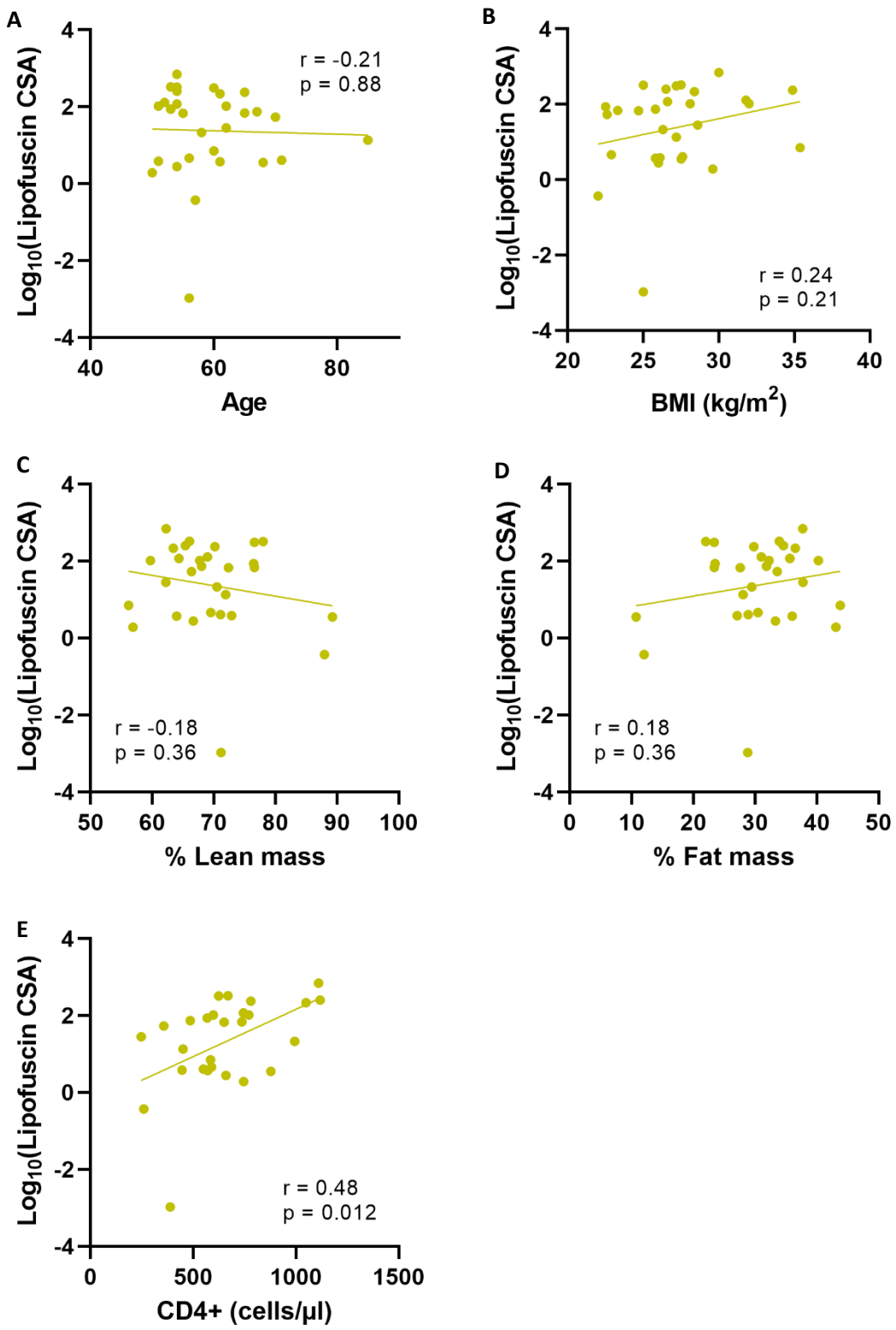

Figure 7.49 - Clinical determinants of lipofuscin accumulation*. Scatter plots depicting the linear regression (Pearson's correlation) between log_{10}(lipofuscin CSA) and (**A**) age, (**B**) BMI (kg/m^2), (**C**) percentage lean mass, (**D**) percentage fat mass, and (**E**) CD4 count (copies/µl) in older PLWH (n = 30). Each dot represents an individual patient.*

7.4.18.2 Physical determinants of lipofuscin accumulation in older PLWH

Next, I sought to determine whether physical parameters significantly predicted increased lipofuscin area in skeletal muscle from the HIV+ group (n = 30). Hence, unadjusted linear regression analysis was performed between lipofuscin area and physical function results (**Table 7.17**). In particular, Pearson's correlation was performed on normalised data sets whilst Spearman's correlation was performed on non-normalised data sets, which is denoted in **Table 7.17**.

Here, there was no significant association between the area covered by lipofuscin granules and any of the physical parameters such as FFP score, SSPB score or grip strength (**Figure 7.50**).

	Log_{10}(Lipofuscin CSA (μm^2))	
	HIV+ (n = 29)	
	r	***p***
FFP score^	-0.14	0.46
SPPB score^	0.20	0.31
MET score^	-0.30	0.11
Grip strength (kg)	-0.11	0.58
ASMI (kg/m^2)	0.22	0.24

Table 7.17 – Physical factors predicting lipofuscin CSA in older PLWH. *Table depicting the associations between log_{10}(lipofuscin CSA), and various physical factors. Linear regression and correlation analysis was determined by Pearson's correlation for normal data and Spearman's correlation for non-normal data (denoted by ^).*

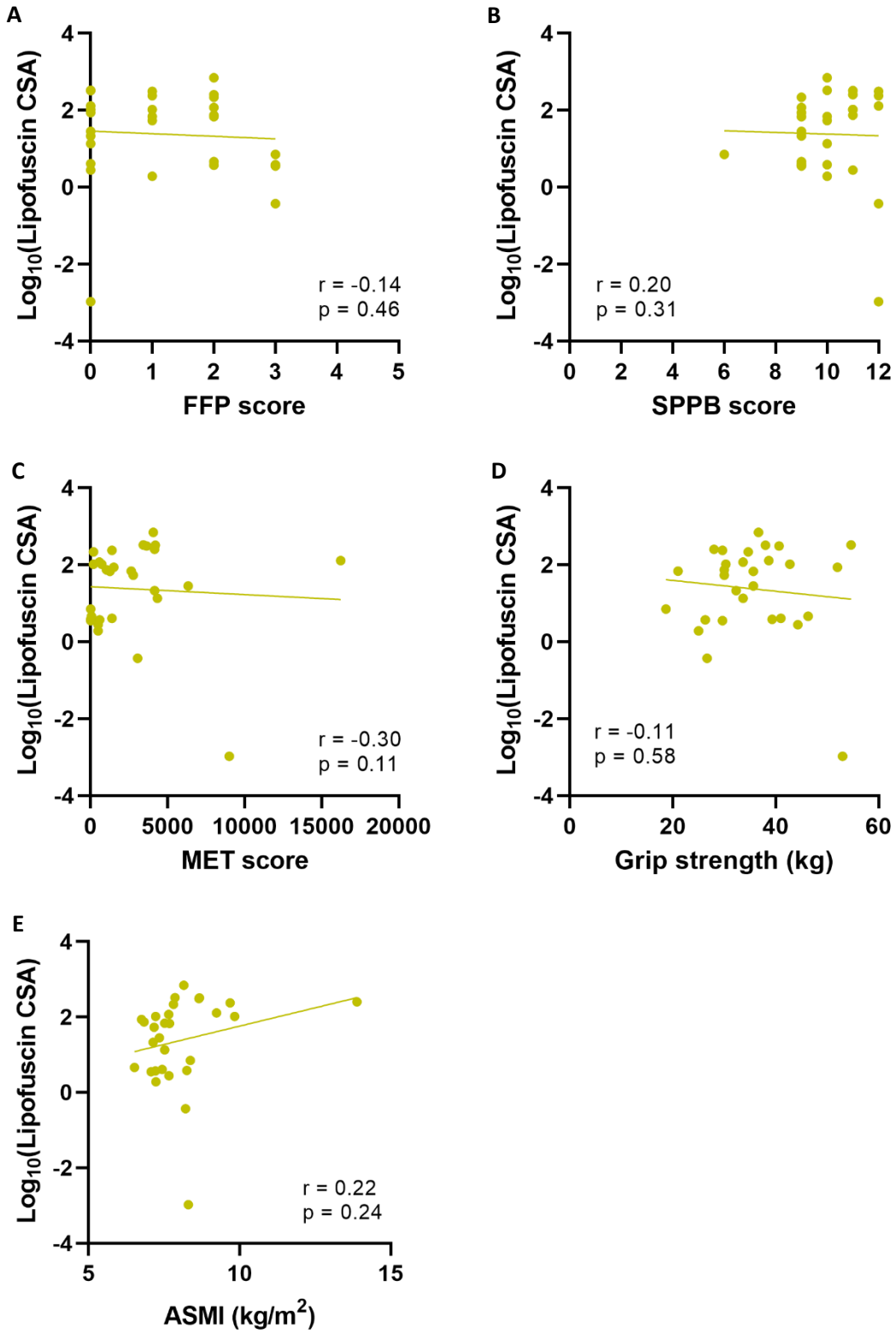

Figure 7.50 – Physical factors predicting lipofuscin accumulation. *Scatter plots depicting the linear regression between log_{10}(lipofuscin CSA (μm^2)) and (**A**) FFP score, (**B**) SPPB score, (**C**) MET score, (**D**) grip strength (kg), and (**E**) ASMI (kg/m^2) in older PLWH (n = 30). Pearson's correlation was performed on parametric data (**D** and **E**), and Spearman's correlation was performed on non-parametric data (**A**, **B**, **C**). Each dot represents an individual patient.*

7.4.18.3 Skeletal muscle pathophysiological determinants of lipofuscin accumulation in older PLWH

Finally, linear regression analysis was undertaken in order to determine whether any of the pathophysiological skeletal muscle factors previously discussed in this chapter significantly predicted an increased area covered by lipofuscin granules (**Table 7.18**).

As demonstrated in the previous sections (**Section 7.4.15.3**), lipofuscin CSA was significantly associated with a lower proportion of degenerated fibres (n = 29; r = -0.60; *p* = 0.001, **Pearson's correlation**) (**Figure 7.51**). Hence, another multivariate linear regression model was developed with lipofuscin CSA as the dependant variable and age, as well as percentage degenerated fibres as the independent variables. Here, the overall model fit was significant (*p* = 0.003) and was predictive of a reasonably modest amount of variation in lipofuscin CSA (r^2 = 0.37). Indeed, the association between lipofuscin CSA and the percentage of degenerated fibres remained significant independently of the effect of age (unstandardised regression coefficient = -1.30; *p* = 0.001, **multivariate linear regression**) (**Table 7.18**).

	Log_{10}(Lipofuscin CSA (μm^2)) HIV+ (n = 29)		
	r	***p***	**Age-adjusted *p***
Type I %	-0.025	0.90	-
Type IIa %	0.11	0.59	-
Type IIx %	-0.12	0.54	-
Fibre CSA (μm^2)	-0.001	0.99	-
Log_{10}(Pax7$^+$ SC)	0.052	0.79	-
Log_{10}(% BodipyAbn)	-0.008	0.97	-
% Regenerated fibres	0.097	0.62	-
% Degenerated fibres	**-0.60**	**0.001**	**0.001**
Log_{10}(% Fibrosis)	0.037	0.85	-

Table 7.18 – Skeletal muscle determinants of lipofuscin accumulation*. Table depicting the associations between the log_{10}(lipofuscin CSA) and various skeletal muscle pathophysiological factors. Linear regression and correlation analysis was determined by Pearson's correlation. Multivariate linear regression with adjustment for age was performed for determinants significantly associated through univariate regression analyses. Statistically significant associations are bold.*

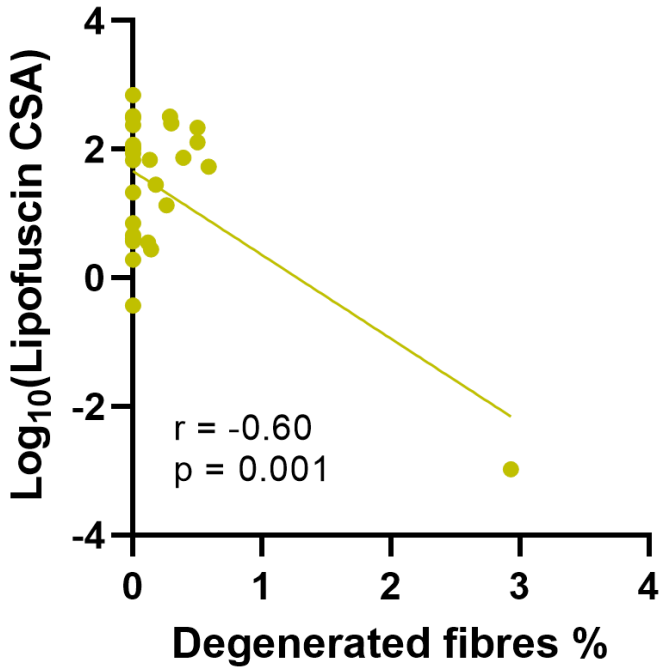

Figure 7.51 – Pathophysiological determinants of lipofuscin accumulation. *Scatter plot depicting linear regression analysis (Pearson's correlation) between log_{10}(lipofuscin CSA (μm^2)) and percentage degenerated fibres. Each dot represents an individual patient.*

7.4.19 Lipofuscin in adverse ageing phenotypes in older PLWH

To investigate whether there is increased skeletal muscle lipofuscin accumulation in older PLWH with adverse ageing phenotypes such as frailty and sarcopenia, I stratified the HIV+ group (n = 29) into frail (n = 4), prefrail (n = 14), and robust (n = 11) HIV+, as well as sarcopenic (n = 5), presarcopenic (n = 5), and non-sarcopenic (n = 19) HIV+ groups.

Here, there was no significant difference in the area covered by lipofuscin granules between frail, prefrail and robust individuals (p = 0.083, **one-way ANOVA**) (**Figure 7.52a**) or sarcopenic, presarcopenic and non-sarcopenic individuals (p = 0.77) (**Figure 7.52c**).

In addition, there was no significant difference in the frequency of lipofuscin granules between frail, prefrail and robust PLWH (p = 0.13) (**Figure 7.52b**), or between sarcopenic, presarcopenic and non-sarcopenic HIV+ individuals (p = 0.99) (**Figure 7.52d**).

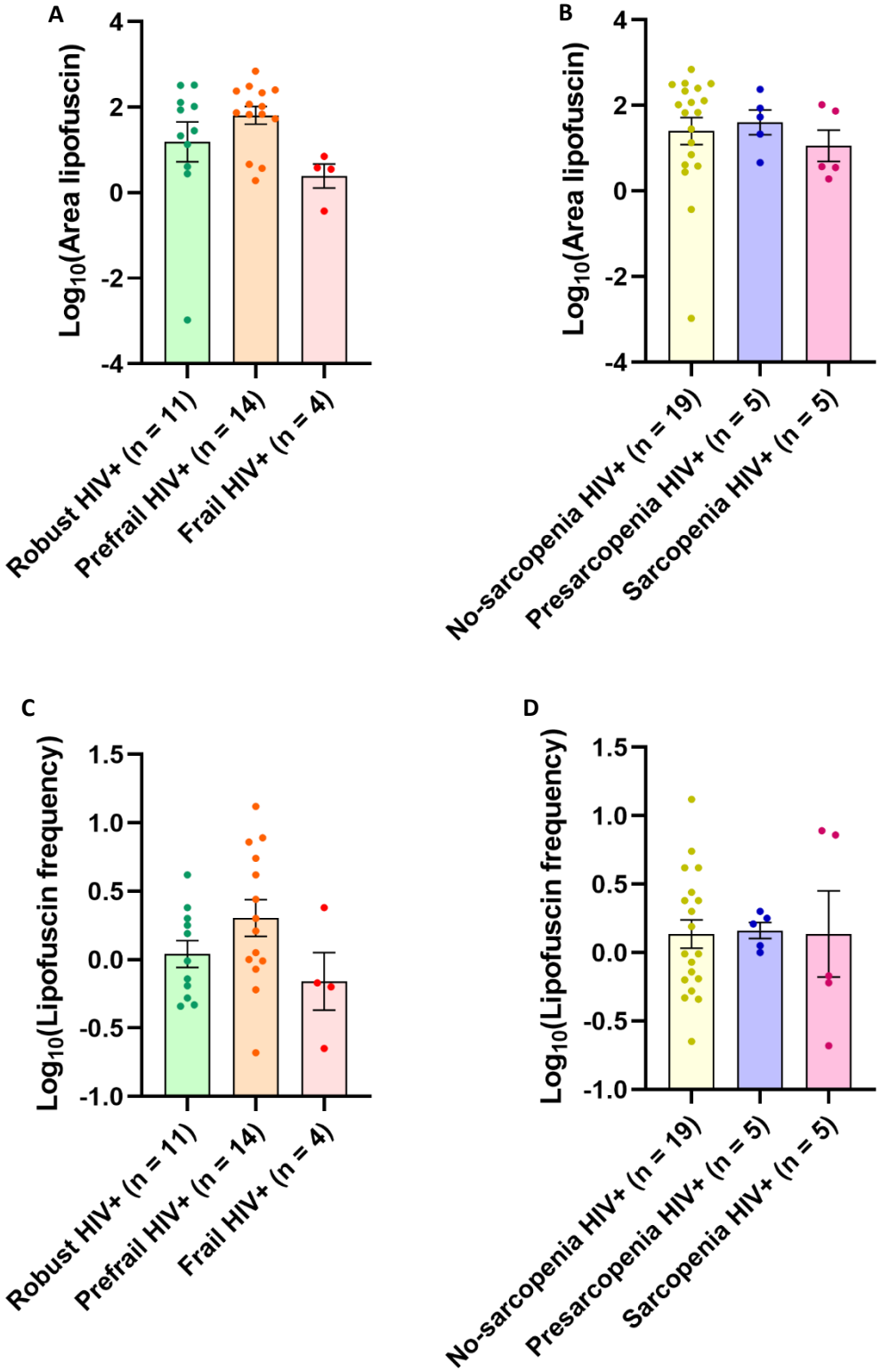

Figure 7.52 – Differences in lipofuscin accumulation across the frailty and sarcopenia spectrum in older PLWH. *Dot plots (mean ± SEM) showing no significant difference between frail (n = 4), prefrail (n = 14) or robust (n = 11) PLWH in either (**A**) log_{10}(lipofuscin CSA (µm²)) or (**C**) log_{10}(lipofuscin frequency); no significant difference between sarcopenic (n = 5), presarcopenic (n = 5) or non-sarcopenic (n = 19) PLWH in either (**B**) log_{10}(lipofuscin CSA (µm²)) or (**D**) log_{10}(lipofuscin frequency). Each dot represents an individual patient.*

Next, I further stratified the HIV+ group into frail/prefrail HIV+ (n = 18) and sarcopenic/presarcopenic HIV+ (n = 10) groups, and compared both the CSA covered by and frequency of lipofuscin granules in the respective groups against robust HIV+ (n = 11) and non-sarcopenic HIV+ individuals (n = 19).

Again, there was no significant difference in either the area covered by lipofuscin granules (p = 0.51, **unpaired t test**) (**Figure 7.53a**), or the frequency of lipofuscin granules (p = 0.37) (**Figure 7.53c**) between the frail/prefrail PLWH (n = 18) and robust PLWH (n = 10). Similarly, there was also no significant difference in the area covered by lipofuscin granules (p = 0.89) (**Figure 7.53b**) or frequency of lipofuscin granules (p = 0.94) (**Figure 7.53d**) between sarcopenic/presarcopenic PLWH (n = 10) and non-sarcopenic PLWH (n = 19).

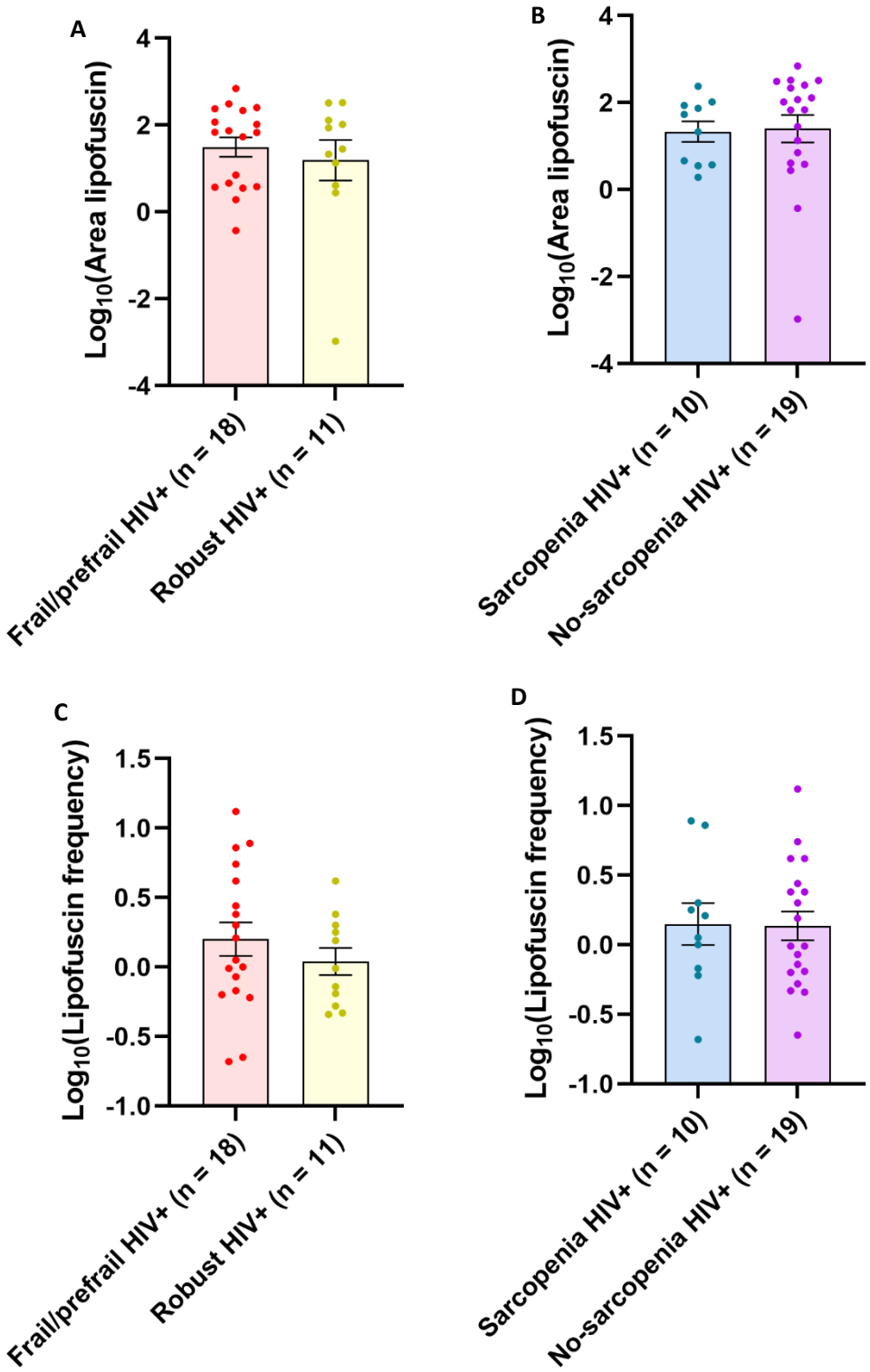

Figure 7.53 – Lipofuscin accumulation in adverse ageing phenotypes in older PLWH. *Dot plots (mean ± SEM) depicting no significant difference in log_{10}(lipofuscin CSA (μm^2)) between (**A**) frail/prefrail PLWH (n = 18) and robust PLWH (n = 11) and, (**B**) sarcopenic/presarcopenic PLWH (n = 10) and non-sarcopenic PLWH (n = 19); no significant difference in the frequency of lipofuscin granules between (**C**) frail/prefrail PLWH and robust PLWH and, (**B**) sarcopenic/presarcopenic PLWH and non-sarcopenic PLWH. Each dot represents an individual patient.*

7.4.20 Links between skeletal muscle mitochondrial dysfunction and pathophysiological skeletal muscle factors

Work undertaken in **Chapter 6** demonstrated that skeletal muscle mitochondrial dysfunction in the form of CI and CIV deficiency was significantly higher in older PLWH compared to age-matched HIV- individuals (**Section 6.4.2**). Here, I sought to assess whether skeletal muscle mitochondrial dysfunction significantly predicted any of the respective skeletal muscle pathophysiological factors previously discussed in this chapter. To this end, I performed linear regression analysis between proportional CI and CIV deficiency, as well as mitochondrial mass (represented as VDAC1 z-score) and the various respective skeletal muscle pathophysiological factors (**Table 7.19**).

Interestingly, proportional CI deficiency significantly predicted a lower percentage of type I fibres in older PLWH (n = 30; r = -0.39; *p* = 0.033, **Pearson's correlation**) (**Figure 7.54a**), as well as a greater percentage of type IIx fibres (r = 0.51; *p* = 0.004) (**Figure 7.54b**).

Subsequently, as both fibre type proportions and mitochondrial dysfunction are linked with age, I developed multivariate linear regression models with either the percentage of type I fibres or the percentage of type IIx fibres as the dependant variable and age, as well as proportional CI deficiency as the independent variables. Here, multivariate linear regression confirmed that the association between proportional CI deficiency and the lower percentage of type I was independent of the effect of age (unstandardised regression coefficient = -12.18; *p* = 0.018, **multivariate linear regression**) (**Table 7.19**). The overall model fit was marginally not significant (*p* = 0.055) and predicted only a small amount of variation in the percentage of type I fibres (r^2 = 0.19).

Next, another multivariate linear regression model with the percentage of type IIx fibres as the dependant variable, and proportional CI deficiency and age as the independent variables demonstrated that the association between the percentage of type IIx fibres and proportional CI deficiency was independent of the effect of age (unstandardised regression coefficient = 6.70; *p* = 0.003) (**Table 7.19**). The overall fit of this model was statistically significant (*p* = 0.012) although was only predictive of a small amount of variation in the percentage of type IIx fibres (r^2 = 0.28).

In addition, as the percentage of type IIx fibres was also significantly predicted by a higher number of comorbidities (**Section 7.4.9.1**), a multivariate linear regression model with the percentage of type IIx fibres as the dependant variable, and independent variables including age, proportional CI deficiency, and number of comorbidities was developed. Here, multivariate linear regression confirmed that the association between proportional CI deficiency and the percentage of type IIx fibres was independent of the effect of age and greater number of comorbidities (unstandardised

regression coefficient = 5.26; *p* = 0.013, **multivariate linear regression**) (**Table 7.20**). In addition, the association between percentage type IIx fibres and greater number of comorbidities remained significant after adjustment for age and proportional CIV deficiency (unstandardised regression coefficient = 0.26; *p* = 0.015) (**Table 7.20**). The overall fit of this model was statistically significant (*p* = 0.002) and predictive of a moderate amount of variation in the percentage of type IIx fibres (r^2 = 0.36).

Finally, proportional CIV deficiency significantly predicted a greater prevalence of quiescent $Pax7^+$ SCs (r = 0.49; *p* = 0.006, **Pearson's correlation**) (**Figure 7.54c**). Again, in a multivariate linear regression model with adjustment for age, the association between proportional CIV deficiency and $Pax7^+$ SC prevalence was demonstrated to be independent on the effect of age (unstandardised regression coefficient = 0.22; *p* = 0.009, **multivariate linear regression**) (**Table 7.19**). Here, the overall fit of this model was significant (*p* = 0.023) although was only predictive of a small amount of variation in $Pax7^+$ SC prevalence (r^2 = 0.24).

	HIV+ (n = 30)							
	CI abnormal			CIV abnormal			VDAC1 z-score	
	r	*p*	Age-adjusted *p*	r	*p*	Age-adjusted *p*	r	*p*
Type I %	**-0.39**	**0.033**	**0.018**	-0.17	0.82	-	-0.059	0.76
Type IIa %	0.21	0.27	-	0.009	0.96	-	0.030	0.88
Type IIx %	**0.51**	**0.004**	**0.003**	0.35	0.061	-	0.078	0.68
Fibre CSA (μm^2)	-0.14	0.47	-	-0.18	0.34	-	-0.18	0.35
Log_{10}(Pax7$^+$ SC)	0.29	0.12	-	**0.49**	**0.006**	**0.009**	-0.081	0.67
Log_{10}(% BodipyAbn)	0.050	0.79	-	0.19	0.31	-	0.024	0.90
% Regenerated fibres	0.19	0.32	-	0.056	0.77	-	0.018	0.93
% Degenerated fibres	0.086	0.65	-	0.11	0.56	-	0.088	0.64
Log_{10}(% Fibrosis)	0.10	0.59	-	0.32	0.085	-	-0.036	0.85
Log_{10}(Lipofuscin CSA)$^+$	-0.093	0.63	-	-0.067	0.73	-	0.031	0.87
Log_{10}(Lipofuscin frequency)$^+$	0.25	0.19	-	0.12	0.54	-	0.044	0.82

Table 7.19 – Skeletal muscle determinants of mitochondrial dysfunction*. Table depicting the associations between the proportion of log_{10}(CI abnormal), log_{10}(CIV abnormal) fibres, as well as average myofibre VDAC! Z-score, and various skeletal muscle pathological factors. Linear regression and correlation analysis was determined by Pearson's correlation. Multivariate linear regression with adjustment for age was performed for determinants significantly associated through univariate regression analyses.+ = data missing from 1 patient. Statistically significant associations are bold.*

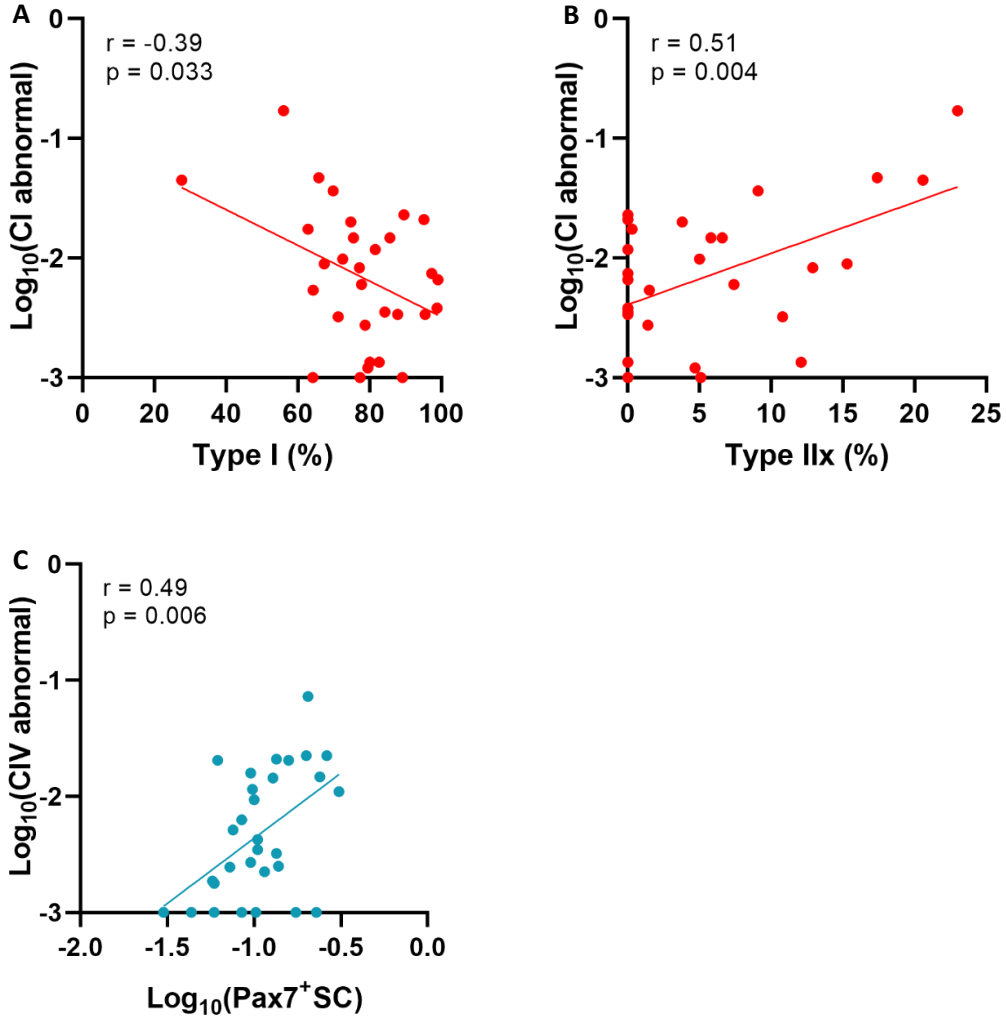

Figure 7.54 - Pathophysiological determinants of skeletal muscle mitochondrial dysfunction*. Scatter plot depicting linear regression analysis (Pearson's correlation) between log_{10}(CI abnormal) and (**A**) percentage type I fibres, and (**B**) percentage type IIx fibres; log_{10}(CIV abnormal) and log_{10}(Pax7^{+} SCs per 100 fibres). Each dot represents an individual patient.*

Dependant variable	Independent variables	Unstandardised regression coefficients			*p*		
		CI abnormal	Age	# Comorbidities	CI abnormal	Age	# Comorbidities
% Type IIx	Age, CI abnormal, # comorbidities,	**5.26**	-0.11	**2.60**	**0.013**	0.42	**0.015**

Table 7.20 – Fibre type IIx multivariate linear regression model*. Table depicting the dependant and independent variables, as well as the unstandardised regression coefficients and p value outputs from a multivariate linear regression model used to determine predictive factors of the percentage of type IIx fibres. Statistically significant results are bold.*

7.4.21 Is there a compensatory upregulation in myofibre regenerative capacity in older PLWH?

Pax7$^+$ SC prevalence was previously demonstrated to be predicted by mitochondrial dysfunction (in particular CIV deficiency) (**Section 7.4.20**), as well as the increased fibrosis in older PLWH (**Section 7.4.6.3**). This therefore suggests that muscle damage through both mitochondrial dysfunction and fibrosis may be stimulating a regenerative response, mediated by an increased prevalence of quiescent satellite cells. As such, through various multivariate linear regression analyses I next investigated the hypothesis that increased fibrosis and CIV deficiency was underpinning an upregulated skeletal muscle regenerative response in older PLWH.

Firstly, I wanted to determine whether a greater prevalence of Pax7$^+$ SCs was dependant on factors found to be significantly predicitive of Pax7$^+$ SC prevalence through unadjusted linear regression analysis. As such, a multivariate linear regression model was developed with Pax7$^+$ SC prevalence as the dependant variable and age, fibrosis, and proportional CIV deficiency as the independent variables. Here, the overall fit of the model was statistically significant (p = 0.002) and predicted a reasonably large amount of variation in Pax7$^+$ SC prevalence (r^2 = 0.37). Interestingly, a greater prevalence of Pax7$^+$ SCs was significantly predicted by proportional CIV deficiency independently of the effect of age and fibrosis (unstandardised regression coefficient = 0.16; p = 0.033, **multivariate linear regression**) (**Table 7.21**). In addition, Pax7$^+$ SCs prevalence was also significantly predicted by fibrosis independently of the effect of age and proportional CIV deficiency (unstandardised regression coefficient = 0.52; p = 0.007) (**Table 7.21**).

Next, I wanted to investigate whether a greater prevalence of regenerated fibres was directly predicted by an increased prevalence of Pax7$^+$ SCs, or whether other factors of muscle damage such as fibrosis independently predicted increased regeneration, irrespective of an increased prevalence of Pax7$^+$ SCs. As such, a multivariate linear regression model was developed with the percentage of regenerated fibres as the dependant variable and age, months untreated HIV infection, proportional CIV deficiency, fibrosis, and Pax7$^+$ SC prevalence as independent variables (**Table 7.22**). Of note, the proportion of degenerated fibres was not included in the model as it was not significantly predictive of the percentage of regenerated fibres.

Here, the overall fit of the model was statistically significant (p = 0.002), and was predictive of a large amount of variation in the percentage of regenerated fibres (r^2 = 0.52). Notably, a greater prevalence of regenerated fibres was indeed significantly predicted by a greater prevalence of Pax7$^+$ SCs independently of the effect of age, greater months untreated HIV infection, fibrosis, and CIV deficiency (unstandardised regression coefficient = 16.43; p = 0.041, **multivariate linear regression**)

(**Table 7.22**). In addition, increased fibrosis also significantly predicted a greater prevalence of regenerated fibres independently of the effects of age, CIV deficiency, months untreated HIV infection, and importantly, Pax7^{+} SC prevalence (unstandardised regression coefficient = 17.72; p = 0.037) (**Table 7.22**).

Dependant variable	Independent variables	Unstandardised regression coefficients			*p*		
		Age	CIV deficiency	Fibrosis	Age	CIV deficiency	Fibrosis
Pax7$^+$ SC	Age, fibrosis, proportional CIV deficiency	-0.002	**0.16**	**0.52**	0.70	**0.033**	**0.007**

Table 7.21 – Pax7$^+$ SC prevalence multivariate linear regression analysis model. *Table depicting the dependant and independent variables included in the multivariate model used to determine factors predictive of the prevalence of Pax7$^+$ SCs. Statistically significant data is bold.*

Dependant variable	Independent variables	Unstandardised regression coefficients					*p*				
		Age	CIV deficiency	Fibrosis	Pax7$^+$ SCs	Months untreated	Age	CIV deficiency	Fibrosis	Pax7$^+$ SCs	Months untreated
Percentage regenerated fibres	Age, Pax7$^+$ SCs, fibrosis, months untreated, proportional CIV deficiency	0.040	-5.30	**17.72**	**16.43**	0.030	0.83	0.093	**0.037**	**0.041**	0.11

Table 7.22 – Skeletal muscle regeneration multivariate linear regression analysis models. *Table depicting the dependant and independent variables included in the multivariate model used to determine whether Pax7$^+$ SC prevalence was directly responsible for skeletal muscle regeneration. Statistically significant data is bold.*

7.5 Discussion

Data on skeletal muscle pathophysiological factors in older (≥ 50 years) PLWH and age-matched HIV- individuals recruited as part of the MAGMA study was presented for the first time in this chapter.

Other studies conducted as part of the MAGMA study and discussed in previous chapters (**Chapter 5 and 6**) demonstrated that older HIV-infected males had a higher prevalence of adverse ageing phenotypes such as frailty and sarcopenia when compared to age and sex-matched HIV-uninfected individuals. In addition, these older HIV+ individuals had a significantly higher proportion of skeletal muscle mitochondrial dysfunction in the form of CI and CIV deficiency compared to the matched HIV- individuals.

However, as this skeletal muscle mitochondrial dysfunction did not appear to directly explain the observed frailty and sarcopenia in older PLWH, I wanted to investigate the effect of other pathogenic muscle factors that are known to be involved in the pathophysiology of age-related muscle decline, such as stem cell availability and intramyocellular lipid accumulation (Wu & Ballantyne, 2017; Collins *et al*., 2007; Sousa-Victor *et* al., 2014). Importantly, I also aimed to determine whether skeletal muscle mitochondrial dysfunction was predictive of any of these pathophysiological factors, and additionally whether any of these factors were implicated in frailty and sarcopenia in older PLWH.

7.5.1 Study findings

7.5.1.1 Insulin resistance and adverse ageing phenotypes in older PLWH

Initially, I sought to investigate the role of insulin resistance (IR) in adverse ageing conditions in older PLWH, as IR has been shown to be associated with physiological decline (Wu & Ballantyne, 2017; Phielix *et al*., 2012). Firstly, I assessed whether there were differences in skeletal muscle IR between the HIV+ and HIV- individuals. Here, by staining skeletal muscle sections with the fluorescent histochemical dye BODIPY (493/503), I quantified a surrogate for IR – IMCL – in both the HIV+ and HIV- individuals and found that there was no statistically significant difference in the proportion of IMCL between the respective serostatus groups. Importantly, this is the first study to demonstrate that there is no significant difference in IMCL at the individual myofibre level between older PLWH and age-matched HIV- individuals.

Next, I assessed whether exposure to particular ARV classes predicted IMCL. Surprisingly, PLWH who had been exposed to older, mitochondrially-toxic nucleoside reverse transcriptase inhibitors (NRTIs) had significantly lower IMCL than PLWH who had not been exposed to these ARVs. As zidovudine (AZT) and stavudine (d4T) in particular have been shown to be associated with fat redistribution

elsewhere in the body (Moyle *et al*., 2006; Jones *et al*., 2005; Glidden *et al*., 2018; Carr *et al*., 1999; Dragovic *et al*., 2014; Miller *et al.*, 2003; McComsey *et al*., 2016), I further stratified the HIV+ group into those who had been exposed to those two NRTIs and those who had not. Again, PLWH who had been exposed to these NRTIs had significantly lower IMCL compared to those who had not. This suggests that any potential abnormalities in fat distribution seen in PLWH exposed to these drugs did not contribute to an increased insulin resistance and IMCL accumulation in skeletal muscle, and exposure to these ARVs may in fact result in increased metabolism of fats in skeletal muscle. It is plausible that because these drugs cause loss of subcutaneous limb fat (lipoatrophy) (Innes *et al*., 2012), they might also reduce IMCL.

Finally, through unadjusted linear regression analysis I demonstrated that increased IMCL was not significantly predicted by any of the clinical, HIV-related, physical, or lifestyle factors assessed as part of the MAGMA study. Even though the average BMI of the HIV- group was significantly higher compared to the HIV+ group, this did not predict IMCL. In addition, IMCL was not significantly altered in PLWH with adverse ageing phenotypes such as frailty and sarcopenia, nor did skeletal muscle mitochondrial dysfunction appear to predict IMCL in the older HIV+ individuals. This was surprising as mitochondrial dysfunction is thought to be associated with IR (Kelley *et* al., 2002; Hwang *et* al., 2010; Heilbronn *et al*., 2007; Ritov *et al*., 2005; Phielix *et al*., 2008), which in turn is a risk factor for the age-associated decline in muscle function (Wu & Ballantyne, 2017). In addition, these results suggest that metabolic abnormalities do not significantly contribute to the pathophysiology of adverse ageing phenotypes in older PLWH, as they do in diabetics (Park *et al*., 2009; Cacciatore *et al*., 2013). As IR is associated with oxidative stress (Rains & Jain, 2011) and chronic inflammation (Patsouris *et al*., 2014), it would therefore be interesting to investigate whether there were differences in systemic, or skeletal muscle specific oxidative stress, as well as inflammatory markers between the HIV+ and HIV- groups.

7.5.1.2 Lipofuscin accumulation does not contribute to the pathophysiology of adverse ageing phenotypes in older PLWH

Another pathophysiological skeletal muscle factor assessed was lipofuscin accumulation. In the general population, age-associated skeletal muscle lipofuscin accumulation has been associated with declining muscle function through proteolytic mechanisms (Hutter *et al*., 2007; Sitte *et al*., 2000; Hohn *et al*., 2011; Sugano *et al*., 2006; Powell *et al*., 2005; Stroiken *et al*., 2004), and there are possible links to the causative role of age-associated mitochondrial dysfunction in this phenomenon (Terman & Brunk, 2006; Konig *et* al., 2016; Terman & Sandberg, 2002; Couve *et al*., 2012). As such, I quantified both the area covered by, and frequency of lipofuscin granules in both the HIV+ and HIV- individuals, and found that there was no significant difference in either parameter between the two

respective groups. In addition, older PLWH with the adverse ageing phenotypes of frailty and sarcopenia did not have a significantly different amount of either parameter compared to age-matched robust and non-sarcopenic PLWH respectively.

The discrepancy between my results and results from previous studies are possibly explained by the fact that I measured lipofuscin accumulation through the quantification of the area covered as well as by the frequency of lipofuscin granules, and imaged lipofuscin autofluorescence in two different channels. In contrast, the Hutter *et al*. (2007) study only measured lipofuscin by the raw autofluorescence intensity in one channel (488nm), and in only 6 individual fibres. The variation in participant ages was also much larger in the Hutter *et al*. (2007) study compared to this study.

Surprisingly, through unadjusted and age-adjusted linear regression analyses it was also demonstrated that an increased area covered by lipofuscin granules was significantly predicted by a higher CD4 count and a lower proportion of degenerated fibres. However, there was no significant association between lipofuscin accumulation and skeletal muscle mitochondrial dysfunction, again contradicting previous studies (Terman & Bunk, 2006).

Notably, this was the first study to investigate skeletal muscle lipofuscin accumulation in the context of ageing in HIV. As such, the demonstration that there was no significant difference either the area covered by or frequency of lipofuscin granules between older PLWH and age-matched HIV- individuals is novel.

7.5.1.3 Skeletal muscle CI deficiency predicts decreased fibre type conversion in older PLWH

In addition to IR and decreased stem cell prevalence, age-related changes in fibre type composition have previously been implicated in the age-associated decline in muscle function (Manini, 2011; Milijkovic *et al*., 2015). In particular, older individuals in the general population have lower proportions of the glycolytic fibre types IIa and IIx, and an increased prevalence in fibre type I proportions, which account for loss of muscle mass and strength with age (Brunner *et al*., 2007; Grimby, 1995; Murgia *et al*., 2017; Ubaida-Mohien *et al*., 2019; Roberts *et al*., 2018; Verdijk *et al*., 2009; 2010; 2012; 2014; McKay *et al*., 2012; 2013). Therefore, in both the HIV+ and HIV- groups, I quantified the proportions of the three fibre types, as well as their cross-sectional area, as this is also associated with muscle function (van Wessel *et al*., 2010; Frontera *et* al., 2000; Milijkovic *et al*., 2015). Whilst the proportion of type I fibres was higher than that of both types IIa and IIx fibres in both the HIV+ and HIV- groups, there was no significant difference in the proportions of the respective fibres types between the HIV+ and HIV- individuals themselves. In addition, there was no significant difference in average fibre cross-sectional area between the HIV and HIV- groups.

Importantly, this study is the first to investigate differences in fibre type proportions between older PLWH and age-matched HIV- individuals.

I then wanted to determine if altered proportions of any of the fibre types or average fibre cross-sectional area was linked to frailty or sarcopenia in older PLWH. Here, frail PLWH had a significantly higher proportion of type IIx fibres compared to both prefrail and robust PLWH, contradicting previous observations (St-Jean Pelletier *et* al., 2017; Sonjak *et al*., 2019).

Additionally, through unadjusted and age-adjusted linear regression analysis, the proportions of the fibre types were investigated in relation to the other pathogenic skeletal muscle factors, as well as clinical, physical, and lifestyle parameters. Here, it was also found that a higher average fibre cross-sectional area was significantly associated with the proportion of regenerated fibres, suggesting that those older PLWH with higher regenerative capacity have increased muscle mass and potentially therefore, muscle strength (Verdijk *et al*., 2007; van Wessel *et al*., 2010). In addition, individuals with a higher prevalence of comorbidities, as well as those prescribed with more medications, had a significantly higher proportion of type IIx fibres. Together, this suggests that increased age-related pathology in older PLWH may impair fibre type switching with age, potentially through increased chronic inflammation or poorer neuromuscular junction dynamics, leading to inadequate fibre type switching (D'Antona *et al*., 2003; Gonzalez-Freire *et al*., 2014). This therefore merits further investigation.

Interestingly, greater proportional skeletal muscle CI deficiency also appeared to predict a higher proportion of type IIx fibres, as well as a lower proportion of type I fibres through unadjusted and age-adjusted linear regression analysis. Further, multivariate linear regression models also demonstrated that greater proportional CI deficiency significantly predicted a lower percentage of type I fibres and a simultaneous increase in the percentage of type IIx fibres, independently of the effect of both age and a greater number of comorbidities. As type IIx fibres have a lower mitochondrial content compared to type I fibres, as well as the fact that type IIx fibres are glycolytic and type I fibres are oxidative (Murgia *et* al., 2019; Howald *et al*., 1985; Picard *et* al., 2012; Picard *et* al., 2008), these findings suggest that age-related skeletal muscle mitochondrial dysfunction may be preserving type IIx fibres from age-related atrophy. Conversely, these findings may also be suggestive of a phenomenon whereby instead type I fibres are preferentially selected for atrophy as a result of metabolic and functional decline (Murgia *et al*., 2017; Murgia *et* al., 2019). Unfortunately it was not possible to precisely determine which of these processes were occurring, or whether both were occurring in the older PLWH, and so further work is required.

7.5.1.4 Elevated skeletal muscle fibrosis does not directly contribute to the onset of adverse ageing phenotypes in older PLWH

Next, as age-associated mitochondrial dysfunction induces skeletal muscle apoptosis and potentially fibrosis (Marzetti *et al*., 2006; Powers *et al*., 2012), I investigated and compared the level of skeletal muscle fibrosis in both the older HIV+ and HIV- individuals. Notably, HIV+ individuals had a significantly higher level of skeletal muscle fibrosis compared to age-matched HIV- individuals. As this was a novel result, I undertook unadjusted and age-adjusted linear regression analysis in order to determine the factors that predicted this increased fibrosis in the older HIV+ individuals.

Surprisingly, greater fibrosis did not seem to be explained by any of the clinical, HIV-related, physical, or lifestyle factors assessed in the MAGMA study. Nor was fibrosis associated with skeletal muscle mitochondrial dysfunction. This later finding is surprising, as mitochondrial dysfunction is linked with increased skeletal muscle atrophy in the general population (Powers *et al*., 2012). However, atrophy is not solely dependent on fibrosis, and other factors not investigated in this study, such as inflammation, may be contributing.

Additionally, by stratifying the HIV+ individuals into whether they were frail/prefrail or sarcopenic/presarcopenic, and comparing levels of fibrosis against robust and non-sarcopenic PLWH, it was demonstrated that there was no significant difference in skeletal muscle fibrosis in PLWH with these adverse ageing phenotypes.

Importantly, as previously mentioned, fibrosis was significantly associated with a higher prevalence of Pax7^{+} SCs and regenerated fibres. In this circumstance, even though a greater prevalence of quiescent Pax7^{+} SCs allows for a greater regeneration potential in response to injury, there will be some abhorrent skeletal muscle healing that results in fibrosis (Mann *et al*., 2011).

7.5.1.5 Older PLWH with adverse ageing phenotypes did not have higher prevalences of regenerated or degenerated fibres compared to normal older PLWH

Loss of muscle mass is a contributing factor to the development of sarcopenia (Cruz-Jentoft *et* al., 2019), and the age-associated decline in muscle regenerative capacity contributes to both the decline in muscle mass and strength (Garcia-Prat *et al*., 2013; Li *et al*., 2019). Here, by subjecting muscle sections to H&E histochemistry, I determined the proportions of regenerated and degenerated muscle fibres in both the HIV+ and HIV- groups. Notably, HIV+ individuals had a significantly lower proportion of regenerated fibres when compared to the HIV- individuals. This is the first time this result has been demonstrated and this novel finding may be explained by the fact that greater duration (months) of untreated HIV infection was significantly predictive of a lower proportion of regenerated fibres in unadjusted and age-adjusted linear regression analysis. Here,

individuals with a greater duration of untreated HIV infection may be predisposed to residual chronic inflammation and immunosenescence, impairing muscle regenerative capabilities (Wilson & Sereti, 2013; Guaraldi *et al*., 2011).

As expected, the proportion of regenerated fibres was also significantly associated with the prevalence of Pax7$^+$ SCs as well as average fibre CSA in unadjusted and age-adjusted linear regression, supporting previous observations (Sambasivan *et al*., 2011). A higher percentage of regenerated fibres was also significantly predicted by fibrosis in unadjusted and age-adjusted linear regression. There were no other significant associations between the proportion of regenerated fibres and any of the clinical, HIV, physical, or lifestyle parameters. Overall, these findings suggest that older PLWH with a long duration of untreated HIV infection have a reduced regenerative capacity. This may be due to an impaired immune system and residual chronic inflammation (Wilson & Sereti, 2013; Guaraldi *et al*., 2011; Fornica *et al*., 2020).

Finally, there was no significant difference in either the proportion of regenerated, or degenerated fibres between PLWH with the adverse ageing phenotypes of frailty and sarcopenia, and those who did not have these adverse ageing phenotypes.

7.5.1.6 Potential compensatory mechanisms inducing the upregulation of skeletal muscle regenerative capacity in older PLWH

Another factor associated with declining muscle and physical function with age is the reduced prevalence of quiescent stem cells (Lopez-Otin *et al*., 2013; Verdijk *et al*., 2007). As such, I sought to investigate the prevalence of Pax7$^+$ satellite cells (SCs) in the older HIV+ and HIV- individuals.

Indeed, there was no statistically significant difference in Pax7$^+$ satellite cell prevalence between the two respective groups. This result is this first demonstration that there is no significant difference in the prevalence of quiescent skeletal muscle stem cells between older PLWH and age-matched HIV- individuals.

I next sought to determine whether the prevalence of Pax7$^+$ SCs was significantly predicted by any of the clinical, HIV-related, or lifestyle parameters. As such, through unadjusted linear regression analysis it was shown that none of these factors significantly predicted the prevalence of Pax7$^+$ SCs. Additionally, linear regression analysis also determined that Pax7$^+$ SC prevalence was not subsequently predictive of physical function or indeed that Pax7$^+$ SC prevalence was significantly different in frail/prefrail or sarcopenic/presarcopenic PLWH compared to robust or non-sarcopenic PLWH.

However, it was determined through unadjusted and age-adjusted linear regression analysis that mechanisms of skeletal muscle damage in the form of mitochondrial dysfunction (specifically CIV deficiency) and fibrosis were both significantly predictive of a greater prevalence of Pax7$^+$ SCs in older PLWH. Indeed, in a multivariate linear regression model developed to determine the predictive value of both CIV deficiency and fibrosis independently of age and the other respective factor, both factors remained statistically significant after adjustment.

Interestingly, as mentioned previously, both increased fibrosis and prevalence of regenerated myofibres were significantly predicted by an increased prevalence of Pax7$^+$ SCs independently of age in older PLWH. Additionally, a higher proportion of regenerated fibres was also significantly predicted by a greater prevalence of Pax7$^+$ SCs following adjustment for the effect of other factors shown to be predictive of fibre regeneration, such as age, greater months untreated HIV infection, fibrosis, and CIV deficiency. Finally, a greater percentage of regenerated fibres was also significantly predicted by increased fibrosis after adjustment for age, months untreated, CIV deficiency, and stem cell prevalence – further supporting the idea that muscle damage is stimulating regeneration.

Altogether, these findings are strongly suggestive of phenomenon in older PLWH whereby both fibrosis and mitochondrial dysfunction are independently inflicting muscle damage, which is subsequently stimulating the compensatory increase in quiescent satellite cell prevalence. However, this increased prevalence of Pax7$^+$ SCs is leading to increased levels of both normal muscle healing, via the regeneration of myofibres, as well as abhorrent healing, in the form of fibrosis formation. This would indicate a reduction in the functional efficiency of Pax7$^+$ SCs in older PLWH, as the Pax7$^+$ SC pool is not necessarily depleted (Sacco *et al*., 2010; Attia *et al*., 2017; Dumont *et al*., 2015). Indeed, elevated residual chronic inflammation as the result of HIV infection may be contributing to this phenomenon (Wanschitz *et al*., 2013; McKay *et al.,* 2013; Rudnicki *et al*., 2008; Collins *et al*., 2007; Yang *et al*., 2011; Conboy *et al*., 2005; Merritt *et al*., 2013). In addition, exhaustion of satellite cells could be due to continued activation in response to muscle damage, as is the case in studies of Duchenne Muscular Dystrophy using the *mdx* mouse model (Lu *et al*., 2014; Sacco *et al*., 2010). Indeed, it is likely that chronic inflammation is a primary driver of continued SC activation and exhaustion (Fornica *et al*., 2020). This therefore requires further investigation.

Finally, as none of fibrosis, the percentage of regenerated fibres, or the prevalence of Pax7$^+$ SCs was significantly different in frail/prefrail or sarcopenic/presarcopenic PLWH compared to robust and non-sarcopenic PLWH, this would suggest that none of these factors are directly responsible for the greater prevalence of adverse ageing conditions seen in PLWH compared to age-matched HIV-individuals. Altogether, these findings subsequently suggest that the proposed compensatory

upregulation in regenerative capacity may not be fully efficient, but is functional enough to attenuate the onset of adverse ageing in PLWH. Indeed, as mentioned several times previously throughout this thesis, it also suggests that other factors known to be present in ART-treated PLWH, such as elevated chronic inflammation or immune senescence, are likely to be playing a significant causative role in age-related pathogenesis.

Importantly, these findings could have significant clinical and therapeutic relevance, as they suggest that age-related muscle decline could potentially be attenuated in older PLWH through exercise regimens (Lo *et al*., 2020; Zampieri *et al*., 2015; Marzetti *et al*., 2008; Rowe *et al*., 2014; Walston *et al.*, 2018; Cameron *et al*., 2013; Silva *et al*., 2017; Li *et al*., 2019). Notably, these findings also support recent studies which have suggested that the transplantation of functional Pax7$^+$ SCs may be beneficial in preventing declining muscle function (Yang *et al*., 2017; Berberoglu *et al.,* 2017).

7.5.1.7 Study conclusions

In conclusion, whilst there were several key age-associated pathogenic skeletal muscle parameters that were significantly altered in older HIV+ individuals compared to age-matched HIV- individuals, such as increased skeletal muscle fibrosis and the decreased proportion of regenerated fibres, only a greater proportion of type IIx fibres appeared to be directly linked to the adverse ageing phenotype of frailty, whilst none were linked to sarcopenia in older PLWH.

Interestingly however, results from this chapter did demonstrate the presence of some potential compensatory regenerative mechanisms in older PLWH. Here, a higher prevalence of quiescent Pax7$^+$ SCs was significantly predicted by both increased proportional CIV deficiency and skeletal muscle fibrosis, suggesting a compensatory upregulation in the stimulation of regeneration. Normally, this increased prevalence of quiescent Pax7$^+$ SCs would consequently then induce increased muscle healing. However, as the increased prevalence of quiescent Pax7$^+$ SCs was significantly predictive of both fibre regeneration and abhorrent healing in the form of increased fibrosis, this would instead suggest that regenerative mechanisms are not fully efficient in older PLWH – most likely to a decline in Pax7$^+$ SC function. Importantly though, as there was not a significantly lower level of quiescent Pax7$^+$ SCs or regenerated fibres in frail and sarcopenic PLWH, these findings together suggest that the attempted compensatory upregulation in muscle regeneration in response to muscle damage is attenuating the pathogenic decline in muscle function and onset of adverse ageing phenotypes in older PLWH. However, these findings do not explain the exact mechanisms behind this compensation. Hence, as chronic inflammation is known to be linked to declining muscle function with age (Perandini *et al*., 2018), as well as the fact that inflammation is

known to regulate stem cell function (McKay *et al.,* 2013; Rudnicki *et al*., 2008; Collins *et al*., 2007; Yang *et al*., 2011; Conboy *et al*., 2005) this should be investigated in future studies.

Another interesting finding was that, through investigations into the proportions of skeletal muscle fibre types, it was demonstrated that mitochondrial dysfunction in the form of CI deficiency significantly predicted a greater proportion of type IIx fibres, independently of the number of comorbidities, as well as a decrease in the proportion of type I fibres. Importantly, the proportion of type IIx fibres was significantly higher in frail PLWH compared to prefrail and robust PLWH. Taken together, as the age-related decrease in the proportion of glycolytic type IIx fibres is associated with declining muscle function (Brunner *et al*., 2007; Grimby, 1995; Murgia *et al*., 2017; Ubaida-Mohien *et al*., 2019; Roberts *et al*., 2018; Verdijk *et al*., 2009; 2010; 2012; 2014; McKay *et al*., 2012; 2013), as well as frailty and prefrailty (St-Jean Pelletier *et* al., 2017; Sonjak *et al*., 2019), these results indicate that another compensatory mechanism could also involve attenuated fibre type switching in response to age-related mitochondrial dysfunction, ultimately slowing down the onset of adverse ageing phenotypes. Alternatively, these findings could also suggest that declining skeletal muscle mitochondrial function may induce the selective atrophy of type I fibres in older PLWH. To better understand this phenomenon, other factors such as chronic inflammation, oxidative stress, immune senescence, and neuromuscular junction decline should be investigated in order to better understand these pathophysiological mechanisms.

The design of the MAGMA study, in particular the range of clinical parameters and skeletal muscle factors investigated, has meant that several novel observations have been made. Of note, this is the first study to simultaneously investigate whether physical parameters such as percentage fat mass or MET score are associated with pathogenic factors such as IMCL or stem cell availability in the context of HIV in ageing. In addition, whether HIV-related clinical parameters such as CD4 count or duration on antiretroviral therapy contributed to these pathogenic factors was also investigated for the first time.

Importantly, the utilisation of a novel immunofluorescence assay which objectively quantifies mitochondrial mass as well as CI and CIV deficiency at the individual myofibre level (Rocha *et al*., 2015) afforded the ability to investigate the role skeletal muscle mitochondrial dysfunction plays in these pathophysiological mechanisms. Whilst previous studies have demonstrated that mitochondrial dysfunction is present in some virally-supressed PLWH (Cote *et* al., 2002; Payne *et* al., 2011; Martin *et* al., 2013; Morse *et* al., 2012; McComsey *et* al., 2008; Samuels *et al*., 2017; Lewis & Dalkas, 2003), this is the first study to assess whether mitochondrial dysfunction is implicated in the

pathophysiology of age-associated skeletal muscle decline and adverse ageing phenotypes in older PLWH.

	Older PLWH	Older HIV- individuals	Conclusions
IMCL	• Comparable to HIV- individuals • No associations with clinical parameters • No difference between frail and robust, or sarcopenic and non-sarcopenic PLWH • Not predicted by mitochondrial dysfunction • ARV regimen did not predict increased IMCL	• Comparable to HIV+ individuals	• IMCL was not significantly different in HIV+ and HIV- individuals • IMCL did not appear to contribute to adverse ageing phenotypes
Quiescent Pax7$^+$ SC prevalence	• Comparable to HIV- individuals • Predictive of age-adjusted fibrosis and regenerated fibre percentage • No difference between frail and robust, or sarcopenic and non-sarcopenic PLWH • Predicted by age-adjusted CIV deficiency and fibrosis, independently of various other pathophysiological factors	• Comparable to HIV+ individuals	• Pax7$^+$ SC prevalence was not significantly different in HIV+ and HIV- individuals • No difference between frail and robust, or sarcopenic and non-sarcopenic PLWH • CIV deficiency appeared to predict greater Pax7$^+$ SC prevalence independently of age-related pathophysiologic factors
Fibre type proportions and fibre CSA	• Comparable to HIV- individuals • Frail PLWH had higher levels of type IIx fibres than prefrail and robust PLWH • Type I percentage was negatively predicted by age-adjusted CI deficiency • Type IIx percentage predicted by age-adjusted CI deficiency, number of comorbidities, and number of medications • Fibre CSA predicted by age-adjusted percentage of regenerated fibres	• Comparable to HIV+ individuals	• Fibre type prevalence and fibre CSA was not significantly different in HIV+ and HIV- individuals • Frail PLWH had higher levels of type IIx fibres than prefrail and robust PLWH • CI deficiency appeared to predict increased type IIx prevalence and decreased type I prevalence, potentially attenuating frailty and sarcopenia onset • Proposed decrease in fibre type switching in response to mitochondrial dysfunction
Fibrosis	• Greater fibrosis than in HIV- individuals • No difference between frail and robust, or sarcopenic and non-sarcopenic PLWH • Predicted by age-associated regenerated fibres and Pax$^+$ SC prevalence • Not predicted by mitochondrial dysfunction	• Significantly lower than in HIV+ individuals	• HIV+ had higher skeletal muscle fibrosis • No difference between frail and robust, or sarcopenic and non-sarcopenic PLWH

Regenerated fibres	• Lower prevalence than in HIV- individuals • No difference between frail and robust, or sarcopenic and non-sarcopenic PLWH • Predicted by months untreated HIV infection, Pax7^{+} SC prevalence, and fibrosis after age-adjustment • Predicted by Pax7^{+} SC prevalence and fibrosis after adjustment for age-related pathophysiological factors • Associated with higher fibre CSA • Not predicted by mitochondrial dysfunction	• Significantly greater than in HIV+ individuals	• HIV+ individuals had a lower prevalence of regenerated fibres • No difference between frail and robust, or sarcopenic and non-sarcopenic PLWH • Fibre regeneration induced by muscle damage in the form of fibrosis • Proposed compensatory upregulation in regenerative capacity
Lipofuscin accumulation	• Comparable to HIV- individuals • No difference between frail and robust, or sarcopenic and non-sarcopenic PLWH • Not predicted by mitochondrial dysfunction • Associated with decreased degenerative fibre prevalence	• Comparable to HIV+ individuals	• Lipofuscin accumulation was not significantly different in HIV+ and HIV- individuals. • No difference between frail and robust, or sarcopenic and non-sarcopenic PLWH • Lipofuscin accumulation did not appear to contribute to adverse ageing phenotypes
Involvement of mitochondrial dysfunction	• Predicted age-adjusted increase in type IIx and decrease in type I percentage • Predicted age-adjusted increase in Pax7^{+} prevalence	• Not investigated	• Appeared to predict a decline in age-related fibre type switching • Predicted compensatory upregulation in stem cell prevalence
Potential pathophysiological mechanisms behind adverse ageing phenotypes in older PLWH	Two distinct potential compensatory mechanisms: 1. Mitochondrial dysfunction predicts a decline in age-related fibre type switching 2. Upregulation in regenerative capacities in response to skeletal muscle damage, in which fibrosis and mitochondrial dysfunction are involved. However, this compensatory regenerative response may not be fully efficient. • Both mechanisms appear to be underpinned by age-related factors not investigated in the present study, such as chronic inflammation		

Table 7.23 – Summary of experimental findings.

7.5.2 Limitations

Whilst this study has several novel aspects, it is limited in the fact that it is not a longitudinal study. An important aspect of this study was the large data set and several parameters assessed, as no previous studies have been able to combine all these parameters. However, this limited the ability to recruit a large cohort. As a result of this, it is difficult to extrapolate whether several of the pathogenic skeletal muscle factors such as mitochondrial dysfunction or increased fibrosis are a consequence or causal factor of the increased prevalence of adverse ageing phenotypes in the HIV+ group. It is acknowledged though that due to the comprehensive nature of tissue acquisition outlined in the study manual, repeated study visits may be difficult to achieve. Additionally, variability in repeat muscle sections would restrict the validity of several muscle biopsies being taken.

Whilst the HIV+ and HIV- groups are well matched for age, another limitation lies in the fact that the two groups are not perfectly matched in body composition. Notably, the HIV- individuals had a higher average BMI and mean percentage fat mass than the HIV+ group. It is not clear whether this was largely explained by differences in lifestyle factors between the groups or whether HIV-associated changes in fat metabolism are implicated. BMI and malnutrition have been shown to affect the onset and progression of frailty in PLWH (Erlandson *et al*., 2017a; Onen *et al*., 2009), although BMI did not however seem to be predictive of any outcome measures in this study. In response, future studies should look to better match the body compositions of the experimental groups. As a low daily protein intake is associated with an increased susceptibility to developing frailty, another potential alteration to the study protocol could have been the addition of a food dairy (Bartali *et al*., 2006).

Importantly, although our cohort size of 45 is large enough to allow us to get a reasonably firm understanding of the cellular and pathophysiological mechanisms underpinning frailty and sarcopenia in HIV+ individuals, a larger cohort size would increase the power afforded to us to make more detailed within-group observations. In addition, our cohort was solely made up of males, as older (≥ 50 years) males are less heterogeneic than older females (Kennedy *et al.,* 2014), as well as the fact that there is a much larger population of older HIV-infected males as opposed to females in the UK, and especially in the North East (Public Health England, 2019). The fact that the MAGMA study recruited majority middle-aged individuals (50-65 years) also meant that the ability to potentially predict the age of onset of adverse ageing phenotypes was more restricted. Hence, future studies should look to study females. In addition, a wider range of age should be included, especially enriching for old (≥65 years) individuals.

7.5.3 Future work

Whilst this study has many novel aspects, there is scope for additional work to be conducted in order to better answer the study's experimental aims. As mentioned above, any future studies should aim to be longitudinal cohort studies. In addition, the sample size should increase and should ideally include younger and old (≥65 years) individuals, in addition to middle-aged (50-65 years) individuals. This would allow for the better understanding of the trajectories of adverse ageing conditions in PLWH, as well as allowing us to better test our compensatory mechanism hypotheses. In addition, HIV+ and HIV- females from various age ranges should be included.

One of the most immediate areas of future work would be to perform proteomics or genomics on individual muscle fibres or homogenate tissue, with a keen interest in comparing the signatures of HIV+ vs HIV- individuals, frail vs robust HIV+ subjects, and individual fibres from HIV+ subjects with mitochondrial dysfunction vs fibres with normal mitochondrial function. This work would expand on several significant recent proteomic and genomic studies done in isolated muscle fibres (Murgia *et al*., 2019) and would completement the existing experimental work.

An additional recent advance being pioneered by our lab is the use of multiplex imaging mass cytometry (IMC) (Warren *et al*., 2020). Here, instead of being limited to four or five channels in which to immunofluorescently stain muscle sections, IMC would allow the simultaneous staining and imaging of up to 40 channels. Any IMC work should be preceded by the proteomic or genomic work, as this will allow us to identify any additional proteins or genes of interest.

One of the interesting findings of this study was that muscle damage in the form of mitochondrial dysfunction and fibrosis were predictive of an increased prevalence of Pax7^{+} SCs. However, whilst this led to increased fibre regeneration, it also predicted a further increase in the formation of tissue fibrosis – indicating a possible defect in Pax7^{+} SC functional efficiency (Sacco *et al*., 2010; Attia *et al*., 2017; Dumont *et al*., 2015). As such, in order to further investigate this phenomenon, investigations should be undertaken into Pax7^{+} SC function in older PLWH. As it would be difficult to fully recapitulate the heterogeneity of older PLWH in mouse models such as the *mdx* mouse model or in *in vitro* studies (Lu *et al*., 2014; Sacco *et al*., 2010), other markers of muscle regeneration, such as MyoD and Myf5 should be investigated in muscle biopsies from older PLWH (Tedesco *et al*., 2010; Almada & Wagers, 2016).

One of the primary research interests of this study was to better understand the role of mitochondrial dysfunction in adverse age-related complications such as frailty and sarcopenia in older PLWH. In this study I utilised a novel assay which allowed us to quantify protein levels of

OXPHOS complexes and mitochondrial mass in individual fibres (Rocha *et al*., 2015). There are however several other experimental methods that could be used to better understand the mitochondrial function in our patients (Hunt & Payne, 2020; Fraizer *et al*., 2020). These include quantifying mitochondrial OXHPOS capacity through physiological assessments such as ^{31}P-MRS. Additionally, specific functions of mitochondria known to be adversely affected by ART and ageing itself such as fission and fusion dynamics, calcium handling, signalling pathway activity, or mitochondrial morphology can be assessed through a range of cellular assays and electron microscopy imaging. In particular, as mitochondrial biogenesis and particularly PGC-1α are involved in fibre type switching (Liu *et al*., 2016), it would be of interest to investigate this specifically. At the molecular level, whole exome sequencing (WES) could be used to screen for pathogenic mtDNA mutations (Taylor *et al*., 2014), or alternatively qPCR and long-range PCR can be used to better assess mtDNA mutations (Hunt & Payne, 2020).

As chronic immunosenescence and other immune system alterations are significantly implicated in the pathology of adverse age-related complications (Dihn *et al*., 2019), future flow cytometry work, with the aim of assessing the cohorts' immune profile, should be conducted. This would complement the existing experimental analyses and allow us to comprehensively assess its role in the majority of pathophysiological factors underpinning adverse age-related complications. In addition, it would be of interest to assess various mitochondrial parameters such as mitochondrial mass or OXPHOS capabilities in certain immune cell subsets of interest.

Another important factor involved in the decline of muscle function with age is increased muscle denervation (Pannerec *et al*., 2016; Morat *et al*., 2016; Always *et al*., 2017). Indeed, as neuromuscular junction decline is associated with deregulated fibre type switching (Gonzalez-Freire *et al*., 2014), and the findings in this study demonstrated a potential alteration in fibre type switching in older PLWH, these investigations would be of interest. In addition, as alluded to previously, general interest in this area has increased over recent years and so it would be interesting to assess whether frail HIV+ individuals have greater levels of muscle denervation compared to robust HIV+ individuals or HIV- individuals.

As both chronic inflammation and oxidative stress at both the systemic and skeletal muscle level have been associated with adverse ageing through a variety of mechanisms (Soysal *et al*., 2016; Leng *et al*., 2007), another interesting aspect of potential future work would be to investigate these factors. Unfortunately, both of these factors are difficult to experimentally investigate at the individual myofibre level, and so homogenate tissue or plasma studies would most likely be conducted.

Finally, as a proxy for a larger cohort size, collaborators at University College London (UCL) possess a database and tissue resource for several thousand PLWH. Ideally, once the future work mentioned above is completed and pathologically defined ageing phenotypes are identified, it is hoped that I can utilise this database and resource to further validate our findings.

Chapter 8 – TDF-induced mitochondrial dysfunction in proximal convoluted tubules

8.1 Introduction

Prior to the advent of ART, HIV-associated kidney disease (HIVAN) was one of the most prevalent comorbidities associated with HIV infection itself (Phair & Palella, 2011; Choi *et al*., 2010; Swanepoel *et al*., 2018). However, ART drastically reduced the onset of HIVAN in PLWH (Ross & Klotman, 2002; Lucas *et al*., 2004; Swanepoel *et al*., 2018), reports of tissue-specific drug-induced toxicities surfaced.

With regard to nephrotoxicities, acute kidney injury (AKI), nephrolithiasis, tubulopathies, and chronic kidney disease (CKD) were reported in virally supressed PLWH (Izzedine *et al*., 2004, Peyriere *et* al., 2004; Izzedine *et al*., 2009, Wong *et al*., 2017; Guaraldi *et al*., 2011). Although the exact pathophysiological mechanisms underpinning these ART-induced nephrotoxicities are yet to be completely understood, it is well regarded that there are multiple potential mechanisms including direct and indirect tubular toxicity, and the precipitation of insoluble drug crystals, and that mitochondrial dysfunction is thought to play a significant role in these pathophysiological mechanisms (Kohler *et al*., 2009; Ramamoorthy *et al*., 2014; Hall, 2011; Zhao *et al*., 2017; Ramamoorthy *et al*., 2018; Samuels *et al*., 2017; Murphy *et al*., 2017).

Although several ARVs of varying classes, including the PI atazanavir (ATV) (ritonavir-boosted) (Ryom *et al*., 2013), have been shown to contribute to the onset of some nephrotoxicities, the NRTI tenofovir has been consistently implicated in several nephrotoxicities occurring in PLWH (Thigpen *et al*., 2012; Gupta *et al*., 2014; Jotwani *et al*., 2016; Hertlitz *et al*., 2010; Samuels *et al*., 2017; Scherzer *et al*., 2012; Winston *et al*., 2006; Ryom *et al.,* 2013; Poizot-Martin *et al*., 2013; Atta *et al*., 2006; Foy *et al*., 2013; Woodward *et al*., 2009; Hamzah *et al*., 2017; Mocroft *et al*., 2016).

Therefore, in this pilot study I sought to better understand the role of mitochondrial dysfunction in nephrotoxicities in TDF-treated PLWH.

8.1.1 Causes and pathology of tenofovir-induced nephrotoxicity

Tenofovir (TFV) disoproxil fumarate (TDF) is a newer oral-prodrug NRTI produced in 2001 in order to overcome issues of earlier NRTIs such as difficult dosing schedules and several tissue-specific adverse effects (Gilead Sciences Inc, 2001). Clinical trials and early *in vitro* studies demonstrated the

advantages of TDF's efficiency, tolerability, convenient dosing, and low toxicity compared to older NRTIs, and as a result TDF is now one of the most commonly used NRTIs in cART (Jimenez-Nacher *et al*., 2008, Izzedine *et al*., 2004; Nelson *et al*., 2007). In fact, a large cohort study of 10,343 TDF-treated PLWH demonstrated that less than 1% of patients developed adverse renal effects after 4 years of use (Nelson *et al*., 2007). Various other cohort studies have calculated that prior to 2008, the incidence of TDF-induced AKI ranged from 1.6 per 100 individuals to 1.5 per 1000 individuals (Antoniou *et al*., 2005; Madeddu *et al*., 2008).

Initial concerns about the potential nephrotoxicity of TDF arose due to its structural similarity to the two acyclic nucleotide analogue drugs adefovir and cidofovir, which are used to treat hepatitis B and cytomegalovirus (CMV) infection (Gallant *et al*., 2004) (**Figure 8.1**). Both adefovir and cidofovir have been shown to cause acute tubular necrosis (ATN) and Fanconi's syndrome, which lead to proximal tubulopathies (Tanji *et al*., 2001; Meier *et al*., 2002). Although the underlying mechanism is yet to be fully elucidated, it is widely believed that adefovir and cidofovir deplete mtDNA content by inhibiting PolG (Tanji *et al*., 2001; Zhao *et al*., 2017). This induces disruptions in proximal tubular mitochondrial function, similarly to how other NRTIs induce tissue-specific mitochondrial toxicities such as zidovudine (AZT)-induced myopathy or zalcitabine (ddC)-induced peripheral neuropathy (Dalkas *et al*., 1990; Dalakas *et al*., 2001). Notably, Fanconi's syndrome and renal tubular acidosis are also reported in various mitochondrial disease patients (Gorman *et al*., 2016).

Controversially, post-marketing studies supported the demonstration of TDF's safe profile (Nelson *et al*., 2007), and early *in vitro* studies showed that TDF induced minimal changes in mtDNA content or cellular expression of the mitochondrial ETC protein cytochrome *c* oxidase in various human cell lines, including proximal renal tubules (Birkus *et al*., 2002; Biesecker *et al*., 2003). *In vitro* studies also demonstrated the significantly lower nephrotoxicity potential of TDF compared to both adefovir and cidofovir (Rodriguez-Nova *et al*., 2010).

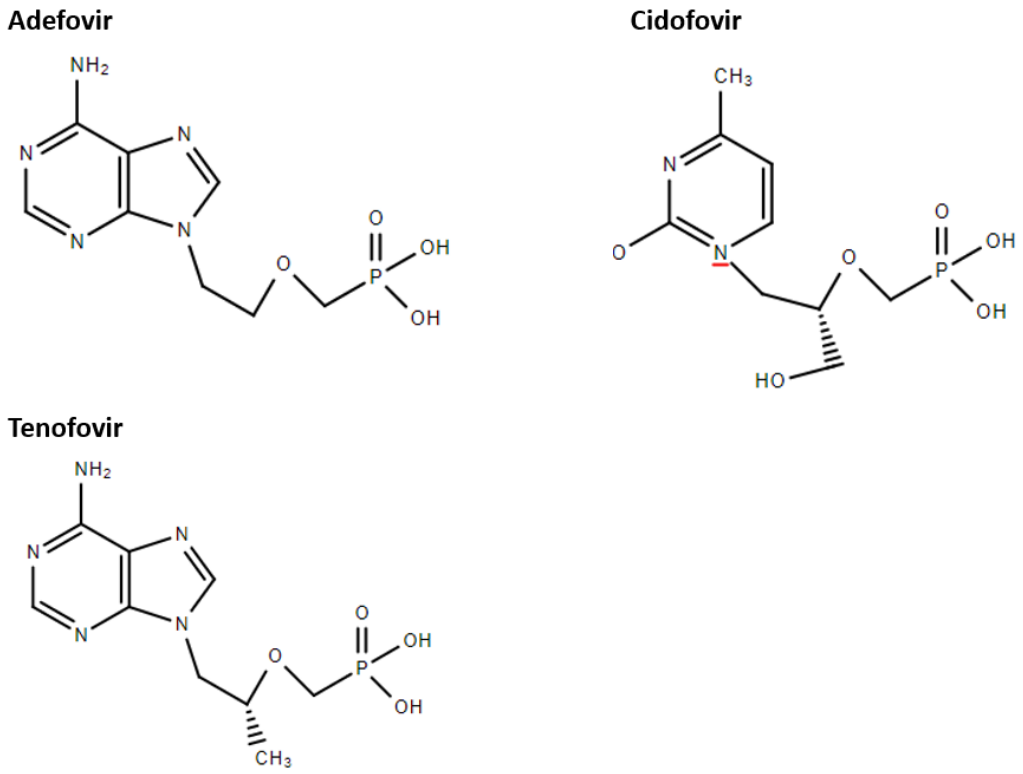

Figure 8.1 – Chemical structures of acyclic nucleotide inhibitors tenofovir, adefovir and cidofovir.

However, reports of AKIs such as ATN and Fanconi's syndrome began to surface from case reports of TDF-treated PLWH following the widespread use of TDF in clinical practice (Rifkin & Perazella 2004; Coca & Perazella 2002, Peyriere *et al*., 2004, Zimmerman *et al*., 2006; Agarwala *et al*., 2010; Hall *et* al., 2011; Quinn, 2010). Proximal tubular injury baring a striking resemblance to adefovir and cidofovir-induced AKI, with characteristics such as loss of brush border, luminal ectasia, and hypereosinophilia, were noted in these renal histopathology investigations. Significantly, alterations in mitochondrial structure such as cristae remodelling, mitochondrial swelling, fragmentation, and reductions in mtDNA content were also observed in PLWH but not HIV- individuals with renal toxicities (Cote *et al*., 2006; Herlitz *et al*., 2010). Conversely however, the same retrospective studies failed to demonstrate a difference in mtDNA content in renal tissue from TDF-treated PLWH compared to TDF-unexposed PLWH (Cote *et* al., 2006; Herlitz *et al*., 2010).

Other studies in rats, monkeys, woodchucks, and mice have supported the demonstration of TDF-induced mtDNA depletion in proximal tubules (Kohler *et al*., 2009; Lebrecht *et al.,* 2009; Biesecker *et al*., 2003) and a study on transgenic HIV+ mice showed, through electron microscopy (EM), that only mice exposed to TDF had ultrastructural changes to mitochondria in proximal tubule cells (Kohler *et al*., 2009). In both studies, the NRTI didanosine (ddI) was also given to the animals and induced

isolated hepatic alterations, but no abnormal renal changes. This further supports the hypothesis that ART-induced nephrotoxicities are caused by TDF-specific mechanisms. In support of this, recent studies demonstrated that chronic TDF exposure induced mitochondrial dysfunction which leads to kidney damage, primarily through ROS and RNS overproduction and oxidative stress (Ramamoorthy *et al*., 2012; Abraham *et al*., 2013; Ramamoorthy *et al*., 2014).

Renal pathologies are complex and difficult to diagnose due to the undesirability of taking renal biopsies in most cases. Several validated biomarkers are therefore used for determining declining kidney function, including proteinuria, low eGFR and serum creatinine. A large cohort study of over 10,000 PLWH demonstrated that TDF is significantly associated with increased proteinuria, rapid decline in eGFR, creatine doubling and incident CKD in PLWH, and that cumulative exposure to TDF increased these risks. The same study also found that these risk factors were not associated with concomitant use of PIs, NNRTIs, or ritonavir-boosted ART regimens (Scherzer *et al*., 2012). The association between TDF, eGFR decline, and serum creatine has also been demonstrated in other studies (Winston *et al*., 2006; Gallant *et al*., 2005; Ryom *et al*., 2013; Poizot-Martin *et al*., 2013; Rifkin & Perazella, 2004).

Whilst the majority of the more recent studies on the effect of TDF on renal function have supported the notion of TDF exposure increasing the susceptibility of developing nephrotoxicities, several studies have argued against this theory (Antoniou *et al*., 2005; Gayet-Ageron *et al*., 2007; Padilla *et al*., 2005; Scott *et al*., 2006). A randomised study investigating the effect of exposure to TDF/emtricitabine (FTC) against abacavir (ABC)/lamivudine (3TC) found no significant differences in estimated glomerular filtration rate (eGFR) between the two groups (Martinez *et al*., 2009). Additionally, TDF was not found to be associated with worsening kidney function over 48 weeks in the multicentre FRAM study (Longenecker *et al*., 2009), whilst a 1 year prospective study of PLWH also failed to find an association between proximal tubular damage and exposure to TDF (Ando *et al*., 2011). These studies mainly determined kidney function through eGFR measurement, and unlike some of the studies mentioned above, did not use clinical observations of kidney damage, therefore limiting their clinical significance. These studies also used patients with short TDF follow-up times and so may not have allowed for the adverse effects of TDF exposure to sufficiently develop. For example, in another retrospective study PLWH who were exposed to TDF for 27 months on average had a significantly steeper decline in eGFR compared to age-matched PLWH who had never been exposed to TDF (Horberg *et al*., 2010).

Although difficult to precisely pin down, the discrepancy between initial clinical trials and later clinical reports and experimental analysis of the potential of TDF to cause nephrotoxicities is partially

explained by the cohorts used in the early trials. These studies generally excluded subjects with pre-existing renal impairments and those with a higher susceptibility to developing adverse renal pathologies (Squires *et al*., 2003; Gallant *et al*., 2004). The discrepancies may also be explained by the lack of consensus regarding the definition of what declining kidney function and kidney disease itself is.

Although there is large heterogeneity in the HIV+ population, cohort studies have identified older age, lower CD4 count, lower BMI, higher serum creatinine levels, and the presence of other comorbidities as risk factors in the development of TDF-induced nephrotoxicities (Campbell *et al*., 2009; Gallant *et al*., 2005; Wever *et* al., 2010; Nartey *et al*., 2019; Nelson *et al*., 2007; Madeddu *et al*., 2008; Guaraldi *et al*., 2011). In the normal population, kidney function, as measured by eGFR, declines 0.4ml/min with every year, and TDF treatment and HIV infection itself both significantly increase this rate (Wetzels *et al*., 2007; Scherezer *et al*., 2012).

8.1.2 Mechanisms of TDF-induced nephrotoxicity

Due to the vast heterogeneity in the HIV+ population, as well as the complexity in kidney biology and disease, the exact pathophysiological mechanism underpinning TDF-induced nephrotoxicity is not completely understood. From *in vivo* and *in vitro* studies of TDF and studies on other acyclic nucleoside inhibitors adefovir and cidofovir, the primary mechanism behind TDF-induced nephrotoxicities is believed to be driven by TDF-induced mitochondrial defects, which are caused by the accumulation of the metabolite TFV in proximal convoluted tubules (Kohler *et al*., 2009; Ramamoorthy *et al*., 2018; Murphy *et al*., 2017) (**Figure 8.2**).

After oral administration, TDF undergoes rapid cleavage into TFV in plasma. TDF is then eliminated from circulation renally through a combination of glomerular filtration and active tubular secretion (Barditch-Crovo *et al*., 2001; Rodriguez-Novoa *et al*., 2009). Normally, active tubular secretion is tightly regulated by uptake transporters on the basolateral membrane and efflux transporters on the apical membrane of proximal convoluted tubules (PCTs) (Ray *et al*., 2006). These transporters mediate the active transport of small molecules from systemic circulation into urine. Initially, TFV is actively taken up by proximal tubular cells at the basolateral membrane through human organic anion transporter 1 (hOAT1) and hOAT3 (Cihlar *et al*., 2001). *In vitro* cell based studies have demonstrated that TFV has a >20 times higher affinity for hOAT1 than hOAT3, but that hOAT3 is significantly more highly expressed than hOAT1 (Cihlar *et al*., 2001). This study also showed that TFV is not a substrate for human organic cation transporter 1 (hOCT1) or hOCT2, and is therefore exclusively taken up by hOAT1 and hOAT3 at the basolateral membrane. After active uptake, TFV is

effluxed primarily by the ATP-binding cassette transporter subfamily member multidrug resistance-associated protein type 4 (MRP4) and to a less potent degree MRP2, but not P glycoprotein (PgP) (Izzedine *et al*., 2004; Klokouzas *et* al., 2003; Reid *et al*., 2003; Schaub *et al*., 1997; van Aubel *et al*., 2002; Ray *et al*., 2006).

In the presence of increased TFV plasma concentration, or when apical efflux is inhibited, TFV accumulates in proximal renal cells. Here, the increased intracellular concentration of TFV becomes toxic and can lead to the partial inhibition of PolG (Lewis *et al*., 2003) and mtDNA depletion (Kohler *et al*., 2009; Cote *et al*., 2006), which subsequently causes defects in OXPHOS and other mitochondrially-mediated processes. Due to the resultant declines in ATP production, proximal tubular cells fail to perform active reabsorption of ions and small molecules such as phosphate, amino acids, and β_2-microglobulin. These molecules are then secreted in abnormal quantities in urine, and thus are characteristic of Fanconi syndrome (Fanconi, 1936; Herlitz *et al*., 2010). Support for this theory was demonstrated through two studies which showed that significantly increased tubular toxicity was associated with polymorphisms in the *MRP2* gene, which led to increased intracellular accumulation of TFV (Izzedine *et al*., 2006; Rodriquez-Novoa *et al*., 2009). A study from our group also provided evidence to support the theory of TDF-induced mitochondrial-dysfunction mediated nephrotoxicity by demonstrating the elevated presence of mtDNA deletions in urine from TDF-treated PLWH compared to PLWH who had not been exposed to TDF (Samuels *et al*., 2017).

In more recent years, studies have suggested that the primary mechanism behind TDF-induced renal toxicities is increased ROS leading to cellular apoptosis and necrosis. This is mediated through mitochondrial abnormalities (Ramamoorthy *et al*., 2018; Murphy *et al*., 2017). Here, as the result of oxidative stress and increased inflammation, activation of apoptosis is upregulated. Neutrophil infiltration then further exacerbates the inflammatory response and oxidative stress, leading to tissue necrosis, hypoxia, kidney dysfunction, and failure (Fernandes Bertocchi *et al*., 2008; Schreiber *et al*., 2006; Kim, 2016; Biro *et al*., 2016; Zoja *et al*., 2009).

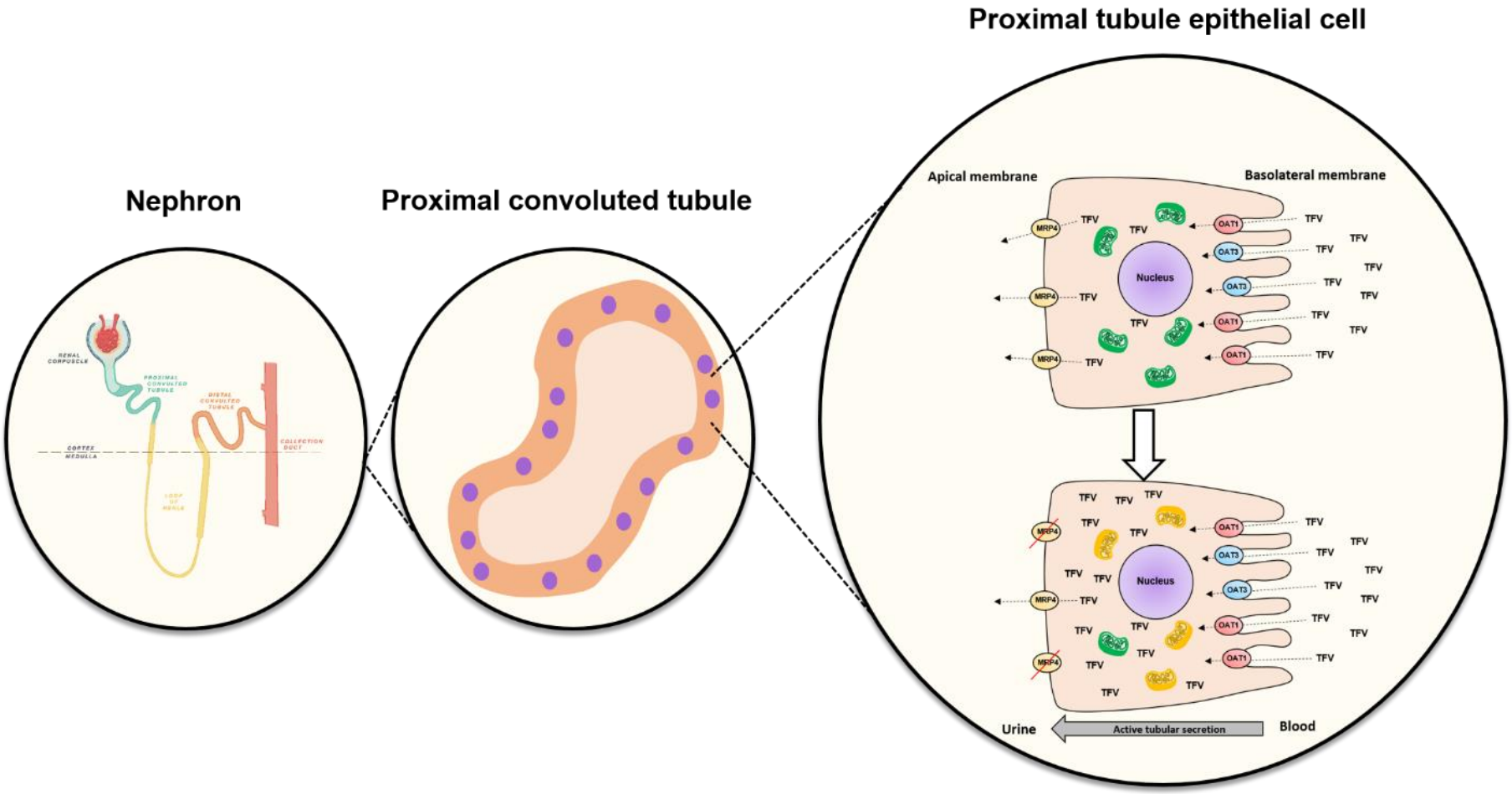

Figure 8.2 – Transport pathway for TDF in proximal tubular cells*. Tenofovir (TFV) is actively taken up into proximal tubular epithelial cells through the organic anion transporter 1 (OAT1) and OAT3 and is effluxed into urine through multidrug resistance protein 2 (MRP2) in individuals with normally functioning kidneys. When TFV accumulates intracellularly, possibly via increased uptake from plasma or decreased efflux into urine, it can cause mitochondrial defects. These defects can arise from mtDNA depletion, large-scale mtDNA deletions, and increased ROS and oxidative stress, leading to declines in energy production and an increased level of mitochondrially-mediated apoptosis.*

8.1.3 Effect of concomitant use of PIs and NNRTIs on nephrotoxicity

8.1.3.1 PIs and nephrotoxicity

Between the roll-out of TDF in 2001 and 2006, the US FDA reported 164 cases of TDF-induced Fanconi syndrome (Gupta, 2014). 74% of those patients were co-exposed to a ritonavir-boosted PI - mainly ritonavir-boosted lopinavir (LPV). However, a more recent systematic review and meta-analysis demonstrated that the risk of eGFR decline in PLWH treated with LPV or ATV was not substantial (Bagnis & Stellbrink, 2015).

In a cohort study, declines in kidney function were more frequent and more pronounced in TDF-treated PLWH who were co-administered with ddI or ritonavir-boosted PI than those TDF-treated PLWH without co-administration (Crane *et al*., 2007). Another study calculated that PLWH who are treated with TDF plus a ritonavir-boosted PI had a 3.7 times higher risk of developing nephrotoxicities than PLWH who were treated with TDF plus an NNRTI (Goicoechea *et al*., 2008). Other PIs such as saquinavir (SQV) and nelfinavir (NFV) have been reported to be associated with nephrotoxicities in both case reports and cohort studies (Rollot *et al*., 2003; Gutmann *et al*., 1999; Engeler *et al.,* 2002; Mocroft *et al*., 2010; Ryom *et al*., 2013). Another large cohort study found that the PI atazanavir (ATV) was associated with an increased risk of the rapid decline in eGFR, but not CKD. In addition, another PI, NFV was associated with a decreased risk of both CKD and proteinuria (Scherzer *et al*., 2013).

Unlike TDF, ARVs in the PI class are not eliminated renally. In fact, they are primarily eliminated through the hepatic cytochrome P450 system and so do not accumulate in proximal tubule cells like TDF (Balani *et al*., 1995). One proposed mechanism behind the adverse effects of ritonavir-boosted PIs is that both ARVs partially inhibit the apical efflux transporter MRP2, leading to decreased efflux and increased intracellular accumulation of TFV (Cihlar *et al*., 2007).

8.1.3.2 Links between NNRTIs as well as other ARV classes and nephrotoxicity

Like the majority of PIs, ARVs in the NNRTI class are also eliminated through the cytochrome P450 system as opposed to renally. There have been no reports of NNRTIs interacting with any of the luminal proximal tubule transporters, and subsequently there have been no reports of an association between NNRTI use and nephrotoxicity (Gallant *et al*., 2005).

Fusion inhibitors and integrase inhibitors are two of the most recently developed classes of ARV. Whilst the majority of ARVs in these two classes have demonstrated a good safety profile and do not induce toxicities like several other ARVs, there have been limited clinical and *in vitro* studies

undertaken in order to assess the nephrotoxicity potential of these drugs. A recent study into the metabolic, mitochondrial and renal impact of the fusion inhibitor enfuvirtide (T20) and the integrase inhibitor raltegravir (RAL) found that these two drugs produce no adverse effects on the factors mentioned above when given as either a monotherapy or in combination with other ARVs (Barroso *et al*., 2019).

8.1.4 Potential treatment of TDF-induced nephrotoxicities

Importantly, PLWH on stable ART should be monitored regularly for CKD in the form of urinalysis, GFR estimation, serum phosphate quantification, and quantification of proteinuria (Yombi *et al*., 2015). If CKD is identified, patients should undergo risk stratification. Referral to nephrology should be conducted in patients with unexplained AKI or CKD, worsening proteinuria, and rapid kidney function decline. Here, a nephrologist will assess the degree of renal impairment and recommend treatments. In addition, patients with CKD stage G3b/G4 should have a biopsy taken and be recommended for kidney replacement therapy (Swanepoel *et al*., 2018).

One of the most obvious treatments for TDF-induced nephrotoxicities is cessation of TDF treatment. Whilst treatment cessation appears to have at least some clinical benefit, the heterogeneity in renal disease type and severity dictates that this method will not always be successful. For example, only 50% of PLWH who had discontinued TDF treatment following the onset of AKI had their renal function return to baseline (Herlitz *et al*. 2010). However, other cohort studies determined that the risk of renal events did not decrease after TDF cessation (Scherzer *et al*., 2012, Monteagudo-Chu *et al*., 2012).

A meta-analysis demonstrated that there is a substantial statistical heterogeneity (I^2 = 66%) between the cohort studies conducted prior and up to 2010 (Cooper *et al*., 2010). As such, due to the heterogeneity of the various studies, it is extremely difficult to reach a firm conclusion with regards to the potential beneficial effect of TDF cessation.

Another viable option is lowering the toxicity of TDF itself (Jose *et al*., 2014; Post *et al*., 2017; Ryom *et al*., 2017; Waheed *et al*., 2015). Tenofovir alafenamide fumarate (TAF) is a recently developed prodrug form of TFV with a far lower plasma exposure than that of TDF (Podany *et al*., 2018). *In vitro* studies have also demonstrated the far lower pathogenic potential of TAF compared to TDF with regards to eGFR decline, general tubular function, as well as on bone mass (Venter *et al*., 2018), and switches from TDF to TAF have been associated with improved kidney function (Jose *et al*., 2014; Post *et al*., 2017; Ryom *et al*., 2017; Waheed *et al*., 2015). However, as TAF is newly administered antiretroviral, the long-term safety is not known.

A potential alternative previously considered was the administration of probenecid, which is commonly used to prevent cidofovir-induced nephrotoxicity. Probenecid is an effective inhibitor of the basolateral membrane transporter hOAT1 and so prevents the nephrotoxic build-up of cidofovir in proximal tubule cells (Izzedine *et al*., 2009; Perazella, 2010). Controversially though, use of probenecid has been associated with dose-limiting toxic side-effects (Lalezari *et al*., 1997).

As the primary mechanism of TDF-induced renal toxicities is thought to be elevated oxidative stress, the potential therapeutic effect of the antioxidant melatonin is currently being investigated (Ramamoorthy *et al*., 2018). As melatonin has been shown to have several beneficial antioxidant effects, such as inhibiting apoptosis (Zhao *et al*., 2015; Perdomo *et al*., 2013), decreasing ROS and RNS levels (Rieter *et al*., 2002; Hardeland, 2005; Ding *et al*., 2014; Rodriguez *et al*., 2004), and improving mitochondrial function (Reiter *et al*., 2008; Kleszcynski *et al*., 2016), it is hoped it may provide a future clinical and therapeutic benefit.

8.2 Experimental aims

In the years following the early clinical trials and *in vitro* studies which demonstrated the safe profile and low PolG-binding affinity of TDF, numerous clinical reports and cohort studies have demonstrated a link between TDF exposure and the development of various nephrotoxicities (Thigpen *et al*., 2012; Gupta *et al*., 2014; Jotwani *et al*., 2016; Hertlitz *et al*., 2010; Samuels *et al*., 2017; Scherzer *et al*., 2012; Winston *et al*., 2006; Ryom *et al.,* 2013; Poizot-Martin *et al*., 2013).

Whilst the exact underlying pathogenic mechanisms behind this phenomenon are yet to be fully elucidated, various studies have suggested a causative role for TDF-induced mitochondrial dysfunction (Kohler *et al*., 2009; Ramamoorthy *et al*., 2014; Hall, 2013; Zhao *et al*., 2017; Ramamoorthy *et al*., 2018; Murphy *et al*., 2017). However, a comprehensive understanding of these mechanisms is limited due to the difficulty in acquiring renal biopsies, as well as extraction of genetic material from renal tubules and tubular cells. Hence, by using renal biopsies acquired from TDF-treated PLWH and matched HIV- individuals in a pilot study, in this chapter I sought to:

- Determine whether the novel immunofluorescence assay developed in our lab (Rocha *et al*., 2015) can be applied to quantify mitochondrial ETC complexes CI, CIII, CIV, CV, and mitochondrial mass in renal tissue.
- Determine whether mtDNA can be successfully extracted from proximal tubules and individual proximal tubule cells following laser capture microdissection.
- Explore whether TDF-treated PLWH had higher levels of proximal tubule mitochondrial CI, CIII, CIV, and CV deficiency compared to HIV- individuals.
- Explore whether TDF-treated PLWH had higher levels of CI, CIII, CIV, and CV deficiency compared to non-TDF-treated PLWH.
- Determine if CI-deficient proximal tubules and tubule cells contained mtDNA deletions or reductions in mtDNA copy number.

8.3 Methods

8.3.1 Patient cohort

This study was approved by the research ethics committee (Newcastle and North Tyneside 2; 17-NE-0015), as described in **Section 3.2.1** and **Section 3.2.5**.

Percutaneous renal biopsies were taken from PLWH (n = 6) (supplied as residual diagnostic tissue from Royal Free London Hospital (RFH) Cellular Pathology Department) and open renal biopsies were taken from HIV- individuals (n = 5) (supplied by Dr Ashwin Sachdeva and Manchester University NHS Biobank), as described in **Section 3.2.5**. All biopsies were formalin-fixed and paraffin-embedded.

Of the PLWH, four were being treated with an ART regimen including TDF at the time of biopsy, while one had never been exposed to TDF, and clinical information was missing for one subject (**Table 8.1**). Of the four TDF-treated PLWH, only patient 3 had discontinued TDF treatment.

8.3.2 Haematoxylin & Eosin histochemistry staining and imaging for renal tissue

In order to visualise the renal biopsies, FFPE sections (4µm) were subjected to H&E histochemistry as described in **Section 3.5.1.**

8.3.3 Multiplex immunofluorescence for OXPHOS complex I, III, IV and V activity in proximal convoluted tubules

To objectively quantify mitochondrial dysfunction in renal tissue, serial FFPE renal sections (4µm) were subjected to both the CI + CIV as well as CIII + CV panels separately (**Table 3.6/3.7**), as described in **Section 3.4.3**.

8.3.4 Image acquisition and determination of ETC complex activity in proximal tubules and proximal tubule epithelial cells

Fluorescent images were acquired as described in **Section 3.4.5**. With regards to quantifying CI and CIV protein levels in individual proximal tubule epithelial cells, 37 putatively OXPHOS-deficient individual PCT cells were manually randomly identified from renal biopsies from PLWH (n = 3). No putatively deficient cells were identified from the HIV- individuals.

8.3.5 Laser microdissection of PCTs and individual PCT epithelial cells

In order to isolate renal tissue for downstream molecular analysis, stained serial 4µm sections were removed from -20°C and left to air-dry for 1 hour at RT. Sections were then incubated in 1% PBS overnight at RT in order to remove cover slips. PCTs and individual PCT epithelial cells of interest were laser microdissected as described in **Section 3.6.2** and captured into 15µm lysis buffer, as described in **Section 3.6.1**.

8.3.6 Quantitative PCR for the detection and quantification of mtDNA mutations

A duplex quantitative real-time PCR assay targeting the mitochondrial genes *MT-ND1* and *MT-ND4* was used to detect and quantify deletions in the mitochondrial genome, as described in **Section 3.7.5**. By assuming that *MT-ND1* was not deleted through mutations I was also able to calculate mtDNA copy number. Details of all primers and standards used as well as their preparation are described in **Section 3.7**.

8.3.7 Statistical analyses

Normality was determined by Shapiro-Wilk tests.

Individual PCTs were then classified into groups based on their z-scores for MTCO1, NDUFB8, UQCRFS1 and ATPB. Respective z-scores were calculated after normalisation to VDAC1 staining intensity: 'positive' ($z > -3$); 'intermediate positive (+)' ($-3 > z > -4.5$); 'intermediate negative (-)' ($-4.5 > z > -6$) and 'deficient' ($z < -6$). Subsequently, the 'deficient', 'intermediate -' and 'intermediate +' groups were pooled together to create the 'deficient' group (i.e. $z < -3$ = deficient). The $\log_{10}$-transformed percentage of PCTs in either category for NDUFB8, UCQRFS1, MTCO1 and ATPB activity were compared between patient groups using unpaired t tests in Prism v5.04. Graphs were also made in Prism v5.04.

The average mitochondrial mass (as indicated through VDAC1 staining intensity z-score) for each subject was also quantified, although not log-transformed. Individual PCTs were then classified into mitochondrial mass groups depending on their z-score: 'very low' ($VDAC1\_z < -3$); 'low' ($-3 < VDAC1\_z < -2$); 'normal' ($-2 < VDAC1\_z < +2$); 'high' ($+2 < VDAC1\_z < +3$) and 'very high' ($3 < VDAC1\_z$).

Unadjusted linear regression analysis (Pearson's correlation) was undertaken in order to assess the relationship between mitochondrial complex deficiency and average mitochondrial mass.

Statistical significance was set at $p \leq 0.05$.

8.4 Results

8.4.1 Cohort clinical characteristics

The clinical characteristics of the HIV-infected subjects are described in **Table 8.1**. Clinical information was missing for patient 6. The mean age of the HIV+ subjects (n = 6) at biopsy was 55.6 (range 47-79) years old and 100% of the subjects were male and white British. Of the HIV- subjects (n = 5), 80% were male and 100% were white British. The average age of the HIV- individuals was 32 years old. Clinical information was missing from the HIV- individuals except for age, gender and ethnicity.

Of the patients with available clinical information (n = 5), four of the five had an eGFR lower than 15 ml/min/1.73m^2, which is indicative of stage 5 kidney disease. The other individual, patient 5, had an eGFR indicative of stage 2 kidney disease. All five HIV+ subjects with available clinical information were virally supressed.

Patient	Age	Ethnicity	CD4 (copies/ml)	Nadir CD4 (copies/ml)	Viral load (copies/ml)	eGFR (ml/min/1.73m²)	ART	Duration on TDF (months)	Duration of HIV infection (months)	Renal pathology	Comorbidities	Potential pathogenic factors
1	50	WB	294	294	50	5	TDF, FTC, ATV/r	18	19	Acute tubular injury	T2D, hyperlipidaemia	Metformin
2	59	WB	214	214	50	9	TDF, FTC, ATV/r	69	176	Acute tubular injury + Diabetic neuropathy	Cellulitis	ACEi, cellulitis
3	43	WB	510	-	40	6	TDF, FTC, EFV, DRV/r	37	218	Acute tubular injury	T2D, hyperlipidaemia	NSAIDs
4	79	WB	296	26	40	6	TDF, FTC, ATV/r	22	115	Tubulointerstitial nephritis + Diabetic neuropathy	Diarrhoea	LRTI
5	47	WB	590	80	50	71	3TC, EFV, SQV/r	N/A	158	Interstitial fibrosis and tubular atrophy	None	None
6	-	-	-	-	-	-	-	-	-	-	-	-

Table 8.1 - Clinical characteristics of the PLWH. *Clinical information was missing for patient 6. T2D = type 2 diabetes; TDF = tenofovir disoproxil fumarate; FTC = emtricitabine; ATV = atazanavir; /r = ritonavir boosted; EFV = efavirenz; DRV = darunavir; 3TC = lamivudine; SQV = saquinavir; ACEi = angiotensin-converting enzyme inhibitor; LRTI = lower respiratory tract infection*

8.4.2 Haematoxylin and Eosin (H&E) histochemistry

Renal biopsies from PLWH (n = 6) and HIV- individuals (n = 5) were subjected to H&E histochemistry in order to determine the robustness of the tissue morphology prior to subjecting the sections to multiplex immunofluorescence and laser microdissection. H&E was also performed in order to detect the presence of any significant tissue abnormalities (**Figure 8.3**).

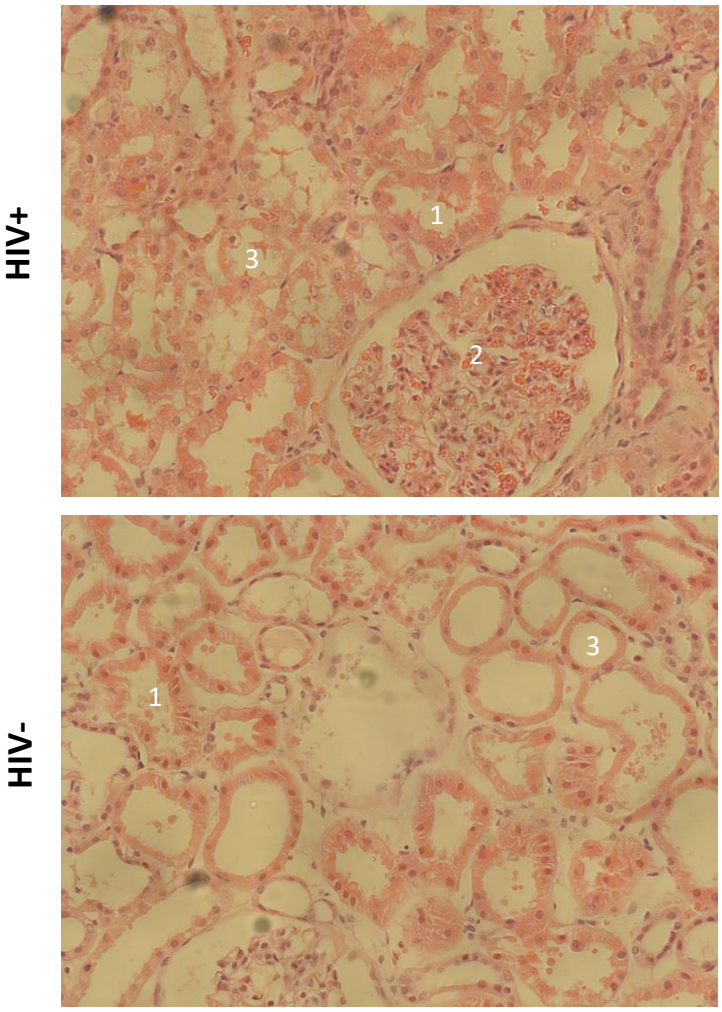

Figure 8.3 – Representative example of a renal needle biopsy taken from a HIV+ and HIV- individual*. (**1**) Proximal convoluted tubule (PCT). (**2**) Glomeruli. (**3**) Distal convoluted tubule (DCT). Proximal tubules exhibit partial loss of brush-border, cytoplasmic simplification and epithelial desquamation. Scale bar = 50μm.*

8.4.3 PCT mitochondrial ETC CI and CV deficiency in PLWH

Protein levels of the four mitochondrially-encoded ETC complexes - CI, CIII, CIV, and CV were quantified in 40 randomly selected PCTs from renal biopsies derived from a cohort of PLWH (n = 6) and HIV- individuals (n = 5) using novel multiplex immunofluorescence assays developed in our lab (Rocha *et al*., 2015) (**Figure 8.4a**). As there is a lack of literature describing immunofluorescence-analysed mitochondrial activity in PCTs, I reported the findings using $z < -3$ as the cut-off for defining deficiency in the respective mitochondrial complexes.

HIV+ patients (n = 6) had a significantly higher proportion of PCTs with CI deficiency ($p = 0.021$, **unpaired t-test**) compared to HIV uninfected individuals (n = 5) (**Figure 8.4d**). There was no significant difference in proportional PCT CIII and CIV deficiency.

Proportional CV deficiency was high in both the HIV+ and HIV- groups. However, there was no statistically significant difference between the respective serostatus groups (**unpaired t test**) (**Figure 8.4d**).

Mitochondrial mass was quantified by background corrected VDAC1 staining intensity in individual PCTs from both groups. Although mean PCT mitochondrial mass was lower in the HIV+ compared to HIV-uninfected subjects, this did not reach statistical significance ($p = 0.18$, **unpaired t test**) (**Figure 8.4e**).

There was no significant correlation between mean PCT mitochondrial mass and proportional CI, CIII, CIV, or CV deficiency (**Pearson's correlation**).

Through immunofluorescence analysis of ETC activity in whole PCTs, it was observed that some individual epithelial cells had a staining pattern indicative of putative CI deficiency (i.e. hyperintensity in the mitochondrial mass channel with simultaneous downregulation of CI channel intensity). Therefore, further work was performed in order to investigate this perceived epithelial cell mitochondrial dysfunction (**Section 8.4.5**).

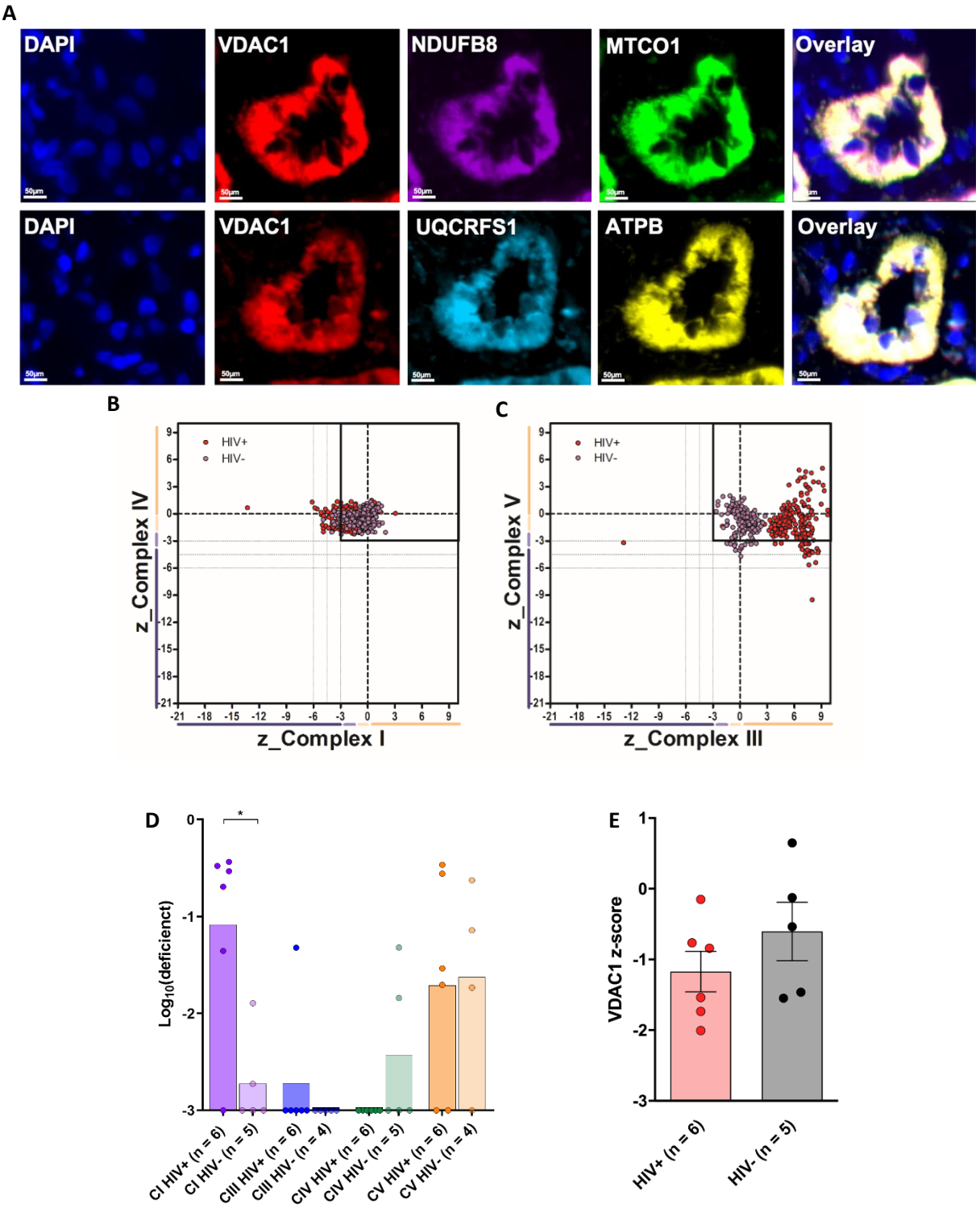

Figure 8.4 – Mitochondrial function in PCTs. *(**A**) Example images of multiplex immunofluorescence stained renal biopsy sections stained for DAPI (nuclear marker), VDAC1 (mitochondrial mass), NDUFB8 (CI subunit), MTCO1 (CIV subunit), UQCRFS1 (CIII subunit), and ATPB (CV subunit). Scale bar = 50µm. (**B-C**) Example plot of (**B**) CI (x-axis) and CIV (y-axis) deficiency in 40 proximal tubules from each of the HIV+ (n = 6) and HIV- (n = 5) individuals; (**C**) CIII (x-axis) and CV (y-axis) deficiency in 40 proximal tubules from each of the HIV+ and HIV- individuals. Each dot represents an individual proximal tubule plotted by z-score. Red dots represent proximal tubules from HIV+ subjects and purple dots represent proximal tubules from HIV- individuals. (**D**) Proportional levels of CI, CIII, CIV and CV deficiency in proximal tubules from the HIV+ and HIV- groups. Each dot represents an individual subject and is plotted by the (log_{10}) proportion of proximal tubules with the respective mitochondrial defects. (**E**) Dot plot (mean ± SEM) depicting mitochondrial mass as measured by normalised VDAC1 staining intensity. Each dot represents an individual subject and is plotted by the average VDAC1 z-score of the 40 proximal tubules analysed. There was no significant difference in mitochondrial mass between the HIV+ and HIV- groups.*

8.4.4 Differences in PCT CI and CV deficiency in PLWH

Due to the large heterogeneity in the HIV+ individuals themselves, differences in PCT mitochondrial function between TDF-treated PLWH and non-TDF-treated PLWH, or PLWH with acute tubular injury (AKI) and those with other nephrotoxicities may be masked when solely comparing the HIV+ and HIV- groups. Therefore, by comparing the levels of PCT mitochondrial dysfunction (in the form of CI and CV deficiency) between the HIV+ individuals with available clinical information (n = 5), I attempted to qualitatively identify differences in the HIV+ group stratified by the above characteristics.

Notably, the only patient not exposed to TDF (patient 5) had a similar level of PCT CI deficiency compared to the TDF-treated individuals (n = 4) (**Figure 8.5a**) as well as having the highest level of CV deficiency (**Figure 8.5b**).

In addition, the two patients not diagnosed with AKI (patients 4 and 5) had comparable levels of PCT CI (**Figure 8.5a**) and CV (**Figure 8.5b**) deficiency compared to the AKI patients (patients 1, 2 and 3).

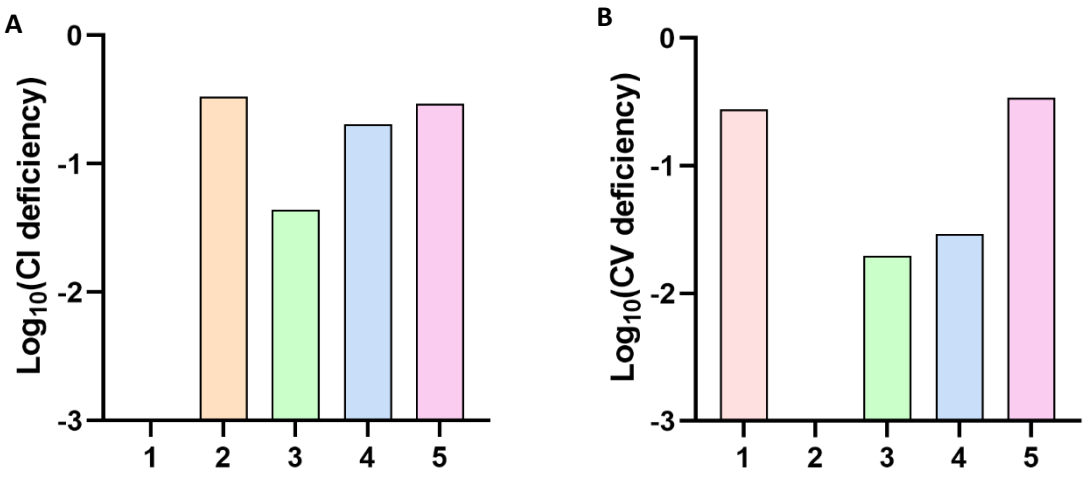

Figure 8.5 – PCT CI and CV deficiency in PLWH*. Bar charts depicting the differences in (**A**) log_{10}(CI deficiency) and (**B**) log_{10}(CV deficiency) between the HIV+ individuals with available clinical information (n = 5). X-axis = patient number.*

8.4.5 PCT epithelial cell mitochondrial dysfunction

Following the observation that there were individual PCT epithelial cells which putatively looked CI deficient within PCTs with 'normal' mitochondrial ETC activity (**Figure 8.6**), I manually identified a maximum of 33 individual cells (all from HIV+ subjects) and quantified their CI and CIV protein levels using methods described previously (**Section 8.3.4**).

All single epithelial cells of interest were subsequently found to have z-scores < -3 for CI when compared to randomly identified epithelial cells with putatively 'normal' CI activity (n = 27) from both the HIV+ (n = 17) and HIV- group (n = 10), and so were classified as CI deficient.

Notably, although proportional CV deficiency was the most prevalent ETC complex deficiency after CI deficiency at the whole PCT level, I was unable to identify any individual epithelial cells with putative CV deficiency.

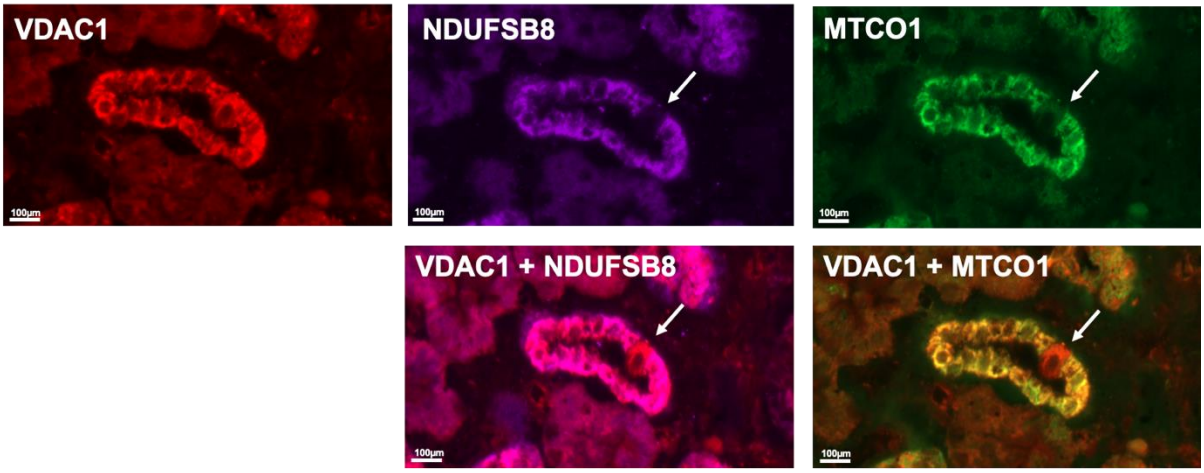

Figure 8.6 – Example image of a PCT epithelial cell with CI and CIV deficiency*. Renal biopsies stained with markers for mitochondrial mass (VDAC1), CI (NDUFB8), and CIV (MTCO1). The arrow indicates a proximal tubule epithelial cell with putative CI and CIV deficiency, characterised by the weak staining intensity of CI and CIV markers in synergy with hyperintensity staining in the VDAC1 channel. Scale bar = 100µm.*

8.4.6 Molecular basis of CI deficiency in PCTs from PLWH

I next wanted to explore the molecular basis of the observed CI deficiency in PCTs from PLWH. After isolating both CI deficient (n = 13), and CI normal (n = 33) PCTs, as well as glomeruli (n = 10) through laser microdissection (**Figure 8.7a**), I amplified genetic material from the lysate and subjected it to qPCR analysis (as described in **Section 3.7.5**) in order to detect and quantify mtDNA mutations.

Initially, mtDNA depletion was excluded as a possible cause of CI deficiency in affected PCTs, as qPCR analysis demonstrated no reduction in mtDNA copy number when compared to CI normal PCTs (**Figure 8.7b**).

Based on previous literature describing TDF-related renal mitochondrial defects, which suggests the predominant cause of mitochondrial dysfunction in TDF-treated PLWH are large-scale mtDNA deletions, I expected this to be the cause of CI deficiency in PCTs from PLWH (Samuels *et al*., 2017). By quantifying the copy number of two mtDNA-encoded genes (*MT-ND1* and *MT-ND4*) I however observed mtDNA deletions in only 15% of CI-deficient PCTs and in 3% of CI-positive PCTs. No deletions were found in the isolated glomeruli (**Figure 8.7c**). These deletions occurred in both the major and minor arc of the mitochondrial genome.

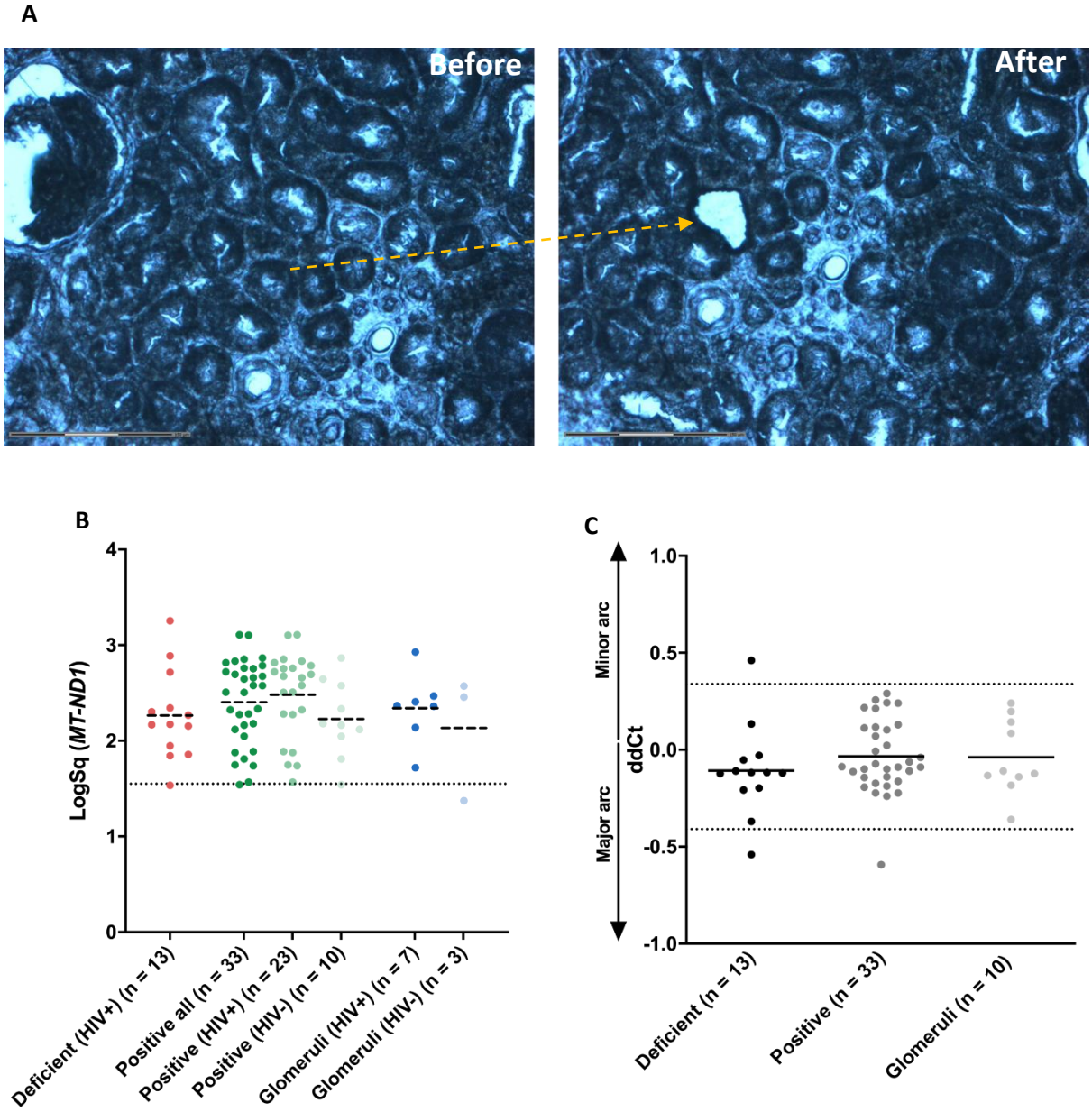

Figure 8.7 – Molecular analysis of mtDNA mutations in laser microdissected proximal tubules. *(**A**) Example image of a renal biopsy from a HIV+ individual with a proximal tubule isolated by laser capture microdissection. Scale bar = 500µm. (**B**) Dot plot (mean) depicting no significant differences in mtDNA content between CI-deficient and CI-normal proximal tubules as well as glomeruli isolated from HIV+ (n = 6) and HIV- (n = 5) individuals. Each dot represents an individual proximal tubule or glomeruli isolated by LCM. The thin dotted line represents 2 standard deviations below the mean MT-ND1 copy number for CI-positive proximal tubules and glomeruli. (**C**) Distribution (mean) of mtDNA deletion levels in CI-deficient (n = 13) and CI-normal (n = 33) proximal tubules as well as glomeruli (n = 10). The dotted lines represent 2 standard deviations away from the mean δδCt of positive PCTs and glomeruli. Dots that lie above the upper dotted line contained a deletion in the minor arc of the mtDNA genome, and dots that lie below the lower dotted line contained a deletion in the major arc of the mtDNA genome.*

8.4.7 Molecular basis of CI deficiency in proximal tubule epithelial cells

I next performed quantitative molecular analyses on individual PCT epithelial cells with either CI deficiency (n = 33) or normal CI activity (n = 27), after isolation by LCM (**Figure 8.8a**).

qPCR analysis again demonstrated no reduction in mtDNA copy number and so mtDNA depletion was excluded as a potential cause of mitochondrial dysfunction (**Figure 8.8b**). In fact, *MT-ND1* copy number was significantly higher in CI-deficient proximal tubular cells (n = 33) compared to CI-normal proximal tubular cells from HIV+ (n = 17; $p = 0.047$, **unpaired t-test**) and HIV- individuals (n = 10; $p = 0.017$), as well as all CI-normal proximal tubular cells from both HIV+ and HIV- individuals (n = 27; $p = 0.013$).

I found that 18% of CI-deficient PCT epithelial cells contained an mtDNA deletion. These deletions occurred in both the major and minor arc of the mitochondrial genome (**Figure 8.8c**).

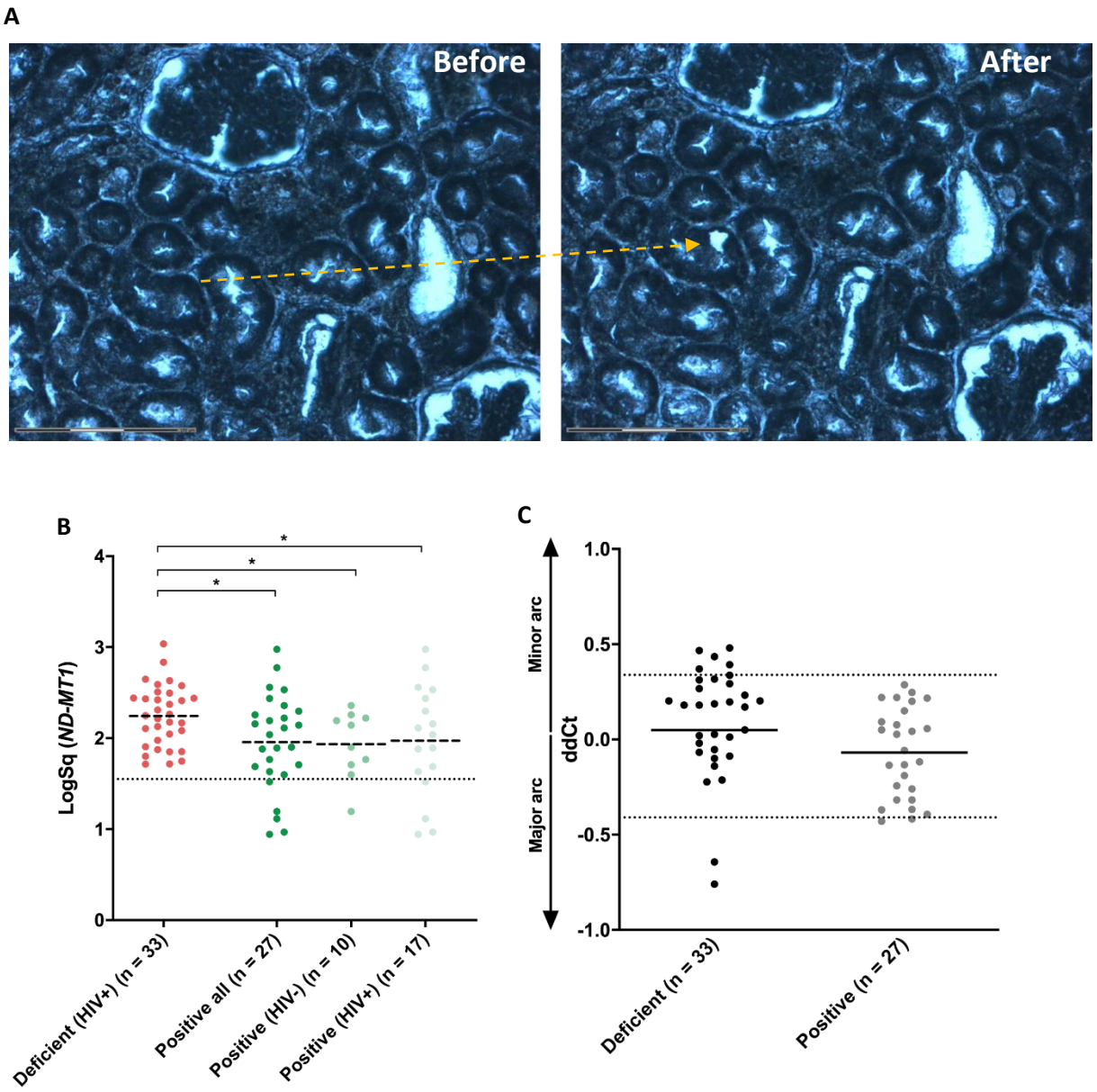

Figure 8.8 – Molecular analysis of isolated individual proximal tubule epithelial cells. *(**A**) Example image of an isolated proximal tubular epithelial cell from a HIV+ individual. Scale bar = 500µm. (**B**) Dot plot (mean) demonstrating significantly higher mtDNA content in CI-deficient proximal tubule cells compared to CI-normal proximal tubular cells overall (n = 27) (p = 0.013), from HIV- individuals (n = 10) (p = 0.017) and HIV+ individuals (n = 17) (p = 0.047). Each dot represents an individual isolated proximal tubule epithelial cell and is plotted by its MT-ND1 copy number. (**C**) Distribution (mean) of mtDNA deletions in isolated CI-deficient (n = 33) and CI-normal (n = 27) proximal tubular epithelial cells. Dotted lines represent 2 standard deviations away from the mean δδCt of positive cells. Dots that lie above the upper dotted line contained a deletion in the minor arc of the mtDNA genome, and dots that lie below the lower dotted line contained a deletion in the major arc of the mtDNA genome.*

8.5 Discussion

In this chapter I assessed cellular and molecular mitochondrial function in whole proximal convoluted tubules and in individual proximal tubule epithelial cells derived from renal biopsies from TDF-treated PLWH who presented with varying clinically significant nephrotoxicities.

8.5.1 Conclusions

8.5.1.1 Successful application of novel immunofluorescence assay to quantify mitochondrial protein levels in renal tissue

As there are limited experimental methods to assess renal mitochondrial function at the cellular level, an important aim of this study was to determine whether a novel multiplex immunofluorescence assay developed in our lab (Rocha *et* al., 2015) could be applied to renal tissue. As such, this immunofluorescence assay, with markers for mitochondrial mass as well as subunits of CI, CIII, CIV and CV of the mitochondrial ETC, was successfully applied to renal tissue from both HIV+ and HIV- individuals. Notably, this was the first study to demonstrate specific CI deficiency in proximal tubules of PLWH who had been treated with TDF at the cellular level, as opposed to in tissue homogenates. This assay also allowed for the quantification of lesser analysed subunits of the ETC - CIII and CV, as well as mitochondrial mass. Hence, I also demonstrated deficiency in CV protein levels in proximal tubules from PLWH. However, the proportional levels of CV deficiency appeared comparable with CV deficiency seen in PCTs in the HIV- group, suggesting CV deficiency could be a universal factor in renal toxicity.

8.5.1.2 Assessment of proximal tubule mitochondrial dysfunction in PLWH

Although the sample size was small and there was heterogeneity between the HIV+ individuals, another aim of this study was to explore whether there appeared to be differences in PCT mitochondrial dysfunction between TDF-treated PLWH and non-TDF-treated PLWH, as well as between PLWH diagnosed with AKI and those with other nephrotoxicities. Interestingly, the only non-TDF-treated patient had comparable levels of CI and CV deficiency compared to the TDF-treated patients, suggesting TDF exposure may not be the only pathogenic HIV-related factor. In addition, levels of PCT CI and CV deficiency were comparable between AKI patients and non-AKI patients, supporting previous observations that mitochondrial dysfunction is not restricted to AKI patients (Samuels *et al*., 2017). It should be stressed that due to the small size of the HIV+ group with available clinical information and the heterogeneity of the group, these observations are not heavily weighted.

Importantly, this is also the first study to demonstrate CI and CIV protein deficiency at the individual proximal tubule epithelial cell level in TDF-induced nephrotoxicities. These results build on previous work which demonstrated the presence of punctate abnormal mitochondria, characterised by swelling

and irregular morphology, in TDF-exposed proximal tubules (Herlitz *et al*., 2010). Whilst highlighting the vast variability in how mitochondrial dysfunction may present in nephrotoxicities, these findings are suggestive of a mechanism by which individual proximal tubule epithelial cells develop mitochondrial dysfunction in a mosaic pattern. Nephrotoxicities then subsequently arise following the accumulation of abnormal epithelial cells, leading to defects in proximal tubule function (Biro *et al*., 2016; Zoja *et al*., 2009).

Importantly, mitochondrial mass was not significantly elevated in the HIV+ group at the proximal tubule level, indicating that there was no compensatory upregulation in mitochondrial content in response to ETC deficiencies. Notably though, there appeared to be hyperintense staining in the VDAC1 channel in individual proximal tubule epithelial cells with putative CI and CIV deficiency, indicative of a compensatory upregulation in mitochondrial mass in those cells. These results appear to indicate that punctate mitochondrial defects at the individual cellular level are compensated at the whole proximal tubule level, revealing unanswered questions regarding the contribution of individual epithelial cells or whole proximal tubules to the pathophysiology of various nephrotoxicities. This finding also argues against the mechanism of mtDNA depletion underpinning TDF-induced renal toxicities (Tanji *et al*., 2001; Cote *et al*. 2006; Kohler *et al*., 2009). In addition, this finding highlights the need for further investigation into whether mitochondrial dysfunction in individual tubule cells expand to neighbouring epithelial cells and whether this leads to whole tubule dysfunction.

8.5.1.3 Molecular basis of proximal tubule mitochondrial dysfunction

Finally, this study is also the first to successfully isolate and amplify mtDNA from individual proximal tubule epithelial cells by LCM and qPCR techniques. Importantly, I found that 18% of CI-deficient proximal tubule epithelial cells harboured an mtDNA deletion in either the major or minor arc of the mtDNA genome, while simultaneously failing to detect evidence of mtDNA depletion in these cells. In fact, the results demonstrate an increase in mtDNA content, presumably as a result of upregulated mitochondrial biogenesis in response to ETC defects. However, a large proportion of CI-deficient tubule cells did not contain a detectable mtDNA deletion or mtDNA depletion and so the underlying mechanisms behind their CI deficiency remains unsolved (Samuels *et al*., 2017). One possibility may be mtDNA point mutations, which have been shown to eventually induce mitochondrial toxicities. mtDNA point mutations have been found in substantia nigra neurons as well as mitotic cells such as colonic crypt cells (Greaves *et al*., 2012; Reeve *et al*., 2009). These point mutations are most likely arising as the result of increased ROS production due to TFV accumulation (Ramamoorthy *et al*., 2012; Abraham *et al*., 2013; Ramamoorthy *et al*., 2014; Ramamoorthy *et al*., 20108). This theory is supported by the strong link between elevated ROS production and the generation of mtDNA point mutations (Taylor & Turnbull, 2005; Chung *et* al., 2014; Caldecott, 2008; Pinz *et* al., 1995; Baines *et* al., 2014). The increase

in ROS and subsequently mtDNA point mutations may be part of a vicious cycle, whereby mtDNA mutations further exacerbate ROS production, leading to further tubular damage through apoptosis and subsequently necrosis (Ramamoorthy *et al*., 2018, Murphy *et al*., 2017, Liu *et al*., 2014; Servais *et al*., 2008; Wang *et al*., 2013). These observations could be significant to future work in the field as they suggest more investigations are needed looking into the mitochondrial effects of TDF, in particular the exacerbatory effects on ROS and inflammation, at the individual epithelial cell level.

8.5.2 Summary of results

	HIV+ individuals	HIV-uninfected individuals	Conclusions
Cellular proximal tubular mitochondrial dysfunction	• High levels of CI and CV proximal tubule deficiency • Comparable levels of CV deficiency compared to HIV- individuals • Individual epithelial cells had CI deficiency inside whole tubules with normal CI levels	• Comparably high levels of CV deficiency compared to HIV+ individuals	• PLWH displayed high levels of CI and CV deficiency in whole proximal tubules • Punctate epithelial cells had CI deficiency
Molecular proximal tubule mitochondrial defects	• Majority of CI-deficient whole tubules or epithelial cells did not contain mtDNA deletions • No evidence of mtDNA depletion	• No tissue extracted for molecular analysis	• CI deficiency at the whole tubule or epithelial cell level was not explained by mtDNA deletions • Most likely caused by mtDNA point mutations
Disparities between TDF-treated PLWH and non-TDF treated PLWH	• Comparable levels of CI and CV deficiency between groups	• Not investigated	• There appeared to be no difference in CI or CV proximal tubule deficiency between TDF and non-TDF-treated PLWH
Disparities between PLWH with AKI and those with other renal pathology	• Comparable levels of CI and CV deficiency between groups	• Not investigated	• No evidence of increased mitochondrial dysfunction in PLWH with AKI

Table 8.2 – Summary of experimental findings.

8.5.3 Limitations

As this was a pilot study there are a few limitations which need to be noted. Most obviously, the greatest limitation lies in the small sample size of both the HIV+ and HIV- groups used in the study. This limitation significantly reduced the power to detect differences between the HIV+ and HIV- groups, as well as restricting the ability to include a HIV+/TDF- comparator group in order to determine how specific to TDF the mitochondrial defects were. Hence, I was unable to extrapolate pathophysiological information about the role chronic HIV-infection itself plays. Ideally, I would also have recruited a cohort with a wider variation in nephrotoxicity diagnoses, in order to better understand the role of mitochondrial defects in those specific pathologies.

Another limitation was missing clinical information. With regards to the HIV+ group in our cohort, although I had information about whether the PLWH had ever been exposed to TDF, ATV/r, SQV, 3TC or FTC ARVs, information regarding current/previous exposure to NNRTIs or older, more mitochondrially-toxic NRTIs such as AZT or ddI was missing. Missing clinical information from patient 6 also reduced our ability to understand potential mechanisms behind mitochondrial defects in their proximal tubules.

Aside from their age, ethnicity and gender, little information was given to us about the HIV- control subjects. Biopsies came from 'normal' tissue adjacent to explanted renal masses, however, I did not know whether these individuals had been diagnosed with any renal pathologies and I had no information about potential co-morbidities or other adverse factors such as certain medications.

Finally, another limitation lies in the fact that these biopsies were taken at one time point and I was therefore unable to extrapolate data directly to drug administration or disease progression. Ideally, biopsies should be taken when the patients eGFR began to decline and then at multiple follow up visits to the clinic. The biopsies used in this study were taken from PLWH who already had well developed nephrotoxicities, and so I was unable to determine whether mitochondrial dysfunction played a causative role in these nephrotoxicities or whether it was consequence of declining tissue homeostasis. However, due to the highly invasive nature of taking kidney biopsies, it is well acknowledged that taking several biopsies from the same individual is not entirely practical.

8.5.4 Future work

Due to the fact that this was a pilot study, there is significant scope for potential future work. The most significant addition to any future work would be to use a much larger cohort in order to increase our power to detect inter- and intragroup differences. As mentioned above, this would ideally include more patients in both the HIV+ and HIV- groups as well as a group of PLWH who had never been exposed to TDF. Ideally, this future cohort should also contain individuals with varying renal pathologies. This

would help extrapolate information about the specific role of mitochondrial dysfunction in the pathogenesis of various nephrotoxicities. In this regard, it would be hugely beneficial to conduct a longitudinal study in which renal biopsies are taken from patients at several time points, including when eGFR initially starts declining (or failing that, when symptoms first develop). As mentioned in the previous section (**Section 8.5.2**), this would help better the understanding of the pathogenesis of nephrotoxicities in TDF-treated PLWH.

One of the most significant findings of this study was the presence of individual proximal tubule epithelial cells deficient in complex I of the ETC within a proximal tubule with normal mitochondrial protein levels. Future work should look to expand the understanding of the significance of punctate mitochondrial dysfunction in the pathogenesis of nephrotoxicities. As recent studies have suggested the potential causative factor of elevated ROS and inflammation in the pathophysiology of TDF-induced renal toxicities (Murphy *et al*., 2017; Ramamoorthy *et al*., 2018), investigations into these factors at the tubular and cellular level would also be of benefit.

Conducting longitudinal studies is not always possible, especially when concerning the invasive nature of renal biopsies. With regards to this, research is steering away from human biopsy and toward non-invasive fluid biomarkers and well-characterised animal models. Abraham *et al*. (2016) recently developed a mouse model with TDF-induced nephrotoxicity similar to that seen in humans. This mouse model has the potential to be hugely beneficial in studies investigating the pathogenic mechanisms behind TDF-induced nephrotoxicity. Additionally, a recent study by our lab investigated mtDNA mutations in the urine of TDF-treated PLWH (Samuels *et al*., 2017). Although urine contains a heterogenous mix of cell types, including non-proximal tubule tissue, it can still be used as a clinically relevant tissue to investigate renal pathology and mtDNA deletions, and may be useful in cases where renal biopsies are unavailable (Blackwood *et al*., 2010).

EM studies should also be performed in any future work. It would be a significant benefit to analyse mitochondrial morphology, particularly in the CI-deficient proximal tubule cells. This would allow for comparisons to be made between these CI-deficient epithelial cells and adjacent cells which do not appear to have mitochondrial defects. This could be performed through super resolution microscopy, which allows for simultaneous detection of fluorescence (to identify CI-deficient tubules) and morphology, or immunofluorescence EM. Limitations lie in the fact that super resolution microscopy does not provide high enough resolution to analyse individual mitochondria to a high standard, and immunofluorescence EM requires no primary controls in order to eliminate the effects of non-specific binding.

Finally, another future study with potential benefit would be one which performs detailed genetic assessment of pathologic proximal tubules through RNA sequencer analysis. Experiments such as this would be hugely informative regarding differences in gene expression between comparator groups and may further our understanding in the pathogenesis behind TDF-induced nephrotoxicities.

Chapter 9 – Conclusions

In this chapter I discuss the main findings with relation to the thesis aims and objectives outlined in **Chapter 2**, as well as the potential impact these findings may have on the current and future work in the field of mitochondrial dysfunction and adverse ageing in the HIV setting.

9.1 Physiological, cellular and molecular skeletal muscle mitochondrial dysfunction in the contemporary ART setting

Several studies conducted over the course of the past three decades have established the link between older antiretrovirals (ARVs) and the development of mitochondrial toxicities such as myopathy or lactic acidosis (Dalakas *et* al., 1990; Arnaudo *et* al., 1991; Samuels *et al*., 2017; Domingo *et al*., 2014; Dragovic *et al*., 2014; Alikhani *et al*., 2019; Carr *et al*., 1999; Lewis, 2003; Brinkman & Kakuda, 2000). These mitochondrial toxicities are tissue-specific and heterogenous in presentation, and are induced by various ARVs of different classes. In particular, the NRTIs zidovudine (AZT), zalcitabine (ddC), didanosine (ddI), and stavudine (d4T) have been shown to induce mitochondrial dysfunction and subsequent toxicities (Dalakas *et al*., 1990; Arnaudo *et* al., 1991; Lim & Copeland, 2001; Lewis, 2003). However, no studies have assessed the impact of newer ARVs such as tenofovir disoproxil fumarate (TDF) and abacavir (ABC), which have been considered as being free from mitochondrial toxicity *in vitro* (Venhoff *et al*., 2007), on skeletal muscle mitochondrial function at the cellular level. This study was therefore the first to do so. In addition, previous studies such as those done by our group have suggested that previous exposure to early NRTIs such as AZT may predispose PLWH to an excess of skeletal muscle mitochondrial defects years after cessation of treatment with the NRTI (Payne *et al*., 2011). As such, I aimed to investigate whether there were differences in skeletal muscle mitochondrial dysfunction in PLWH stratified by the type of antiretrovirals they have been exposed to, in an effort to better understand skeletal muscle mitochondrial dysfunction in the contemporary ART era.

Notably, this study was the first to demonstrate skeletal muscle mitochondrial defects in the form of CI deficiency in PLWH who have only been exposed to newer, supposedly non-mitochondrially toxic ARVs (**Chapter 4**). Here, using a novel immunofluorescence assay developed in our lab (Rocha *et al*., 2015) I demonstrated that PLWH who had been exposed to mitochondrially-toxic NRTIs had a significantly higher proportion of myofibres with CI deficiency than treatment-naïve PLWH. In addition, PLWH who had only been exposed to newer NRTIs also had a significantly higher proportion of CI and CIV deficient fibres than ART-naïve PLWH, and a comparable level to historical NRTI-treated PLWH. Finally, results presented in **Chapter 6** using age-matched older HIV+ and HIV- individuals supported the notion that

skeletal muscle mitochondrial dysfunction in PLWH in the contemporary ART era is not primarily age related, and there are therefore other pathogenic mechanisms driving this mitochondrial dysfunction.

Through qPCR analysis I then demonstrated that the majority of CI-deficient myofibres contained mtDNA deletions, supporting previous work (Payne *et al*,. 2011). As CI is the largest mtDNA-encoded complex of the electron transport chain, it is more likely to be affected by large-scale mtDNA deletions. The cellular and molecular work was also supported by *in vivo* functional evidence from previously obtained ^{31}P-MRS data (Payne *et al*., 2014).

The final aim of the study conducted in **Chapter 4** was to determine whether there was the presence of a 'legacy effect' in PLWH who have previously been exposed to older NRTIs such as AZT, ddC, ddI, d4T (Hunt & Payne, 2020). Surprisingly, data presented in **Chapter 4** seemingly argues against the existence of this phenomenon, at least in skeletal muscle. Support for this observation centres around the fact that PLWH who had been exposed to these older NRTIs had comparable levels of skeletal muscle mitochondrial defects compared to age-matched PLWH who had never been exposed to the older NRTIs. Importantly, the majority of these cellular mitochondrial defects were underpinned by mtDNA deletions in both sets of ART-treated PLWH. Indeed, as PLWH treated only with newer NRTIs over a long duration had comparable levels of skeletal muscle mitochondrial defects compared to those treated with the older NRTIs, the mechanisms behind this mitochondrial dysfunction could therefore be underpinned by other factors seen in long-term ART-treated PLWH, such as chronic inflammation or oxidative stress (Melov *et al*., 1999; Zorov *et al*., 2014; Rao *et al*., 2014; Massaad & Klann, 2011; Deeks, 2011).

9.2 Older PLWH have a higher prevalence of frailty and sarcopenia compared to age-matched HIV- individuals

The advent of cART has greatly reduced the mortality rate of PLWH as well as considerably extending their lifespan. As a result, the average age of the HIV+ population is now ~50 years old, with this number still increasing (Public Health England, 2019; Smit *et al*., 2015). Consequently, whilst the mortality rate and prevalence of HIV-associated comorbidities has decreased, the prevalence of age-associated conditions such as frailty or cardiovascular diseases in PLWH has increased (Desquilbet *et* al., 2007; Nou *et al*., 2016; Leng *et al*., 2015; Guaraldi *et al*., 2011; Smit *et al*., 2015; Chow *et al*., 2012; Althoff *et* al., 2014; Drummond *et al*., 2014; Kirk *et al*., 2013; Shiels *et al*., 2009; Sico *et al*., 2015; Silverberg *et al*., 2015).

Work in **Chapter 5** using data obtained from the MAGMA study supported observations from previous studies which demonstrated the increased prevalence of both frailty and sarcopenia in PLWH compared

to age-matched HIV- individuals (Desquilbet *et al*., 2007; 2009; Hanlon *et* al., 2018; Brothers *et* al., 2017; Erlandson *et al*., 2015; Echeverria *et al*., 2018; Pinto Neto *et al*., 2016; Oliveria *et al*., 2020).

Interestingly, metabolic expenditure (MET) score was significantly lower in frail/prefrail PLWH compared to robust PLWH. As this was a cross-sectional study I cannot be certain whether low MET score was a cause or consequence of frailty in older PLWH. However, as lower MET score was also seen in prefrailty this may suggest that decreased metabolic expenditure predates the onset of frailty. In addition, whilst none of the clinical or lifestyle parameters were associated with either frailty or sarcopenia in older PLWH themselves, a longer duration of untreated HIV infection, adjusted for age, significantly predicted weaker grip strength, which is well-recognised to be a very important measure of declining physical function. In addition, a poorer immune function in the form of CD4 count significantly predicted poorer muscle mass adjusted for height (ASMI). The link between these factors may well be mediated through increased inflammation and immune senescence (Deeks, 2011; Baylis *et al*., 2013; Shaw *et al*., 2010), however further work is required.

Altogether, these findings suggest that poorer immune function, possibly as the result of delayed initiation of ART after initial HIV infection, may contribute to reduced muscle strength in older PLWH. This, among potentially other untested factors, is responsible for the greater prevalence of adverse ageing phenotypes in older PLWH compared to the age-matched general population. Importantly, these findings suggest that physical activity interventions aimed at improving muscle strength would likely to be beneficial to older PLWH who are more susceptible to developing adverse ageing phenotypes, supporting previous data from the general population (Landi *et al*., 2014; Zubala *et al*., 2017; Lo *et al*., 2020).

9.3 Skeletal muscle mitochondrial dysfunction in frail and sarcopenic PLWH

One of the important aims of this thesis was to determine whether older PLWH had greater levels of skeletal muscle mitochondrial dysfunction compared to age-matched HIV- individuals.

Hence, a major finding from the study in **Chapter 6** was the demonstration of significantly higher skeletal muscle mitochondrial dysfunction in older PLWH compared to age-matched HIV- individuals. Specifically, individuals in the HIV+ group had a significantly higher proportion of myofibres with CI and CIV deficiency compared to the HIV- individuals, although there was no difference in mean skeletal muscle mitochondrial mass. This mitochondrial dysfunction did not seem to be explained by exposure to particular ARVs including NRTIs such as AZT and ddC, or protease inhibitors (PIs), supporting work

from **Chapter 4**. Neither could this mitochondrial dysfunction be explained by other HIV-related factors such as duration on ART in adjusted linear regression models.

Whilst average myofibre mitochondrial mass was not significantly different between the HIV+ and HIV- individuals, it was notable that increased myofibre mitochondrial mass was significantly associated with a decline in fat mass in the older PLWH. This observation may suggest that obesity adversely impacts mitochondrial content, reducing skeletal muscle quality, and resulting in physical decline (Shetty *et* al., 2009; Winalawansa, 2019; Li *et al*.,2017; Slawik & Vidal-Puig, 2006). In addition, this finding supports the idea that increased physical exercise, in this instance particularly aerobic exercise resulting in a reduction in fat mass, may be beneficial in improving mitochondrial function in older PLWH (Marzetti *et al*., 2008; Rowe *et al*., 2014).

Following the demonstration of a greater prevalence of adverse ageing phenotypes in older PLWH compared to the HIV- individuals in **Chapter 5**, and owing to the link between mitochondrial dysfunction and these phenotypes in both frailty and sarcopenia (Chistiakov *et al*. 2014; Andreux *et* al., 2018; Sayeed *et* al., 2018), I also sought to assess whether increased mitochondrial dysfunction contributed to frailty and sarcopenia in PLWH.

Somewhat surprisingly, it was demonstrated that frail and sarcopenic PLWH did not have a significantly higher level of skeletal muscle mitochondrial dysfunction compared to robust and non-sarcopenic PLWH – suggesting that mitochondrial dysfunction alone is not driving these adverse ageing phenotypes in older PLWH. However, this finding should be treated with caution, owing to the relatively small numbers of frail and sarcopenic individuals. Furthermore, mitochondrial dysfunction can be measured through different parameters (Hunt & Payne, 2020; Fraizer *et al*., 2020). In addition, other pathophysiological factors that were not analysed in this study, such as chronic inflammation or immunosenescence, may also be driving adverse ageing phenotypes in PLWH (Deeks, 2011; Baylis *et al*., 2013; Shaw *et al*., 2010; Soysal *et al*., 2016).

9.4 Analysis of age-associated cellular skeletal muscle pathophysiological decline and its associations with adverse ageing phenotypes

Due to the fact that the pathophysiology of declining muscle function in frailty and sarcopenia is extremely heterogenic in the general population (Fried *et al.,* 2009; Cruz-Jentoft *et al*., 2019), and the fact that skeletal muscle pathology is little studied in PLWH, I sought to better understand these pathophysiological mechanisms in the context of ageing with HIV. As such, one aim of the work

conducted in **Chapter 7** was to compare the levels of several skeletal muscle pathophysiologic factors in older HIV+ and HIV- individuals.

The most notable aspect of the study conducted in **Chapter 7** using data and tissue collected as part of the MAGMA study is the fact that it is the first study to assess a range of pathophysiological factors such as satellite (stem) cell availability and fibrosis in the skeletal muscle of older PLWH. The comprehensive nature of this study allowed for a wider understanding of the factors that are at play in age-related physiological decline in older PLWH.

Notably, I failed to find any significant difference in several of these factors between the HIV+ and HIV- groups, including, intramyocellular lipid accumulation, $Pax7^+$ satellite cell (muscle stem cell) prevalence, fibre type proportions, average fibre size, lipofuscin accumulation, or proportion of degenerated fibres. I did however demonstrate that older PLWH had a significantly greater level of skeletal muscle fibrosis and significantly lower percentage of regenerated fibres compared to age-matched HIV- individuals.

In addition, it was demonstrated that except for an increased prevalence of type IIx fibres, none of these pathophysiological factors were significantly altered in frail PLWH compared to robust and prefrail PLWH. Interestingly, no skeletal muscle pathophysiological factor appeared to be altered in sarcopenic PLWH compared to non-sarcopenic PLWH. Importantly, these were novel findings in the context of skeletal muscle function in older PLWH.

9.5 Role of skeletal muscle mitochondrial dysfunction in muscle pathophysiological factors, and the combined role in adverse ageing phenotypes in older PLWH – potential compensatory mechanisms?

After investigating whether there were differences in several skeletal muscle pathophysiological factors between the age-matched HIV+ and HIV- groups, I next sought to determine whether there was any association between mitochondrial dysfunction and these other factors in the skeletal muscle of older PLWH.

Importantly, the only factors that appeared to be predicted by skeletal muscle mitochondrial dysfunction was the relative fibre type proportions, and an increased $Pax7^+$ satellite cell (SC) prevalence.

In particular, greater proportional CI deficiency was significantly predictive of a lower proportion of oxidative type I fibres, and therefore a greater proportion of glycolytic type IIx fibres, both after adjustment for age. These novel findings suggest that skeletal muscle mitochondrial dysfunction may be compensated in older PLWH by a reduction in the usual pattern of age-associated fibre type

switching (from type II to type I). This preservation of glycolytic fibres might partially compensate for a loss of oxidative metabolism, and therefore diminish the onset of adverse ageing phenotypes (Wang *et al*., 2013; Maughan *et al*., 1983; Anderson, 2003; Phillips & Leeuwenburgh, 2005). Conversely though, mitochondrial dysfunction may be leading to selective atrophy of type I fibres. As it was not possible to fully elucidate which mechanisms were occurring, future studies should investigate neuromuscular junction efficiency and fibre apoptosis.

Furthermore, mitochondrial dysfunction (in the form of proportional CIV deficiency) predicted a higher prevalence of $Pax7^+$ SCs in the older PLWH. This may again suggest the presence of a compensatory mechanism whereby an intact stem cell population allows skeletal muscle to respond to the adverse effects of mitochondrial dysfunction. However, a greater prevalence of $Pax7^+$ SCs predicted not only a greater level of regenerated fibres, but also increased fibrosis. This may suggest an impairment in the regenerative function of quiescent satellite cells in older PLWH, with some muscle damage being resolved by scarring (fibrosis) rather than regeneration.

With regard to potential clinical or therapeutic implications of these findings, they support previous work in the general population which has suggested that increased exercise is the most effective mechanism in preventing the onset of adverse ageing conditions (Walston *et al.*, 2018; Cameron *et al*., 2013; Silva *et al*., 2017). For example, resistance and aerobic exercise is known to improve muscle function (Cesari *et al*., 2015; Suetta *et al*., 2008; Binder *et al*., 2005; Campbell *et al*., 2002; Benito *et al*., 2020), muscle mitochondrial function (Zampieri *et al*., 2015; Marzetti *et al*., 2008; Rowe *et al*., 2014), improve stem cell function (Yang *et al*., 2017; Berberoglu *et al.,* 2017), metabolic function (Kang & Krauss, 2010), and a greater proportion of type I fibres is known to be associated with poorer physical performance (Kitada *et al*., 2015). Future studies should therefore investigate the role of exercise in preventing or treating declining muscle function in older PLWH.

9.6 Novel investigations of mitochondrial function at the cellular and molecular level in renal tissue

Chronic kidney disease (CKD) remains an important comorbidity in older PLWH. In recent years, there has been particular concern about the renal toxicities of tenofovir disoproxil fumarate (TDF) (Atta *et al*., 2006; Foy *et al*., 2013; Woodward *et al*., 2009; Hamzah *et al*., 2017; Mocroft *et al*., 2016; Guaraldi *et al*., 2011). Although TDF has been shown to have a low binding affinity to the mitochondrial polymerase – PolG – it is nevertheless considered that the most likely pathological mechanism underpinning these renal-specific toxicities is TDF-induced mitochondrial dysfunction (Kohler *et al*., 2009; Samuels *et al*., 2017; Murphy *et al*., 2017; Ramamoorthy *et al*., 2018).

However, due to limitations around the ability to firstly acquire renal tissue in TDF-treated PLWH, and secondly investigate mitochondrial function at the individual cellular level (as opposed to homogenate studies), the underlying mechanisms remain poorly understood. In addition, whilst *in vitro* models allow for the assessment of these factors in specific renal cells, they fail to fully recapitulate the real effects of TDF in human renal toxicity in PLWH.

Hence, after acquiring renal biopsies from TDF and non-TDF-treated PLWH, as well as HIV- individuals who all presented with varying renal pathologies, I sought to determine whether renal mitochondrial function can be better assessed using novel validated cellular and molecular techniques pioneered in our lab (Rocha *et al*., 2015).

Indeed, the novel immunofluorescence assay which quantifies protein levels of CI, CIII, CIV, CV and mitochondrial mass, previously used on skeletal muscle (Rocha *et al*., 2015; Ahmed *et al*., 2017; Warren *et al*., 2020; Lehmann *et al*., 2019; **Chapter 4**; **Chapter 6**), brain (Hatton *et al*., 2020), and colon/intestinal tissue (Smith *et al*., 2020) was successfully applied to renal tissue, as discussed in **Chapter 8**.

In addition, individual proximal tubules and proximal tubule epithelial cells were successfully isolated by laser capture microdissection (LCM). Finally, using a quantitative real-time PCR assay with mtDNA gene targets, mtDNA deletions were investigated in isolated renal proximal tubules and single renal tubular epithelial cells for the first time. Hence, the work conducted as part of **Chapter 8** contained several novel experimental protocols which could have beneficial implications for future work aiming to better understand the pathophysiological mechanisms behind TDF-induced mitochondrial dysfunction and renal pathology.

9.7 Potential underlying mechanisms of mitochondrial dysfunction in older PLWH

A clear finding throughout this thesis was that mitochondrial dysfunction is implicated in age-related pathophysiology in older PLWH. Although specific CI dysfunction was demonstrated in both renal tissue (in **Chapter 8**) and skeletal muscle tissue (**Chapter 4**, **Chapter 6**), the mechanisms underpinning these phenomena are most likely different.

Whilst it is heavily suspected that the cause of skeletal muscle CI (and to a lesser extent CIV) deficiency in the HIV+ individuals was somatic large-scale mtDNA deletions that have clonally expanded and subsequently accumulated to a point exceeding the threshold for biochemical function (Payne *et al*., 2011), this was likely not the case for the CI and CV renal dysfunction. Instead, although this was not proven through the data collected as part of **Chapter 8**, the most likely genetic mechanisms

underpinning this CI and CV deficiency are somatic mtDNA point mutations. These *de novo* mtDNA point mutations could be the result of increased ROS production and subsequent oxidative stress, which is known to induce mtDNA point mutations (Taylor & Turnbull, 2005; Chung *et al*., 2014; Caldecott, 2008; Pinz *et al*., 1995; Baines *et al*., 2014). Indeed, more recent work in the field has suggested the role of enhanced oxidative stress in renal tubules leading to higher levels of mitochondrially-mediated apoptosis (Murphy *et al*., 2017; Ramamoorthy *et al*., 2018). Although CV is not a commonly affected ETC complex in age-associated mitochondrial dysfunction, preliminary work from our collaborators has suggested through genomic analyses of *in vitro* nephrotoxicity cell models that there is an upregulation in cristae remodelling genes and a downregulation of CV genes in TDF-exposed renal cells. They/we suggest that TDF proximal tubule accumulation induces enhanced ROS production, which would lead to mitochondrial stress and cristae remodelling (Cole *et al*., 2011; Cogliati *et al*., 2016), ultimately leading to a dysregulation in CV activity (Geromel *et al*., 2001; Ide *et al*., 1999). This model would also explain the formation of mtDNA point mutations, which subsequently could be affecting CI activity (Taylor & Turnbull, 2005).

9.8 Final conclusions

In this thesis, I have presented the first comprehensive analysis of skeletal muscle function in older PLWH, combining histopathological data with physical function, body composition and clinical parameters. This approach has allowed several novel observations to be made. Many of which provide a basis for future work, and some of which could have potential future clinical and therapeutic implications.

Firstly, I have shown that older PLWH in the contemporary ART era have an excess of skeletal muscle mitochondrial dysfunction. However, in contrast to the historical literature (Dalakas *et al*., 1990; Arnaudo *et al*., 1991; Lim & Copeland, 2001), this skeletal muscle mitochondrial dysfunction in PLWH was not solely predicted by ART exposure. In fact, the findings suggest that other potential factors such as chronic inflammation, oxidative stress, or immunosenescence are driving skeletal muscle mitochondrial dysfunction in older PLWH in the contemporary ART era.

Importantly, skeletal muscle function in older PLWH, including frail and sarcopenic PLWH, was comprehensively studied. Overall, these studies have significantly advanced our understanding of the potential pathophysiological mechanisms contributing to adverse ageing phenotypes in older PLWH. Of note, it was demonstrated that older PLWH experience dysregulated fibre type switching, in which mitochondrial dysfunction is playing a significant role. In addition, I demonstrated that older PLWH have an excess of skeletal muscle fibrosis. Both mitochondrial dysfunction and fibrosis were correlated with myofibre regeneration, suggesting an adaptive response to muscle damage.

However, neither mitochondrial dysfunction nor fibrosis appeared to directly explain the greater prevalence of frailty and sarcopenia in PLWH compared to age-matched HIV- individuals. This suggests that other HIV-related factors such as chronic inflammation are likely to also be playing a causative role in these adverse ageing phenotypes.

With regard to potential clinical impacts, these findings suggest that targeted exercise regimes may be beneficial in attenuating age-related physiological decline in older PLWH.

In conclusion, the work described in this thesis has demonstrated the importance of several aspects of skeletal muscle function in older people living with HIV, including mitochondrial function. Future work should attempt to link muscle and mitochondrial dysfunction with chronic inflammation in PLWH, and explore therapeutic strategies to improve these factors.

Chapter 10 – Appendices

Appendix 1 – MAGMA study protocol

'**M**uscle **Ag**eing and **A**nti-retroviral Study'

Chief Investigator: Dr Brendan Payne

REC reference: 17/NE/0015
IRAS ref: 212276

Protocol version: 1.21 (22.5.2017)
Funder: Wellcome Trust

Sponsor: Newcastle-upon-Tyne Hospitals NHS Foundation Trust (Ref.: 8149)

wellcome trust centre for Mitochondrial Research
Newcastle University
The Newcastle Upon Tyne Hospitals NHS Foundation Trust

Protocol Contacts

Chief Investigator:
Dr Brendan Payne, Honorary Consultant in Infectious Diseases & Virology
Wellcome Trust Centre for Mitochondrial Research, Institute of Genetic Medicine, Newcastle University, Newcastle-upon-Tyne.
Department of Infection & Tropical Medicine, Royal Victoria Infirmary, Newcastle-upon-Tyne.
0191 282 1161 / 0771 7531935
brendan.payne@ncl.ac.uk

Co-Investigator:
Dr Alan Winston, Reader in Genitourinary Medicine
Winston Churchill Wing, St. Mary's Campus, Imperial College London.
a.winston@imperial.ac.uk

Protocol Summary

Short title:	*MAGMA*
Protocol version: 1.21	
Protocol date:	*22.5.2017*
Chief Investigator:	*Dr Brendan Payne*
Sponsor:	*Newcastle-upon-Tyne Hospitals NHS Foundation Trust*
Funder:	*Wellcome Trust*
Study design:	*Observational, cross-sectional*
Primary objective:	*To determine whether anti-retroviral treated HIV-infected older people have an excess of mitochondrial defects in skeletal muscle compared with age-matched uninfected people.*
Secondary objectives:	*To determine whether mitochondrial defects in HIV-infected older people are in keeping with accelerated clonal expansion of mitochondrial DNA mutations.* *To determine whether mitochondrial defects in older HIV-infected people correlate with clinical parameters, anti-retroviral treatment, or markers of systemic inflammation.* *To determine whether muscle mitochondrial defects in HIV-infected people correlate with reduced physical function.*
Number of study sites: 2	
Study population/size:	*45*
Study duration:	*36 months*

Background

Anti-retroviral treated HIV-infected persons achieve good immune reconstitution, but nevertheless experience an increase in many of the common diseases and physiological changes of older age (1-3). Given the known links between mitochondria and ageing (4-8), and mitochondria and HIV infection (9-12), it is plausible that increased mitochondrial damage may be a biological mediator of ageing in HIV.

We have previously demonstrated that younger (aged <50) anti-retroviral treated persons have an excess of cells containing mtDNA mutations, but the mechanism remains to be determined (13). Our modelling suggests that the increase may be consistent with an acceleration of clonal expansion of mtDNA mutations within cells, particularly in the setting of exposure to certain NRTI anti-retroviral drugs. Conversely, other authors have suggested that HIV infection or therapy may be mutagenic for mtDNA (14-16). Which model is correct will dictate the natural history of the mitochondrial defect in later life.

Hypotheses

1) Anti-retroviral treated HIV-infected older men will have an excess of mitochondrial defects in skeletal muscle compared with age-matched HIV-uninfected men.
2) The pattern of mitochondrial defects found in HIV-infected men will be consistent with a mechanism of accelerated clonal expansion of mtDNA mutations.
3) Correlates of mitochondrial damage will include: increased age (>60 years), longer history of treated HIV infection (>15 years), increased systemic inflammation.
4) Increased mitochondrial damage will correlate with decreased physical function in HIV-infected men.

Objectives

Primary objective: To determine whether anti-retroviral treated HIV-infected older men have an excess of mitochondrial defects in skeletal muscle compared with age-matched uninfected men.

Secondary objectives: To determine whether mitochondrial defects in HIV-infected older men are in keeping with accelerated clonal expansion of mitochondrial DNA mutations.

To determine whether mitochondrial defects in HIV-infected men correlate with clinical parameters, anti-retroviral treatment, or markers of systemic inflammation.

To determine whether muscle mitochondrial defects in HIV-infected men correlate with reduced physical function.

Study Design

This is an observational cross-sectional study.

Primary outcome measures:

The proportion of skeletal muscle fibres with functional mitochondrial COX (cytochrome c oxidase) defects.

The level of mtDNA mutations in skeletal muscle.

Secondary outcome measures:

The plasma levels of inflammatory cytokines.

Physical performance as measured by a testing battery.

Definition of end of study:

For the purposes of recruitment, the end of study will be the last participant's final study contact. Recruitment is expected to take approximately 12 months.

Ethical permission will include ongoing analyses and storage of samples beyond that date.

Study of archived tissue:

The ethical and HRA permission for this study also allows for similar mitochondrial analyses to be performed on anonymised archival tissue samples obtained from research tissue banks and residual tissue from NHS histopathology departments.

Study of these tissues will allow cellular and molecular findings from the muscle biopsies to be extended to other tissues.

Tissues studied may include (but are not limited to): brain, bowel, cardiac, renal, plasma/serum, urine.

Samples requested may be from HIV positive subjects or healthy controls.

Samples will be supplied in anonymised form.

Tissue may be supplied as blocks or as slides (10µm sections, 2 sections per slide, 10 slides per case) at the preference of the supplying site.

Participants

A total of 45 subjects will be recruited:

HIV-infected n = 30.
HIV-uninfected n = 15.

Inclusion criteria

- Patient has provided written informed consent for participation in the study prior to any study specific procedures
- Age ≥50 years at time of study visit.
- Male
- Willing to travel to one of the study sites
- Willing to have muscle biopsy

HIV-infected group only:

- Documented positive HIV status at study entry

HIV-uninfected group only:

- Documented negative HIV test at study entry

Exclusion criteria

- Female
- Inability to give informed consent
- In the opinion of the investigator, those unable or unwilling to comply with the requirements of the study
- Life expectancy <6 months
- Known coagulation disorder or taking anti-coagulant medication
- Known or suspected neuromuscular disorder of a genetic basis
- Unable to walk 4 metres (use of a stick or walking frame is permitted)

Screening, Recruitment and Consent

Identification and screening of participants

Different processes will apply at the two study sites (Newcastle-upon-Tyne Hospitals, Imperial College Healthcare NHS Trust as follows):

Imperial College

- All subjects recruited will already be part of an existing longitudinal study of ageing in HIV ('POPPY').
- Potential subjects will be identified by a member of the POPPY study team, or the normal clinical team at site.
- This mechanism applies to both HIV-infected and uninfected subjects.

Newcastle

- Potential HIV-infected participants will be identified through screening of clinical records by a member of the study team who is also a member of the usual clinical team (the PI, or a colleague with documented, delegated responsibility).
- Potential HIV-infected participants will also be eligible if they receive their usual HIV care at other clinics within the Northeast HIV Network. In these cases those sites will serve as PIC sites. At these sites potential participants will be identified by a member of the usual clinical team at site.
- Potential HIV-uninfected subjects will be identified through genitourinary medicine clinics within the Northeast HIV Network (operating as PIC sites, as described above).
- Potential HIV-infected and uninfected subjects may also be peer referred.

Recruitment procedures

Imperial College

Potential participants from POPPY can be approached at the time of their routine clinic appointment, or a planned POPPY study visit. They may also be contacted by email or letter. A study Participant Information Sheet will be provided at this time and the patient allowed time to read it. At least 24 hours later this will be followed up by a telephone call to allow the patient to ask further questions, and if they are then agreeable, to book the study visit.

If a patient declines to participate this will be recorded to avoid them being approached again.

Newcastle

Eligible participants will be invited to participate by a member of the study team, who is also a member of the clinical team, during their routine consultation. A study Participant Information Sheet will be provided at this time and the patient allowed time to read it. Where prior consent exists to contact the patient by email or by letter a PIS may also be sent out in this manner. At least 24 hours later this will be followed up by a telephone call to allow the patient to ask further questions, and if they are then agreeable, to book the study visit.

If a patient declines to participate this will be recorded in the medical notes to avoid them being approached again.

Age bands

Whilst (for practical reasons) there is no specific stratification of recruitment target by age bands, sites will be specifically encouraged to identify older subjects, aged over 60, in addition to those aged 50-60 years.

In the case of HIV-uninfected subjects, these will be specifically age (by 5 year bands: 50-54, 55-59, 60-64, 65+) and sex matched with HIV-infected cases. This will be facilitated by identification of potential HIV-uninfected participants at the St Mary's site.

Consent procedures

Informed consent discussions will be untaken only by the investigator who is to perform the study procedures. Opportunity will be given for participants to ask any questions. Those wishing to take part will provide written informed consent by signing and dating the study consent form, which will be witnessed and dated by a member of the research team with documented, delegated responsibility to do so. Written informed consent should always be obtained prior to study specific investigations. The original signed consent form will be retained in the Investigator Site File, with a copy in the clinical notes and a copy provided to the participant. The participant will specifically consent to their GP being informed of their participation in the study. The right to refuse to participate without giving reasons must be respected.

Due to the small subject population, the information sheet and consent form for the study will be available only in English. Interpreters will be arranged for all visits of patients who require them via local NHS arrangements. Qualified interpreters will be used to explain the consent form and information sheet, and great priority will be placed on finding the most direct communication.

Consent will be taken at the time of the study visit, which in all cases will be at least 24 hours after receipt of the PIS by the patient.

Study Data

Study procedures

There will be some differences in the number of study procedures performed at the two study sites as those subjects attending the Imperial site will have already had some procedures performed as part of the POPPY study (procedures not required for these participants indicated *) and those data will be available for this study. HIV-specific data is not required for HIV uninfected participants (indicated †).

Subjects will attend for a single study visit, where the following will be performed:

- Written informed consent
- Completion of health and treatment questionnaires:
    - Demographics (age, self-reported ethnicity, country of birth, sexual orientation)*
    - Lifestyle factors (smoking, alcohol, drug use history), past medical history, current (non-HIV) medications*
    - General health and wellbeing (frailty assessment questions)
    - Current HIV treatment†
    - Past HIV treatment*†
    - HIV history (duration of infection, nadir CD4)†
- Completion of physical activity questionnaire
- Anthropometric measurements: height, weight, BMI, waist circumference
- Collection of serum, whole blood and urine samples, for immune / inflammatory cytokine profiling, mitochondrial DNA analyses, and storage for possible future metabolic profiling.
- Lean muscle mass assessment by whole body DXA*
- Short physical performance battery (17)
- Percutaneous skeletal muscle biopsy (from leg muscle) for mitochondrial analyses and gene expression profiling.

See study appendix for details of procedures.

Timings

All procedures will be performed in a single study visit, approximately as follows:

- Consent, collection of clinical data and blood samples: 30 mins
- Completion of questionnaires: 20 mins
- DXA scan: 20 mins
- Physical performance assessments: 20 mins
- Muscle biopsy: 20 mins
- Rest / observation after biopsy: 120 mins

All procedures should be completed within ~4hr.

Clinical laboratory data

Clinical and past treatment data for subjects in POPPY will be obtained by a data download. Only those parameters marked (†) will need verifying at the time of study visit.

In addition to those data collected by questionnaire (as above), clinical disease and treatment data will be collected by case-note review by a member of the study team who is also a member of the

clinical team. The following will be recorded:

- Current CD4 lymphocyte count†
- Current HIV RNA plasma viral load†
- Most recent laboratory tests will be recorded (in the HIV-infected cohort): renal, liver, lipid and bone profiles, glucose, full blood count. These tests should have been performed within a year of the clinic visit.

Data Handling & Record Keeping

A Study File will be maintained at each of the two study sites by the PI / Co-I in a locked office. Only members of the study team will have access to this file. This will contain a copy of the screening log and copies of the consent forms for enrolled subjects. This file will also contain a key of patient identifiers linked to anonymised study code for each subject.

All patient-identifiable data will be handled at the two clinical study sites and all samples and data handled at the University site will use anonymised codes only.

The PI has overall responsibility for data management.

Statistical Considerations

The primary analysis is the between-group comparison (HIV-infected vs. uninfected) of mtDNA mutation burden. The chosen sample sizes are well-powered to detect a mean difference of 0.33 $\log_{10}$ between groups (α 0.05, 1-β 0.92), based on past experience of SD for this measure.

Secondary analyses will include within group (HIV-infected) correlation between treatment parameters and mtDNA defect. The selected sample size will allow detection of a moderate (r 0.5) correlation (α 0.05, 1-β 0.8) (18).

Withdrawal

Participants have the right to withdraw from the study at any time for any reason, and without giving a reason. Should a patient decide to withdraw from the study, all efforts will be made to report the reason for withdrawal as thoroughly as possible.

As the study is a single visit, a request to withdrawal from the study will mean that no data is used for that patient, up until the point of publication of the study results.

Incidental findings

All blood results on HIV-infected subjects will already have been performed as part of routine clinical care and will have been actioned already if required.

Although not the primary purpose of performing the test, DXA scans may produce clinically actionable results regarding bone mineral density. This will be communicated to the patient's usual physician and GP.

The molecular analyses performed on mtDNA are such that no genetic information of potential relevance to the patient or their family would be discovered.

Adverse events

Adverse event reporting for this study will be as follows:

All Adverse Events (AE) that are related to any of the study procedures outlined in the protocol (e.g. during muscle biopsy, physical function testing, DXA scanning) will be reported to the sponsor. (Discomfort and bruising in line with that expected for the muscle biopsy or venepuncture does not count as an AE.)

As such AEs may present up to a few days after the study procedures, if the patient reports any AE with reference to the study visit then this will be recorded.

All Serious Adverse Events (SAE) will be reported to the sponsor (both those related to study procedures and those which may not be related to study procedures).

All study-related adverse events, however minor, will be documented. An adverse event is any untoward medical occurrence in a subject administered a pharmaceutical product or, in the case of this study, in a subject undergoing a study procedure (including events that do not necessarily have a

causal relationship with the study procedure). Adverse events observed by the Investigator, or reported by the subject, and any remedial action taken, will be recorded in the subject's CRF and should be verifiable in the subject's notes throughout the study. The nature of each event, time of onset (if known), after undergoing a study procedure will be documented together with in the Investigator's opinion of the causal relationship to the study procedure (unrelated, unlikely, possible, probable, definite and not assessable). All subjects experiencing adverse events, whether considered associated with study procedures or not, must be monitored until the symptoms subside.

Severity should be recorded and graded according to the AIDS Clinical Trial Group (ACTG) Grading Scale. Moreover, adverse events should be assessed in relation to their intensity, defined as follows:

MILD: the adverse event does not interfere with subject's usual function

MODERATE: the adverse event interferes to some extent with subject's usual function

SEVERE: the adverse event interferes significantly with subject's usual function

Serious Adverse Events (SAE)

A SAE is any untoward medical occurrence or effect that:

- Results in death
- Is life-threatening – refers to an event in which the subject was at risk of death at the time of the event; it does not refer to an event which hypothetically might have caused death if it were more severe
- Requires hospitalisation, or prolongation of existing inpatients' hospitalisation
- Results in persistent or significant disability or incapacity – there is a substantial disruption of a person's ability to carry out normal life functions
- Is a congenital abnormality or birth defect

An SAE form should be completed and faxed to for all SAEs within 24 hours of notification about the event. The ICTU / CRF will inform the following individuals within 24 hours of receiving notice of them:

- The Sponsor (Newcastle-upon-Tyne Hospitals)
- The Chief Investigator (Dr Brendan Payne)

Given the observational and nature of this study, no additional information on SAEs will be captured.

All SAEs and AEs will be recorded on the annual study reports that are sent to the REC.

Also, given the observational and non-interventional nature of this study, no serious, unexpected adverse drug reactions (SUSARs) reporting will be undertaken. As all subjects continue with their general clinical care, which is unaltered during the course of this study, the 'yellow card' reporting will be unaffected.

Ethics & Regulatory Issues

The conduct of this study will be in accordance with the recommendations for physicians involved in research on human subjects adopted by the 18th World Medical Assembly, Helsinki 1964 and later revisions.

Favourable ethical opinion from an appropriate REC and NHS R&D approval will be obtained prior to commencement of the study.

Information sheets will be provided to all eligible subjects and written informed consent obtained prior to any study procedures.

Study management

A study management group will be convened which will meet quarterly or as required (in person or by teleconference). This will include the CI, Co-I, research nurses involved in the study.

Confidentiality

Personal data will be regarded as strictly confidential. To preserve anonymity, any data leaving the site will identify participants by a unique study identification code only. The study will comply with the Data Protection Act, 1998. All study records and Investigator Site Files will be kept at site in a locked filing cabinet with restricted access.

Insurance

The Newcastle-upon-Tyne Hospitals NHS Foundation Trust has liability for clinical negligence that harms individuals toward whom they have a duty of care. NHS Indemnity covers NHS staff and medical academic staff with honorary contracts conducting the trial for potential liability in respect of negligent harm arising from the conduct of the study. The Trust is Sponsor and through the Sponsor, NHS indemnity is provided in respect of potential liability and negligent harm arising from study management. Indemnity in respect of potential liability arising from negligent harm related to study design is provided by NHS schemes for those protocol authors who have their substantive contracts of employment with the NHS and by Newcastle University Insurance schemes for those protocol authors who have their substantive contract of employment with the University. This is a non-commercial study and there are no arrangements for non-negligent compensation.

Study Report / Publications

The data will be the property of the Chief Investigator and Co-Investigators. Publication will be the responsibility of the Chief Investigator.

It is planned to publish this study in peer review articles and to present data at national and international meetings. Results of the study will also be reported to the Sponsor and Funder. All

manuscripts, abstracts or other modes of presentation will be reviewed by the Trial Steering Committee and Funder prior to submission. Individuals will not be identified from any study report.

Participants will be informed about their treatment and their contribution to the study at the end of the study, including a lay summary of the results.

References

1. Oursler KK, Sorkin JD, Smith BA, Katzel LI. Reduced aerobic capacity and physical functioning in older HIV-infected men. AIDS research and human retroviruses. 2006 Nov;22(11):1113-21. PubMed PMID: 17147498. Epub 2006/12/07. eng.

2. Desquilbet L, Jacobson LP, Fried LP, Phair JP, Jamieson BD, Holloway M, et al. HIV- 1 infection is associated with an earlier occurrence of a phenotype related to frailty. J Gerontol A Biol Sci Med Sci. 2007 Nov;62(11):1279-86. PubMed PMID: 18000149. Epub 2007/11/15. eng.

3. Erlandson KM, Allshouse AA, Jankowski CM, Mawhinney S, Kohrt WM, Campbell TB. Functional Impairment is Associated with Low Bone and Muscle Mass among Persons Aging with HIV-Infection. Journal of acquired immune deficiency syndromes (1999). 2013 Feb 7. PubMed PMID: 23392468.

4. Brierley EJ, Johnson MA, Lightowlers RN, James OF, Turnbull DM. Role of mitochondrial DNA mutations in human aging: implications for the central nervous system and muscle. Annals of neurology. 1998 Feb;43(2):217-23. PubMed PMID: 9485063. eng.

5. Bua E, Johnson J, Herbst A, Delong B, McKenzie D, Salamat S, et al. Mitochondrial DNA-deletion mutations accumulate intracellularly to detrimental levels in aged human skeletal muscle fibers. American journal of human genetics. 2006 Sep;79(3):469-80. PubMed PMID: 16909385. eng.

6. Kujoth GC, Hiona A, Pugh TD, Someya S, Panzer K, Wohlgemuth SE, et al. Mitochondrial DNA mutations, oxidative stress, and apoptosis in mammalian aging. Science (New York, NY. 2005 Jul 15;309(5733):481-4. PubMed PMID: 16020738. eng.

7. Short KR, Bigelow ML, Kahl J, Singh R, Coenen-Schimke J, Raghavakaimal S, et al. Decline in skeletal muscle mitochondrial function with aging in humans. Proceedings of the National Academy of Sciences of the United States of America. 2005 Apr 12;102(15):5618- 23. PubMed PMID: 15800038. Epub 2005/04/01. eng.

8. Taylor RW, Barron MJ, Borthwick GM, Gospel A, Chinnery PF, Samuels DC, et al. Mitochondrial DNA mutations in human colonic crypt stem cells. The Journal of clinical investigation. 2003 Nov;112(9):1351-60. PubMed PMID: 14597761. eng.

9. Arnaudo E, Dalakas M, Shanske S, Moraes CT, DiMauro S, Schon EA. Depletion of muscle mitochondrial DNA in AIDS patients with zidovudine-induced myopathy. Lancet. 1991 Mar 2;337(8740):508-10. PubMed PMID: 1671889. eng.

10. Shikuma CM, Hu N, Milne C, Yost F, Waslien C, Shimizu S, et al. Mitochondrial DNA decrease in subcutaneous adipose tissue of HIV-infected individuals with peripheral lipoatrophy. AIDS (London, England). 2001 Sep 28;15(14):1801-9. PubMed PMID: 11579242. eng.

11. Cote HC, Brumme ZL, Craib KJ, Alexander CS, Wynhoven B, Ting L, et al. Changes in mitochondrial DNA as a marker of nucleoside toxicity in HIV-infected patients. The New England journal of medicine. 2002 Mar 14;346(11):811-20. PubMed PMID: 11893792. Epub 2002/03/15. eng.

12. Miura T, Goto M, Hosoya N, Odawara T, Kitamura Y, Nakamura T, et al. Depletion of mitochondrial DNA in HIV-1-infected patients and its amelioration by antiretroviral therapy. Journal of medical virology. 2003 Aug;70(4):497-505. PubMed PMID: 12794710. eng.

13. Payne BA, Wilson IJ, Hateley CA, Horvath R, Santibanez-Koref M, Samuels DC, et al. Mitochondrial aging is accelerated by anti-retroviral therapy through the clonal expansion

of mtDNA mutations. Nature genetics. 2011 Aug;43(8):806-10. PubMed PMID: 21706004. Pubmed Central PMCID: 3223397. Epub 2011/06/28. eng.

14. Martin AM, Hammond E, Nolan D, Pace C, Den Boer M, Taylor L, et al. Accumulation of mitochondrial DNA mutations in human immunodeficiency virus-infected patients treated with nucleoside-analogue reverse-transcriptase inhibitors. American journal of human genetics. 2003 Mar;72(3):549-60. PubMed PMID: 12587093. eng.

15. Walker DM, Poirier MC, Campen MJ, Cook DL, Jr., Divi RL, Nagashima K, et al. Persistence of mitochondrial toxicity in hearts of female B6C3F1 mice exposed in utero to 3'- azido-3'-deoxythymidine. Cardiovascular toxicology. 2004;4(2):133-53. PubMed PMID: 15371630. Epub 2004/09/17. eng.

16. Jitratkosol MH, Sattha B, Maan EJ, Gadawski I, Harrigan PR, Forbes JC, et al. Blood mitochondrial DNA mutations in HIV-infected women and their infants exposed to HAART during pregnancy. AIDS (London, England). 2012 Mar 27;26(6):675-83. PubMed PMID: 22436539. Epub 2012/03/23. Eng.

17. Erlandson KM, Allshouse AA, Jankowski CM, Duong S, Mawhinney S, Kohrt WM, et al. Comparison of functional status instruments in HIV-infected adults on effective antiretroviral therapy. HIV clinical trials. 2012 Nov-Dec;13(6):324-34. PubMed PMID: 23195670. Pubmed Central PMCID: 4379206.

18. Lachin JM. Introduction to sample size determination and power analysis for clinical trials. Controlled clinical trials. 1981 Jun;2(2):93-113. PubMed PMID: 7273794.

Appendix 2 – Health Questionnaire

Instructions to Clinical Research Nurse:

Please ask the participant to complete the following forms.

This questionnaire is in 5 sections. **Not all participants need to complete all sections**. Please check the top of each section before giving it to the participant.

Please write the participant code number on the top of each sheet before giving them to the participant.

The table below shows which forms are required for each group of participants:

HIV positive participant at Newcastle site	**HIV positive participant at St Mary's site**
Section 1 Section 2 Section 3 Section 4 Section 5	Section 2 Section 3 Section 5
HIV negative participant at Newcastle site	**HIV negative participant at St Mary's site**
Section 1 Section 2	Section 2

Section 1 – questions about your medical history

Note to research nurse: this section is for participants at Newcastle site only.

Please complete this questionnaire as best as you can. Please ask the research nurse / doctor if you are uncertain. This section contains 3 sides of questions.

General questions:

What is your age in years? _____

What country were you born in? _____

How would you describe your ethnic group (e.g. black African, white British etc.)?

(*leave blank if prefer not to say*) _____

How would you describe your sexual orientation?

Gay ☐ Bisexual ☐

Straight ☐ Other / prefer not to say ☐

Lifestyle questions:

Have you ever smoked? (Please tick one answer): I

am a current smoker ☐

I am a social smoker I ☐

am an ex-smoker ☐

I have never smoked ☐

Do you drink alcohol?

Yes currently ☐

Previously but not currently ☐

Never / almost never ☐

If you drink alcohol currently, how much do you drink in an average **week**? (Please write the number of each drink per week in the box):

Beer or cider (pints) ☐

Wine (glasses) ☐

Spirits (single measures) ☐

Have you used any recreational drugs **in the last 6 months**? (Please tick one answer):

Yes ☐ No ☐

If yes, please list which _____

Please turn over for the next set of questions

Medical history:

Below is a list of common types of medical conditions, with examples of each type. Please tick any that you have ever suffered from. Please give any further details in the right hand column where indicated.

Medical condition	**Tick if here you have been affected**	**Further details**
Heart disease *Includes: myocardial infarction ('heart attack'), angina, acute coronary syndrome, coronary artery bypass, coronary artery stenting, cardiac arrhythmias (abnormal heart rhythms), cardiac arrest, heart failure (congestive cardiac failure)*		*Please state type of cardiovascular disease:*
Peripheral vascular disease *Includes: claudication, bypass grafts of legs, stents to legs, aortic aneurysm*		*Please state type of peripheral vascular disease:*
Stroke *Includes: 'mini stroke', TIA*		*Please state type:*
Renal (kidney) disease		*Please state type:*
Liver disease *Includes: hepatitis, hep B, hep C*		*Please state type:*
Diabetes		
Cancer		*Please state type:*
Joint disease (arthritis) or joint replacements		*Please state type of arthritis and any joints that have been replaced:*
Fractures (broken bones)		*Please state which bones:*
Osteoporosis		
Falls		*Please state number of falls that you think you have had* ***in the last 12 months****:*

Medications

Please list below all the medications that you currently take. Please list both prescribed medications and ones that you buy over-the-counter.

Tick here if you do not take any medications ☐

Thank you for completing this form. Please hand it back to the research nurse / doctor.

Section 2 – questions about your general health and wellbeing

Note to research nurse: this section is for all participants

Please complete the following questions. It is not a test! Please just choose the answer that you think fits best for you. If you are not sure, please ask the research nurse / doctor.

1. In **the last 12 months** has your weight decreased, increased or has it stayed about the same? (Please tick one answer):

1-Decreased ☐ 2-Increased ☐ 3-Stayed about the same ☐

If you chose answer 1, go to question 2.

If you chose answer 2 or 3, go straight to question 3.

2. Was your weight loss intentional, for example, you were dieting? (Please tick):

1-Yes ☐ 2-No ☐

If you answered 'Yes', go to question 3.

If you answered 'No', continue with this question.

a. Approximately how much weight did you lose **over the last 12 months**? (You can give your answer in either kg **or** lbs):

..... kg .....lbs

3. Does your health limit you in vigorous activities, such as running, lifting heavy objects, or participating in strenuous sports? (Please tick one answer):

1-Yes, limited a lot ☐ 2-Yes, limited a little ☐ 3-No, not limited at all ☐

For the following statement, tick the answer that best describes how often you felt or behaved this way **during the past week**:

4. Everything I did was an effort:

1-Rarely or none of the time (<1 day) ☐

2-Some or a little of the time (1-2 days) ☐

3-Occasionally or a moderate amount of time (3-4 days) ☐

4-Most or all of the time (5-7 days) ☐

For the following statement, tick the answer that best describes how often you felt or behaved this way **during the past week**:

5. I could not get going:

1-Rarely or none of the time (<1 day) ☐

2-Some or a little of the time (1-2 days) ☐

3-Occasionally or a moderate amount of time (3-4 days) ☐

4-Most or all of the time (5-7 days) ☐

Section 3 – questions about your current HIV treatment

Note for research nurse: this section is for HIV positive participants only

Please write the names of all the HIV drugs that you are **currently** taking in the table below. We just need drug names, not doses or how many times per day.

If you cannot remember the date that you started a drug please just put a ? in the relevant box (e.g. ??/12 for sometime in 2012, or ??/?? if you have no idea). If you are not sure about how to complete this form, please ask the research nurse or doctor. Thank you.

HIV treatment name	**Date started (MM/YY)**	**Date stopped (MM/YY)**

Thank you for completing this form. Please hand it back to the research nurse / doctor.

Section 4 – questions about your previous HIV treatment

Note for research nurse: this section is for HIV positive participants at the Newcastle site only.

We would like you to try and remember the details of any HIV treatment that you may have had in the past. Please include all previous HIV treatments but **do not** include the treatment you are on now. We just need drug names, not doses or how many times per day.

If you cannot remember the dates please just put a ? in the relevant box (e.g. ??/12 for sometime in 2012, or ??/?? if you have no idea). If you are not sure about how to complete this form, please ask the research nurse or doctor. Thank you.

If your current HIV treatment is your first ever regimen then please tick this box (you do not need to complete the rest of this page). ☐

If you have had other HIV treatment regimens in the past but cannot remember any of them please tick this box (we will try to confirm them from your medical records). ☐

HIV treatment name	Date started (MM/YY)	Date stopped (MM/YY)

If you have any other comments about past HIV treatments you have taken please write them here:

Thank you for completing this form. Please hand it back to the research nurse / doctor.

Section 5 – questions about your HIV

Note for research nurse: this section is for HIV positive participants only

Please try and complete the three questions below.

If you cannot remember the dates please just put a ? in the relevant box (e.g. ??/12 for sometime in 2012, or ??/?? if you have no idea). If you are not sure about how to complete this form, please ask the research nurse or doctor. Thank you.

When were you first diagnosed with HIV? (MM/YY) _ _ / _ _

When do you think you became HIV positive? (MM/YY) _ _ / _ _

What is the **lowest** CD4 count that you can ever remember having (please tick the relevant box)?

- Between 0 and 100 ☐
- Between 100 and 200 ☐
- Between 200 and 350 ☐
- More than 350 ☐
- Don't know ☐

Thank you for completing this form. Please hand it back to the research nurse / doctor.

Appendix 3 – Physical performance assessment

Scoring sheets

Single Chair Rise, Repeated Chair Rise

1) "*This is a test of strength in your legs in which you stand up without using your arms*."
2) "*Fold your arms across your chest, like this, and stand when I say GO, keeping your arms in this position. OK*? Ready, go!"

   Able to rise 1 time? **Yes / No**

3) If able to rise… ***"This time, I want you to stand up ten times as quickly as you can, keeping your arms folded across your chest. When you stand up, come to a full standing position each time, and when you sit down, sit all the way down each time. I'll demonstrate two chair stands to show you how it is done."*** Rise two times as quickly as you can, counting as you sit down each time. Cross your arms over your chest and emphasize full standing position, all the way down.

4) ***"When I say 'Go' stand ten times in a row, as quickly as you can, without stopping. Stand up all the way, and sit all the way down each time. Ready? Go!"*** Start timing as soon as you say "*Go*." Count aloud: "*1, 2, 3, 4, 5, 6, 7, 8, 9, 10*" when the participant **sits down** each time. **After the participant sits down for the fifth time, depress the split button on the stopwatch**. When the participant stops for the tenth time, then "stop" the stopwatch.

5 x chair rise ____:_____seconds

10x chair rise_____:_____seconds

__Unable to complete 5 chair stands

__Complete > 5 but < 10 stands

 ___# completed_____:_____sec

Balance Test

1. "*I'm going to ask you to stand in several different positions that test your balance. I'll demonstrate each* position and then ask you to try to stand in each position for up to 30 seconds. I'll be near you to provide support, and the wall is close enough to prevent you from falling if you lose your balance. Do you have any questions?"

2. ***"First I would like you to try to stand with your feet together, side-by side, for 30 seconds. Please watch while I demonstrate."*** Demonstrate while you say: ***"You may use your arms, bend your knees, or move your body to maintain your balance, but try not to move your feet. Try to hold your feet in this position until I say stop."***

3. Begin the test. Allow the participant to hold onto your arm to get balanced. ***"Hold onto the chair while you get in position. When you are ready, let go and I'll start timing. Ready? Go!"*** Start timing when the participant lets go. (If the participant does not hold onto your arm, start timing when he/she is in position. Stop the stopwatch if he/she takes a step or grabs for support. Record to 0.01 second the time the participant could hold this position. **Say, "STOP" after 30 seconds.**

___Side-by-side x 10 sec

___Side-by-side x 30 sec

Time (if other than 30 sec)

____: ____

If side-by-side test is 10 seconds or longer, proceed with the next test:

4. "***Now I would like you to try to stand with the side of the heel of one foot touching the big toe of the other foot for 30 seconds. Please watch while I demonstrate."*** Demonstrate and say: ***"You may put either foot in front, whichever is more comfortable. You can use your arms and body to maintain your balance. Try to hold your feet in position until I say stop. If you lose your balance, take a step like this. Hold onto the chair while you get in position. When you are ready, let go and I'll start timing. Ready? Go!"*** Start timing when the participant lets go. (If the participant does not hold onto your arm, start timing when he/she is in position. Stop the stopwatch if he/she takes a step or grabs for support. Record to 0.01 second the time the participant could hold this position. Say, "STOP" after 30 seconds.

___Semi-tandem x 10 sec

___ Semi-tandem x 30 sec

Time (if other than 30 sec)

____: ____

___Not attempted

If able to hold semi-tandem for 10 seconds or longer, proceed with next test:

5. **"Now I would like you to try to stand with the heel of one foot in front of and touching the toes of the other foot. I'll demonstrate."** Demonstrate, and say: **"Again, you may use your arms and body to maintain your balance. Try to hold your feet in position until I say stop. If you lose your balance, take a step, like this. Hold onto the chair while you get in position. When you are ready, let go and I'll start timing. Ready? Go!"** Start timing when the participant lets go. Stop the stopwatch if he/she takes a step or grabs for support. Record to 0.01 second how long the participant is able to hold this position. Say, "STOP" after 30 seconds.

___ Tandem x 10 sec

___ Tandem x 30 sec

Time (if other than 30 sec)

____: ____

6. If the participant holds the position for *at least 10 seconds*, go to the Single Leg Stand. If the participant attempts the Tandem Stand and is unable or cannot hold it *for at least one second*, perform a second trial of the Tandem Stand. "Now, let's try that again. Hold onto my arm while you get into position. When you are ready, let go and I'll start timing."

If able to hold tandem stand for 10 seconds or longer, proceed with the next test:

7. ***"For the last position, I would like you to try to stand on one leg for 30 seconds. You may stand on either leg, whichever is more comfortable. I'll demonstrate.***" Demonstrate the single leg stand by lifting the heel of one leg so that the toes are about 2 inches off the floor. The knee should be flexed and hip should remain straight (so that the foot goes behind the participant rather than in front). Demonstrate and say: ***"Try to stand on one leg until I say stop. If you lose your balance, then put your foot down. Hold onto my arm while you get in position. When you are ready, let go, and I'll start timing. Ready? Go!"*** Start timing when the participant lets go. Stop the stopwatch if he/she takes a step or grabs for support. Record to 0.01 second how long participant is able to hold this position. Say, "STOP" after 30 seconds.

8. If the position is held for less than 30 seconds, *for this test only*, perform a second trial of the Single Leg Stand. "***Now, let's try the same thing one more time."***

___ One-leg x 30 sec on 1st try

___ One-leg x 30 sec on 2nd try

Time (if not 30 sec) on 1st try_____:_____

Time (if not 30 sec) on 2nd try_____: _____

___ Not attempted

Grip Strength

Assess whether the participant can complete the Grip Strength Test.

Script: "In this exercise, I am going to use this instrument to measure the strength in your dominant hand."

Dominant Hand: Right / Left

1) ***"Are you right handed or left handed?"***
2) ***"Have you had any recent pain in your wrist or hand, or any acute flare-up in your wrist or hand from conditions like arthritis, tendonitis or carpel tunnel syndrome? Do you think that squeezing this instrument would cause you to have pain"?***
3) ***"Have you had any surgery on your hands or arms during the last 3 months?"***
4) ***"Do you think you can safely squeeze this instrument as hard as you can with your [right/left] hand?"***

Instructions and Demonstration

While the examiner is demonstrating the procedure, read the following script: "***I'd like you to take your dominant arm, press your arm against your side and grab the two pieces of metal together like this***." (Examiner should be holding the dynamometer in the correct position).

"When I say 'squeeze,' squeeze as hard as you can (examiner demonstrates). The two pieces of metal do not move, but I will be able to read the force of your grip on the dial (examiner points to the dial). I will ask you to do this three times. If you feel any pain or discomfort, tell me. Do you have any questions?"

Performance and Scoring

1. Hand the dynamometer to the participant and place the wrist strap around his/her wrist.
2. Script: "***Press your arm against your side and grip the two pieces of metal with your dominant hand. Your wrist should be straight. "Ready? Go! Squeeze, squeeze, squeeze!!*** When the needle starts to go down, tell the subject to stop.
3. Record the strength in kilograms (round DOWN to the nearest line). Reset the dynamometer to zero.
4. "***Now we will test your strength a second time. When I say 'squeeze,' squeeze as hard as you can. Ready? Go! Squeeze, squeeze, squeeze!*** When the needle starts to go down, tell the subject to stop.
5. Record the strength in kilograms (round DOWN to the nearest line). Reset the dynamometer to zero.
6. ***"Now we will test your strength a third and final time. When I say 'squeeze,' squeeze as hard as you can. Ready? Go! Squeeze, squeeze, squeeze!*** When the needle starts to go down, tell the subject to stop.

Attempt #1_____kg

Attempt #2_____kg

Attempt #3_____kg

If unable, indicate why he/she was unable to complete the grip strength test and STOP TESTING. If attempted, but unable physically, STOP TESTING.

METER WALK

Script*: **"In this test, I would like you to walk at your usual pace from this red line to the other red line. Do you think you could do that? Good. Can you see the tape? Good. Let me demonstrate what I want you to do**."* Read the following script while demonstrating the procedure for the participant: ***"To do this test, place your toes behind the tape. I will time you. When I say 'Go!' walk at your usual pace past the line*** (examiner walks the 4 meters past the other piece of tape). ***Do you have any questions?"***

Record if participant regularly uses an assistive device (cane/walking stick, walker, wheelchair, scooter, or other) when walking? Y / N

Device:_____

Performance and Scoring

1. The tester will stay at the finish line to time the test. When you are in position, say***: "Now we will begin the test. Please start with your toes behind the piece of tape."***

2. When the participant is properly at the starting tape, say "***Ready? Go!"*** and start the stopwatch when you say go (even if the participant has a pause before he/she begins). Stop the stopwatch when the participant's **first foot** is completely across the finish line.

3. Record the time and reset the stopwatch to 0. Ask the participant to return to the starting line.

4. Script: "Now, I'd like you to try this test a second time. Start with your toes behind the piece of tape.

   When I say *"Go!" walk at your usual pace to the line."*

4. When the participant is properly at the cone, say ***"Ready, go!"*** and start the stopwatch when you say go. Stop the stopwatch when the participant's first foot is completely across the finish line.

_____

Walk attempted? Y / N If no, record reason(s)
Walk #1_____._____seconds
Walk #2_____._____seconds

"Thank you. This is the end of this test."

Appendix 4 – Physical activity questionnaire

We are interested in finding out about the kinds of physical activities that people do aspart of their everyday lives. The questions will ask you about the time you spent beingphysically active in the **last 7 days**. Please answer each question even if you do not consider yourself to be an active person. Please think about the activities you do at work, as part of your house and garden work, to get from place to place, and in your spare time for recreation, exercise or sport.

Think about all the **vigorous** activities that you did in the **last 7 days**. **Vigorous** physical activities refer to activities that take hard physical effort and make you breathemuch harder than normal. Think *only* about those physical activities that you did for atleast 10 minutes at a time.

1. During the **last 7 days**, on how many days did you do **vigorous** physical activities like heavy lifting, digging, aerobics, or fast bicycling?

_____days per week

☐ No vigorous physical activities → ***Skip to question 3***

2. How much time did you usually spend doing **vigorous** physical activities on oneof those days?

_____**hours per day**

_____**minutes per day**

☐ Don't know/Not sure

Think about all the **moderate** activities that you did in the **last 7 days**. **Moderate** activities refer to activities that take moderate physical effort and make you breathe somewhat harder than normal. Think only about those physical activities that you didfor at least 10 minutes at a time.

3. During the **last 7 days**, on how many days did you do **moderate** physical activities like carrying light loads, bicycling at a regular pace, or doubles tennis?Do not include walking.

_____days per week

☐ No moderate physical activities → ***Skip to question 5***

4. How much time did you usually spend doing **moderate** physical activities on oneof those days?

_____**hours per day**

_____**minutes per day**

☐ Don't know/Not sure

Think about the time you spent **walking** in the **last 7 days**. This includes at work and athome, walking to travel from place to place, and any other walking that you have done solely for recreation, sport, exercise, or leisure.

5. During the **last 7 days**, on how many days did you **walk** for at least 10 minutesat a time?

_____days per week

☐ No walking → ***Skip to question 7***

6. How much time did you usually spend **walking** on one of those days?

_____**hours per day**

_____**minutes per day**

☐ Don't know/Not sure

The last question is about the time you spent **sitting** on weekdays during the **last 7 days**. Include time spent at work, at home, while doing course work and during leisuretime. This may include time spent sitting at a desk, visiting friends, reading, or sitting orlying down to watch television.

7. During the **last 7 days**, how much time did you spend **sitting** on a **week day**?

_____**hours per day**

_____**minutes per day**

☐ Don't know/Not sure

This is the end of the questionnaire, thank you. Please hand it back tothe nurse / doctor.

Appendix 5 – IRAS approval

17 March 2017

Dear Dr Payne

Letter of HRA Approval

Study title:	**Muscle Ageing and Anti-retroviral study**
IRAS project ID:	**212276**
REC reference:	**17/NE/0015**
Sponsor	**Newcastle-upon-Tyne Hospitals NHS Foundation Trust**

I am pleased to confirm that **HRA Approval** has been given for the above referenced study, on the basis described in the application form, protocol, supporting documentation and any clarifications noted in this letter.

Participation of NHS Organisations in England

The sponsor should now provide a copy of this letter to all participating NHS organisations in England.

Appendix B provides important information for sponsors and participating NHS organisations in England for arranging and confirming capacity and capability. **Please read *Appendix B* carefully**, in particular the following sections:

- *Participating NHS organisations in England* – this clarifies the types of participating organisations in the study and whether or not all organisations will be undertaking the same activities
- *Confirmation of capacity and capability* - this confirms whether or not each type of participating NHS organisation in England is expected to give formal confirmation of capacity and capability. Where formal confirmation is not expected, the section also provides details on the time limit given to participating organisations to opt out of the study, or request additional time, before their participation is assumed.
- *Allocation of responsibilities and rights are agreed and documented (4.1 of HRA assessment criteria)* - this provides detail on the form of agreement to be used in the study to confirm capacity and capability, where applicable.

Further information on funding, HR processes, and compliance with HRA criteria and standards is also provided.

It is critical that you involve both the research management function (e.g. R&D office) supporting each

organisation and the local research team (where there is one) in setting up your study. Contact details and further information about working with the research management function for each organisation can be accessed from www.hra.nhs.uk/hra-approval.

Appendices

The HRA Approval letter contains the following appendices:

- A – List of documents reviewed during HRA assessment
- B – Summary of HRA assessment

After HRA Approval

The document *"After Ethical Review – guidance for sponsors and investigators",* issued with your REC favourable opinion, gives detailed guidance on reporting expectations for studies, including:

- Registration of research
- Notifying amendments
- Notifying the end of the study

The HRA website also provides guidance on these topics, and is updated in the light of changes in reporting expectations or procedures.

In addition to the guidance in the above, please note the following:

- HRA Approval applies for the duration of your REC favourable opinion, unless otherwise notified in writing by the HRA.
- Substantial amendments should be submitted directly to the Research Ethics Committee, as detailed in the *After Ethical Review* document. Non-substantial amendments should be submitted for review by the HRA using the form provided on the HRA website, and emailed to hra.amendments@nhs.net.
- The HRA will categorise amendments (substantial and non-substantial) and issue confirmation of continued HRA Approval. Further details can be found on the HRA website.

Scope

HRA Approval provides an approval for research involving patients or staff in NHS organisations in England.

If your study involves NHS organisations in other countries in the UK, please contact the relevant national coordinating functions for support and advice. Further information can be found at http://www.hra.nhs.uk/resources/applying-for-reviews/nhs-hsc-rd-review/.

If there are participating non-NHS organisations, local agreement should be obtained in accordance with the procedures of the local participating non-NHS organisation.

User Feedback

The Health Research Authority is continually striving to provide a high quality service to all applicants and sponsors. You are invited to give your view of the service you have received and the application

procedure. If you wish to make your views known please use the feedback form available on the HRA website: http://www.hra.nhs.uk/about-the-hra/governance/quality-assurance/.

HRA Training

We are pleased to welcome researchers and research management staff at our training days – see details at http://www.hra.nhs.uk/hra-training/

Your IRAS project ID is **212276**. Please quote this on all correspondence. Yours

sincerely

Alison Thorpe

Senior Assessor

Email: hra.approval@nhs.net

Copy to: *Mr Andrew Johnston , RM&G Manager, Newcastle Joint Research Office*

Appendix A - List of Documents

The final document set assessed and approved by HRA Approval is listed below.

Document	*Version*	*Date*
Contract/Study Agreement [Template Agreement]		24 December 2016
Copies of advertisement materials for research participants [Poster]	1.0	06 December 2016
Covering letter on headed paper		12 December 2016
Covering letter on headed paper		10 February 2017
Evidence of Sponsor insurance or indemnity (non NHS Sponsors only) [Indemnity for study design - Newcastle University]		19 July 2016
GP/consultant information sheets or letters	1.0	06 December 2016
IRAS Application Form [IRAS_Form_21122016]		21 December 2016
IRAS Application Form XML file [IRAS_Form_21122016]		21 December 2016
Laboratory Manual [Skeletal muscle biopsy]	1.1	10 February 2017
Laboratory Manual [Physical performance assessment - instructions]	1.0	06 December 2016
Laboratory Manual [Physical performance assessment - record]	1.0	06 December 2016
Letter from funder [Fellowship award letter - Wellcome Trust]		18 December 2015
Letters of invitation to participant [Letter of invitation]	1.1	10 February 2017
Non-validated questionnaire [Health questionnaire]	1.0	06 December 2016
Other [SoA PIC Sites]	1.0	10 February 2017
Other [SoA Study Sites]	1.1	10 February 2017
Other [SoE PIC Sites]	1.0	10 February 2017
Other [SoE Study Sites]	1.0	10 February 2017
Participant consent form	1.0	06 December 2016
Participant information sheet (PIS) [Newcastle site]	1.3	08 March 2017
Participant information sheet (PIS) [St Mary's Site]	1.3	08 March 2017
Referee's report or other scientific critique report [Reviewer's comments - Wellcome Trust]		
Research protocol or project proposal	1.2	10 February 2017
Summary CV for Chief Investigator (CI)		06 December 2016
Validated questionnaire [Physical activity questionnaire]	1.0	

Appendix B - Summary of HRA Assessment

This appendix provides assurance to you, the sponsor and the NHS in England that the study, as reviewed for HRA Approval, is compliant with relevant standards. It also provides information and clarification, where appropriate, to participating NHS organisations in England to assist in assessing and arranging capacity and capability.

For information on how the sponsor should be working with participating NHS organisations in England, please refer to the, *participating NHS organisations, capacity and capability* and *Allocation of responsibilities and rights are agreed and documented (4.1 of HRA assessment criteria)* sections in this appendix.

The following person is the sponsor contact for the purpose of addressing participating organisation questions relating to the study:

Name: Andrew Johnston

Tel: 0191 282 5969

Email: andrew.johnston@nuth.nhs.uk

HRA assessment criteria

Section	HRA Assessment Criteria	Compliant with Standards	Comments
1.1	IRAS application completed correctly	Yes	No comments
2.1	Participant information/consent documents and consent process	Yes	No comments
3.1	Protocol assessment	Yes	No comments
4.1	Allocation of responsibilities and rights are agreed and documented	Yes	The sponsor intends that an unmodified mNCA acts as the agreement between the sponsor and the research site. The statement of activities will act as the agreement for participant identification centres (PICs), there will be no funding provided by the sponsor to the PICs.
4.2	Insurance/indemnity	Yes	Where applicable, independent

Section	HRA Assessment Criteria	Compliant with Standards	Comments
	arrangements assessed		contractors (e.g. General Practitioners) should ensure that the professional indemnity provided by their medical defence organisation covers the activities expected of them for this research study
4.3	Financial arrangements assessed	Yes	Financial arrangements for research sites are detailed in the mNCA. There is no funding available from the sponsor for the PICs.
5.1	Compliance with the Data Protection Act and data security issues assessed	Yes	No comments
5.2	CTIMPS – Arrangements for compliance with the Clinical Trials Regulations assessed	Not Applicable	No comments
5.3	Compliance with any applicable laws or regulations	Yes	Human Tissue Act – the applicant confirmed that any samples imported for the study would have the appropriate consent in place taken in the country of origin.
6.1	NHS Research Ethics Committee favourable opinion received for applicable studies	Yes	No comments
6.2	CTIMPS – Clinical Trials Authorisation (CTA) letter received	Not Applicable	No comments
6.3	Devices – MHRA notice of no objection received	Not Applicable	No comments
6.4	Other regulatory approvals and authorisations received	Not Applicable	No comments

Participating NHS Organisations in England

This provides detail on the types of participating NHS organisations in the study and a statement as to whether the activities at all organisations are the same or different.
There are two types of participating NHS organisations. 1) Research sites will identify, recruit and consent participants and conduct the study interventions including blood and urine samples, muscle biopsies and DXA scans. 2) PICs will identify and approach potential participants regarding their participation in the study. The Chief Investigator or sponsor should share relevant study documents with participating NHS organisations in England in order to put arrangements in place to deliver the study. The documents should be sent to both the local study team, where applicable, and the office providing the research management function at the participating organisation. For NIHR CRN Portfolio studies, the Local LCRN contact should also be copied into this correspondence. For further guidance on working with participating NHS organisations please see the HRA website. If chief investigators, sponsors or principal investigators are asked to complete site level forms for participating NHS organisations in England which are not provided in IRAS or on the HRA website, the chief investigator, sponsor or principal investigator should notify the HRA immediately at hra.approval@nhs.net. The HRA will work with these organisations to achieve a consistent approach to information provision.

Confirmation of Capacity and Capability

This describes whether formal confirmation of capacity and capability is expected from participating NHS organisations in England.
Participating NHS organisations in England **will be expected to formally confirm their capacity and capability to host this research**. • Following issue of this letter, participating NHS organisations in England may now confirm to the sponsor their capacity and capability to host this research, when ready to do so. How capacity and capacity will be confirmed is detailed in the *Allocation of responsibilities and rights are agreed and documented (4.1 of HRA assessment criteria)* section of this appendix. • The Assessing, Arranging, and Confirming document on the HRA website provides further information for the sponsor and NHS organisations on assessing, arranging and confirming capacity and capability.

Principal Investigator Suitability

This confirms whether the sponsor position on whether a PI, LC or neither should be in place is correct for each type of participating NHS organisation in England and the minimum expectations for education, training and experience that PIs should meet (where applicable).
PIs have been identified at the research sites, neither local collaborators nor PIs are expected at the PICs. GCP training is not a generic training expectation, in line with the HRA statement on training

expectations.

HR Good Practice Resource Pack Expectations

This confirms the HR Good Practice Resource Pack expectations for the study and the pre-engagement checks that should and should not be undertaken
Where arrangements are not already in place, network staff (or similar) undertaking any research activities that may impact on the quality of care of the participant (such as blood sampling, informed consent procedures), would be expected to obtain an honorary research contract from one NHS organisation (if university employed), followed by Letters of Access for subsequent organisations. This would be on the basis of a Research Passport (if university employed) or an NHS to NHS confirmation of pre-engagement checks letter (if NHS employed). These should confirm enhanced DBS checks, including appropriate barred list checks, and occupational health clearance. For research team members undertaking activities that do not impact on the quality of care of the participant (for example, administering questionnaires) a Letter of Access based on standard DBS checks and occupational health clearance would be appropriate.

Other Information to Aid Study Set-up

This details any other information that may be helpful to sponsors and participating NHS organisations in England to aid study set-up.
• The applicant has indicated that they intend to apply for inclusion on the NIHR CRN Portfolio.

Appendix 6 – Hunt & Payne, 2020

REVIEW

Mitochondria and ageing with HIV

Matthew Hunt[a,b] *and Brendan A.I. Payne*[a,c]

Purpose of review
Some older people living with HIV (PLWH) exhibit features of unsuccessful ageing, such as frailty. Mitochondrial dysfunction is one of the best characterized ageing mechanisms. There has been recent interest in whether some people ageing with HIV may have an excess of mitochondrial dysfunction. This review aims to address this question through: analogy with ageing and chronic disease; discussion of the key unknowns; suggested ways that measures of mitochondrial dysfunction might be incorporated into HIV research studies.

Recent findings
Recent data suggest that mitochondrial dysfunction in PLWH may not be wholly a legacy effect of historical nucleoside analog reverse transcriptase inhibitor exposures. Research in the non-HIV setting has altered our understanding of the important mediators of mitochondrial dysfunction in ageing.

Summary
Mitochondrial dysfunction is a very plausible driver of adverse ageing phenotypes in some older PLWH. As such it may be a target for therapeutic interventions. Currently, however, there remain considerable uncertainties around the extent of this phenomenon, and its relative importance. Current studies are likely to clarify these questions over the next few years.

Keywords
ageing, antiretroviral therapy, HIV, mitochondria, mitochondrial DNA

INTRODUCTION

One of the best characterized pathways of human ageing is mitochondrial dysfunction [1]. Given the well established role of mitochondrial dysfunction in the toxicity of some older antiretroviral therapy (ART), it deserves particular attention as a possible driver of unsuccessful ageing in older people living with HIV (PLWH) [2].

In this review, we will address three key questions. How might mitochondrial dysfunction be measured in studies of PLWH? To what extent does mitochondrial dysfunction in HIV mirror that seen in ageing and chronic diseases? What are the key unknowns?

HOW SHOULD WE MEASURE MITOCHONDRIAL FUNCTION IN PEOPLE LIVING WITH HIV?

Mitochondrial function can be measured at the physiological, cellular and molecular level. To develop a comprehensive picture we likely need complementary studies at all these levels. We will discuss the commonly used methods for assessing mitochondrial function and give suggestions as to what methods could be used in future studies in the HIV setting, and are summarized in Table 1. Figure 1 illustrates a hypothetical PLWH participating in a mitochondrial research study and the potential use of various assays.

Physiological measures

There are two frequently used in-vivo methods which measure oxidative capacity: phosphorus magnetic resonance spectroscopy (^{31}P-MRS) and near-infrared spectroscopy (NIRS). ^{31}P-MRS allows estimation of energy (ATP) metabolism through measurement of phosphorus spectra, usually in

[a]Wellcome Centre for Mitochondrial Research, Translational and Clinical Research Institute, Newcastle University, [b]NIHR Newcastle Biomedical Research Centre and [c]Department of Infection and Tropical Medicine, Newcastle upon Tyne Hospitals NHS Foundation Trust, Newcastle upon Tyne, UK

Correspondence to Dr Brendan A.I. Payne, Medical School, 4th Floor Cookson Building, Framlington Place, Newcastle upon Tyne NE2 4HH, UK. Tel: +44 191 208 5295; e-mail: Brendan.Payne@ncl.ac.uk

Curr Opin HIV AIDS 2019, 14:000–000
DOI:10.1097/COH.0000000000000607

KEY POINTS

- Mitochondrial dysfunction is a plausible mechanism driving adverse ageing phenotypes in some older PLWH.
- Some older PLWH may have a 'legacy effect' of historical NRTI exposures, but the importance of this remains to be fully defined.
- Emerging evidence suggests there may also be a more general phenomenon of mitochondrial dysfunction in combination antiretroviral therapy-treated PLWH.
- Tissue-specificity and a lack of minimally invasive biomarkers are barriers to large studies of mitochondrial dysfunction in PLWH.

skeletal muscle. Typically the rate of ATP production through oxidative phosphorylation is inferred from the recovery of phosphocreatine following sub-threshold exertion. It is reasonably well validated and has been used in longitudinal studies of patients with inherited mitochondrial diseases [3]. Limited studies by our group and others suggest that this may be a useful technique in PLWH [4,5]. ^{31}P-MRS is however expensive, requires specialist equipment (coils for phosphorus spectral acquisition) and software, and is not well suited to large multicenter studies. ATP defects detected are unlikely to be entirely specific to mitochondrial dysfunction and may also be affected by vascular supply for example.

NIRS offers a rather simpler noninvasive measurement of oxidative metabolism within tissues. To

Table 1. Selected methods for measuring mitochondrial dysfunction

Type of assessment	Experimental method	Assessing	Type of tissue	Advantages	Limitations
In-vivo	^{31}P-MRS	Oxidative capacity	Usually skeletal muscle	Well validated and reproducible method	Not suited to patients who can't perform physical exercise
	NIRS	Oxidative capacity	Systemic measure	Simultaneous multiple measurements in various tissue groups; cheap; easy to use	Not as well validated in research setting
Cellular	COX histochemistry	Enzyme levels of complex IV	Cryosections; cells	Cheap; quick and easy to perform	No normalization of COX intensity; some interference with molecular assays
	NBTx histochemistry	Enzyme levels of complex IV	Cryosections; cells	Visualizes CIV deficiency; does not interfere with molecular assays	Assesses CIV activity only; subjective quantification
	Multiplex fluorescent immunohistochemistry	ETC complexes protein abundance	FFPE sections; cryosections; cells	Automated; simultaneous quantification of complexes I, III, IV and V and mitochondrial mass	Quantification of protein not enzyme; antibody sets expensive
	Flow cytometry	Mitochondrial protein content, ROS, apoptosis, $\Delta\Psi m$	Tissue homogenates; cells	High-throughput; well validated; noninvasive; live cell capabilities	Potential issues with mitochondrial integrity
	Seahorse XF	Mitochondrial respiration (basal, maximal, spare capacity) and proton leak	Tissue homogenates; cells	Noninvasive; medium-throughput; live cell capability	Expensive; machine accessibility
	Oroboros O2k	Mitochondrial respiration, $\Delta\Psi m$	Tissue homogenates; cells	Noninvasive; live cell capability	Labour intensive; low-throughput
	Enzymatic cycling	NAD+ and NADH abundance and rate of metabolism in tissue homogenates	Tissue homogenates	Numerous commercial kits available; quick and easy to perform	Can only assess NAD+/NADH ratio in tissue homogenates; tissue preparation may impact various substrate levels
	LC–MS/HPLC	Protein quantification (including NAD+, NADH and complexes of the ETC)	Tissue homogenates; cells	High-throughput; simultaneous measurements of several variables	Technically demanding; tissue preparation may impact various substrate levels
Molecular	Massively parallel (next generation) sequencing	Identification of mtDNA point mutations and heteroplasmy levels	DNA extract	High-throughput; great breadth and depth of coverage	Technically demanding; expensive
	qPCR	Detection and quantification of large-scale mtDNA mutations; mtDNA copy number quantification	DNA extract	Quick; well validated	Run-to-run variability; may not detect whole mutational burden
	smPCR	Detection and quantification of point mutations or deletions	DNA extract	Low rate of noise	Technically demanding; time-consuming; samples only a limited pool of mitochondria

Preference has been given to those methods which may be more suited to studies in people living with HIV. ^{31}P-MRS, phosphorus magnetic resonance spectroscopy; CIV, complex IV; COX, cytochrome c oxidase; ETC, electron transport chain; FFPE, formalin fixed paraffin embedded; HPLC, high performance liquid chromatography; LC-MS, liquid chromatography-mass spectrometry; mtDNA, mitochondrial DNA; NAD+, nicotinamide adenine dinucleotide; NADH, reduced nicotinamide adenine dinucleotide; NBTx, nitrotetrazolium blue exclusion assay; NIRS, near-infrared spectroscopy; qPCR, quantitative real-time PCR; ROS, reactive oxygen species; smPCR, single-molecule PCR.

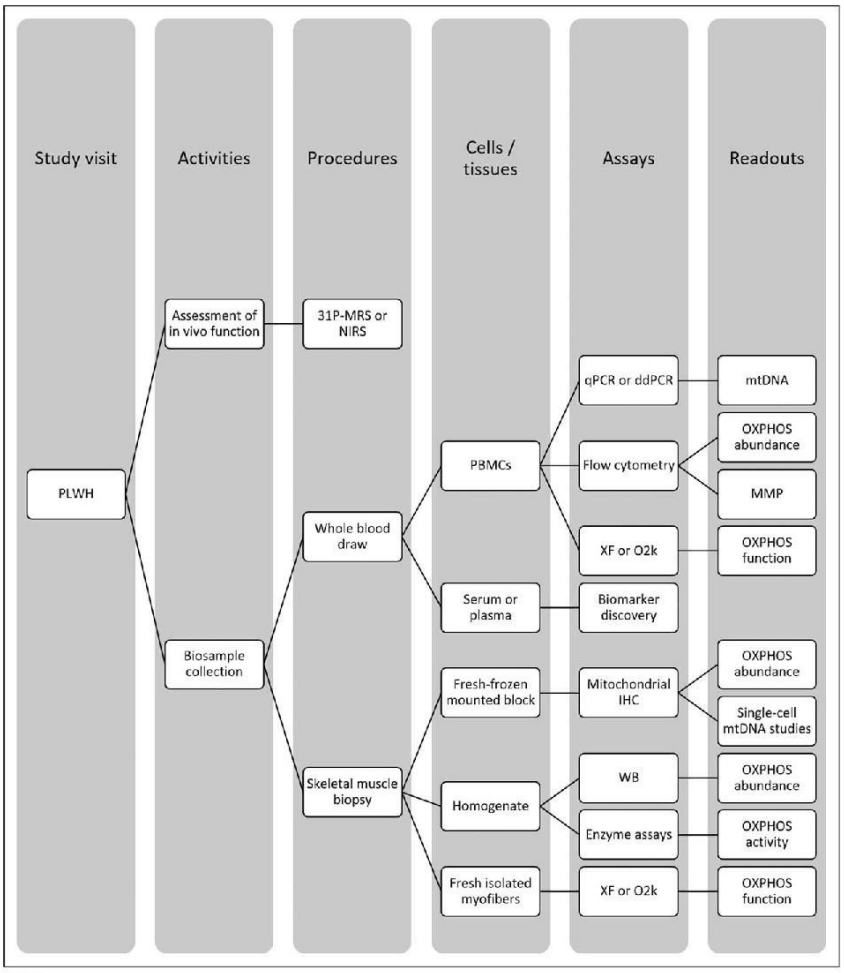

FIGURE 1. Putative approach for a mitochondrial study in people living with HIV. It is not envisaged that all these assays would necessarily be feasible. ^{31}P-MRS, phosphorus magnetic resonance spectroscopy; ddPCR, digital droplet PCR; IHC, immunohistochemistry; MMP, mitochondrial membrane potential; mtDNA, mitochondrial DNA; NIRS, near-infrared spectroscopy; O2k, Oroborus analyzer; OXPHOS, oxidative phosphorylation (mitochondrial respiratory chain); PBMC, peripheral blood mononuclear cell; qPCR, quantitative real-time PCR; WB, western blot; XF, Seahorse analyzer.

measure mitochondrial function the NIRS probe is applied to the skin overlying a muscle. A period of ischaemia is then induced by rapid inflation of a cuff to a suprasystolic pressure and the change in oxygenation of haemoglobin is determined. Ultimately, the much smaller size of the NIRS apparatus means that multiple measurements can be taken at the same muscle site, or at different muscle groups, or different tissue altogether [6]. It also means that NIRS may be more suited to larger multicenter

studies and more easily incorporated into clinical trial protocols.

Cellular assessments

Cellular assessments are vital in furthering the understanding of the biochemical consequences of mitochondrial dysfunction and allow the linking of mitochondrial genetic abnormalities to their physiological consequences. In general, however, assessment of a tissue yields information that is relatively specific to that tissue. The gold standard tissue for mitochondrial analyses remains skeletal muscle. The evidence that mitochondrial measurements on more easily accessible tissues such as peripheral blood can inform function of skeletal muscle remains limited. While historically muscle biopsy has not been considered feasible for large studies, greater recognition of its safety and utility has led to it now being employed in large interventional studies such as Molecular Transducers of Physical Activity Consortium.

In our opinion, histochemical techniques have an advantage over tissue homogenate studies in that they can assess mitochondrial function at an individual cellular level. This allows us to capture the mosaic nature of mitochondrial defects seen in ageing [7]. Until recently, the standard technique for assessing mitochondrial defects in frozen tissue was through histochemical staining for the enzymatic activity of cytochrome *c* oxidase (COX). We have successfully employed this technique in PLWH, and correlated defects of mitochondrial enzyme function with molecular defects at the single cell level [8]. However, COX histochemistry only quantifies activity of complex IV of the mitochondrial electron transport chain (ETC) and will fail to detect defects in the other ETC complexes. Thus, colleagues in our lab recently developed a multiplex fluorescence immunohistochemistry assay which allows for the automated and objective quantification of ETC complexes I, III, IV and V, and mitochondrial mass [9].

In recent years, the Seahorse XF Extracellular Flux Analyzer (Agilent, Santa Clara, CA, US) has become a frequently used method to measure mitochondrial respiration (oxygen consumption rate) *in vitro* or *ex vivo* [10]. Seahorse XF analysis offers a reliable, medium-throughput method of quantifying mitochondrial health. While originally applied to cultured cells, this technique could be considered for use on primary cells collected in HIV studies, including PBMCs (peripheral blood mononuclear cells) and even isolated skeletal muscle fibres. However, it is likely to require the ability to process samples immediately on collection, rather than freeze and store and thus is not suitable for use on tissue collected for histochemistry for example. The O2k (Oroboros Instruments GmbH, Innsbruck, Austria) platform also measures oxidative phosphorylation in similar sample types. Compared with Seahorse it is cheaper, but more labour intensive. It can additionally measure mitochondrial membrane potential ($\Delta\Psi m$).

The use of flow cytometry for the investigation of mitochondrial function has become increasingly popular, owing to the greater commercial availability of suitable reagents. Flow cytometry can be used to study several relevant cellular markers, often in parallel, such as $\Delta\Psi m$, mitochondrial mass, reactive oxygen species (ROS) and apoptosis [11,12,13▪]. The high-throughput and noninvasive nature of flow cytometry mean it would be a potentially useful method in future large cohort studies looking to investigate certain aspects mitochondrial dysfunction in the HIV setting. Furthermore, PBMCs are often collected as part of existing clinical HIV study protocols.

Simple serum/plasma biomarkers of mitochondrial dysfunction are not currently available. In the setting of inherited mitochondrial disease FGF-21 (fibroblast growth factor 21) and growth/differentiation factor 15 have shown some promise, but are most useful in children with myopathic phenotypes [14,15]. We have examined the use of FGF-21 in PLWH and it did not predict mitochondrial dysfunction in skeletal muscle [16].

Finally, fat biopsy might also be considered in mitochondrial studies of PLWH given the historical links between lipodystrophy and ART-induced mitochondrial dysfunction. This might help better define the extent to which mitochondrial dysfunction in adipose tissue relates to systemic metabolism.

Molecular assessments

Abnormalities of mitochondrial function at the organismal or cellular level can often be linked to changes at the molecular level. Most molecular assessments quantify mitochondrial DNA (mtDNA) content, and sometimes measure mtDNA mutations. Commonly used methods have previously been reviewed in the context of mtDNA changes in HIV [17]. Changes in mtDNA content are readily measured in accessible tissues such as stored PBMCs. Most studies use quantitative real-time PCR or digital droplet PCR. Recent novel approaches include inferring mtDNA copy number and mutations from whole genome data [18▪▪]. In the non-HIV setting, changes in blood mtDNA content have been associated with systemic phenotypes such as frailty, but it is unclear exactly how these parameters are mechanistically linked [19]. Furthermore, mtDNA content is likely

to vary between different cell types (e.g. between different leucocyte populations) and this may complicate interpretation of apparent changes [20]. Finally both decreases and increases in cellular mtDNA content have been considered as pathogenic.

MITOCHONDRIAL FUNCTION IN PEOPLE AGEING WITH HIV: A SPECIAL CASE?

Ageing, comorbidity, HIV and ART are all highly heterogeneous. This heterogeneity tends to increase with age. All may contribute to the overall burden of mitochondrial dysfunction in older PLWH.

Changes in mitochondrial function with ageing

The presence of damaged and dysfunctional mitochondria in aged tissues is well established. Furthermore, recent data appear to indicate a causal link between frailty and mitochondrial dysfunction [21••]. These abnormalities include alterations in mitochondrial morphology and abundance as well as a decline in energy producing capacity and increased oxidative damage as a result of elevated electron leak and ROS production. The changes have been reviewed extensively [22] and are summarized in Fig. 2. These mitochondrial defects were initially suspected to be the result of a 'vicious cycle' of increased ROS production and subsequent oxidative damage [23]. However, this theory has been disputed over recent years, due to the demonstration in humans and mouse models that directly manipulating ROS and antioxidant levels show no effects on the ageing process or lifespan [24]. Many studies now favour the theory that the accumulation of mutated mtDNA plays a causal role in mitochondrial dysfunction with ageing. These mtDNA mutations may lead to abnormalities in cellular energy conversion leading to tissue dysfunction and age-related phenotypes [25]. Much recent work has focused on the signalling pathways mediating mitochondrial dysfunction in ageing. In particular, NAD+ (nicotinamide adenine dinucleotide) appears to be a potent and potentially modifiable regulator [26••,27•].

To what extent are these abnormalities of mitochondria which are seen in ageing mirrored by those seen in HIV or ART? Decline in mitochondrial abundance (often measured as cellular mtDNA content) is well described in patients receiving treatment with certain older NRTIs (nucleoside reverse transcriptase inhibitors) which inhibit the mtDNA polymerase, pol γ (zalcitabine, didanosine, stavudine and to a lesser extent zidovudine) [28]. However, this effect is thought to be reversible on switching off the culprit NRTI [29]. MtDNA mutations have been less extensively studied in PLWH, but our group and others have shown that some PLWH do have an excess of mtDNA mutations, both point mutations and deletions [8,30]. Significantly, the pattern of these mutations appears to be very similar to that seen in normal ageing.

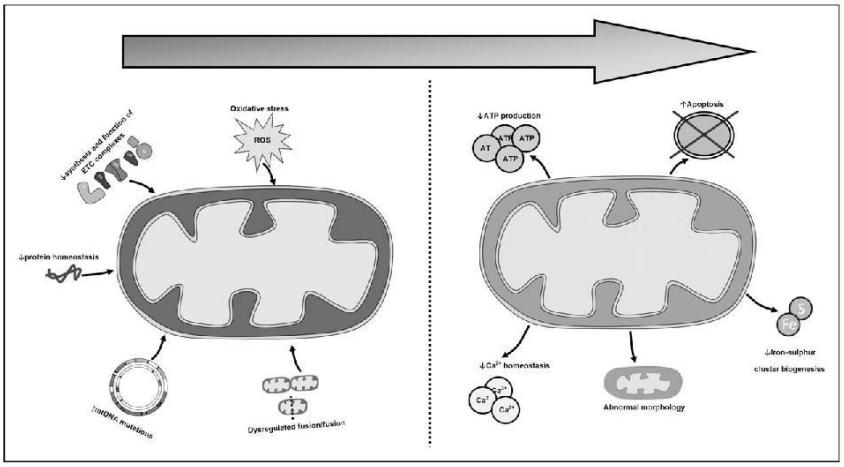

FIGURE 2. Causes and consequences of mitochondrial dysfunction in ageing.

Stem cell exhaustion is common in ageing and results in an impaired regenerative capacity in response to stressors. While historically mitochondria were considered to be of prime importance in postmitotic tissues with high energy demands such as brain and muscle, accumulating evidence now points to a critical role for mitochondria in stem cell function [31,32••]. It remains to be determined whether mitochondrially mediated stem cell exhaustion significantly contributes to accelerated ageing in PLWH.

Mitochondrial dysfunction in chronic disease

Comorbid disease is extremely prevalent among older PLWH and is more common than expected for age [33]. In addition, adverse metabolic phenotypes such as central obesity and insulin resistance are common [34]. There is a wealth of published data demonstrating mitochondrial dysfunction in many different tissues in a range of chronic diseases. Perhaps the best example is type 2 diabetes mellitus (T2DM). Most studies in T2DM have examined mitochondria in skeletal muscle. Findings from both human and rodent studies include decreased mitochondrial biogenesis, decreased oxidative metabolism and decreased lipid metabolism. However, other studies have shown little change in these parameters, or indeed a compensatory increase in oxidative metabolism in response to increased lipid supply. It remains unclear to what extent observed changes are a cause or a consequence of insulin resistance, but overall is seems unlikely that mitochondrial dysfunction is an absolute prerequisite for insulin resistance. This topic has been reviewed extensively elsewhere [35].

WHAT ARE THE KEY UNKNOWNS?

In attempting to understand the role of mitochondrial dysfunction in the health of people ageing with HIV, there remain many gaps in our knowledge, summarized in Fig. 3. We will outline four of the key questions below.

Is there a legacy effect of historical antiretroviral therapy exposure?

Most PLWH who were diagnosed in the 1980s or 1990s will have received exposure to ART that exhibited considerably greater toxicity than that in use today. Several of the historical NRTIs are well established to have effects on mtDNA [28]. During therapy with these agents, PLWH were at risk of developing mitochondrially mediated toxicities [36,37]. The risk of these toxicities appears to be modified by mtDNA haplogroup, reinforcing the aetiological role for mitochondrial dysfunction [38]. In our previous work, we have shown that PLWH who have been exposed to these NRTIs have an excess of mtDNA mutations in skeletal muscle, leading to defects of mitochondrial function in individual myofibres [8]. Critically, this effect was detectable even years after stopping the relevant drugs. These observations therefore give a sound basis for the hypothesis that there could be a legacy effect of historical NRTI exposure leading to an increase in mitochondrial dysfunction in a subgroup of older PLWH. This concept has significant resonance both among HIV care providers and PLWH.

While historical NRTI exposures have the most clear mechanistic basis for a legacy effect, there could be other contributing factors. For example, the older protease inhibitors were associated with adverse changes in body composition, including lipohypertrophy, as well as insulin resistance [39]. Again, these effects are often persistent after stopping the relevant protease inhibitor. These metabolic abnormalities could affect mitochondrial dysfunction, in line with those effects seen in T2DM. Finally, PLWH first treated before the combination ART (cART) era will be very likely to have had more prolonged periods of uncontrolled viraemia.

To determine the importance of such a legacy effect we must firstly establish whether there are health consequences of this excess of mitochondrial dysfunction, especially as related to ageing phenotypes such as frailty. These studies also need to be supplemented by better longitudinal studies, designed to tease out any legacy effects.

Is modern combination antiretroviral therapy blameless?

Is has been traditionally assumed that contemporary ART is free from mitochondrial toxicity. In the case of nucleoside/nucleotide analog reverse transcriptase inhibitors in current usage this notion is supported by in-vitro studies [40]. This lack of effect on mtDNA may not however apply to all cell types. For example, we and others have shown that tenofovir disoproxil fumarate can cause mitochondrial dysfunction in the renal tract [41,42•].

Less is known about the effects of other contemporary ART classes on mitochondrial function. In-vitro studies have demonstrated mitochondrial toxicity of non-nucleoside reverse transcriptase inhibitors (NNRTIs), especially efavirenz [43,44•]. The mechanisms of these effects probably differ from that of NRTIs. To date these findings have not been

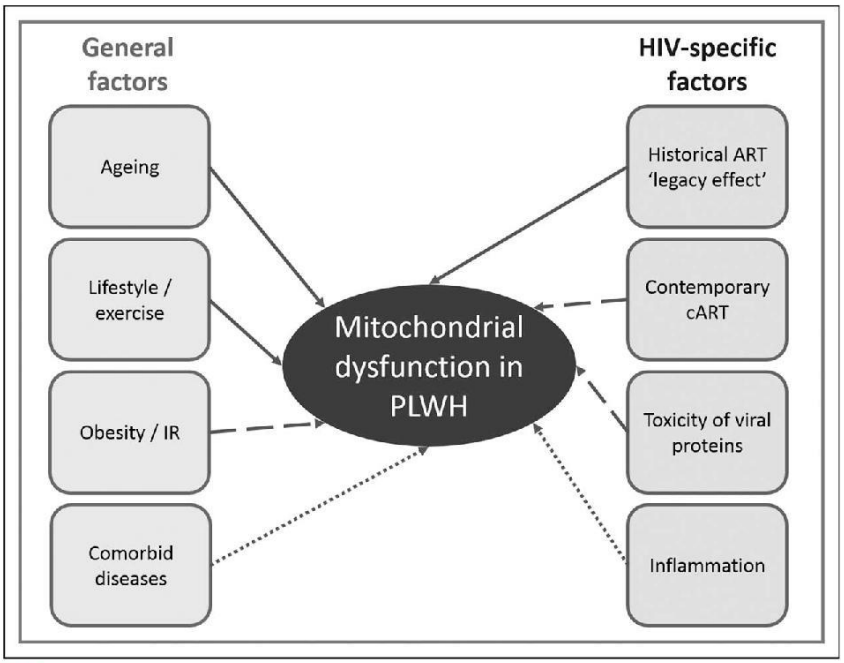

FIGURE 3. Probable and possible mediators of mitochondrial dysfunction in older people living with HIV. Solid lines indicate associations for which there is good empirical evidence of an effect. Dashed lines represent associations for which there is more limited evidence. Dotted lines are hypothetical effects. IR, insulin resistance.

confirmed in human studies. INSTIs (integrase strand transfer inhibitors) have become 3rd agents of choice in many cART regimens in recent years, and this ART class is generally considered to show very favourable toxicity profiles. Data on mitochondrial function with INSTI exposure are however currently very limited [45▪].

In support of a concept of a broader effect of ART-treated HIV on mitochondrial function, we have previously investigated in-vivo mitochondrial function in skeletal muscle of PLWH using ^{31}P-MRS [5]. We showed a significant abnormality of resting state mitochondrial metabolism in PLWH. However, this effect did not appear to be explained by historical NRTI exposures, suggesting that ART-treated PLWH may show impaired mitochondrial function as a more general phenomenon.

Current research studies will hopefully indicate whether more subtle effects of contemporary ART exist. Such studies should include HIV negative individuals, who are not only age-matched but, in so far as possible, lifestyle matched. This will go some way to controlling for the numerous non-HIV-specific drivers of mitochondrial dysfunction in older people. For example, the UK-based 'POPPY' study of ageing in HIV was specifically designed with these considerations in mind [46▪▪]. While not specifically designed as 'ageing' studies, several very large US cohorts (MACS/WIHS, VACS, ALIVE) also contain demographically matched controls. Nevertheless, given the heterogeneity of older PLWH, it is extremely difficult to dissect out effects of individual ART exposures.

Does HIV itself contribute to mitochondrial dysfunction?

In-vitro and rodent studies suggest that certain HIV proteins may cause mitochondrially mediated cellular toxicity, especially in neurons [47▪,48,49].

Equivalent studies are more challenging to perform in PLWH; however, we have recently demonstrated that brain samples of PLWH show changes in mtDNA which accentuate those seen in normal human ageing [50▪]. This effect appeared to be driven by HIV infection itself, rather than by ART exposures.

Pragmatically, in contemporary HIV practice, almost all PLWH are on suppressive cART. This means that dissecting out the relative contributions of ART and HIV to mitochondrial dysfunction is problematic. One possible indirect approach is to consider using measures of residual HIV activity such as persistent inflammation, and to examine whether these correlate with mitochondrial dysfunction. Furthermore, there is now strong evidence that HIV infection induces alterations in mitochondrial metabolism within immune cells [51▪,52▪].

Does HIV affect mitochondrial responsiveness to therapy?

Therapeutics for mitochondrial dysfunction is very much in its infancy. The majority of putative strategies are focused on enhancing mitochondrial biogenesis through a number of signalling pathways which converge on peroxisome proliferator-activated receptor gamma coactivator 1-alpha. The intervention with the best evidence base is endurance exercise. Recent data suggest that older individuals have a metabolic 'block' of ADP/ATP signalling which limits response to training [32▪▪]. Lack of mitochondrial responsiveness to training has also recently been reported in PLWH [53▪]. Other promising avenues in ageing and chronic disease include augmenting NAD+/NADH (oxidized/reduced nicotinamide adenine dinucleotide) ratio [26▪▪].

CONCLUSION

A key challenge for the next decade of HIV care will be improving healthspan in those PLWH who exhibit unsuccessful ageing phenotypes. An important component of this approach is to reach a better understanding of those mechanisms that may drive these phenotypes at the molecular, cellular, organ and organismal levels. Mitochondrial dysfunction is a strong candidate for such studies, especially as novel therapies are emerging that may be able to improve mitochondrial function [26▪▪]. Studying mitochondrial dysfunction in older PLWH is however complex because of considerable heterogeneity and a lack of good noninvasive markers. Nevertheless, a combination of focused mechanistic studies, combined with large studies that include surrogate markers of mitochondrial dysfunction is likely to significantly improve our understanding of this area in the next few years.

Acknowledgements

None.

Financial support and sponsorship

B.A.I.P. is funded by the Wellcome Trust (109975/Z/15/Z, 203105/Z/16/Z). M.H. is funded by the National Institute for Health Research (NIHR) Newcastle Biomedical Research Centre.

Conflicts of interest

There are no conflicts of interest.

REFERENCES AND RECOMMENDED READING

Papers of particular interest, published within the annual period of review, have been highlighted as:
▪ of special interest
▪▪ of outstanding interest

1. Short KR, Bigelow ML, Kahl J, *et al.* Decline in skeletal muscle mitochondrial function with aging in humans. Proc Natl Acad Sci U S A 2005; 102:5618–5623.
2. Cote HC, Brumme ZL, Craib KJ, *et al.* Changes in mitochondrial DNA as a marker of nucleoside toxicity in HIV-infected patients. N Engl J Med 2002; 346:811–820.
3. Trenell MI, Sue CM, Kemp GJ, *et al.* Aerobic exercise and muscle metabolism in patients with mitochondrial myopathy. Muscle Nerve 2006; 33:524–531.
4. Sinnwell TM, Sivakumar K, Soueidan S, *et al.* Metabolic abnormalities in skeletal muscle of patients receiving zidovudine therapy observed by 31P in vivo magnetic resonance spectroscopy. J Clin Invest 1995; 96:126–131.
5. Payne BA, Hollingsworth KG, Baxter J, *et al.* In vivo mitochondrial function in HIV-infected persons treated with contemporary antiretroviral therapy: a magnetic resonance spectroscopy study. PLoS One 2014; 9:e84678.
6. Willingham TB, McCully KK. In vivo assessment of mitochondrial dysfunction in clinical populations using near-infrared spectroscopy. Front Physiol 2017; 8:689.
7. Bua E, Johnson J, Herbst A, *et al.* Mitochondrial DNA-deletion mutations accumulate intracellularly to detrimental levels in aged human skeletal muscle fibers. Am J Hum Genet 2006; 79:469–480.
8. Payne BA, Wilson IJ, Hateley CA, *et al.* Mitochondrial aging is accelerated by antiretroviral therapy through the clonal expansion of mtDNA mutations. Nat Genet 2011; 43:806–810.
9. Rocha MC, Grady JP, Grunewald A, *et al.* A novel immunofluorescent assay to investigate oxidative phosphorylation deficiency in mitochondrial myopathy: understanding mechanisms and improving diagnosis. Sci Rep 2015; 5:15037.
10. Salabei JK, Gibb AA, Hill BG. Comprehensive measurement of respiratory activity in permeabilized cells using extracellular flux analysis. Nat Protoc 2014; 9:421–438.
11. Ronot X, Benel L, Adolphe M, Mounolou JC. Mitochondrial analysis in living cells: the use of rhodamine 123 and flow cytometry. Biol Cell 1986; 57:1–7.
12. Doherty E, Perl A. Measurement of mitochondrial mass by flow cytometry during oxidative stress. React Oxyg Species (Apex) 2017; 4:275–283.
13. ▪ Clutton G, Mollan K, Hudgens M, Goonetilleke N. A reproducible, objective method using MitoTracker(R) fluorescent dyes to assess mitochondrial mass in T cells by flow cytometry. Cytometry A 2019; 95:450–456.
An important demonstration of the utility of flow cytometry for measuring mitochondrial parameters. Potentially very tractable to HIV studies.
14. Suomalainen A, Elo JM, Pietilainen KH, *et al.* FGF-21 as a biomarker for muscle-manifesting mitochondrial respiratory chain deficiencies: a diagnostic study. Lancet Neurol 2011; 10:806–818.
15. Montero R, Yubero D, Villarroya J, *et al.* GDF-15 is elevated in children with mitochondrial diseases and is induced by mitochondrial dysfunction. PLoS One 2016; 11:e0148709.
16. Payne BAI, Price DA, Chinnery PF. Elevated serum fibroblast growth factor 21 levels correlate with immune recovery but not mitochondrial dysfunction in HIV infection. AIDS Res Ther 2013; 10:27.

17. Payne BA, Gardner K, Chinnery PF. Mitochondrial DNA mutations in ageing and disease: implications for HIV? Antivir Ther 2015; 20:109–120.
18. ■■ Hulgan T, Kallianpur AR, Guo Y, *et al.* Peripheral blood mitochondrial DNA copy number obtained from genome-wide genotype data is associated with neurocognitive impairment in persons with chronic HIV infection. J Acquir Immune Defic Syndr 2019; 80:e95–e102.
Evidence that blood mitochondrial DNA (mtDNA) content is associated with an adverse ageing phenotype (NCI, neurocognitive impairment) in another tissue. This article also shows how mtDNA levels can be inferred from available genomic data.
19. Ashar FN, Moes A, Moore AZ, *et al.* Association of mitochondrial DNA levels with frailty and all-cause mortality. J Mol Med 2015; 93:177–186.
20. Pyle A, Burn DJ, Gordon C, *et al.* Fall in circulating mononuclear cell mitochondrial DNA content in human sepsis. Intensive Care Med 2010; 36:956–962.
21. ■■ Andreux PA, van Diemen MPJ, Heezen MR, *et al.* Mitochondrial function is impaired in the skeletal muscle of prefrail elderly. Sci Rep 2018; 8:8548.
While extensive evidence correlates mitochondrial dysfunction with ageing, this study is one of the first in humans to show that this association is probably causal.
22. Brierley EJ, Johnson MA, Lightowlers RN, *et al.* Role of mitochondrial DNA mutations in human aging: implications for the central nervous system and muscle. Ann Neurol 1998; 43:217–223.
23. Harman D. Aging: a theory based on free radical and radiation chemistry. J Gerontol 1956; 11:298–300.
24. Ristow MSS. Extending life span by increasing oxidative stress. Free Radic Biol Med 2011; 51:327–336.
25. Kujoth GC, Hiona A, Pugh HA, *et al.* Mitochondrial DNA mutations, oxidative stress, and apoptosis in mammalian aging. Science 2005; 309:481–484.
26. ■■ Elhassan YS, Kluckova K, Fletcher RS, *et al.* Nicotinamide riboside augments the aged human skeletal muscle NAD(+) metabolome and induces transcriptomic and anti-inflammatory signatures. Cell Rep 2019; 28:1717–1728.e6.
The article shows that not only does nicotinamide adenine dinucleotide supplementation affect the metabolic profile of skeletal muscle but it also had unexpected beneficial effects on inflammation.
27. ■ Katsyuba E, Mottis A, Zietak M, *et al.* De novo NAD(+) synthesis enhances mitochondrial function and improves health. Nature 2018; 563:354–359.
28. Lim SE, Copeland WC. Differential incorporation and removal of antiviral deoxynucleotides by human DNA polymerase gamma. J Biol Chem 2001; 276:23616–23623.
29. McComsey GA, Paulsen DM, Lonergan JT, *et al.* Improvements in lipoatrophy, mitochondrial DNA levels and fat apoptosis after replacing stavudine with abacavir or zidovudine. AIDS 2005; 19:15–23.
30. Martin AM, Hammond E, Nolan D, *et al.* Accumulation of mitochondrial DNA mutations in human immunodeficiency virus-infected patients treated with nucleoside-analogue reverse-transcriptase inhibitors. Am J Hum Genet 2003; 72:549–560.
31. Taylor RW, Barron MJ, Borthwick GM, *et al.* Mitochondrial DNA mutations in human colonic crypt stem cells. J Clin Invest 2003; 112:1351–1360.
32. ■■ Holloway GP, Holwerda AM, Miotto PM, *et al.* Age-associated impairments in mitochondrial ADP sensitivity contribute to redox stress in senescent human skeletal muscle. Cell Rep 2018; 22:2837–2848.
Provides evidence that older person may have a mitochondrial metabolic block to training response.
33. Goulet JL, Fultz SL, Rimland D, *et al.* Aging and infectious diseases: do patterns of comorbidity vary by HIV status, age, and HIV severity? Clin Infect Dis 2007; 45:1593–1601.
34. Grunfeld C, Rimland D, Gibert CL, *et al.* Association of upper trunk and visceral adipose tissue volume with insulin resistance in control and HIV-infected subjects in the FRAM study. J Acquir Immune Defic Syndr 2007; 46:283–290.
35. Szendroedi J, Phielix E, Roden M. The role of mitochondria in insulin resistance and type 2 diabetes mellitus. Nat Rev Endocrinol 2011; 8:92–103.
36. Dalakas MC, Illa I, Pezeshkpour GH, *et al.* Mitochondrial myopathy caused by long-term zidovudine therapy. N Engl J Med 1990; 322:1098–1105.
37. Carr A, Miller J, Law M, Cooper DA. A syndrome of lipoatrophy, lactic acidaemia and liver dysfunction associated with HIV nucleoside analogue therapy: contribution to protease inhibitor-related lipodystrophy syndrome. AIDS 2000; 14:F25–F32.
38. Hendrickson SL, Kingsley LA, Ruiz-Pesini E, *et al.* Mitochondrial DNA haplogroups influence lipoatrophy after highly active antiretroviral therapy. J Acquir Immune Defic Syndr 2009; 51:111–116.
39. Gan SK, Samaras K, Thompson CH, *et al.* Altered myocellular and abdominal fat partitioning predict disturbance in insulin action in HIV protease inhibitor-related lipodystrophy. Diabetes 2002; 51:3163–3169.
40. Birkus G, Hitchcock MJ, Cihlar T. Assessment of mitochondrial toxicity in human cells treated with tenofovir: comparison with other nucleoside reverse transcriptase inhibitors. Antimicrob Agents Chemother 2002; 46:716–723.
41. Samuels R, Bayerri CR, Sayer JA, *et al.* Tenofovir disoproxil fumarate-associated renal tubular dysfunction: noninvasive assessment of mitochondrial injury. AIDS 2017; 31:1297–1301.
42. ■ Ramamoorthy H, Abraham P, Isaac B, Selvakumar D. Mitochondrial pathway of apoptosis and necrosis contribute to tenofovir disoproxil fumarate-induced renal damage in rats. Hum Exp Toxicol 2019; 38:288–302.
43. Funes HA, Apostolova N, Alegre F, *et al.* Neuronal bioenergetics and acute mitochondrial dysfunction: a clue to understanding the central nervous system side effects of efavirenz. J Infect Dis 2014; 210:1385–1395.
44. ■ Martinez-Arroyo O, Gruevska A, Victor VM, *et al.* Mitophagy in human astrocytes treated with the antiretroviral drug efavirenz: lack of evidence or evidence of the lack. Antiviral Res 2019; 168:36–50.
45. ■ Barroso S, Moren C, Gonzalez-Segura A, *et al.* Metabolic, mitochondrial, renal and hepatic safety of enfuvirtide and raltegravir antiretroviral administration: randomized crossover clinical trial in healthy volunteers. PLoS One 2019; 14:e0216712.
46. ■■ Bagkeris E, Burgess L, Mallon PW, *et al.* Cohort profile: the Pharmacokinetic and clinical Observations in PeoPle over fiftY (POPPY) study. Int J Epidemiol 2018; 47:1391–1392.
A description of the 'POPPY' cohort design which is a model for good design of HIV ageing studies.
47. ■ Cotto B, Natarajanseenivasan K, Langford D. HIV-1 infection alters energy metabolism in the brain: contributions to HIV-associated neurocognitive disorders. Prog Neurobiol 2019; 181:101616.
48. Cheung JY, Gordon J, Wang J, *et al.* Mitochondrial dysfunction in human immunodeficiency virus-1 transgenic mouse cardiac myocytes. J Cell Physiol 2019; 234:4432–4444.
49. Teodorof-Diedrich C, Spector SA. Human immunodeficiency virus type 1 gp120 and tat induce mitochondrial fragmentation and incomplete mitophagy in human neurons. J Virol 2018; 92:e00993-18.
50. ■ Roca Bayerri C, Payne BAI. Mitochondrial DNA damage in brain associated with HIV infection 7th international workshop on HIV and aging; Washington, DC; 2016.
51. ■ Castellano P, Prevedel L, Valdebenito S, Eugenin EA. HIV infection and latency induce a unique metabolic signature in human macrophages. Sci Rep 2019; 9:3941.
52. ■ Younes SA, Talla A, Pereira Ribeiro S, *et al.* Cycling CD4+ T cells in HIV-infected immune nonresponders have mitochondrial dysfunction. J Clin Invest 2018; 128:5083–5094.
53. ■ Jankowski CM, Wilson MP, Mawhinney S, *et al.*, editors. Blunted muscle mitochondrial responses to exercise training in older adults with HIV. Conference on retroviruses and opportunistic infections; 2019; Boston, MA.

Appendix 7 – Smith et al., 2020

nature cancer

ARTICLES

https://doi.org/10.1038/s43018-020-00112-5

Check for updates

Age-associated mitochondrial DNA mutations cause metabolic remodeling that contributes to accelerated intestinal tumorigenesis

Anna L. M. Smith[1,2,10], Julia C. Whitehall[1,2,10], Carla Bradshaw[1,2], David Gay[3,4], Fiona Robertson[1,5], Alasdair P. Blain[1,5], Gavin Hudson[1,2], Angela Pyle[1,2], David Houghton[1,5], Matthew Hunt[1,5], James N. Sampson[1,5], Craig Stamp[1,2], Grace Mallett[5], Shoba Amarnath[5], Jack Leslie[6], Fiona Oakley[6], Laura Wilson[7], Angela Baker[1,5], Oliver M. Russell[1,5], Riem Johnson[1,5], Claire A. Richardson[5], Bhavana Gupta[1,2], Iain McCallum[5], Stuart A. C. McDonald[8], Seamus Kelly[5], John C. Mathers[9], Rakesh Heer[7], Robert W. Taylor[1,5], Neil D. Perkins[2], Doug M. Turnbull[1,5], Owen J. Sansom[3,4] and Laura C. Greaves[1,2] ✉

Oxidative phosphorylation (OXPHOS) defects caused by somatic mitochondrial DNA mutations increase with age in human colorectal epithelium and are prevalent in colorectal tumors, but whether they actively contribute to tumorigenesis remains unknown. Here we demonstrate that mitochondrial DNA mutations causing OXPHOS defects are enriched during the human adenoma/carcinoma sequence, suggesting that they may confer a metabolic advantage. To test this, we deleted the tumor suppressor *Apc* in OXPHOS-deficient intestinal stem cells in mice. The resulting tumors were larger than in control mice due to accelerated cell proliferation and reduced apoptosis. We show that both normal crypts and tumors undergo metabolic remodeling in response to OXPHOS deficiency by upregulating the de novo serine synthesis pathway. Moreover, normal human colonic crypts upregulate the serine synthesis pathway in response to OXPHOS deficiency before tumorigenesis. Our data show that age-associated OXPHOS deficiency causes metabolic remodeling that can functionally contribute to accelerated intestinal cancer development.

Fundamental changes in the cellular metabolism of tumor cells were first observed in 1956 by Otto Warburg, who showed that tumor cells preferentially utilize glycolysis for ATP production over mitochondrial oxidative phosphorylation (OXPHOS)[1,2]. This was termed aerobic glycolysis, or the Warburg effect. Warburg suggested that a key event in carcinogenesis was injury to the respiratory machinery, and subsequent analysis of mitochondrial function showed that OXPHOS was frequently downregulated in many tumors[3]. This shift to glycolysis results in less efficient production of ATP, but has been shown to confer selective advantages during oncogenesis via other mitochondrial processes such as resistance to apoptosis[4], diversion of glycolytic intermediates into pathways required for cellular biomass production via one-carbon metabolism[5], and reactive oxygen species (ROS) production[6].

Defects in the OXPHOS system are also a common feature in a number of human aging tissues[7–10]. The colorectal epithelium is particularly susceptible to the accumulation of crypts deficient in complexes I and IV[11–13], with an average of 15% of crypts being OXPHOS deficient at the age of 70 years[13]. The underlying causes of the OXPHOS defects in the aging colonic epithelium are somatic mutations of the mitochondrial DNA (mtDNA). Human mtDNA is a circular, multicopy genome of ~16.6 kilobases that is found within the mitochondrial matrix and encodes 13 essential subunits of the OXPHOS system, together with 22 transfer RNAs and two ribosomal RNAs, to support the synthesis of mtDNA-encoded proteins within the organelle. As there are multiple copies of mtDNA in individual cells, mutant and wild-type mtDNA can co-exist in a situation termed heteroplasmy, or all copies can be the same, termed homoplasmy. Most mtDNA mutations are functionally recessive; somatic mtDNA mutations must clonally expand to high levels of heteroplasmy within an individual cell before a defect in the OXPHOS system becomes manifest[14]. The downstream metabolic consequences of such mutations in the rapidly proliferating colonic epithelial cells are largely unknown, although studies of other proliferative cell lines taken from patients with primary mtDNA disease have shown evidence of metabolic rewiring similar to that of cancer cells as a compensatory response to promote cell survival[15]. mtDNA mutations at very high levels of heteroplasmy, or homoplasmy, have also been detected in a number of tumor types[16], including in 60–70% of colorectal cancers[17–19]. In silico predictions have suggested that

[1]Wellcome Centre for Mitochondrial Research, Newcastle University, Newcastle upon Tyne, UK. [2]Biosciences Institute, Newcastle University, Newcastle upon Tyne, UK. [3]Cancer Research UK Beatson Institute, Glasgow, UK. [4]Institute of Cancer Sciences, University of Glasgow, Glasgow, UK. [5]Translational and Clinical Research Institute, Newcastle University, Newcastle upon Tyne, UK. [6]Newcastle Fibrosis Research Group, Biosciences Institute, Newcastle upon Tyne, UK. [7]Newcastle Cancer Centre, Translational and Clinical Research Institute, Newcastle University, Newcastle upon Tyne, UK. [8]Centre for Tumour Biology, Barts Cancer Institute, Queen Mary University of London, London, UK. [9]Human Nutrition Research Centre, Population Health Sciences Institute, Newcastle University, Newcastle upon Tyne, UK. [10]These authors contributed equally: Anna L. M. Smith, Julia C. Whitehall.
✉e-mail: laura.greaves@ncl.ac.uk

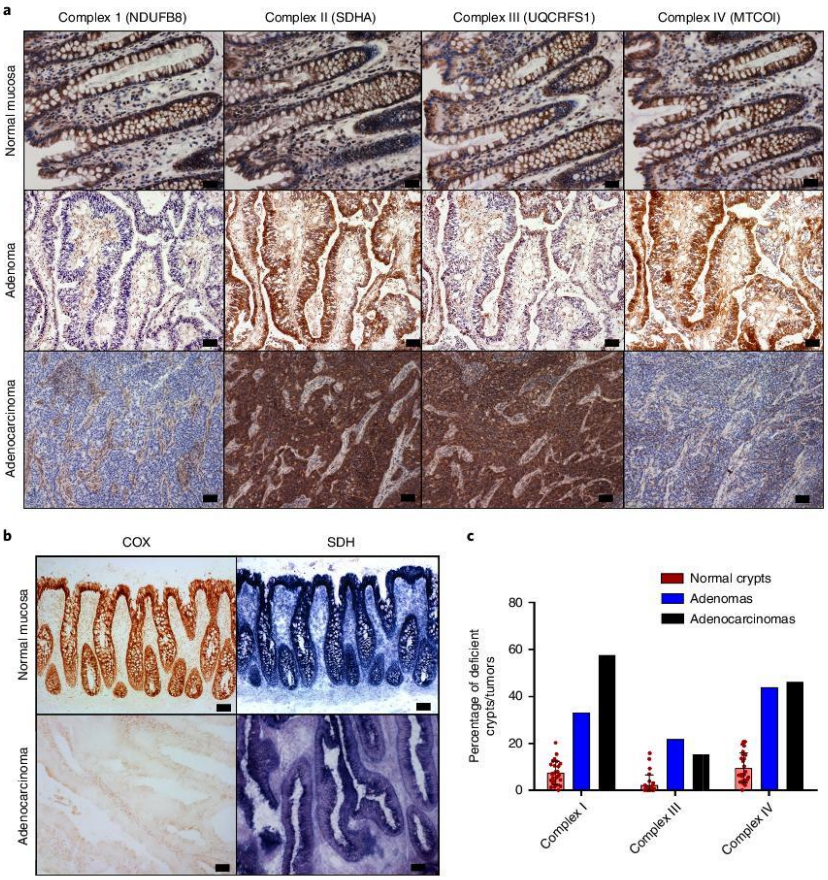

Fig. 1 | OXPHOS subunit IHC and histochemical analysis of human colorectal adenomas and adenocarcinomas. a, IHC was performed on 26 adenocarcinoma samples and patient-matched normal mucosa and nine colonic adenoma samples. Representative images show OXPHOS subunit expression in normal mucosa (CSC024), an adenoma (AD07) and an adenocarcinoma (CSC024). **b**, COX and SDH histochemistry was performed on the same samples as in **a**. Representative images of normal colonic mucosa and adenocarcinoma from CRC009 are shown. **c**, Quantification of the mean percentage of normal crypts per subject with defects in the specified OXPHOS subunits (each dot represents the mean percentage of OXPHOS-deficient crypts in each subject; $n = 26$ subjects; error bars are s.e.m.) and the percentage of adenomas ($n = 9$) and adenocarcinomas ($n = 26$) analyzed with defects in the specified OXPHOS subunits. Scale bars, 20 μm (**a**) and 50 μm (**b**).

mtDNA mutations that are likely to be detrimental to OXPHOS function are particularly enriched in colorectal tumors[16]. Age is the biggest risk factor for colorectal cancer development[20], and given the fact that pathogenic mtDNA mutations are a common feature of both normal aging colorectal crypts and colorectal tumors, we wanted to address the question of whether age-related mtDNA mutations are playing a role in colorectal cancer development.

Results

We hypothesized that if age-related mtDNA mutations present in non-transformed colonic epithelium[13,21] contribute to colorectal cancer development, a similar spectrum of mtDNA mutations (and downstream mitochondrial OXPHOS deficiency) would be present and enriched in colorectal tumors. To investigate this, we assessed mitochondrial OXPHOS subunit protein levels and enzyme activities in nine adenomatous polyps and 26 adenocarcinomas and their patient-matched normal mucosa (Fig. 1a,b). We performed in situ immunohistochemistry (IHC) analysis to ensure we only analyzed the epithelial compartment without contamination by muscle, stromal or immune cells or the non-transformed mucosa. Four out of nine (44%) of the adenomas and 18 out of 26 (69%) of the adenocarcinomas had decreased levels, or absence, of one or more OXPHOS subunits and/or loss of histochemical cytochrome *c* oxidase (COX) reactivity (Fig. 1 and Supplementary Table 1) compared with an average of 10% of normal crypts (Fig. 1c). Sequencing of the mtDNA of laser microdissected tumor epithelium, and either patient-matched normal mucosa or stromal tissue from the tumor section (to provide the germline mitochondrial genotype of each subject), detected tumor-specific, clonally expanded mtDNA point mutations in four out of nine adenomas and 22 out of 26

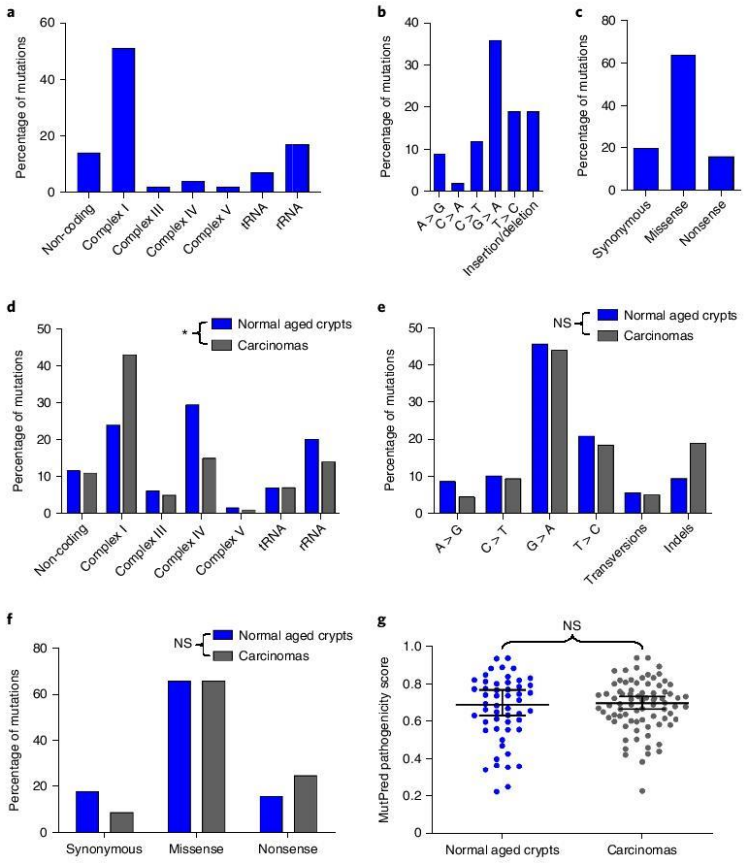

Fig. 2 | Analysis of mtDNA mutations detected in 26 colorectal adenocarcinomas compared with normal aged crypts. a–c, Location (**a**), type (**b**) and consequences (**c**) of mtDNA mutations detected in colorectal adenocarcinomas in this study ($n = 41$ mutations). rRNA, ribosomal RNA; tRNA, transfer RNA. **d–f**, Comparison of the location (**d**), types (**e**) and functional consequences (**f**) of mtDNA mutations in previously published normal crypts ($n = 129$ mutations) and adenocarcinomas[11,13,21,23] ($n = 182$ mutations). There was a significant difference in the location of the mtDNA mutations in adenocarcinomas compared with normal aged crypts ($P = 0.0123$; chi-squared analysis (**d**)), but no significant differences were detected in the types of mutations ($P = 0.2264$; chi-squared analysis (**e**)) or the predicted functional consequences ($P = 0.1504$; chi-squared analysis (**f**)). NS, not significant. **g**, Comparison of MutPred pathogenicity scores for missense mutations in protein-encoding genes in normal aging crypts ($n = 52$ mutations) and adenocarcinomas ($n = 80$ mutations). Statistical significance was determined by two-tailed Mann-Whitney *U*-test ($P = 0.8138$; medians ± 95% confidence intervals are shown). $^*P < 0.05$.

adenocarcinomas (47 mutations in total) (Supplementary Table 2 and Fig. 2). Of the 22 OXPHOS-deficient tumors, 18 had one or more mtDNA mutations at high levels of heteroplasmy correlating with the IHC profile (Supplementary Table 2). mtDNA mutations detected in tumors with normal OXPHOS protein levels were either present at <50% heteroplasmy or were known polymorphic variants predicted not to affect OXPHOS[14]. This highlights the fact that mtDNA mutations are functionally recessive and must reach high levels of heteroplasmy before an OXPHOS defect will become manifest. In four of the tumors with OXPHOS defects, mtDNA mutations were not detected, similar to our previous analyses of normal crypts[13], suggesting that nuclear factors can also contribute to age-related OXPHOS deficiency. Combining the mtDNA mutations detected in the human adenocarcinomas here with those published by others[17–19,22] (Supplementary Table 3), we observed a similar mtDNA mutation spectrum in tumors and normal aging colonic crypts[11,13,21,23] (Supplementary Table 4 and Fig. 2), with the only significant difference being a higher proportion of complex I subunit mutations in the tumors (Fig. 2d, $P = 0.0123$). Given the similarities between the mutational spectrum and OXPHOS defects in normal crypts and tumors, and the very high prevalence of OXPHOS defects in the tumors, we hypothesized that pre-existing OXPHOS defects in normal crypts may provide a selective metabolic advantage during tumorigenesis.

To test this hypothesis, we crossed an inducible intestinal tumor mouse model (*Lgr5-creER*;*Apc*$^{fl/fl}$)[24] with a model of accelerated mtDNA mutagenesis (*PolgA*$^{mut/mut}$)[25,26] (Extended Data Fig. 1a). By 6 months of age, the *PolgA*$^{mut/mut}$ mice have a high frequency of intestinal crypts with OXPHOS dysfunction caused by clonally

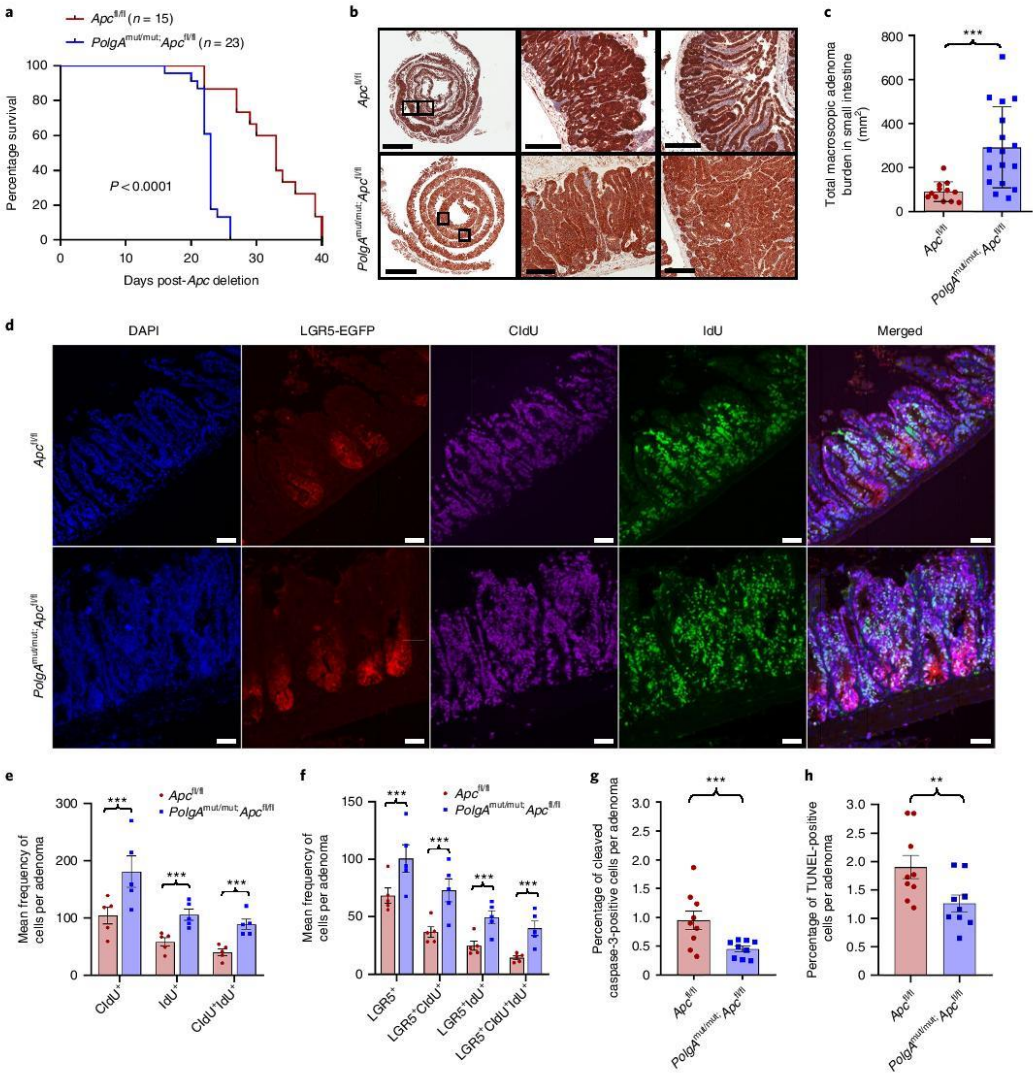

Fig. 3 | *PolgA*$^{mut/mut}$;*Apc*$^{fl/fl}$ mice have a reduced lifespan and enhanced tumor growth due to accelerated cell proliferation and reduced apoptosis compared with *Apc*$^{fl/fl}$ mice. a, Kaplan–Meier survival curve showing survival times post-*Apc* deletion (two-sided Mantel–Cox (log-rank) test; $P<0.0001$; n = number of mice). **b**, β-catenin IHC on small intestinal sections. Scale bars, 3 mm (first column) and 200 μm (second and third columns). IHC was performed on *PolgA*$^{mut/mut}$;*Apc*$^{fl/fl}$ ($n=17$) and *Apc*$^{fl/fl}$ ($n=12$) mice 23 d post-*Apc* deletion. Representative images are shown. **c**, Tumor burden in the small intestines of *PolgA*$^{mut/mut}$;*Apc*$^{fl/fl}$ ($n=17$) and *Apc*$^{fl/fl}$ ($n=12$) mice 23 d post-*Apc* deletion (unpaired, two-tailed *t*-test; error bars show s.d.; $P=0.0010$). **d**, Immunoflourescence images showing LGR5$^+$ cells and cells that had incorporated CldU and IdU. Scale bars, 50 μm. Immunofluorescence was performed on $n=5$ mice per group and representative images are shown. **e**,**f**, Quantification of the frequency of thymidine analog incorporation in all cells per adenoma (**e**) and LGR5$^+$ cells per adenoma per mouse (**f**) ($n=5$ mice per group with 20 adenomas analyzed per mouse; two-sided linear mixed-effects regression model with mouse ID as a random effect; $P<0.001$ in all comparisons). **g**,**h**, Apoptotic cells were identified and quantified using cleaved caspase-3 IHC (**g**) and TUNEL labeling (**h**) in mice 23 d post-*Apc* deletion ($n=9$ mice per group with a minimum of ten adenomas analyzed per mouse; two-sided linear mixed-effects regression model with mouse ID as a random effect; $P<0.001$ for cleaved caspase-3; $P=0.008$ for TUNEL; mean percentages of apoptotic cells per adenoma per mouse are shown ± s.e.m). $^{**}P<0.01$; $^{***}P<0.001$.

expanded mtDNA mutations[27]. Furthermore, modeling studies support a similar mechanism of clonal expansion of mtDNA mutations through random genetic drift with age in intestinal crypts of *PolgA*$^{mut/mut}$ mice[27] and humans[28]. Intestinal tumors were induced in *PolgA*$^{mut/mut}$;*Lgr5-creER*;*Apc*$^{fl/fl}$ (hereafter denoted *PolgA*$^{mut/mut}$;*Apc*$^{fl/fl}$) and *Lgr5-creER*;*Apc*$^{fl/fl}$ (hereafter denoted *Apc*$^{fl/fl}$) mice by tamoxifen activation of the Cre recombinase at 6 months of age. *PolgA*$^{mut/mut}$;*Apc*$^{fl/fl}$ mice had a significantly shorter lifespan than *Apc*$^{fl/fl}$ mice, with median survival times post-*Apc* deletion of 23 and 33 d, respectively (Fig. 3a, $P<0.0001$). We confirmed that the dose of the inducing agent tamoxifen was not toxic when given to mice that did not express Cre recombinase (Extended Data Fig. 1b). To compare tumor growth rates, *Apc* deletion was induced in *PolgA*$^{mut/mut}$;*Apc*$^{fl/fl}$ and *Apc*$^{fl/fl}$ mice at 6 months of age, and all mice were killed 23 d later (the median lifespan of the *PolgA*$^{mut/mut}$;*Apc*$^{fl/fl}$ line). The total tumor burden in the small intestine of *PolgA*$^{mut/mut}$;*Apc*$^{fl/fl}$ mice was significantly higher than in *Apc*$^{fl/fl}$ mice (Fig. 3b,c, $P=0.0010$). β-catenin IHC showed no significant difference in the number of microscopic β-catenin^{high} foci in the colon between the two groups (Extended Data Fig. 1c,d, $P=0.7444$). However, foci in *PolgA*$^{mut/mut}$;*Apc*$^{fl/fl}$ mice were almost twice the size of those in *Apc*$^{fl/fl}$ mice (Extended Data Fig. 1e, $P<0.0001$). These data suggest that mitochondrial dysfunction in intestinal epithelial cells of *PolgA*$^{mut/mut}$;*Apc*$^{fl/fl}$ mice promotes tumor cell growth after transformation by *Apc* deletion.

To investigate the underlying cause of the increased tumor size in the *PolgA*$^{mut/mut}$;*Apc*$^{fl/fl}$ mice, we compared proliferation rates of all cells in the adenomas, and specifically in the leucine-rich repeat-containing G protein-coupled receptor 5-positive (LGR5^{+}) stem cells, from both groups of animals using multiple thymidine analog labeling (Fig. 3d). We noted a significantly higher frequency of cells incorporating 5-chloro-2′-deoxyuridine (CldU) and 5-iodo-2′-deoxyuridine (IdU), both individually and together, in adenomas of the small intestine (Fig. 3e, $P<0.001$ in all cases) and colon (Extended Data Fig. 1f, $P<0.001$ in all cases) of the *PolgA*$^{mut/mut}$;*Apc*$^{fl/fl}$ mice. Incorporation of both thymidine analogs identifies cells that have divided twice within the 28 h period, providing evidence that the cells are proliferating faster in *PolgA*$^{mut/mut}$;*Apc*$^{fl/fl}$ adenomas. In the small intestine, both the frequency of LGR5^{+} cells per adenoma and their levels of thymidine analog incorporation were significantly higher in the *PolgA*$^{mut/mut}$;*Apc*$^{fl/fl}$ mice compared with the *Apc*$^{fl/fl}$ mice, indicative of a higher proliferative index (Fig. 3f, $P<0.001$ in all cases). Despite an increase in LGR5^{+} stem cells in colonic adenomas (Extended Data Fig. 1g, $P<0.001$, no significant differences in LGR5^{+} stem cell proliferation rates were noted (Extended Data Fig. 1g). Using cleaved caspase-3 IHC and terminal deoxynucleotidyl transferase (TdT)-mediated dUTP nick end (TUNEL) labeling, we detected a significantly lower frequency of apoptotic cells in adenomas from the *PolgA*$^{mut/mut}$;*Apc*$^{fl/fl}$ mice in both the small intestine (Fig. 3g,h, $P<0.001$ for cleaved caspase 3 and $P=0.008$ for TUNEL) and colon (Extended Data Fig. 1h,i, $P=0.0092$ for cleaved caspase 3 and $P=0.002$ for TUNEL). These data suggest that mitochondrial dysfunction leads to increased cell proliferation and decreased apoptosis, resulting in accelerated tumor growth.

Next, we investigated the pattern of OXPHOS deficiency in intestinal adenomas from *PolgA*$^{mut/mut}$;*Apc*$^{fl/fl}$ and *Apc*$^{fl/fl}$ mice using quantitative quadruple immunofluorescence[29] (Fig. 4a–e and Extended Data Fig. 2a–e). OXPHOS proteins were normalized to the mitochondrial mass marker TOMM20, with *Apc*$^{fl/fl}$ adenomas acting as controls. In the small intestine, >85% of *PolgA*$^{mut/mut}$;*Apc*$^{fl/fl}$ adenomas were classified as NADH:ubiquinone oxidoreductase subunit B8 (NDUFB8; complex I) deficient, whereas mitochondrially encoded cytochrome *c* oxidase I (MTCO1; complex IV) and ubiquinol–cytochrome *c* reductase, Rieske iron-sulfur polypeptide 1 (UQCRFS1; complex III) labeling only revealed minimal deficiency (Fig. 4e). Similar patterns of OXPHOS deficiency were detected in colonic adenomas (Extended Data Fig. 2e). To determine whether *Apc* deletion affected mitochondrial OXPHOS protein abundance, we compared normal (non-recombined) small intestine and colonic mucosa of the *PolgA*$^{mut/mut}$;*Apc*$^{fl/fl}$ and *Apc*$^{fl/fl}$ mice with the adenomas (Fig. 4f and Extended Data Fig. 2f–h). In both tissues, mitochondrial density increased significantly following *Apc* deletion in both mouse models ($P<0.0001$ all cases). There were no significant differences in NDUFB8 or UQCRFS1 between the crypts and adenomas of the *PolgA*$^{mut/mut}$;*Apc*$^{fl/fl}$ mice in both small intestine and colon, but MTCO1 and ATP synthase subunit beta (ATPB) levels were significantly lower in the adenomas (MTCO1, $P<0.0001$ in the small intestine and $P=0.007$ in the colon; ATPB, $P<0.0001$ in both tissues). In the *Apc*$^{fl/fl}$ mice, OXPHOS proteins were significantly lower in the adenomas than in the normal mucosa in both colon and small intestine ($P<0.0001$ in all cases), supporting previous studies showing Wnt-mediated downregulation of mitochondrial OXPHOS as a tumor-promoting mechanism[30]. Our data suggest that this mechanism is accelerated in *PolgA*$^{mut/mut}$;*Apc*$^{fl/fl}$ mice.

To investigate whether somatic mtDNA mutations were responsible for the OXPHOS deficiencies in the mice, individual adenomas were laser microdissected from *PolgA*$^{mut/mut}$;*Apc*$^{fl/fl}$ and *Apc*$^{fl/fl}$ mice and the mtDNA was sequenced. *PolgA*$^{mut/mut}$;*Apc*$^{fl/fl}$ adenomas harbored an average of 13–14 variants present at 30–70% heteroplasmy (Supplementary Table 5), whereas in *Apc*$^{fl/fl}$ adenomas, none were detected at >5%. The mutational spectrum was consistent with the random mutagenesis model previously described in colonic crypts of the *PolgA*$^{mut/+}$ mice[27] (Extended Data Fig. 3). Unlike our human dataset, no homoplasmic mtDNA variants were detected; however, this is not unexpected given the age of the mice and the predictions of the time required for an mtDNA variant to reach homoplasmy[27]. These data strongly infer that multiple heteroplasmic clonally expanded mtDNA mutations are the underlying cause of the OXPHOS defects detected in *PolgA*$^{mut/mut}$;*Apc*$^{fl/fl}$ adenomas.

Next, we used RNA sequencing (RNA-Seq) to investigate the mechanism by which OXPHOS dysfunction in the normal aging

Fig. 4 | Small intestinal adenomas from *PolgA*$^{mut/mut}$;*Apc*$^{fl/fl}$ mice are deficient in mitochondrial complex I, but the majority retain expression of subunits of complexes III, IV and V. a,**c**, Immunofluorescence was performed to quantify levels of OXPHOS proteins on $n=9$ *PolgA*$^{mut/mut}$;*Apc*$^{fl/fl}$ mice and $n=10$ *Apc*$^{fl/fl}$ mice. Representative images are shown. Scale bars, 50 μm. In **a**, white dashed lines show an adenoma region deficient in complexes I and III and red dashed lines highlight deficiency in complex I only. In **c**, white dashed lines show an adenoma region deficient in complex IV and red dashed lines show normal complex IV. **b**,**d**, Dot plots showing relative *Z* scores for complexes I and III (**b**) and IV and V (**d**), calculated following quantification of mitochondrial OXPHOS protein levels in adenomas from *PolgA*$^{mut/mut}$;*Apc*$^{fl/fl}$ ($n=9$) and *Apc*$^{fl/fl}$ ($n=10$) mice using the method described in ref. [29] ($n=20$ adenomas quantified per mouse). The dashed lines indicate *Z* scores of −3, −4.5 and −6, which are used in the categorical analsyis of OXPHOS protein levels in **e**. **e**, Categorical analysis of OXPHOS protein levels in *PolgA*$^{mut/mut}$;*Apc*$^{fl/fl}$ ($n=9$) mice. Data points show individual mice ± s.d. **f**, Dot plots showing raw densitometry values for mitochondrial protein levels. For the adenomas, $n=9$ *PolgA*$^{mut/mut}$;*Apc*$^{fl/fl}$ and $n=10$ *Apc*$^{fl/fl}$ mice with 20 adenomas analyzed per mouse. For the normal crypts, $n=5$ mice were analyzed per group with a minimum of 13 crypts quantified per mouse. Statistical significance was determined by one-way ANOVA with Tukey's post-hoc test. *P* values for within-genotype comparisons between normal crypts and adenomas were as follows: TOMM20: $P<0.0001$ (*Apc*$^{fl/fl}$); $P<0.0001$ (*PolgA*$^{mut/mut}$;*Apc*$^{fl/fl}$); NDUFB8: $P<0.0001$ (*Apc*$^{fl/fl}$); $P=0.9995$ (*PolgA*$^{mut/mut}$;*Apc*$^{fl/fl}$); UQCRFS1: $P<0.0001$ (*Apc*$^{fl/fl}$); $P=0.1302$ (*PolgA*$^{mut/mut}$;*Apc*$^{fl/fl}$), MTCO1: $P<0.0001$ (*Apc*$^{fl/fl}$); $P=0.0001$ (*PolgA*$^{mut/mut}$;*Apc*$^{fl/fl}$); ATPB: $P<0.0001$ (*Apc*$^{fl/fl}$); $P<0.0001$ (*PolgA*$^{mut/mut}$;*Apc*$^{fl/fl}$). ***$P<0.001$. Error bars show s.e.m.

intestinal epithelium accelerates tumor development. Normal epithelial crypts from the distal end of the small intestine (where the majority of adenomas occur) were isolated from 6-month-old *PolgA*$^{mut/mut}$ and *PolgA*$^{+/+}$ mice. Comparison of differentially expressed genes revealed that the most significantly upregulated genes (*Phgdh*, *Psat1*, *Psph*, *Mthfd2*, *Slc1a4* and *Aldh1l2*) were

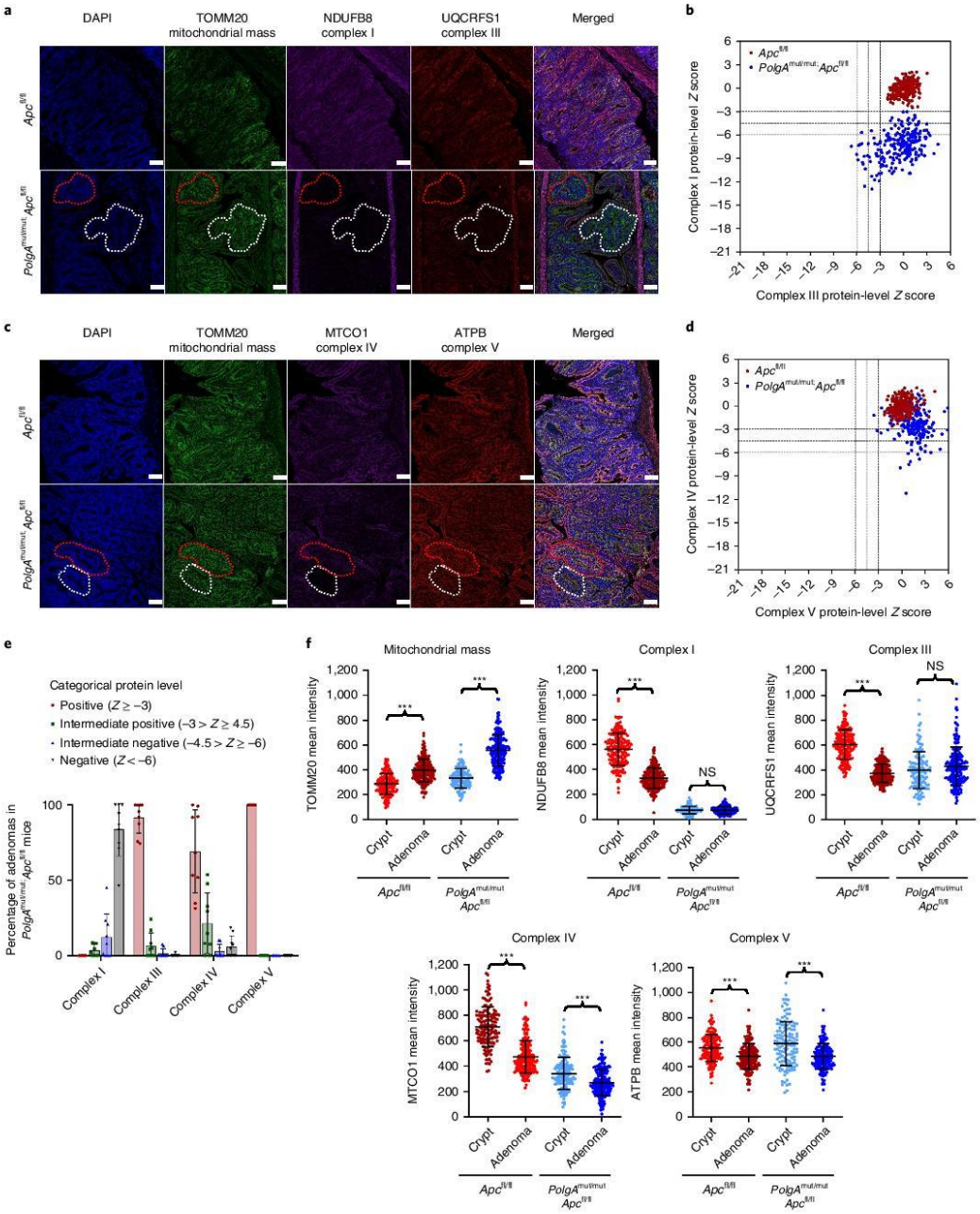

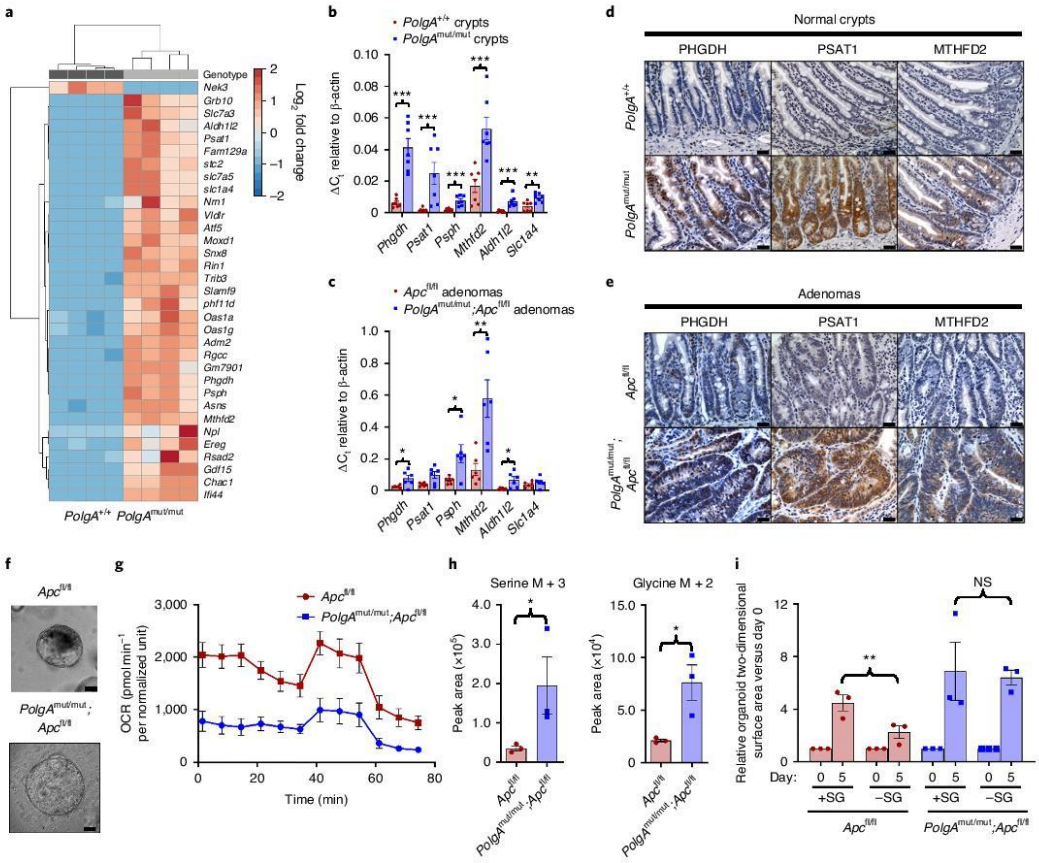

Fig. 5 | Mitochondrial OXPHOS dysfunction causes upregulation of denovo serine synthesis in both non-transformed crypts and adenomas from mice. **a**, Heat map showing differential gene expression in non-transformed crypt homogenates from the small intestines of *PolgA*$^{+/+}$ and *PolgA*$^{mut/mut}$ mice ($n=4$ mice per group). **b**, Mean relative expression of the SSP genes by RT-PCR that were identified to be upregulated by RNA-Seq analysis in normal crypts ($n=7$ mice per group; one-way Mann–Whitney *U*-test; $P=0.0003$ for all genes except *Slc1a4*, where $P=0.0035$; error bars show s.e.m.). **c**, Mean relative expression of the SSP genes by RT-PCR that were identified to be upregulated by RNA-Seq analysis in laser microdissected adenomas ($n=6$ mice per group; one-way Mann–Whitney *U*-test; *P* values as follows: $P=0.0325$ (*Phgdh*); $P=0.066$ (*Psat1*); $P=0.0130$ (*Psph*); $P=0.0043$ (*Mthfd2*); $P=0.0130$ (*Aldh1l2*), $P=0.1548$ (*Slc1a4*); error bars show s.e.m.). **d**,**e**, IHC images showing in situ levels of SSP proteins in the non-transformed normal small intestinal mucosa (**d**) and adenomas (**e**). IHC was performed on $n=4$ mice per genotype and representative images are shown. Scale bars, 50 μm. **f**, Organoids were generated from $n=3$ *PolgA*$^{mut/mut}$;*Apc*$^{fl/fl}$ and $n=3$ *Apc*$^{fl/fl}$ mice. Representative images of adenoma organoids are shown. Scale bars, 100 μm. **g**, OCRs measured by Seahorse analysis in adenoma organoids ($n=3$ mice per genotype; $n=8$ technical replicates per mouse; means ± s.e.m per mouse are shown). **h**, Quantification of major mass isotopomers detected in adenoma organoids following growth in the presence of $^{13}C_6$ glucose for 24 h. ^{13}C labeling is shown as M + 3 (serine) or M + 2 (glycine) ($n=3$ mice per group with $n=3$ technical replicates performed per mouse; one-way unpaired *t*-test; $P=0.0143$ for labeled serine and $P=0.0151$ for labeled glycine; data are means per mouse ± s.e.m). **i**, Quantification of the growth of adenoma organoids in medium with (+SG) or without (−SG) serine and glycine for 5 d. Data are normalized to organoid area on day 0. Mean organoid sizes per mouse relative to day 0 ± s.e.m are shown ($n=3$ mice per group; unpaired, two-tailed *t*-test; $P=0.0021$ for *Apc*$^{fl/fl}$; $P=0.4140$ for *PolgA*$^{mut/mut}$;*Apc*$^{fl/fl}$). $^{*}P<0.05$; $^{**}P<0.01$; $^{***}P<0.001$.

involved in pathways relating to serine biosynthesis, uptake and metabolism (Fig. 5a and Supplementary Table 6). These data were confirmed by quantitative reverse-transcriptase PCR (qRT-PCR; Fig. 5b, $P=0.0003$ for all genes except *Slc1a4*, where $P=0.0035$). RNA extracted from laser microdissected adenoma tissue from the small intestine of both groups of animals showed significant upregulation of *Phgdh*, *Psph*, *Mthfd2* and *Aldh1l2* in the adenomas from *PolgA*$^{mut/mut}$;*Apc*$^{fl/fl}$ mice (Fig. 5c, $P=0.0325$ (*Phgdh*), $P=0.0130$ (*Psph*), $P=0.0043$ (*Mthfd2*), $P=0.0130$ (*Aldh1l2*)). These findings were confirmed at the protein level for phosphoglycerate dehydrogenase (PHGDH), phosphoserine aminotransferase 1 (PSAT1) and methylenetetrahydrofolate dehydrogenase (NADP^{+} dependent) 2, methenyltetrahydrofolate cyclohydrolase (MTHFD2) by IHC in the small intestine (Fig. 5d,e) and colon (Extended Data Fig. 4a,b).

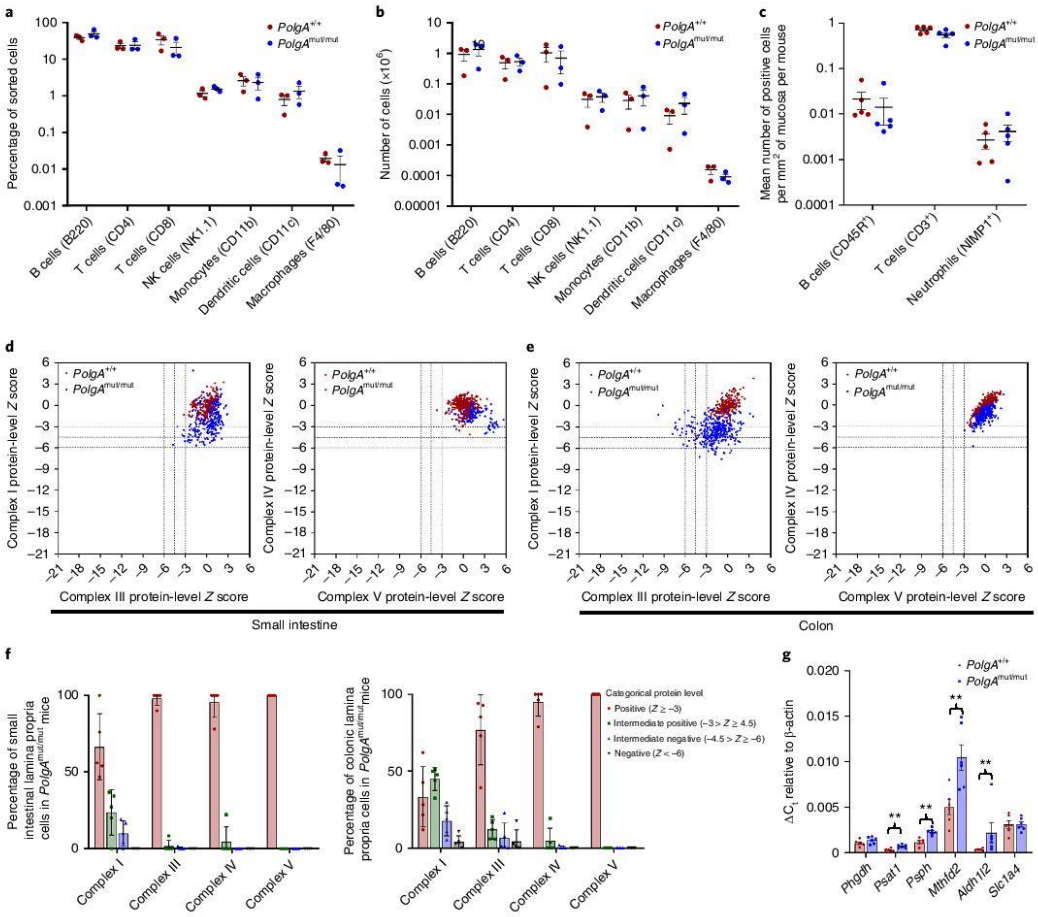

Fig. 6 | Characterization of the immune microenvironment in the lamina propria of the small intestine of *PolgA*$^{mut/mut}$ and *PolgA*$^{+/+}$ mice at 6 months of age, before tumor induction. a,b, Immune cell infiltration within the distal third of the small intestine was analyzed by flow cytometry. Relative proportions (**a**) and absolute numbers (**b**) of each cell type are shown. No significant differences were found between the two groups ($n=3$ mice per group; one-way ANOVA with Tukey's post-hoc test). NK, natural killer. **c**, Mean frequency of B cells, T cells and neutrophils per mm^2 of small intestinal epithelium, as quantified by IHC ($n=5$ mice per group). No significant differences were detected by one-way ANOVA with Tukey's post-hoc test. **d,e**, Dot plots showing *Z* scores, for complex 1 versus complex III (left) and complex IV versus complex V (right), calculated following quantification of mitochondrial OXPHOS protein levels in small groups of lamina propria cells in the small intestine (**d**) and colon (**e**) of *PolgA*$^{mut/mut}$ and *PolgA*$^{+/+}$ mice ($n=5$ mice per group; a minimum of 50 areas per mouse were analyzed). **f**, Categorical analysis of OXPHOS protein levels in the small intestine (left) and colon (right) of *PolgA*$^{mut/mut}$ mice ($n=5$ mice per group). **g**, Relative expression of the SSP genes in the lamina propria of the small intestine by RT-PCR that had been identified to be upregulated by RNA-Seq analysis in the crypts ($n=6$ mice per group; one-way Mann–Whitney *U*-test). *P* values are as follows: $P=0.1201$ (*Phgdh*); $P=0.0043$ (*Psat1*); $P=0.0011$ (*Psph*); $P=0.0043$ (*Mthfd2*); $P=0.0022$ (*Aldh1l2*); $P=0.500$ (*Slc1a4*). Mean values per mouse ± s.e.m are shown. $^{**}P<0.01$.

Supporting the hypothesis that these proteins are upregulated in response to age-related accumulation of OXPHOS defects in the *PolgA*$^{mut/mut}$ mice, we observed an age-related increase in serine synthesis pathway (SSP) protein levels in the normal small intestine crypts of *PolgA*$^{mut/mut}$ mice between 1 and 12 months of age (Extended Data Fig. 5).

We investigated the functional consequences of changes in gene expression and protein levels in the *PolgA*$^{mut/mut}$;*Apc*$^{fl/fl}$ adenomas by generating in vitro adenoma organoids from mice from the two groups (Fig. 5f). We were unable to investigate this in non-transformed normal small intestinal organoids as it has been shown previously (as is our own experience) that these do not grow from the *PolgA*$^{mut/mut}$ mice in vitro[31]. The baseline oxygen consumption rate (OCR) was lower in organoids derived from *PolgA*$^{mut/mut}$; *Apc*$^{fl/fl}$ adenomas compared with *Apc*$^{fl/fl}$ adenomas, confirming that in vivo OXPHOS defects were manifest in the in vitro model (Fig. 5g).

Following growth in $^{13}C_6$-labeled glucose for 24 h, we found that labeled serine (M+3) and glycine (M+2) (derived from the labeled glucose through the SSP) were significantly higher in *PolgA*$^{mut/mut}$; *Apc*$^{fl/fl}$ organoids, indicating increased rates of de novo serine synthesis (Fig. 5h, $P=0.0143$ (serine), $P=0.0151$ (glycine)). No significant differences were observed in the levels of labeled glucose per se, suggesting equal uptake, nor were there differences in the levels of unlabeled (M+0) serine or glycine (Extended Data Fig. 6a). Growth rates in the absence of serine and glycine (−SG) were significantly impaired in the *Apc*$^{fl/fl}$ organoids ($P=0.0021$), whereas *PolgA*$^{mut/mut}$; *Apc*$^{fl/fl}$ organoids maintained their growth (Fig. 5i, $P=0.4140$), suggesting that complex I deficiency induces the SSP, conferring a significant growth advantage to adenomas. Next, we investigated the effect of the biguanide metformin, which has been shown to inhibit complex I[32,33], on the growth of *Apc*$^{fl/fl}$ organoids. There was a notable increase in organoid growth rate when they were dosed with metformin compared with vehicle controls (Extended Data Fig. 6b), confirming that pharmacological inhibition of complex I can also enhance adenoma organoid growth[34].

Since the *PolgA*$^{mut/mut}$ model is a whole body knock-in, we evaluated changes in the intestinal immune microenvironment at 6 months of age before tumor induction to determine any contribution to accelerated tumor growth. In-depth fluorescence-activated cell sorting (FACS) analysis of immune cell types in the distal end of the small intestine revealed no significant differences between either the proportions or the absolute numbers of the sorted immune cells between the two groups (Fig. 6a,b and Supplementary Fig. 1). This was confirmed in a subset of immune cells by IHC (Fig. 6c). Furthermore, in contrast with our crypt data, we detected little evidence of OXPHOS deficiency within the lamina propria of *PolgA*$^{mut/mut}$ mice; 66% of small intestinal cells showed normal NDUFB8 levels while 95% had normal MTCO1 levels (Fig. 6d–f). Gene expression studies revealed significant upregulation of *Psat1*, *Psph*, *Mthfd2* and *Aldh1l2*, but not *Phgdh* (Fig. 6g, $P=0.0043$ (*Psat1*), $P=0.0011$ (*Psph*), $P=0.0043$ (*Mthfd2*), $P=0.0022$ (*Aldh1l2*)), providing evidence that there is mitochondrial dysfunction and metabolic remodeling in the epithelial tissue microenvironment, but this is less marked than in epithelial cells.

Our mouse experiments have provided evidence that mitochondrial OXPHOS dysfunction can induce metabolic remodeling in the mouse small intestine and colon. Finally, it was important to see whether these findings were translatable to humans. We tested this by quantifying levels of PHGDH, PSAT1 and MTHFD2 in individual OXPHOS-normal and OXPHOS-deficient crypts from aged human samples by immunofluorescence. Levels of all three enzymes were significantly higher in crypts with OXPHOS defects than those with normal OXPHOS function (Fig. 7a–d, $P<0.0001$ for all enzymes), suggesting that normal aged human crypts expressing OXPHOS deficiency upregulate the de novo SSP as a pro-survival mechanism.

Discussion

Our data show that age-related mitochondrial OXPHOS dysfunction caused by mtDNA mutations in both humans and mice causes metabolic remodeling in intestinal epithelial cells, with specific upregulation of the de novo SSP, and the mouse model shows that this provides a metabolically favorable environment for tumor growth (Fig. 7e). Our human mtDNA sequencing data show that mtDNA mutations are not a requirement for tumorigenesis as they were not present in all adenocarcinomas studied, highlighting diverse mitochondrial genetic heterogeneity between tumors. In addition, the specific mtDNA mutation and its level of heteroplasmy are important determinants of whether an mtDNA mutation is actively contributing to a favorable metabolic phenotype for the tumor or whether it is simply a passenger mutation. Only those mtDNA mutations that are present both at functionally important sites and at a high enough level of heteroplasmy to cause OXPHOS defects result in a favorable metabolic shift, which, as we have shown in the mouse, can accelerate tumor cell growth. We believe that it is the biochemical change rather than the mutational event per se providing the advantage. In contrast, mtDNA mutations that are present at low levels of heteroplasmy, or ones that do not cause a biochemical defect, fall into the passenger mutation category and examples of these were also detected in our study.

The pathways we show to be upregulated in OXPHOS-deficient crypts in both our human and mouse data are well recognized as being critical for biomass production during tumor growth[34]. It is well accepted that only a small proportion of human adenomas go on to become adenocarcinomas[35] and that the larger the adenoma the higher the risk of carcinogenesis[36]. Therefore, the selective advantage of OXPHOS dysfunction for tumor growth, acting in synergy with nuclear DNA mutations, would be reflected in their increasing prevalence in clinically detectable large adenomas and adenocarcinomas, which is in line with our data. Although our mouse data specifically identified the contribution of pre-existing mtDNA mutations to tumorigenesis, it is also possible that tumor cells can acquire new mtDNA mutations that randomly clonally expand to high levels of heteroplasmy in individual cells during the tumorigenic process. If these mutations cause an OXPHOS defect, together with the associated favorable metabolic phenotype, those cells may outcompete others and become dominant within the tumor. Additional data to support a pro-tumorigenic role for pathogenic mtDNA mutations can be found in a recent pan-cancer analysis of mtDNA by the Pancancer Analysis of Whole Genomes Consortium[16]. This study showed selective enrichment of truncating mtDNA mutations in the protein-encoding genes at high levels of heteroplasmy (>60%), specifically in colorectal cancers. This was not seen in most other cancer types, with the authors suggesting that these mtDNA mutations could have oncogenic effects by altering signaling pathways[16].

In the normal aging intestine, this metabolic shift in response to OXPHOS deficiency may represent a response to mitochondrial stress, particularly if there are increased mitochondrial ROS levels; diversion of glucose through the SSP to increase glutathione production to help detoxify mitochondrial ROS is documented in mitochondrial disease models[37]. In addition, mitochondrial ROS play a significant role as signaling molecules in LGR5$^+$ stem cell

Fig. 7 | Mitochondrial OXPHOS dysfunction causes upregulation of de novo serine synthesis in normal aging human colonic crypts. a, Immunoflourescent images showing co-labeling of OXPHOS proteins and SSP enzymes in normal human colonic epithelium. CI (Complex I), CIV (Complex IV). White dashed lines highlight crypts that are NDUFB8 and MTCO1 deficient and have upregulation of PHGDH, PSAT1 or MTHFD2. Scale bars, 50 μm. Immunofluorescence was performed for each antibody on $n=12$ human samples. Representative images are shown. **b**–**d**, Quantification of the levels of PHGDH (**b**), PSAT1 (**c**) and MTHFD2 (**d**) in individual human crypts. Every OXPHOS-deficient crypt on the section was quantified, and OXPHOS-normal crypts on the same section were randomly sampled. In **b**, the numbers of crypts analyzed from left to right are: $n=45$, 46, 40, 62, 43, 50, 28, 29, 21, 16, 16, 17, 33, 31, 41, 17, 20, 8, 32, 27, 15, 17, 24 and 24. In **c**, the numbers of crypts analyzed from left to right are: $n=47$, 57, 58, 70, 44, 56, 54, 39, 73, 11, 21, 20, 33, 33, 39, 16, 30, 8, 61, 45, 31, 22, 51 and 49. In **d**, the numbers of crypts analyzed from left to right are: $n=23$, 67, 40, 61, 44, 47, 42, 32, 108, 15, 37, 38, 59, 60, 58, 26, 62, 10, 48, 40, 31, 24, 60 and 59. Error bars show means ± s.d. Data were analyzed using a two-sided linear mixed-effects regression model with mouse ID as a random effect. $P<0.0001$ in all comparisons. e, Schematic showing the hypothesized mechanism by which mtDNA mutations and OXPHOS defects contribute to tumorigenesis. ***$P<0.001$.

maintenance and crypt differentiation, highlighting the importance of maintaining the required ROS levels for normal crypt cell homeostasis[38,39]. Through its role as a precursor for the synthesis of nucleic acids, proteins and lipids, as well as antioxidants, serine is critical to support metabolic processes for cellular growth and survival in cancer development[40]. Therefore, the apparently protective cellular response to OXPHOS deficiency during aging may provide a distinct metabolic advantage for tumor growth when those cells are transformed. The OXPHOS deficiency observed in our mouse model provoked a similar metabolic response (that is, resistance to serine starvation due to upregulation of the SSP) to that seen in a model with activating *Kras* mutations in the presence of *Apc* deletion[34].

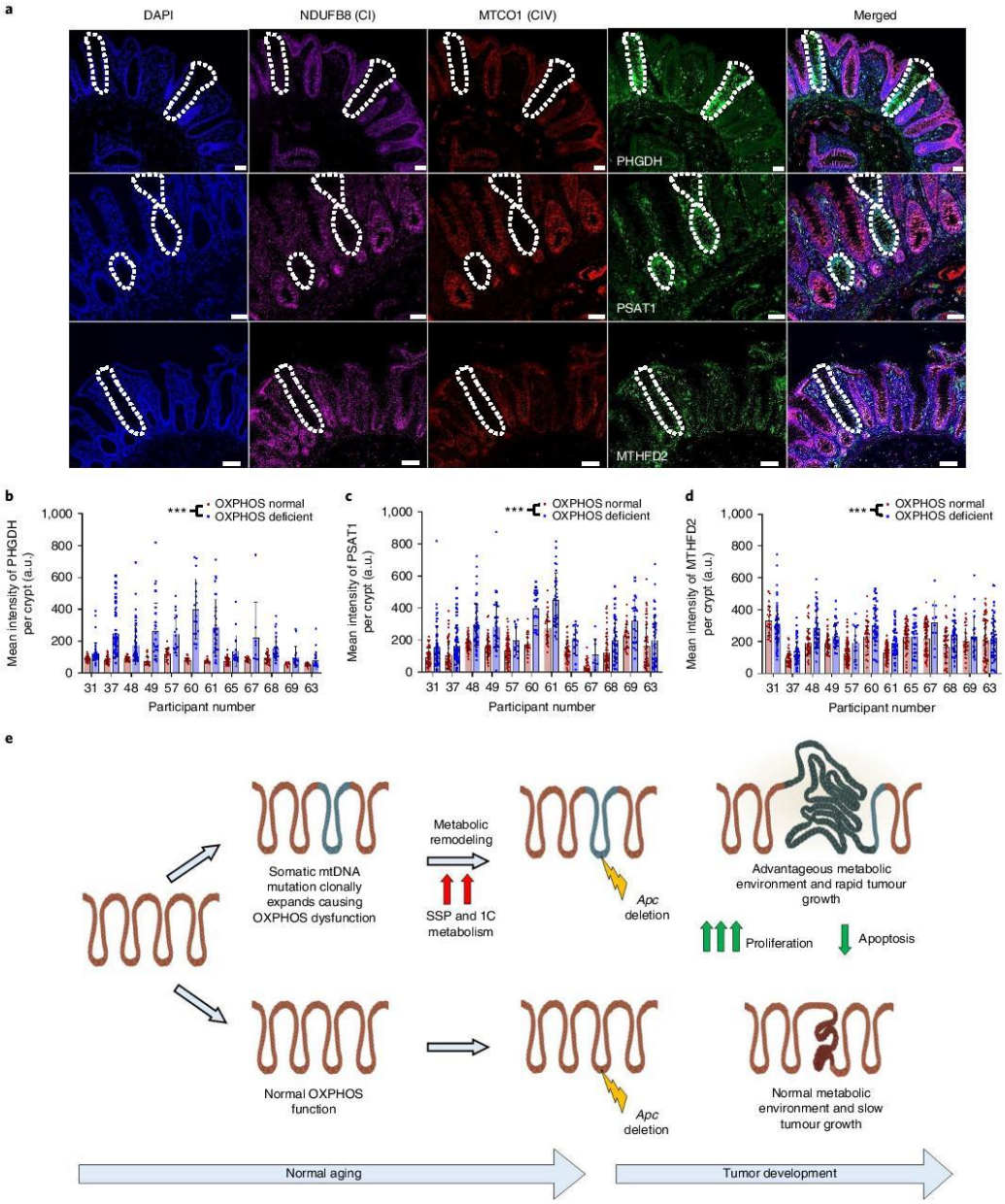

Furthermore, metabolic rewiring has been shown to occur in gliomas containing oncogenic *IDH1* mutations in response to oxidative stress, suggesting that mechanisms to maintain cellular redox balance are important for cancer cell survival[41]. Although we found no significant differences in either the absolute numbers or proportions of immune cell types in our model, we found evidence of low-level OXPHOS defects and a compensatory increase in SSP gene expression in cells of the lamina propria. Therefore, in addition to definitive evidence of the cell intrinsic effect of OXPHOS defects on tumor cell growth, it is possible that the aged microenvironment also plays a role.

We stress that our observations do not indicate that mtDNA-driven OXPHOS deficiency alone is able to initiate cancer as *PolgA*$^{mut/mut}$ mice do not have a higher tumor incidence compared with age-matched wild-type controls[25,26]. Rather, we hypothesize that age-related mtDNA mutations act synergistically with driver mutations, which are present in ~1% of normal crypts in middle-aged individuals[32], providing an advantageous metabolic environment during the pervasive process of neoplastic change during the colorectal adenoma–carcinoma sequence[35]. This hypothesis is supported by evidence of an increasing frequency of mtDNA mutations and OXPHOS defects from normal aged human crypts to adenoma to carcinoma.

A logical question arising from our studies is whether there is an increased incidence of colorectal cancer in patients with inherited pathogenic mtDNA mutations causing mitochondrial disease. Although there are no published studies addressing this question, in our clinical experience, we see no evidence to suggest that the patients have an increased incidence of cancer over their lifetime. However, a number of studies have shown that there is rapid loss of inherited pathogenic mtDNA mutations in human replicating tissues with age[43–48]. This is supported by similar findings in mouse models of inherited mtDNA disease[49,50]. Specifically looking at data from the gut, this loss of inherited mtDNA mutations results in the frequency of crypts with OXPHOS defects being similar to age-matched controls[48,51]. We currently do not understand the mechanism by which this selective loss is happening; however, loss of OXPHOS-deficient cells from the rapidly proliferating tissues would mean that any metabolic advantage for cancer cells would also be lost. This could explain why these patients do not appear to be at a higher risk of cancer. These observations suggest that inherited and age-associated somatic mtDNA mutations are behaving differently, highlighting the value of using the *PolgA*$^{mut/mut}$ mouse model in our study to model the aging human phenotype.

In conclusion, we propose that age-related mitochondrial OXPHOS defects can contribute to accelerated intestinal cancer cell growth and survival through upregulation of serine biosynthetic pathways. Metabolic pathways are attractive targets for therapeutic intervention, and the inherent reliance on the SSP in intestinal tumors with OXPHOS defects may make them selectively vulnerable to SSP inhibition and worthy of future investigation.

Methods

Patients and samples. Normal colonic epithelial and colorectal adenocarcinoma tissue was obtained from 26 patients undergoing surgical resection for a histopathologically graded adenocarcinoma diagnosis and from nine patients undergoing surgery for the removal of adenomatous polyps (age range: 52–82 years; 20 male; 15 female). Informed written consent was obtained before surgery and samples were coded to maintain confidentiality. This project was approved by the Joint Ethics Committee of Newcastle and North Tyneside Health Authority (2001/188) and the London–Stanmore National Research Ethics Committee (11/LO/1613).

Genetically engineered mouse models. *Lgr5-EGFP-IRES-creERT2*, *Apc*$^{fl/fl}$ (ref. [24]) and *PolgA*$^{+/mut}$ (ref. [25]) mice were cross-bred to generate *PolgA*$^{mut/mut}$;*Lgr5-creER*;*Apc*$^{fl/fl}$ and *Lgr5-creER*;*Apc*$^{fl/fl}$ mice, as shown in Extended Data Fig. 1. Mice were maintained on a C57BL/6 background, both sexes were used and researchers were blinded to genotypes. Mice were housed in single-sex cages at 20 ± 2 °C under a 12 h light/12 h dark photoperiod with the lights on at 07:00. All animal work was carried out in line with the Animals (Scientific Procedures) Act 1986 and the EU Directive 2010 in compliance with the UK Home Office (PPL P3052AD70) and the Newcastle University Animal Welfare Ethical Review Board (AWERB 425). Both sexes were used in all experiments (except RNA-Seq, for which all mice were female) and all mice were 6 months old unless otherwise stated.

COX/succinate dehydrogenase (SDH) histochemistry. Human colon samples were mounted for sectioning and frozen in isopentane pre-cooled to −190 °C in liquid nitrogen. Cryostat sections (12 μm) were cut onto glass slides and COX/SDH histochemistry was performed as previously described[13].

OXPHOS subunit IHC (human samples). Sections of 10 μm were cut from all samples described above and air dried for 1 h at room temperature. IHC was performed as previously described[13] using the antibodies complex I NDUFB8 (1:50), complex II SDHA (1:1,000), complex III UQCRFS1 (1:1,000) and complex IV MTCO1 (1:1,000) combined with a polymer detection system (Menarini Diagnostics). Protein levels were qualitatively scored in tumors compared with patient-matched colonic epithelium by two independent scorers (+++ normal levels, ++ intermediate levels, + low levels, – absence of protein). For adenoma samples, patient-matched normal epithelium was not available; therefore, we compared the samples with at least five samples of normal epithelium from the adenocarcinoma cohort. All normal crypts on each tissue section were analyzed (mean: 243 per section; range: 43–769).

DNA isolation from tumor epithelium and normal tissue. Human colon tumor samples or murine small intestinal adenomas were mounted for sectioning and frozen in isopentane pre-cooled to −190 °C in liquid nitrogen. Cryostat sections (20 μm) were mounted on polyethylene naphthalate membrane slides (Leica Microsystems). Sections were subjected to SDH histochemistry followed by ethanol dehydration and were then air dried for 1 h. Areas of tumor epithelium were cut into sterile 0.5-ml PCR tubes using a Zeiss PALM microdissection system and lysed as previously described[13]. DNA was extracted from whole tissue from matched normal colon using an EZ1 DNA extraction system (Qiagen).

Human mtDNA sequencing. The entire mtDNA sequence was determined from the adenocarcinoma tissue and matched normal colon. mtDNA was PCR amplified and sequenced using the ABI 3130xl Genetic Analyzer system with ABI 3130 Data Collection Software version 4 and analyzed as previously described using SeqScape software version 2.6 (ref. [13]). Human adenoma tissue was sequenced as previously described[32].

Mouse mtDNA sequencing. mtDNA was PCR amplified in two overlapping 9-kilobase fragments using the primer sets 1628F (5′-AGAAAGCGTTCAAGCT CAAC-3′) and 10737R (5′-CCATGAAGCGTCTAAGGTGTG-3′) and 10059F (5′-ACCATCTTAGTTTTCGCAGC-3′ and 2315R (5′-CACTTTGACTTGTAAG TCTAGG-3′) (numbers correspond to NC_005089.1). The PCR parameters were: an initial denaturation at 94 °C for 10 min followed by 30 cycles of denaturation at 94 °C for 20 s, primer annealing at 68 °C for 20 s, extension for 9 min at 68 °C and a final extension at 72 °C for 5 min. PCR products were purified and sequenced on an MiSeq system (Illumina) using MiSeq control software, and bioinformatics analysis was performed as previously described[32], with the exception that the mouse mtDNA reference sequence was used (NC_005089.1 and MM10). The software used in the bioinformatics analysis was as follows: BWA version 0.7, SAMtools version 0.1.18, Picard version 1.85, VarScan version 2.3.8, LoFreq version 0.6.1, ANNOVAR version 529 and Haplogrep version 2.

Tamoxifen induction. *PolgA*$^{mut/mut}$;*Lgr5-creER*;*Apc*$^{fl/fl}$ and *Lgr5-creER*;*Apc*$^{fl/fl}$ mice aged 6 months were injected intraperitoneally with four doses of tamoxifen in sunflower oil at 10 mg ml^{-1} over four consecutive days (300, 200, 200 and 200 μl).

Scoring of macroscopic adenomas. Mice were culled 23 d post-tamoxifen administration. Their intestines were removed, flushed with 10% neutral-buffered formalin, opened up and pinned out as intestinal whole mounts. Using a dissecting microscope, intestinal adenomas (minimum: 1 mm × 1 mm) were counted and their areas were measured. For fused adenomas, the total area was measured. For comparative analysis between *PolgA*$^{mut/mut}$;*Apc*$^{fl/fl}$ ($n = 17$) and *Apc*$^{fl/fl}$ ($n = 12$) mice, the total sum of the adenomatous area was calculated. Adenomas were counted blind by two independent scorers.

IHC. Sections (4 μm) were de-paraffinized and rehydrated as standard. Antigen retrieval was performed by pressure cooking in either 1 mM EDTA pH 8.0 (β-catenin, CD3 and OXPHOS antibodies) or 10 mM sodium citrate pH 6.0 (PSAT1, PHGDH, MTHFD2, cleaved caspase-3, CD45R and neutrophil) for 20 min. Standard IHC was performed using the following antibodies: rabbit anti-β-catenin (1:1,000), anti-MTHFD2 (1:600), anti-PSAT1 (1:600), anti-PHGDH (1:4,000), anti-cleaved caspase-3 (1:35), rat anti-CD45R (1:200), anti-CD3 (1:100) and anti-neutrophil (1:100). Rabbit primary antibodies were visualized using the EnVision Anti-Rabbit HRP Polymer Kit (Dako), per the manufacturer's instructions. Rat primary antibodies were detected and visualized using goat

anti-IgG:Biotin and a HRP-conjugated ABC kit (Vector Laboratories). All IHC slides were imaged using the Aperio virtual pathology system (Leica Microsystems) and analyzed using Aperio ImageScope version 12.4.

Immunofluorescence. Sections were prepared and antigen retrieval performed as for IHC. Sections were incubated in primary antibodies at 4 °C overnight. The primary antibodies used were: anti-NDUFB8 (1:50), anti-UQCRFS1 (1:100), anti-MTCO1 (1:100), anti-ATPB (1:100), anti-TOMM20 (1:100), anti-IdU (1:100), anti-BrdU (1:100), anti-GFP biotin (1:100), anti-MTHFD2 (mouse: 1:300; human: 1:90), anti-PSAT1 (mouse: 1:300; human: 1:90) and anti-PHGDH (mouse: 1:2,000; human: 1:300). Sections were washed in 1× Tris-buffered saline with 0.1% Tween 20 and incubated in secondary antibodies for 2 h at room temperature. Secondary antibodies (all diluted 1:200 unless otherwise stated) were: goat anti-mouse IgG1 biotin, goat anti-mouse IgG2b-546, goat anti-rabbit IgG-488, goat anti-mouse IgG2a-546, goat anti-mouse IgG1-647, donkey anti-mouse IgG-488 (1:150), donkey anti-rat IgG-Cy5, streptavidin-546 and donkey anti-rabbit-750. Sections were then washed. For anti-NDUFB8, sections were also incubated in tertiary antibody: streptavidin-647 for 2 h at room temperature. All sections were stained with Hoechst 33342 (Invitrogen).

TUNEL labeling. TUNEL labeling was performed using an In Situ Cell Death Detection kit (Merck; 11684817910) per the manufacturer's standard protocol with the following exceptions: the enzyme solution was diluted 1:40 in TUNEL dilution buffer (Merck; 11966006001) and the convertor POD was diluted 1:2 in phosphate-buffered saline (PBS).

OXPHOS protein quantification, image analysis and *Z* score generation (mice). Sections were imaged using a Nikon A1R inverted confocal microscope and were analyzed using ImageJ software (NIH). Adenomas ($n=9$ *PolgA*$^{mut/mut}$;*Lgr5-creER*;*Apc*$^{fl/fl}$ mice per group; $n=10$ *Lgr5-creER*;*Apc*$^{fl/fl}$ mice per group; minimum of 20 crypts per mouse), normal crypts ($n=5$ mice per group; minimum of ten crypts per mouse) or small areas of lamina propria containing approximately 5–10 stromal cells ($n=5$ mice per group; minimum of 50 areas per mouse) were selected as regions of interest and fluorophore mean intensity values were recorded for each channel. Values were background corrected by subtracting the mean intensity of a no primary control from the regions of interest mean. *Z* scores were generated using in-house software (available at http://mito.ncl.ac.uk/immuno/), as previously described[29].

OXPHOS/SSP protein quantification, image analysis and *Z* score generation (humans). OXPHOS and OXPHOS/SSP immunofluorescence was performed as above on four serial sections per subject ($n=12$). The first section was labeled with antibodies against NDUFB8, MTCO1 and TOMM20. OXPHOS proteins were quantified and crypts were categorized as OXPHOS positive or deficient based on their *Z* scores. The second to fourth sections were labeled with antibodies against NDUFB8, MTCO1 and one of either PHGDH, PSAT1 or MTHFD2. The same crypts were identified in all serial sections and levels of SSP enzymes were quantified. Data were binned into OXPHOS normal or OXPHOS deficient and SSP enzyme protein levels were compared. Every OXPHOS-deficient crypt on the section was quantified (range: $n=8$–108) and OXPHOS-normal crypts on the same section were randomly selected based on the 4′,6-diamidino-2-phenylindole (DAPI) channel and quantified.

Thymidine analog labeling, immunofluorescence and analysis. At 16 d post-*Apc* deletion, mice ($n=5$ per group) were injected with 300 µl CldU (C6891; Sigma–Aldrich) 28 and 20 h before death. At 4 h before death, mice were injected with 300 µl IdU (I7125; Sigma–Aldrich). Immunofluorescence was performed as above. Twenty adenomas per mouse were manually identified and imaged using a Zeiss Axio Imager M1 fluorescence microscope. Zeiss ZEN Lite (Blue Edition) was used to quantify cells labeled with a single antibody and cells in which co-localization of >1 antibody was observed.

Scoring of β-catenin^{high} foci. Two serial sections were taken for scoring β-catenin^{high} foci; the first was subjected to β-catenin IHC and the adjacent section was subjected to standard hematoxylin and eosin staining, as previously described[13]. β-catenin^{high} foci were scored as clusters of cells that showed increases in both nuclear and cytoplasmic β-catenin compared with surrounding cells. Hematoxylin and eosin sections were used to confirm the dysplastic nature of the cells. Areas of β-catenin^{high} cell clusters were measured, with cells being classed as belonging to the same cluster or foci if there were no normal crypts separating them. Sections were scored blind by two people independently.

Scoring of apoptotic cells. Apoptotic cells were labeled in colon and small intestine tissue sections from $n=9$ mice per group using two methods: cleaved caspase-3 IHC and TUNEL assay. For the small intestine, $n=9$ mice were analyzed per assay per group. For the colon, $n=7$ *PolgA*$^{mut/mut}$;*Lgr5-creER*;*Apc*$^{fl/fl}$ mice and $n=9$ *Lgr5-creER*;*Apc*$^{fl/fl}$ mice were analyzed per group using cleaved caspase-3 IHC and $n=9$ mice per group were analyzed for the TUNEL assay. A minimum of ten adenomas were analyzed per mouse. Apoptotic cells were counted and presented as the percentage of total nuclei in the adenoma.

Quantification of CD3$^+$, CD45R$^+$ and NIMP1$^+$ cells. Small intestine sections from $n=5$ *PolgA*$^{mut/mut}$ and *PolgA*$^{+/+}$ mice underwent IHC as above to identify CD3$^+$, CD45R$^+$ and NIMP1$^+$ cells. Ten random ×20 magnification images were taken per section and the number of positive cells per field of view were counted. The total area of epithelium was measured and the frequency of positive cells per mm^2 was calculated. Areas containing Peyer's patches were excluded.

Small intestinal crypt and stromal RNA extraction. Small intestine crypts were isolated from the stroma from the distal small intestine as previously described[53]. Crypt pellets and stromal pellets were flash frozen in liquid nitrogen and stored at −80 °C. RNA was extracted using the RNeasy Mini Kit with DNase (Qiagen) using the manufacturer's protocol. Sample RNA integrity scores were analyzed on a 2100 Bioanlyzer (Agilent) using the RNA 600 Nanokit and 2100 Expert software version B02.9.

RNA-Seq. Crypt RNA from *Polg*$^{mut/mut}$ ($n=4$) and *PolgA*$^{+/+}$ ($n=4$) mice with an RNA integrity score of >7.0 (range: 7.5–9.2) were used in differential gene expression analysis. Crypt messenger RNA (mRNA) libraries were prepared using the TruSeq Stranded mRNA library kit (Illumina). Samples were analyzed using the NextSeq 500 system (Illumina) with 16 million 75-base pair single reads per sample. All samples were quality assessed using FASTQC version 0.11.7, before processing in accordance with the protocol in refs. [54–57] using StringTie version 1.3.4 and Ballgown version 3.8. Alignment and annotation used the Hisat2 mm10 genome build (Hisat2 version 2.1.0) and the Ensembl GTF version GRCm38.92, respectively. The resultant gene lists were then submitted to Enrichr webserver[58,59] to obtain ontology information.

Small intestine adenoma RNA extraction. The distal small intestine was extracted from 6-month-old *PolgA*$^{mut/mut}$;*Lgr5-creER*;*Apc*$^{fl/fl}$ and *Lgr5-creER*;*Apc*$^{fl/fl}$ mice at 23 d post-tamoxifen induction. Tissue was flushed with PBS, opened longitudinally and rolled up, followed by freezing in isopentane cooled to −190 °C in liquid nitrogen. Small intestine tissue sections (15 µM) were cut on polyethylene naphthalate membrane slides. Sections were fixed in 75% ethanol and stained in 1% cresyl violet acetate (in 50% ethanol). Sections were dehydrated in a graded ethanol series and air dried for 5 min. Laser microdissection of adenomas was performed using the Zeiss PALM microdissection system. Adenoma RNA was isolated using the RNeasy Micro kit with DNase (Qiagen).

qRT-PCR. A High-Capacity cDNA Reverse Transcription Kit (Applied Biosystems) was used to reverse transcribe RNA from crypt, stromal and adenoma samples. qRT-PCR was performed in triplicate using validated TaqMan assays for *Phgdh*, *Psat1*, *Psph*, *Mthfd2*, *Aldh1l2* and *Slc1a4* with TaqMan Universal PCR Master Mix (Applied Biosystems) on the Applied Biosystems StepOnePlus Real-Time PCR system. In total, 14 crypt samples ($n=7$ per group), 12 stromal samples ($n=6$ per group) and 12 adenoma samples ($n=6$ per group) were analyzed by StepOne Software version 2.1. The comparative C_t method was used with *Actb* mRNA as a reference to generate ΔC_t values in Microsoft Excel 2016.

Adenoma organoid generation. *Lgr5-creER*;*Apc*$^{fl/fl}$ and *PolgA*$^{mut/mut}$;*Lgr5-creER*;*Apc*$^{fl/fl}$ mice were induced with tamoxifen across 4 d (3, 2, 2 and 2 mg) at 6 months and small intestine adenomas were isolated ~3 weeks after induction. Organoids were generated and maintained as previously described[34].

Growth analysis in SG medium. Adenoma cultures from *Apc*$^{fl/fl}$ ($n=3$) and *PolgA*$^{mut/mut}$;*Apc*$^{fl/fl}$ ($n=3$) mice were collected in PBS, pelleted and resuspended in 50% Matrigel (vol/vol) in PBS in a 96-well plate. Amino acid-free Advanced DMEM/F-12 (Life Technologies) was reconstituted with the appropriate concentrations of amino acids. Cultures were grown in complete (+SG) or serine and glycine free (−SG) medium for 5 d at 37 °C and 5% CO_2, with the media refreshed after 3 d. Images of four points per well were taken every 2 h using Incucyte ZOOM (Essen BioScience) equipped with their Dual Color Filter Cube (4459) and a Nikon 10× objective, using Incucyte ZOOM 2018A (version 20181.1.6628.28170) software. Organoid two-dimensional areas on day 0 and day 5 were measured using ImageJ version 1.51.

Mitochondrial functional assay. The XF Cell Mito Stress Test Kit (Seahorse Bioscience) was performed using the adenoma organoids. One day before the assay, 96-well plates were prepared with Matrigel as previously described[60]. Intestinal adenoma cultures from *Apc*$^{fl/fl}$ ($n=3$) and *PolgA*$^{mut/mut}$;*Apc*$^{fl/fl}$ mice ($n=3$) were collected 3 d post-seeding, pooled, washed and pelleted. Pellets were resuspended in Mito XF medium. The Mito Stress Test was performed per the manufacturer's standard protocol on a Seahorse XF96 Extracellular Flux analyzer. Data were collected using Agilent Seahorse Wave software version 2.4. Following analysis, organoids were fixed in 10% neutral-buffered formalin for 30 min at room temperature. Formalin was then removed and the plates were left to air dry overnight. Organoids were incubated in cresyl violet at room temperature for 30 min, then washed in dH_2O overnight followed by incubation in 10 mM acetic acid on a shaker at room temperature for 30 min. The optical intensity was measured at 562 nm and read-outs were used to normalize OCR measurements.

Metabolomics analysis. Organoid cultures were plated in technical triplicates in 24-well plates and 3 d post-seeding the medium was changed to include $^{13}C_6$-labeled glucose (Cambridge Isotope Laboratories) minus HEPES and nystatin. Samples were prepared and underwent liquid chromatography–mass spectrometry (LC-MS) as previously described[34]. Metabolite peak areas were determined using Thermo TraceFinder (version 3.2). Commercial standards of all metabolites detected had been previously analyzed on this LC-MS system with the pHLIC column. ^{13}C labeling patterns were determined by measuring peak areas for the accurate mass of each isotopolog of many metabolites. Metabolite levels were normalized to total cell protein. The LC-MS protocol was adapted from ref. [61].

Complex I inhibition of adenoma organoids with metformin. Adenoma organoids from *Apc*$^{fl/fl}$ mice ($n=3$) were washed in PBS, resuspended in 100 µl CellTracker Green CMFDA (1:200 in media) and incubated at 37 °C for 10 min. Afterwards, the cells were pelleted, washed and resuspended in Matrigel, then seeded in 96-well plates, and complete media was added. Cells were imaged on a Zeiss LSM 800 confocal microscope at 2.5× magnification to generate 1-mm-thick Z-stacks of 25 slices. Organoids were then dosed with 0–500 µM metformin in dimethyl sulfoxide (three technical replicates per dose per mouse). On the fifth day, organoids were stained with DAPI (1:200), washed and imaged as above. Images were stitched using ZEN version 2.6 and channels were deconvolved using Huygens Software version 18.04. Surfaces were created in Imaris version 9.0 using the CellTracker or DAPI labeling. A threshold of >200,000 µm^2 was applied and the volumetric size of organoids on day 5 was normalized to day 1.

FACS analysis of small intestinal lymphocytes. Lamina propria lymphocytes were extracted from 6-month-old *PolgA*$^{+/+}$ and *PolgA*$^{mut/mut}$ mice ($n=3$ per genotype) as follows: small intestines were extracted, cleared of mesentery, fat and Peyer's patches, cut into pieces and washed in Hank's balanced salt solution without calcium and magnesium. Intraepithelial lymphocytes were removed by agitation for 15 min in Hank's balanced salt solution with 20 mM HEPES and 2% fetal calf serum. The remaining tissue was digested in serum-free medium containing Liberase TL (250 µg ml^{-1}; Roche) and 0.05% DNase I (Roche) for 15 min. Lamina propria lymphocytes were separated from epithelial cells by centrifugation in 40% Percoll and cell pellets were collected.

Lymphocytes were washed once with PBS and then stained with LIVE/DEAD stain (Invitrogen; 34961) for 30 min at 40 °C. Cells were then washed once with PBS and labeled with the following cell-surface antibodies: CD4, CD8, CD45R/B220, NK1.1, CD11b, CD11c, F4/80 and Class II (anti-mouse I-A/I-E). Cells were analyzed using LSR II (FACSDiva version 8 software) and FlowJo version 10 software.

Statistics and reproducibility. Statistical comparisons for survival data were performed using GraphPad Prism (version 8.3.1) software using a Mantel–Cox (log-rank) test. Unpaired *t*-tests and Mann–Whitney *U*-tests were performed using GraphPad Prism (version 8.3.1). Where no predication was made about the direction of a potential difference, two-tailed tests were used (for example, Fig. 3c). Where pre-existing data supported a prediction in the direction of a difference between samples, a one-tailed *t*-test was used (for example, Fig. 5b,c). Where multiple comparisons were made, one-way analysis of variance (ANOVA) was calculated using GraphPad Prism (version 8.3.1), followed by Tukey's post-hoc test (for example, Fig. 4f). Linear mixed-effects models were employed to compare the tumor sizes, cell proliferation apoptotic and immune cell (IHC) frequencies for each group (for example, Fig. 3e–h). This allowed variation between individual mice and sample location to be accounted for as random effects within the model structure. Tumor data were logged to approximate a normal distribution. For analysis of organoids following metformin dosing, estimation graphics for observed organoid sizes were displayed on Gardner–Altman plots[62]. This allows the distribution of the mean difference to be observed though bootstrapping[63], generating a robust sampling-error curve with a 95% confidence interval. Analysis was conducted using the R programming language (code available on request)[64] (R Studio version 3.4.0). In all figures where the data shown are the means per mouse or human of multiple measurements, error bars represent s.e.m. Where they are a single data point per mouse or human, error bars represent s.d. All *P* values are: $^*P<0.05$; $^{**}P<0.01$; $^{***}P<0.001$.

Sample sizes were chosen based on previous studies and our experience using these models, which had shown robust statistical power. No statistical methods were used to predetermine sample size. All experiments were successfully replicated. For the mouse studies, a minimum of four mice were used; organoid cultures were generated from three different animals; and a minimum of three independent cultures per mouse were used in each experiment. All mouse and organoid work was replicated in at least two independent experiments. For the IHC or immunofluorescence experiments, preliminary staining was performed on $n=3$–5 samples, then optimized staining was performed on the entire cohort (minimum $n=3$ biological replicates (for example, three murine or human samples) per experiment) at the same time. Image analysis was performed at the same time for each experiment. Mouse experiments were not randomized; animals were allocated to experimental groups based on their genotype. Investigators were blinded to the genotypes of the animals during the experiments and data analysis.

Reporting Summary. Further information on research design is available in the Nature Research Reporting Summary linked to this article.

Data availability

RNA-Seq and DNA next-generation sequencing data have been deposited in the Sequence Read Archive under BioProject accession code PRJNA645504. All other data supporting the findings of this study are available from the corresponding author upon reasonable request. Source data are provided with this paper.

Code availability

Code used to generate the mitochondrial OXPHOS *Z* scores and dot pots is freely available at http://mito.ncl.ac.uk/immuno/. The R programming code used in the linear regression mixed-effects modeling is available upon request.

Received: 5 June 2020; Accepted: 5 August 2020;
Published online: 21 September 2020

References

1. Warburg, O. On the origin of cancer cells. *Science* **123**, 309–314 (1956).
2. Warburg, O. On respiratory impairment in cancer cells. *Science* **124**, 269–270 (1956).
3. Pedersen, P. L. Tumor mitochondria and the bioenergetics of cancer cells. *Prog. Exp. Tumor Res.* **22**, 190–274 (1978).
4. Marchetti, P. et al. Mitochondrial permeability transition is a central coordinating event of apoptosis. *J. Exp. Med.* **184**, 1155–1160 (1996).
5. Rosenzweig, A., Blenis, J. & Gomes, A. P. Beyond the Warburg effect: how do cancer cells regulate one-carbon metabolism? *Front. Cell Dev. Biol.* https://doi.org/10.3389/fcell.2018.00090 (2018).
6. Diebold, L. & Chandel, N. S. Mitochondrial ROS regulation of proliferating cells. *Free Radic. Biol. Med.* **100**, 86–93 (2016).
7. Bender, A. et al. High levels of mitochondrial DNA deletions in substantia nigra neurons in aging and Parkinson disease. *Nat. Genet.* **38**, 515–517 (2006).
8. Fellous, T. G. et al. Locating the stem cell niche and tracing hepatocyte lineages in human liver. *Hepatology* **49**, 1655–1663 (2009).
9. Muller-Hocker, J. Cytochrome-*c*-oxidase deficient cardiomyocytes in the human heart—an age-related phenomenon. A histochemical ultracytochemical study. *Am. J. Pathol.* **134**, 1167–1173 (1989).
10. Muller-Hocker, J. Cytochrome *c* oxidase deficient fibres in the limb muscle and diaphragm of man without muscular disease: an age-related alteration. *J. Neurol. Sci.* **100**, 14–21 (1990).
11. Greaves, L. C. et al. Defects in multiple complexes of the respiratory chain are present in ageing human colonic crypts. *Exp. Gerontol.* **45**, 573–579 (2010).
12. Greaves, L. C. et al. Clonal expansion of early to mid-life mitochondrial DNA point mutations drives mitochondrial dysfunction during human ageing. *PLoS Genet.* **10**, e1004620 (2014).
13. Taylor, R. W. et al. Mitochondrial DNA mutations in human colonic crypt stem cells. *J. Clin. Invest.* **112**, 1351–1360 (2003).
14. Lightowlers, R. N., Chinnery, P. F., Turnbull, D. M. & Howell, N. Mammalian mitochondrial genetics: heredity, heteroplasmy and disease. *Trends Genet.* **13**, 450–455 (1997).
15. Bao, X. R. et al. Mitochondrial dysfunction remodels one-carbon metabolism in human cells. *eLife* **5**, e10575 (2016).
16. Yuan, Y. et al. Comprehensive molecular characterization of mitochondrial genomes in human cancers. *Nat. Genet.* **52**, 342–352 (2020).
17. He, Y. et al. Heteroplasmic mitochondrial DNA mutations in normal and tumour cells. *Nature* **464**, 610–614 (2010).
18. Larman, T. C. et al. Spectrum of somatic mitochondrial mutations in five cancers. *Proc. Natl Acad. Sci. USA* **109**, 14087–14091 (2012).
19. Polyak, K. et al. Somatic mutations of the mitochondrial genome in human colorectal tumours. *Nat. Genet.* **20**, 291–293 (1998).
20. *Bowel Cancer Statistics* (CRUK); http://www.cancerresearchuk.org/health-professional/cancer-statistics/statistics-by-cancer-type/bowel-cancer (accessed March 2020).
21. Greaves, L. C. et al. Comparison of mitochondrial mutation spectra in ageing human colonic epithelium and disease: absence of evidence for purifying selection in somatic mitochondrial DNA point mutations. *PLoS Genet.* **8**, e1003082 (2012).
22. Ericson, N. G. et al. Decreased mitochondrial DNA mutagenesis in human colorectal cancer. *PLoS Genet.* **8**, e1002689 (2012).
23. Greaves, L. C. et al. Mitochondrial DNA mutations are established in human colonic stem cells, and mutated clones expand by crypt fission. *Proc. Natl Acad. Sci. USA* **103**, 714–719 (2006).
24. Barker, N. et al. Crypt stem cells as the cells-of-origin of intestinal cancer. *Nature* **457**, 608–611 (2009).
25. Kujoth, G. C. et al. Mitochondrial DNA mutations, oxidative stress, and apoptosis in mammalian aging. *Science* **309**, 481–484 (2005).
26. Trifunovic, A. et al. Premature ageing in mice expressing defective mitochondrial DNA polymerase. *Nature* **429**, 417–423 (2004).

27. Baines, H. L. et al. Similar patterns of clonally expanded somatic mtDNA mutations in the colon of heterozygous mtDNA mutator mice and ageing humans. *Mech. Ageing Dev.* **139**, 22–30 (2014).
28. Stamp, C. et al. Predominant asymmetrical stem cell fate outcome limits the rate of niche succession in human colonic crypts. *EBioMedicine* **31**, 166–173 (2018).
29. Rocha, M. C. et al. A novel immunofluorescent assay to investigate oxidative phosphorylation deficiency in mitochondrial myopathy: understanding mechanisms and improving diagnosis. *Sci. Rep.* **5**, 15037 (2015).
30. Pate, K. T. et al. Wnt signaling directs a metabolic program of glycolysis and angiogenesis in colon cancer. *EMBO J.* **33**, 1454–1473 (2014).
31. Fox, R. G., Magness, S., Jujoth, G. C., Prolla, T. A. & Maeda, N. Mitochondrial DNA polymerase editing mutation, *Polg*^{D257A}, disturbs stem-progenitor cell cycling in the small intestine and restricts excess fat absorption. *Am. J. Physiol. Gastrointest. Liver Physiol.* **302**, G914–G924 (2012).
32. El-Mir, M. Y. et al. Dimethylbiguanide inhibits cell respiration via an indirect effect targeted on the respiratory chain complex I. *J. Biol. Chem.* **275**, 223–228 (2000).
33. Owen, M. R., Doran, E. & Halestrap, A. P. Evidence that metformin exerts its anti-diabetic effects through inhibition of complex 1 of the mitochondrial respiratory chain. *Biochem. J.* **348**, 607–614 (2000).
34. Maddocks, O. D. K. et al. Modulating the therapeutic response of tumours to dietary serine and glycine starvation. *Nature* **544**, 372–376 (2017).
35. Fearon, E. R. & Vogelstein, B. A genetic model for colorectal tumorigenesis. *Cell* **61**, 759–767 (1990).
36. Winawer, S. J. et al. Colorectal cancer screening: clinical guidelines and rationale. *Gastroenterology* **112**, 594–642 (1997).
37. Nikkanen, J. et al. Mitochondrial DNA replication defects disturb cellular dNTP pools and remodel one-carbon metabolism. *Cell Metab.* **23**, 635–648 (2016).
38. Rodriguez-Colman, M. J. et al. Interplay between metabolic identities in the intestinal crypt supports stem cell function. *Nature* **543**, 424–427 (2017).
39. Stringari, C. et al. Metabolic trajectory of cellular differentiation in small intestine by Phasor Fluorescence Lifetime Microscopy of NADH. *Sci. Rep.* **2**, 568 (2012).
40. Yang, M. & Vousden, K. H. Serine and one-carbon metabolism in cancer. *Nat. Rev. Cancer* **16**, 650–662 (2016).
41. Hollinshead, K. E. R. et al. Oncogenic *IDH1* mutations promote enhanced proline synthesis through PYCR1 to support the maintenance of mitochondrial redox homeostasis. *Cell Rep.* **22**, 3107–3114 (2018).
42. Lee-Six, H. et al. The landscape of somatic mutation in normal colorectal epithelial cells. *Nature* **574**, 532–537 (2019).
43. De Laat, P. et al. Clinical features and heteroplasmy in blood, urine and saliva in 34 Dutch families carrying the m.3243A > G mutation. *J. Inherit. Metab. Dis.* **35**, 1059–1069 (2012).
44. Frederiksen, A. L. et al. Tissue specific distribution of the 3243A→G mtDNA mutation. *J. Med. Genet.* **43**, 671–677 (2006).
45. Grady, J. P. et al. mtDNA heteroplasmy level and copy number indicate disease burden in m.3243A>G mitochondrial disease. *EMBO Mol. Med.* https://doi.org/10.15252/emmm.201708262 (2018).
46. Olsson, C. et al. The level of the mitochondrial mutation A3243G decreases upon ageing in epithelial cells from individuals with diabetes and deafness. *Eur. J. Hum. Genet.* **9**, 917–921 (2001).
47. Rahman, S., Poulton, J., Marchington, D. & Suomalainen, A. Decrease of 3243 A>G mtDNA mutation from blood in MELAS syndrome: a longitudinal study. *Am. J. Hum. Genet.* **68**, 238–240 (2001).
48. Su, T. et al. Inherited pathogenic mitochondrial DNA mutations and gastrointestinal stem cell populations. *J. Pathol.* **246**, 427–432 (2018).
49. Filograna, R. et al. Modulation of mtDNA copy number ameliorates the pathological consequences of a heteroplasmic mtDNA mutation in the mouse. *Sci. Adv.* **5**, eaav9824 (2019).
50. Kauppila, J. H. K. et al. A phenotype-driven approach to generate mouse models with pathogenic mtDNA mutations causing mitochondrial disease. *Cell Rep.* **16**, 2980–2990 (2016).
51. Betts, J. et al. Gastrointestinal tract involvement associated with the 3243A>G mitochondrial DNA mutation. *Neurology* **70**, 1290–1292 (2008).
52. Coxhead, J. et al. Somatic mtDNA variation is an important component of Parkinson's disease. *Neurobiol. Aging* **38**, 217.e1–217.e6 (2016).
53. Sato, T. et al. Single Lgr5 stem cells build crypt–villus structures in vitro without a mesenchymal niche. *Nature* **459**, 262–265 (2009).
54. Pertea, M., Kim, D., Pertea, G. M., Leek, J. T. & Salzberg, S. L. Transcript-level expression analysis of RNA-seq experiments with HISAT, StringTie and Ballgown. *Nat. Protocols* **11**, 1650–1667 (2016).
55. Pertea, M. et al. StringTie enables improved reconstruction of a transcriptome from RNA-seq reads. *Nat. Biotechnol.* **33**, 290–295 (2015).
56. Frazee, A. C. et al. Ballgown bridges the gap between transcriptome assembly and expression analysis. *Nat. Biotechnol.* **33**, 243–246 (2015).
57. Kim, D., Langmead, B. & Salzberg, S. L. HISAT: a fast spliced aligner with low memory requirements. *Nat. Methods* **12**, 357–360 (2015).
58. Chen, E. Y. et al. Enrichr: interactive and collaborative HTML5 gene list enrichment analysis tool. *BMC Bioinformatics* **14**, 128 (2013).
59. Kuleshov, M. V. et al. Enrichr: a comprehensive gene set enrichment analysis web server 2016 update. *Nucleic Acids Res.* **44**, W90–W97 (2016).
60. Fan, Y. Y. et al. A bioassay to measure energy metabolism in mouse colonic crypts, organoids, and sorted stem cells. *Am. J. Physiol. Gastrointest. Liver Physiol.* **309**, G1–G9 (2015).
61. Gonzalez, P. S. et al. Mannose impairs tumour growth and enhances chemotherapy. *Nature* **563**, 719–723 (2018).
62. Ho, J., Tumkaya, T., Aryal, S., Choi, H. & Claridge-Chang, A. Moving beyond *P* values: data analysis with estimation graphics. *Nat. Methods* **16**, 565–566 (2019).
63. Efron, B. & Tibshirani, R. J. *An Introduction to the Bootstrap* (CRC Press, 1994).
64. R Development Core Team *R: A Language and Environment for Statistical Computing* (R Foundation for Statistical Computing, 2018).
65. Ross, J. M. et al. Germline mitochondrial DNA mutations aggravate ageing and can impair brain development. *Nature* **501**, 412–415 (2013).

Acknowledgements

We thank T. Prolla (University of Wisconsin, Washington, United States) for donating the *PolgA*$^{+/mut}$ mice. We thank C. Alston for assistance with the analysis of mtDNA mutations and staff at the Newcastle University Comparative Biology Centre for animal husbandry. This work was supported by the Wellcome Centre for Mitochondrial Research (203105/Z/16/Z), Newcastle University Centre for Ageing and Vitality (supported by the Biotechnology and Biological Sciences Research Council, Engineering and Physical Sciences Research Council, Economic and Social Research Council and Medical Research Council (MR/L016354/1)), UK NIHR Biomedical Research Centre Age and Age Related Diseases award (to the Newcastle upon Tyne Hospitals NHS Foundation Trust) and NC3Rs (to C.A.R.; NC/K500513/1). O.J.S. is supported by Cancer Research UK grants (A25045, A17196, A12481 and A21139). O.J.S. and D.G. were supported by ERC starting grant 311301 awarded to O.J.S. F.O. is supported by the Medical Research Council (MR/R023026/1). J.L. is supported by Cancer Research UK (C18342/A23390).

Author contributions

L.C.G., C.B., C.S. and C.A.R. performed the breeding and phenotypic analyses of mice. A.L.M.S., D.H., M.H., J.N.S. and A.B. performed the histology, IHC, immunofluorescence and analysis of mouse and human samples. L.C.G., O.M.R., R.J. and B.G. performed the sequencing and histological analysis of human samples. S.A.C.M., I.M., S.K. and J.C.M. collected and processed the human samples. J.C.W. performed the molecular biology and cell culture experiments. G.H. and A.P. performed the sequencing and bioinformatics analyses of the mouse and human adenomas. Flow cytometric immunophenotyping of the small intestine was carried out by S.A. and G.M. J.L. and F.O. performed the immune cell IHC. L.W. carried out the imaging and analysis of the immune cell IHC. F.R. performed the statistical analysis of the RNA-Seq data. A.P.B. performed the statistical analysis of the experimental data. D.G., J.C.W. and O.J.S. performed the metabolomics analyses and analyzed the data. L.C.G., R.W.T., R.H., D.M.T., N.D.P. and O.J.S. conceived of the ideas, designed the experiments and interpreted the data. All authors contributed to writing and revising the paper.

Competing interests

F.O. is a director of Fibrofind. J.L. and F.O. are shareholders in Fibrofind. The other authors declare no competing interests.

Additional information

Extended data is available for this paper at https://doi.org/10.1038/s43018-020-00112-5.

Supplementary information is available for this paper at https://doi.org/10.1038/s43018-020-00112-5.

Correspondence and requests for materials should be addressed to L.C.G.

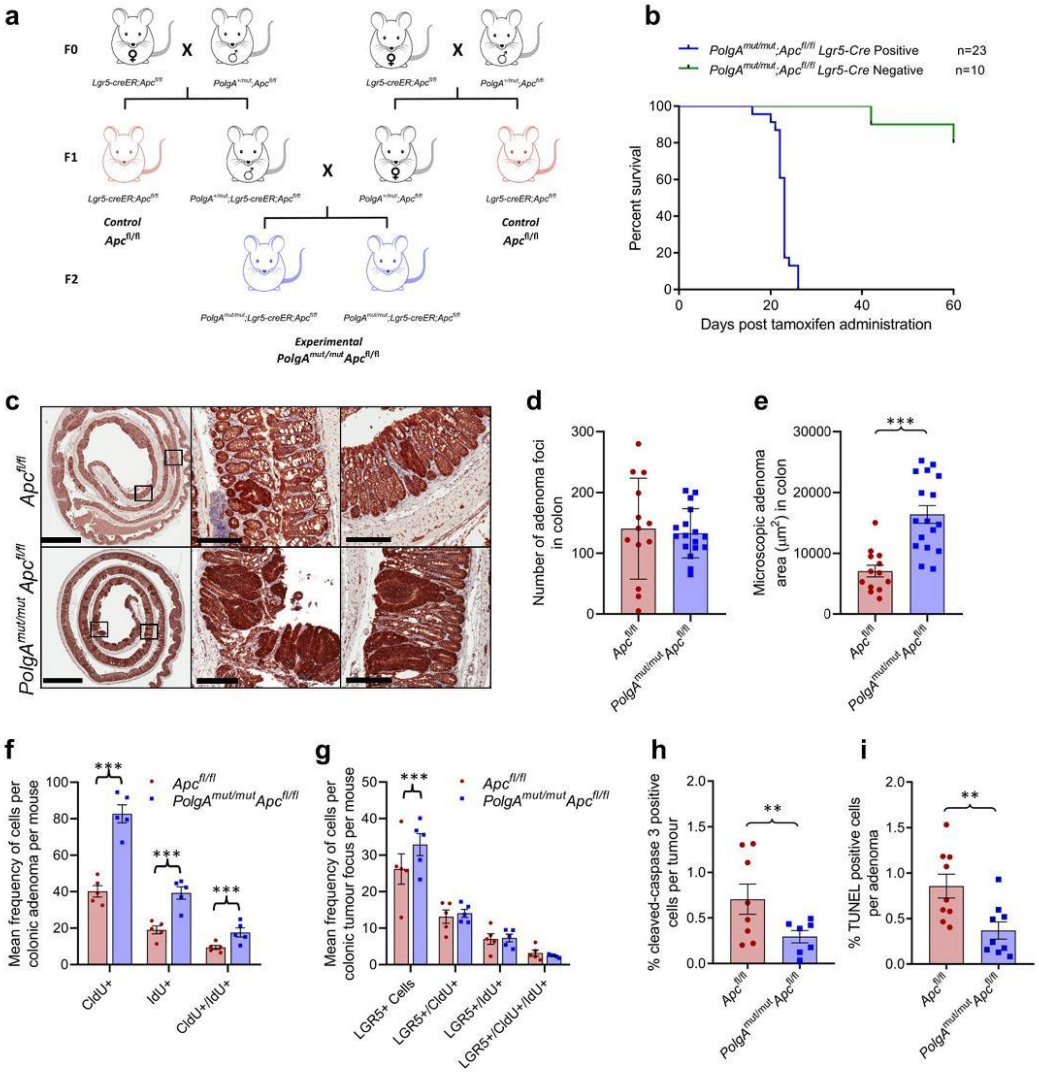

Extended Data Fig. 1 | Generation of *PolgA*$^{mut/mut}$;*Lgr5-creER;Apc*$^{fl/fl}$ and *Lgr5-creER;Apc*$^{fl/fl}$ mice and analysis of colonic adenomas. a: Breeding scheme. MtDNA mutations can be transmitted down the maternal germline[10] therefore it was essential that only *Lgr5-creER;Apc*$^{fl/fl}$ (red) mice from a wild-type *PolgA* mother used as controls. **b**: Kaplan-Meier survival curve showing survival time following tamoxifen administration in *PolgA*$^{mut/mut}$ mice. Survival to clinical endpoint or experimental endpoint of 60 days is shown, 'n' = number of mice. **c**: β-Catenin immunohistochemistry was performed on colon sections from n = 17 *PolgA*$^{mut/mut}$;*Apc*$^{fl/fl}$ mice and n = 13 *Apc*$^{fl/fl}$ mice. Representative images are shown (scale bars 3 mm (first column) and 200 μm). **d**: Frequency of adenomas in the colon 23 days post-*Apc* deletion (unpaired, two tailed, t-test, p = 0.7444), n = 17 *PolgA*$^{mut/mut}$;*Apc*$^{fl/fl}$ mice and n = 13 *Apc*$^{fl/fl}$ mice, data are mean ±s.d. **e**: Mean adenoma size in the colon in n = 17 *PolgA*$^{mut/mut}$;*Apc*$^{fl/fl}$ mice and n = 13 *Apc*$^{fl/fl}$ mice 23 days post-*Apc* deletion. All adenomas on a section were quantified ranging from 5 to 280, mean per mouse ± s.e.m are shown. Two-sided linear mixed effect regression model with mouse ID as a random effect, $P < 0.0001$. **f-g**: Quantification of the frequency of thymidine analogue incorporation in all cells per colonic adenoma (**f**) and LGR5 + cells per colon adenoma per mouse (**g**). n = 5 mice per group with 18 adenomas analysed per mouse. Mean frequency per adenoma per mouse ± s.e.m is shown. Two-sided linear mixed effect regression model with mouse ID as a random effect, $P < 0.001$. **h**, **i**: Apoptotic cells were quantified using (**h**) cleaved caspase 3 (CC3) immunohistochemistry n = 7 *PolgA*$^{mut/mut}$;*Apc*$^{fl/fl}$ mice and n = 9 *Apc*$^{fl/fl}$ mice and (**i**) TUNEL labelling (n = 9 mice per group) in mice 23 days post-*Apc* deletion. A minimum of 10 adenomas were analysed per mouse, mean percentage of apoptotic cells per adenoma per mouse ±s.e.m is shown. Two-sided linear mixed effect regression model with mouse ID as a random effect, CC3 $P = 0.0092$, TUNEL $P = 0.002$. * $P < 0.05$, ** $P < 0.01$, *** $P < 0.001$.

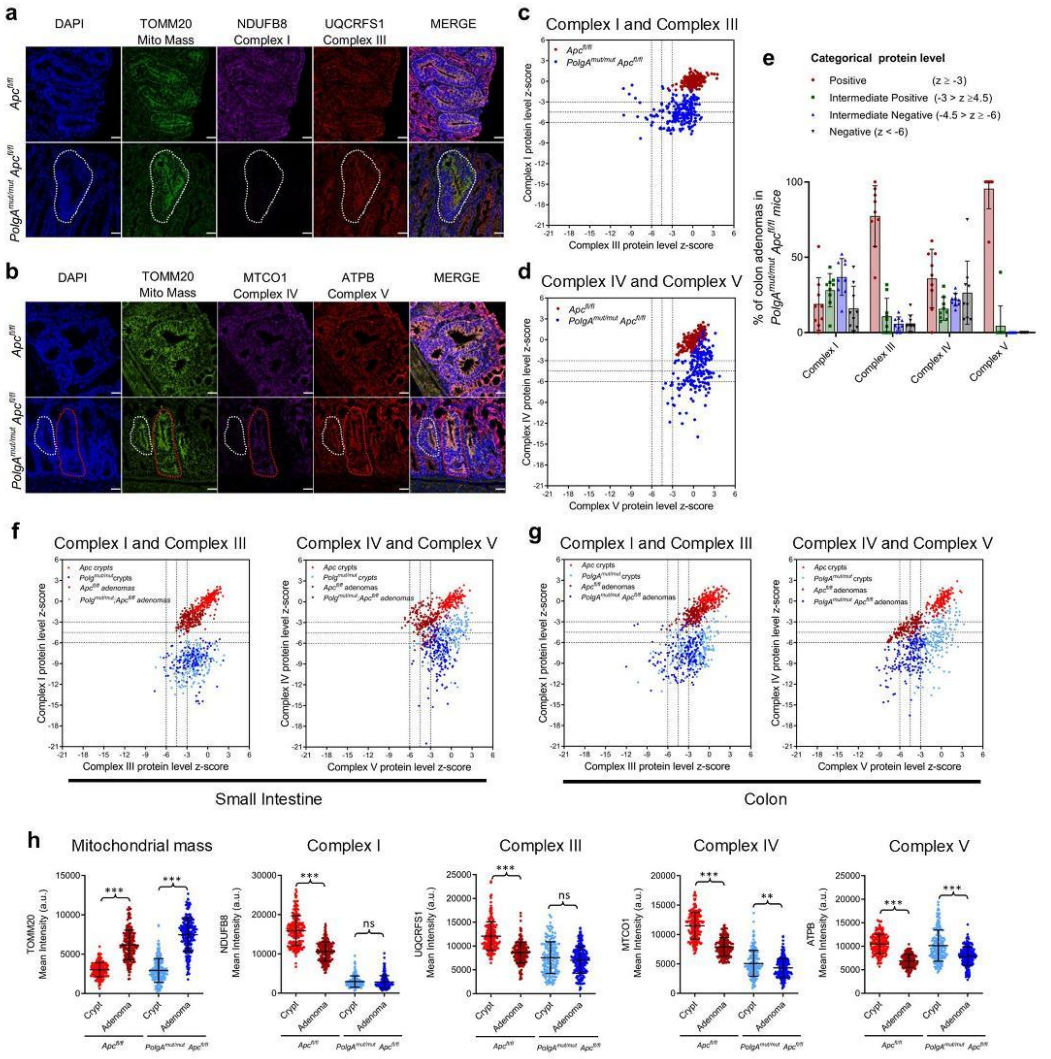

Extended Data Fig. 2 | Colonic adenomas from *PolgA*$^{mut/mut}$;*Apc*$^{fl/fl}$ mice are deficient in mitochondrial complex I, but the majority retain expression of subunits of complexes III, IV and V. a, **b**: Immunofluorescence was performed to quantify levels of OXPHOS proteins in n = 9 *PolgA*$^{mut/mut}$;*Apc*$^{fl/fl}$ mice and n = 9 *Apc*$^{fl/fl}$ mice. Representative images are shown. Scale bars 50 µm. An adenoma deficient in complex I is highlighted by the white dashed line in **a**. The white dashed line highlights an adenoma deficient in complex IV, and red dashed line shows one with normal complex IV in **b**–**d**: dot plots showing Z-scores calculated following quantification of mitochondrial OXPHOS protein levels in adenomas from n = 9 *PolgA*$^{mut/mut}$;*Apc*$^{fl/fl}$ and n = 9 *Apc*$^{fl/fl}$ mice with 20 adenomas quantified per mouse. **e**: Categorical analysis of OXPHOS protein levels in *PolgA*$^{mut/mut}$;*Apc*$^{fl/fl}$ (n = 9) and *Apc*$^{fl/fl}$ (n = 9) mice, error bars show mean ±s.d. **f**, **g**: dot plots showing Z-scores calculated following quantification of mitochondrial OXPHOS protein levels in normal crypts and adenomas in the small intestine (**f**) and the colon (**g**). **f**: For the adenomas: n = 9 *PolgA*$^{mut/mut}$;*Apc*$^{fl/fl}$ and n = 10 *Apc*$^{fl/fl}$ mice were analysed with 20 adenomas quantified per mouse. For the normal crypts, n = 5 mice were analysed with a minimum of 13 crypts quantified per mouse. **g**: For the colonic adenomas: n = 9 mice per group were analysed with a minimum of 20 adenomas quantified per mouse. For the normal crypts, n = 6 *Apc*$^{fl/fl}$ mice and n = 7 *PolgA*$^{mut/mut}$;*Apc*$^{fl/fl}$ mice were analysed with a minimum of 22 crypts quantified per mouse. **h** Dot plots showing raw densitometry values for mitochondrial protein levels in the colon (n numbers same as in **g**, error bars are s.d.). One-way ANOVA with Tukey's post-test. *P* values for within genotype comparisons between normal crypts and adenomas were as follows: TOMM20: *Apc*$^{fl/fl}$ $P < 0.0001$, *PolgA*$^{mut/mut}$;*Apc*$^{fl/fl}$ $P < 0.0001$, NDUFB8: *Apc*$^{fl/fl}$ $P < 0.0001$, *PolgA*$^{mut/mut}$;*Apc*$^{fl/fl}$ $P = 0.9761$, UQCRFS1: *Apc*$^{fl/fl}$ $P < 0.0001$, *PolgA*$^{mut/mut}$;*Apc*$^{fl/fl}$ $P = 0.2901$, MTCO1: *Apc*$^{fl/fl}$ $P < 0.0001$, *PolgA*$^{mut/mut}$;*Apc*$^{fl/fl}$ $P = 0.007$, ATPB: *Apc*$^{fl/fl}$ $P < 0.0001$, *PolgA*$^{mut/mut}$;*Apc*$^{fl/fl}$ $P < 0.0001$. For all panels: * $P < 0.05$, ** $P < 0.01$, *** $P < 0.001$.

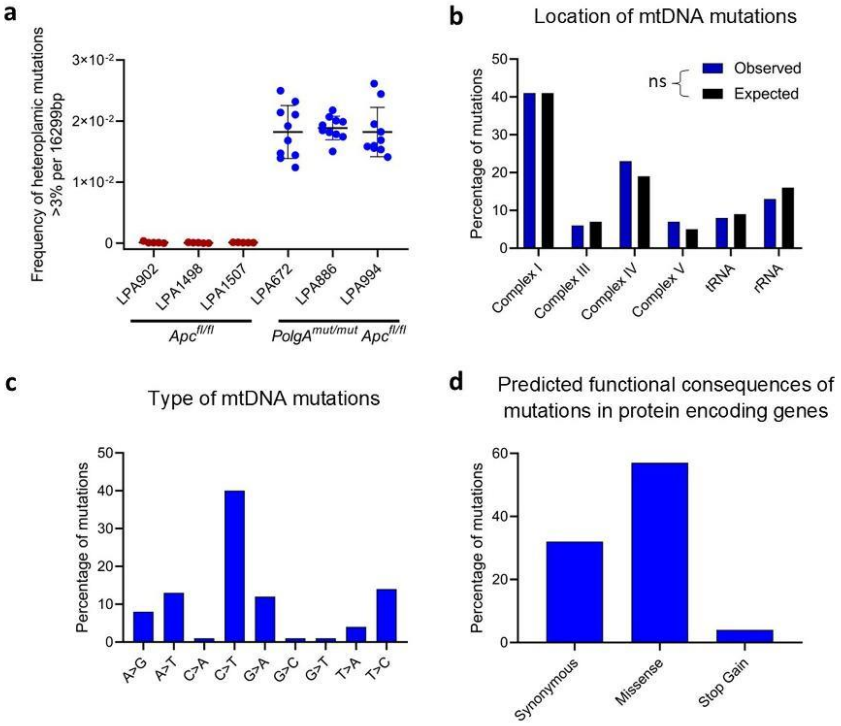

Extended Data Fig. 3 | Analysis of mitochondrial DNA (mtDNA) mutations detected in individual small intestinal adenomas from *PolgA*$^{mut/mut}$;*Apc*$^{fl/fl}$ and *Apc*$^{fl/fl}$ mice. a: The frequency of heteroplasmic variants >3% detected in adenomas from *PolgA*$^{mut/mut}$;*Apc*$^{fl/fl}$ (n = 3 mice per group and n = 10 adenomas per mouse) and *Apc*$^{fl/fl}$ mice (n = 3 mice per group, n = 5 adenomas per mouse), mean ±s.d. are shown. **b–d**: Analysis of mtDNA variants present at >30% heteroplasmy in individual adenomas from *PolgA*$^{mut/mut}$;*Apc*$^{fl/fl}$ mice (n = 413 mtDNA mutations in total). For location (**b**), expected values were calculated based on the proportion of the mitochondrial genome taken up by each gene category and observed and expected values compared using Chi-squared analysis. No significant deviation from the expected frequencies was detected ($P = 0.4744$).

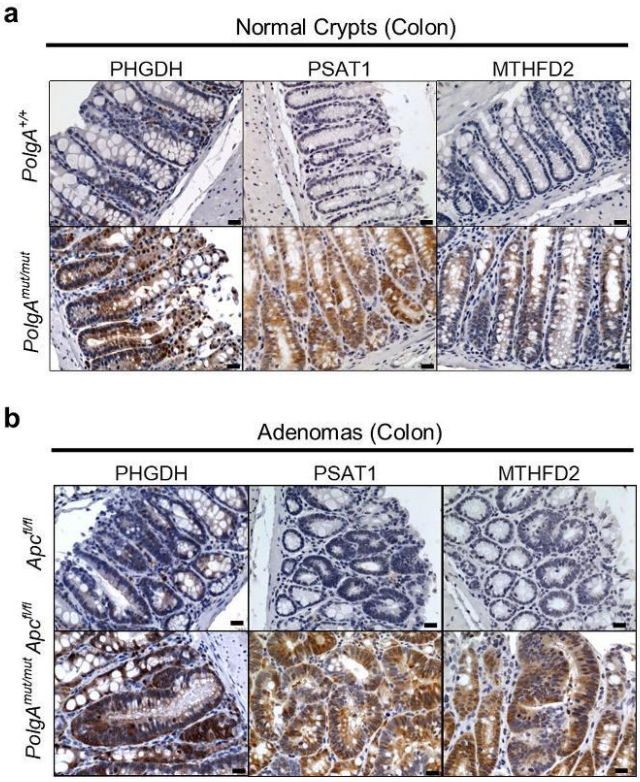

Extended Data Fig. 4 | Mitochondrial OXPHOS dysfunction causes upregulation of de novo serine synthesis *in vivo* in the mouse colon. Immunohistochemistry images showing in situ levels of SSP proteins in the non-transformed normal colonic mucosa (**a**) and adenomas (**b**) of *PolgA*$^{+/+}$ and *PolgA*$^{mut/mut}$ mice. Immunohistochemistry was performed on n = 4 mice per group. Representative images are shown. Scale bars 50 µm.

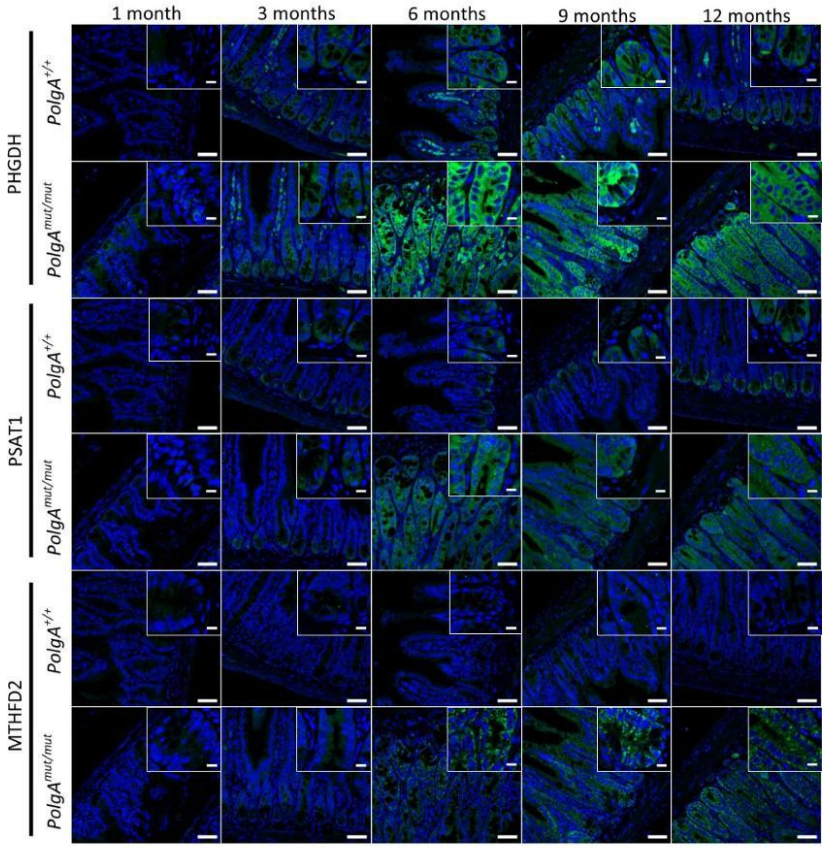

Extended Data Fig. 5 | Immunofluorescent images showing the levels of PHGDH, PSAT1 and MTHFD2 in *PolgA*$^{+/+}$ and *PolgA*$^{mut/mut}$ mice from 1–12 months of age. Immunofluorescence was performed on n = 3 mice per group at each time point. Representative images are shown. Scale bars 50 μm.

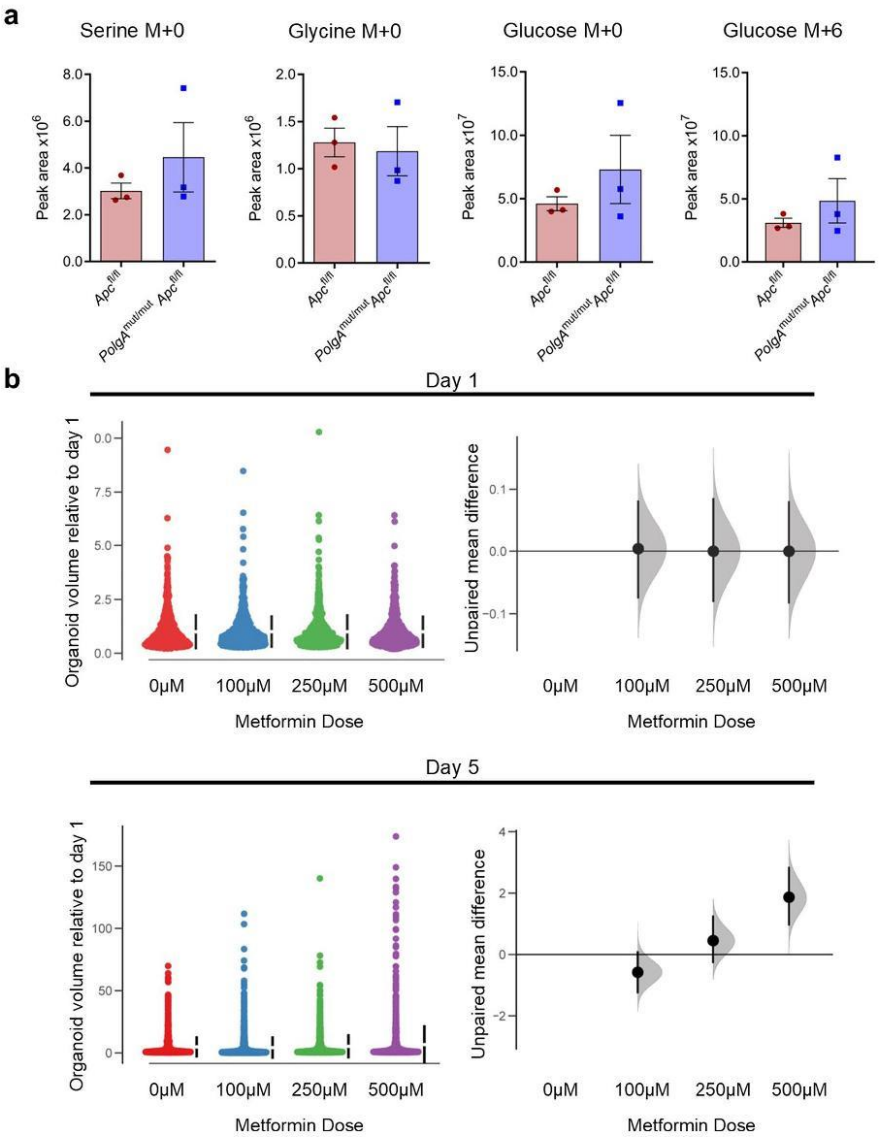

Extended Data Fig. 6 | Quantification of major mass isotopomers following growth of adenoma organods in $^{13}C_6$-glucose and adenoma organoid growth in to the presence of metformin. a: Quantification of major mass isotopomers following growth in the presence of $^{13}C_6$-glucose for 24 h. ^{13}C labelling is shown as M + 6 (glucose) and M + 0 denotes no labelling. No significant differences were found between organoids from *Apc*$^{fl/fl}$ mice compared with *PolgA*$^{mut/mut}$;*Apc*$^{fl/fl}$ mice by one-tailed unpaired t-test. n = 3 mice per group with 3 technical replicates performed per mouse. Error bars show s.e.m. **b**: A shared group estimation plot comparing the effect of metformin on the volume of individual adenoma organoids generated from *Apc*$^{fl/fl}$ mice (n = 3) on days 1 and 5 post seeding. Volume data are normalised to day 1. On day 1 the numbers of organoids measured were: 0 μM: n = 739, 100 μM: n = 796, 250 μM: n = 711, 500 μM: n = 652. On day 5 the numbers of organoids measured were: 0 μM: n = 1060, 100 μM: n = 1515, 250 μM: n = 1088, 500 μM: n = 1431. Bootstrap estimation of group mean differences (circle) and 95% confidence intervals (vertical bars) are plotted as a sampling distribution.

Chapter 11 - References

Abbatecola AA, Paolisso G (2008). 'Is there a relationship between insulin resistance and frailty syndrome?'. Current Pharmaceutical Designs 14:405-410.

Abdul-Ghani MA, Muller F, Liu Y, Chavez AO, Balas B, Zuo P, Chang Z, Tripathy D, Jani R, Molina-Carrion M, Monroy A, Folli F, Van Remmen H, DeFronzo RA (2008). 'Deleterious action of FA metabolites on ATP synthesis: possible link between lipotoxicity, mitochondrial dysfunction, and insulin resistance'. Am J Physiol Endocrinol Metab 295:678-685.

Abraham P, Isaac B (2016). 'A reliable and reproducible rodent model of tenofovir disoproxil fumarate (TDF) (anti-HIV drug) nephrotoxicity that resembles human TDF tubulopathy'. Biochemical Research 27(1):84-92.

Abraham P, Ramamoorthy H, Isaac B (2013). 'Depletion of the cellular antioxidant system contributes to tenofovir disoproxil fumarate-induced mitochondrial damage and increased oxido-nitrosative stress in the kidney'. J Biomed Sci 20:61–70.

Adams PF, Marano MA (1995). 'Current Estimates from the National Health Interview Survey'. Vital Health Stat 10 (193 Pt1):1-260.

Adelnia F, Bergeron CM, Fishbein KW, et al. (2019). 'The role of muscle perfusion in the age-associated decline of mitochondrial function in healthy individuals'. Front Physiol 10.

Agarwala R, Herlitz L, et al. (2010). '41-year-old HIV patient with proteinuria and progressive renal dysfunction.' Kidney Int 77: 475–476.

Agostini F, Rittweger J, Mazzucco S, Jurdana M, Mekjavic IB, et al. (2010). 'Effects of inactivity on human muscle glutathione synthesis by a doubletracer and single-biopsy approach'. J Physiol 588: 5089e5104.

Aguilar-Navarro SG, Gutierrez-Robledo LM, AvilaFunes JA (2015). 'Frailty among Mexican community-dwelling elderly: a story told 11 years later. The Mexican Health and Aging Study'. Salud Publica Mex 57:S62e69.

Ahlqvist KJ, Hamalainen RH, Yatsuga S, Uutela M, Terzioglu M, Gotz A, Forsstrom S, Salven P, Angers-Loustau A, Kopra OH, Tyynismaa H, Larsson N-G, Wartiovaara K, Prolla T, Trifunovic A, Suomalainen A (2012). 'Somatic progenitor cell vulnerability to mitochondrial DNA mutagenesis underlies progeroid phenotypes in polg mutator mice'. Cell Metab 15:100–109.

Ahmed N, Mandel LR, Fain M (2007). 'Frailty: An Emerging Geriatric Syndrome'. American Journal of Medicine 120:748-753.

Ahmed ST, Alston CL, Hopton S, et al. (2017). 'Using a quantitative quadruple immunofluorescent assay to diagnose isolated mitochondrial complex I deficiency'. Sci Rep 7:15676.

Ainsworth BE, Haskell WL, Whitt MC, et al. (2000). 'Compendium of Physical Activities: an update of activity codes and MET intensities'. Medicine and Science in Sports and Exercise 32:S498–S516.

Ainsworth BE, Leon AS, et al. (1993). 'Compendium of physical activities: classification of energy costs of human physical activities'. Medicine and Science in Sports and Exercise 25:71–8

Akgun KM, et al. (2014). ‘An adapted frailty-related phenotype and the VACS Index as predictors of hospitalization and mortality in HIV-infected and uninfected individuals’. J Acquir Immune Defic Syndr 67(4):397-404.

Al Rawi S, et al. (2011). ‘Postfertilization autophagy of sperm organelles prevents paternal mitochondrial DNA transmission’. Science 334:1144–1147.

Alexander C, et al. (2000). ‘OPA1, encoding a dynamin-related GTPase, is mutated in autosomal dominant optic atrophy linked to chromosome 3q28’. Nat. Genet 26:211–215.

Alikhani A, Morin H, Matte S, et al. (2019). ‘Association between lipodystrophy and length of exposure to ARTs in adult HIV-1 infected patients in Montreal’. BMC Infectious Diseases 19:820.

Almada AE, Wagers AJ (2016). ‘Molecular circuitry of stem cell fate in skeletal muscle regeneration, ageing and disease’. Nat. Rev. Mol. Cell Biol 17:267–279.

Althof KN, McGinnis KA, Wyatt CM, Freiberg MS, Gilbert C, Oursler KK, et al. (2015). ‘Comparison of risk and age at diagnosis of myocardial infarction, end-stage renal disease, and non-AIDSdefning cancer in HIV-infected versus uninfected adults’. Clin Infect Dis 60: 627–638.

Althoff KN, Jacobson LP, Cranston RD, et al. (2014). ‘Age, comorbidities, and AIDS predict a frailty phenotype in men who have sex with men’. J Gerontol A Biol Sci Med Sci 69:189-198.

Alvarez-Rios AI, Guerrero JM, Garcia-Garcia FJ, et al. (2015). ‘Associations between frailty and serum N-terminal propeptide of type I procollagen and 25-hydroxyvitamin D in older Spanish women: The Toledo Study for Healthy Aging’. Exp gerontol 69:79-84.

Alway SE, Mohamed JS, Myers MJ (2017). ‘Mitochondria initiate and regulate sarcopenia’. Exerc Sport Sci Rev 45:58-69.

Amati-Bonneau P, Valentino ML, Reynier P, Gallardo ME, Bornstein B, Boissiere A, Campos Y, Rivera H, de la Aleja JG, et al. (2008). ‘OPA1 mutations induce mitochondrial DNA instability and optic atrophy 'plus' phenotypes’. Brain 131:338-351.

Ambagtsheer RC, Beilby J, Dabravolskaj J, Abbasi M, Archibald M, Dent E (2019). ‘Application of an electronic frailty index in Australian primary care: data quality and feasibility assessment’. Aging Clin Exp Res 31:653-660.

Ameling S, Kacprowski T, Chilukoti RK, Malsch C, Liebscher V, Suhre K, Pietzner M, Friedrich N, Homuth G, Hammer E, Völker U (2015). ‘Associations of circulating plasma microRNAs with age, body mass index and sex in a population-based study’. BMC Med. Genomics 8:61.

Andersen JL (2003). ‘Muscle fibre type adaptation in elderly human muscle’. Scand J Med Sci Sport 13:40-47.

Anderson EJ, Lustig ME, Boyle KE, Woodlief TL, Kane DA, Lin CT, et al. (2009). ‘Mitochondrial H_2O_2 emission and cellular redox state link excess fat intake to insulin resistance in both rodents and humans’. J. Clin. Invest. 119:573–581.

Anderson S, Bankier AT, Barrell BG, de Bruijn MH, Coulson AR, Drouin J, Eperon IC, Nierlich DP, et al. (1981). ‘Sequence and organization of the human mitochondrial genome’. Nature 290:457-465.

Ando M, Yanagisawa N, Ajisawa A, Tsuchiya K, Nitta K (2011). ‘Kidney tubular damage in the absence of glomerular defects in HIV-infected patients on highly active antiretroviral therapy.’ Nephrol Dial Transplant 26:3224-3229.

Andreazza AC, Shao L, Wang JF, et al. (2010). 'Mitochondrial complex I activity and oxidative damage to mitochondrial proteins in the prefrontal cortex of patients with bipolar disorder'. Arch Gen Psychiatry. 67(4):360–368.

Andreux PA, et al. (2018). 'Mitochondrial function is impaired in the skeletal muscle of pre-frail elderly'. Scientific Reports 8:8548.

Antoniou T, Raboud J, Chirhin S, Yoong D, Govan V, Gough K, Rachlis A, Loutfy M (2005). 'Incidence of and risk factors for tenofovir-induced nephrotoxicity: A retrospective cohort study'. HIV Med 6: 284–290.

Apostolo J, Bobrowicz-Campos E, et al. (2018). 'Effectiveness of interventions to prevent pre-frailty and frailty progression in older adults: a systematic review'. JBI Database System Rev Implement Rep 16:140–232.

Apostolova N, et al. (2011). 'Compromising mitochondrial function with the antiretroviral drug efavirenz induces cell survival-promoting autophagy'. Hepatology 54(3).

Apostolova N, Gomez-Sucerquia LJ, Moran A, Alvarez A, Blas-Garcia A, Esplugues JV. (2010). 'Enhanced oxidative stress and increased mitochondrial mass during efavirenz-induced apoptosis in human hepatic cells'. British journal of pharmacology. 160:2069–84.

Arnaudo E, Dalakas M, Shanske S, DiMauro S, Schon EA, Moraes CT (1991). 'Depletion of muscle mitochondrial DNA in AIDS patients with zidovudine-induced myopathy'. The Lancet 337(8740):508-510.

Arts EJ, Hazuda DJ (2012). 'HIV-1 Antiretroviral Drug Therapy'. Cold Spring Harb Perspect Med 2: e007161.

Ashar F, Moes A, Moore A, Grove M, Chaves PM, Coresh J, Newman A, Matteini A, Bandeen-Roche K, Boerwinkle E, et al. (2015). 'Association of mitochondrial DNA levels with frailty and all-cause mortality'. J Mol Med 93:177-186.

Ashar FN, Moes A, Moore AZ, et al. (2015). 'Association of mitochondrial DNA levels with frailty and all-cause mortality'. J Mol Med 93:177-186.

Asp P, Blum R, Vethantham V (2011). 'Genome-wide remodelling of the epigenetic landscape during myogenic differentiation'. Proc Natl Acad Sci USA 108:E149-E158.

Atta MG, Gallant JE, Rahman MH, et al. (2006). 'Antiretroviral therapy in the treatment of HIV-associated nephropathy'. Nephrol Dial Transplant. 21:2809–2813.

Attia M, Maurer M, Robinet M, Le Grand F, Fadel E, Le Panse R, et al. (2017). 'Muscle satellite cells are functionally impaired in myasthenia gravis: consequences on muscle regeneration'. Acta Neuropathol 134:869–888.

Augustin S, Nolden M, Muler S, Hardt O, Arnold I, Langer T (2005). 'Characterization of peptides released from mitochondria'. J. Biol. Chem 280:2691–2699.

Austin RL, Rune A, Bouzakri K, Zierath JR, Krook A (2008). 'siRNA-mediated reduction of inhibitor of nuclear factor-κB kinase prevents tumor necrosis factor-alpha-induced insulin resistance in human skeletal muscle'. Diabetes 57:2066–2073.

Autran B, Carcelain G, Li TS, et al. (1999). 'Restoration of the immune system with anti-retroviral therapy'. Immunol Lett 66:207–11.

Avdoshina V, Fields JA, Castellano P, et al. (2016). 'The HIV Protein gp120 Alters Mitochondrial Dynamics in Neurons'. Neurotox Res 29:583-593

Aversa Z, Penna F, Costelli P, Di Rienzo G, Lacitignola A, et al. (2012). 'Changes in myostatin signaling in non-weight-losing cancer patients'. Ann Surg Oncol 19:1350e1356.

Ayanga BA, Badal SS, Wang Y, et al. (2016). 'Dynamin-related protein 1 deficiency improves mitochondrial fitness and protects against progression of diabetic nephropathy'. J Am Soc Nephrol. 27:2733–2747.

Badley AD (2005). 'In vitro and in vivo effects of HIV protease inhibitors on apoptosis'. Cell Death Differ 1:924-31.

Bagkeris E, Burgess L, Mallon PW, et al. (2018). 'Cohort profile: the pharmacokinetic and clinical observations in PeoPle over fifty (POPP) study'. Int J Epidemiol 47:1391-1392.

Bagnis CI, Stellbrink H-K (2015). 'Protease inhibitors and renal function in patients with HIV infection a systematic review'. Infec Dis Ther 4:15-50.

Bahat G, Ilhan B (2016). 'Sarcopenia and the cardiometabolic syndrome: a narrative review'. Eur Geriatr Med 6: 20–23.

Baines HL, Stewart JB, Stamp C, Greaves LC (2014). 'Similar patterns of clonally expanded somatic mtDNA mutations in the colon of heterozygous mtDNA mutator mice and ageing humans'. Mech. Ageing Dev, 139:22-30

Balaban RS, Nemoto S, Finkel T (2005). 'Mitochondria, oxidants, and aging'. Cell 120: 483– 495.

Balani SK, Mathai L, et al. (1995). 'Metabolites of L-735,524, a potent HIV-1 protease inhibitor, in human urine'. Drug Metab. Dispos 23:266-270.

Baltgalvis KA, Berger FG, Pena M, Davis JM, Muga SJ, Carson JA (2008). 'Interleukin-6 and cachexia in ApcMin/+ mice'. Am. J. Physiol. Regul. Integr. Comp. Physiol 294:R393–R401.

Banci L, Cefaro C, Ciofi-Baffoni S, Gallo A, et al. (2009). 'MIA40 is an oxidoreductase that catalyzes oxidative protein folding in mitochondria'. Nat. Struct. Mol. Biol 16:198–206.

Bandeen-Roche K, Seplaki CL, Huang J, Buta B, Kalyani RR, Varadhan R, et al. (2015). 'Frailty in older adults: a nationally representative profile in the United States'. J Gerontol A Biol Sci Med Sci. 70(11): 1427–34.

Baptista G, Dupuy AM, Jaussent A, Durant R, Ventura E, Sauguet P, Picot MC, Jeandel C, Cristol JP (2012). 'Low-grade chronic inflammation and superoxide anion production by NADPH oxidase are the main determinants of physical frailty in older adults'. Free Radic. Res 46:1108–1114.

Baradaran R, Berrisford JM, Minhas GS, Sazanov LA (2013). 'Crystal structure of the entire respiratory complex I'. Nature 494:443–448.

Barazzoni R, Short KR, Nair KS (2000). 'Effects of aging on mitochondrial DNA copy number and cytochrome c oxidase gene expression in rat skeletal muscle, liver, and heart'. Journal of Biological Chemistry 275(5):3343–3347.

Barbat-Artigas S, Pion CH, Leduc-Gaudet JP, et al. (2014). 'Exploring the role of muscle mass, obesity, and age in the relationship between muscle quality and physical function'. J Am Med Dir Assoc 303: e13–20.

Barbosa SG, Mansur HN, Colugnate FAB (2017). ‘Impacts of frailty on the negative health outcomes of elderly Brazilians’. Revista Brasileira de Geriatria e Gerontologia 20(6).

Barditch-Crovo P, Deeks SG, Collier A, Safrin S, Coakley DF, Miller M, Kearney BP, Coleman RL, Lamy PD, Kahn JO, McGowan I, Lietman PS (2001). ‘Phase I/II trial of the pharmacokinetics, safety, and antiretroviral activity of tenofovir disoproxil fumarate in human immunodeficiency virus-infected adults’. Antimicrob. Agents Chemother 45:2733–2739.

Barre-Sinoussi F, Chermann JC, Rey F, et al. (1983). ‘Isolation of a T-lymphotropic retrovirus from a patient at risk for acquired immune deficiency syndrome (AIDS)’. Science 20:868-871.

Barrett EF, Barrett JN, David G (2011). ‘Mitochondria in motor nerve terminals: function in health and in mutant superoxide dismutase 1 mouse models of familial ALS’. J. Bioenerg. Biomembr 43: 581–586.

Barroso S, Gonzalez-Segura A, RIba N, et al. (2019). ‘Metabolic, mitochondrial, renal and hepatic saftey of enfuvirtide and raltegravir antiretroviral administration: randomised crossover clinical trial in healthy volunteers’. PLOS ONE 15(5):e0216712.

Barruet E, Striedinger K, Wu J, et al. (2020). ‘Functionally heterogeneous human satellite cells identified by single cell RNA sequencing’. eLife 9:e51576.

Barshad G, Marom S, Cohen T, Mishmar D (2018). ‘Mitochondrial DNA Transcription and Its Regulation: An Evolutionary Perspective’. Trends in Genetics 34:682-692.

Bartali B, Bandinelli S, Lauretani F, Semba RD, Fried LP, Ferrucci L (2006). ‘Low nutrient intake is an essential component of frailty in older persons’. J Gerontol A Biol Sci Med Sci 61:589-593.

Bartali B, Frongillo EA, Bandinelli S, Lauretani F, Semba RD, Fried LP, Ferrucci L (2013). ‘Protein intake and muscle strength in older persons: does inflammation matter’. J Am Geriatr Soc 60:480-484.

Bartz R, Suliman HB, Piantadosi CA (2015). ‘Redox mechanisms of cardiomyocyte mitochondrial protection’. Frontiers in Physiology 6:291.

Basic D, Shanley C (2015). ‘Frailty in an Older Inpatient Population: Using the Clinical Frailty Scale to Predict Patient Outcomes’. Journal of Aging and Health 27:670-685.

Baumann CW, Kwak D, Liu HM, et al. (2016). ‘Age-induced oxidative stress: how does it influence skeletal muscle quantity and quality?’ Journal of Applied Physiology 121:1047-1052.

Baylis D, Bartlett DB, Patel HP, Roberts HC (2013). ‘Understanding how we age: insights into inflammaging’. Longev Healthspan 2:1-8.

Beaudart C, Buckinx F, Rabenda V, Gillain S, Cavalier E, Slomian J, et al. (2014). ’The effects of vitamin D on skeletal muscle strength, muscle mass, and muscle power : a systematic review and meta-analysis of randomized controlled trials’. J. Clin. Endocrinol. Metab. 99:4336–4345.

Beaudart C, Cruz-Jentoft A, et al. (2018). ‘Assessment of muscle function and physical performance in daily clinical practice’. Calif Tissue Int 105:1-14.

Beaudart C, McCloskey E, Bruyere O, et al. (2016). ‘Sarcopenia in daily practice: assessment and management’. BMC Geriatr 16:170

Beinert H, Holm RH, Munck E (1997). ‘Iron-Sulfur Clusters: Nature's Modular, Multipurpose Structures’. Science 277:653-659.

Benedetti C, Haynes CM, Yang Y, Harding HP, Ron D (2006). 'Ubiquitin-like protein 5 positively regulates chaperone gene expression in the mitochondrial unfolded protein response'. Genetics 174:229–239.

Benit P, Lebon S, Rustin P (2009). 'Respiratory-chain diseases related to complex III deficiency'. Biochimica et Biophysica Acta (BBA) - Molecular Cell Research 1793:181-185.

Benito PJ, Cupeiro R, Ramos-Campo DJ, et al. (2020). 'A systematic review with meta-analysis of the effect of resistance training on whole-body muscle growth in health adult males'. Int Journal of Environmental Research and Public Health 17:1285.

Berberoglu MA, Gallagher TL, Morrow ZT, J, et al. (2017).'Satellite-like cells contribute to pax7-dependent skeletal muscle repair in adult zebrafish'. Dev Biol, 424 (2):162-180.

Bereiter-Hahn J, Voth M (1994). 'Dynamics of mitochondria in living cells: shape changes, dislocations, fusion, and fission of mitochondria'. Microsc Res Tech 27:198-219.

Berg JM, Tymockzko JL, Gatto GJ, Stryer L (2015a). 'Glycolysis and gluconeogenesis'. Biochemistry 8th Edition.

Berg JM, Tymockzko JL, Gatto GJ, Stryer L (2015b). 'Citric acid acycle'. Biochemistry 8th Edition: 495-5

Bertrand L, Dygert L, Toborek M (2016). 'Antiretroviral treatment with efavirenz disrupts the blood-brain barrier integrity and increases stroke severity'. Sci Rep 6:39738.

Bhargava K, Spremulli LL (2005). 'Role of the N- and C-terminal extensions on the activity of mammalian mitochondrial translational initiation factor 3'. Nucleic Acids Research 33:7011-7018.

Bian AL, Hu HY, Rong YD, Wang J, Wang JX, Zhou XZ (2017). 'A study on relationship between elderly sarcopenia and inflammatory factors IL-6 and TNF-α'. Eur. J. Med. Res. 22:25.

Biesecker G, Karimi S, Desjardins J, Meyer D, Abbott B, Bendele R, Richardson F (2003). 'Evaluation of mitochondrial DNA content and enzyme levels in tenofovir DF-treated rats, rhesus monkeys and woodchucks'. Antiviral Research 58:217-225.

Bigler M, Odriozola A, Halm S, Tschanz S A, Zakrzewicz A, et al. (2016). 'Morphometry of skeletal muscle capillaries: the relationship between capillary ultrastructure and ageing in humans'. Acta Physiol 218: 98–111.

Binder EF, Yarasheski KE, Steger-May K, Sinacore DR, Brown M, Schechtman KB, Holloszy JO (2005). 'Effects of progressive resistance training on body composition in frail older adults: results of a randomized, controlled trial'. J Gerontol A Biol Sci Med Sci 60:1425–1431.

Binkley N, Krueger D, Buehring B (2013). 'What's in a name revisited: should osteoporosis and sarcopenia be considered components of 'dysmobility syndrome?''. Osteoporos Int 24:2955e2959.

Biolo G, Stulle M, Piccoli A, Lorenzon S, Dal Mas V, et al. (2005). 'Metabolic consequences of physical inactivity'. J Ren Nutr 15:49e53.

Birkus G, Hitchcock MJ, Cihlar T (2002). 'Assessment of mitochondrial toxicity in human cells treated with tenofovir: comparison with other nucleoside reverse transcriptase inhibitors'. Antimicrob Agents Chemother 46:716–723.

Biro A, Vaknine H, Cohen-Armon M, et al. (2016). 'The effect of poly (ADP-ribose) polymerase inhibition on aminoglycoside-induced acute tubular necrosis in rats'. Clin Nephrol 85:226–234.

Bischoff-Ferrari HA, Orav JE, Kanis JA, et al. (2015). 'Comparative performance of current definitions of sarcopenia against the prospective incidence of falls among community-dwelling seniors age 65 and older'. Osteoporos Int 26:2793–802.

Blackwood JK, Whittaker RG, Blakely EL, Alston CL, Turnbull DM, Taylor RW (2010). 'The investigation and diagnosis of pathogenic mitochondrial DNA mutations in human urothelial cells'. Biochemical and Biophysical Research Communications 393:740-745.

Blas-Garcia A, et al. (2010). 'Inhibition of mitochondrial function by efavirenz increases lipid content in hepatic cells'. Hepatology 52:115–25.

Blau HM, Cosgrove BD, Ho ATV (2015). 'The central role of muscle stem cells in regenerative failure with aging'. Nat. Med 21:854–862.

Blaum CS, Xue QL, Michelon E, Semba R, Fried LP (2005). 'The association between obesity and the frailty syndrome in older women: The Women's Health and Aging Study'. Journal of the American Geriatric Society 53(6):927-934.

Ble A, Cherubini A, Volpato S, Bartali B, Walston JD, Windham BG, Bandinelli S, Lauretani F, Guralnik JM, Ferrucci L. (2006). 'Lower plasma vitamin E levels are associated with the frailty syndrome: the InCHIANTI study'. J Gerontol A Biol Sci Med Sci. 61:278–83.

Bloch-Damti A, Bashan N (2005). 'Proposed mechanisms for the induction of insulin resistance by oxidative stress'. Antioxid Redox Signal 7:1553-1567.

Bloom I, Shand C, Cooper C, et al. (2018). 'Diet quality and sarcopenia in older adults: a systematic review'. Nutrients 10.

Boden G, Chen X (1995). 'Effects of fat on glucose uptake and utilization in patients with non-insulin-dependent diabetes'. J Clin Invest 96:1261-1268.

Bogenhagen D, Clayton DA (1977). 'Mouse L cell mitochondrial DNA molecules are selected randomly for replication throughout the cell cycle'. Cell 11:719-727.

Bohannon RW. (2015). 'Muscle strength: clinical and prognostic value of hand-grip dynamometry'. Curr Opinion Clin Nutr. 18(5):465–470.

Bohr VA. (2002). 'Repair of oxidative DNA damage in nuclear and mitochondrial DNA, and some changes with aging in mammalian cells'. Free Radic. Biol.Med 32:804–812.

Bohuszewicz O, Low HH (2018). 'Structure of a mitochondrial fission dynamin in the closed conformation'. Nat. Struct. Mol. Biol 25:722–731.

Bone AE, Hepgul N, Kon S, et al. (2017). 'Sarcopenia and frailty in chronic respiratory disease'. Chron Respir Dis 14:85–99.

Bonetto A, Aversa Z, Mercantini P, Baccino F M, Costelli P, et al. (2013). 'Early changes of muscle insulin-like growth factor-1 and myostatin gene expression in gastric cancer patients'. Muscle Nerve 48:387e392.

Bongiovanni M, Bini T, Chiesa E, et al. (2004). 'Lopinavir/ritonavir vs. indinavir/ritonavir in antiretroviral naive HIV-infected patients: immunovirological outcome and side effects'. Antiviral Research 62:53-56.

Bonjoch A, Juega J, Puig J, Pérez-Alvarez N, Aiestarán A, Echeverría P, Pérez V, Clotet B, Romero R, Bonet J, Negredo E (2014). 'High prevalence of signs of renal damage despite normal renal function in a cohort of HIV-infected patients: Evaluation of associated factors'. AIDS Patient Care STDS 28: 524–529.

Bonn F, Tatsuta T, Petrungaro C, Riemer J, Langer T (2011). 'Presequence-dependent folding ensures MrpL32 processing by the m-AAA protease in mitochondria'. EMBO J 30:2545–2556.

Bonnard C, Durand A, Peyrol S, Chanseaume E, Chauvin MA, Morio B, Vidal H, Rieusset J (2008). 'Mitochondrial dysfunction results from oxidative stress in the skeletal muscle of diet-induced insulin-resistant mice'. J Clin Invest 118:789-800.

Boppart MD, Asp S, Wojtaszewski JF, Fielding RA, Mohr T, Goodyear LJ (2000). 'Marathon running transiently increases c-Jun NH2-terminal kinase and p38 activities in human skeletal muscle'. J. Physiol Rev 526:663–669.

Bortoli S, Renault V, Eveno E, Auffray C, Butler-Browne G, Pietu G (2003). 'Gene expression profiling of human satellite cells during muscular aging using cDNA arrays'. Gene 321:145– 154.

Bortz WM. (2002). 'A conceptual framework of frailty'. Journal of Gerontology 57(5):283-288.

Bourgeron T, Chretien D, Birch-Machin M, et al. (1995). 'Mutation of a nuclear succinate dehydrogenase gene results in mitochondrial respiratory chain deficiency'. Nat Genet 11:144-149.

Boyle PA, Buchman AS, Wilson RS, Leurgans SE, Bennett DA (2010). 'Physical frailty is associated with incident mild cognitive impairment in community-based older persons'. J. Am. Geriatr. Soc. 58:248–255.

Brack AS, Conboy MJ, Roy S, Lee M, Kuo CJ, Keller C, et al. (2007). 'Increased Wnt signaling during aging alters muscle stem cell fate and increases fibrosis'. Science 317:807–810.

Bradley AD (2005). 'In vitro and in vivo effects of HIV protease inhibitors on apoptosis'. Cell Death Differ 12:924-931.

Branas F, Jimenez Z, Sanchez-Conde M, Dronda F, LopezBernaldo De Quiros JC, Perez-Elias MJ, et al. (2017). 'Frailty and physical function in older HIV-infected adults'. Age Ageing 46(3):522–6

Braymer J, Lill R (2017). 'Iron-sulfur cluster biogenesis and trafficking in mitochondria'. J Biol Chem 272:12754-12763.

Brehm A, Krssak M, Schmid AI, Nowotny P, Waldhäusl W, Roden M (2006). 'Increased lipid availability impairs insulin-stimulated ATP synthesis in human skeletal muscle'. Diabetes 55:136-140.

Breitling LP, Saum KU, Perna L, Schöttker B, Holleczek B, Brenner H (2016). 'Frailty is associated with the epigenetic clock but not with telomere length in a German cohort'. Clin. Epigenetics 8:1-8.

Brierley EJ, Johnson MA, Lightowlers RN, et al. (2998). 'Role of mitochondrial DNA mutations in human aging: implications for the central nervous system and muscle'. Ann Neurol 43:217–223

Brini M, Carafoli E (2009). 'Calcium Pumps in Health and Disease'. Physiological Reviews 89:1341-1378

Brinkman K, Smeitink JA, Romijn JA, Reiss P (1999). 'Mitochondrial toxicity induced by nucleoside-analogue reverse-transcriptase inhibitors is a key factor in the pathogenesis of antiretroviral-therapy-related lipodystrophy'. Lancet 354:1112-1115.

British Geriatrics Society (2017). 'Fit for frailty'. Available online: https://www.bgs.org.uk/sites/default/files/ content/resources/files/2018-05-14/fff2_short.pdf. (Assessed 14 November 2020).

Brocca L, Coletto L, Biolo G, Sandri M, Bottinelli R, et al. (2012). 'The time course of the adaptations of human muscle proteome to bed rest and the underlying mechanisms'. J Physiol 590:5211e5230.

Brothers TD, Guaraldi G, Falutz J, Theou O, Johnston B L, et al. (2014). 'Frailty in people aging with human immunodeficiency virus (HIV) infection'. J Infect Dis 210(8):1170-1179.

Brothers TD, Kirkland S, Theou O, Zona S, Malagoli A, Wallace LMK, et al. (2017). 'Predictors of transitions in frailty severity and mortality among people aging with HIV'. PLoS One 12(10): e0185352.

Brown DT, Michael EM, Turnbull DM, Chinnery PF (2001). 'Random genetic drift determines the level of mutant mtDNA in human primary oocytes'. J Hum Genet Am 68:533-536.

Brown TA, Ceccconi C, Tkachuk AN, Bustamante C, Clayton DA (2005). 'Replication of mitochondrial DNA occurs by strand displacement with alternative light-strand origins, not via a strand-coupled mechanism'. Genes & Development 19:2466-2476.

Brown WM, George M, Wilson AC (1979). 'Rapid evolution of animal mitochondrial DNA'. Proceedings of the National Academy of Sciences of the United States of America 76:1967-1971.

Brownlee M. (2005). 'The pathobiology of diabetic complications: a unifying mechanism'. Diabetes. 54:1615–1625.

Bruning A, Friese K, Burges A, Mylonas L (2010). 'Tamoxifen enhances the cytotoxic effects of nelfinavir in breast cancer cells'. Breast Cancer Res 12(R45).

Brunk UT, Truman A (2002). 'Lipofuscin: mechanisms of age-related accumulation and influence on cell function'. Free Radic Biol Med 33:611-619.

Brunner F, Sheikhzadeh A, Nordin M, Yoon J, Frankel V (2007). 'Effects of aging on Type II muscle fibers: a systematic review of the literature'. J. Aging Phys. Act. 15:336–348.

Bruunsgaard H, Anderson-Ranberg K, Pedersen Hjelmborg JvB, et al. (2003). 'Elevated levels of tumor necrosis factor alpha and mortality in centenarians'. Am J Med 115:278–283.

Bua E, Johnson J, Herbst A, et al. (2006). 'Mitochondrial DNA-deletion mutations accumulate intracellularly to detrimental levels in aged human skeletal muscle fibres'. Am J Hum Genet 79:469-480.

Burin des Roziers N, Sotto A, Arnaud A, Saissi G, Nasar O, Jourdan J (1995). 'Kinetics of detection of antibodies to HIV-1 and plasma p24 antigens during a severe primary HIV-1 infection'. AIDS 9:528–529.

Burke RE, Levine DN, Zajac FE III (1971). 'Mammalian motor units: physiological-histochemical correlation in three types in cat gastrocnemius'. Science 174:709–712.

Bury AG, Pyle A, Elson JL, Greaves L (2017). 'Mitochondrial DNA changes in pedunculopontine cholinergic neurons in Parkinson's Disease'. Annuals of Neurology 82:1016-21.

Buta BJ, Walston JD, Godino JG, Park M, KalyaniR R, Xue Q L, et al. (2015). 'Frailty assessment instruments: systematic characterization of the uses and contexts of highly-cited instruments'. Ageing Res Rev 26:53-61.

Cacciatore F, Testa G, Galizia G, Della-Morte D, Mazzella F, Langellotto A, et al. (2013). 'Clinical frailty and long-term mortality in elderly subjects with diabetes'. Acta Diabetol 50:251-60.

Cadore EL, Rodriguez-Manas L, Sinclair A, Izquierdo M (2013). 'Effects of different exercise interventions on risk of falls, gait ability, and balance in physically frail older adults: a systematic review'. Rejuvenation Res 16:105-114.

Cai YC, Bullard JM, Thompson NL, Spremulli L (2000). 'Interaction of mitochondrial elongation factor Tu with aminoacyl-tRNA and elongation factor Ts'. J Biol Chem 275:20308-20314.

Cain K, Bratton SB, Cohen GM (2002). 'The Apaf-1 apoptosome: a large caspase-activating complex'. Biochimie 84:203-214.

Caldecott KW (2008). 'Single-strand break repair and genetic disease'. Nat. Rev. Genet. 9:619-631

Calvani R, landi F, et al. (2013). 'Current nutritional recommendations and novel dietary strategies to manage sarcopenia'. J Frailty Aging 2:38-53.

Calvo SE, Clauser KR, Mootha VK (2016). 'MitoCarta2.0: an updated inventory of mammalian mitochondrial proteins'. Nucleic Acids Research 44:D1251-D1257.

Cameron ID, et al. (2013). 'A multifactorial interdisciplinary intervention reduces frailty in older people: randomized trial'. BMC Med 11.

Campbell G, Krishnan KJ, Deschauer M, Taylor RW, Turnbull DM (2014). 'Dissecting the mechanisms underlying the accumulation of mitochondrial DNA deletions in human skeletal muscle'. Hum Mol Genet 23:4612-4620.

Campbell LJ, Ibrahim F, Fisher M, Holt SG, Hendry BM, Post FA (2009). 'Spectrum of chronic kidney disease in HIV-infected patients'. HIV Med 10:329-336.

Campbell W, Trappe TA, Jozsi AC, Kruskall LJ, Wolfe R, Evans WJ (2002). 'Dietary protein adequacy and lower body versus whole body resistive training in older humans'. J Physiol 542:631–642.

Canon ME, Crimmins EM (2011). 'Sex differences in the association between muscle quality, inflammatory markers, and cognitive decline'. J. Nutr. Health Aging 15:695-698.

Canto C, Gerhart-Hines Z, Feige JN, Lagouge M, Noriega L, Milne JC, Elliott PJ, Puigserver P, Auwerx J (2009). 'AMPK regulates energy expenditure by modulating NAD+ metabolism and SIRT1 activity'. Nature 458:1056-1060.

Cappola AR, Xue QL, Ferrucci L, Guralnik JM, Volpato S, Fried LP (2003). 'Insulin-like growth factor I and interleukin-6 contribute synergistically to disability and mortality in older women'. Journal of Clinical Endocrinology and Metabolism 88:2019-2025.

Carlson ME, Suetta C, Conboy MJ, Aagaard P, Mackey A, Kjaer M, et al. (2009). 'Molecular aging and rejuvenation of human muscle stem cells'. EMBO Mol. Med. 1:381–391.

Caron M, et al. (2007). 'Human lipodystrophies linked to mutations in A-type lamins and to HIV protease inhibitor therapy are both associated with prelamin A accumulation, oxidative stress and premature cellular senescence'. Cell Death Differ 14:1759-1767.

Carr A, Samaras K, Thorisdottir A, Kaufmann GR, Chisholm DJ, Cooper DA (1999). 'Diagnosis, prediction, and natural course of HIV-1 protease-inhibitor-associated lipodystrophy, hyperlipidaemia, and diabetes mellitus: a cohort study'. Lancet (London, England) 353(9170):2093–9.

Carrio E, Lois S, Mallona I, et al. (2015). 'Deconstruction of DNA methylation patterns during myogenesis reveals specific epigenetic events in the establishment of skeletal muscle lineage'. Stem Cell 10.

Carrio E, Munoz M, et al. (2016). 'Muscle cell identity requires Pax7-mediated lineage-specific DNA demetehylation'. BMC Biology 14.

Carrol J, Fearnley IM, Skehel JM, Shannon RJ, Hirst J, Walker JE (2006). 'Bovine complex I is a complex of 45 different subunits'. J Biol Chem 281:32724-32727.

Cartee GD, Hepple RT, Bamman M, Zierath JR (2016). 'Exercise promotes healthy aging of skeletal muscle'. Cell Metab 23:1034–1047.

Carvalho-Filho MA, Ueno M, Hirabara SM, Seabra AB, Carvalheira JB, de Oliveira MG, Velloso LA, Curi R, Saad MJ (2005). 'S-nitrosation of the insulin receptor, insulin receptor substrate 1, and protein kinase B/Akt: a novel mechanism of insulin resistance'. Diabetes 54:959-967.

Castro Mdel R, Suarez E, Kraiselburd E, et al. (2012). 'Aging increases mitochondrial DNA damage and oxidative stress in liver of rhesus monkeys'. Exp Gerontol 47(1):29–37.

Cavalier-Smith T (1987). 'Eukaryotes with no mitochondria'. Nature 326:332-333.

Cawthon PM, Lui LY, Taylor BC, et al. (2017). 'Clinical definitions of sarcopenia and risk of hospitalization in community-dwelling older men: the osteoporotic fractures in men study'. J Gerontol A Biol Sci Med Sci 72:1383–89.

Cawthon PM, Peters KE, et al. (2019). 'Strong relation between muscle mass determined by D3-creatine dilution, physical performance and incidence of falls and mobility limitations in a prospective cohort of older men'. J Gerontol A Biol Sci Med Sci 74:844-852.

CDC (1981). 'Pneumocystis pneumonia — Los Angeles'. MMWR 30:250-252.

Cecchini G. (2003). 'Function and Structure of Complex II of the Respiratory Chain'. Annual Review of Biochemistry 72:77-109.

Cederholm T, Barazzoni R, Austin P, et al. (2017). 'ESPEN guidelines on definitions and terminology of clinical nutrition'. Clin Nutr 36:49–64

Cederholm T, Jensen GL, Correia M, et al. (2019). 'GLIM criteria for the diagnosis of malnutrition - A consensus report from the global clinical nutrition community'. Clin Nutr 38:1-9.

Cesari M, et al. (2002). 'Inflammatory markers and physical performance in older persons: the InCHIANTI Study'. J. Gerontol. A Biol. Sci. Med. Sci 59:M242–M248.

Cesari M, Hsu F-C, et al. (2015). 'A physcial activity intervention to treat the frailty syndrome in older persons- results from the LIPE-P study'. Journals of Gerontology 70(2):216-222.

Chaban Y, Boekema EJ, Dudkina NV (2014). 'Structures of mitochondrial oxidative phosphorylation supercomplexes and mechanisms for their stabilisation'. Biochim. Biophys. Acta 1837:428-426.

Chan NC, et al. (2011). 'Broad activation of the ubiquitin-proteasome system by Parkin is critical for mitophagy'. Hum. Mol. Genet 20:1726–1737.

Chandel NS, Jasper H, Ho T, Passegue E (2016). 'Metabolic regulation of stem cell function in tissue homeostasis and organismal ageing'. Nat Cell Biol 18:823-832.

Chandel NS, Maltepe E, Goldwasser E, Mathieu CE, Simon MC, Schumacker PT (1998). 'Mitochondrial reactive oxygen species trigger hypoxia-induced transcription'. Proceedings of the National Academy of Sciences of the United States of America 95:11715-11720.

Chang D, Clayton DA (1984). 'Precise identification of individual promoters for transcription of each strand of human mitochondrial DNA'. Cell 36:635-643.

Chang KV, Hsu TH, Wu WT et al. (2016). 'Association between sarcopenia and cognitive impairment: a systematic review and meta-analysis'. J Am Med Dir Assoc 17:1164.e7–64.e15.

Chang S, Weiss CO, Xue QL, Fried LP (2012). 'Association between inflammatory-related disease burden and frailty: Results from the Women's Health and Aging Studies (WHAS) I and II'. Arch Gerontol Geriatr 54:9-15.

Chang SF, Lin HC, Cheng CL (2018). 'The relationship of frailty and hospitalisation among older people: evidence from a meta-analysis'. J Nurs Scholarsh 50:383-391.

Charge SB, Brack AS, Hughes SM (2002). 'Aging-related satellite cell differentiation defect occurs prematurely after Ski-induced muscle hypertrophy'. Am J Physiol Cell Physiol 283:C1228– C1241.

Chavez JA, Summers SA (2003). 'Characterizing the effects of saturated fatty acids on insulin signaling and ceramide and diacylglycerol accumulation in 3T3-L1 adipocytes and C2C12 myotubes'. Arch Biochem Biophys 419:101-109.

Chawla A, Wang C, Patton C, et al. (2018). 'A review of long-term toxicity of antiretroviral treatment regimens and implications for an aging population'. Infect Dis Ther 7:183-195.

Chawla LS, Eggers PW, Star RA, Kimmel PL (2014). 'Acute kidney injury and chronic kidney disease as interconnected syndromes'. N Engl J Med. 371(1):58–66.

Chen H, Chomyn A, Chan DC (2005). 'Disruption of fusion results in mitochondrial heterogeneity and dysfunction'. J Biol Chem 280:26185-26192.

Chen H, Vermulst M, Wang YE, Chomyn A, Prolla TA, McCaffery JM, Chan DC (2010). 'Mitochondrial fusion is required for mtDNA stability in skeletal muscle and tolerance of mtDNA mutations'. Cell 141:280-289.

Chen J, Chen JK, Harris RC. (2015). 'EGF receptor deletion in podocytes attenuates diabetic nephropathy'. J Am Soc Nephrol 26:1115–1125.

Chen J-F, Mandel EM, Thomson JM, et al. (2006). 'The role of microRNA-1 and microRNA-133 in skeletal muscle proliferation and differentiation'. Nat Genet 38:228-233.

Chen J-F, Tao Y, Li J, Deng Z, et al. (2010). 'microRNA-1 and microRNA-206 regulate skeletal muscle satellite cell proliferation and differentiation by repressing Pax7'. Mol Cell Biol 31:203-214.

Chin ER, Olson EN, Richardson JA, Yang Q, Humphries C, Shelton JM, Wu H, Zhu W, BasselDuby R, Williams RS (1998). 'A calcineurin-dependent transcriptional pathway controls skeletal muscle fiber type'. Genes Dev 12:2499–2509.

Chinnery PF, Samuels DC (1999). 'Relaxed replication of mtDNA: a model with implications for the expression of disease'. Am. J. Hum. Genet 64:1158–1165.

Chistiakov DA, Sobenin IA, Revin V, Orekhov AN, Bobryshev YV (2014). 'Mitochondrial aging and age-related dysfunction of mitochondria'. Biomed Res Int 238463.

Choi AI, Li Y, Parikh, et al. (2010). 'Long-term clinical consequences of acute kidney injury in the HIV-infected'. Kidney Int 78:478-485.

Choi S, Reiter DA, Shardell M, Simonsick EM, Studenski S, Spencer RG, Fishbein KW, Ferrucci L (2016). '31P magnetic resonance spectroscopy assessment of muscle bioenergetics as a predictor of gait speed in the Baltimore longitudinal study of aging'. J. Gerontol. A Biol. Sci. Med. Sci. 71:1638-1645.

Chow DC, Bernas MA, Gangcuangco LM, et al. (2020). 'Frailty is associated with insulin resistance in chronic HIV'. Clin Infec Dis 71:1127-1128.

Chow FC, Feske S, Meigs JB, Grinspoon SK, Triant VA (2012). 'Comparison of ischemic stroke incidence in HIV-infected and non-HIV-infected patients in a US health care system'. J Acquir Immune Defic Syndr 60(4):351-358.

Chung YJ, Robert C, Gough SM, et al. (2014). 'Oxidative stress leads to increased mutation frequency in a murine model of myelodysplastic syndrome'. Leuk Res 38(1) 95-102.

Ciccosanti F, Corazzari M, Soldani F (2010). 'Proteomic analysis identifies prohibitin down-regulation as a crucial event in the mitochondrial damage observed in HIV-infected patients'. Antivir Ther 15: 377-90.

Cihlar T, Ho ES, Lin DC, Mulato AS (2001). 'Human renal organic anion transporter 1 (hOAT1) and its role in the nephrotoxicity of antiviral nucleotide analogs'. Nucleosides, Nucleotides and Nucleic Acids 20:641–648.

Cihlar T, Ray AS, Laflamme G, Vela JE, Tong L, Fuller MD, Roy A, Rhodes GR (2007). 'Molecular assessment of the potential for renal drug interactions between tenofovir and HIV protease inhibitors'. Antivir Ther 12:267–272.

Cipolat SO, Dal Zilio B, Scorrano L (2004). 'OPA1 requires mitofusin 1 to promote mitochondrial fusion'. Proc. Natl Acad. Sci. USA 101:15927–15932

Clayden P (2018). 'Fit for Purpose: Antiretroviral Treatment Optimisation'. London: HIV i-Base.

Clayton A (1982). 'Replication of animal mitochondrial DNA'. Cell 28:693-705.

Clegg A, Hassan-Smith (2018). 'Frailty and the endocrine system'. Lancet Diab Endocrinol 6:743-752.

Clegg A, Young J, Iliffe S, Rikkert MO, Rockwood K (2013). 'Frailty in elderly people'. Lancet 381:752-762.

Coca S, Perazella MA (2002). 'Acute renal failure associated with tenofovir: evidence of drug-induced nephrotoxicity'. Am J Med Sci 324:342–344.

Coca SG, Cho KC, Hsu CY (2011). 'Acute kidney injury in the elderly: predisposition to chronic kidney disease and vice versa'. Nephron Clinical practice. 119(Suppl 1):c19–24.

Coen PM, Jubrias SA, Distefano G, Amati F, Mackey DC, Glynn NW, Manini TM, Wohlgemuth SE, Leeuwenburgh C, Cummings SR (2013). 'Skeletal muscle mitochondrial energetics are associated with maximal aerobic capacity and walking speed in older adults'. J Gerontol A Biol Sci Med Sci 68: 447-455.

Cogliati S, Enriquez JA, Scorrano L (2016). 'Mitochondrial cristae: where beauty meets functionality'. Mitochondrial & Metabolism 41:261-273.

Cogswell AM, Stevens RJ, Hood DA (1993). 'Properties of skeletal muscle mitochondria isolated from subsarcolemmal and intermyofibrillar regions'. Am J Physiol 264:C383-C389.

Cohen AH, Nast CC (1988). 'HIV-associated nephropathy. A unique combined glomerular, tubular, and interstitial lesion'. Mod Pathol. 1:87–97.

Cole NB, Daniels MP, Levine RL, Kim G (2011). 'Oxidative stress causes reversible changes in mitochondrial permeability and structure'. Exp Gereontol 45:596-602.

Collard RM, Boter H, Schoevers RA, Oude Voshaar RC (2012). 'Prevalence of frailty in community-dwelling older persons: a systematic review'. J Am Geriatr Soc 60:1487-1492.

Collerton J, Van Otterdijk SD, Davies K, Martin-Ruiz C, Von Zglinicki T, Kirkwood TBL, Jagger C, Mathers J , Strathdee G (2014). 'Acquisition of aberrant DNA methylation is associated with frailty in the very old: findings from the Newcastle 85+ study'. Biogerontology 15:317–328.

Collins CA, Zammit PA, Ruiz AP, Morgan JE, Partridge TA. (2007). 'A population of myogenic stem cells that survives skeletal muscle aging'. Stem Cell 25 (4):885-894

Conboy IM, Conboy MJ, Smythe GM, Rando TA (2003). 'Notch-mediated restoration of regenerative potential to aged muscle'. Science 302:1575– 1577.

Conboy IM, Conboy MJ, Wagers AJ, Girma ER, Weissman IL, Rando TA. (2005). 'Rejuvenation of aged progenitor cells by exposure to a young systemic environment'. Nature 433:760–764.

Concepcion-Huertas M, Chirosa LJ, de Haro T, Chirosa IJ, Romero V, AguilarMartinez D, Leonardo-Mendonça RC, Doerrier C, Escames G, Acuña, Castroviejo D (2013). 'Changes in the redox status and inflammatory response in handball players during one-year of competition and training'. J. Sports Sci 31:1197–1207.

Consitt LA, Bell JA, Houmard JA (2009). 'Intramuscular lipid metabolism, insulin action, and obesity'. IUBMB Life 61:47-55.

Contreras L, Drago I, Zampase E, Pozzan T (2010). 'Mitochondria: The calcium connection'. Biochim. Biophys. Acta 1797:6070618.

Cooper RD, Wiebe N, Smith N, Keiser P, Naicker S, Tonelli M (2010). 'Systematic review and meta-analysis: Renal safety of tenofovir disoproxil fumarate in HIV-infected patients'. Clin Infect Dis 51: 496–505.

Coppé JP, Patil CK, Rodier F, Sun Y, Muñoz DP, Goldstein J, Nelson PS, Desprez PY, Campisi J (2008). 'Senescence-associated secretory phenotypes reveal cell-nonautonomous functions of oncogenic RAS and the p53 tumor suppressor'. PLoS Biol 6.

Corral-Debrinski M, Stepien G, Shoffner JM, Lott MT, Kanter K, Wallace DC (1991). 'Hypoxemia is associated with mitochondrial DNA damage and gene induction. Implications for cardiac disease'. JAMA 266:1812–1816.

Cory S, Adams JM (2002). 'The Bcl2 family: regulators of the cellular life-or-death switch'. Nat Rev Cancer 2:647-656.

Cote HCF (2005). 'Possible ways nucleoside analogues can affect mitochondrial DNA content and gene expression during HIV therapy'. Antivir Ther 10.

Cote HCF, et al. (2008). 'Perinatal exposure to antiretroviral therapy is associated with increased blood mitochondrial DNA levels and decreased mitochondrial gene expression in infants'. J Infec Dis 198:851-859.

Cote HCF, Magil A, Harris M, et al. (2006). 'Exploring mitochondrial nephrotoxicity as a potential mechanism of kidney dysfunction among HIV-infected patients on highly active antiretroviral therapy'. Antivir Ther 11:79–86.

Couve E, Osorio R, Schmachtenberg O (2012). 'Mitochondrial autophagy and lipofuscin accumulation in aging odontoblasts'. J. Dent. Res. 91:696–701.

Crane HM, Kestenbaum B, Harrington RD, Kitahata MM (2007). 'Amprenavir and didanosine are associated with declining kidney function among patients receiving tenofovir'. AIDS 21:1431–1439.

Cree LM, Samuels DC, de Sousa Lopes SC, Rajasimha HK, Wonnapinij P, Mann JR, Dahl H-HM, Chinnery PF (2008). 'A reduction of mitochondrial DNA molecules during embryogenesis explains the rapid segregation of genotypes'. Nat Genet 40:249-254.

Crocker TF, Brown L, Clegg A, Farley K, Franklin M, Simpkins S, Young J (2019). 'Quality of life is substantially worse for community-dwelling older people living with frailty: systematic review and meta-analysis'. Qual Life Res 28:2041-2056.

Croston TL, Thapa D, Holden AA, Tveter KJ, Lewis SE, Shepherd DL, Nichols CE, Long DM, Olfert IM, Jagannathan R, et al. (2014). 'Functional deficiencies of subsarcolemmal mitochondria in the type 2 diabetic human heart'. Am. J. Physiol. Heart Circ. Physiol. 307:H54–H65.

Cruz-Jentoft AJ, Bauer J, et al. (2019). 'Sarcopenia: revised European consensus on definition and diagnosis'. Age and Ageing 48:16-31.

Cruz-Jentoft AJ, Schneider SM, Zuniga C, et al. (2014). 'Prevalence of and interventions for sarcopenia in ageing adults: a systematic review. Report of the International Sarcopenia Initiative (EWGSOP and IWGS)'. Age Ageing 43:748-759.

Cruz-Jentoft AJ, Topinkova E, Michel J-P (2010). 'Understanding sarcopenia as a geriatric syndrome'. Current Opinion in Clinical Nutrition and Metabolic Care 131:1-7.

Cui H, Kong Y, Zhang H (2012). 'Oxidative Stress, Mitochondrial Dysfunction, and Aging'. Journal of Signal Transduction 13.

Cupler EJ, Danon MJ, Jay C, et al. (1996). 'Early features of zidovudine-associated myopathy: histopathological findings and clinical correlations'. Acta Neuropathol 90:1-6.

Curcio F, Ferro G, Basile C, et al. (2016). 'Biomarkers in sarcopenia: a multifactorial approach'. Exp Gerontol 85: 1–8.

D’Agati V, Suh JI, Carbone L, et al. (1989). ‘Pathology of HIV-associated nephropathy: a detailed morphologic and comparative study’. Kidney Int. 35:1358–1370.

D’Arcy MS (2019). ‘Cell death: a review of the major forms of apoptosis, necrosis and autophagy’. Cell Biol Int 43.

da Silva VD, Tribess S, Meneguci J, Sasaki JE, et al. (2019). ‘Association between frailty and the combination of physcial activity level and sedentary behaviour in older adults’. BMC Public Health 19:709.

Daems WT, Wisse E (1966). ‘Shape and attachment of the cristae mitochondriales in mouse hepatic cell mitochondria’. J Ultrastructure 16:123-140.

Dalakas MC, Semino-Mora C, Leon-Monzon M (2001). ‘Mitochondrial alterations with mitochondrial DNA depletion in the nerves of AIDS patients with peripheral neuropathy induced by 2’3’-dideoxycytidine (ddC)’. Lab Invest 81:1537-44.

Dali-Youcef N, Mecili M, Ricci R, Andres E (2013). ‘Metabolic inflammation: connecting obesity and insulin resistance’. Ann Med. 45(3):242–253.

D'Antona G, Pellegrino MA, Adami R, Rossi R, Carlizzi CN, Canepari M, et al. (2003). ‘The effect of ageing and immobilization on structure and function of human skeletal muscle fibres’. J Physiol 552(Pt 2):499–511.

Das A, Bonkowski MS, Longchamp A, Li C, Schultz MB, et al. (2018). ‘Impairment of an endothelial NAD(+)-H2S signaling network is a reversible cause of vascular aging.’ Cell 173:74e20–89e20.

Davidson AJ (2009). ‘Mouse kidney development’. Harvard Stem Cell Institute (Cambridge, MA).

Day K, Shefer G, Shearer A, Yablonka-Reuveni Z (2010). ‘The depletion of skeletal muscle satellite cells with age is concomitant with reduced capacity of single progenitors to produce reserve progeny’. Dev Biol 340:330– 343.

de Brito OM, Scorrano L. (2008). ‘Mitofusin 2 tethers endoplasmic reticulum to mitochondria’. Nature 456:605–610.

de Brito-Neto JG, de Andrade MF, de Almeida VD, et al. (2019). ‘Strength training improves body composition, muscle strength and increases CD4+ T lymphocyte levels in people living with HIV/AIDS’. Infect Dis Rep, 11:7925.

De Buyser SL, Petrovic M, Taes YE, et al. (2016). ’Validation of the FNIH sarcopenia criteria and SOF frailty index as predictors of long-term mortality in ambulatory older men’. Age Ageing 45:602–8.

De Fanis U, Fedarko NS, Walston JD, Casolaro V, Leng SX (2008). ‘T lymphocytes expressing CC chemokine receptor-5 are increased in frail older adults’. J. Am. Geriatr. Soc. 59:904-908.

de Grey AD (1997). ‘A proposed refinement of the mitochondrial free radical theory of aging’. Bioessays 19:161-166.

de Labra C, Guimaraes-Pinheiro C, Maseda A, Lorenzo T, Millan-Calenti JC (2015). ‘Effects of physical exercise interventions in frail older adults: a systematic review of randomized controlled trials’. BMC Geriatr 15:154.

De Martinis M, Franceschi C, Monti D, Ginaldi L (2006). ‘Inflammation markers predicting frailty and mortality in the elderly’. Exp. Mol. Pathol. 80:219–227.

de Waal R, Cohen K, Maartens G (2013). 'Systematic review of antiretroviral-associated lipodystrophy: lipoatrophy, but not central fat gain, is an antiretroviral adverse drug reaction'. PLoS One. 8(5):e63623.

Dedeyne L, Deschodt M, Verschueren S, Tournoy J, Gielen E (2017). 'Effects of multi-domain interventions in (pre)frail elderly on frailty, functional, and cognitive status: a systematic review'. Clin Interv Aging 12:873–896

Deeks SG (2011). 'HIV infection, inflammation, immunosenescence, and aging'. Ann Rev Med 62: 141-155.

Delettre C, et al. (2000). 'Nuclear gene OPA1, encoding a mitochondrial dynamin-related protein, is mutated in dominant optic atrophy'. Nat. Genet 26:207–210.

Dell'Orso S, Juan AH, Ko K-D, Naz F, et al. (2019). 'Single cell analysis of adult mouse skeletal muscle stem cells in homeostatic and regenerative conditions'. Techniques and resources 146.

Delmonico MJ, Harris TB, Visser M, et al. (2009). 'Longitudinal study of muscle strength, quality, and adipose tissue infiltration'. Am J Clin Nur 90:1579-1585.

Demongeot J, Glade N, Hansen O, Moreira A (2007). 'An open issue: the inner mitochondrial membrane (IMM) as a free boundary problem'. Biochimie 89:1049–1057

Deng W, Baki L, Yin J, Zhou H, Baumgarten CM. (2010). 'HIV protease inhibitors elicit volume-sensitive Cl- current in cardiac myocytes via mitochondrial ROS. Journal of molecular and cellular cardiology'. 49:746–52.

Deniaud A, Brenner C, Kroemer G (2004). 'Mitochondrial membrane permeabilization by HIV-1 Vpr'. Mitochondrion 4:223-233.

Dent E, Bergman H, Woo J, Romero-Ortuno R, Walston J D (2019). 'Management of frailty: opportunities, challenges, and future directions'. Lancet 394:1376-1386.

Denton RM (2009). 'Regulation of mitochondrial dehydrogenases by calcium ions'. Biochim. Biophys. Acta 1787:1309–1316.

Desai VG, et al. (2008). 'Effect of short-term exposure to zidovudine (AZT) on the expression of mitochondria-related genes in skeletal muscle of neonatal mice'. Mitochondrion 9:9-16.

Desco MC, Asensi M, Marquez R, Martinez-Valls J, Vento M, Pallardo FV, Sastre J, Vina J (2002). 'Xanthine oxidase is involved in free radical production in type 1 diabetes: protection by allopurinol'. Diabetes 51:1118-1124.

Desquilbet L, et al. (2007). 'HIV-1 infection is associated with an earlier occurrence of a phenotype related to frailty'. J Gerontol A Biol Sci Med Sci 62(1):1279-1286.

Desquilbet L, et al. (2009). 'Relationship between a frailty-related phenotype and progressive deterioration of the immune system in HIV-infected men'. J Acquir Immune Defic Syndr 50(3):299-306.

DeVay RM, Dominguez-Ramirez L, Lackner LL, Hoppins S, Stahlberg H, Nunnari J (2009). 'Coassembly of Mgm1 isoforms requires cardiolipin and mediates mitochondrial inner membrane fusion'. J Cell Biol 186:793-803.

Devenish RJ, Prescott M, Rodgers AJ (2008). 'The Structure and Function of Mitochondrial F1F0-ATP Synthases'. International Review of Cell and Molecular Biology 267:1-58.

Di Girolamo FG, Situlin R, Mazzucco S, Valentini R, Toigo G, Biolo G (2014). 'Omega-3 fatty acids and protein metabolism: enhancement of anabolic interventions for sarcopenia'. Curr Opin Clin Nutr Metab Care 17:145–150.

Di Nottia N, Carrozzo A, et al. (2017). 'Novel mutation in mitochondrial Elongation Factor EF-Tu associated to dysplastic leukoencephalopathy and defective mitochondrial DNA translation'. Biochim. Biophys. Acta 1863:961-967.

Diaz F (2010). 'Cytochrome c oxidase deficiency: Patients and animal models'. Biochimica et Biophysica Acta (BBA) - Molecular Basis of Disease 1802:100-110.

Dieter BP, Alicic RZ, Meek RL, et al. (2015). 'Novel therapies for diabetic kidney disease: Storied past and forward paths'. Diabetes Spectr 28:167–174.

Dihn HC, Bautmans I, Beyer I, et al. (2019). 'Association between immunosenescence phenotypes and pre-frailty in older subjects: does cytomegalovirus play a role?'. Journals of Gerontology 74:480-488.

Ding K, Wang H, Xu J, et al. (2014). 'Melatonin stimulates antioxidant enzymes and reduces oxidative stress in experimental traumatic brain injury: the Nrf2-ARE signaling pathway as a potential mechanism'. Free Radic Biol Med 73: 1–11.

Distefano G, Standley RA, Zhang X, et al. (2018). 'Physical activity unveils the relationship between mitochondrial energetics, muscle quality, and physical function in older adults'. J Cachexia Sarcopenia Muscle 9:279-294.

Distelmaier F, Visch H-J, Smeitink JAM, Mayatepek E, Koopman WJ, Willems PH (2009). 'The antioxidant Trolox restores mitochondrial membrane potential and Ca^{2+}-stimulated ATP production in human complex I deficiency'. J. Mol. Med. 87:515-522

Divo MJ, Martinez CH, Mannino DM (2016). 'Ageing and the epidemiology of multimorbidity'. Eur Respir J 44:1055-1068.

Dodds R, Sayer AA (2015).'Sarcopenia and frailty: new challenges for clinical practice'. Clin Med 15(suppl 6):88e91.

Dodds RM, Syddall HE, Cooper R et al. (2014). 'Grip strength across the life course: normative data from twelve British studies'. PLoS One 9:e113637.

Domenech E, Esteban-Martinez L, Partida D, Pascual R, Fernandez-Miranda G, Seco E, Campos-Olivas R, Perez M, Megias D, Allen K, Lopez M, Saha A K, Velasco G, Rial E, Mendez R, Boya P, Salazar-Roa M, Malumbres M (2015). 'AMPK and PFKFB3 mediate glycolysis and survival in response to mitophagy during mitotic arrest'. Nat Cell Biol 17:1304-1316.

Domingo P, Gutierrez Mdel M, Gallego-Escuredo JM, Torres F, Mateo GM, Villarroya J, et al. (2014). 'Effects of switching from stavudine to raltegravir on subcutaneous adipose tissue in HIV-infected patients with HIV/HAART-associated lipodystrophy syndrome (HALS). A clinical and molecular study'. PLoS One 9(2):e89088.

Dorshkind K, Montecino-Rodriquez E, Signer RA (2009). 'The ageing immune system: is it ever too old to become young again?'. Nat Rev Immunol 9:57– 62.

dos Santos L, Antunes M, Santos DA, Sardinha LB (2017). 'Sarcopenia and physical independence in older adults: the independent and synergic role of muscle mass and muscle function'. Journal of Cachexia, Sarcopenia and Muscle 8:245-250.

Dragic T, Thompson A, Cormier EG, et al. (2000). 'A binding pocket for a small molecule inhibitor of HIV-1 entry within the transmembrane helices of CCR5'. Proc Natl Acad Sci USA 97:5639-5644.

Dragovic G, Danilovic D, Dimic A, Jevtovic D (2014). 'Lipodystrophy induced by combination antiretroviral therapy in HIV/AIDS patients: a Belgrade cohort study'. Vojnosanit Pregl. 71(8):746–50.

Dresner A, Marcucci M, Griffin ME, Dufour S, Cline GW, Slezak LA, Andersen DK, Hundal RS, Rothman DL, Petersen KF, Shulman GI (1999). 'Effects of free fatty acids on glucose transport and IRS-1-associated phosphatidylinositol 3-kinase activity'. J Clin Invest 103:253-259.

Dreyer HC, Fujita S, Cadenas JG, Chinkes DL, Volpi E, Rasmussen BB (2006). 'Resistance exercise increases AMPK activity and reduces 4E-BP1 phosphorylation and protein synthesis in human skeletal muscle'. J Physiol 576:613–624.

Drummond MB, Kirk GD (2014). 'HIV-associated obstructive lung diseases: insights and implications for the clinician'. Lancet Respir Med. 2(7):583–92.

Dudzinska-Griszek J, Szuster K, Szeqieczek J (2017). 'Grip strength as a frailty diagnostic component in geriatric patients'. Clin Interv Aging 12:1151-1157.

Dugan LL, You YH, Ali SS, et al. (2013). 'AMPK dysregulation promotes diabetes-related reduction of superoxide and mitochondrial function'. J Clin Invest 123:4888–4899.

Dumont NA, Wang YX, von Maltzahn J, Pasut A, Bentzinger CF, Brun CE, et al. (2015). 'Dystrophin expression in muscle stem cells regulates their polarity and asymmetric division'. Nat Med 21:1455–1463.

Durieux J, Wolff S, Dillin A (2011). 'The cell-non-autonomous nature of electron transport chain-mediated longevity'. Cell 144:79–91.

Echeverria P, Bonjoch A, Puig J, et al. (2018). 'High prevalence of sarcopenia in HIV-infected individuals'. BioMed Research International :5074923.

Elmore S (2007). 'Apoptosis: A Review of Programmed Cell Death'. Toxicologic Pathology 35:495-516.

Elson JL, Samuels DC, Turnbull DM, Chinnery PF (2001). 'Random intracellular drift explains the clonal expansion of mitochondrial DNA mutations with age'. Am J Hum Genet 68:802-806.

Engeler DS, John H, Rentsch KM, Ruef C, Oertle D, Suter S (2002). 'Nelfinavir urinary stones'. J. Urol 167:1384-1385.

Enomoto L, Anderson PL, et al. (2011). 'Effect of nucleoside and nucleotide analog reverse transcriptase inhibitors on cell-mediated immune function'. AIDS Res Hum Retroviruses 27:47-55.

Ensrud KE, Schousboe JT, et al. (2018). 'Frailty phenotype and healthcare costs and utilization in older women'. J Am Geriatr Soc 66:1276–1283.

Ensrud KE, Taylor BC, Fink HA, et al. (2007). 'Frailty and Risk of Falls, Fracture, and Mortality in Older Women: The Study of Osteoporotic Fractures'. J Gerontol A Biol Sci Med Sci 62(7):744-751.

Erdei N, Toth A, Pasztor ET, Papp Z, Edes I, Koller A, Bagi Z (2006). 'High-fat diet induced reduction in nitric oxide-dependent arteriolar dilation in rats: role of xanthine oxidase-derived superoxide anion'. Am J Physiol Heart Circulatory Physiol 291:H2107-H2115.

Erlandson KM, Allshouse AA, Jankowski CM, Lee EJ, Rufner KM, Palmer BE, et al. (2013). 'Association of functional impairment with inflammation and immune activation in HIV type 1-infected adults receiving effective antiretroviral therapy'. J Infect Dis. 208(2):249–259.

Erlandson KM, et al. (2012a). 'Comparison of functional status instruments in HIV-infected adults on effective antiretroviral therapy'. HIV Clin Trials 13(6):324-334.

Erlandson KM, et al. (2012b). 'Risk factors for falls in HIV-infected persons'. J Acquir Immune Defic Syndr 61(4):484-489.

Erlandson KM, Karris MY (2019). 'HIV and Aging: Reconsidering the Approach to Management of Comorbidities'. Infect Dis Clin North Am 33(3):769-786.

Erlandson KM, Ng DK, Jacobson LP, Margolick JB, Dobs AS, Palella FJ Jr, et al. (2017a). 'Inflammation, immune activation, immunosenescence, and hormonal biomarkers in the frailty related phenotype of men with or at risk for HIV infection'. J Infect Dis. 215(2):228–37.

Erlandson KM, Shrack JA, Jankowski CM, Brown TT, Campbell TB (2014). 'Functional impairment, disability, and frailty in adults aging with HIV-infection'. Curr HIV/AIDS Rep 11:279-290.

Erlandson KM, Wu K, Koletar SL, Kalayjian RC, Ellis RJ, Taiwo B, et al. (2017b). 'Association between frailty and components of the frailty phenotype with modifiable risk factors and antiretroviral therapy'. J Infect Dis. 215(6):933–7

Escota GV, et al. (2016). 'High Prevalence of Low Bone Mineral Density and Substantial Bone Loss over 4 Years Among HIV-Infected Persons in the Era of Modern Antiretroviral Therapy'. AIDS Res Hum Retroviruses 32:59-67.

Escribese MM, Casas M, Corbi AL (2012). 'Influence of low oxygen tensions on macrophage polarization'. Immunobiology 217:1233-1240.

Eshleman SH, Mracna M, Guay LA, et al. (2001). 'Selection and fading of resistance mutations in women and infants receiving nevirapine to prevent HIV-1 vertical transmission (HIVNET 012)'. AIDS 15(15):1951–1957.

Esteban-Martinez L, Sierra-Filardi E, McGreal RS, et al. (2017). 'Programmed mitophagy is essential for the glycolytic switch during cell differentiation'. EMBO J 36.

Etman A, Van der Cammen TJ, et al. (2012). 'Socio-demographic determinants of worsening in frailty among community-dwelling older people in 11 European countries'. J Epidemiol Community Health 66:1116-1121.

Fabbri E, An Y, Zoli M, et al. (2015). 'Aging and the burden of multimorbidity: associations with inflammatory and anabolic hormonal biomarkers'. J Gerontol A Biol Sci Med Sci 70:63–70.

Fabbri E, Spencer RG, Fishbein KW, et al. (2017). 'Insulin resistance is assocaited with reduced mitochondrial oxidative capacity measured by 31P-magnetic resonance spectroscopy in participants without diabetes from the Baltimore Longitudinal Study of Aging'. Diabetes 66:170-176.

Fairhall N, Sherrington C, Lord SR, et al. (2014). 'Effect of a multifactorial, interdisciplinary intervention on risk factors for falls and fall rate in frail older people: A randomised controlled trial'. Age Ageing 43:616e622.

Falkenberg M (2018). 'Mitochondrial DNA replication in mammalian cells: overview of the pathway'. Essays in Biochemistry 62:287-296.

Falkenberg M, Gaspari M, Rantanen A, Trifunovic A, Larsson N-G, Gustafsson CM (2002). 'Mitochondrial transcription factors B1 and B2 activate transcription of human mtDNA'. Nat Genet 31:289-294.

Fan J, Kou X, Yang Y, Chen N (2016). 'MicroRNA-regulated proinflammatory cytokines in sarcopenia'. Mediat. Inflamm. 1438686.

Fan L, Farr CL, Schaefer KT, Randolph KM, Tainer JA, et al. (2006). 'A novel processive mechanism for DNA synthesis revealed by structure, modelling and mutagenesis of the accessory subunit of human mitochondrial DNA polymerase'. J. Mol. Biol 358:1229–1243.

Fanconi G (1936). 'Fruhinfantile nephrotiscglyko-surische Zwergwuch mit hypophosphatamischer rachitis'. Jahrbuch Ninderhrilkunde 147:299.

Faria NR, Rambaut A, Suchard MA, Baele G, Bedford T, Ward MJ, Tatem AJ, Sousa JD, Arinaminpathy N, Pépin J, Posada D, Peeters M, Pybus OG, Lemey P (2014). 'HIV epidemiology. The early spread and epidemic ignition of HIV-1 in human populations'. Science 346:56–61.

Fassone E, Rahman S (2012). 'Complex I deficiency: clinical features, biochemistry and molecular genetics'. J Med Genet. 249:578-590.

Fatti G, Mothibi E, Meintjes G, Grimwood A (2014). 'Antiretroviral treatment outcomes amongst older adults in a large multicentre cohort in South Africa'. PLoS One 9:e100273.

FDA (1987). 'Approval of small molecule Retrovir Capsules'.

Feeney ER, Mallon P (2010). 'Impact of mitochondrial toxicity of HIV-1 antiretroviral drugs on lipodystrophy and metabolic dysregulation'. Curr Pharm Des 16:3339-3351.

Feng Z, Lugtenberg M, Franse, *et al*.. (2017). 'Risk factors and protective factors associated with incident or increase of frailty among community-dwelling older adults: a systematic review of longitudinal studies'. PLos One 12:e0178383.

Fernandes Bertocchi AP, Campanhole G, Wang PH, et al. (2008). 'A role for galectin-3 in renal tissue damage triggered by ischemia and reperfusion injury'. Trans Int 21:999–1007.

Fernandez-Checa JC, Kaplowitz N, Garcia-Ruiz C, Colell A (1998). 'Mitochondrial glutathione: importance and transport'. Semin Liver Dis 18:389-401.

Fernandez-Garrido J, Ruiz-Ros V, Navarro-Martínez R, Buigues C, Martínez M, Verdejo Y, Sanantonio-Camps L, Mascarós M C, Cauli O (2018). 'Frailty and leucocyte count are predictors of all-cause mortality and hospitalization length in non-demented institutionalized older women.' Exp. Gerontol 103:80-86.

Fernando SK, Finkelstein FO, Moore BA, Weissman S (2008). 'Prevalence of chronic kidney disease in an urban HIV infected population'. Am J Med Sci 355:89–94.

Ferreira R, Alves RMP, et al. (2010). 'Subsarcolemmal and intermyofibrillar mitochondria proteome differences disclose functional specializations in skeletal muscle'. Proteomics 10:3142-54.

Ferri KF, Blanco J, et al. (2000). 'Apoptosis Control in Syncytia Induced by the HIV Type 1–Envelope Glycoprotein Complex'. JEM 192:1081-1092.

Ferrucci L, et al. (2002). 'Change in muscle strength explains accelerated decline of physical function in older women with high interleukin-6 serum levels'. J. Am. Geriatr. Soc 50:1947–1954.

Fevrier M, Dorgham K, Rebollo (2011). 'CD4+ T cell depletion in human immunodeficiency virus (HIV) infection: role of apoptosis'. Viruses 3:586-612.

Fielding RA, Evans WJ, Bhasin S, Morley JE, Newman AB, et al. (2011). 'Sarcopenia: an undiagnosed condition in older adults. Current consensus definition: prevalence, etiology, and consequences. International working group on sarcopenia'. J Am Med Dir Assoc 12:249-256.

Fields JA, Campos S, et al. (2016). 'HIV alters neuronal mitochondrial fission/fusion in the brain during HIV-Associated Neurocognitive Disorders'. Neurobiol Dis 86:154-169.

Fields JA, Swinton MK, Carson A, et al (2019). 'Tenofovir disoproxil fumarate induced peripheral neuropathy and alters inflammation and mitochondrial biogenesis in the brains of mice'. Sci Rep 9:17158.

Filippin L, Magalhaes PJ, Di Benedetto G, Colella M, Pozzan T (2003). 'Stable interactions between mitochondria and endoplasmic reticulum allow rapid accumulation of calcium in a subpopulation of mitochondria'. J. Biol. Chem 278:39224–39234.

Fink LN, et al. (2014). 'Pro-inflammatory macrophages increase in skeletal muscle of high fat-fed mice and correlate with metabolic risk markers in humans'. Obesity 22:747–757.

Fiorese CJ, Haynes CM (2017). 'Integrating the UPR(mt) into the mitochondrial maintenance network'. Crit. Rev. Biochem. Mol. Biol 52:304–313.

Flandre P, Pugliese P, Cuzin L, Bagnis CI, Tack I, Cabié A, Poizot-Martin I, Katlama C, Brunet-François C, Yazdanpanah Y, Dellamonica P (2011). 'New AIDS Data group : Risk factors of chronic kidney disease in HIV-infected patients'. Clin J Am Soc Nephrol 6:1700–1707.

Flores I, Canela A, Vera E, Tejera A, Cotsarelis G, Blasco MA (2008). 'The longest telomeres: a general signature of adult stem cell compartments'. Gene Dev 22:654– 667.

Fornica L, Cosntino M, Musaro A (2020). 'Mechanisms regulating muscle regeneration: insights into the interrelated and time-dependant phases of tissue healing'. Cells 9:1297.

Foy MC, Estrella MM, Lucas GM, et al. (2013). 'Comparison of risk factors and outcomes in HIV immune complex kidney disease and HIV-associated nephropathy'. Clin J Am Soc Nephrol. 8:1524–1532.

Fraizer AE, Thornburn DR, Compton AG (2019). 'Mitochondrial energy generation disorders: genes, mechanisms, and clues to pathology'. Journal of Biological Chemistry 294:5386-5395.

Fraizer AE, Vincent AE, Turnbull DM, et al. (2020). 'Chapter 5 – Assessment of mitochondrial respiratory chain enzymes in cells and tissues'. Methods in Cell Biology 155:121-156.

Franceschi C, Bonafe M, Valensin S, Olivieri F, De LM, Ottaviani E, et al. (2000). 'Inflamm-aging. An evolutionary perspective on immunosenescence'. Ann N Y Acad Sci. 908:244–254.

Franco I, Johansson A, Olsson K, et al. (2018). 'Somatic mutagenesis in satellite cells associates with human skeletal muscle aging'. Nat Comm 9.

Franco-Iborra S, Vila M, Perier C (2016). 'The Parkinson disease mitochondrial hypothesis: where are we at?'. Neuroscientist 22:266– 277.

Fratter C, Raman P, Alston CL, Blakely EL, et al. (2011). 'RRM2B mutations are frequent in familial PEO with multiple mtDNA deletions'. Neurology 76:2032-2034.

Fried LP (1998). 'Principles of Geriatric Medicine and Gerontology'. New York, McGraw Hill Health Professions Divisions (4th edn), McGraw-Hill, New York, NY:1387-1402.

Fried LP, Cappola AR, Ferrucci L, Chaves P, Varadhan R, Guralnik JM, Leng SX, Semba RD, Walston JD (2009). 'Nonlinear multisystem physiological dysregulation associated with frailty in older women: Implications for etiology and treatment'. J Gerontol A Biol Sci Med Sci 64:1049-1057.

Fried LP, F. L., Darer J, Williamson JD, Anderson G. (2004). 'Untangling the concepts of disability, frailty, and comorbidity: implications for improved targeting and care'. J Gerontol A Biol Sci Med Sci 59(3):255-263.

Fried LP, Tangen CM, Walston J, et al. (2001). 'Frailty in older adults: evidence for a phenotype'. J Gerontol A Biol Sci Med Sci 56:M146-156.

Friedlander AL, Butterfield GE, Moynihan S, et al. (2001). 'One year of insulin like growth factor I treatment does not affect bone density, body composition, or psychological measures in postmenopausal women'. J Clin Endocrinol Metab 86:1496–1503.

Friedman JR, Nunnari J (2014). 'Mitochondrial form and function'. Nature 505:335-343.

Frontera WR, Suh D, Krivickas LS, Hughes VA, Goldstein R, Roubenoff R (2000). 'Skeletal muscle fiber quality in older men and women'. Am J Physiol Cell Physiol 279:C611-8.

Frost R, Jovicic A, et al. (2017). 'Health promotion interventions for community-dwelling older people with mild or pre-frailty: a systematic review and meta-analysis'. BMC Geriatr 17:157.

Fry C, et al. (2015). 'Inducible depletion of satellite cells in adult, sedentary mice impairs muscle regenerative capacity without affecting sarcopenia'. Nat. Med 21:76–80.

Fu Y, Zhu JY, Richman A, et al. (2017). 'APOL1-G1 in Nephrocytes Induces Hypertrophy and Accelerates Cell Death'. J Am Soc Nephrol 28:1106–1116.

Fukui H, Moraes CT. (2009). 'Mechanisms of formation and accumulation of mitochondrial DNA deletions in aging neurons'. Hum Mol Genet 18:1028-1036.

Funes HA, Apostolova N, Alegre F, et al. (2014). 'Neuronal bioenergetics and acute mitochondrial dysfunction: a clue to understanding the central nervous system side effects of efavirenz'. J Infect Dis 210:1385-95.

Gale CR, Westbury L, Cooper C (2018). 'Social isolation and loneliness as risk factors for the progression of frailty: the English Longitudinal Study of Ageing'. Age Ageing 47(3):392-397.

Gallant JE, Parish MA, Keruly JC, Moore RD (2005). 'Changes in renal function associated with tenofovir disoproxil fumarate treatment, compared with nucleoside reverse-transcriptase inhibitor treatment'. Clin Infect Dis 40:1194–1198.

Gallant JE, Pozniak AL, DeJesus E, Suleiman JM, Miller MD, et al. (2004). 'Efficacy and safety of tenofovir DF vs stavudine in combination therapy in antiretroviral-naive patients: a 3-year randomized trial'. JAMA 292:191–201.

Galloway CA, Lee H, Nejjar S, et al. (2012). 'Transgenic control of mitochondrial fission induces mitochondrial uncoupling and relieves diabetic oxidative stress'. Diabetes. 61:2093–2104.

Gao F, Bailes E, Robertson DL, Chen Y, Rodenburg CM, Michael SF, Cummins LB, Arthur LO, Peeters M, Shaw GM, Sharp PM, Hahn BH (1999). 'Origin of HIV-1 in the chimpanzee Pan troglodytes'. Nature 397:436–441.

Garcia ML, Fernandez A, Solas MT (2013). 'Mitochondria, motor neurons and aging'. J. Neurol. Sci 330:18–26.

Garcia-Prat L, Sousa-Victor P, Munoz-Canoves P (2013). 'Functional dysregulation of stem cells during aging: a focus on skeletal muscle stem cells'. FEBS J, 280 (17) (2013), pp. 4051-4062.
Gatica D, L. V., Klionsky D J (2018). 'Cargo recognition and degradation by selective autophagy'. Nat. Cell Biol 20:233–242.

Gaut JP, Liapis H (2020). 'Acute kidney injury pathology and pathophysiology: a retrospective review'. Clinical Kidney Journal, sfaa142.

Gayet-Ageron A, Ananworanich J, Jupimai T, Chetchotisakd P, Prasithsirikul W, Ubolyam S, Le Braz M, Ruxrungtham K, Rooney JF, Hirschel B, Staccato Study Group (2007). 'No change in calculated creatinine clearance after tenofovir initiation among Thai patients'. J Antimicrob Chemother 59: 1034–1037.

GBD collaborators (2019). 'Global, regional, and national incidence, prevalence, and mortality of HIV, 1980–2017, and forecasts to 2030, for 195 countries and territories: a systematic analysis for the Global Burden of Diseases, Injuries, and Risk Factors Study 2017'. Lancet HIV 6:E831-E859.

Gellerich FN, Gizatullina Z, Arandarcikaite O, Jerzembek D, Vielhaber S, Seppet E, Striggow F (2009). 'Extramitochondrial Ca2+ in the nanomolar range regulates glutamate-dependent oxidative phosphorylation on demand'. PLOS ONE 4:e8181.

Genton L, Karsegard VL, Chevalley T, Kossovsky MP, Darmon P, Pichard C (2011). 'Body composition changes over 9 years in healthy elderly subjects and impact of physical activity'. Clin Nutr 30: 436e442.

Gerasimenko JV, Tepikin AV, Petersen OH, Gerasimenko OV (1998). 'Calcium uptake via endocytosis with rapid release from acidifying endosomes'. Curr Biol 8:1335-1338.

Giacca M (2005). 'HIV-1 Tat, apoptosis and the mitochondria: a tubulin link?'. Retrovirology 2:7.

Giacomello M, Pyakurel A, Glytsou C, Scorrano L (2020). 'The cell biology of mitochondrial membrane dynamics'. Nat Rev Mol Cell Biol 21:204-224.

Gilbert T, Kraindler J, et al (2018). 'Development and validation of a Hospital Frailty Risk Score focusing on older people in acute care settings using electronic hospital records: an observational study'. Lancet 391:1775-1782.

Gilead Sciences Inc (2001). 'Drug approval package for NDA 21–356: VIREAD (tenofovir disoproxil fumarate). US Food and Drug Administration FDA Report'. Pharmacology review, 2001.

Giles RE, Blanc H, Cann HM, Wallace DC (1980). 'Maternal inheritance of human mitochondrial DNA'. Proc Natl Acad Sci USA 77:6715-6719.

Gill TM, Gahbauer EA, Allore HG, Han L (2006). 'Transitions between frailty states among community-living older persons'. Arch Intern Med 166:418–423.

Gine-Garriga M, Roque-Figuls M, Coll-Planas L, Sitja-Rabert M, Salva A (2014). 'Physical exercise interventions for improving performance-based measures of physical function in community-dwelling, frail older adults: a systematic review and meta-analysis'. Arch Phys Med Rehabil 95:753–769.e753.

Giuliani A, Prattichizzo F, Mensà E, Fulgenzi G, Sabbatinelli J, Graciotti L, Olivieri F, Procopio A D, Tiano L, Rippo M R (2018). 'The mitomiR/Bcl-2 axis affects mitochondrial function and autophagic vacuole formation in senescent endothelial cells'. Aging (Albany. NY) 10:2855–2873.

Glancy B, et al. (2015). 'Mitochondrial reticulum for cellular energy distribution in muscle'. Nature 523:617–620.

Glass DJ (2010). 'PI3 kinase regulation of skeletal muscle hypertrophy and atrophy'. Curr Top Microbiol Immunol 346:267–278.

Glidden DV, Mulligan K, McMahan V, Anderson PL, Guanira J, Chariyalertsak S, Buchbinder SP, Bekker LG, Schechter M, Grinsztejn B, Grant RM. (2018). 'Metabolic Effects of Preexposure Prophylaxis With Coformulated Tenofovir Disoproxil Fumarate and Emtricitabine'. Clin Infect Dis. 67(3):411-419.

Go AS, Chertow GM, Fan D, McCulloch CE, Hsu CY (2004). 'Chronic kidney disease and the risks of death, cardiovascular events, and hospitalization'. New England Journal of Medicine 351(13):1296–1370.

Goicoechea M, Best B, et al. (2008). 'Greater tenofovir-associated renal function decline with protease inhibitor-based versus nonnucleoside reverse-transcriptase inhibitor-based therapy'. Journal of Infectious Diseases 197(1):102–108.

Gonen O, Toledano H (2014). 'Why adult stem cell functionality declines with age? Studies from the fruit fly Drosophila melanogaster model organism'. Curr Genomics 15(3):231-236

Gonzalez-Freire M, de Cabo R, Studenski SA, Ferrucci L (2014). 'The neuromuscular junction: aging at the crossroad between nerves and muscle'. Front Aging Neuroscience 6.

Goodpaster BH, Harris TB, Kritchevsky SB, Nevitt M, Schwartz AV, et al. (2006). 'The loss of skeletal muscle strength, mass, and quality in older adults: the health, aging and body composition study'. J Gerontol A Biol Sci Med Sci 61:1059-1064.

Gopinath SD, Rando TA (2008). 'Stem cell review series: aging of the skeletal muscle stem cell niche'. Aging Cell 7:590-598.

Gorman GS, DiMauro S, Hirano M, Koga Y, McFarlannd R et al. (2016). 'Mitochondrial diseases'. Nature Reviews Disease Primers 2:1-22.

Gorman GS, Ng Y, Gomez N, Blakely E L, Alston C L, Feeney C, Horvath R, et al. (2015). 'Prevalence of nuclear and mitochondrial DNA mutations related to adult mitochondrial disease'. Ann Neurol 77: 753-759.

Goudenege S, Huot NB, Dufour C, Fujii I, Gekas J, et al. (2012). 'Myoblasts derived from normal hESCs and dystrophic hiPSCs efficiently fuse with existing muscle fibers following transplantation'. Molecular therapy: the journal of the American Society of Gene Therapy 20:2153–2167.

Grady JP, Greaves LC, Ratnaike T, Blakely E L, et al. (2014). 'Disease progression in patients with single, large-scale mitochondrial DNA deletions'. Brain: A Journal of Neurology 137:323-334.

Gray H, Wong TW (1992). 'Purification and identification of subunit structure of the human mitochondrial DNA polymerase'. J. Biol. Chem 267:5835–5841.

Greaves LC, Elson JL, Nooteboom M, Grady J P, Taylor G A, Taylor R W, Mathers J C, Kirkwood T B L, Turnbull D M (2012). 'Comparison of mitochondrial mutation spectra in ageing human colonic epithelium and disease: Absence of evidence for purifying selection in somatic mitochondrial DNA point mutations'. PLoS Genet 8:e1003082.

Greene M, Valcour V, et al. (2015). 'Geriatric Syndromes in Older HIV-Infected Adults'. J Acquir Immune Defic Syndr 69:161-167.

Griffin ME, Marcucci MJ, Cline GW, Bell K, Barucci N, Lee D, Goodyear LJ, Kraegen EW, White MF, Shulman GI (1999). 'Free fatty acid-induced insulin resistance is associated with activation of protein kinase C theta and alterations in the insulin signaling cascade'. Diabetes 48:1270-1274.

Grimby G (1995). 'Muscle performance and structure in the elderly as studied cross-sectionally and longitudinally'. J. Gerontol. A Biol. Sci. Med. Sci. 50:17–22.

Grobbler JA, Hu B, Witmer M, Felock P, et al. (2002). 'Diketo acid inhibitor mechanism and HIV-1 integrase: Implications for metal binding in the active site of phosphotransferase enzymes'. PNAS 99:6661-6666.

Guadalupe M, Reay E, Sankaran S, Prindiville T (2003). 'Severe CD4+ T-cell depletion in gut lymphoid tissue during primary human immunodeficiency virus type 1 infection and substantial delay in restoration following highly active antiretroviral therapy'. J Virol 77:11708-11717.

Guaraldi G, et al. (2015). 'A frailty index predicts survival and incident multimorbidity independent of markers of HIV disease severity'. AIDS 29(13):1633-1641.

Guaraldi G, et al. (2019b). 'The interplay between age and frailty in people living with HIV: results from an 11-year follow-up observational study'. Open Forum Infectious Diseases 6(5):ofz199.

Guaraldi G, Malagoli A, Theou O, Brothers TD, Wallace L, Torelli R, et al. (2017). 'Correlates of frailty phenotype and frailty index and their associations with clinical outcomes'. HIV Med 18(10):764– 71

Guaraldi G, Orlando G, Zona S, Menozzi M, Carli F, Garlassi E, et al. (2011). 'Premature age-related comorbidities among HIV-infected persons compared with the general population'. Clin Infect Dis 53:1120–1126

Guaraldi G, Zona S, Silva AR, Menozzi M, Dolci G, Milic J, et al. (2019a). 'The dynamic association between frailty, CD4 and CD4/CD8 ratio in people aging with HIV'. PLoS One 14(2):e0212283

Guillet C, Masgrau A, Walrand S, Boirie Y (2012). 'Impaired protein metabolism: interlinks between obesity, insulin resistance and inflammation'. Obes Rev 13:51e57.

Gulick RM (2018). 'New HIV drugs: 2018 and beyond'. Curr Opin HIV AIDS 13:291–293.

Guo LJ, Oshida Y, Fuku N, Takeyasu T, Fujita Y, Kurata M, Sato Y, Ito M, Tanaka M (2005). 'Mitochondrial genome polymorphisms associated with type-2 diabetes or obesity'. Mitochondrion 5:15-33.

Gupta SK (2008). 'Tenofovir-associated Fanconi syndrome: Review of the FDA adverse event reporting system'. AIDS Patient Care STDS 22:99–103.

Gupta SK, Anderson AM, Ebrahimi R, Fralich T, Graham H, Scharen-Guivel V, Flaherty JF, Fortin C, Kalayjian RC, Rachlis A, Wyatt CM (2014). 'Fanconi syndrome accompanied by renal function decline with tenofovir disoproxil fumarate: A prospective, case-control study of predictors and resolution in HIV-infected patients'. PLoS One 9:e92717

Guralnik JM, Simonsick EM, Ferrucci L, Glynn RJ, Berkman LF, Blazer DG, Scherr PA, Wallace RB (1994). 'A short physical performance battery assessing lower extremity function: Association with self-reported disability and prediction of mortality and nursing home admission'. Gerontology 49: M85–M94.

Gutmann H, Fricker G, Drewe J, Toeroek M, Miller DS (1999). 'Interactions of HIV protease inhibitors with ATP-dependent drug export proteins'. Mol. Pharmacol 56:383-389.

Guzman N, Vijayan V (2020). 'HIV-associated lipodystrophy'. StatPearls Publishing.

Gwyther H, Bobrowicz-Campos E, Luis Alves Apostolo J, Marcucci M, Cano A, Holland C (2018). 'A realist review to understand the efficacy and outcomes of interventions designed to minimise, reverse or prevent the progression of frailty'. Health Psychol Rev 12:382-404.

Haas DW, Geraghty DE, Andersen J, et al. (2006). 'Immunogenetics of CD4 lymphocyte count recovery during antiretroviral therapy: an AIDS Clinical Trials Group study'. J Infect Dis 194:1098–107.

Habets P, Franco D, Ruijter JM, Sargeant AJ, Pereira J, Moorman AFM (1999). 'RNA content differs in slow and fast muscle fibers: implications for interpretation of changes in muscle gene expression'. J Histochem Cytochem 47 995–1004.

Hackenbrock CR (1966). 'Ultrastructural bases for metabolically linked mechanical activity in mitochondria. I. reversible ultrastructural changes with change in metabolic steady state in isolated liver mitochondria'. J. Cell Biol 30:269–297.

Hall AM (2013). 'Update on tenofovir toxicity in the kidney'. Pediatric Nephrology 28: 1011–1023.

Hall AM, Hendry BM, Nitsch D, Connolly JO (2011). 'Tenofovir-associated kidney toxicity in HIV-infected patients: A review of the evidence'. Am J Kidney Dis 57: 773–780.

Hamzah L, Jose S, Booth JW, et al. (2017). 'Treatment-limiting renal tubulopathy in patients treated with tenofovir disoproxil fumarate'. J Infect. 74:492–500.

Han XJ, Lu YF, Li SA, et al. (2008). 'CaM kinase I alpha-induced phosphorylation of Drp1 regulates mitochondrial morphology'. J Cell Biol 182:573–585.

Handforth C, Young C, et al. (2015). 'The prevalence and outcomes of frailty in older cancer patients: a systematic review'. Ann Oncol 26:1091-1101.

Hanlon P, Nicholl BI, Jani BD, Lee D, McQueenie R, Mair FS (2018). 'Frailty and pre-frailty in middle-aged and older adults and its association with multimorbidity and mortality: a prospective analysis of 493 737 UK Biobank participants'. Lancet Public Health 3:e323–332.

Hanlon PH, Nicholl BI, Jani BD (2018). 'Frailty and prefrailty in middle-aged and older adults and its association with multimorbidity and mortality: a prospective analysis of 493,737 UK biobank participants'. Lancet Public Health 3:e323-332.

Hanoken AH, Isohanni P, Paetau A, Herva R, Suomalainen A (2007). 'Recessive Twinkle mutations in early onset encephalopathy with mtDNA depletion'. Brain 130:3032-3040.

Hardeland R (2005). 'Antioxidative protection by melatonin: multiplicity of mechanisms from radical detoxification to radical avoidance'. Endocrine 27:119–130.

Hardie DG (2007). 'AMP-activated/SNF1 protein kinases: conserved guardians of cellular energy'. Nat. Rev. Mol. Cell Biol 8:774–785.

Harman D (1956). 'Aging: a theory based on free radical and radiation chemistry'. Journal of gerontology 11:289-300.

Harman D (1972). 'The biologic clock: the mitochondria?'. Journal of American Geriatric Society 20(4):145-147.

Harper JW, Ordureau A, Heo JM (2018). 'Building and decoding ubiquitin chains for mitophagy'. Nat. Rev. Mol. Cell Biol. 19:93–108.

Hartleben B, Godel M, Meyer-Schwesinger C, et al. (2010). 'Autophagy influences glomerular disease susceptibility and maintains podocyte homeostasis in aging mice'. J Clin Invest. 120:1084–1096.

Hasegawa K, Wakino S, Simic P, et al. (2013). 'Renal tubular Sirt1 attenuates diabetic albuminuria by epigenetically suppressing Claudin-1 overexpression in podocytes'. Nat Med. 19:1496–1504.

Hatton C, Reeve AK, Lax NZ, Erskine D, et al. (2020). 'Complex I reductions in the nucleus basalis of Meynert in Lewy body dementia the role of lew bodies'. Acta Neuropatho Comm 8:103.

Håversen L, Danielsson KN, Fogelstrand L, Wiklund O (2009). 'Induction of proinflammatory cytokines by long-chain saturated fatty acids in human macrophages'. Atherosclerosis 202:382-393.

Hawley JA, Burke LM, Angus DJ, Fallon KE, Martin DT, Febbraio MA (2000). 'Effect of altering substrate availability on metabolism and performance during intense exercise'. Br J Nutr 84:829-838.

Hayes JD, Dinkova-Kostova T, Tew KD (2020). 'Oxidative stress in cancer'. Cancer Cell 38:167-197.

Haynes CM, Petrova K, Benedetti C, Yang Y, Ron D (2007). 'ClpP mediates activation of a mitochondrial unfolded protein response in C. elegans'. Dev. Cell 13:467–480.

He L, Chinnery PF, Durham SE, et al. (2002). 'Detection and quantification of mitochondrial DNA deletions in individual cells by real-time PCR'. Nucleic Acids Research 30:e68.

He L, Pan X, Dou Z, Huang P, Zhou X, Peng Z, et al. (2016). 'The Factors Related to CD4+ T-Cell Recovery and Viral Suppression in Patients Who Have Low CD4+ T Cell Counts at the Initiation of HAART: A Retrospective Study of the National HIV Treatment Sub-Database of Zhejiang Province, China'. PLoS One 11:e0148915.

Heilbronn LK, Gan SK, Turner N, Campbell LV, Chisholm DJ. (2007). 'Markers of mitochondrial biogenesis and metabolism are lower in overweight and obese insulin-resistant subjects'. Journal of Clinical Endocrinology and Metabolism 92:1467–1473.

Hepple RT, Rice CL (2016). 'Innervation and neuromuscular control in ageing skeletal muscle'. J Physiol 594(8).

Herlitz LC, Mohan S, Stokes MB, Radhakrishnan J, D'Agati VD, Markowitz GS (2010). 'Tenofovir nephrotoxicity: acute tubular necrosis with distinctive clinical, pathological, and mitochondrial abnormalities'. Kidney International 78:1171-1177.

Hershberger KA, Martin AS, Hirschey MD (2017). 'Role of NAD+ and mitochondrial sirtuins in cardiac and renal diseases'. Nat Rev Nephrol 13:213–225.

Hirabara SM, Curi R, Maechler P (2010). 'Saturated fatty acid-induced insulin resistance is associated with mitochondrial dysfunction in skeletal muscle cells'. J Cell Physiol 222:187-194.

Hirabara SM, Silveira LR, Abdulkader F, Carvalho CR, Procopio J, Curi R (2007). 'Time-dependent effects of fatty acids on skeletal muscle metabolism'. Cell Physiol 210:7-15.

Hirsch C, Newman A, Kop W, Jackson S, et al. (2006). 'The association of race with frailty: the cardiovascular health study'. Ann Epidemiol 16:545-553.

Hoehn KL, Hohnen-Behrens C, Turner N, Hoy A J, Maghzal G J, Stocker R, Van Remmen H, Kraegen E W, Cooney G J, et al. (2009). 'Insulin resistance is a cellular antioxidant defence mechanism'. PNAS 106:17787–17792.

Hohn A, Grune T (2013). 'Lipofuscin: formation, effects and role of macroautophagy'. Redox Biology 1:140-144.

Höhn A, Jung T, Grimm S, Catalgol B, Weber D, Grune T. (2011). 'Lipofuscin inhibits the proteasome by binding to surface motifs'. Free Radic. Biol. Med. 50:585–591.

Höhn A, Jung T, Grimm S, Grune, T. (2010). 'Lipofuscin-bound iron is a major intracellular source of oxidants: role in senescent cells'. Free Radic. Biol. Med. 48:1100–1108.

Holland WL, Summers SA (2008). 'Sphingolipids, insulin resistance, and metabolic disease: new insights from in vivo manipulation of sphingolipid metabolism'. Endocr Rev 29:381-402.

Hollensworth SB, Shen C, Sim JE, et al. (2000). 'Glial cell type-specific responses to menadione-induced oxidative stress'. Free Radic Biol Med 28(8):1161–1174.

Holloway GP, Thrish AB, Heigenhauser GJ, Tandon NN, Dyck DJ, Bonen A, Spriet LL (2007). 'Skeletal muscle mitochondrial FAT/CD36 content and palmitate oxidation are not decreased in obese women'. Am J Physiol Endocrinol Metab 292:1782-1789.

Holt IJ, Harding AE, Cooper JM, Schapira AH, Toscano A, Clark JB, Morgan-Hughes JA (1989). 'Mitochondrial myopathies: clinical and biochemical features of 30 patients with major deletions of muscle mitochondrial DNA'. Ann Neurol 26:699-708.

Holt IJ, Lorimer HE, Jacobs HT (2000). 'Coupled Leading- and Lagging-Strand Synthesis of Mammalian Mitochondrial DNA'. Cell 100:515-524.

Holt IJ, Reyes A (2012). 'Human Mitochondrial DNA Replication'. Cold Spring Harbor Perspectives in Biology 4:a012971.

Hong EG, et al. (2009). 'Interleukin-10 prevents diet-induced insulin resistance by attenuating macrophage and cytokine response in skeletal muscle'. Diabetes 58:2525–2535.

Hood DA (2001). 'Contractile activity-induced mitochondrial biogenesis in skeletal muscle.' J App Physiol 90:1137-1157.

Hoogendijk EO, R. K., Theou O, et al. (2018). 'Tracking changes in frailty throughout later life: results from a 17-year longitudinal study in the Netherlands'. Age Ageing 47:727–733.

Hopman P, Forjaz M J, et al. (2016). 'Effectiveness of comprehensive care programs for patients with multiple chronic conditions or frailty: a systematic literature review'. Health Policy 120:818–832.

Horberg M, Tang B, Towner W, Silverberg M, Bersoff-Matcha S, Hurley L, et al. (2010). 'Impact of tenofovir on renal function in HIV-infected, antiretroviral-naive patients'. J Acquir Immune Defic Syndr 53:62–69.

Hoschele D (2006). 'Cell culture models for the investigation of NRTI-induced mitochondrial toxicity. Relevance for the prediction of clinical toxicity'. Toxicology in vitro: an international journal published in association with BIBRA 20:535–546.

Hotamisligil GS, Shargill NS, Spiegelman BM (1993). 'Adipose expression of tumor necrosis factor-alpha: direct role in obesity-linked insulin resistance'. Science 259:87-91.

Houstis N, Rosen ED, Lander ES (2006). 'Reactive oxygen species have a causal role in multiple forms of insulin resistance'. Nature:944–948.

Houston DK, Ding J, Harris TB, Tylavsky FA, Newman AB, et al. (2008). 'Dietary protein intake is associated with lean mass change in older, community dwelling adults: the Health, Aging, and Body Composition (Health ABC) Study'. Am J Clin Nutr 87:150–155.

Houtkooper RH, Mouchiroud L, Ryu D, Moullan N, Katsyuba E, Knott G, Williams RW, Auwerx J (2013). 'Mitonuclear protein imbalance as a conserved longevity mechanism'. Nature 497:451–457.

Howald H, Hoppeler H, Claassen H, Mathieu O, Straub R. (1985). 'Influence of endurance training on the ultrastructure composition of different muscle fiber types in humans'. Pflügers Arch 403:369–376.

Howell N, Chinnery PF, Ghosh SS, Fahy E, Turnbull DM (2000). 'Transmission of the human mitochondrial genome'. Hum Reprod 15:235-245.

Howlett SE, Rockwood K (2013). 'New horizons in frailty: ageing and the deficit-scaling problem'. Age Ageing 42:416–23.

Huang CY, Hwang AC, Liu LK, Lee WJ, Chen LY, Peng LN, et al. (2015). 'Association of dynapenia, sarcopenia and cognitive impairment among community-dwelling older Taiwanese'. Rejuvenation Res 19:71-78.

Huang L-J, et al. (2012). 'Attenuation of mitochondrial unfolded protein response is associated with hepatic dysfunction in septic rats'. Shock 38:642-648.

Hubbard RE, Andrew MK, Fallah N, Rockwood K. (2010). 'Comparison of the prognostic importance of diagnosed diabetes, co-morbidity and frailty in older people'. Diabet Med 27:603-6.

Hubbard RE, O'Mahony MS, Savva GM, Calver BL, Woodhouse KW (2009). 'Inflammation and frailty measures in older people'. J Cell Mol Med 13.

Hughes AL, Hughes CE, Henderson KA, Yazvenko N, Gottschling DE (2016). 'Selective sorting and destruction of mitochondrial membrane proteins in aged yeast'. eLife 5:e13943.

Hulver MW, Berggren JR, Cortright RN, Dudek RW, Thompson RP, Pories WJ, MacDonald KG, Cline G W, Shulman GI, Dohm GL, Houmard JA (2003). 'Skeletal muscle lipid metabolism with obesity'. Am J Physiol Endocrinol Metab 284:741-747.

Hung WW, Ross JS, Boockvar KS, Siu AL (2011). 'Recent trends in chronic disease, impairment and disability among older adults in the United States'. BMC Geriatr 11.

Hunt M, Payne BAI (2020). 'Mitochondria and ageing with HIV'. Curr HIV/AIDS Rep 14.

Hurst SA, Appelgren KE, Kourtis AP (2016). 'Prevention of mother-to-child transmission of human immunodeficiency virus type I (HIV): the role of neonatal and infant prophylaxis'. Expert Rev Anti Infect Ther 13:169-181.

Hutter E, et al. (2007). 'Oxidative stress and mitochondrial impairment can be separated from lipofuscin accumulation in aged human skeletal muscle'. Aging Cell 6(2).

Hwang H, Bowen BP, Lefort N, Flynn CR, De Filippis EA, Roberts C, Smoke CC, Meyer C, Højlund K, Yi Z, et al. (2010). 'Proteomics analysis of human skeletal muscle reveals novel abnormalities in obesity and type 2 diabetes'. Diabetes 59:33–42.

Ianas V, et al. (2013). 'Antiretroviral therapy protects against frailty in HIV-1 infection'. J Int Assoc Provid AIDS Care 12(1):62-66.

Ibrahim K, Patel HP, et al. (2016). 'A feasibility study of implementing grip strength measurement into routine hospital practice (GRImP): study protocol'. Pilot Feasibility Stud 2.

Ida S, Kaneko R, Imatake K, Murata K (2019). 'Relationship between frailty and mortality, hospitalization, and cardiovascular diseases in diabetes: a systematic review and meta-analysis'. Cardiovascular Diabetology 18:81.

Igney FH, Krammer PH (2002). 'Death and anti-death: tumour resistance to apoptosis'. Nat Rev Cancer 2:277-288.

Igoudjil A, Begriche K, Pessayre D, Fromenty B (2006). 'Mitochondrial, metabolic and genotoxic effects of antiretroviral nucleoside reverse-transcriptase inhibitors'. Anti-Infective Agents in Medicinal Chemistry 5:273-292.

Ingles M, Gambini J, Carnicero JA, et al. (2014). 'Oxidative stress is related to frailty, not to age or sex, in a geriatric population: lipid and protein oxidation as biomarkers of frailty'. J Am Geriatr Soc 62:1324-1328.

Inglés M, Gambini J, Carnicero JA, García-García FJ, Rodríguez-Mañas L, Olaso-González G, Dromant M, Borrás C, Viña J. (2014). 'Oxidative stress is related to frailty, not to age or sex, in a geriatric population: lipid and protein oxidation as biomarkers of frailty'. J Am Geriatr Soc. 62:1324–28.

Innes S, et al. (2012). 'High prevalence of objectively verified clinical lipoatrophy in pre-pubertal children is associated with stavudine-the clock is ticking: sub-Saharan Africa'. 19th Conference on Retroviruses and Opportunistic Infections, Seattle, poster 972, 2012.

Ipson BR, Fletcher MB, Espinoza SE, Fisher AL (2018). 'Identifying exosome-derived MicroRNAs as candidate biomarkers of frailty'. J. Frailty Aging 7:100-103.

Ishihara N, Eura Y, Mihara K (2004). 'Mitofusin 1 and 2 play distinct roles in mitochondrial fusion reactions via GTPase activity'. J. Cell Sci 117:6535–6546.

Iwuji CC, Churchill D, Gilleece Y, Weiss HA, Fisher M (2013). 'Older HIV-infected individuals present late and have a higher mortality. Brighton, UK cohort study'. BMC Public Health 13:397.

Izzedine H, Harris M, Perazella MA (2009). 'The nephrotoxic effects of HAART.' Nat Rev Nephrol 5: 563–573.

Izzedine H, Hulot JS et al. (2004). 'Renal safety of tenofovir in HIV treatment-experienced patients'. AIDS 18:1074–1076.

Izzedine H, Hulot J-S, Villard E, Goyenvalle C, Dominguez S, Ghosn J, Valantin MA, Lechat P, Deray A G (2006). 'Association between ABCC2 gene haplotypes and tenofovir-induced proximal tubulopathy'. J Infect Dis 194:1481–1491.

Jamaluddin MS, Lin P, Chen YC (2010). 'Non-nucleoside reverse transcriptase inhibitor efavirenz increases monolayer permeability of human coronary artery endothelial cells'. Atherosclerosis 208: 104-111.

James DI, Parone PA, Mattenberger Y, Martinou JC (2003). 'hFis1, a novel component of the mammalian mitochondrial fission machinery'. J. Biol. Chem 278:36373–36379

Jang JC, Sinha M, Cerletti M, Dall'Osso C, Wagers AJ. (2011). 'Skeletal muscle stem cells: effects of aging and metabolism on muscle regenerative function'. Cold Spring Harbor Symp Quant Biol 76:101-111

Jankowski CM, Wilson MP, Erlandson KM, et al (2019). 'Blunted muscle mitochondrial responses to exercise training in older adults with HIV'. CROI 2019: abstract number 701.

Janzen V, Forkert R, Fleming HE, Saito Y, Waring MT, Dombkowski DM, Cheng T, DePinho RA, Sharpless NE, Scadden DT (2006). 'Stem-cell ageing modified by the cyclin-dependent kinase inhibitor p16INK4a'. Nature 443:421-426.

Jasper H, Kennedy BK (2012). 'Niche science: the aging stem cell'. Cell Cycle 11: 2959-2960.

Jemsek JG, Arathoon E, Arlotti M, Perez C, Sosa N, et al. (2006). 'Body fat and other metabolic effects of atazanavir and efavirenz, each administered in combination with zidovudine plus lamivudine, in antiretroviral-naive HIV-infected patients'. Clin Infect Dis 42:273–280.

Jenkins AB, Storlien LH, Chisholm DJ, Kraegen EW (1988). 'Effects of nonesterified fatty acid availability on tissue-specific glucose utilization in rats in vivo'. J Clin Invest 82:293-299.

Jia Y, Shibanuma M, et al (2001). 'Identification and characterisation of the hic-5/ARA55 as an hsp27 binding protein'. J Biol Chem 276:39911-39918.

Jimenez-Nacher I, Garcia B, Barreiro P, et al. (2008). 'Trends in the prescription of antiretroviral drugs and impact on plasma HIV-RNA measurements'. J Antimicrob Chemother 62:816–822.

Jin SM, LM, Wang C, et al. (2010). 'Mitochondrial membrane potential regulates PINK1 import and proteolytic destabilization by PARL'. J Cell Biol 191:933-942.

Johnson ML, Distelmaier K, Lanza IR, Irving BA, Robinson MM. Konopka AR, Shulman GI, Nair KS. (2016). 'Mechanism by which caloric restriction improves insulin sensitivity in sedentary obese adults'. Diabetes 65:74–84.

Johnson Stoklossa CA, Forhan M, et al. (2017). 'Prevalence of sarcopenic obesity in adults with class II/III obesity using different diagnostic criteria'. J Nutr Metab 7307618.

Jonckheere AI, Smeitink JAM, Rodenburg RJT (2012). 'Mitochondrial ATP synthase: architecture, function and pathology'. Journal of Inherited Metabolic Disease 35:211-225.

Jones D, Song X, Mitnitski, et al. (2005). 'Evaluation of a frailty index based on a comprehensive geriatric assessment in a population based study of elderly Canadians'. Aging Clin Exp Res 17:465-471.

Jones DL, Rando TA (2011). 'Emerging models and paradigms for stem cell ageing'. Nat Cell Biol 13: 506-512.

Jones DM, Song X, Rockwood K (2004). 'Operationalizing a frailty index from a standard comprehensive geriatric assessment'. J Am Geriatr Soc 52:1929-1933.

Jones R, Sawleshwarkar S, et al. (2005). 'Impact of antiretroviral choice on hypercholesterolaemia events: the role of the nucleoside reverse transcriptase inhibitor backbone'. HIV Med 6:396-402.

Jordheim LP, Dumontet C (2007). 'Review of recent studies on resistance to cytotoxic deoxynucleoside analogues'. Biochim Biophys Acta 1776:138-159.

Jose S, Hamzah L, Campbell LJ, et al. (2014). 'Incomplete reversibility of estimated glomerular filtration rate decline following tenofovir disoproxil fumarate exposure'. J Infect Dis 210:363–373.

Jotwani V, Scherzer R, Estrella MM, Jacobson LP, Witt MD, Palella F, Macatangay B, Bennett M, Parikh CR, Ix JH, Shlipak M. (2016). 'Brief report: Cumulative tenofovir disoproxil fumarate exposure is associated with biomarkers of tubular injury and fibrosis in HIV-infected men'. J Acquir Immune Defic Syndr 73:177–181

Joza N, Daugas E, et al. (2001). 'Essential role of the mitochondrial apoptosis-inducing factor in programmed cell death'. Nature 410:549-554.

Juo SHH, Lu MY, Bai RK, Liao YC, Trieu RB, Yu ML, Wong LJC (2010). 'A common mitochondrial polymorphism 10398A > G is associated metabolic syndrome in a Chinese population'. Mitochondrion 10:294-299.

Justice AG, et al. (2014). 'Predictive Accuracy of the Veterans Aging Cohort Study (VACS) Index for Mortality with HIV Infection: A North American Cross Cohort Analysis'. J Acquir Immune Defic Syndr 62(2):149-163.

Kahle KM, Steger HK, Root MJ (2009). 'Asymmetric Deactivation of HIV-1 gp41 following Fusion Inhibitor Binding'. PLoS Pathog 5:e1000674.

Kakuda TN, Brundage R, Anderson PL, Fletcher CV (2000). 'Nucleoside reverse transcriptase inhibitor-induced mitochondrial toxicity as an etiology for lipodystrophy'. AIDS 13:2311–2312.

Kalia R, et al. (2018). 'Structural basis of mitochondrial receptor binding and constriction by DRP1'. Nature 558:401–405

Kalinkovich A, Livshits G (2017). 'Sarcopenic obesity or obese sarcopenia: A cross talk between age-associated adipose tissue and skeletal muscle inflammation as a main mechanism of the pathogenesis'. Ageing Res Rev 35:200-221.

Kalyani RR, Corriere M, Ferrucci L (2014). 'Age-related and disease-related muscle loss: the effect of diabetes, obesity, and other diseases'. Lancet Diabetes Endocrinol 2:819-29

Kalyani RR, Tian J, Xue QL, Walston J, Cappola AR, Fried LP, Brancati FL, Blaum CS (2012). 'Hyperglycemia and incidence of frailty and lower extremity mobility limitations in older women'. J Am Geriatr Soc 60:1701-1707.

Kane AE, Sinclair DA. (2019). 'Frailty biomarkers in humans and rodents: current approaches and future advances'. Mech Ageing Dev 180:117–28.

Kang E, Tippner-Hedges R, Ma H, Folmes Clifford D L, Gutierrez Nuria M, et al. (2016). 'Age-Related Accumulation of Somatic Mitochondrial DNA Mutations in Adult-Derived Human iPSCs'. Cell Stem Cell 5:625-36.

Kang JS, Krauss RS (2010). 'Muscle stem cells in developmental and regenerative myogenesis'. Curr Opin Clin Nutr Metab Care 13:243-248.

Kanki T, Wang K, Cao Y, Baba M, Klionsky DJ (2009). 'Atg32 is a mitochondrial protein that confers selectivity during mitophagy'. Dev. Cell 17:98–109.

Kasamatsu H, Vinograd J (1973). 'Unidirectionality of replication in mouse mitochondrial DNA'. Nature New Biol 241:103-105.

Kasembeli AN, Duarte R, Ramsay M, et al. (2015). 'APOL1 Risk Variants Are Strongly Associated with HIV-Associated Nephropathy in Black South Africans'. J Am Soc Nephrol 26:2882–2890.

Katunin VI, Savelsbergh A, Rodnina MV, Wintermeyer W (2002). 'Coupling of GTP Hydrolysis by Elongation Factor G to Translocation and Factor Recycling on the Ribosome'. Biochemistry 41: 12806-12812.

Kauppila TES, Kauppila JH, Larsson NG (2017). 'Mammalian mitochondria and ageing: an update'. Cell Metab 25:57-71.

Kelley DE, He J, Menshikova EV, Ritov VB. (2002). 'Dysfunction of mitochondria in human skeletal muscle in type 2 diabetes'. Diabetes 51:2944–2950.

Kelly SG, Wu K, Tassiopoulos K, Erlandson KM, Koletar SL, Palella FJ (2019). 'Frailty is an independent risk factor for mortality, cardiovascular disease, bone disease, and diabetes among aging adults with human immunodeficiency virus'. Clin Infect Dis 69(8):1370–6

Kennedy BK, et al. (2014). 'Geroscience: Linking aging to chronic disease'. Cell 159:709–713.

Kennedy SR, Salk J, Schmitt MW, Loeb LA (2013). 'Ultra-Sensitive Sequencing Reveals an Age-Related Increase in Somatic Mitochondrial Mutations That Are Inconsistent with Oxidative Damage'. PLOS Genetics 9(9):e1003794.

Kenny AM, Kleppniger A, Annis K, Rathier M, Browner B, Judge JO, McGee D (2010). 'Effects of transdermal testosterone on bone and muscle in older men with low bioavailable testosterone levels, low bone mass, and physical frailty'. J Am Geriatr Soc 58:1134-1143.

Kerr JFR, Wyllie AH, Currie AR (1972). 'Apoptosis: a basic biological phenomenon with wide-ranging implications in tissue kinetics'. Br J Cancer 26:239.

Khaminets A, Behl C, Dikic I (2016). 'Ubiquitin-dependent And independent signals in selective autophagy'. Trends Cell Biol 26:6–16.

Khan IM, et al. (2015). 'Intermuscular and perimuscular fat expansion in obesity correlates with skeletal muscle T cell and macrophage infiltration and insulin resistance'. Int J Obes 39:1607–1618.

Kim DH, Avorn J, et al. (2019). 'Validation of a claims-based frailty index against physical performance and adverse health outcomes in the Health and Retirement Study'. J Gerontol A Biol Sci Med Sci 74:1271–1276.

Kim GH, Kim JE, Rhie SJ, Yoon S (2015). 'The role of oxidative stress in neurodegenerative diseases'. Exp Neurobiol 24:325-340.

Kim J (2016). 'Poly (ADP-ribose) polymerase activation induces high mobility group box 1 release from proximal tubular cells during cisplatin nephrotoxicity'. Physiol Res 65:333–340.

Kim JY, Hickner RC, Cortright RL, Dohm GL, Houmard JA (2000). 'Lipid oxidation is reduced in obese human skeletal muscle'. Am J Physiol Endocrinol Metab 279:1039-1044.

Kimura M (1968). 'Evolutionary rate at the molecular level'. Nature 217:624–626.

Kirichok Y, Krapivinsky G, Clapham DE (2004). 'The mitochondrial calcium uniporter is a highly selective ion channel'. Nature 427:360–364.

Kirk GD, Mehta SH, Astemborski J, Galai N, Washington J, Higgins Y, et al. (2013). 'HIV, age, and the severity of hepatitis C virus-related liver disease: a cohort study'. Ann Intern Med 158(9):658–66.

Kirkwood TB (1977). 'Evolution of ageing'. Nature Cell Biology 270:301-304.

Kirkwood TB (2005). 'Understanding the odd science of aging'. Cell 120(4):437-447.

Klein BE, Klein R, Knudtson MD, Lee KE (2005). 'Frailty, morbidity and survival'. Archives of Gerontology and Geriatrics 41:141-149.

Kleszczynski K, Zillikens D, Fischer TW (2016). 'Melatonin enhances mitochondrial ATP synthesis, reduces reactive oxygen species formation, and mediates translocation of the nuclear erythroid 2-related factor 2 resulting in activation of phase-2 antioxidant enzymes (g-GCS, HO-1, NQO1) in ultraviolet radiation-treated normal human epidermal keratinocytes (NHEK)'. J Pineal Res 61:187–197.

Klokouzas A, Chung-Pu W, van Veen HW, Barrand MA, Hladky SB (2003). 'cGMP and glutathione-conjugate transport in human erythrocytes'. Eur. J. Biochem 270:3696–3708.

Kohler J, Hoying-Brandt A, et al. (2009). 'Tenofovir renal toxicity targets mitochondria of renal proximal tubules'. Lab Invest 89:513–519.

Kohlstaedt LA, Wang J, Friedman JM, Rice PA, Steitz TA (1992). 'Crystal structure at 3.5 A resolution of HIV-1 reverse transcriptase complexed with an inhibitor'. Science 26:1783-1790.

Kojima G (2015). 'Prevalence of frailty in nursing homes: a systematic review and meta-analysis'. J Am Med Dir Assoc 16:940-945.

Kojima G (2017). 'Prevalence of frailty in end-stage renal disease: a systematic review and meta-analysis'. Int Urol Nephrol 49:1989-1997.

Kojima G, Avgerinou C, Iliffe S, Walters K (2018). 'Adherence to Mediterranean diet reduces incident frailty risk: systematic review and meta-analysis'. J. Am. Geriatr. Soc. 66:783–788.

Kong P, Lei P, Zhang S, Li D, Zhao J, Zhang B (2018). 'Integrated microarray analysis provided a new insight of the pathogenesis of Parkinson's disease'. Neurosci. Lett 662:51–58.

Konig J, Hugo M, Jung T, et al. (2017). 'Mitochondrial contribution to lipofuscin formation'. Redox Biology 11:673-681.

Kooij KW, Wit FWNM, Schouten J, et al. (2016). 'HIV infection is independently associated with frailty in middle-aged HIV type 1-infected individuals compared with similar uninfected controls'. AIDS 30:241-250.

Koopman R, van Loon LJ (2009). 'Aging, exercise, and muscle protein metabolism'. J Appl Physiol 106:2040–2048.

Koopman WJ, Nijtmans L, Dieteren CE, Roestenberg P, Valsecchi F, Smeitink JA, Willems PH (2010). 'Mammalian mitochondrial complex I: biogenesis, regulation, and reactive oxygen species generation'. Antioxid Redox Signal 12(12):1431-1470.

Kopp JB, Winkler C (2003). 'HIV-associated nephropathy in African Americans'. Kidney Int Suppl. S43–49.

Koshiba T, Detmer SA, Kaiser JT, Chen H, McCaffery JM, Chan DC (2004). 'Structural Basis of Mitochondrial Tethering by Mitofusin Complexes'. Science 305:858-862.

Koster JC, Remedi M, et al. (2003). 'HIV protease inhibitors acutely impair glucose-stimulated insulin release'. Diabetes 52:1695-1700.

Kourtis AP, Bulterys M (2010). 'Mother-to-child transmission of HIV: pathogenesis, mechanisms and pathways'. Clin. Perinatol. 37(4):721–737

Kowald A, Kirkwood TBL (2014). 'Transcription could be the key to the selection advantage of mitochondrial deletion mutants in aging'. Proc. Natl Acad. Sci. USA 111:2972–2977.

Kowald A, Kirkwood TBL (2018). 'Resolving the enigma of the clonal expansion of mtDNA deletions'. Genes 9:126.

Kraytsberg Y, Kudryavtseva E, McKee AC, Geula C, Kowall NW, Khrapko K (2006). 'Mitochondrial DNA deletions are abundant and cause functional impairment in aged human substantia nigra neurons'. Nat Genet 38:518– 520.

Krentz AJ, Viljoen A, Sinclair A. (2013). 'Insulin resistance: a risk marker for disease and disability in the older person'. Diabet Med 30:535-48.

Krishnan KJ, Greaves LC, Reeves AK, Turnbull DM (2007). 'The ageing mitochondrial genome'. Nucleic Acids Res 35:7399–7405.

Krishnan KJ, Reeves AK, Samuels DC, Chinnery PF, Blackwood JK, Taylor RW, Wanrooij S, Spelbrink J N, Lightowlers RN, Turnbull DM (2008). 'What causes mitochondrial DNA deletions in human cells?'. Nat Genet 40:275-279.

Kroemer G, Galluzzi L, Brenner C (2007). 'Mitochondrial membrane permeabilization in cell death'. Physiol. Rev 87:99–163.

Kruzel-Davila E, Shemer R, Ofir A, et al. (2017). 'APOL1-Mediated Cell Injury Involves Disruption of Conserved Trafficking Processes'. J Am Soc Nephrol. 28:1117–1130.

Kuang S, Charge SB, Seale P, Huh M, Rudnicki MA (2006). 'Distinct roles for Pax7 and Pax3 in adult regenerative myogenesis'. J Cell Biol 172:103–113.

Kujoth GC, Pugh T D, Someya S, Panzer K, Wohlgemuth S E, et al. (2005). 'Mitochondrial DNA mutations, oxidative stress, and apoptosis in mammalian aging'. Science 309:481–484.

Kukielka E, Dicker E, Cederbaum AI (1994). 'Increased production of reactive oxygen species by rat liver mitochondria after chronic ethanol treatment'. Arch Biochem Biophys 309:377–386.

Kulawiak B, Gebert M, et al. (2013). 'The mitochondrial protein import machinery has multiple connections to the respiratory chain'. Biochimica et Biophysica Acta 1827:612-626.

Kumar P, Trudel N, et al. (2010). 'Nelfinavir, an HIV-1 Protease Inhibitor, Induces Oxidative Stress–Mediated, Caspase-Independent Apoptosis in Leishmania Amastigotes.' PLOS.

Kumashiro N, Tamura Y, Uchida T, Ogihara T, Fujitani Y, Hirose T, Mochizuki H, Kawamori R, Watada H (2008). 'Impact of oxidative stress and peroxisome proliferator-activated receptor gamma coactivator-1alpha in hepatic insulin resistance'. Diabetes 57:2083-2091.

Kummer E, L. M., Rackham O, Lee R G, Boehringer D, Filipovsaka A, Ban N K (2018). 'Unique features of mammalian mitochondrial translation initiation revealed by cryo-EM'. Nature 560:263-267.

Kunkel TA, Leibundgut LA. (1981). 'Fidelity of mammalian DNA polymerases'. Science 213:765-776.

Kwon JB, Vankara A, Ettyreddy AR, Bohning JD, Gerbach CA (2020). 'Myogenic progenitor cell lineage specification by CRISPR/Cas9-based transcriptional activators'. Stem Cell Reports 14:1-15.

Lachin JM (1981). 'Introduction to sample size determination and power analysis for clinical trials'. Controlled clinical trials 2(2):93-113

Lagathu C, Eustace B, Prot M, et al. (2007). 'Some HIV antiretrovirals increase oxidative stress and alter chemokine, cytokine or adiponectin production in human adipocytes and macrophages'. Antivir Ther 12:489-500.

Lalezari JP, Kuppermann BD, et al. (1997). 'Intravenous cidofovir for peripheral cytomegalovirus retinitis in patients with AIDS: a randomized, controlled trial'. Annals of Internal Medicine 126(4): 257–263.

Landi F, Calvani R, Tosato M, Martone AM, Ortolani E, Savera G, Sisto A, Marzetti E (2016). 'Anorexia of aging: Risk factors, consequences, and potential treatments'. Nutrients 8:69.

Landi F, Marzetti E, Martone AM, Bernabei R, Onder G (2014). 'Exercise as a remedy for sarcopenia'. Curr Opin Clin Nutr Metab Care 17:25-31.

Lang P, Michel J-P, Zekry D (2009). 'Frailty syndrome: A transitional state in a dynamic process'. Gerontology 55:539-549.

Langen RC, Van Der Velden JLJ, Schols AM, Kelders MC, Wouters EF, JanssenHeininger YM (2004). 'Tumor necrosis factor alpha inhibits myogenic differentiation through MyoD protein destabilization'. FASEB J 18:227-237.

Larrick JW, Mendelsohn AR (2017). 'Mesenchymal Stem Cells for Frailty?'. Rejuvenation Res 20(6):525-529.

Larsson L, Degens H, Li M, Salviati L, Lee YI, Thompson W, Kirkland JL & Sandri M (2019). 'Sarcopenia: aging-related loss of muscle mass and function'. Physiol Rev 99:427–511.

Laskus T, Radkowski M, Piasek A, et al. (2000). 'Hepatitis C virus in lymphoid cells of patients coinfected with human immunodeficiency virus type 1: evidence of active replication in monocytes/macrophages and lymphocytes'. J Infect Dis 181:442–8.

Laskus T, Radkowski M, Wang LF, Vargas H, Rakela J (1998). 'The presence of active hepatitis C virus replication in lymphoid tissue in patients coinfected with human immunodeficiency virus type 1'. J Infect Dis 178:1189–92.

Lawless C, Greaves L, Reeve AK, Turnbull DM, Vincent AE (2020). 'The rise and rise of mitochondrial DNA mutations'. Open Biol 10:200061.

Lazarou M, Jin SM., Kane LA, Youle RJ (2012). 'Role of PINK1 binding to the TOM complex and alternate intracellular membranes in recruitment and activation of the E3 ligase Parkin'. Dev Cell 22: 320-333.

Lebrecht D, Kirschner J, et al. (2009). 'Mitochondrial tubulopathy in tenofovir disoproxil fumarate-treated rats'. J Acquir Immune Defic Syndr 51:158–163.

Lee H, Smith SB, Yoon Y (2017). 'The short variant of the mitochondrial dynamin OPA1 maintains mitochondrial energetics and cristae structure'. J Biol Chem 292:7115-7130.

Lee JE, Westrate LM, Wu H, Page C, Voeltz GK (2016). 'Multiple dynamin family members collaborate to drive mitochondrial division'. Nature 540:139–143

Lee JS, Kwok T, et al. (2007). 'Associated factors and health impact of sarcopenia in older Chinese men and women: a cross-sectional study'. Gerontology 53:404-410.

Lee S, Lee S, Harada K, Bae S, Makizako H, Doi T, et al. (2017). 'Relationship between chronic kidney disease with diabetes or hypertension and frailty in community-dwelling Japanese older adults'. Geriatr Gerontol Int 17:1527-33.

Lee YS, et al. (2011). 'Inflammation is necessary for long-term but not short-term high-fat diet-induced insulin resistance'. Diabetes 60:2474–2483.

Legros F, Manuel R, et al. (2002). 'Mitochondrial Fusion in Human Cells Is Efficient, Requires the Inner Membrane Potential, and Is Mediated by Mitofusins'. Mol Biol Cell 13:4343-4354.

Lehmann D, Tuppen HAL, Vincent AE, et al. (2019). 'Understanding mitochondrial DNA maintenance disorders at the single muscle fibre level'. Nuc Acids Res. 47:7430-7443.

Lehmann J, Baar MP, de Keizer PLJ (2018). 'Senescent cells drive frailty through systemic signals'. Trends In Molecular Medicine 24:917-918.

Lemmon MA, Schlessinger J (2010). 'Cell signalling by receptor-tyrosine kinases'. Cell 141:1117-1134.

Lenassi M, Cagney G, Liao M, et al. (2009). 'HIV Nef is Secreted in Exosomes and Triggers Apoptosis in Bystander CD4+ T Cells'. Traffic 11(1).

Leng SX, Hung W, Cappola AR, Yu Q, Xue QL, Fried LP (2009). 'White blood cell counts, insulin-like growth factor-1 levels, and frailty in community-dwelling older women'. J Gerontol A Biol Sci Med Sci. 64:499–502.

Leng SX, Margolick JB (2015). 'Understanding frailty, aging, and inflammation in HIV infection'. Curr HIV/AIDS Rep 12(1):25-32.

Leng SX, Tian X, Matteini A, Li H, Hughes J, Jain A, et al. (2011). 'IL-6-independent association of elevated serum neopterin levels with prevalent frailty in community-dwelling older adults'. Age Ageing 40(4):475–481.

Leng SX, Xue Q-L., Tian J, Walston JD, Fried LP (2007). 'Inflammation and frailty in older women.' J. Am. Geriatr. Soc. 55:864-871.

Leong DP, Rangarajan S, et al. (2015). 'Prognostic value of grip strength: findings from the Prospective Urban Rural Epidemiology (PURE) study'. Lancet 386:266–273.

Levett T, Alford K, Roberts, et al. (2020). 'Evaluation of a combined HIV and geriatrics clinic for older people living with HIV: the Silver Clinic in Brighton, UK'. Geriatrics 5(4):81.

Levett T, Cresswell FV, Malik MA et al. (2016). 'Systematic review of prevalence and predictors of frailty in individuals with human immunodeficiency virus'. J Am Geriatr Soc 64:1006-1014.

Levett TJ, Cresswell FV, Malik MA et al. (2016). 'Systematic review of prevalence and predictors of frailty in individuals with Human Immunodeficiency Virus'. J Am Ger Soc 64(5).

Levy JA (2007). 'HIV and the Pathogenesis of AIDS 3rd ed.'

Lewis W (2003). 'Mitochondrial DNA replication, nucleoside reverse-transcriptase inhibitors, and AIDS cardiomyopathy'. Prog Cardiovasc Dis 45:305-318.

Lewis W, Dalkas MC (1995). 'Mitochondrial toxicity of antiviral drugs'. Nat Med 1:417–422.

Lewis W, Gonzalez B, Chomyn A, Papoian T (1992). 'Zidovudine induces molecular, biochemical, and ultrastructural changes in rat skeletal muscle mitochondria'. J Clin Invest 89: 1354–1360.

Lewis W, Levine E, Griniuviene B, Tankersley KO, Colacino JM, Sommadossi JP, Watanabe KA, Perrino FW (1996). 'Fialuridine and its metabolites inhibit DNA polymerase gamma at sites of multiple adjacent analog incorporation, decrease mtDNA abundance, and cause mitochondrial structural defects in cultured hepatoblasts'. Proc Natl Acad Sci USA 93:3592–3597.

Lexell J, Henriksson-Larsen K, Winblad B, Sjostrom M (1983). 'Distribution of different fiber types in human skeletal muscles: effects of aging studied in whole muscle cross sections'. Muscle Nerve 6: 588–595

Li C, Lin CH, Lin WY, Liu CS, Chang C, Meng NH, Lee YD, Li TC, Lin CC (2014). 'Successful aging defined by health-related quality of life and its determinants in community-dwelling elders'. BMC Public Health 14:1013.

Li CW, Yu K, Shyh-Chang N, Li G-X, Jiang LJ, Yu SL, Xu LY, Liu RJ, Guo ZJ, Xie HY, et al. (2019). 'Circulating factors associated with sarcopenia during ageing and after intensive lifestyle intervention'. J. Cachexia Sarcopenia Muscle 10:586–600.

Li CW, Yu K, Shyh-Chang N, et al. (2019). 'Circulating factors associated with sarcopenia during ageing and after intensive lifestyle intervention'. J Cachexia Sarcopenia Muscle 10(3):586-600.
Li H, M. S., Kumar A (2008). 'Nuclear factor-kappa B signalling in skeletal muscle'. J Mol Med 86:1113-1126.

Li M, Foli Y, Liu Z, Wang G, Hu Y, Lu Q, et al. (2017). 'High frequency of mitochondrial DNA mutations in HIV-infected treatment-experienced individuals'. HIV Med 18(1):45–55.

Li QOT, Soro-Arnaiz I, Aragones J (2019). 'Age-dependant obesity and mitochondrial dysfunction'. Adipocyte 6:161-166.

Li Y, Shlipak MG, Grunfeld C, Choi AI. (2012). ’Incidence and risk factors for acute kidney injury in HIV infection’. Am J Nephrol 35(4):327–334.

Libório AB, Andrade L, Pereira LVB, Sanches TRC, Shimizu MH, Seguro AC (2008). ‘Rosiglitazone reverses tenofovir-induced nephrotoxicity’. Kidney International 74(7):910–918.

Lieber MR (2010). ‘The mechanism of double-strand DNA break repair by the nonhomologous DNA end joining pathway’. Annu. Rev. Biochem 79:181–211.

Lieber RL, Ward SR (2011). ‘Skeletal muscle design to meet functional demands.’ Philosophical Transactions of the Royal Society B 366: 1466-1476.

Lill R (2009). ‘Function and biogenesis of iron–sulphur proteins’. Nature 460:831.

Lill R, Hoffmann B, Molik S, Pierik A J, Rietzschel N, et al. (2012). ‘The role of mitochondria in cellular iron-sulfur protein biogenesis and iron metabolism.’ Biochim. Biophys. Acta 1823:1491–1508.

Lim S, Park KS, Kim MS, Cho BY, Lee HK (2001). ‘Relationship between various surrogate indices of insulin resistance and mitochondrial DNA content in the peripheral blood of 18 healthy volunteers’. Mitochondrion 1:71-77.

Lim SE, Copeland WC (2001). ‘Differential incorporation and removal of antiviral deoxynucleotides by human DNA polymerase gamma’. J Biol Chem 276:23616–23623.

Lipina C, Hundal HS (2011). ‘Sphingolipids: agents provocateurs in the pathogenesis of insulin resistance’. Diabetologia 54:1596-1607.

Liu CK, Lyass A, Larson MG, Massaro JM, Wang N, D’Agostino RB Sr, Benjamin EJ, Murabito JM. (2016). ‘Biomarkers of oxidative stress are associated with frailty: the Framingham offspring study’. Age (Dordr) 38:1.

Liu CK, Lyass A, Larson MG, Massaro JM, Wang N, D'Agostino RB, Benjamin EJ, Murabito JM (2016). ‘Biomarkers of oxidative stress are associated with frailty: the Framingham offspring study’. Age (Omaha) 38:1-10.

Liu J, Liang X, Zhou D, et al. (2016). ‘Coupling of mitochondrial function and skeletal muscle fibre type by a miR-499/Fnip1/AMPK circuit’. EMBO Mol Med 8:1212-1228.

Liu L, et al. (2012). ‘Mitochondrial outer-membrane protein FUNDC1 mediates hypoxia-induced mitophagy in mammalian cells’. Nat Cell Biol 14:177–185.

Llibre JM, Hung CC, Brinson C, Castelli F, Girard PM, Kahl LP, et al. (2018). ‘Efficacy, safety, and tolerability of dolutegravir-rilpivirine for the maintenance of virological suppression in adults with HIV-1: phase 3, randomised, non-inferiority SWORD-1 and SWORD-2 studies’. Lancet 391(10123):839–849

Lo J H-T, U KP, You Y, et al. (2020). ‘Sarcopenia: current treatments and new regenerative therapeutic approaches’. J Ortho Translation 23:38-52.

Longenecker CT, Scherzer R, Bacchetti P, Lewis CE, Grunfeld C, Shlipak MG (2009). ‘HIV viremia and changes in kidney function’. AIDS 23:1089–1096.

López IP, Marti FI, Martí A, Moreno-Aliaga MJ, Martínez JA, De Miguel C (2004). ‘Gene expression changes in rat white adipose tissue after a high-fat diet determined by differential display’. Biochem Biophys Res Commun 318:234-239.

Lopez-Gallardo E, Lopez-Perez MJ, Montoya J, Ruiz-Pesini E (2009). 'CPEO and KSS differ in the percentage and location of the mtDNA deletion'. Mitochondrion 9:314-317.

Lorenzo-López L, Maseda A, de Labra C, Regueiro-Folgueira L, Rodríguez-Villamil JL, Millán-Calenti JC (2017). 'Nutritional determinants of frailty in older adults: a systematic review'. BMC Geriatr 17: 108.

Loson OC, Song Z, Chen H, Chan DC (2013). 'Fis1, Mff, MiD49, and MiD51 mediate Drp1 recruitment in mitochondrial fission'. Mol. Biol. Cell 24:659–667.

Lu A, Poddar M, Tang Y, Proto JD, Sohn J, Mu X, et al (2014). 'Rapid depletion of muscle progenitor cells in dystrophic mdx/utrophin-/-mice'. Hum Mol Genet 23:4786–4800.

Lucas GM, Jing Y, Sulkowski M, et al. (2013). 'Hepatitis C viremia and the risk of chronic kidney disease in HIV-infected individuals'. J Infect Dis. 208:1240–1249.

Lucas GM, Ross MJ, Stock PG, et al. (2014). 'Executive summary: clinical practice guideline for the management of chronic kidney disease in patients infected with HIV: 2014 update by the HIV Medicine Association of the Infectious Diseases Society of America'. Clin Infect Dis 59(9):1203–1207.

Lucas GM, Sozio S, Mentari EK, et al. (2004). 'Highly active antiretroviral therapy and the incidence of HIV-1 associated nephropathy: a 12-year cohort study'. AIDS 18:541-546.

Luciw PA (1996). 'Human immunodeficiency viruses and their replication.' in Fields BN (ed): Virology, 3rd ed. Philadelphia, Lippincott-Raven: 1881-1952.

Luger E, Dorner TE, Haider S, et al. (2016). 'Effects of a Home-Based and Volunteer Administered Physical Training, Nutritional, and Social Support Program on Malnutrition and Frailty in Older Persons: A Randomized Controlled Trial'. J Am Med Dir Assoc 17:671.e9e671.e16.

Lund KC, Wallace K (2008). 'Adenosine 3',5'-cyclic monophosphate (cAMP)-dependent phosphoregulation of mitochondrial complex I is inhibited by nucleoside reverse transcriptase inhibitors'. Toxicol Appl Pharmacol 226:94-106.

Luo S, Valencia CA, Zhang J, Lee N-C, Slone J (2018). 'Biparental Inheritance of Mitochondrial DNA in Humans'. Proceedings of the National Academy of Sciences of the United States of America 115: 13039-13044.

Ma H, Lee Y, Hayama T, et al. (2018). 'Germline and somatic mtDNA mutations in mouse aging'. PLOS ONE 13:e0201304.

Ma J, Spremulli LL (1996). 'Expression, purification, and mechanistic studies of bovine mitochondrial translational initiation factor 2'. J Biol Chem 271:5805-5011.

Ma L, Chou JW, Snipes JA, et al. (2017). 'APOL1 Renal-Risk Variants Induce Mitochondrial Dysfunction'. J Am Soc Nephrol 28:1093–1105.

Ma L, Sha G, Zhang Y, Li Y (2018). 'Elevated serum IL-6 and adiponectin levels are associated with frailty and physical function in Chinese older adults'. Clin. Interv. Aging 13:2013–2020.

Maagaard A, et al. (2005). 'Depletion of mitochondrial DNA copies/cell in peripheral blood mononuclear cells in HIV-1-infected treatment-naïve patients'. HIV Medicine 7(1).

Maagaard A, Kvale D (2009). 'Mitochondrial toxicity in HIV-infected patients both off and on antiretroviral treatment: a continuum or distinct underlying mechanisms?'. J Antimicrob Chemother 64:901-9.

Mackenzie RM, Salt IP, Miller WH, Logan A, Ibrahim HA, Degasperi A, Dymott JA, Hamilton CA, Murphy MP., Delles C, et al. (2013). 'Mitochondrial reactive oxygen species enhance AMP-activated protein kinase activation in the endothelium of patients with coronary artery disease and diabetes'. Clin. Sci. 124:403–411.

Maddalozzo GF, Edwards CH, et al. (2009). 'Alcohol alters whole body composition, inhibits bone formation, and increases bone marrow adiposity in rats'. Osteoporos Int 20:1529-1538.

Maddux BA, See W, Lawrence JC Jr, Goldfine AL, Goldfine ID, Evans JL (2001). 'Protection against oxidative stress-induced insulin resistance in rat L6 muscle cells by mircomolar concentrations of alpha-lipoic acid'. Diabetes 50:404-410.

Madeddu G, Bonfanti P, De Socio GV, Carradori S, Grosso C, Marconi P, Penco G, Rosella E, Miccolis S, Melzi S, Mura MS, Landonio S, Ricci E, Quirino T, CISAI Group (2008). 'Tenofovir renal safety in HIV-infected patients: Results from the SCOLTA Project.' Biomed Pharmacother 62:6–11.

Magner M, Kolarova H, Honzik T, Svandova I, Zeman J (2015). 'Clinical manifestation of mitochondrial diseases'. Dev Period Med 19:441-449.

Maher D, Wu X, Schacker T, Horbul J, Southern P (2005). 'HIV binding, penetration, and primary infection in human cervicovaginal tissue'. Proc Natl Acad Sci U S A 102:11504–11509.

Mai N, Chrzanowska-Lightowlers ZM, Lightowlers RN (2017). 'The process of mammalian mitochondrial protein synthesis'. Cell and Tissue Research 367:5-20.

Makary MA, Pronovost PJ, Syin D, Bandeen-Roche K, Patel P, et al. (2010). 'Frailty as a predictor of surgical outcomes in older patients'. J Am Coll Surg 210(6):901-908.

Makizako H, Shimada H, Doi T, Tsutsumimoto K, Suzuki T (2015). 'Impact of physical frailty on disability in community dwelling older adults: a prospective cohort study'. BMJ Open 5:e008462.

Mallipattu SK, Liu R, Zhong Y, et al. (2013). 'Expression of HIV transgene aggravates kidney injury in diabetic mice'. Kidney Int 83(4):626–634.

Maman D, Pujades-Rodriguez M, Subtil F, Pinoges L, McGuire M, Ecochard R, et al. (2012) 'Gender differences in immune reconstitution: a multicentric cohort analysis in sub-Saharan Africa'. PLoS One 7:e31078.

Mancuso M, Angelini C, Bertini E, Carelli V, Comi GP, Donati MA, Federico A, Minetti C, Moggio M, et al. (2015). 'Redefining phenotypes associated with mitochondrial DNA single deletion'. J Neurol 262: 1301-1309.

Mancuso M, Angelini C, Bertini E, Carelli V, Comi GP, Minetti C, Moggio M, Mongini T, Servidei S, Tonin P, et al. (2013). 'Phenotypic heterogeneity of the 8344A>G mtDNA 'MERRF' mutation'. Neurology 80:2049-2054.

Manini TM (2010). 'Energy expenditure and aging'. Ageing Res Rev 9:1e11.

Manini TM, Clark BC (2012). 'Dynapenia and aging: an update'. J Gerontol A Biol Sci Med Sci 67: 28e40.

Mann CJ, Perdiguero E, Kharraz Y, et al. (2011). 'Aberrant repair and fibrosis development in skeletal muscle'. Skeletal muscle 1:21.

Mannella CA, et al. (2001). 'Topology of the mitochondrial inner membrane: dynamics and bioenergetic implications'. IUBMB Life 52:93–100.

Maranzana E, Barbero G, Falasca A I, Lenaz G, Genova ML (2013). 'Mitochondrial Respiratory Supercomplex Association Limits Production of Reactive Oxygen Species from Complex I'. Antioxidants & Redox Signaling 19:1469-1480.

Marciniak C, Marechal X, Montaigne D, Neviere R, Lancel S (2014). 'Cardiac contractile function and mitochondrial respiration in diabetes-related mouse models'. Cardiovasc. Diabetol. 13:118.

Marcos-Pérez D, Sanchez-Flores M, Maseda A, Lorenzo-López L, Millán-Calenti JC, Gostner JM, Fuchs D, Pásaro E, Laffon B, Valdiglesias V (2018). 'Frailty in older adults is associated with plasma concentrations of inflammatory mediators but not with lymphocyte subpopulations'. Front Immunol 9.

Margolick JB, Bream JH, Martinez-Maza O, Lopez J, Li X, Phair JP, et al. (2017). 'Frailty and circulating markers of inflammation in HIV+ and HIV- men in the Multicenter AIDS cohort study'. J Acquir Immune Defic Syndr 74(4):407–17

Margolick JB, Chadwick KR, et al. (1992). 'Comparison of lymphocyte immunophenotyes obtained simultaneously from two different data acquisition and analysis systems on the same flow cytomete'. Cytometry 13(2).

Margolick JB, Martinez-Maza O, Jacobson L, Lopez J, Li X, Phair J, et al. (2013). 'Frailty and circulating markers of inflammation in HIV-infected and -uninfected men in the Multicenter AIDS Cohort Study (MACS)'. Presented at the 20th Conference on Retroviruses and Opportunistic Infections; Atlanta, GA. March 2013

Margolis AM, Heverling G, Pham PA, Stolbach A (2014). 'A Review of the Toxicity of HIV Medications'. J Med Toxicol 10(1):26-29.

Margolis DA, Gonzalez-Garcia J, Stellbrink H-J, Eron JJ, Yazdanpanah Y, Podzamczer D, et al. (2017). 'Long-acting intramuscular cabotegravir and rilpivirine in adults with HIV-1 infection (LATTE-2): 96-week results of a randomised, open-label, phase 2b, non-inferiority trial'. Lancet 390(10101):1499–1510.

Martin W, Muller M (1989). 'The hydrogen hypothesis for the first eukaryote'. Nature 392:37-41.

Martinez E, Podzamczer D, Lonca M, Sanz J, Barragan P, et al. (2009). 'A simplification trial switching from nucleoside reverse transcriptase inhibitors to once-daily fixed-dose abacavir/lamivudine or tenofovir/emtricitabine in HIV-1-infected patients with virological suppression'. J Acquir Immune Defic Syndr 51:290–297.

Martins R, Lithgow GJ, Link W (2016). 'Long live. Unraveling the role of FOXO proteins in aging and longevity'. Aging Cell 15:196-207.

Martinus RD, Garth GP, Webster TL, Cartwright P, Naylor DJ, Høj PB, Hoogenraad NJ (1996). 'Selective induction of mitochondrial chaperones in response to loss of the mitochondrial genome'. Eur. J. Biochem 240:98–103.

Martone AM, Onder G, Vetrano DL, Ortolani E, Tosato M, Marzetti E, Landi F (2013). 'Anorexia of aging: A modifiable risk factor for frailty'. Nutrients 5:4126–4133

Marttila S, Jylhava J, Kananen L, Hervonen A, Jylhä M, Hurme M (2014). 'Molecular mechanisms associated with the strength of the anti-CMV response in nonagenarians'. Immun Ageing 11:2.

Marzetti E, Lawler JM, Hiona A, Manini T, Seo AY, Leeuwenburgh C (2008). 'Modulation of age-induced apoptotic signaling and cellular remodelling by exercise and calorie restriction in skeletal muscle'. Free Radic Biol Med 44:160-168.

Marzetti E, Leeuwenburgh C (2006). 'Skeletal muscle apoptosis, sarcopenia and frailty at old age'. Exp Gerontol 41:1234-8.
Masgrau A, Murakami H, Beaufrère A M, Walrand S, Giraudet C, et al. (2012). 'Time-course changes of muscle protein synthesis associated with obesity-induced lipotoxicity'. J Physiol 590:5199e5210.

Massaad CA, Klann E (2011). 'Reactive oxygen species in the regulation of synaptic plasticity and memory'. Antioxid Redox Signal 14:2013– 2054.

Matsuda N, Sato S, Shiba K, Okatsu K, Saisho K, Gautier CA, Sou Y-S, Saiki S, Kawajiri S, Sato F, Kimura M, Komatsu M, Hattori N, Tanaka K (2010). 'PINK1 stabilized by mitochondrial depolarization recruits Parkin to damaged mitochondria and activates latent Parkin for mitophagy'. J. Cell Biol 189: 211–221.

Maughan RJ, Watson JC, Weir J (1983). 'Strength and cross-sectional area of human skeletal muscle'. J Physiol 338:37-49.

Mauro A (1961). 'Satellite cell of skeletal muscle fibres'. J Biophys Biochem Cytol 9:493-495.

Mayot G, Vidal K, Combaret L, et al. (2007). 'Presence of low-grade inflammation in old rats does not worsen skeletal muscle loss under an endotoxemic and dietary stress'. Exp Gerontol 42:1167–1175

Mazzucco S, Agostini F, Mangogna A, Cattin L, Biolo G (2010). 'Prolonged inactivity up-regulates cholesteryl ester transfer protein independently of body fat changes in humans'. J Clin Endocrinol Metab 95:2508e2512.

McComsey G, Tan D-J, Lederman M, Wilson E, Wong LJ (2002). 'Analysis of the mitochondrial DNA genome in the peripheral blood leukocytes of HIV-infected patients with or without lipoatrophy'. AIDS 16:513–518.

McComsey GA, et al. (2008). 'Mitochondrial RNA and DNA alterations in HIV lipoatrophy are linked to antiretroviral therapy and not to HIV infection'. Antivir Ther 13:715–722.

McComsey GA, Moser C, Currier J, Ribaudo HJ, Paczuski P, Dube MP, et al. (2016). 'Body composition changes after initiation of Raltegravir or protease inhibitors: ACTG A5260s'. Clin Infect Dis 62(7):853–62.

McKay BR, Ogborn DI, Baker JM, Toth KG, Tarnopolsky MA, Parise G (2013). 'Elevated SOCS3 and altered IL-6 signaling is associated with age-related human muscle stem cell dysfunction'. Am. J. Physiol. Cell Physiol. 304:C717–C728.

McKinney EA, Oliveira MT (2013). 'Replicating animal mitochondrial DNA'. Genetics and Molecular Biology 36:308-315.

McLelland G-L, Soubannier V, Chen CX, McBride HM, Fon EA (2014). 'Parkin and PINK1 function in a vesicular trafficking pathway regulating mitochondrial quality control'. EMBO J 33:282–295.

Mears JA, Lackner LL, Fang S, Ingerman E, Nunnari J, Hinshaw JE (2011). 'Conformational changes in Dnm1 support a contractile mechanism for mitochondrial fission'. Nat Struct Mol Biol 18:20-26.

Medapalli RK, Parikh CR, Gordon K, et al. (2012). ’Comorbid diabetes and the risk of progressive chronic kidney disease in HIV-infected adults: data from the Veterans Aging Cohort Study’. JAIDS 60(4):393–399.

Medwar PB (1952). ‘An unsolved problem in biology’. HK Lewis, London.

Meeusen S, DeVay R, Block J, Cassidy-Stone A, Wayson S, McCaffery JM, Nunnari J (2006). ‘Mitochondrial inner-membrane fusion and crista maintenance requires the dynamin-related GTPase Mgm1’. Cell 127:383-95.

Meex RCR, Schrauwen-Hinderling VB, Moonen-Kornips E, Schaart G, Mensink M, Phielix E, van de Weijer T, Sels J-P, Schrauwen P, Hesselink MKC (2010). ‘Restoration of muscle mitochondrial function and metabolic flexibility in type 2 diabetes by exercise training is paralleled by increased myocellular fat storage and improved insulin sensitivity’. Diabetes 59:572–579.

Meier P, Dautheville-Guibal S, Ronco PM, Rossert J (2002). ‘Cidofovir-induced end-stage renal failure’. Nephrol. Dial. Transplant 1:148-149.

Mekli K, Marshall A, Nazroo J, Vanhoutte B, Pendleton N (2015). ‘Genetic variant of Interleukin-18 gene is associated with the Frailty Index in the English Longitudinal Study of Ageing’. Age Ageing 44: 937-942.

Melov S, Schneider JA, Day BJ, et al. (1999). ‘A novel neurological phenotype in mice lacking mitochondrial manganese superoxide dismutase’. Nature Genetics 18:159–163.

Menshikova EV, Ritov VB, Fairfull L, et al. (2006). ‘Effects of exercise on mitochondrial content and function in aging human skeletal muscle’. J Gerontol A Biol Sci Med Sci 61:534-540.

Messi ML, Li T, Wang ZM, Marsh AP, Nicklas B, Delbono O (2016). ‘Resistance training enhances skeletal muscle innervation without modifying the number of satellite cells or their myofiber association in obese older adults’. J Gerontol A Biol Sci Med Sci 71:1273–1280.

Mijnarends DM, Koster A, Schols JM, et al. (2016). ‘Physical activity and incidence of sarcopenia: the population-based AGESReykjavik Study’. Age Ageing 45:614–20.

Milenkovic D, Matic S, Kuhl I, Ruzzenente B, Freyer C, Jemt E, Park CB, Falkenberg M, Larsson N-G (2013). ‘TWINKLE is an essential mitochondrial helicase required for synthesis of nascent D-loop strands and complete mtDNA replication’. Human Molecular Genetics 22:1983-1993.

Miljkovic N, Lim J-Y, Miljkovic I, et al. (2015). ‘Aging of skeletal muscle fibres’. Ann Rehabil Med 39: 155-162.

Miller FJ, Rosenfeldt FL, Zhang C, Linnane AW, Nagley P (2003). ‘Precise determination of mitochondrial DNA copy number in human skeletal and cardiac muscle by a PCR-based assay: lack of change of copy number with age’. Nucleic Acids Research 31:e61-e61.

Miller J, Carr A, Emery S, Law M, Mallal S, Baker D, et al. (2003). ‘HIV lipodystrophy: prevalence, severity and correlates of risk in Australia’. HIV medicine 4(3):293–301.

Miquel J, Economos AC, Fleming J, Johnson Jr JE (1980). ‘Mitochondrial role in cell aging’. Exp. Gerontol. 15 575–591.

Mishra P, Varuzhanyan G, Pham AH, Chan DC (2014). ‘Mitochondrial Dynamics is a Distinguishing Feature of Skeletal Muscle Fiber Types and Regulates Organellar Compartmentalization’. Cell Metab 22:1033-1044.

Mitchell WK, Williams J, Atherton P, Larvin M, Lund J, Narici M (2012). 'Sarcopenia, dynapenia, and the impact of advancing age on human skeletal muscle size and strength; a quantitative review'. Front Physiol 3:260.

Mitnitski AB, Mogilner AJ, Rockwood K (2001). 'Accumulation of deficits as a proxy measure of aging'. Scientific World Journal 1:323-336.

Mocroft A, Johnson MA, Phillips AN (1996). 'Factors affecting survival in patients with the acquired immunodeficiency syndrome'. AIDS 10:1057–1065.

Mocroft A, Lundgren JD, Ross M, et al. (2016). 'Cumulative and current exposure to potentially nephrotoxic antiretrovirals and development of chronic kidney disease in HIV-positive individuals with a normal baseline estimated glomerular filtration rate: a prospective international cohort study'. Lancet HIV 3:e23–32.

Mocroft A, Neuhaus J, Peters L, et al. (2012). 'Hepatitis B and C co-infection are independent predictors of progressive kidney disease in HIV-positive, antiretroviral-treated adults'. PLoS One 7:e40245.

Moehle EA, Shen K, Dillin A (2018). 'Mitochondrial proteostasis in the context of cellular and organismal health and aging'. J. Bio Chem 294:5396-5407.

Moir S, Chun T-W, Fauci AS (2011). 'Pathogenic mechanisms of HIV disease'. Annu Rev Pathol 6: 233-248.

Molina J-M, et al. (2018). 'Doravirine versus ritonavir-boosted darunavir in antiretroviral-naive adults with HIV-1 (DRIVE-FORWARD): 48-week results of a randomised, double-blind, phase 3, non-inferiority trial'. Lancet HIV 5:e211-e220.

Mondi A, Fabbiani M, Ciccarelli N, Colafigli M, D'Avino A, Borghetti A, et al. (2015). 'Efficacy and safety of treatment simplification to atazanavir/ritonavir + lamivudine in HIV-infected patients with virological suppression: 144 week follow-up of the AtLaS pilot study'. J Antimicrob Chemother 70(6):1843–1849.

Montaigne D, Marechal X, Coisne A, Debry N, Modine T, Fayad G, Potelle C, El Arid J, Mouton S, Sebti Y, et al. (2014). 'Myocardial contractile dysfunction is associated with impaired mitochondrial function and dynamics in type 2 diabetic but not in obese patients'. Circulation 130:554–564.

Monteagudo-Chu MO, Monteaudo-Chu H, Fung HB, Bräu N (2012). 'Renal toxicity of long-term therapy with tenofovir in HIV-infected patients'. J Pharm Pract 25:552–559.

Moore AZ, Matteini A, O'Connor A, McGuire S, Beamer BA, Fallin MD, Fried LP, Walston J, Chakravarti A, et al. (2010). 'Polymorphisms in the mitochondrial DNA control region and frailty in older adults'. PLOS ONE 5:e11069.

Moore AZ, Metter EJ, et al. (2014). 'Difference in muscle quality over the adult life span and biological correlates in the Baltimore Longtitudinal Study of Aging'. J Am Geriatr Soc 62:230-236.

Moraes CT, Shanske S, Tritschler HJ, Aprille JR, Andreetta F, Bonilla E, Schon EA, DiMauro S (1991). 'mtDNA depletion with variable tissue expression: A novel genetic abnormality in mitochondrial diseases'. Am J Hum Genet 48:492–501.

Morat T, Gilmore KJ, Rice CL (2016). 'Neuromuscular function in different stages of sarcopenia'. Exp Gerontol 81:28-36.

Morely JE, Malmstrom TK (2013). 'Frailty, sarcopenia, and hormones'. Endocrinology & Metabolism Clinics 42:391-405.

Moreno-Garcia A, Kun A, Calero M (2018). 'An overview of the role of lipofuscin in age-related neurodegeneration'. Front Neuro 12.

Morigi M, Perico L, Rota C, et al. (2015). 'Sirtuin 3-dependent mitochondrial dynamic improvements protect against acute kidney injury'. J Clin Invest 125:715–726.

Morley JE, Anker SD, von Haehling S (2014). 'Prevalence, incidence, and clinical impact of sarcopenia: facts, numbers, and epidemiology-update 2014'. J Cachexia Sarcopenia Muscle 5:253-259.

Morley JE, Kim MJ, Haren MT, Kevorkian R, Banks WA (2005). 'Frailty and the aging male'. Aging Male 8:135-140.

Morley JE, Malmstrom TK, Rodriguez-Manas L, Sinclair AJ (2014). 'Frailty, sarcopenia and diabetes'. J Am Med Dir Assoc 15:853-9.

Morley JE, Vellas B, et al. (2014). 'Frailty consensus: a call to action'. J Am Med Dir Assoc 14(6):392-397.

Morozov YI, Parshin AV, Agaronyan K, Alan CM, Anikin M, Cramer P, Temiakov D (2015). 'A model for transcription initiation in human mitochondria'. Nucleic Acids Research 43:3726-3735.

Morse CG, Voss JG, Rakocevic G, et al. (2012). 'HIV infection and antiretroviral therapy have divergent effects on mitochondria in adipose tissue'. J Infect Dis 205(12):1778- 1787.

Moslemi A-R, Tulinius M, Holme E, Oldfors A (1998). 'Threshold expression of the tRNALys A8344G mutation in single muscle fibres'. Neuromuscular Disorders 8:345-349.

Mosole S, Carraro U, Kern H, Loefler S, Fruhmann H, Vogelauer M, Burggraf S, Mayr W, Krenn M, Paternostro-Sluga T, Hamar D, Cvecka J, Sedliak M, Tirpakova V, Sarabon N, Musaro A, Sandri M, Protasi F, Nori A, Pond A, Zampieri S (2014). 'Long-term high-level exercise promotes muscle reinnervation with age'. J Neuropathol Exp Neurol 73:284–294.

Mossmann D, Meisinger C, Vogtle FN (2012). 'Processing of mitochondrial presequences'. Biochimica et Biophysica Acta 1819:1098–1106.

Mott JL, Zhang D, Stevens M, Chang S, Denniger G, Zassenhaus HP (2001). 'Oxidative stress is not an obligate mediator of disease provoked by mitochondrial DNA mutations'. Mutation Research 475: 35-45.

Mountjoy CQ, Harrington C, et al. (2005). 'Characteristics of neuronal lipofuscin in the superior temporal gyrus in Alzheimer's disease do not differ from non-diseased controls: a comparison with disease-related changes in the superior frontal gyrus'. Acta Neuropathol 109:490-496.

Mourtzakis M, Lieffers JR, et al. (2008). 'A practical and precise approach to quantification of body composition in cancer patients using computed tomography images acquired during routine care'. Appl Physiol Nutr Metab 33:997–1006.

Moyle GJ, Andrade-Villanueva J, Girard PM, Antinori A, Salvato P, et al. (2012) 'A randomized comparative 96-week trial of boosted atazanavir versus continued boosted protease inhibitor in HIV-1 patients with abdominal adiposity'. Antivir Ther 17:689–700.

Moyle GJ, Sabin CA, Cartledge J, et al. (2006). 'A randomized comparative trial of tenofovir DF or abacavir as replacement for a thymidine analogue in persons with lipoatrophy'. Acquir Immune Defic Syndr 20:2043-50.

Muir S W, Montero-Odasso M (2011). 'Effect of vitamin D supplementation on muscle strength, gait and balance in older adults: a systematic review and meta-analysis'. J. Am. Geriatr. Soc. 59:2291–2300.

Mukhopadhyay A, Zullo SJ, et al. (2002). 'In vitro evidence of inhibition of mitochondrial protease processing by HIV-1 protease inhibitors in yeast: a possible contribution to lipodystrophy syndrome'. Mitochondrion 1:511-518.

Müller MJ, Wang Z, Heymsfield SB, Schautz B, Bosy-Westphal A (2013). 'Advances in the understanding of specific metabolic rates of major organs and tissues in humans'. Curr Opin Clin Nutr Metab Care 16:501e508.

Murgia M, Nagaraj N, et al. (2017). 'Single muscle fibre proteomics reveals fibre-type-specific features of human muscle aging'. Cell Reports 19:2396-2409.

Murphy JL, Ratnaike TE, Shang ES, Falkous G, Blakely EL, Alston CL, Taivassalo T, Haller RG, Taylor RW, Turnbull DM (2012). 'Cytochrome c oxidase-intermediate fibres: Importance in understanding the pathogenesis and treatment of mitochondrial myopathy'. Neuromuscular Disorders **22**(8):690-698.

Murphy RA, Stafford RM, Petrasovits BA, et al. (2017). 'Establishment of HK-2 cells as a relevant model to study tenofovir-induced cytotoxicity'. Int J Mol Sci 18(3):pii: E531.

Muscaritoli M, Anker SD, Argiles J, et al. (2010). 'Consensus definition of sarcopenia, cachexia and pre-cachexia: joint document elaborated by Special Interest Groups (SIG) 'cachexiaanorexia in chronic wasting diseases' and 'nutrition in geriatrics''. Clin Nutr 29: 154–9.

Nadkarni GN, Patel AA, Yacoub R, et al. (2015). 'The burden of dialysis-requiring acute kidney injury among hospitalized adults with HIV infection: a nationwide inpatient sample analysis'. AIDS 29(9): 1061–1066.

Naif HM (2013). 'Pathogenesis of HIV Infection'. Infect Dis Rep 5:e6.

Nakatani Y, Inagi R. (2016). 'Epigenetic regulation through SIRT1 in podocytes'. Curr Hypertens Rev 12:89–94.

Namioka N, Hanyu H, Hirose D, Hatanaka H, Sato T, Shimizu S (2017). 'Oxidative stress and inflammation are associated with physical frailty in patients with Alzheimer's disease'. Geriatr Gerontol Int 17:913–18.

Nansseu JR, Tounouga DN, Noubiap JJ, Bigna JJ (2020). 'Changes in smoking patterns after HIV diagnosis or antiretroviral treatment initiation: a global systematic review and meta-analysis'. Infect Dis Poverty 9:35.

Nargund AM, Fiorese CJ, Pellegrino MW, Deng P, Haynes CM (2015). 'Mitochondrial and nuclear accumulation of the transcription factor ATFS-1 promotes OXPHOS recovery during the UPR'. Mol Cell 58:123–133.

Narici MV, Maffulli N (2010). 'Sarcopenia: characteristics, mechanisms and functional significance'. Br Med Bull 95:139-159.

Nartey ET, Yankey BA, et al. (2019). 'Tenofovir-associated renal toxicity in a cohort of HIV infected patients in Ghana'. BMC Research Notes 12:1-6.

National Institute for Excellence (2016). 'Multimorbidity: clinical assessment and management: NICE guideline'.

Naviaux RK, Nguyen KV (2005). 'POLG mutations associated with Alpers syndrome and mitochondrial DNA depletion'. Ann Neurol 58:491.

Nelson MR, Montaner JS, et al. (2007). 'The safety of tenofovir disoproxil fumarate for the treatment of HIV infection in adults: the first 4 years'. AIDS 21:1273–1281.

Nerurkar PV, Shikuma CM, Nerurkar VR (2001). 'Sterol regulatory element-binding proteins and reactive oxygen species: potential role in highly-active antiretroviral therapy (HAART)-associated lipodystrophy'. Clin Biochem 34:519-29.

Nesbitt V, McFarland R. (2011). 'Phenotypic spectrum of m.3243A>G mitochondrial DNA mutation in children'. Archives of Disease in Childhood 96:A28.

Nesbitt V, Turnbull DM, Taylor RW, et al. (2013). 'The UK MRC Mitochondrial Disease Patient Cohort Study: clinical phenotypes associated with the m.3243A>G mutation--implications for diagnosis and management'. J Neurol Neurosurg Psychiatry 84:936-938.

Nguyen MT, et al. (2007). 'A subpopulation of macrophages infiltrates hypertrophic adipose tissue and is activated by free fatty acids via Toll-like receptors 2 and 4 and JNK-dependent pathways'. J Biol Chem 282:35279–35292.

NHS (2020). 'Identifying frailty'. Available at https://www. england.nhs.uk/ourwork/clinical-policy/older-people/frailty/ frailty-risk-identification/. (Accessed 24/11/20).

NHS England (2017). 'Supporting routine frailty identification and frailty through the GP contract 2017/2018'.

Nielsen J, Holmberg HC, Schrøder HD, Saltin B, Ørtenblad N (2011). 'Human skeletal muscle glycogen utilization in exhaustive exercise: role of subcellular localization and fiber type'. J. Physiol. 589:2871–2885.

Nielsen J, Suetta C, Hvid LG, Schrøder HD, Aagaard P, Ørtenblad N (2010). 'Subcellular localization dependent decrements in skeletal muscle glycogen and mitochondria content following short-term disuse in young and old men'. Am. J. Physiol. 299:E1053–E1060.

Nightingale S, Letendre S, Michael BD, McArthur JC, Khoo S, et al. (2014). 'Controversies in HIV-associated neurocognitive disorders'. Lancet Neurol 13(11):1139-1151.

Nisoli E, Clementi E, Paolucci C, Cozzi V, Tonello C, Sciorati C, Bracale R, Valerio A, Francolini M, Moncada S, Carruba MO (2003). 'Mitochondrial biogenesis in mammals: the role of endogenous nitric oxide'. Science 299:896–899.

Nissanka N, Minczuk M, Moraes CT (2019). 'Mechanisms of mitochondrial DNA deletion formation'. Trends Genet 35:235–244.

Nooteboom M, Johnson R, Taylor RW, Greaves LC, et al. (2010). 'Age-associated mitochondrial DNA mutations lead to small but significant changes in cell proliferation and apoptosis in human colonic crypts'. Aging Cell 9:96-99.

Nosraty, L, Sarkeala T, Hervonen A, Jylha M (2012). 'Is there successful aging for nonagenarians? The vitality 90+ study'. J Aging Res 868797

Nou E, Lo J, Hadigan C, Grinspoon SK (2016). 'Pathophysiology and management of cardiovascular disease in patients with HIV'. Lancet Diabetes Endocrinol 4:598-610.

Novak I, et al. (2010). 'Nix is a selective autophagy receptor for mitochondrial clearance'. EMBO Rep 1:45–51

Ntanasi E, Kosmidis MH, et al. (2018). 'Adherence to Mediterranean diet and frailty'. J Am Med Dir Assoc 19:315-322.

Ofiri-Asenso R, Chin KL, Mazidi M, et al. (2019). 'Global incidence of frailty and prefrailty among community-dwelling older adults'. JAMA 2:e198398.

Ojala D, Montoya J, Attardi G (1981). 'tRNA punctuation model of RNA processing in human mitochondria'. Nature 290:470-474.

Okusa MD, Davenport A (2014). 'Reading between the (guide)lines-the KDIGO practice guidelines on acute kidney injury in the individual patient'. Kidney Int 855:39-48.

Oldfors A, Moslemi AR, Fyhr IM (1995). 'Mitochondrial DNA deletions in muscle fibres in inclusion body myositis'. J Neuropathol Exp Neurol 54:581-7.

Olefsky JM, Glass CK (2010). 'Macrophages, inflammation, and insulin resistance'. Annu Rev Physiol 72:219–246.

Oliveira VHF, Borsari AL, Webel AR, et al. (2020). 'Sarcopenia in people living with the human immunodeficiency virus: a systematic review and meta-analysis'. European Journal of Clinical Nutrition 74:1009-1021.

Olsen RH, Krogh-Madsen R, Thomsen C, Booth FW, Pedersen BK (2008). 'Metabolic responses to reduced daily steps in healthy nonexercising men'. J Am Med Assoc 299:1261e1263.

Önen NF, Patel P, Baker J, Conley L, Brooks JT, Bush T, et al (2014). 'Frailty and pre-frailty in a contemporary cohort of HIVinfected adults'. J Frailty Aging 3:158–165.

Onen NF, Shacham E, et al. (2009). 'Frailty among HIV-infected persons in an urban outpatient care setting'. J Infect 59:346-352.

Ortiz A, J. P., Sanz A, Melero R, Caramelo C, Guerrero M F, Strutz F, Müller G, Barat A, Egido J (2005). 'Tubular cell apoptosis and cidofovir-induced acute renal failure'. Antivir Ther 10:185–190.

Orvedahl A, et al. (2011). 'Image-based genome-wide siRNA screen identifies selective autophagy factors'. Nature 480:113–117.

Otera H, et al. (2010). 'Mff is an essential factor for mitochondrial recruitment of Drp1 during mitochondrial fission in mammalian cells'. J. Cell Biol 191:1141–1158.

Ottenbacher KJ, Graham JE, Al Snih S, Raji M, Samper-Ternent R, Ostir GV, et al. (2009). 'Mexican Americans and frailty: findings from the Hispanic established populations epidemiologic studies of the elderly'. Am J Public Health 99:673-9.

Otto-Buczkowska E, Dworzecki T (2003). 'The role of skeletal muscle in the regulation of glucose homeostasis.' Endokrynol Diabetol Chor Przemiany Materii Wieku Rozw 9:93-97.

Oustanina S, Hause G, Braun T (2004). 'Pax7 directs postnatal renewal and propagation of myogenic satellite cells but not their specification'. EMBO J 23:3430–3439.

Padilla S, Gutierrez F, Masiá M, Cánovas V, Orozco C (2005). 'Low frequency of renal function impairment during one-year of therapy with tenofovir-containing regimens in the real-world: A case-control study'. AIDS Patient Care STDS 19:421–424.

Palade GE (1953). 'An electron microscope study of the mitochondrial structure'. Journal of Histochemistry & Cytochemistry 1:188-211.

Palau F, Estela A, Pla-Martin D, Sanchez-Piris M (2009). 'The role of mitochondrial network dynamics in the pathogenesis of Charcot-Marie-Tooth disease'. Adv Exp Med Biol 652:129-137.

Palikaras K, Lionaki E, Tavernarakis N (2018). 'Mechanisms of mitophagy in cellular homeostasis, physiology and pathology'. Nature Cell Biology 20:1013-1022.

Pannerec A, Springer M, Migliavacca E, Ireland A, Piasecki M, Karaz S, et al. (2016). 'A robust neuromuscular system protects rat and human skeletal muscle from sarcopenia'. Aging 8:712-729.

Pannu N (2012). 'Bidirectional relationships between acute kidney injury and chronic kidney disease'. Curr Opin Nephrol Hypertens 22(3):351–356.

Panza F, Barulli MR, et al. (2015). 'Cognitive frailty: a systematic review of epidemiological and neurobiological evidence of an age-related clinical condition'. Rejuvenation Res 18:389–412.

Panza F, Lozupone M, Solfrizzi V, et al. (2018). 'Different cognitive frailty models and heath- and cognitive related outcomes in older age: from epidemiology to prevention'. J Alzheimers Dis 62:993-1012.

Paravicini TM, Touyz RM (2006). 'Redox signaling in hypertension'. Cardiovasc Res 71:247–258.

Park CB, Larsson NG (2011). 'Mitochondrial DNA mutations in disease and aging'. J Cell Biol 193:809–818.

Park J, Morrow CD (1993). 'Mutations in the protease gene of human immunodeficiency virus type 1 affect release and stability of virus particles'. Virology 194:843-850.

Park SW, Lee JS, Kuller LH, Boudreau R, de Rekeneire N, Harris TB, Kritchevsky S, Tylavsky FA, Nevitt M, et al. (2009). 'Excessive loss of skeletal muscle mass in older adults with type 2 diabetes'. Diabetes Care 32.

Pathai S, Weiss HA, et al. (2013). 'Ocular parameters of biological ageing in HIV-infected individuals in South Africa: Relationship with chronological age and systemic biomarkers of ageing'. Mech Ageing Dev 134:400-406.

Patsouris D, et al. (2014). 'Insulin resistance is associated with MCP1-mediated macrophage accumulation in skeletal muscle in mice and humans'. PLOS ONE 9.

Paulo TRS, Sasaki JE, et al. (2016). 'A cross-sectional study of the relationship of physcial activity with depression and cognitive deficit in older adults'. J Aging Phys Act 24:311-321.

Pavasini R, Brown JC, et al. (2016). 'Short physical performance battery and all-cause mortality: systematic review and meta-analysis'. BMC Med 14.

Payne BAI, Hollingsworth K, Baxter J, Wilkins E, Lee V, Price DA, Trenell M, Chinnery PF (2014). 'In Vivo Mitochondrial Function in HIV-Infected Persons Treated with Contemporary Anti-Retroviral Therapy: A Magnetic Resonance Spectroscopy Study'. PLOS ONE 9(1):e84678.

Payne BAI, Wilson IJ, Hateley CA, et al. (2011). 'Mitochondrial aging is accelerated by anti-retroviral therapy through the clonal expansion of mtDNA mutations'. Nat Genet 43:806-810.

Perandini LA, Chimin P, Lutkemeyer DDS, Camara NOS (2018). 'Chronic inflammation in skeletal muscle impairs satellite cells function during regeneration: can physical exercise restore the satellite cell niche?'. FEBS J 285(11):1973-1984

Perazella MA. (2010). 'Tenofovir-induced kidney disease: an acquired renal tubular mitochondriopathy'. Kidney International 78(11):1060-1063.

Perdomo J, Cabrera J, Estevez F, et al. (2013). 'Melatonin induces apoptosis through a caspase-dependent but reactive oxygen species-independent mechanism in human leukemia Molt-3 cells'. J Pineal Res 55:195–206.

Pereira AS, Gerber JG, et al. (2002). 'The Pharmacokinetics of Amprenavir, Zidovudine, and Lamivudine in the Genital Tracts of Men Infected with Human Immunodeficiency Virus Type 1 (AIDS Clinical Trials Group Study 850)'. Journal of Infectious Diseases 186:198-204.

Perez-Molina J, Rubio R, Rivero A, Pasquau J, Suárez-Lozano I, Riera M, et al. (2017). 'Simplification to dual therapy (atazanavir/ritonavir + lamivudine) versus standard triple therapy [atazanavir/ritonavir + two nucleos(t)ides] in virologically stable patients on antiretroviral therapy: 96 week results from an open-label, non-inferiority, randomized clinical trial (SALT study)'. J Antimicrob Chemother 72(1):246–253.

Pérez-Suárez TG, Gutierrez-Robledo LM, Ávila-Funes JA, Acosta JL, EscamillaTilch M, Padilla-Gutiérrez JR, Torres-Carrillo N, Torres-Castro S, López-Ortega M, Muñoz-Valle JF, Torres-Carrillo NM (2016). 'VNTR polymorphisms of the IL-4 and IL-1RN genes and their relationship with frailty syndrome in Mexican community-dwelling elderly'. Aging Clin. Exp. Res 28:823-832.

Perez-Tasigchana RF, Leon-Munoz LM, Lopez-Garcia E, et al. (2017). 'Metabolic syndrome and insulin resistance are associated with frailty in older adults: a prospective cohort study'. Age Ageing 46:807-812.

Perico L, Morigi M, Benigni A (2016). 'Mitochondrial Sirtuin 3 and renal diseases'. Nephron 134:14–19.

Perkins G, Renken C, Martone ME, Young SJ, Ellisman M, Frey T (1997). 'Electron tomography of neuronal mitochondria: three-dimensional structure and organization of cristae and membrane contacts'. J Struct Biol 119(3):260-272.

Perkisas S, Vandewoude M (2016). 'Where frailty meets diabetes'. Diabetes Metab Res Rev 32 Suppl 1:261- 7

Persson Ö, et al. (2019). 'Copy-choice recombination during mitochondrial L-strand synthesis causes DNA deletions'. Nat. Commun 10:75.

Peter P (2004). 'Pharmacokinetic properties of nucleoside/nucleotide reverse transcriptase inhibitors'. JAIDS 37:s2-12.

Petersen KF, et al. (2007). 'The role of skeletal muscle insulin resistance in the pathogenesis of the metabolic syndrome'. Proc Natl Acad Sci U S A 104:12587–12594.

Petersen KF, Shulman GI (2002). 'Pathogenesis of skeletal muscle insulin resistance in type 2 diabetes mellitus'. Am J Cardiol 90:11G–18G.

Peterson CM, Johannsen DL, Ravussin E (2012). 'Skeletal muscle mitochondria and aging: a review'. J. Aging Res 194821.

Peyriere H, Rouanet I, et al. (2004). 'Renal tubular dysfunction associated with tenofovir therapy: report of 7 cases'. J Aquir Immune Defic Syndr 35:269–273.

Phair J, Palella F (2011). 'Renal disease in HIV-infected individuals.' Curr Opin HIV AIDS 6(4):285-289.

Phielix E, Meex R, Ouwens DM, Sparks L, Hoeks J, Schaart G, et al. (2012). 'High oxidative capacity due to chronic exercise training attenuates lipid-induced insulin resistance'. Diabetes 61:2472–2478.

Phielix E, Schrauwen-Hinderling VB, Mensink M, Lenaers E, Meex R, Hoeks J, Kooi ME, Moonen-Kornips E, Sels JP, Hesselink MK, et al. (2008). 'Lower intrinsic ADP-stimulated mitochondrial respiration underlies *in vivo* mitochondrial dysfunction in muscle of male type 2 diabetic patients'. Diabetes 57:2943–2949.

Phillips T, Leeuwenburgh C (2005). 'Muscle fiber specific apoptosis and TNF-alpha signaling in sarcopenia are attenuated by life-long calorie restriction'. Faseb J 19(6):668-670

Picard M, Csukly K, Robillard ME, et al. (2008). "Resistance to Ca^{2+}-induced opening of the permeability transition pore differs in mitochondria from glycolytic and oxidative muscles'. Am J Physiol Regul Integr Comp Physiol *295*:R659–R668.

Picard M, Hepple RT, Burelle Y (2012). 'Mitochondrial functional specialisation in glycolytic and oxidative muscle fibres: tailoring and organelle for optimal function'. Am J Physiol: Cell Physiol 15:C629-41.

Pickett SJ, Ng Y, Gorman GS, et al. (2018). 'Phenotypic heterogeneity in m.3243A>G mitochondrial disease: The role of nuclear factors'. Annals of clinical and translational neurology 5:333-345.

Pickles S, Vigie P, Youle RJ (2018). 'Mitophagy and quality control mechanisms in mitochondrial maintenance'. Curr. Biol 28:R170–R185.

Pierce GB, Parchment RE, Lewellyn AL (1991). 'Hydrogen peroxide as a mediator of programmed cell death in the blastocyst'. Differentiation 46:181-186.

Pietrangelo T, Puglielli C, Mancinelli R, Beccafico S, Fano G, Fulle S (2009). 'Molecular basis of the myogenic profile of aged human skeletal muscle satellite cells during differentiation'. Exp Gerontol 44:523– 531.

Piggott DA, Mehta SR, et al. (2013). 'Frailty, HIV infection, and mortality in an aging cohort of injection drug users'. PLOS ONE 8:e54910.

Piggott DA, Varadhan R, Metha SH, et al. (2015). 'Frailty, inflammation, and mortality among persons aging with HIV infection and injection drug use'. J Gerontol A Biol Sci Med Sci 70:1542-7.

Pilon AA, et al. (2002). 'Induction of Apoptosis by a Nonnucleoside Human Immunodeficiency Virus Type 1 Reverse Transcriptase Inhibitor'. Antimicrobial Agents and Chemotherapy.

Pinto Neto LFDS, Sales MC, Scaramussa ES (2016). 'Human immunodeficiency virus infection and its association with sarcopenia'. The Brazilian Journal of Infectious Diseases 20:99–102.

Pinton P, Pozzan T, Rizzuto R (1998). 'The Golgi apparatus is an inositol 1, 4, 5- trisphosphate-sensitive Ca2+ store, with functional properties distinct from those of the endoplasmic reticulum'. EMBO J 17:5298–5308.

Pinz KG, Shibutani S, Bogenhagen DF (1995). 'Action of mitochondrial DNA polymerase gamma at sites of base loss or oxidative damage'. J. Biol. Chem. 270:9202-9206

Platt C, Coward RJ. (2017). 'Peroxisome proliferator activating receptor-gamma and the podocyte'. Nephrol Dial Transplant 32:423–433.

Podany AT, Bares SH, Havens J, et al. (2018). 'Plasma and intracellular pharmacokinetics of tenofovir in patients switched from tenofovir disoproxil fumarate to tenofovir alafenamide'. AIDS 32:761-765.

Poizot-Martin I, Solas C, Allemand JOR, et al. (2013). 'Renal impairment in patients receiving a tenofovir–cART regimen: impact of tenofovir concentration'. J Acquir Immune Defic Syndr 62(4): 375–380.

Pollack LR, Cawthon PM, et al. (2017). 'Patterns and predictors of frailty transitions in older men: the Osteoporotic Fractures in Men study'. J Am Geriatr Soc 65:2473–2479.

Ponnalagu D, Farber J, et al. (2016). 'Molecular identity of cardiac mitochondrial chloride intracellular channel proteins'. Mitochondrion 27:6-14.

Popovic M, Sarngadharan MG, Read E, Gallo RC (1984). 'Detection, isolation, and continuous production of cytopathic retroviruses (HTLV-III) from patients with AIDS and pre-AIDS'. Science 224: 497-500.

Porpiglia E, Samusik N, Ho ATV, Cosgrove BD, Mai T, Davis KL, Jager A, Nolan GP, Bendall SC, Fantl WJ, Blau HM (2017). 'High-resolution myogenic lineage mapping by single-cell mass cytometry'. Nature Cell Biology 19:558–567.

Porteous WK, James AM, Sheard PW, Porteous CM, Packer MA, Hyslop SJ, Melton JV, Pang C-Y, Wei Y-H, Murphy MP (1998). 'Bioenergetic consequences of accumulating the common 4977-bp mitochondrial DNA deletion'. European Journal of Biochemistry 257:192-201.

Post FA, Tebas P, Clarke A, et al. (2017). 'Brief Report: Switching to Tenofovir Alafenamide, Coformulated With Elvitegravir, Cobicistat, and Emtricitabine, in HIV-Infected Adults With Renal Impairment: 96-Week Results From a Single-Arm, Multicenter, Open-Label Phase 3 Study'. J Acquir Immune Defic Syndr 74:180–184.

Powell SR, Wang P, Divald A, Teichberg S, Haridas V, McCloskey TW, Davies KJ, Katzeff H (2005). 'Aggregates of oxidized proteins (lipofuscin) induce apoptosis through proteasome inhibition and dysregulation of proapoptotic proteins'. Free Radic. Biol. Med. 38:1093–1101

Powers SK, Ji LL, Kavazis AN, Jackson MJ (2011). 'Reactive oxygen species: impact on skeletal muscle'. Compr. Physiol 1:941-969.

Powers SK, Wiggs MP, Duarte JA, et al. (2012). 'Mitochondrial signalling contributes to disuse muscle atrophy'. Am J Physiol E31-E39.

Preston L, Campbell F, Cantrell A, Turner J, Goyder E (2018). 'What evidence is there for the identification and management of frail older people in the emergency department? A systematic mapping review'. Health Serv Delivery Res:1–142.

Prior SJ, Ryan AS, Blumenthal JB, Watson JM, Katzel LI, Goldberg AP (2016). 'Sarcopenia is associated with lower skeletal muscle capillarization and exercise capacity in older adults'. J. Gerontol. A Biol. Sci. Med. Sci. 71:1096-1101.

Pryde KR, Smith HL, Chau KY, Schapira AH (2016). 'PINK1 disables the anti-fission machinery to segregate damaged mitochondria for mitophagy'. J. Cell Biol 213:163–171.

Public Health England (2019). 'HIV in the United Kingdom: towards zero HIV transmissions by 2030.'

Puts MT, Visser M, Twisk JW, Deeg DJ, Lips P (2005). 'Endocrine and inflammatory markers as predictors of frailty'. Clin Endocrinol (Oxf). 63:403–411.

Qi Y, et al. (2016). 'Structures of human mitofusin 1 provide insight into mitochondrial tethering'. J. Cell Biol 215:621–629.

Quinn KJ (2010). 'Incidence of proximal renal tubular dysfunction inpatients on tenofovir disoproxil fumarate'. Int J STD AIDS 21:150–151

Quinsay MN, Thomas RL, Lee Y, Gustafsson AB (2010). 'Bnip3-mediated mitochondrial autophagy is independent of the mitochondrial permeability transition pore'. Autophagy 6:855–862.

Rabøl R, Svendsen PF, Skovbro M, Boushel R, Haugaard SB, Schjerling P, Schrauwen P, Hesselink MKC, Nilas L, Madsbad S, Dela F (2009). 'Reduced skeletal muscle mitochondrial respiration and improved glucose metabolism in nondiabetic obese women during a very low calorie dietary intervention leading to rapid weight loss'. Metab. Clin. Exp. 58:1145–1152.

Raiche M, Hebert R, Dubois M-F (2008). 'PRISMA-7: A case-finding tool to identify older adults with moderate to severe disabilities'. Archives of Gerontology and Geriatrics 47(1):9-18.

Rains JL, Jain SK (2011). 'Oxidative stress, insulin signaling, and diabetes'. Free Radic Biol Med 50: 567-575.

Rajasekaran NS, Shelar S, Jones DP, Hoidal JR (2020). 'Reductive stress impairs myogenic differentiation'. Redox Biology 34.

Ramamoorthy H, Abraham P, Isaac B (2014). 'Mitochondrial dysfunction and electron transport chain complex defect in a rat model of tenofovir disoproxil fumarate nephrotoxicity'. Journal of Biochemical and Molecular Toxicology 28, 246–255.

Ramamoorthy H, Abraham P, Isaac B, Selvakumar D (2018). 'Mitochondrial pathway of apoptosis and necrosis contribute to tenofovir disoproxil fumarate-induced renal damage in rats'. Human & Exper Toxicol 38:288-302.

Ramamoorthy H, Isaac B, Abraham P (2012). 'Evidence for the roles of oxidative stress, nitrosative stress and Nf-Kb activation in Tenofovir Disoproxil Fumarate (TDF) induced renal damage in rats'. BMC Infect Dis 12(suppl 1): P6

Randle PJ (1998). 'Regulatory interactions between lipids and carbohydrates: the glucose fatty acid cycle after 35 years'. Diabetes Metab Rev 14:263-283.

Randle PJ, Garland PB, Hales CN, Newsholme EA (1963). 'The glucose fatty-acid cycle. Its role in insulin sensitivity and the metabolic disturbances of diabetes mellitus'. Lancet 1:785-789.

Rando TA, Chang HY (2012). 'Aging, rejuvenation, and epigenetic reprogramming: resetting the aging clock'. Cell 148,46–57.

Rao PK, Kumar RM, Farkhondeh M, Baskerville S, Lodish HF (2006). 'Myogenic factors that regulate expression of muscle-specific microRNAs'. Proc Natl Acad Sci USA 103:8721-8726.

Rao VK, Carlson EA, Yan SS (2014). 'Mitochondrial permeability transition pore is a potential drug target for neurodegeneration'. Biochim Biophys Acta 1842:1267-1272.

Ray AS, Robinson KL, et al. (2006). 'Mechanism of active renal tubular efflux of tenofovir'. Antimicrobial Agents and Chemotherapy 50(10):3297–3304.

Ray PD, Huang B-W, Tsuji Y (2012). 'Reactive oxygen species (ROS) homeostasis and redox regulation in cellular signaling'. Cell Signal 24:981-990.

Reeg S, Grune T (2015). 'Protein oxidation in aging: does it play a role in aging progression?'. Antioxid. Redox Signal. 23:239–255.

Reeve AK, Krishnan KJ, Elson JL, Morris CM, Bender A, Lightowlers RN, Turnbull DM (2008). 'Nature of mitochondrial DNA deletions in substantia nigra neurons'. Am. J. Hum. Genet 82:228–235.

Reeve AK, Krishnan KJ, Taylor G, Elson JL, Bender A, Taylor RW, Morris CM, Turnbull DM (2009). 'The low abundance of clonally expanded mitochondrial DNA point mutations in aged substantia nigra neurons'. Aging Cell 8:496–498.

Regidor DL, Detels R, Breen EC, Widney DP, Jacobson LP, Palella F, et al. (2011). 'Effect of highly active antiretroviral therapy on biomarkers of B-lymphocyte activation and inflammation'. AIDS 25(3):303–314.

Reid G, Wielinga P, Zelcer N, De Haas M, Van Deemter L, Wijnholds J, Balzarini J, Borst P (2003). 'Characterization of the transport of nucleoside analog drugs by the human multidrug resistance proteins MRP4 and MRP5'. Mol. Pharmacol 63:1094–1103.

Reiter RJ, Paredes SD, Korkmaz A, et al. (2008). 'Melatonin combats molecular terrorism at the mitochondrial level'. Interdiscip Toxicol 1(2): 137–149.

Reiter RJ, Tan D, Burkhardt S (2004). 'Reactive oxygen and nitrogen species and cellular and organismal decline: amelioration with melatonin'. Mech Ageing Dev 123: 1007–1019.

Richman DD (2011). 'Introduction: challenges to finding a cure for HIV infection'. Curr Opin HIV AIDS 6: 1-3.

Richter C, Park JW, Ames BN (1988). 'Normal oxidative damage to mitochondrial and nuclear DNA is extensive'. Proc Natl Acad Sci U S A. 85:6465–6467.

Richter R, Pajak A, Dennerlein S, Rozanska A, Lightowlers RN, Chrzanowska-Lightowlers ZMA (2010). 'Translation termination in human mitochondrial ribosomes'. Biochemical Society Transactions 38: 1523-1526.

Rifkin BS, Perazella MA. (2004). 'Tenofovir-associated nephrotoxicity: Fanconi syndrome and renal failure'. Am J Med 117:282–284.

Riley JS, Cloix C, et al. (2018). 'Mitochondrial inner membrane permeabilisation enables mtDNA release during apoptosis'. EMBO J 37:e99238.

Ristow MSS. (2011). 'Extending life span by increasing oxidative stress'. Free Radic Biol Med 51:327–336.

Ritov VB, Menshikova EV, He J, Ferrell RE, Goodpaster BH, Kelley DE (2005). 'Deficiency of subsarcolemmal mitochondria in obesity and type 2 diabetes'. Diabetes 54:8–14.

Ritz P, Gachon P, Vico L, Bernard JJ, Alexandre C, et al. (1998). 'Energy and substrate metabolism during a 42-day bed-rest in a head-down tilt position in humans'. Eur J Appl Physiol Occup Physiol 78:308e314.

Robberson DL, Kasamatsu H, Vinograd J (1972). 'Replication of Mitochondrial DNA. Circular Replicative Intermediates in Mouse L Cells'. Proceedings of the National Academy of Sciences of the United States of America 69:737-741.

Roberts BM, Lavin KM, Many GM, Thalacker-Mercer A, Merritt EK, Bickel CS, Mayhew DL, Tuggle SC, Cross JM, Kosek DJ, Petrella JK, Brown CJ, Hunter GR, Windham ST, Allman RM, Bamman MM (2018). 'Human neuromuscular aging: sex differences revealed at the myocellular level'. Exp Gerontol 106: 116–124.

Rocha MC, Grady JP, et al. (2018). 'Pathological mechanisms underlying single large-scale mitochondrial DNA deletions'. Annals of Neurology 83:115-130.

Rocha MC, Grady JP, Grunewald A, et al. (2015). 'A novel immunofluorescent assay to investigate oxidative phosphorylation deficiency in mitochondrial myopathy: understanding mechanisms and improving diagnosis'. Scientific Reports 5:15037.

Rockwood K (2005b). 'What would make a definition of frailty successful?'. Age Ageing 34(5):432-4.

Rockwood K, MacKnight C, Bergman H, et al. (2005). 'A global clinical measure of fitness and frailty in elderly people'. CMAJ 173(5):489-495.

Rockwood K, Mitniski A. (2007). 'Frailty in relation to the accumulation of deficits'. J Gerontol A Biol Sci Med Sci 62:722-727.

Rockwood K, Mitnitski A (2011). 'Frailty defined by deficit accumulation and geriatric medicine defined by frailty'. Clin Ger Med 27:17-26.

Rockwood K, Rockwood MRH, Mitnitski A (2010). 'Physiological Redundancy in Older Adults in Relation to the Change With Age in the Slope of a Frailty Index'. J Am Geriatr Soc 58(2):318-323.

Rockwood K, Song X, MacKnight C, Bergman H, Hogan DB, McDowell I, Mitnitski A (2005a). 'A global clinical measure of fitness and frailty in elderly people'. Canadian Medical Association Journal 173:489-495.

Roden M, Perseghin TB, Perseghin G, Petersen KF, Rothman DL, Cline GW, Shulman GI (1996). 'Mechanism of free fatty acid-induced insulin resistance in humans'. J Clin Invest 97:2859-2865

Rodenburg RJ (2016). 'Mitochondrial complex I-linked disease'. Biochemica et Biophysica Acta – Bioenergetics 1857:938-945.

Rodolfo C, Campello S, Cecconi F (2018). 'Mitophagy in neurodegenerative diseases'. Neurochem. Int. 117:156–166.

Rodrigues-Laso A, Galluzzo L, Carcaillon-Bentata L, Beltzer N, Macijauskiene J, et al. (2018). 'Population screening, monitoring and surveillance for frailty: Three systematic reviews and a grey literature review'. Annali Dell'Istituto Superiore di Sanita 54:253-262.

Rodriguez A, Webster P, Ortego J, Andrews NW (1997). 'Lysosomes behave as Ca2+- regulated exocytic vesicles in fibroblasts and epithelial cells'. J. Cell Biol 137:93–104.

Rodriguez C, Mayo JC, Sainz RM, et al. (2004). 'Regulation of antioxidant enzymes: a significant role for melatonin'. J. Pineal Res 36:1–9

Rodriguez-Nvoa S, Alvarez E, Labarga P, Soriano V (2010). 'Renal toxicity associated with tenofovir use'. Expert Opinion on Drug Safety 9(4):545–559.

Roger AJ, Munoz-Gomez SA, Kamikawa R (2017). 'The Origin and Diversification of Mitochondria'. Curr Biol 27(21):R1177-R1192.

Rojansky R, Cha MY, Chan DC (2016). 'Elimination of paternal mitochondria in mouse embryos occurs through autophagic degradation dependent on PARKIN and MUL1'. eLife 5: e17896.

Rojas-Rivera J, De La Piedra C, Ramos A, Ortiz A, Egido J (2010). 'The expanding spectrum of biological actions of vitamin D'. Nephrology Dialysis Transplantation 25(9):2850–2865.

Rolfson DB, Majumdar SR, Tsuyuki RT, Tahir A, Rockwood K (2006). 'Validity and Reliability of the Edmonton Frail Scale'. Age Ageing 35:526-529.

Rollot F, Chauvelot-Moachon L, et al. (2003). 'Tenofovir-related Fanconi syndrome with nephrogenic diabetes insipidus in a patient with acquired immunodeficiency syndrome: the role of lopinavir-ritonavir-didanosine'. Clin. Infect. Dis 37:e174-e176.

Romera-Liebana L, Segura J M, et al. (2018). 'Effects of a primary-care based multifactorial intervention on physical and cognitive function in frail, elderly individuals: a randomized controlled trial'. J Gerontol A Biol Sci Med Sci 73:1668–1674.

Rorbach J, Richter R, Wessels HJ, Wydro M, Pekalski M, Farhoud M, Kuhl I, Gaisne M, Bonnefoy N, Smeitink JA, Lightowlers RN, Chrzanowska-Lightowlers ZM (2008). 'The human mitochondrial ribosome recycling factor is essential for cell viability'. Nucleic Acids Research 36:5787-5799.

Rose AJ, Bisiani B, Vistisen B, Kiens B, Richter EA (2009). 'Skeletal muscle eEF2 and 4EBP1 phosphorylation during endurance exercise is dependent on intensity and muscle fiber type'. Am. J. Physiol. Regul. Integr. Comp. Physiol. 296:R326–R333.

Ross JM, Stewart JB, Hagstrom E, Brene S, Mourier A, Coppotelli G, Freyer C, Lagouge M, Hoffer BJ, Olson L, Larsson N-G (2013). 'Germline mitochondrial DNA mutations aggravate ageing and can impair brain development'. Nature 501:412–415.

Ross MJ, Klotman PE (2002). 'Recent progress in HIV-associated nephropathy'. J Am Soc Nephrol 13: 2997-3004.

Rossi DJ, Seita J, Czechowicz A, Bhattacharya D, Bryder D, Weissman IL (2007). 'Hematopoietic stem cell quiescence attenuates DNA damage response and permits DNA damage accumulation during aging'. Cell Cycle 6:2371– 2376.

Rossignol R, Faustin B, Rocher C, Malgat M, Mazat JP, Letellier T (2003). 'Mitochondrial threshold effects'. Biochem J 370:751-762.

Roth SM, Martel GF, Ivey FM, Lemmer JT, Metter EJ, Hurley BF, Rogers MA (2000). 'Skeletal muscle satellite cell populations in healthy young and older men and women'. Anat Rec 260:351– 358.

Rothman DL, Shulman RG, Shulman GI (1992). '31P nuclear magnetic resonance measurements of muscle glucose-6-phosphate. Evidence for reduced insulin-dependent muscle glucose transport or phosphorylation activity in non-insulin-dependent diabetes mellitus'. J Clin Invest 89:1069-1075

Rouault TA (2012). 'Biogenesis of the iron-sulfur clusters in mammalian cells: new insights and relevance to human disease'. Disease Models & Mechanisms 5:155-164.

Roubenoff R, Parise H, Payette HA, Abad LW, D'Agostino R, Jacques PF, et al. (2003). 'Cytokines, insulin-like growth factor 1, sarcopenia, and mortality in very old community-dwelling men and women: the Framingham Heart Study'. Am J Med. 115(6):429–435.

Roumier T, et al. (2006). 'HIV-1 protease inhibitors and cytomegalovirus vMIA induce mitochondrial fragmentation without triggering apoptosis'. Cell Death Differ 13:348-351.

Rouzier C, Bannwarth S, Chaussenot A, Chevrollier A, Verschueren A, Bonello-Palot N, Fragaki K, Cano A, Pouget J, Pellissier JF, Procaccio V, Chabrol B, Paquis-Flucklinger V (2012). 'The MFN2 gene is responsible for mitochondrial DNA instability and optic atrophy 'plus phenotype'. Brain 135:23-34.

Rowan SL, Rygiel K, Purves-Smith FM, Solbak NM, Turnbull DM, Hepple RT (2012). 'Denervation causes fiber atrophy and myosin heavy chain co-expression in senescent skeletal muscle'. PLOS ONE 7.

Rowe GC, Safdar A, Arany Z (2014). 'Running forward: new frontiers in endurance exercise biology'. Circulation 129:798–810.

Rozzi SJ, Avdoshina V, Fields JA, Mocchetti I (2018). 'Human immunodeficiency virus Tat impairs mitochondrial fission in neurons'. Cell Death Discov 4.

Ruan Q, D'onofrio G, Wu T, Greco A, Sancarlo D, Yu Z1 (2017). 'Sexual dimorphism of frailty and cognitive impairment: Potential underlying mechanisms'. Mol Med Rep 16(3):3023-3033.

Rubenstein AB, Smith GR, Raue U, Begue G, Minchev K, Ruf-Zamojski F, Nair VD, Wang X, Zhou L, Zaslavsky E, Trappe TA, Trappe S, Sealfon SC (2020). 'Single-cell transcriptional profiles in human skeletal muscle'. Scientific Reports 10.

Rudnicki MA, Le Grand F, McKinnell I, Kuang S (2008) 'The molecular regulation of muscle stem cell function'. Cold Spring Harbor Symp Quant Biol 73:323-331

Ruegsegger GN, Creo AL, Cortes TM, Dasari S, Nair KS (2018). 'Altered mitochondrial function in insulin-deficient and insulin-resistant states'. J. Clin. Invest. 128:3671–3681.

Ruggiero C, Metter EJ, Cherubini A, Maggio M, Sen R, Najjar SS, Windham GB, Ble A, Senin U, Ferrucci L (2007). 'White blood cell count and mortality in the Baltimore Longitudinal Study of Aging'. Am Coll Cardiol 49:1841-1850.

Rumlova M, Keprova A, et al. (2014). 'HIV-1 protease-induced apoptosis'. Retrovirology 11.

Russell OM, Rai PK, et al. (2018). 'Preferential amplification of a human mitochondrial DNA deletion in vitro and in vivo'. Scientific Reports 8:1-10.

Rutten IJG, Kruitwagen R, et al. (2017). 'Psoas muscle area is not representative of total skeletal muscle area in the assessment of sarcopenia in ovarian cancer'. J Cachexia Sarcopenia Muscle 8: 630–638.

Ryder JW, Bassel-Duby R, Olson EN, Zierath JR (2003). 'Skeletal muscle reprogramming by activation of calcineurin improves insulin action on metabolic pathways'. J. Biol. Chem 278:44298–44304.

Rygiel KA, Grady JP, Turnbull DM (2014). 'Respiratory chain deficiency in aged spinal motor neurons'. Neurobiol Aging 35:2230-2238.

Ryhänen T, Hyttinen JMT, Kopitz J, Rilla K, Kuusisto E, Mannermaa E, et al. (2009). 'Crosstalk between Hsp70 molecular chaperone, lysosomes and proteasomes in autophagy-mediated proteolysis in human retinal pigment epithelial cells'. J. Cell. Mol. Med. 13:3616–3631.

Ryom L, Kirk O, Worm SW, et al. (2013). 'Association between antiretroviral exposure and renal impairment among HIV-positive persons with normal baseline renal function: the D:A:D study'. Journal of Infectious Diseases 207:1359-1369.

Ryom L, Mocroft A, Kirk O, et al. (2017). 'Predictors of estimated glomerular filtration rate progression, stabilization or improvement after chronic renal impairment in HIV-positive individuals'. AIDS 31:1261–1270.

Sacco A, Mourkioti F, Tran R, Choi J, Llewellyn M, Kraft P, et al (2010). 'Short telomeres and stem cell exhaustion model Duchenne muscular dystrophy in mdx/mTR mice'. Cell 143:1059–1071.

Sagan L (1967). 'On the origin of mitosing cells'. Journal of Theoretical Biology 14(3):225-274.

Sakamoto K, Holman GD (2008). 'Emerging role for AS160/TBC1D4 and TBC1D1 in the regulation of GLUT4 traffic'. Am J Physiol Endocrinol Metab 295:29-37.

Sakellariou GK, Pye D, Vasilaki A, Zibrik L, Palomero J, Kabayo T, et al. (2011). 'Role of superoxide-nitric oxide interactions in the accelerated age-related loss of muscle mass in mice lacking Cu,Zn superoxide dismutase'. Aging Cell 10:749–760.

Sambasivan R, Yao R, Kissenpfennig A, Van Wittenberghe L, Paldi A, Gayraud-Morel B, et al. (2011). 'Pax7-expressing satellite cells are indispensable for adult skeletal muscle regeneration'. Development 138:3647–3656.

Samuels R, Roca-Bayerri C, Sayer JA, D. A Price, Payne BAI (2017). 'Tenofovir disoproxil fumarate-associated renal tubular dysfunction: non-invasive assessment of mitochondrial injury'. AIDS 31: 1297-1301.

Sandoval H, et al. (2008). 'Essential role for Nix in autophagic maturation of erythroid cells'. Nature 454:232–235.

Santos-Eggimann B, Cuénoud P, Spagnoli J, Junod J (2009). 'Prevalence of frailty in middle-aged and older community-dwelling Europeans living in 10 countries'. J. Gerontol. A Biol. Sci. Med. Sci 64: 675–681

Sarraf SA, et al. (2013). 'Landscape of the PARKIN-dependent ubiquitylome in response to mitochondrial depolarization'. Nature 496:372–376.

Sato M, Motomura T, Aramaki H, Matsuda T, et al. (2006). 'Novel HIV-1 integrase inhibitors derived from quinolone antibiotics'. J Med Chem 49:1506-1508.

Satoh M, Kuroiwa T (1991). 'Organization of multiple nucleoids and DNA molecules in mitochondria of a human cell'. Experimental Cell Research 196:137-140.

Saum KU, Dieffenbach AK, Jansen EHJM, Schöttker B, Holleczek B, Hauer K, Brenner H (2015). 'Association between oxidative stress and frailty in an elderly German population: results from the ESTHER cohort study'. Gerontology 61:407–415.

Saum KU, Dieffenbach AK, Muller H, Holleczek B, Hauer K, Brenner H (2014). 'Frailty prevalence and 10-year survival in community-dwelling older adults: results from the ESTHER cohort study'. Eur J Epidemiol 29:171-9

Sauter D, Vogl M, Usmani S M, Heigele A, Kluge SF, Hermkes E, Moll M, Barker E, Peeters M, Learn G H, Bibollet-Ruche F, Fritz JV, Fackler OT, Hahn BH, Kirchhoff F (2012). 'Human tetherin exerts strong selection pressure on the HIV-1 group N Vpu protein'. PLoS Pathog 8:e1003093.

Savage DB, Petersen KF, Shulman GI (2007). 'Disordered lipid metabolism and the pathogenesis of insulin resistance'. Physiol Rev 87:507-520.

Sayed RKA, Fernandez-Ortiz M, Diaz-Casado ME, Rusanova I, Rahim I, Escames G, López LC, Mokhtar DM, Acuña-Castroviejo D (2018). 'The protective effect of melatonin against age-associated, sarcopenia-dependent tubular aggregate formation, lactate depletion, and mitochondrial changes'. J. Gerontol. A Biol. Sci. Med. Sci. 73:1330–1338.

Sayegh JF, Lajtha A (1989). 'In vivo rates of protein synthesis in brain, muscle, and liver of 5 vertebrate species'. Neurochem Res 14:1165–1168.

Sayer AA, Kirkwood TBL (2015). 'Grip strength and mortality: a biomarker of ageing?'. Lancet. 386(9990):226–227.

Scarpulla RC (2008). 'Transcriptional paradigms in mammalian mitochondrial biogenesis and function'. Physiol Rev 88:611-638.

Schaap LA, Koster A, Visser M (2013). 'Adiposity, muscle mass, and muscle strength in relation to functional decline in older persons'. Epidemiol Rev 35:51-65.

Schaap LA, van Schoor NM, Lips P, et al. (2018). 'Associations of sarcopenia definitions, and their components, with the incidence of recurrent falling and fractures: the longitudinal aging study Amsterdam'. J Gerontol A Biol Sci Med Sci 73:1199–204.

Schägger H, Pfeiffer K (2000). 'Supercomplexes in the respiratory chains of yeast and mammalian mitochondria'. EMBO J 19:1777–1783.

Schaub TP, Kartenbeck J, Konig J, Vogel O, Witzgall R, Kriz W, Keppler D (1997). 'Expression of the conjugate export pump encoded by themrp2 gene in the apical membrane of kidney proximal tubules'. J. Am. Soc Nephrol 8:1213–1221.

Scherzer R, Estrella M, Li Y, Deeks SG, Grunfeld C, Shlipak M G (2012). 'Association of Tenofovir Exposure with Kidney Disease Risk in HIV Infection'. AIDS 26(7):867-875.

Scherz-Shouval R, Shvets E, Fass E, Shorer H, Gil L, Elaza Z (2007). 'Reactive oxygen species are essential for autophagy and specifically regulate the activity of Atg4'. EMBO Journal 26:1749-1760.

Schieber M, Chandel NS (2014). 'ROS function in detox signalling and oxidative stress'. Curr Biol 24:R453-462.

Schlegel TF, Hawkins RJ, Lewis CW, Motta T, Turner AS (2006). 'The effects of augmentation with swine small intestine submucosa on tendon healing under tension: histologic and mechanical evaluations in sheep'. Am. J. Sports Med 34, 275–280.

Schmaltz HN, Fried LP, Xue QL, Walston J, Leng SX, Semba RD (2005). 'Chronic cytomegalovirus infection and inflammation are associated with prevalent frailty in community-dwelling older women'. J Am Ger Soc 53:747-754.

Schmitz-Peiffer C, Biden TJ (2008). 'Protein kinase C function in muscle, liver, and β-cells and its therapeutic implications for type 2 diabetes'. Diabetes 57:1774–1783.

Schnyder S, Handschin C (2015). 'Skeletal muscle as an endocrine organ: PGC-1alpha, myokines and exercise'. Bone 80:115–125.

Schon EA, Rizzuti R, Moreas CT, Nakase H, Zeviani M, DiMauro S (1989). 'A direct repeat is a hotspot for large-scale deletion of human mitochondrial DNA'. Science 244:346-349.

Schrauwen-Hinderling VB, Kooi ME, Hesselink MK, Jeneson JA, Backes WH, van Echteld CJ, van Engelshoven JM, Mensink M, Schrauwen P (2007). 'Impaired in vivo mitochondrial function but similar intramyocellular lipid content in patients with type 2 diabetes mellitus and BMI-matched control subjects'. Diabetologia 50:113-120.

Schreiber V, Dantzer F, Ame JC, et al. (2006). 'Poly (ADP-ribose): novel functions for an old molecule'. Nat Rev Mol Cell Biol 7:517–528.

Schrempft S, Jackowska M, Hamer M, Steptoe A (2019). 'Associations between social isolation, loneliness, and objective physical activity in older men and women'. BMC Public Health 19:74.

Schweers RL, et al. (2007). 'NIX is required for programmed mitochondrial clearance during reticulocyte maturation'. Proc. Natl Acad. Sci. USA 104:19500–19505.

Sciacco M, Bonilla E, Schon EA, DiMauro S, Moraes CT (1994). 'Distribution of wild-type and common deletion forms of mtDNA in normal and respiration-deficient muscle fibers from patients with mitochondrial myopathy'. Hum Mol Genet 3:13-19.

Scorrano L, et al. (2002). 'A distinct pathway remodels mitochondrial cristae and mobilizes cytochrome c during apoptosis'. Dev. Cell 2:55–67

Scott D, Sanders KM, Aitken D, Hayes A, Ebeling PR, Jones G (2014). 'Sarcopenic obesity and dynapenic obesity: 5-year associations with falls risk in middle-aged and older adults'. Obesity 22: 1568-1574.

Scott JD, Wolfe PR, Bolan RK, Guyer B (2006). 'Serious renal impairment occurs rarely with use of tenofovir DF'. HIV Clin Trials 7:55-58.

Scott W, Stevens J, Binder-Macleod SA (2001). 'Human skeletal muscle fibre type classifications'. Physical therapy 81:1810-1816.

Searle SD, Mitnitski AB, Gahbauer EA, et al. (2008). 'A standard procedure for creating a frailty index'. BMC Geriatr 8:24.

Sekine S, Youle RJ (2018). 'PINK1 import regulation; a fine system to convey mitochondrial stress to the cytosol'. BMC Biol. 16: 2.

Selvaraj S, Ghebremichael M, Li M (2014). 'Antiretroviral Therapy-Induced Mitochondrial Toxicity: Potential Mechanisms Beyond Polymerase-γ Inhibition'. Clin Pharmacol Ther 96(1):110-120.

Semba RD, Margolick JB, Leng S, Walston J, Ricks MO, Fried LP (2005). 'T cell subsets and mortality in older community-dwelling women'. Exp Gerontol 40:81-87.

Serra-Prat M, Domenich R, et al. (2017). 'Effectiveness of an intervention to prevent frailty in pre-frail community-dwelling older people consulting in primary care: a randomised controlled trial'. Age Ageing 46:401–407.

Servais H, Ortiz A, Devuyst O, et al. (2008). 'Renal cell apoptosis induced by nephrotoxic drugs: cellular and molecular mechanisms and potential approaches to modulation'. Apoptosis 13:11–32.

Serviddio G, Romano AD, Greco A, Rollo T, Bellanti F, Altomare E, Vendemiale G. (2009). 'Frailty syndrome is associated with altered circulating redox balance and increased markers of oxidative stress'. Int J Immunopathol Pharmacol. 22:819–27.

Shadel GS, Clayton DA (1997). 'Mitochondrial DNA maintenance in vertebrates'. Annu Rev Biochem 66:409-435.

Shadrach JL, Wagers AJ (2011). 'Stem cells for skeletal muscle repair'. Phil Trans R Soc Lond B 366: 2297– 2306.

Shaffer N, Chuachoowong R, Mock PA, et al. (1999). 'Short-course zidovudine for perinatal HIV-1 transmission in Bangkok, Thailand: a randomised controlled trial. Bangkok Collaborative Perinatal HIV Transmission Study Group'. Lancet 353(9155):773–780.

Shah K, Hilton TN, Myers L, Pinto JF, et al. (2012). 'A new frailty syndrome: central obesity and frailty in older adults with the human immunodeficiency virus'. J Am Geriatr Soc 60:545-9.

Shankaran M, Fessler C, et al. (2018). 'Dilution of oral D3-creatine to measure creatine pool size and estimate skeletal muscle mass: development of a correction algorithm'. J Cachexia Sarcopenia Muscle 9:540–546.

Sharp PM, Hahn BH (2011). 'Origins of HIV and the AIDS pandemic'. Cold Spring Harb Perspect Med 1:a006841.

Shaw AC, Joshi H, Greenwood A, et al. (2010). 'Aging of the innate immune system'. Curr Opin Immunol 22:507-513.

Shefer G, Van de Mark DP, Richardson JB, Yablonka-Reuveni Z (2006). 'Satellite-cell pool size does matter: defining the myogenic potency of aging skeletal muscle'. Dev Biol 294:50– 66.

Shetty S, et al. (2009). 'Adiponectin in health and disease: evaluation of adiponectin-targeted drug development strategies'. Trends Pharmacol. Sci. 30:234–239.

Shivappa N, Stubbs B, Hébert JR, Cesari M, Schofield P, Soysal P, Maggi S, Veronese N (2018). 'The relationship between the dietary inflammatory index and incident frailty: a longitudinal cohort study'. J. Am. Med. Dir. Assoc 19:77-82.

Shoffner JM, Lott MT, Lezza AMS, Seibel P, Ballinger SW, Wallace DC (1989). 'Myoclonic epilepsy and ragged-red fiber disease (MERRF) is associated with a mitochondrial DNA tRNALys mutation'. Cell 61:931-937.

Short KR, Bigelow ML, Kahl J, Singh R, et al. (2005). 'Decline in skeletal muscle mitochondrial function with aging in humans'. PNAS 102:5618-5623.

Shoubridge EA, Wai T (2007). 'Mitochondrial DNA and the mammalian oocyte'. Curr Top Dev Biol 77:87-111.

Shukla V, Mishra SK, Pant HC (2011). 'Oxidative stress in neurodegeneration'. Adv Pharmacol Sci 572634.

Sickmann A, Reinders J, Wagner Y, Joppich C, Zahedi R, et al. (2003). 'The proteome of Saccharomyces cerevisiae mitochondria'. Proc. Natl. Acad. Sci. USA 100:13207–13212.

Sico JJ, Chang CC, So-Armah K, Justice AC, Hylek E, Skanderson M, et al. (2015). 'HIV status and the risk of ischemic stroke among men'. Neurology 84(19):1933–40

Sies H (2015). 'Oxidative stress: a concept in redox biology and medicine'. Redox Biol 4:180-183.

Silva RB, Aldoradin-Cabeza H, Eslick GD, Phu S, Duque G (2017). 'The effect of physical exercise on frail older persons: a systematic review'. J Frailty Aging 6:91-96.

Silverberg MJ, Lau B, Achenbach CJ, Jing Y, Althoff KN, D'Souza G, et al. (2015). 'Cumulative incidence of cancer among persons with HIV in North America: a cohort study'. Ann Intern Med 163(7):507–18.

Simms V, Rylance S, Bandason T, Dauya E, McHugh G, Munyati S, et al. (2018). 'CD4 count recovery following initiation of HIV antiretroviral therapy in older childhood and adolescence'. AIDS 32:1977-1982.

Sims CR, MacMillan-Crow LA, Mayeux PR (2014). 'Targeting mitochondrial oxidants may facilitate recovery of renal function during infant sepsis'. Clin Pharmacol Ther 96:662–664.

Sitte N, Huber M, Grune T, Ladhoff A, Doecke WD, Von Zglinicki T, Davies KJ (2000). 'Proteasome inhibition by lipofuscin/ceroid during postmitotic aging of fibroblasts'. FASEB J. Off. Publ. Fed. Am. Soc. Exp. Biol. 14:1490–1498.

Slawik M, Vidal-Puig AJ (2006). 'Lipotoxicity, overnutrition and energy metabolism in aging'. Ageing Res Rev 5(2):144-64

Smirnova E, Griparic L, Shurland DL, van der Bliek AM (2001). 'Dynamin-related protein Drp1 is required for mitochondrial division in mammalian cells'. Mol. Biol. Cell 12:2245–2256

Smit M, Geerlings S, Smit C, Thyagarajan K, Sighem A, et al. (2015). 'Future challenges for clinical care of an ageing population infected with HIV: a modelling study'. Lancet Infect Dis 15(7):810-818.

Smith ALM, Whitehall JC, Greaves LC, Hunt M, et al. (2020). 'Age-associated mitochondrial DNA mutations cause metabolic remodelling that contributes to accelerated intestinal tumorigenesis'. Nat Cancer 1:976-989.

Smith GI, Reeds D N, Mohammed B S, Rankin D, Rennie M J, et al. (2011). 'Omega-3 polyunsaturated fatty acids augment the muscle protein anabolic response to hyperinsulinaemiahyperaminoacidaemia in healthy young and middle-aged men and women'. Clin Sci 121:267-278.

Smith HW (1952). 'The Kidney: structure and function in heath and disease'. Postgraduate Medical Journal 28:191-192.

Snyder PJ, Hannoush P, Berlin JA, Loh L, Lenrow DA, Holmes JH, Dlewati A, Santanna J, Rosen CJ, et al. (1999). 'Effect of testosterone treatment on body composition and muscle strength in men over 65 years of age'. J Clin Endocrinol Metab 84:2647-2653.

Sonjak V, Jacob K, Morais JA, et al. (2019). 'Fidelity of muscle fibre reinnervation modulates ageing muscle impact in elderly women'. J Physiol 597.

Soubannier V, Rippstain P, Kaufman BA, Shoubridge EA, McBride HM (2012). 'Reconstitution of Mitochondria Derived Vesicle Formation Demonstrates Selective Enrichment of Oxidized Cargo'. PLOS ONE:e52830.

Sousa-Victor P, Garcia-Prat L, et al. (2014). 'Geriatric muscle stem cells switch reversible quiescence into senescence'. Nature 506:316-330.

Sousa-Victor P, Munoz-Canoves P (2017). 'Regenerative decline of stem cells in sarcopenia'. Mol Aspects Med 50:109-117.

Soysal P, Isik AT, Carvalho AF, Fernandes BS, Solmi M, Schofield P, Veronese N, Stubbs B (2017). 'Oxidative stress and frailty: a systematic review and synthesis of the best evidence'. Maturitas 99:66–72.

Soysal P, Stubbs B, Lucato P, Luchini C Solmi M, Peluso R, Sergi G, Isik AT, Manzato E, Maggi S, Maggio M, Prina AM, Cosco TD, Wu Y-T, Veronese N (2016). 'Inflammation and frailty in the elderly: a systematic review and meta-analysis'. Ageing Res. Rev 31:1-8.

Sparks LM, Xie H, Koza RA, Mynatt R, Hulver MW, Bray GA, Smith SR (2005). 'A high-fat diet coordinately downregulates genes required for mitochondrial oxidative phosphorylation in skeletal muscle'. Diabetes 54:1926-1933.

Speakman JR, Westerterp KR (2010). 'Associations between energy demands, physcial activity, and body composition in adult humans between 18 and 96 y of age'. The American Journal of Clinical Nutrition 92:826-834.

Spelbrink JN, Nikali K, et al. (2001). 'Human mitochondrial DNA deletions associated with mutations in the gene encoding Twinkle, a phage T7 gene 4-like protein localized in mitochondria'. Nat Genet 28:223-231.

Spendiff S, Gouspillou G, et al. (2016). 'Denervation drives mitochondrial dysfunction in skeletal muscle of octogenarians'. J Physiol 594:7361-7379.

Squires K, Pierone G, Jr., Steinhart C R, Berger D, Bellos N C, et al. (2003). 'Tenofovir disoproxil fumarate in nucleoside-resistant HIV-1 infection: a randomized trial'. Ann Intern Med 139:313–320.

Standley RA, Liu SZ, Jemiolo B, Trappe SW, Trappe TA (2013). 'Prostaglandin E2 induces transcription of skeletal muscle mass regulators interleukin-6 and muscle RING finger-1 in humans'. Prostaglandins Leukot. Essent. Fat. Acids 88:361–364.

Steffl M, Sima J, Shiells K, et al. (2017). 'The increase in health care costs associated with muscle weakness in older people without long-term illnesses in the Czech Republic: results from the Survey of Health, Ageing and Retirement in Europe (SHARE)'. Clin Interv Aging 12:2003–07

Stenholm S, Ferrucci L, Vahtera J, et al. (2019). 'Natural course of frailty components in people who develop frailty syndrome: evidence from two cohort studies'. J Gerontol A Biol Sci Med Sci 74:667-674

Stiles AR, Stover A, et al. (2016). 'Mutations in TFAM, encoding mitochondrial transcription factor A, cause neonatal liver failure associated with mtDNA depletion'. Mol Genet Metab 119:91-09.

St-Jean-Pelletier F, Pion CH, Leduc-Gaudet JP, Sgarioto N, Zovile I, Barbat-Artigas S, Reynaud O, Alkaterji F, Lemieux FC, Grenon A, Gaudreau P, Hepple RT, Chevalier S, Belanger M, Morais JA, Aubertin-Leheudre M, Gouspillou G (2017). 'The impact of ageing, physical activity, and pre-frailty on

skeletal muscle phenotype, mitochondrial content, and intramyocellular lipids in men'. J Cachexia Sarcopenia Muscle 8:213–228.

Stock D, Gibbons C, Arechaga I, Leslie AG, Walker JE (2000). 'The rotary mechanism of ATP synthase'. Curr. Opin. Struct. Biol 10:672–679.

Stroikin Y, Dalen H, Loof S, Terman A (2004). 'Inhibition of autophagy with 3-methyladenine results in impaired turnover of lysosomes and accumulation of lipofuscin-like material'. Eur. J. Cell Biol. 83:583–590.

Studenski SA, Peters KW, Alley DE (2014). 'The FNIH sarcopenia project: rationale, study description, conference recommendations, and final estimates'. Journal of Gerontology 69(5):547-558.

Stumpf JD, Copeland WC (2013). 'The Exonuclease Activity of the Yeast Mitochondrial DNA Polymerase γ Suppresses Mitochondrial DNA Deletions Between Short Direct Repeats in Saccharomyces cerevisiae'. Genetics 194:519-522.

Suda T, Takubo K, Semenza GL (2011). 'Metabolic regulation of hematopoietic stem cells in the hypoxic niche'. Cell Stem Cell 9:298-310.

Suetta C, Andersen JL, Dalgas U, Berget J, Koskinen S, Aagaard P, Magnusson SP, Kjaer M (2008). 'Resistance training induces qualitative changes in muscle morphology, muscle architecture, and muscle function in elderly postoperative patients'. J Appl Physiol 105:180–186.

Sugimoto T, Sakurai T, Ono R, Kimura A, Saji N, Niida S, et al. (2018). 'Epidemiological and clinical significance of cognitive frailty: a mini review'. Ageing Res. Rev. 44 1–7.

Sun N, Youle RJ, Finkel T (2016). 'The mitochondrial basis of aging'. Mol Cell 61:654-666.

Sutovsky P, Moreno RD, Ramalho-Santos J, Dominko T, Simerly C, Shatten G (2000). 'Ubiquitinated sperm mitochondria, selective proteolysis, and the regulation of mitochondrial inheritance in mammalian embryos'. Biol Reprod 63:582-590.

Swanepoel CR, Atta MG, D'Agati VD, et al. (2018). 'Kidney disease in the setting of HIV infection: conclusions from a kidney disease: Improving global outcomes (KDIGO) controversies conference'. Kidney Int 93:545-559.

Swiecicka A, Eendebak RJAH, Lunt M, et al. (2018). 'Reproductive hormone levels predict changes in frailty status in community-dwelling older men: European Male Ageing Study Prospective Data'. Journal of Clinical Endocrinology & Metabolism 103:701-709.

Sykora P, Akbari M, Kulikowicz T, Baptiste BA, Leandro GS, et al. (2017). 'DNA polymerase beta participates in mitochondrial DNA repair'. Mol. Cell. Biol 10.

Szabados E, Fischer G, Toth K, Csete B, Nemeti B, Trombitas K, Habon T, Endrei D, Sumegi B (1999). 'Role of reactive oxygen species and poly-ADP-ribose polymerase in the development of AZT-induced cardiomyopathy in rat'. Free Radic Biol Med 26:309–317.

Szendroedi J, Kloock L, et al. (2014). 'Lower fasting muscle mitochondrial activity related to hepatic steatosis in humans'. Diabetes Care 37:468-474.

Szendroedi J, Schmid AI, Meyerspeer M, Cervin C, Kacerovsky M, Smekal G, Graser-Lang S, Groop L, Roden M (2009). 'Impaired mitochondrial function and insulin resistance of skeletal muscle in mitochondrial diabetes'. Diabetes Care 32:677-679.

Taaffe DR, Sipila S, Cheng S, Puolakka J, Toivanen J, Suominen H (2005). 'The effect of hormone replacement therapy and/or exercise on skeletal muscle attenuation in postmenopausal women: A yearlong intervention'. Clin Physiol Funct Imaging 25:297-304.

Tadi SK, Sebastian R, Dahal S, Babu R K, Choudhary B, Raghavan SC (2016). 'Microhomology-mediated end joining is the principal mediator of double strand break repair during mitochondrial DNA lesions'. Mol. Biol. Cell 27:223–235.

Tanaka A, et al. (2010). 'Proteasome and p97 mediate mitophagy and degradation of mitofusins induced by Parkin'. J. Cell Biol 191:1367–1380.

Tanji N, Tanji K, Kambham N, et al. (2001). 'Adefovir nephrotoxicity: possible role of mitochondrial DNA depletion'. Hum Pathol 32:734–740.

Tantillo C, Jocobo-Molina A, Nanni RG, et al. (1994). 'Locations of anti-AIDS drug binding sites and resistance mutations in the three-dimensional structure of HIV-1 reverse transcriptase. Implications for mechanisms of drug inhibition and resistance'. J Mol Biol 243:369-387.

Tate JP, Justice AC, Hughes MD, Bonnet F, Reiss P, Mocroft A, Nattermann J, Lampe FC, Bucher HC, Sterling TR, et al. (2013). 'An internationally generalizable risk index for mortality after one year of antiretroviral therapy'. AIDS 27:563–72.

Taylor RW, et al. (2003). 'Mitochondrial DNA mutations in human colonic crypt stem cells'. J. Clin. Invest 112:1351–1360.

Taylor RW, Pyle A, Griffin H, et al. (2014). 'Use of whole exome sequencing to determine the genetic basis of multiple mitochondrial respiratory chain complex deficiency'. JAMA 312:68-77.

Taylor RW, Turnbull DM (2005). 'Mitochondrial DNA mutations in human disease'. Nat Rev Genet 6(5):389-402.

Taylor-Jones JM, McGehee RE, Rando TA, Lecka-Czernik B, Lipschitz DA, Peterson CA (2002). 'Activation of an adipogenic program in adult myoblasts with age'. Mech Ageing Dev 123:649– 661.

Tedesco FS, Dellavalle A, Diaz-Manera J, Messina G, Cossu G (2010). 'Repairing skeletal muscle: regenerative potential of skeletal muscle stem cells'. J Clin Invest. 120:11-19.

Tengan CH, Moraes CT (1998). 'Duplication and triplication with staggered breakpoints in human mitchondrial DNA'. Biochimica et Biophysica Acta 1406:73-80.

Terman A, Bunk UT (2004). 'Lipofuscin'. Int J Biochem Cell Biol 36:1400-1404.

Terman A, Sandberg S (2002). 'Proteasome inhibition enhances lipofuscin formation'. Ann. N. Y. Acad. Sci. 973:309–312.

Terzian AS, et al. (2009). 'Factors associated with preclinical disability and frailty among HIV-infected and HIV-uninfected women in the era of cART'. J Womens Health 18:1965-1974.

Theou O, Brothers TD, Rockwood MR, Haardt D, Mitnitski A, Rockwood K (2013). 'Exploring the relationship between national economic indicators and relative fitness and frailty in middle-aged and older Europeans'. Age Ageing 42(5):614-619.

Thigpen MC, Kebaabetswe PM, Paxton LA, Smith DK, Rose CE, Segolodi TM, Henderson FL, Pathak SR, Soud FA, Chillag KL, Mutanhaurwa R, Chirwa LI, Kasonde M, Abebe D, Buliva E, Gvetadze RJ, Johnson S, Sukalac T, Thomas VT, Hart C, Johnson JA, Malotte CK, Hendrix CW, Brooks JT (2012).

‘TDF2 Study Group : Antiretroviral preexposure prophylaxis for heterosexual HIV transmission in Botswana’. N Engl J Med 367:423–434

Thillainadesan J, Scott IA, Le Couteur DG (2020). ‘Frailty, a multisystem ageing syndrome’. Age and Ageing 49:758-763.

Thompson C, Dodds RM (2020). ‘The ageing syndromes of sarcopenia and frailty’. Medicine.

Tieland M, Trouwborst I, Clark BC (2018). ‘Skeletal muscle performance and ageing’. Journal of Cachexia, Sarcopenia and Muscle 9:3-19.

Tolea MI, Galvin JE (2015). ‘Sarcopenia and impairment in cognitive and physical performance’. Clin Interv Aging 10:663-671.

Toth MJ, Tchernof A (2006). ‘Effect of age on skeletal muscle myofibrillar mRNA abundance: relationship to myosin heavy chain protein synthesis rate’. Exp Gerontol 41:1195–1200.

Toth MJ, Tracy RP, et al. (2005). ‘Age-related differences in skeletal muscle protein synthesis: relation to markers of immune activation’. Am J Physiol Endocrinol Metab 288:E883-E891.

Trachootham D, Alexandre J, Huang P (2009). ‘Targeting cancer cells by ROS-mediated mechanisms: a radical therapeutic approach?’. Nat Rev Drug Discov 8:579–591.

Tran MT, Zsengeller ZK, Berg AH, et al. (2016). ‘PGC1alpha drives NAD biosynthesis linking oxidative metabolism to renal protection’. Nature 531:528–532.

Trevisan C, Veronese N, Maggi S, et al. (2017). ‘Factors Influencing Transitions Between Frailty States in Elderly Adults: The Progetto Veneto Anziani Longitudinal Study’. J Am Geriatr Soc 65:179-184.

Trifunovic A, Larsson N-G (2008). ‘Mitochondrial dysfunction as a cause of ageing’. J. Int. Med 263: 167–178.

Trifunovic A, Wredenberg A, Falkenberg M, Spelbrink N, Rovio AT, Bruder CE, et al. (2004). ‘Premature ageing in mice expressing defective mitochondrial DNA polymerase’. Nature 429:417-423.

Trounce I, Byrne E, Marzuki S (1989). ‘Decline in skeletal muscle mitochondrial respiratory chain function: possible factor in ageing’. Lancet 25:637-639.

Tsamis F, Gavrilov S, Kajumo F, Seibert C et al. (2003). ‘Analysis of the mechanism by which the small-molecule CCR5 antagonists SCH-351125 and SCH-350581 inhibit human immunodeficiency virus type 1 entry’. J Virol 77:5201-5208.

Tsuboi M, Morita H, Nozaki Y, Akama K, Ueda T, Ito K, Nierhaus KH, Takeuchi N (2009). ‘EF-G2mt is an exclusive recycling factor in mammalian mitochondrial protein synthesis’. Mol Cell 35:502-510.

Turrens JF (2003). ‘Mitochondrial formation of reactive oxygen species’. The Journal of Physiology 552:335-344.

Tyynismaa H, Ylikallio E, Patel M, Molnar MJ, Haller RG, Suomalainen A (2009). ‘A heterozygous truncating mutation in RRM2B causes autosomal-dominant progressive external ophthalmoplegia with multiple mtDNA deletions’. Am J Hum Genet 85:290-295.

Ukropcova B, McNeil M, Sereda O, de Jonge L, Xie H, Bray GA, Smith SR (2005). ‘Dynamic changes in fat oxidation in human primary myocytes mirror metabolic characteristics of the donor’. J Clin Invest 115:1934-1941.

Ulfig N (1989). ‘Altered lipofuscin pigmentation in the basal nucleus (Meynert) in Parkinson's disease’. Neurosci Res 6:456-462.

United Nations (2015). ’World population ageing’. 2015.

Urata M, Wada Y, Kim S H, Chumpia W, Kayamori Y, Hamasaki N, Kang D (2004). ‘High-sensitivity detection of the A3243G mutation of mitochondrial DNA by a combination of allele-specific PCR and peptide nucleic acid-directed PCR clamping’. Clin Chem 50:2045-2051.

Valsecchi F, Esseling JJ, Koopman WJ, Willems PH (2009) ‘Calcium and ATP handling in human NADH:ubiquinone oxidoreductase deficiency’. Biochim. Biophys. Acta 1792:1130-1137

van Aubel RA, Smeets PHE, Peters JG, Bindels RJ, Russel FG (2002). ‘The MRP4/ABCC4 gene encodes a novel apical organic anion transporter in human kidney proximal tubules: putative efflux pump for urinary cAMP and cGMP’. J. Am. Soc. Nephrol 13:595–603.

Van Der Laarse WJ, Des Tombe AL, Lee-de Groot MBE, Diegenbach PC (1998). ‘Size principle of striated muscle cells’. Neth J Zool 48:213–223.

Van Goethem G, Dermaut B, Lofgren A, Maring JJ, Van Broeckhoven (2001). ‘Mutation of POLG is associated with progressive external ophthalmoplegia characterized by mtDNA deletions’. Nat Genet 28:211-212.

Van Laar VS, Berman SB (2009). ‘Mitochondrial dynamics in Parkinson's disease’. Exp Neurol 218:247-56.

Van Rompay AR, Johansson M, Karlsson A (2000). ‘Phosphorylation of nucleosides and nucleoside analogs by mammalian nucleoside monophosphate kinases’. Pharm & Therap 87:189-198.

Vanhoutte G, van de Wiel M, Peeters M, et al. (2016). ‘Cachexia in cancer: what is in the definition’. BMJ Open Gastroenterology 3.

Varma V, et al. (2009). ‘Muscle inflammatory response and insulin resistance: synergistic interaction between macrophages and fatty acids leads to impaired insulin action’. Am J Physiol Endocrinol Metab 296:E1300–E1310.

Vazquez EJ, Berthiaume JM, Kamath V, Achike O, Buchanan E, Montano MM, Chandler MP, Miyagi M, Rosca MG (2015). ‘Mitochondrial complex I defect and increased fatty acid oxidation enhance protein lysine acetylation in the diabetic heart’. Cardiovasc. Res. 107:453–465.

Vellas B, Fielding RA, Bens C, et al. (2018). ‘Implications of ICD-10 for sarcopenia clinical practice and clinical trials: report by the International Conference on Frailty and Sarcopenia Research Task Force’. J Frailty Aging 7:2-9.

Venhoff N, Setzer B, Melkaoui K, Walker UA (2007). ‘Mitochondrial toxicity of tenofovir, emtricitabine and abacavir alone and in combination with additional nucleoside reverse transcriptase inhibitors’. Antivir Ther 12:1075-85.

Venter WDF, Fabian J, Charles F (2018). ‘An overview of tenofovir and renal disease for the HIV-treating clinician’. South African Journal of HIV Medicine 19(1):a817.

Venter WDF, Kambugu A, Chersich MF, et al. (2019). ‘Efficacy and Safety of Tenofovir Disoproxil Fumarate Versus Low-Dose Stavudine Over 96 Weeks: A Multicountry Randomized, Noninferiority Trial’. J Acquir Immune Defic Syndr 80:224.

Venturelli M, Muti E, Naro F, Cancellara L, Toniolo L, et al. (2015). 'In vivo and in vitro evidence that intrinsic upper- and lower-limb skeletal muscle function is unaffected by ageing and disuse in oldestold humans'. Acta Physiol (Oxf) 215:58-71.

Verdijk LB, Dirks ML, Snijders T, Prompers JJ, Beelen M, Jonkers RA, et al. (2012). 'Reduced satellite cell numbers with spinal cord injury and aging in humans'. Med. Sci. Sports Exerc. 44:2322–2330.

Verdijk LB, Gleeson BG, Jonkers RA, Meijer K, Savelberg HH, Dendale P, et al. (2009). 'Skeletal muscle hypertrophy following resistance training is accompanied by a fiber type-specific increase in satellite cell content in elderly men'. J. Geront. Ser. A Biol. Sci. Med. Sci. 64:332–339.

Verdijk LB, Koopman R, Schaart G, Meijer K, Savelberg HH, van Loon LJ (2007). 'Satellite cell content is specifically reduced in type II skeletal muscle fibers in the elderly'. Am J Physiol Endocrinol Metab 292:E151-7.

Verdijk LB, Snijders T, Beelen M, Savelberg HH, Meijer K, Kuipers H, et al. (2010). 'Characteristics of muscle fiber type are predictive of skeletal muscle mass and strength in elderly men'. J. Am. Geriatr. Soc. 58:2069–2075.

Verdijk LB, Snijders T, Drost M, Delhaas T, Kadi F, van Loon LJ (2014). 'Satellite cells in human skeletal muscle; from birth to old age'. Age 36:545–547.

Veronese N, Berton L, Carraro S, Bolzetta F, De Rui M, Perissinotto E, et al. (2014). 'Effect of oral magnesium supplementation on physical performance in healthy elderly women involved in a weekly exercise program: a randomized controlled trial'. Am J Clin Nutr 100:974–981.

Vertano DL, Palmer K, Marengoni A, et al. (2019). 'Frailty and Multimorbidity: A Systematic Review and Meta-analysis'. J Gerontol A Biol Sci Med Sci 74:659-666.

Viengchareun S, Caron M, et al. (2007). 'Mitochondrial toxicity of indinavir, stavudine and zidovudine involves multiple cellular targets in white and brown adipocytes'. Antivir Ther 12:919-929.

Viña J, Borras C, Gomez-Cabrera MC. (2018). 'A free radical theory of frailty'. Free Radic Biol Med 124:358–63.

Viña J, Tarazona-Santabalbina FJ, Pérez-Ros P, Martínez-Arnau FM, Borras C, Olaso-Gonzalez G, Salvador-Pascual A, Gomez-Cabrera MC (2016). 'Biology of frailty: modulation of ageing genes and its importance to prevent age-associated loss of function'. Mol. Asp. Med. 50:88-108.

Vincent AE, et al. (2018). 'Subcellular origin of mitochondrial DNA deletions in human skeletal muscle'. Ann. Neurol 84:289–301.

Virbasius JV, Scarpulla RC (1994). 'Activation of the human mitochondrial transcription factor A gene by nuclear respiratory factors: a potential regulatory link between nuclear and mitochondrial gene expression in organelle biogenesis'. Proceedings of the National Academy of Sciences of the United States of America 91:1309-1313.

Virtuoso VE Jr, Paulo TRS, Martins CA, et al. (2012). 'Physcial activity as an indicator of predicitive functional disability in elderly'. Rev Lat Am Enfermagem 20:259-265.

Virués-Ortega J, de Pedro-Cuesta J, Seijo-Martínez M, Saz P, Sánchez-Sánchez F, Rojo-Pérez F, del Barrio JL (2011). 'Prevalence of disability in a composite ≥ 75 year-old population in Spain: A screening survey based on the International Classification of Functioning'. BMC Public Health 11: 176.

Visser M, et al. (2002). 'Relationship of interleukin-6 and tumor necrosis factor-α with muscle nass and muscle strength in elderly men and women: the Health ABC Study'. J. Gerontol. A Biol. Sci. Med. Sci 57:M326–M332.

Vitoria M, Ford N, et al. (2018). 'The transition to dolutegravir and other new antiretrovirals in low- and middle-income countries: what are the issues?'. AIDS 32:1551–1561.

Vitoria M, Rangaraj A, Ford N, Doherty M (2019). 'Current and future priorities for the development of optimal HIV drugs'. Curr Opin HIV AIDS 14:143-149.

Voets AM, Huigsloot M, Lindsey PJ, et al. (2012). 'Transcriptional changes in OXPHOS complex I deficiency are related to anti-oxidant pathways and could explain the disturbed calcium homeostasis'. Biochim Biophys Acta 1822(7):1161–1168.

Vogel F, Bornhovd C, Reichert S, et al. (2006). 'Dynamic sub compartmentalisation of the mitochondrial inner membrane'. J Cell Biol 175:237-247.

Vogtle FN, Kellermann J, Lottspeich F, Pfanner N, et al. (2011). 'Mitochondrial protein turnover: role of the precursor intermediate peptidase Oct1 in protein stabilization'. Mol. Biol. Cell 22:2135–2143.

Volkert D, Beck AM, Cederholm T, Cruz-Jentoft A, Goisser S, Hooper L, Kiesswetter E, Maggio M, Raynaud-Simon A, Sieber CC, et al. (2019). 'ESPEN guideline on clinical nutrition and hydration in geriatrics'. Clin. Nutr. 38:10–47.

Volt H, Garcia JA, Doerrier C, Díaz-Casado ME, Guerra-Librero A, Lõpez LC, Escames G, Tresguerres J A, Acuña-Castroviejo D (2016). 'Same molecule but different expression: aging and sepsis trigger NLRP3 inflammasome activation, a target of melatonin'. J. Pineal Res 60:193–205.

Wada NI, Jacobson LP, Margolick JB, Breen EB, Macatangay B, Penugonda S, et al. (2015). 'The effect of HAART-induced HIV suppression on circulating markers of inflammation and immune activation'. AIDS 29:463-71.

Waheed S, Attia D, Estrella MM, et al. (2015). 'Proximal tubular dysfunction and kidney injury associated with tenofovir in HIV patients: a case series'. Clin Kidney J 8:420–425.

Wallace DC (1989). 'Mitochondrial DNA mutations and neuromuscular disease'. Trends Genet 5:9-13.

Wallace DC (1992). 'Diseases of the mitochondrial DNA'. Annu Rev Biochem 61:1175–1212.

Wallace DC (2007). 'Why do we still have a maternally inherited mitochondrial DNA? Insights from evolutionary medicine'. Annu Rev Biochem 76:781-821.

Wallace LMK, et. al. (2015). 'Social vulnerability as a predictor of mortality and disability: cross-country differences in the survey of health, aging, and retirement in Europe (SHARE)'. Aging Clin Exp Res 27(3):365-372.

Walston J, Buta B, Xue Q-L (2018). 'Frailty screening and interventions: considerations for clinical practice'. Clin Geriatr Med 34:25-38.

Walston J, McBurnie MA, Newman A, et al. (2002). 'Frailty and activation of the inflammation and coagulation systems with and without clinical comorbidities: results from the Cardiovascular Health Study'. Arch Intern Med 162:2333–2341.

Walston JD (2012). 'Sarcopenia in older adults'. Curr Opin Rheumatol 24:623-627.

Wang C, Youle R (2009). 'The Role of Mitochondria in Apoptosis'. Ann Rev Gen 43:95-118.

Wang H, Lemire B, Cass CE, Weiner JH, Michalak M, Penn AM, Fliegel L (1996). 'Zidovudine and dideoxynucleosides deplete wild-type mitochondrial DNA levels and increase deleted mitochondrial DNA levels in cultured Kearns-Sayre syndrome fibroblasts'. Biochim Biophys Acta 1316:51–59.

Wang W, Wang Y, Long J, et al. (2012). 'Mitochondrial fission triggered by hyperglycemia is mediated by ROCK1 activation in podocytes and endothelial cells'. Cell Metab 15:186–200.

Wang Y, Pessin JE (2013). 'Mechanisms for fiber-type specificity of skeletal muscle atrophy'. Curr Opin Clin Nutr Metab Care 16:243–250.

Wanschitz JV, Dubourg O, Lacene E, Fischer MB, Höftberger R, Budka H, et al. (2013). 'Expression of myogenic regulatory factors and myo-endothelial remodelling in sporadic inclusion body myositis'. Neuromuscul Disord 23:75–83.

Ward JL, Liu Y, Vidoni E D, Maletsky R, Poole D C, et al. (2018). 'Effect of healthy aging and sex on middle cerebral artery blood velocity dynamics during moderate-intensity exercise'. Am. J. Physiol. Heart Circ. Physiol 315:H492–H501.

Warren C, McDonald D, Capaldi R, et al. (2020). 'Decoding mitochondrial heterogeneity in single muscle fibres by imaging mass cytometry'. Sci Rep 10:15336.

Wasserman P, Segal-Maurer S, Rubin DS (2014). 'High prevalence of low skeletal muscle mass associated with male gender in midlife and older HIV-infected persons despite cd4 cell reconstitution and viral suppression'. Journal of the International Association of Providers of AIDS Care 13:145–152.

Weckbecker D, Longen S, Riemer J, Herrmann JM (2012). 'Atp23 biogenesis reveals a chaperone-like folding activity of Mia40 in the IMS of mitochondria'. EMBO J 31:4348–4358.

Weilner S, Grillari-Voguauer R, Redl H, Grillari J, Nau T (2015). 'The role of microRNAs in cellular senescence and age- related conditions of cartilage and bone a review'. Acta Orthop 82:92-99.

Weissman IL (2000). 'Translating stem and progenitor cell biology to the clinic: barriers and opportunities'. Science 287:1442– 1446.

Welle S, Bhatt K, Shah B, Needler N, Delehanty JM, Thornton CA (2003). 'Reduced amount of mitochondrial DNA in aged human muscle'. Journal of Applied Physiology 94:1479–1484.

Wen H, Gris D, Lei Y, Jha S, Zhang L, Huang MT, Brickey WJ, Ting JP (2011). 'Fatty acid-induced NLRP3-ASC inflammasome activation interferes with insulin signaling'. Nat Immunol 12: 408-415

West AP, Brodsky IE, Rahner C, Woo DK, Erdjument-Bromage H, Tempst P, Walsh MC, Choi Y, Shadel GS, Ghosh S (2011). 'TLR signalling augments macrophage bactericidal activity through mitochondrial ROS'. Nature 472:476-480.

Wetzels JF, Kiemeney LA, Swinkels DW, Willems HL, den Heijer M (2007). 'Age- and gender-specific reference values of estimated GFR in Caucasians: The Nijmegen Biomedical Study'. Kidney Int 72:632–637.

Wever K, van Agtmael MA, Carr A (2010). 'Incomplete reversibility of tenofovir-related renal toxicity in HIV-infected men'. J Acquir Immune Defic Syndr 55:78–81.

White SL, Shanske S, McGill JJ, Mountain H, Geraghty MT, DiMauro S, Dahl HH, Throburn D R (1999). 'Mitochondrial DNA mutations at nucleotide 8993 show a lack of tissue- or age-related variation'. J Inherit Metab Dis 22:899-914.

WHO (2016). 'Consolidated Guidelines on the Use of Antiretroviral Drugs for Treating and Preventing HIV Infection'. Recommendations for a Public Health Approach2nd ed.

WHO (2020). 'World health statistics - monitoring health for the SDGs'.

Williams GC (1957). 'Pleiotropy, natural selection, and the evolution of senescence'. Evolution 11: 398-411.

Williams SL, Mash DC, Zuchner S, Moraes CT (2013). 'Somatic mtDNA mutation spectra in the aging human putamen'. PLoS Genet 9:e1003990.

Wilson EMP, Sereti I (2013). 'Immune restoration after antiretroviral therapy: the pitfalls of hasty or incomplete repairs'. Immunol Rev 254:343-354.

Wimalawansa SJ (2019). 'Vitamin d deficiency: Effects on oxidative stress, epigenetics, gene regulation, and aging'. Biology 8:30.

Winston A, Amin J, Mallon P, et al. (2006). 'Minor changes in calculated creatinine clearance and anion-gap are associated with tenofovir disoproxil fumarate-containing highly active antiretroviral therapy'. HIV Med; 7:105–111

Wirthensohn G, Guder WG (1986). 'Renal substrate metabolism'. Physiol Rev 66:469–497.

Wisnovsky S, Jean SR, Kelley SO (2016). 'Mitochondrial DNA repair and replication proteins revealed by targeted chemical probes'. Nat. Chem. Biol 12:567–573.

Womack JA, et al. (2013). 'Physiologic frailty and fragility fracture in HIV-infected male veterans'. Clin Infect Dis 56:1498-1504.

Won JC, Lee JH, Kim JH, Kang ES, Won KC, Kim DJ, et al. (2018). 'Diabetes fact sheet in Korea, 2016: an appraisal of current status'. Diabetes Metab J 42:415-24

Wong C, Gange SJ, Buchacz K, Moore RD, Justice AC, Horberg MA, Gill MJ, Koethe JR, Rebeiro PF, Silverberg MJ, Palella FJ, Patel P, Kitahata MM, Crane HM, Abraham AG, Samji H, Napravnik S, Ahmed T, Thorne JE, Bosch RJ, Mayor AM, Althoff KN. (2017) 'North American AIDS Cohort Collaboration on Research and Design (NA-ACCORD): First occurrence of diabetes, chronic kidney disease, and hypertension among north American HIV-infected adults, 2000-2013'. Clin Infect Dis 64:459–467.

Woodward CL, Hall AM, Williams IG, et al. (2009). 'Tenofovir-associated renal and bone toxicity'. HIV Med 10:482–487.

Wu H, Ballantyne CM (2017). 'Skeletal muscle inflammation and insulin resistance in obesity'. Journal of Clinical Investigation 127:43-54.

Wu H, Kanatous SB, Thurmond FA, Gallardo T, Isotani E, Bassel-Duby R, Williams RS (2002). 'Regulation of mitochondrial biogenesis in skeletal muscle by CaMK'. Science 296:349–352.

Wu H, Naya FJ, McKinsey TA, Mercer B, Shelton JM, Chin ER, Simard AR, Michel RN, BasselDuby R, Olson EN, Williams RS (2000). 'MEF2 responds to multiple calcium-regulated signals in the control of skeletal muscle fiber type'. EMBO J 19:1963–1973.

Wu IC, Shiesh S-C, Kuo PH, Lin XZ (2009). 'High oxidative stress is correlated with frailty in elderly Chinese'. J. Am. Geriatr. Soc. 57:1666-1671.

Wu Z, Puigserver P, Andersson U, Zhang C, Adelmant G, Mootha V, Troy A, Cinti S, Lowell B, Scarpulla RC, Spielgelman BM, (1999). 'Mechanisms controlling mitochondrial biogenesis and respiration through the thermogenic coactivator PGC1'. Cell 98:115-124.

Wyatt CM (2017). 'Kidney disease and HIV infection'. Kidney Disease and HIV 24(1):13-16.

Xia Z, Cholewa J, Zhao Y, Shang H-Y, Yang Y-Q, Araujo Pessoa K, et al. (2017). 'Targeting inflammation and downstream protein metabolism in sarcopenia: a brief up-dated description of concurrent exercise and leucine-based multimodal intervention'. Front. Physiol. 8:434.

Xu J, Han J, Epstein PN, Liu YQ (2006). 'Regulation of PDK mRNA by high fatty acid and glucose in pancreatic islets'. Biochem Biophys Res Commun 344:827-833.

Xu M, et al. (2018). 'Senolytics improve physical function and increase lifespan in old age'. Nat Med 24:1246-1256.

Xue Q-L, Walston JD, Fried LP, et al. (2011). 'Prediction of risk of falling, physical disability, and frailty by rate of decline in grip strength: The women's Heath and Ageing Study'. JAMA 171:1119-1121.

Yakubovskaya E, Byrnes J, Hambardjieva E, Garcia-Diaz M (2010). 'Helix unwinding and base flipping enable human MTERF1 to terminate mitochondrial transcription'. Cell 141:982-993.

Yamamoto M, Biswas AA, et al. (2018). 'Loss of MyoD and Myf5 in skeletal muscle stem cells results in altered myogenic programming and failed regeneration'. Stem Cell Reports 10:956-96

Yamashita S, Nishino I, Nonaka I, Goto Y (2008). 'Genotype and phenotype analyses in 136 patients with single large-scale mitochondrial DNA deletions'. J Hum Genet 53:598-606.

Yan W, Zhang H, Liu P, Wang H, Liu J, Gao C, Liu Y, Lian K, Yang L, Sun L, et al. (2013). 'Impaired mitochondrial biogenesis due to dysfunctional adiponectin-AMPK-PGC-1α signaling contributing to increased vulnerability in diabetic heart'. Basic Res. Cardiol. 108:329.

Yang D, Oyaizu Y, Oyaizu H, Olsen GJ, Woese CR (1985). 'Mitochondrial origins'. PNAS 82(13):4443-4447.

Yang J, Liu H, Wang K, et al. (2017). 'Isolation, culture and biological characteristics of multipotent porcine skeletal muscle satellite cells'. Cell Tissue Bank 18(4):513-525

Yang MY, Bowmaker M, Reyes A, Vergani L, Angeli P, Gringeri E, Jacobs HT, Holt IJ (2002). 'Biased incorporation of ribonucleotides on the mitochondrial Lstrand accounts for apparent strand-asymmetric DNA replication'. Cell 495-505.

Yao C-H, Wang R, Wang Y, Kung C-P, Weber JD, Patti GJ (2019). 'Mitochondrial fusion supports increased oxidative phosphorylation during cell proliferation'. eLife 8:e41351.

Yao X, Li H, Leng SX. (2011). 'Inflammation and immune system alterations in frailty'. Clin Geriatr Med 27(1):79–87.

Yin H, Price F, Rudnicki MA (2013). 'Satellite cells and the muscle stem cell niche'. Physiol Rev 93: 23–67.

Yombi JC, Jones R, Pozniak A, et al. (2015). 'Monitoring of kidney function in HIV-positive patients'. HIV Med 16:457–467.

Yoneda M, Chomyn A, Martinuzzi A, Hurko O, Attardi G (1992). 'Marked replicative advantage of human mtDNA carrying a point mutation that causes the MELAS encephalomyopathy'. Proc. Natl Acad. Sci. USA 89:164–168.

Yoo JI, Park JS, Kim RB, Seo AR, Park YJ, Kim MJ, Park KS (2018). 'WHO disability assessment schedule 2.0 is related to upper and lower extremity disease-specific quality of life'. Qual Life Res : Int J Qual Life Aspects Treat, Care Rehabil 27:2243e2250.

Young JC, Hoogenraad NJ, Hartl FU (2003). 'Molecular chaperones Hsp90 and Hsp70 deliver preproteins to the mitochondrial import receptor Tom70'. Cell 112:41–50.

Young MJ, Copeland WC (2016). 'Human mitochondrial DNA replication machinery and disease'. Current Opinion in Genetics & Development 38:52-62.

Yu C, Chen Y, Cline GW, Zhang D, Zong H, Wang Y, Bergeron R, Kim JK, Cushman SW, Cooney GJ, Atcheson B, White MF, Kraegen EW, Shulman GI (2002). 'Mechanism by which fatty acids inhibit insulin activation of insulin receptor substrate-1 (IRS-1)-associated phosphatidylinositol 3-kinase activity in muscle'. J Biol Chem 277:50230-50236.

Yuan Y, Huang S, Wang W, et al. (2012). 'Activation of peroxisome proliferator-activated receptor-gamma coactivator 1alpha ameliorates mitochondrial dysfunction and protects podocytes from aldosterone-induced injury'. Kidney Int 82:771–789.

Yuzefovych L, Wilson G, Rachek L (2010). 'Different effects of oleate vs. palmitate on mitochondrial function, apoptosis, and insulin signaling in L6 skeletal muscle cells: role of oxidative stress'. Am J Physiol Endocrinol Metab 299:1096-1105.

Zaera MG, et al. (2001). 'Mitochondrial involvement in antiretroviral therapy-related lipodystrophy'. AIDS 15:1643-1651.

Zakeri ZF, Ahuja HS (1997). 'Cell death/apoptosis: normal, chemically induced, and teratogenic effect'. Mtat Res 396:149-161.

Zampieri S, Loefler S, Fruhmann H, Vogelauer M, Burggraf S, Pond A, Grim-Stieger M, Cvecka J, Sedliak M, et al. (2015). 'Lifelong physical exercise delays age-associated skeletal muscle decline'. J Gerontol A Biol Sci Med Sci 70:163-173.

Zane AC, Shardell M, Cameron D, Simonsick EM, Fishbein KW, et al. (2017). 'Muscle strength mediates the relationship between mitochondrial energetics and walking performance'. Aging Cell 16:461–468.

Zanetti HR, da Cruz LG, et al. (2016). 'Nonlinear resistance training enhances the lipid profile and reduces inflammation marker in people living with HIV: a randomised clinical trial'. J Phys Act Health 13:765-70.

Zeballos D, Lins L, Brites C (2019). 'Frailty and its association with health related quality of life in older HIV patients, in Salvador'. Brazil AIDS Res Hum Retroviruses 35(11–12):1074–81

Zhan M, Usman IM, Sun L, et al. (2015). 'Disruption of renal tubular mitochondrial quality control by Myo-inositol oxygenase in diabetic kidney disease'. J Am Soc Nephrol 26:1304–1321.

Zhang W, Nilles TL, Johnson JR, Margolick JB (2015). 'Regulatory T cells, frailty, and immune activation in men who have sex with men in the multicenter AIDS cohort study'. J Gerontol A Biol Sci Med Sci 70(12):1533–41.

Zhao L, An R, Yang Y, et al. (2015). 'Melatonin alleviates brain injury in mice subjected to cecal ligation and puncture via attenuating inflammation, apoptosis, and oxidative stress: the role of SIRT1 signaling'. J Pineal Res 59:230–239.

Zhao Z, Sun K, Lan Z et al. (2017). 'Tenofovir and adefovir down-regulate mitochondrial chaperone TRAP1 and succinate dehydrogenase subunit B to metabolically reprogram glucose metabolism and induce nephrotoxicity'. Scientific reports 7:46344.

Zimmerman A, Bedford J, et al. (2006). 'Tenofovir-associated acute and chronic kidney disease: a case of multiple drug interactions'. Clin Infect Dis 42:283–290.

Zisman A, Abel ED, Michael MD, Mauvais-Jarvis F, Lowell BB, Wojtaszewski JF, Hirshman MF, Virkamaki A, Goodyear LJ, et al. (2000). 'Targeted disruption of the glucose transporter 4 selectively in muscle causes insulin resistance and glucose intolerance'. Nature Medicine 6:924–928.

Zoja C, Garcia PB, Remuzzi G. (2009). 'The role of chemokines in progressive renal disease'. Front Biosci (Landmark Ed) 14:1815–1822.

Zollo O, Tiranti V, Sondheimer N (2012). 'Transcriptional requirements of the distal heavy-strand promoter of mtDNA'. Proceedings of the National Academy of Sciences of the United States of America 109:6508-6512.

Zorov DB, Juhaszova M, Sollott SJ (2014). 'Mitochondrial reactive oxygen species (ROS) and ROS-induced ROS release'. Physiol Rev 94:909– 950.

Zubala A, MacGillivray S, Frost H, *et al*. (2017). 'Promotion of physical activity interventions for community dwelling older adults: a systematic review of reviews'. PLoS One 12:e0180902.

Zuchner S, et al. (2004). 'Mutations in the mitochondrial GTPase mitofusin 2 cause Charcot-Marie-Tooth neuropathy type 2A'. Nat. Genet 36:449–451.

Zwetsloot KA, Childs TE, Gilpin LT, Booth FW (2013). 'Non-passaged muscle precursor cells from 32-month old rat skeletal muscle have delayed proliferation and differentiation'. Cell Prolif 46:45– 57.